GULF OF MEXICO SEAFLOOR STABILITY AND GAS HYDRATE MONITORING STATION PROJECT

FINAL TECHNICAL PROGRESS REPORT

FOR THE 12TH QUARTER
1 October 2003 through 31 March 2004

PREPARED BY THE MANAGEMENT TEAM
THE CENTER FOR MARINE RESOURCES & ENVIRONMENTAL TECHNOLOGY

NOVEMBER 2004

COOPERATIVE AGREEMENT NUMBER:
DE-FC26-00NT40920

Prepared by
The Center for Marine Resources and Environmental Technology
of
The University of Mississippi

This report was prepared with the support of the United States Department of Energy, under award No. DE-FC26-00NT40920. However, any opinions, findings, conclusions, or recommendations expressed herein are those of the authors and do not necessarily reflect the views of the DOE. DOE Award Number DE-FC26-00NT40920 is managed by the U.S. Department of Energy's National Energy Technology Laboratory.

Subcontractors:

J. Robert Woolsey, Thomas M. McGee, Robin C. Buchannon, 220 Old Chemistry, University of Mississippi, University, MS 38677
Task 1: Program Development

Harry Roberts, Coastal Studies Institute, Louisiana State University, 331 Old Geology Complex, Baton Rouge, LA, 70803
Task 2: Site Selection

Roger Sassen, Geochemical and Environmental Research Group, College of Geosciences, Texas A&M University, 833 Graham Road, College Station, TX 77845
Task 3: Site Selection and the Characterization of Vent Gas, Gas Hydrate and Associated Sediments

James M. Brooks, TDI-Brooks International, 1902 Pinon Drive, College Station, TX 77845 and Ian MacDonald and Bernie Bernard, Geochemical and Environmental Research Group, College of Geosciences, Texas A&M University, 833 Graham Road, College Station, TX 77845
Task 4: Heat Flow and Temperature Studies at "Bush Hill" Other and Other Hydrate Sites Using the Submersible Johnson Sea Link

Rudy Rogers, Department of Chemical Engineering, Mississippi State University, PO Drawer 9595, Mississippi State, MS 39762
Task 5: Gas Hydrate Formation and Decomposition in Ocean Sediments

Jean Whelan, Department of Marine Chemistry and Geochemistry, Fye Building MS #4, Woods Hole Oceanographic Institution, 360 Woods Hole Road, Woods Hole, MA 02543
Task 6: Gas Hydrates - Organic Geochemistry

Jeffrey P. Chanton, Department of Oceanography, Florida State University, Tallahassee, FL 32306 and Christopher S. Martens, Department of Marine Sciences, University of North Carolina-Chapel Hill, Chapel Hill, NC 27599
Task 7: Monitoring Biogeochemical Processes Controlling Gas Hydrate Formation, Deposition and Composition in the Gulf of Mexico

Marc Slattery, National Center for Natural Products Research, University of Mississippi, University, MS 38677
Task 8: Deep-Sea Microbes as sources of Biomedically Important Natural Products

Douglass Bartlett and Miriam Kastner, Scripps Institution of Oceanography, University of California-San Diego, La Jolla, CA 92093
Task 9: Scripps Institution of Oceanography Microbiology and Geochemistry

Joel S. Kuszmaul, Department of Geology and Geological Engineering, 118-A Carrier Hall, University of Mississippi, University, MS
Task 10: Establishing the Parameters Required for Spatial Models of Gas Hydrate Collections

DISCLAIMER

This report was prepared as an account of work sponsored by an agency of the United States Government. Neither the United States Government nor any agency thereof, nor any of their employees, makes any warranty, express or implied, or assumes any legal liability or responsibility for the accuracy, completeness, or usefulness of any information, apparatus, product, or process disclosed, or represents that its use would not infringe privately owned rights. Reference herein to any specific commercial product, process, or service by trade name, trademark, manufacturer, or otherwise does not necessarily constitute or imply its endorsement, recommendation, or favoring by the United States Government or any agency thereof. The views and opinions of authors expressed herein do not necessarily state or reflect those of the United States Government or any agency thereof.

ABSTRACT

The gas hydrates research Consortium (HRC), established and administered at the University if Mississippi's Center for Marine Research and Environmental Technology (CMRET) has been active on many fronts in FY 03. Extension of the original contract through March 2004, has allowed completion of many projects that were incomplete at the end of the original project period due, primarily, to severe weather and difficulties in rescheduling test cruises. The primary objective of the Consortium, to design and emplace a remote sea floor station for the monitoring of gas hydrates in the Gulf of Mexico by the year 2005 remains intact. However, the possibility of levering HRC research off of the Joint Industries Program (JIP) became a possibility that has demanded reevaluation of some of the fundamental assumptions of the station format. These provisions are discussed in Appendix A.

Landmark achievements of FY03 include:

- Continuation of Consortium development with new researchers and additional areas of research contribution being incorporated into the project. During this period, NOAA's National Undersea Research Program's (NURP) National Institute for Undersea Science and Technology (NIUST) became a Consortium funding partner, joining DOE and Minerals Management Service (MMS),
- Very successful annual and semiannual meetings in Oxford Mississippi in February and September, 2003,
- Collection of piston cores from MC798 in support of the effort to evaluate the site for possible monitoring station installation,
- Completion of the site evaluation effort including reports of all localities in the northern Gulf of Mexico where hydrates have been documented or are strongly suspected to exist on the sea floor or in the shallow subsurface,
- Collection and preliminary evaluation of vent gases and core samples of hydrate from sites in Green Canyon and Mississippi Canyon, northern Gulf of Mexico,
- Monitoring of gas activity on the sea floor, acoustically and thermally,
- Design, construction, and successful deployment of an *in situ* pore-water sampling device,
- Improvements to the original Raman spectrometer (methane sensor),
- Laboratory demonstration of the impact of bacterially-produced surfactants' rates of hydrate formation,
- Construction and sea floor emplacement and testing - with both watergun and ship noise sources - of the prototypal vertical line array (VLA),
- Initiation of studies of spatial controls on hydrates,
- Compilation and analyses of seismic data, including mapping of surface anomalies,
- Additional field verification (bottom samples recovered), in support of the site selection effort,
- Collection and preliminary analyses of gas hydrates from new sites that exhibit variant structures,
- Initial shear wave tests carried out in shallow water,
- Isolation of microbes for potential medicinal products development,
- Preliminary modeling of occurrences of gas hydrates.

TABLE OF CONTENTS Page

SUBCONTRACTORS…..…..……..ii
DISCLAIMER.....iii
ABSTRACT.....iv
TABLE OF CONTENTS.....v
LIST OF GRAPHICAL MATERIALS.....v
INTRODUCTION.....1
EXECUTIVE SUMMARY.....2
EXPERIMENTAL.....3
RESULTS AND DISCUSSION.....3
CONCLUSION.....3
REFERENCES.....3
LIST OF ACRONYMS AND ABBREVIATIONS.....3
APPENDIX: STATUS/PROGRESS REPORTS SUBMITTED BY THE SUBCONTRACTORS
Task 1: Program Development…….……..5
Task 2: Site Selection…..……....12
Task 3: Site Selection and Characterization of vent gas, gas hydrate and Associated Sediments ……....12
Task 4: Heat Flow and Temperature Studies at Bush Hill and other Hydrate Sites using the Submersible, Johnson Sea Link……..……..…228
Task 5: Gas Hydrate Formation and Decomposition in Ocean Sediments……..……..265
Task 6: Gas Hydrates - Organic Geochemistry…….....277
Task 7: Monitoring Biogeochemical Processes Controlling Gas Hydrate Formation, Deposition and Composition in the Gulf of Mexico...……..314
Task 8: Deep Sea Microbes as Sources of Biomedically-Important Natural Products….334
Task 9: Scripps Institute of Oceanography Microbiology and Geochemistry……....341
Task 10: Establishing the Parameters Required for Spatial Models of Gas Hydrate Collections……...……..…356

LIST OF GRAPHICAL MATERIALS

Figures appropriate to the individual subcontractor's research appear in those researchers' reports listed by task number.

INTRODUCTION

Established in1999, the objective of the Gulf of Mexico gas hydrate monitoring station project is to emplace a remote, multi-sensor monitoring station at a selected location within the hydrate stability zone of the northern Gulf of Mexico. Plans for the station have produced subsets of research related to the establishment, emplacement and maintenance of the facility. These include physical, chemical, and biological components of the hydrocarbon system, location of the station, both geographically and within the water column, and means of accessing, assessing, and archiving the acquired data. Eventually this data base will be made available to groups investigating gas hydrate for energy resource potential and environmental impact.

Responsibility for oversight of each activity of the project is vested in a member of the project's Scientific Supervisory Board. The FY2002 board members were:

- Managing Director: Bob Woolsey, Center for Marine Resources and Environmental Technology, University of Mississippi, Oxford, MS.
- Geologic Setting: Harry Roberts, Coastal Studies Institute, Louisiana State University, Baton Rouge, LA.
- Vertical Line Arrays: Ross Chapman, School of Earth and Ocean Sciences, University of Victoria, British Columbia, Canada
- Water Currents: Vernon Asper, School of Marine Sciences, University of Southern Mississippi, Stennis Space Center, MS.
- Gas Bubble Studies: Ralph Goodman, School of Marine Sciences, University of Southern Mississippi, Stennis Space Center, MS.
- Geoelectric Systems: Rob Evans, Woods Hole Oceanographic Institution, Woods Hole, MA.
- Geochemistry: Roger Sassen, Geochemical and Environmental Research Group, Texas A&M University, College Station, TX.
- Water Chemistry: Jean Whelan, Woods Hole Oceanographic Institute, Woods Hole, MA.
- Pore Water Chemistry: Jeff Chanton, Department of Oceanography, Florida State University, Tallahassee, FL.
- Laboratory Studies: Rudy Rogers, Chemical Engineering Department, Mississippi State University, Starkville, MS.
- Heat Flow Studies: Bernie Bernard, TDI-Brooks International Inc., College Station, TX.
- Pharmaceuticals: Marc Slattery, Pharmacognosy Department, University of Mississippi, Oxford, MS.
- Comparative Studies: Camelia Diaconescu, Department of Geological Sciences,University of South Carolina, Columbia, SC.
- Data Recovery: Paul Higley, Specialty Devices Inc. (SDI), Plano, TX.
- Site Surveys: Tom McGee, CMRET, University of Mississippi, Oxford, MS.

EXECUTIVE SUMMARY

During FY 2003 all tasks described in the original contracts were either completed or funds were redirected to carry out research related to the eventual completion and installation of the monitoring station. Due to complications of funding and scheduling of research activities, the project work period was extended, mid-year, to March 31, 2003. Therefore, most component research activities had not been completed by the close fiscal year 2002. However, a number of significant achievements had been made and others were in progress at the close of the FY02 reporting period.

A large quantity of hydrocarbon fluids floats on the surface of the Gulf of Mexico. At certain locations, oil slicks are extensive enough to be seen from space. The origins of these slicks are natural seeps on the sea floor. Much of the oil rides up on gas bubbles, some of which may originate from the dissociation of natural gas hydrates. This is the basis of concern that drives a significant portion of the hydrate research being done in the Gulf. The Consortium continues to include studies of the properties of bubbles as priority investigation. While the study of the acoustical properties of bubbles, funded in FY01, is not a component of this report, the funding and the studies will resume in FY03. In addition, the Consortium is pursuing other possible bubble investigations, including the mechanical properties of bubbles, at great depth.

Hydrates have been observed and investigated directly by Consortium participants. Temperature probes were inserted directly into outcropping mounds on the sea floor of the Gulf of Mexico (GOM) as well as into nearby mud. Temperatures obtained from the hydrate mounds, the mud, and the water column directly above these sites will serve to advance current knowledge and thinking regarding thermal conductivity of hydrate deposits and their surroundings.

A device for sampling pore water in the upper meter of sea-floor sediment and returning the samples to the surface under *in situ* pressure was designed and built. This device was deployed, successfully, from the Johnson Sea Link. Initial results reveal the highest concentrations of dissolved hydrocarbons yet reported.

Design modifications to improve the resolution of the Raman spectrometer, built with DOE FY01 funding, were made. The device is intended to be mounted on a submersible vehicle so that it can be deployed to analyze hydrocarbons near sea-floor seeps. Outstanding obstacles include the need for this instrument to make measurements extremely rapidly so that variations can be detected over very small distances.

Laboratory studies of hydrate formation continue at Mississippi State University. This work has already demonstrated the significant impact of bacterially produced surfactants on the rate of hydrate formation. New studies address hydrate formation in relation to composition and configuration of host particles.

The prototype vertical line array (VLA) was completed, deployed and tested during FY02. Test tracks were run using both an 80 in^3 water gun and ship noise as acoustic sources. The VLA was deployed in 830 meters of water at a site where previous heat-flow measurements indicated that the base of the hydrate stability zone (BHSZ) is located about 400 meters below the sea floor. A deep-towed hydrophone was also deployed to provide surface-source/deep-receiver (SS/DR) profiles simultaneously with the VLA recordings. The data sets will be processed, analyzed for possible hydrate-related features, and compared.

The University of Mississippi and the University of Wales (Bangor) carried out shear wave studies using a hydrophone and a 3-component accelerometer mounted in a probe that was pushed into sediments of the shallow water in Mississippi Sound. Difficulties encountered in this test form the basis for work aimed at continuing to improve the sensitivity of this instrument.

A variety of samples was recovered from a number of environments known to contain gas hydrates. Testing of these samples is ongoing with plans to use the produced data to determine a sampling protocol for the summer 2003.

Spatial analyses of hydrate-bearing deposits has begun and occurrences of hydrates in the Gulf of Mexico are being compared to those in other marine deposits in an effort to characterize these deposits.

Two problems that have not yet been addressed adequately by the consortium are:

1) supplying electrical power to sensors on the sea floor and
2) telemetering the resulting data to an onshore facility.

The possibility of using an existing oil production platform to solve both has been discussed but has not seemed very appealing because it would seriously limit the choice of monitoring station sites. Alternative solutions have been identified, tentatively, during the past few months:

1) Total power requirements would be rather modest if power generation could be done on the sea floor because the loss associated with transmission from surface to sea floor would be avoided. Sea-floor generation may be feasible using a type of microbial battery that has been under development for some years by Naval Research Laboratory (NRL).
2) The NOAA National Data Buoy Center at Stennis Space Center has expressed an interest in providing a buoy to bring the data to the surface. An interest has also been expressed in engineering the transmission of data over the NOAA satellite system to the Stennis facility.

EXPERIMENTAL: CONTAINED IN PROGRESS-REPORTS FROM THE SUBCONTRACTORS THAT FOLLOW "RESULTS AND DISCUSSION"

RESULTS AND DISCUSSION: CONTAINED IN THE FOLLOWING PROGRESS-REPORTS FROM THE SUBCONTRACTORS

CONCLUSIONS

The work of the HRC is now supported, approximately equally, by three federal agencies: MMS, DOE, and NIUST (NOAA-NURP). Sensor development has advanced to, in most cases, the sea-trials phase. Data acquisition and transfer needs are just beginning to be addressed and will have to be incorporated into the next round of proposals and funding requests. Affiliation with the JIP has necessitated changes in the plan for the Monitoring Station/Sea Floor Observatory (MS/SFO) deployment scheduling as well as many of the details of configuration.

REFERENCES: LISTED IN THE INDIVIDUAL REPORTS OF THE SUBCONTRACTS

LIST OF ACRONYMS AND ABBREVIATIONS

BHSZ – Base of the Hydrate Stability Zone
BLA – borehole vertical line array
CD – compact disk
CMC – critical micellar concentration
CMRET – Center for Marine Resources and Environmental Technology
DIC – dissolved inorganic carbon
DOE – Department of Energy
DRS – data recovery system
FSU – Florida State University
FY - fiscal year
GC – gas chromatography
GC(#) – Green Canyon (followed by block number)

GHASTLI – Gas Hydrate and Sediment Test Laboratory Instrument
GOM – Gulf of Mexico
HRC – Hydrates Research Consortium
HSZ – Hydrate Stability Zone
IDP – integrated data power unit
IRMS – isotope ratio mass spectrometer
JIP – Joint Industries Project
JSL – Johnson Sea Link
MC – Mississippi Canyon
METS – methane sensor available commercially
MMS – Minerals Management Service
MS/SFO – monitoring station or sea floor observatory
NIUST – National Institute for Undersea Science and Technology
NOAA – National Oceanographic and Atmospheric Administration
NRL – Naval Research Laboratory
NURP – National Undersea Research Program
PCB – pressure compensated battery
PI – Principal Investigator
PVC – polyvinyl chloride
ROV – Remotely Operated Vehicle
RV = R/V – Research Vessel
SDS – sodium dodecyl sulfate
SFO – Sea floor observatory
SRR – sulfate reduction rates
SS/DR – surface source/deep receiver
SSD – station service device
TOC – total sedimentary organic carbon
UM/UMiss – University of Mississippi
UNC – University of North Carolina
USGS – United States Geological Survey
UVic – University of Victoria (British Columbia)
VLA – Vertical Line Array

GULF OF MEXICO SEAFLOOR STABILITY AND GAS HYDRATE MONITORING STATION PROJECT

Task 1: Program Development

FINAL TECHNICAL PROGRESS REPORT
DECEMBER 2003

FOR THE 12TH QUARTER
1 July 2003 through 30 September 2003

Principal Investigators: J.R. Woolsey, T.M. McGee, Robin Buchannon, Carol Blanton Lutken
Mississippi Mineral Resources Institute and the Center for Marine Resources and Environmental Technology, University of Mississippi
220 Old Chemistry Building
University, Mississippi 38677

DOE Award DE-FC26-00NT40920

ABSTRACT

Program development in FY03 included all proposal organization and reporting to the Department of Energy. The Annual Meeting of the Consortium, hosted by the Center for Marine Resources and Environmental Technology (CMRET), was held in Oxford, Mississippi, February 17-18, 2003 to define future needs. A semiannual meeting, also held in Oxford, was attended by some 30 participants, September 10-11, 2003, and served as a midyear evaluation point for the group. Since the FY02 contract had been extended to 30 September, 2003, then again to 31 March, 2004, progress reports were given by Consortium participants funded under both FY02 and FY03 DOE grants.

Program Development highlights include:

- A shallow (500-1000m water depth) and a deeper (>1000m water depth) water site are being further characterized,

- The funding granted by DOE to support investigation of the use of an established, industrial platform in the Gulf of Mexico was successfully redirected to fund a cruise to recover cores from the Mississippi Canyon, Northern Gulf of Mexico. Ten 2-8m cores were recovered from the Mississippi Canyon in January of 2004. The cores have been sampled and are currently being evaluated for various properties including age and their ability to "grow" hydrate in the laboratory.

- Establishment of the ChevronTexaco Joint Industries Project (JIP) has influenced many aspects of the Hydrates Monitoring Station research, including site selection. Scientists from the Consortium are playing active roles in the selection of the site that the JIP is scheduled to drill in the Gulf of Mexico in 2004.

TABLE OF CONTENTS

TITLE PAGE
ABSTRACT
TABLE OF CONTENTS
GRAPHICAL MATERIALS
INTRODUCTION
EXECUTIVE SUMMARY
EXPERIMENTAL
RESULTS AND DISCUSSION
CONCLUSION
REFERENCES
ACRONYMS/ABBREVIATIONS

GRAPHICAL MATERIALS

Figure 1-1. Diagram of the component parts of the monitoring station/sea floor observatory.

INTRODUCTION

Established in1999, the objective of the Gulf of Mexico gas hydrate monitoring station project is to emplace a remote, multi-sensor monitoring station at a selected location within the hydrate stability zone of the northern Gulf of Mexico. Plans for the station have produced subsets of research related to the establishment, emplacement and maintenance of the facility. These include physical, chemical, and biological components of the hydrocarbon system, location of the station, both geographically and within the water column, and means of accessing, assessing, and archiving the acquired data. Eventually this data base will be made available to groups investigating gas hydrate for energy resource potential and environmental impact.

The CMRET, as the administrator of the Consortium, organizes an annual and a semiannual meeting each year, usually held in Oxford, Mississippi. The principal goals of these meetings are to maintain communications between investigators and to keep the project on task and on schedule. Attendees include researchers from academia as well as from industry and government and representatives from the Consortium funding agencies, MMS, DOE and, now, the National Oceanic and Atmospheric Administration's National Undersea Research Program's National Institute for Undersea Science and Technology (NOAA-NURP-NIUST). In addition, a compact disk including the agenda, attendees and contact information, presentations and related information from the meeting is produced and distributed to attendees and other interested parties.

The final project of this funding cycle involved the replacement of Conoco's platform-based work with the acquisition of cores from the sea floor in an area from which no core data were available. These cores, subsampled in June, 2004, will be used to establish dates of deposition for shallow units in Mississippi Canyon and to attempt to characterize the sediments in terms of potential for hosting hydrates.

EXECUTIVE SUMMARY

Program development in FY03 included all proposal organization and reporting to the Department of Energy. The Annual Meeting of the Consortium, hosted by the Center for Marine Resources and Environmental Technology (CMRET), was held in Oxford, Mississippi, February 17-18, 2003. This meeting was attended by over 40 active Consortium participants who collaborated on evaluation of the project to date and in defining future needs. Many of the needs were incorporated into summer research plans. A semiannual meeting, also held in Oxford, was attended by some 30 participants, September 10-11, 2003, and served as a midyear evaluation point for the group. Compact disks (CDs) including each meeting's agenda, presentations, attendees and contact information were produced and distributed to those who attended the meeting. The CDs have also been made available to any Consortium member who has requested them. Since the FY02 contract had been extended to 30 September, 2003, then again to 31 March, 2004, progress reports were given by Consortium participants funded under both FY02 and FY03 DOE grants. The following sections comprise highlights of the progress reported at these two meetings.

- Site selection has progressed to the point that a shallow (500-1000m water depth) and a deeper (>1000m water depth) water site are being further characterized. Hydrates are now known to occur either at the surface or within the shallow subsurface at both sites.

- The funding granted by DOE to support investigation of the use of an established, industrial platform in the Gulf of Mexico was successfully redirected to fund a cruise to recover cores from the Mississippi Canyon, Northern Gulf of Mexico. This is an area of known hydrate occurrence (Neurauter and Bryant, 1989) and one from which the

CMRET has acquired much seismic data and had already contracted TDI Brooks, International to acquire heat flow data. No core data were available from this area so when the Conoco contract was negated with the August 30, 2002 merger transaction between Conoco Inc. and Phillips Petroleum, the CMRET applied to DOE to allow the redirection of funds. The result is that ten 2-8m cores were recovered from the Mississippi Canyon in January of 2004. The cores have been sampled and are currently being evaluated for various properties including age (University of Southern Mississippi) and their ability to "grow" hydrate in the laboratory (Mississippi State University). Other researchers will perform additional investigations pending the results of these first studies.

- Establishment of the ChevronTexaco Joint Industries Project (JIP) has influenced many aspects of the Hydrates Monitoring Station research, including site selection. Scientists from the Consortium are playing active roles in the selection of the site that the JIP scheduled to drill in the Gulf of Mexico in 2004. Details of the major changes that cooperation with the JIP has necessitated follow:

EXPERIMENTAL

RECOVERY OF CORE MATERIAL FROM MISSISSIPPI CANYON 798

Carol Lutken, CMRET geologist and Charlotte Brunner, University of Southern Mississippi paleontologist and faculty member at Stennis Space Center campus, participated in the January cruise aboard TDI Brooks, International RV J.W. Powell (for vessel specifications, go to http://www.tdi-bi.com/vessels/powell.htm) in the northern Gulf of Mexico. The purposes of the cruise were several but the Consortium contracted with TDI for 3 days' coring time, waiving transit time as a favor, in support of the research efforts of the Consortium.

Core sites were selected following runs across features observed on 1998 Huntec boomer data and confirmed with onboard chirp sonar. Ten cores were recovered for the following reasons:

- The location was proximal to an area of reported hydrate outcrop,
- The location was distant from areas of reported hydrate outcrop and appeared, on the chirp records to represent continuous deposition and minimal deformation,
- The location was shown on chirp records to be an acoustic wipe-out zone,
- The location appeared, on chirp records, to have had younger units missing and so recovered samples might represent stratigraphically older units,
- The location was coincident with that of a vertical array deployment in 2002 or 2003.

All cores were recovered using 3-inch diameter core-liners in the piston coring apparatus deployed from the Powell's starboard a-frame. Recovery ranged from 1.97m to 7.13m. Following recovery, all cores were cut into 120cm sections, capped, labeled and stored upright until they were off-loaded at Venice, La. Following their trip to Oxford, they were returned to Stennis where they were logged using the Naval Research Laboratory's logger. They were stored in an enclosed, temperature-controlled facility. In June, the core sections were split and one half archived. The other half was photographed, sampled, wrapped, and stored for possible future sampling. The samples were transported to Mississippi State University and to the University of Southern Mississippi, Stennis Space Center via automobile where they will be analyzed with regard to hydrate-producing/hosting potential and age analyses.

CHANGES IN THE SFO DESIGN AND DEPLOYMENT SCHEDULE

ARRAY DESIGN AND DEVELOPMENT

A most important development is the opportunity to deploy an array of sensors in a borehole that will be drilled by the Department of Energy/Joint Industry Project (DOE/JIP) Consortium. The borehole vertical line array (BLA) will consist of hydrophones, three-component accelerometers and temperature sensors that would remain in the hole after the drill stem is recovered, letting the hole collapse and making the installation permanent and thus providing a sub-seafloor component to the station.

The BLA has been funded, separately, by the DOE/JIP and it would not represent a cost increase to the station. The Consortium is, however, investigating the possibility of adding horizontal arrays to the station configuration. This would provide three-dimensional coverage of the water column, seafloor and sub-seafloor at the monitoring station site. It may be that some of the vertical arrays can be converted to horizontal arrays if this route is pursued.

DATA RECOVERY

External factors have also impacted the way monitoring station data will be recovered. For some time it has been hoped that a commercial service would be available in 2004 which would allow the station data-collecting unit to stream data onto an optic-fiber link for near-to-real time transmission to shore. It was learned in the autumn of 2003, however, that the service would not become available until 2006 or later.

The use of a remotely operated vehicle (ROV) to download data directly from the station's data loggers was found to be prohibitively expensive due to the depth of water and the weight of the battery packs that would need to be exchanged. Therefore, until the optic fiber link becomes available, an integrated data power (IDP) module will stream data onto an optic-fiber data recovery system (DRS) which will be connected via optic fiber to an access connector. Whenever downloading is required, a system of buoys will bring the DRS access connector to the surface so that the data can be downloaded onto a computer in a boat. The system has been used successfully before and involves far less expense than repeated use of a deep-water ROV. The system has been dubbed the "Big M" and is illustrated in Fig.1-1.

ELECTRICAL POWER FOR THE MS/SFO

The Gulf of Mexico Hydrates Research Consortium funds the development of microbial batteries but it will be some time before this emerging technology can provide sufficient electrical power to the monitoring station. In the meantime, the IDP module will supply electricity to the station by exchanging the pressure compensated battery (PCB) component about once a year. This will involve unplugging the depleted PCB from the IDP and plugging in a fresh one. The emplacement and exchange of PCBs will be accomplished by a station service device (SSD). The SSD is a ROV-like system, especially designed for the task, that utilizes the power and weight of the payload PCB to supplement the maneuvering of the surface vessel to dock and enable the PCB exchange. The design somewhat restricts the radius of operation, but eliminates the costly power umbilical required by conventional deep ocean ROV's.

A docking station will be incorporated into the IDP module to facilitate changing the PCB's. The SSD will carry the recharged PCB unit to the sea floor and return with the depleted unit. In addition, the SSD will be capable of conducting other tasks such as taking pressure retained short cores and *in situ* pore-fluid samples. Perhaps most significantly, the SSD will be the means by which all station systems are connected to the IDP for data recovery and electrical power.

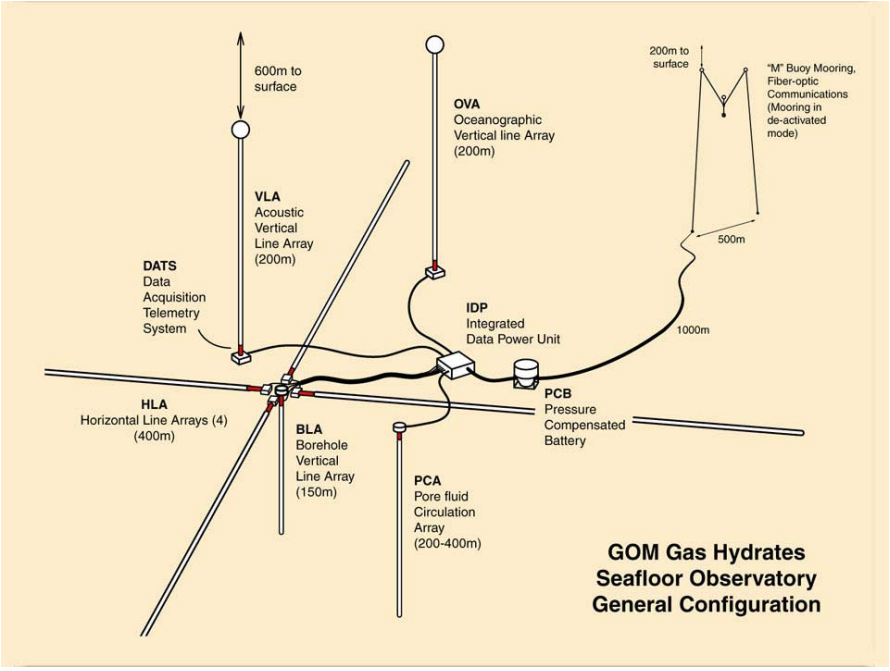

Figure 1-1. Diagram of the component parts of the monitoring station/sea floor observatory

RESULTS AND DISCUSSION

The Mississippi Canyon sample-analyses are underway. Preliminary indications are that the sediments recovered produce hydrates under laboratory conditions and that there are pre-Holocene sediments in our samples. More detail will appear in future reports.

Results of the JIP decisions are, as yet, unknown. Drilling location discussions are still underway.

CONCLUSIONS

Two meetings were held at which Consortium members presented results of their research and made significant progress toward surmounting some of the major obstacles remaining to MS/SFO installation on the sea floor. Small group sessions enabled new and continuing cooperations to be established or advance.

The first samples to which consortium members have had access have been recovered from the sea floor in Mississippi Canyon 798. Evaluation of these samples has commenced and will be included in FY03 reporting.

MS/SFO scheduling and physical modifications discussed herein are not intended to change the basic concepts, overall plans and mission for the monitoring station. Instead, they are expected to enhance the accomplishment of that mission. The MS/SFO will gain a significant degree of autonomy, provide time on the learning curve to deal with the large data sets generated by the station, provide an ROV-like SSD capable of conducting a wide range of support activities, and, probably most important, keep on task towards station deployment in 2005 and operation by 2006.

REFERENCES

Neurauter, T.W. and W.R.Bryant, 1989, "Gas hydrates and their association with mud diapir/mud volcanos on the Louisiana continental slope," Proc. 21st Offshore Tech. Conf., Paper No. 5944, **vol.1**, 599-607.

LIST OF ACRONYMS AND ABBREVIATIONS

BLA – borehole vertical line array
CD – compact disk
CMRET – Center for Marine Resources and Environmental Technology
DOE – Department of Energy
DRS – data recovery system
FY - fiscal year
GOM – Gulf of Mexico
HRC – Hydrates Research Consortium
IDP – integrated data power unit
JIP – Joint Industries Project
MC – Mississippi Canyon
MMS – Minerals Management Service
MS/SFO – monitoring station or sea floor observatory
NIUST – National Institute for Undersea Science and Technology
NOAA – National Oceanographic and Atmospheric Administration
NURP – National Undersea Research Program
PCB – pressure compensated battery
ROV – Remotely Operated Vehicle
RV = R/V – Research Vessel
SFO – Sea floor observatory = MS/SFO
SSD – station service device
UM/UMiss – University of Mississippi
VLA – Vertical Line Array

Tasks 2 and 3

Site Selection and Characterization of Vent Gas, Gas Hydrate and Associated Sediments

Annual Technical Report
January 1, 2002 – June 30, 2004

Roger Sassen, Geochemical and Environmental Research Group, Texas A&M University, College Station, Texas 77845
and
Harry H. Roberts, Department of Oceanography and Coastal Studies, Louisiana State University, Baton Rouge, Louisiana 70803

June 28, 2004
DOE Award # DE-FC26-00NT40920

SITE SELECTION AND CHARACTERIZATION OF VENT GAS, GAS HYDRATE AND ASSOCIATED SEDIMENTS

Principal Investigators: Roger Sassen, Geochemical and Environmental Research Group, Texas A&M University, College Station, Texas 77845
and
Harry H. Roberts, Department of Oceanography and Coastal Studies, Louisiana State University, Baton Rouge, Louisiana 70803

Table of Contents

Abstract
Introduction
Executive Summary
Geologic Setting and Deep Fluid Sources
Review of Gas Hydrate in the Gulf of Mexico Slope
Experimental
Results and Discussion
Descriptions of JSL Sites with Gas Hydrate
Descriptions of JSL Sites without Gas Hydrate
Geochemistry of Vent Gas, Gas Hydrate, and Sediment Gas
Biodegradation of Crude Oil
Isotopic Properties of Authigenic Carbonate Rock
Sites Lacking Gas Hydrate
Conclusions
References
Bibliography
Acronyms and Abbreviations
List of Graphics

ABSTRACT

The total volume of the gas hydrate resource in the Gulf of Mexico slope is estimated to be equivalent to ~1.0-1.4 x 10 m^3 of gas at STP including methane and other hydrate-forming hydrocarbons. The estimate of the Gulf slope hydrate resource is based solely on gas hydrate proven to occur in the mud matrix. There is no evidence as yet that gas hydrate fills pore-space in sands of the Gulf slope. Research on gas hydrate as an alternate energy source or drilling hazard in the Gulf slope should focus on mud as the dominant "reservoir" for gas hydrate. Bottom Simulating Reflectors (BSR) may be a secondary issue in the total energy resource estimate.

The discovery of gas hydrate at the sea floor greatly increases the probability of deep gas hydrate accumulations in the same area. As part of the present study, samples of intact massive gas hydrate were successfully collected from three (3) main sites along with the vent gas from which the gas hydrate crystallized and associated sediment to include

authigenic carbonate rock strongly depleted in ^{13}C. The sites from which intact gas hydrate and vent gas were successfully recovered are Green Canyon (GC) Block 234, GC 232, and Mississippi Canyon (MC) Block 118. The combination of 38 kHz imagery showing large gas plumes in the water column with conventional shallow seismic amplitudes may improve the probability of discovering new gas hydrate sites.

The molecular properties of vent gas provide strong evidence that gas hydrate is not decomposing at a significant rate in the Gulf of Mexico. Some minor decomposition of extremely shallow gas hydrate is likely to occur but deeply buried gas hydrate appears stable over long spans of time. Exposed or shallow gas hydrate may be affected by sea water temperature changes, but overall gas hydrate is apparently accumulating in the Gulf of Mexico slope at present. Thus monitoring of gas hydrate by seismic arrays should focus on the upper few meters of study sites.

Three "control" sites with strong geophysical anomalies were also sampled to determine why no gas hydrate occurs. The apparent lack of gas hydrate at the VK 826 and MC 885 sites may be partially attributed to low hydrocarbon gas flux but the carbonate-rich sites are also too shallow and warm for structure I or II gas hydrate to be stable. In addition, brines are likely to retard gas hydrate crystallization. The MC 709 is a major geophysical anomaly and may or may not contain any gas hydrate although there are areas with intermediate hydrocarbon flux within the Gas Hydrate Stability Zone. The main reason for the lack of abundant gas hydrate at MC 709 may be brine poisoning. More than 160 major gas seeps identified in the deep Gulf of Mexico slope appear to lack gas hydrate. Additional research on factors that prevent gas hydrate crystallization is justified.

INTRODUCTION

In multidisciplinary study of natural gas hydrate, one of the fundamental aspects is to document the basic molecular and isotopic properties of vent gas at the sea floor that gives rise to gas hydrate, the gas hydrate itself, and the sediments intimately associated with gas hydrate. All other research studies depend upon this type of basic information on gas hydrate for their context. This task was undertaken with collaboration from Dr. Harry Roberts of Louisiana State University, who apportioned dive time in the Johnson Sea-Link (JSL) research submersible during the mid-summer of 2002.

Samples of intact gas hydrate were successfully collected from three (3) main sites along with the vent gas from which the gas hydrate crystallized and associated sediment. The sites from which intact gas hydrate and vent gas were successfully recovered are Green Canyon (GC) Block 234, GC 232, and Mississippi Canyon (MC) Block 118 (Fig. 1). Specialized sampling equipment was used to include a high-pressure vessel designed to recover gas hydrate from the sea floor and to return it to the surface intact at temperature and pressure conditions approximately ambient to the deep sea floor.

The GC 234 site has been visited before and new data can be set in the context of previously published research to assess any detectable change in the gas hydrate system at this site. In contrast, gas hydrate was recovered for the first time from GC 232 and

from MC 118. GC 232 is similar to the GC 234 site; the MC 118 site is the most eastward gas hydrate site ever discovered in the Gulf of Mexico. Preliminary molecular and isotopic analyses were performed to characterize the samples as examples of gas hydrate sites. The gas hydrate from these sites can be compared to gas hydrate from other sites in the Gulf of Mexico.

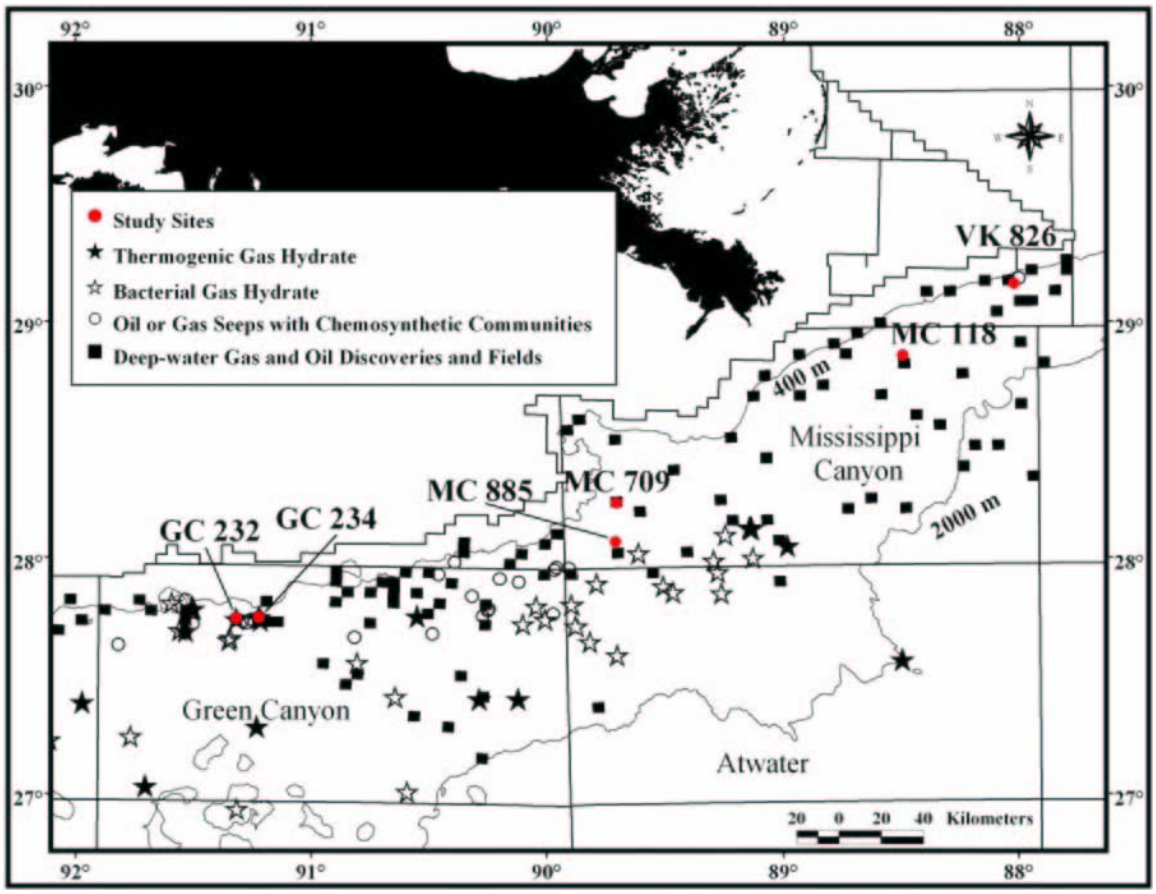

Figure 1. Map showing locations of main study sites of the Gulf slope with gas hydrate (GC 234, GC 232, and MC 118) within a region of has hydrate occurrences, seeps with chemosynthetic communities, and subsurface accumulations of oil and gas. Other study sites used as control sites without gas hydrate are also shown (MC 709, MC 885, VK 826). Hydrate map modified from Sassen et al. (2001a) and sites of chemosynthetic communities from MacDonald et al. (1996).

It is important to emphasized that piston cores taken at many gas-rich sites (>160) within the Gas Hydrate Stability zone (GHSZ) of the Gulf of Mexico have not recovered gas hydrate (Sassen et al., 2002). Such sites are obvious geophysical anomalies and contain abundant free methane and other gases that form hydrate under proper conditions. The ratio of known gassy sites without gas hydrate to sites with gas hydrate is ~2:1. Geophysics has limitations at present in direct sensing of gas hydrate that are not widely recognized. Why no hydrate occurs within the GHSZ where abundant free gas is available is an important question that demands a scientific explanation.

A series of "control" sites lacking gas hydrate were characterized and sampled by the JSL dives in 2002 in order to assess the characteristics of sites that do not show any evidence of gas hydrate near the surface of the sea floor. The JSL sites without gas hydrate include MC 709, MC 885, and Viosca Knoll (VK) 826 (Fig. 1).

The ultimate rationale for the studies is to help determine characteristics of known sites for gas hydrate suitable for further study to include vertical seismic arrays intended to show changes related to instability. The question presupposes that gas hydrate can be directly detected by geophysics and that instability of gas hydrate is sufficient to be detectable. Another ultimate goal is to high-grade sites for deep rotary coring that will provide maximum information on gas hydrate as a drilling hazard and in terms of economic geology. The results of the present study are surprising.

EXECUTIVE SUMMARY

The total volume of the gas hydrate resource in the Gulf slope is estimated to be equivalent to ~1.0-1.4 x 10^{13} m^3 of gas at STP including methane and other hydrate-forming hydrocarbons. The estimate of the Gulf slope hydrate resource is based solely on gas hydrate proven to occur in the mud matrix. It should be emphasized that nearly all known occurrences of gas hydrate in the Gulf of Mexico occur as vein-fillings and thick pavements of nearly pure gas hydrate in hemipelagic mud. Rarely, gas hydrate fills vuggy porosity in authigenic carbonate rock. There is no evidence, as yet, that gas hydrate fills pore-space in sands of the Gulf of Mexico slope. Thus, research on gas hydrate as an alternate energy source or drilling hazard in the Gulf slope should focus on mud and carbonate rock as the dominant "reservoir" for gas hydrate in the Gulf of Mexico. The study of Bottom Simulating Reflectors (BSR) may be a secondary issue when estimating the total hydrate energy resource of the Gulf of Mexico because they are so rare and are of limited size in the Gulf of Mexico slope.

As part of the present study, samples of intact massive gas hydrate were successfully collected from three (3) main sites along with the vent gas from which the gas hydrate crystallized and associated sediment to include authigenic carbonate rock strongly depleted in ^{13}C. The sites from which intact gas hydrate and vent gas were successfully recovered are Green Canyon (GC) Block 234, GC 232, and Mississippi Canyon (MC) Block 118 (Fig. 1). The study sites appear representative of most other gas hydrate sites discovered elsewhere in the Gulf slope. It is now possible to synthesize available data to address important issues relating to gas hydrate as a potential energy source, and to suggest the best ways to study gas hydrate in the unique geologic setting of the Gulf of Mexico slope.

It has been suggested that decomposition of gas hydrate is an important process in nature at this point in geologic time, but there is no geochemical evidence to support the concept in the Gulf of Mexico. If gas is observed venting from over buried gas hydrate, it is sometimes assumed that the vent gas is from decomposition of gas hydrate. It should be emphasized that the composition of vent gas from all sites thus far studied in the Gulf of Mexico slope is consistent with gas hydrate stability over recent geologic time. If gas

hydrate decomposition was geologically significant, then vent gas would show enrichment of hydrate-forming hydrocarbon gases such as ethane and propane. This molecular distribution is not observed, providing strong evidence that gas hydrate is not decomposing at a significant rate in the Gulf of Mexico. Instead, gas hydrate is apparently accumulating in the Gulf at present.

Some decomposition of extremely shallow gas hydrate is likely to occur but deeply buried gas hydrate appears stable in the Gulf of Mexico over long spans of time. Exposed or shallow gas may be affected by sea water temperature changes. The irregular surface of the sea floor at gas hydrate sites is partly the result of cyclical gas hydrate crystallization and decomposition in only a thin-layer nearest the sea floor. Thus, seismic evidence of gas hydrate instability is most likely to be observed in the top ~2 meters of sediment nearest the sea floor whereas deeper sediment should not show evidence of change on any short time scale.

Only a fraction of shallow amplitudes are likely to be related to gas hydrate because several factors appear to retard gas hydrate crystallization in complex natural settings. Brine poisoning may prevent gas from crystallizing as gas hydrate and may help explain >160 known gas seeps in the Gulf that lack any evidence of gas hydrate. Localized heating or insufficient gas flux may also contribute to the observed lack of gas hydrate.

The discovery of gas hydrate at the sea floor greatly increases the probability of deep gas hydrate accumulations in the same area. There are limits to the application of conventional seismic techniques because they do not directly indicate gas hydrate in shallow sediment of the Gulf of Mexico. It is more reasonable to suggest that seismic techniques can identify gassy seeps as sea floor amplitudes. The combination of 38 kHz imagery showing large gas plumes in the water column with conventional shallow seismic amplitudes may improve the probability of discovering new gas hydrate sites.

Additional research to explain why gas hydrate fails to crystallize at many gas seeps in the Gulf of Mexico slope is justified. Although the VK 826 and MC 885 sites display obvious geophysical anomalies, no gas hydrate is present. The apparent lack of gas hydrate at the VK 826 and MC 885 sites may be partially attributed to insufficient hydrocarbon gas flux but the carbonate-rich sites are too shallow and warm for structure I or II gas hydrate to be stable. In addition, brines are present at both sites that are likely to retard gas hydrate crystallization. The MC 709 is a major geophysical anomaly and may or may not contain any gas hydrate although there are areas with intermediate hydrocarbon flux within the GHSZ. The main reason for the lack of abundant gas hydrate at MC 709 may be brine poisoning.

GEOLOGIC SETTING AND DEEP FLUID SOURCES

The main structural features of the northern Gulf of Mexico are salt basins including the large Gulf of Mexico Salt Basin that extends from the coastal salt-dome province to the lower continental slope, and a series of smaller interior salt basins that extend onshore from south Texas to Alabama. The basins formed during Late Triassic rifting and were

floored by salt (Louanne/Werner formations) during Middle Jurassic marine incursions (Salvador, 1987). Structural style is profoundly influenced by the effects of salt movement driven by rapid deposition of siliciclastic sediment. The Gulf of Mexico continental shelf is now characterized by numerous salt domes, whereas the continental slope is affected by large sheet-like salt thrusts that extend from the shelf edge across the continental slope to the Sigsbee Escarpment, near the upper limit of the abyssal plain (Worrall and Snelson, 1989).

The geology of the Gulf of Mexico slope is conducive to seepage and venting from deeply buried petroleum systems to the sea floor because hydrocarbon generation is geologically recent within the deep sediment section beneath the salt thrust and on the upper abyssal plain (Sassen et al., 2001a,b,c,d). The framework of deep hydrocarbon migration involves vertical migration through salt withdrawal basins that pierce the large salt thrusts (Fig. 2). Rapid sedimentation in Pleistocene depocenters (Galloway et al., 2000) activates migration conduits from depth to the sea floor within the salt basins. Fracture zones associated with moving salt sheets, as well as active faults, provide efficient migration conduits for fluid flow to the sea floor including gas, oil, and brines. In some brine seeps, which may be associated with limited chemosynthetic communities, mineral assemblages include strontium-rich barite and radium (Fu and Aharon, 1998).

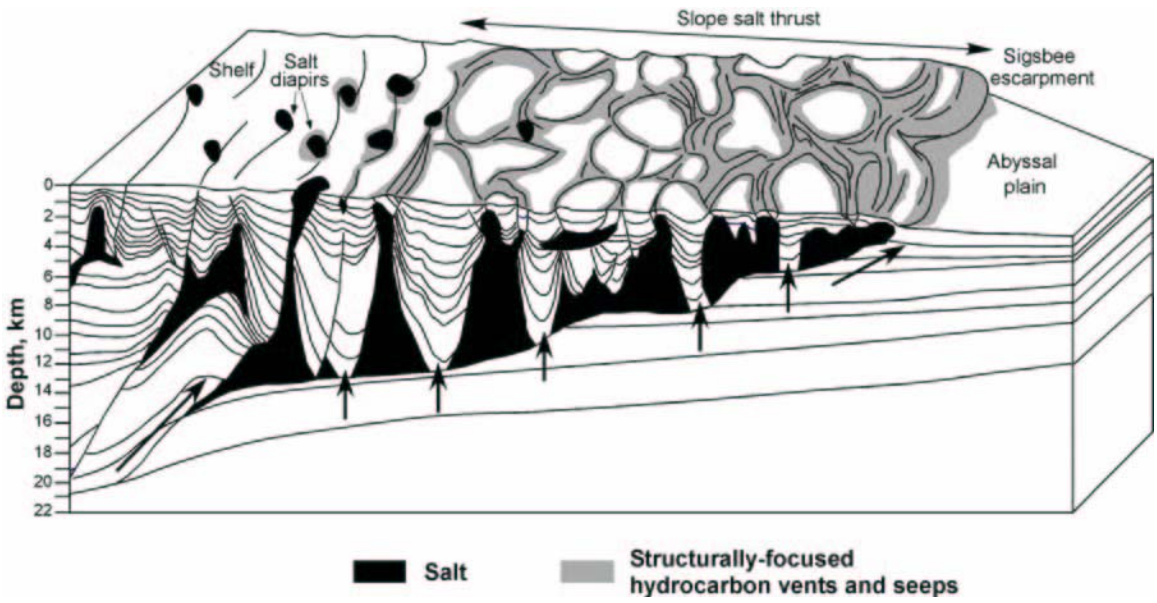

Figure 2. A conceptualized north-south cross-section of central Gulf slope from the shelf to the abyssal plain is shown. Numerous geologically young basins formed by salt withdrawal pierce the slope salt thrust. The drainage areas of recently mature Mesozoic source rocks are deeply buried beneath the allochthonous salt. Fluids migrate upward through holes in the salt thrust (arrows). Within basins, salt and related faults provide conduits for vertical migration of fluids to reservoirs and to the seafloor. Hydrocarbon vents and seeps are focused by the structure near the rims of salt withdrawal basins. Modified from Milkov and Sassen (2001).

The sea floor shows markedly irregular bathymetry from structural deformation, faulting, fracturing, and slumping (Roberts and Carney, 1997). Massive hydrocarbon seepage manifests itself at the Gulf sea floor as gas hydrate, oil-stained sediments, authigenic carbonate rock with carbon depleted in ^{13}C, and hydrocarbon-driven chemosynthetic communities (e.g. Aharon et al., 1997; Roberts and Aharon, 1994; MacDonald et al., 1989; Roberts and Carney, 1997; Sassen et al., 1999a).

Seeps and vents are not uniformly distributed across the Gulf slope. Because fluid flow from great depth is structurally focused, gas hydrate and chemosynthetic communities are concentrated along the rims of salt-withdrawal basins, over salt ridges, and near the faulted and folded margin of the Sigsbee Escarpment at the downdip limit of the Gulf of Mexico Salt Basin (Fig. 2). Seep-related features are infrequently observed within salt withdrawal basins themselves because such sediments are less deformed and usually lack major migration conduits to shallow sediments or the sea floor (Fig. 2).

REVIEW OF GAS HYDRATE IN THE GULF OF MEXICO SLOPE

The total volume of gas hydrate in the Gulf slope is estimated to be equivalent to ~1.0-1.4 x 10^{13} m^3 of gas at STP including methane and other hydrate-forming hydrocarbons (Milkov and Sassen, 2001). The estimate of the Gulf slope hydrate resource is based solely on gas hydrate proven to occur in the mud matrix (e.g. Sassen et al., 1999a). All known occurrences of gas hydrate in the Gulf of Mexico occur as vein-fillings and thick pavements of nearly pure gas hydrate in hemipelagic mud. Occasionally, gas hydrate occur filling vuggy porosity in authigenic carbonate rock. There is no evidence that gas hydrate occurs as pore-space fillings in sands of the Gulf of Mexico slope. Thus, research in the Gulf slope should focus on mud and carbonate rock as “reservoirs” for gas hydrate in sediment.

This volume of gas in geologically shallow sediment dwarfs the volume of conventional reserves of oil and gas in deep subsurface reservoirs of the Gulf slope (Milkov and Sassen, 2002). It should be emphasized that the entire estimate of the Gulf of Mexico gas hydrate resource is based on vein-fillings and pavements of nearly pure gas hydrate in mud. None of this estimate includes gas hydrate in the pore throats of sand and none is related to Bottom Simulating Reflectors (BSRs). There is as yet no evidence of any gas hydrate in a BSR or in sand facies of the Gulf of Mexico.

Thermogenic (oil-related) gas and crude oil from the subsurface hydrocarbon system vents at the sea floor of the Gulf of Mexico continental slope, entering the water column as oil-coated bubbles that rise to the sea surface (Sassen et al., 2001a, b). Much of the thermogenic gas, strongly enriched in 13C relative to bacterial methane, bypasses sediment and vents to the water column and the atmosphere. Because research submersible platforms allow direct sampling of gas vents within 0.5 m of sea floor orifices (see Fig. 3), the molecular and isotopic properties of the hydrocarbon vent gas are well constrained. Some fraction of the vent gas crystallizes near the sea floor as structure II gas hydrate. Vent gas is the starting material from which other major carbon pools at chemosynthetic communities (Fig. 4) are derived, mainly by complex microbial

processes that lead ultimately to geologically significant sequestration of carbon as authigenic carbonate rock depleted in 13C (Fig. 5).

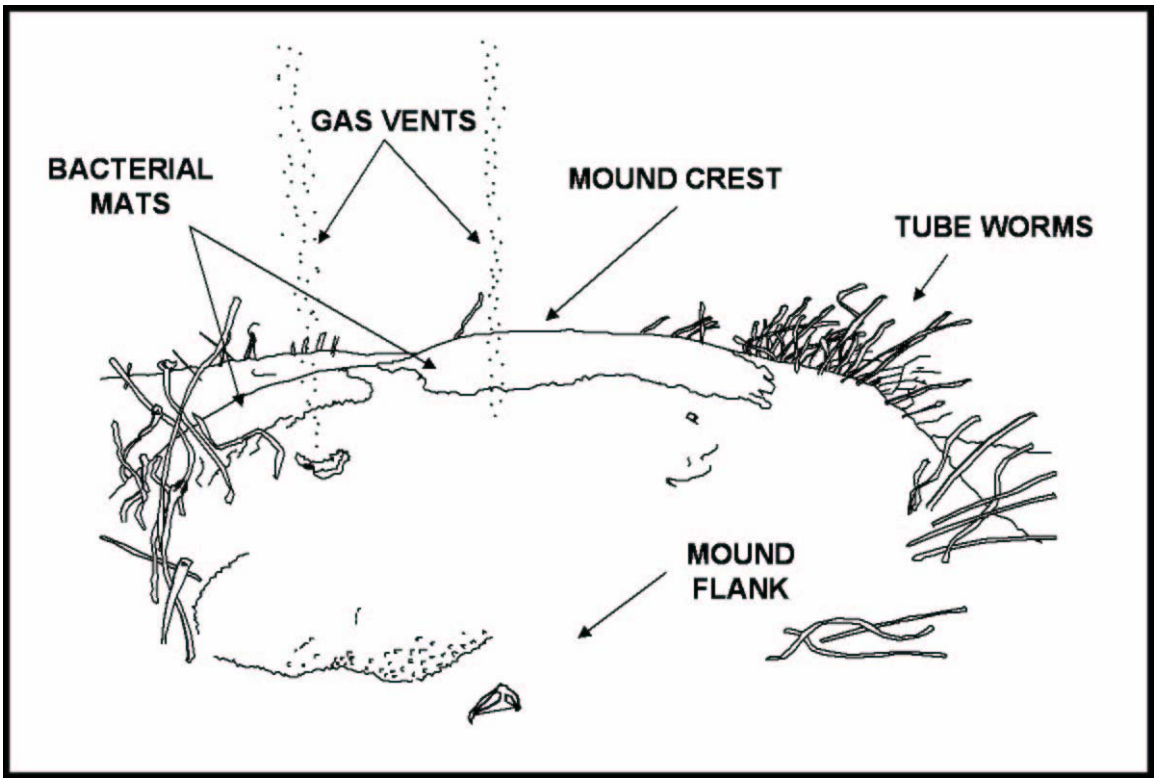

Figure 3. Features of a typical gas hydrate mound (~ 2 m across) with gas vents and nearby chemosynthetic community of tubeworms (Sassen et al.,1999b).

Gas hydrate is an ice-like crystalline mineral in which hydrocarbon gases and nonhydrocarbon gases are held within rigid cages of water molecules (Fig. 6). Structure I gas hydrate has a body-centered cubic lattice, structure II gas hydrate has a diamond lattice, and structure H gas hydrate has a hexagonal lattice (Sloan, 1998). Structure I gas hydrate, which occurs in many basins, is usually predominately bacterial methane (Kvenvolden, 1993; 1995). The ™^{13}C and ™D of bacterial methane from seafloor gas vents and structure I gas hydrate from the Gulf slope is thus far consistent with a source from methanogenesis via CO_2 reduction in geologically shallow sediment (Sassen et al., 1999a, b). Both structure II and structure H gas hydrate are believed to co-exist in the Gulf at water depths as shallow as ~540 m (Sassen and MacDonald, 1997). Structure II gas hydrate generally includes C_1-C_4 hydrocarbons (methane through isobutane) whereas structure H gas hydrate generally includes C_1-C_5 hydrocarbons (methane through isopentane) as significant components (Sloan, 1998).

The total number of documented gas hydrate sites on the deep Gulf of Mexico sea floor is ~65 but this is a minimum number. Known shallow or outcropping gas hydrate sites extend along the Gulf slope offshore Texas and Louisiana over a distance >500 km, and the maximum width of the belt is >100 km. Solid gas hydrate has been recovered from

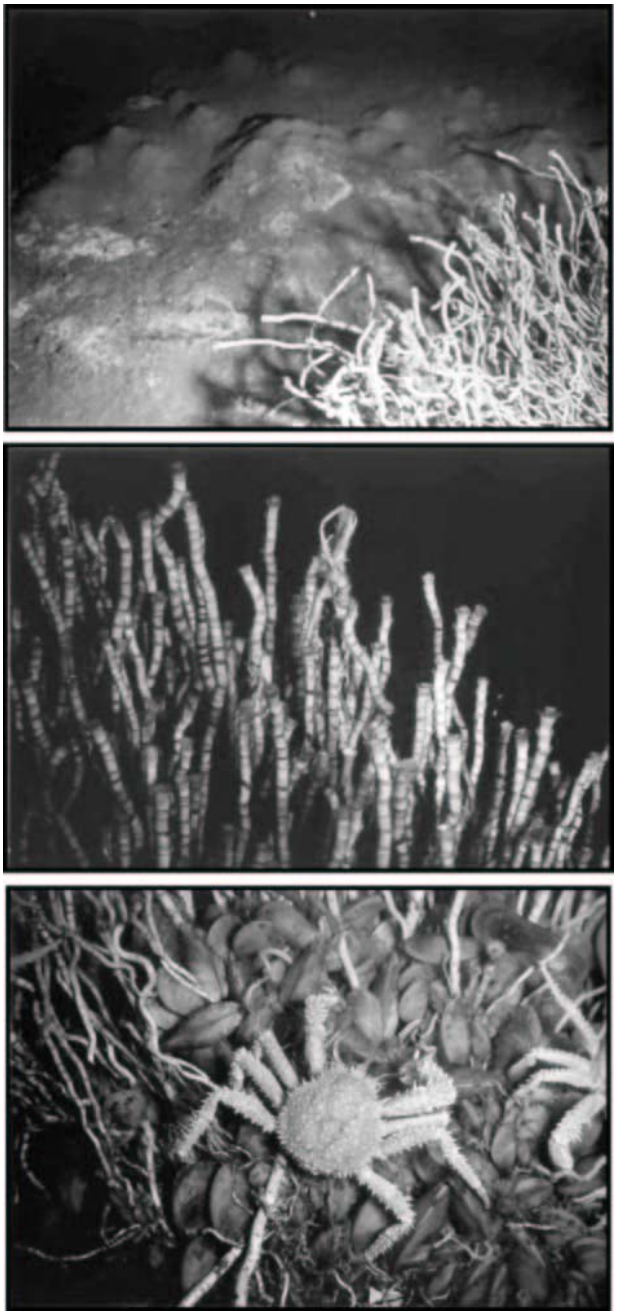

Figure 4. Photographs of tube worms and seep mussels from chemosynthetic communities are shown.

shallow sediments (< 6 m) by piston coring and by research submersibles from > 50 localities on the Gulf slope (Fig. 1). The distribution of mapped gas hydrate sites corresponds to a late Pleistocene depocenter (Galloway et al., 2000). The minimum observed water depth of occurrence of gas hydrate in the Gulf of Mexico is ~ 440 m and the maximum depth is > 2,400 m (Sassen et al., 1999a). The thickness of the gas hydrate stability zone (GHSZ) increases with water depth. Calculations of stability, based on free gas with 90.4% methane, suggest that the thickness of the GHSZ in sediment may be as

much as ~ 450 m at 540 m water depth, and > 1 km at 1930 m water depth in the Gulf (Milkov and Sassen, 2000).

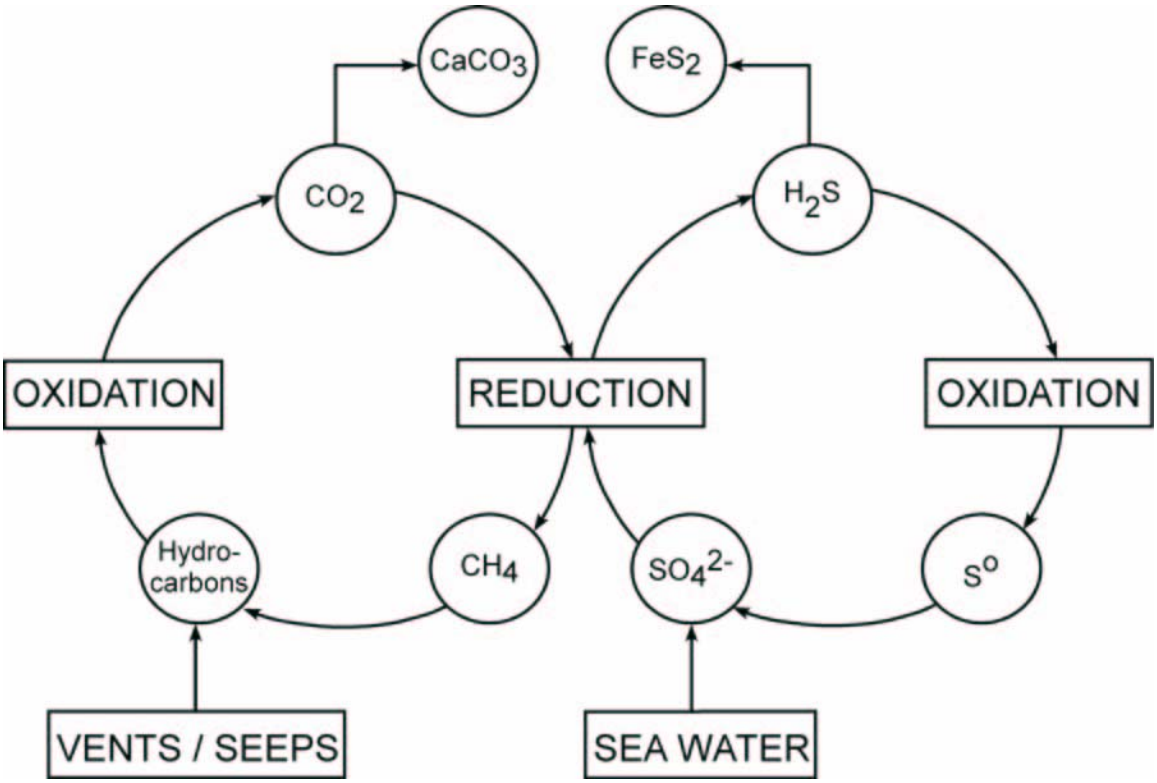

Figure 5. Summary diagram of the microbially-mediated carbon and sulfur cycles associated with hydrate-related chemosynthetic communities. These basic biogeochemical processes are generalized to occur at many other hydrocarbon vent, seep, gas hydrate, and chemosynthetic community sites globally.

In contrast to simple bacterial methane hydrate, thermogenic gas hydrate (methane through pentanes) preserves more complex information on source and stability because numerous hydrocarbon molecules of varying chemical properties are held within crystal lattices. The vent gas and gas hydrate are intimately associated with complex chemosynthetic communities whose initiation and stability depend upon hydrocarbon-driven microbial processes in sediment, which include microbial hydrocarbon oxidation, reduction of CO_2 via methanogenesis, sulfate reduction, and sulfide oxidation (Sassen et al., 1993, 1994, 1999b). The molecular and isotopic properties of vent gas, intact gas hydrate, and free hydrocarbons in sediment trace the effects of microbial hydrocarbon oxidation and CO_2 reduction in anaerobic sediment rich in H_2S (Fig. 5).

The gas hydrate environment encourages microbial activity. New perspectives on anaerobic methane oxidation result from studies in which methane represents the entire hydrocarbon pool (Valentine and Reeburgh, 2000). However, methane may be less abundant relative to total C_2-C_5 hydrocarbons in sediment of some Gulf slope chemosynthetic communities associated with structure II gas hydrate (Sassen et al.,

1999b). Fatty acid biomarkers strongly depleted in ^{13}C (Zhang et al., 2002) and RNA characterization (Lanoil et al., 2001) suggest the presence of methanogens (*Archaea*) in sediment associated with gas hydrate and chemosynthetic communities, where independent geochemical evidence of methane oxidation is compelling. However, there is also geochemical evidence that the C_2-C_5 hydrocarbons may be altered by microbial oxidation (Sassen et al., 1999b) in the same anaerobic setting.

Figure 6. Photograph of structure II gas hydrate on a freshly exposed fault surface at GC 234. Massive vein-fillings of gas hydrate are separated by deformed hemipelagic mud, and the base of the exposure is under cut by flow of free gas. Note scale bar. Photograph by C.F. Fisher.

EXPERIMENTAL

Vent gas was collected using a research submersible by allowing the gas to displace ambient seawater in gas-tight sampling vessels within 0.5 to 1 m of the sea floor. Upon recovery to the sea surface, large aliquots of the gas sample (~240 ml) were transferred from the sampling vessel to pre-evacuated aluminum vacuum containers using a 60 ml gas-tight syringe, and held at –20° C until analysis. Sediment samples were collected using 30-cm push cores on the sea floor. Sediment was immediately canned and frozen for later gas analysis. Analytical procedures for C_1-C_5 gas chromatography, and measurement of isotopic properties of hydrocarbon vent gases, and C_{15+} chromatography of oil from sediment are described by Sassen et al. (2004). An aliquot of sediment was

frozen at collection, and later extracted in the laboratory with hexane (Soxhlet apparatus, 24 hours) to yield solvent-soluble components, mainly a mixture of crude oil with minor recent microbial lipids. The technique of Kennicutt et al. (1992) was used for C_{15}+ chromatography of sediment extracts. Biomarker analyses were also performed by gas chromatography mass spectrometry (GCMS) using the techniques described by Sassen et al. (2001d). Authigenic carbonate, other authigenic minerals, and associated microbes were collected using the robot arm of the JSL research submersible. The d13C of carbonate was determined by Dr. Ethan Grossman of the Department of Geology and Geophysics, Texas A&M University. Precision of C_1-C_5 gas chromatography is ± 5%. The ™^{13}C values are reported as parts per thousand (‰) relative to the PeeDee Belemnite standard (precision = ± 0.2‰), and the ™D values are reported as ‰ relative to the standard mean ocean water (SMOW) standard (precision = ± 5‰).

RESULTS AND DISCUSSION

DESCRIPTIONS OF JSL SITES WITH GAS HYDRATE

Green Canyon 234

1. GC 234 hydrate site is a useful case history with abundant gas hydrate: The GC 234 site has been well-documented by previous studies and serves as a useful example of a typical gas hydrate accumulation in the Gulf of Mexico slope. The location is (27° 44.8' N and 91° 13.3' W). Research on the GC 234 site is extensive and shows great similarity to the better studied Bush Hill site (GC 185) which is nearby (27° 45.7' N and 91° 30.5' W). Refer to Sassen et al. (2004) for an updated comparison of the GC 234 and Bush Hill gas hydrate sites. Water depth of both sites is ~540 meters and temperatures vary in the approximate 6-11° C range. Salinity of sediment pore water shows variation but overall is similar to that of sea water except in immediate proximity to gas hydrate surfaces.
2. Method of discovery: The first identification of the site was based on recovery of intact gas variant structure II gas hydrate by a piston core directed at a sea floor geophysical anomaly. No bottom simulating reflector (BSR) is detected although this is a major gas hydrate site. The finding by piston core led to further study by research submersibles. A gas hydrate outcrop literally covered with “ice worms” was described in 1997 by Fisher et al. (2000).
3. Gas Hydrate fabric: Gas hydrate outcrops on the sea floor where it forms as a consequence of active venting of oil-related gas from the deep subsurface. Veins and pavements of pure gas hydrate are up to tens of centimeters in thickness are most obvious (Fig. 6). Gas hydrate also occurs as nodules in sediment. Maximum depth in sediment known from piston cores of gas hydrate is >4 meters.
4. Gas Hydrate stability: In conformity with stability models (Milkov and Sassen, 2000; Milkov et al., 2000), water depth and temperatures suggest thermogenic gas hydrate (structure II and H hydrate) is stable while biogenic methane (structure I) is not. No structure I gas hydrate has been found at the GC 234 site.
5. Effects of water temperature fluctuations. The upper 0-2 meters of the gas hydrate is relatively unstable because of changes in sea water temperature (Fig 6; Milkov

et al., 2000). Deeper gas hydrate is believed to be stable geologically. Research suggests that from the geologic perspective, GC 234 is not at equilibrium. Instead, venting drives gas hydrate accumulation. The volume of gas hydrate is increasing slowly at this point in geologic time as at the Bush Hill site (Sassen et al., 2001a). There is no geochemical evidence of significant gas hydrate decomposition below the shallow zone of instability (~0 to 2 meters).

6. Geologic occurrence: The gas hydrate occurs as veins and as laterally extensive pavements of nearly pure gas hydrate that apparently extend as a circular feature ~100 meters in diameter as determined from sea floor navigation and by 38 kHz imagery of the sea floor. The host sediment is ~100% hemipelagic clay with no detectably sand. Some hydrate occupies vuggy porosity in authigenic carbonate rock. No discrete sand is present. Salinity of sediment pore water varies but approximates that of normal sea water. The site is old, perhaps thousands of years in age.
7. Gas venting: The hydrate forms when thermogenic (oil-related C_1-C_5 hydrocarbons) gas vents from the deep surface petroleum system and the hydrocarbon gases react with water to crystallize as a mineral. The area shows a near-surface geophysical anomaly and is remotely sensed by 38 kHz imagery (Fig. 7) which is consistent with an intermediate level of fluid flux including deep formation water, gas, and oil (see Roberts and Carney, 1997).

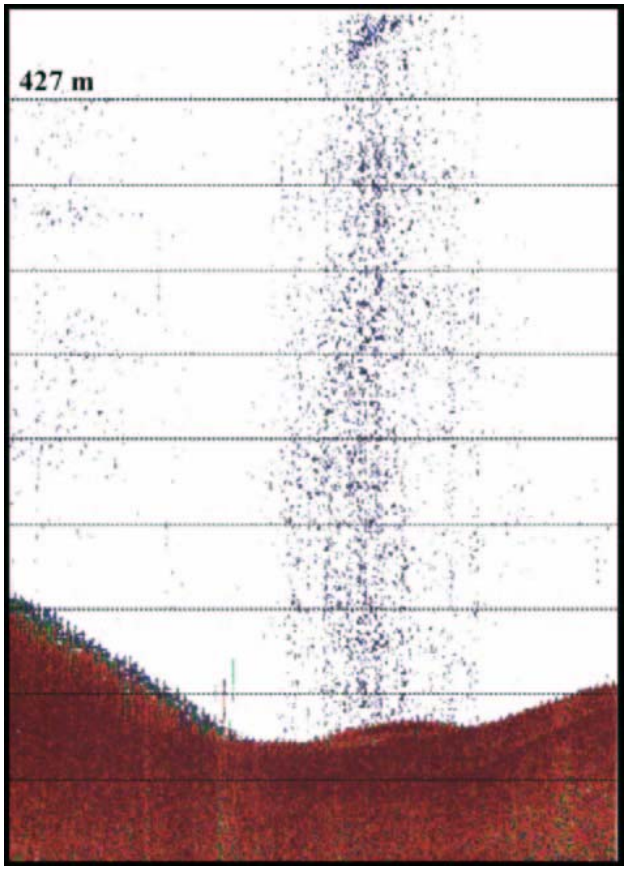

Figure 7. The 38 kHz image shows rapid gas venting to the water column from the GC 234 site.

8. Hydrocarbon Geochemistry: Thermogenic hydrocarbons vent from the deepsubsurface petroleum system to the sea floor. The C_1-C_5 hydrocarbons plus biodegraded crude oil vent from the deep subsurface through gas hydrate mounds ~0.5 to 1 meter across. Sediment is oil-stained. A review of data on gas hydrate, vent gas, and sediment samples is provided by Sassen et al. (2004).
9. Ecology: The GC 234 site has a lush chemosynthetic community dominated by white and orange bacterial mats (*Beggiatoa*), tube worms and mussels plus numerous other species similar to Bush Hill.
10. JSL samples: During JSL dives 4406 and 4407 in 2002, new samples of vent gas and intact gas hydrate were recovered intact from the sea floor. Push-core samples of gassy mud were collected at depths (<30 cm) in sediment. Authigenic carbonate rock samples were also collected.

Green Canyon 232

1. GC 232 hydrate site is a useful case history with abundant gas hydrate: The existence of GC 232 has been known for some time from piston cores (unpublished data) but no samples of vent gas or gas hydrate had been collected or subjected to molecular and isotopic analyses prior to the 2002 JSL dives. In many respects, GC 232 is a "twin" of the nearby GC 234 and Bush Hills sites, only being smaller in size. The location is (~27° 44.5' N and 91° 19.1' W). Water depth is ~ 570 meters. A variant structure II gas hydrate with a component of structure H hydrate (a crystal intergrowth) occurs at GC 232.
2. Method of discovery: The first identification of the site was based on recovery of intact gas variant structure II gas hydrate by a piston core directed at a sea floor geophysical anomaly (unpublished data). No BSR is detected although this is a major gas hydrate site. The finding of gas hydrate by piston core led to further study by research submersibles.
3. Gas Hydrate fabric: Gas hydrate outcrops on the sea floor where it forms as a consequence of active venting of oil-related gas from the deep subsurface. Veins and pavements of pure gas hydrate are up to tens of centimeters in thickness are most obvious because they are exposed at the sea floor. Gas hydrate also occurs as isolated nodules in sediment and filling porosity in authigenic carbonate rock. Maximum depth of gas hydrate in sediment is unknown because no deeppenetration coring has been done at the site.
4. Gas Hydrate stability: Water depth and temperatures suggest thermogenic gas hydrate (structure II and H hydrate) is stable. Gas hydrate composed of pure biogenic methane (structure I) is not. Structure II/H gas hydrate has been recovered intact but no structure I gas hydrate has been found at the GC 232 site. The site is relatively old, perhaps thousands or tens of thousands of years in age.
5. Effects of water temperature changes: The upper 1-2 meters of the gas hydrate is relatively unstable because of changes in sea water temperature (see Milkov et al., 2000). This is readily apparent between dives because the morphology of gas hydrate outcrops changes in response to changes in water temperature. Deeper gas hydrate is believed to be stable geologically. The volume of gas hydrate is thought

to be increasing slowly at this point in geologic time as at the Bush Hill site (Sassen et al., 2001a).

6. Geologic occurrence: The gas hydrate occurs as mounds, veins and as laterally extensive pavements of nearly pure gas hydrate that apparently extend as a circular feature ~50 to 75 meters in diameter as estimated from sea floor navigation and by 38 kHz imagery of the sea floor. The host sediment is ~100% hemipelagic clay with no detectable sand. Salinity is normal. Sediment contains abundant H_2S and is sometimes visibly oil-stained.
7. Gas venting: The hydrate forms when thermogenic (oil-related C_1-C_5 hydrocarbons) gas vents from the deep surface petroleum system and the hydrocarbon gases react with water to crystallize as a mineral. The area shows a near-surface geophysical anomaly and is remotely sensed by 38 kHz imagery which shows a reproducible bubble plume in the water column (Fig. 8). Fluid including deep formation water, gas, and oil are introduced to shallow sediment and the water column. Flux of fluid is intermediate according to the classification of Roberts and Carney (1997).

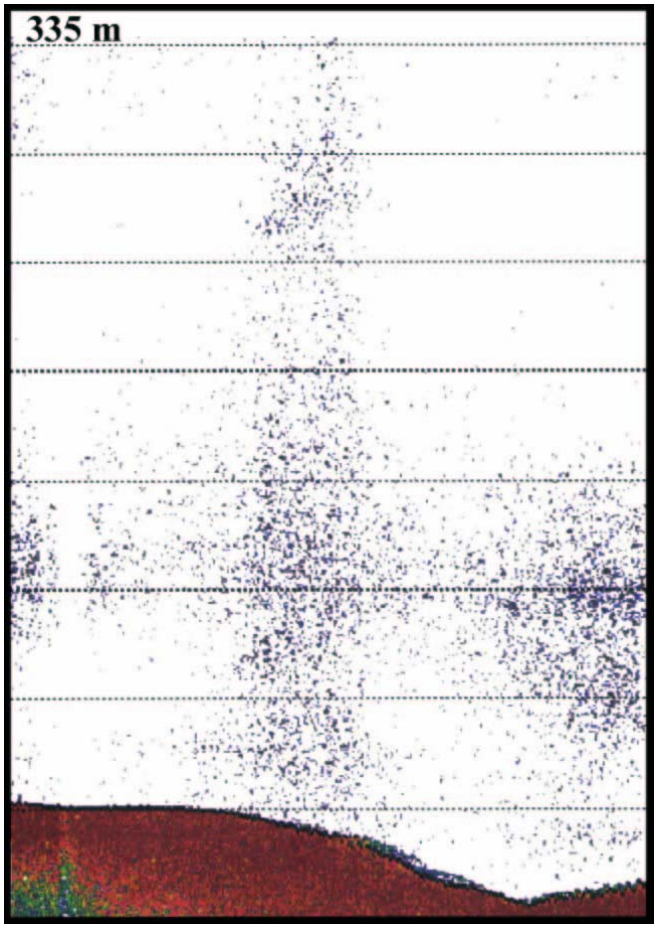

Figure 8. The 38 kHz imagery shows gas venting to the water column from the sea floor at GC 232.

8. Ecology: The GC 232 site has a lush chemosynthetic community dominated by white and orange bacterial mats (*Beggiatoa*), tube worms and mussels plus numerous other species similar to both GC 234 and to Bush Hill. Ice worms were noted at the site in direct association with gas hydrate.
9. JSL samples: During JSL dives in 2002 (4401, 4402/4403, 4404, 4405 and later dives on other JSL cruises that year), new samples of vent gas and intact gas hydrate were recovered intact from the sea floor. Push-core samples of gassy mud were collected at depths (<30 cm) in sediment. Authigenic carbonate rock samples were also collected.

Mississippi Canyon 118

1. The MC 118 site contains significant gas hydrate: The MC 118 site has received little scientific study previously. Because the site is in an area distant from other known gas hydrate discoveries, the hydrocarbons from the MC 188 site may be from a different source rock and petroleum system that gave rise to gas hydrate in Green Canyon. MC 118 is the easternmost discovery of gas hydrate in the Gulf of Mexico slope. The location of the MC 118 site is ~28° 51.4' N and 88° 29.5' W. Maximum water depth at the site during JSL dives is ~890 meters. No samples of vent gas or gas hydrate had been collected or subjected to molecular and isotopic analyses prior to the 2002 JSL dives.
2. Method of discovery: The first identification of the site was on the basis of a sea floor geophysical anomaly in the form of bright amplitudes near the sea floor (unpublished data). There are no reported BSR's near the known hydrate site at MC 118. The geophysical finding led to further study by research submersible and in 2003 by the U.S. Navy nuclear research submarine NR-1 in a grant to Roger Sassen.
3. Gas Hydrate fabric: Gas hydrate outcrops on the sea floor where it forms as a consequence of slow venting of oil-related gas from the deep subsurface. Veins of pure gas hydrate outcrop in mud. Gas hydrate also occurs as small nodules in sediment. Maximum depth of gas hydrate in sediment is unknown.
4. Gas Hydrate stability: The upper 1-2 meters of the gas hydrate is relatively unstable because of changes in sea water temperature, but hypothesized deeper gas hydrate is believed to be stable over a relatively short span of geologic time, perhaps thousands of years.
5. Geologic occurrence: The gas hydrate occurs as mounds, veins of nearly pure gas hydrate that forms a circular sea floor feature only ~ 25 meters in diameter as estimated from sea floor navigation and by a later dive to the site by the U.S. Navy NR1 nuclear research submarine (unpublished data). The host sediment is ~100% hemipelagic clay with no detectably sand. Authigenic carbonate rock is present. H_2S is present in sediment. Salinity is normal.
6. Gas venting: The hydrate forms when thermogenic gas rapidly vents from the deep surface petroleum system and the hydrocarbon gases react with water to crystallize structure II gas hydrate. Fluid flux, including deep formation water, gas, and oil is low to intermediate. Sediment is visibly oil-stained.

7. Ecology: The MC 118 site has a complex chemosynthetic community dominated by bacterial mats (*Beggiatoa*), tube worms and mussels plus other species similar to both GC 234 and to Bush Hill.
8. JSL samples: During JSL dives in 2002, new samples of vent gas and intact gas hydrate were recovered from the sea floor. Push-core samples of gassy mud were collected in sediment (<30 cm).

DESCRIPTIONS OF JSL SITES WITHOUT GAS HYDRATE

Mississippi Canyon 709

1. The MC 709 site, although well studied, is not proven to contain gas hydrate: The site is characterized by intermediate flux gas and oil seepage and by complex chemosynthetic communities. The MC 709 area consists of a sea floor high over shallow salt that is draped with hemipelagic mud. The location is ~28° 13.9' N and 89° 42.5' W. Maximum water depth at the site during JSL dives is ~658 meters. Sea floor temperature is recorded at 6.8° C on JSL dive 4412. Sea water salinity is normal but many brine seeps and brine pools are present in sediment at the site.
2. Method of discovery: The MC 709 site was first characterized as a gas and oil seep site by piston core and has been studied by research submersible for over a decade (see Roberts and Carney, 1997).
3. Gas hydrate stability: Free gas is present at the MC 709 site but no gas hydrate has been proven to occur there. Given water depth and temperature, all three types of gas hydrate are potentially stable in sediment at MC 709. Application of 38 kHz imagery to detect significant gas bubble trains in the water column has been unsuccessful. The apparent lack of gas hydrate at the MC 709 site may relate to brine poisoning that retards the crystallization of gas hydrate. Gas may occur in high concentrations and oil-staining occurs in sediment.
4. Geologic occurrence: The host sediment is largely hemipelagic clay with no sand. Authigenic carbonate rock is present in abundance. Salinity appears to vary widely across the site as a consequence of active dissolution of the underlying salt. However, areas with high flux seepage are associated with extensive brine pools and flows of dense brine that erode gullies down slope.
5. Gas venting: Fluid flux from the deep subsurface is intermediate according to the classification of Roberts and Carney (1997). Small but active vents of gas are observed at several sites and the concentration of oil in sediments is sometimes high.
6. Ecology: The MC 709 site is characterized by white bacteria mats (*Beggiatoa*) and both chemosynthetic tubes worms and mussels. In brine seep areas, mussels may predominate and tube worms are absent. Gorgonians and coral are also present on carbonate outcrops along the periphery of the site. The site has a complex chemosynthetic community with some bacterial mats (*Beggiatoa*), tube worms and mussels, but the area is dissimilar to the classic chemosynthetic communities at GC 234, GC 232, and GC 185.

7. JSL samples: During JSL dives late in 2002 (4412, 4413) samples of sediment were recovered intact from the sea floor using push-cores (<30 cm). Authigenic carbonate rock samples were also collected.

Mississippi Canyon 885

1. The MC 885 site contains no known gas hydrate: The MC 885 is a large diameter site composed of hemipelagic mud, H_2S, and abundant authigenic carbonate rock. The location is ~28° 04.1' N and 89° 43.3' W). Maximum water depth at the site during JSL dives is ~708 meters. Sea floor temperature is recorded at 6.8° C on JSL dive 4409.
2. Method of discovery: The first identification of the site was on the basis of a sea floor geophysical anomaly (unpublished data). The geophysical finding led to further study by research submersible because of its unique biology.
3. Gas Hydrate stability: Free gas is present at the MC 885 site but no gas hydrate has been proven to occur there. Given water depth and temperature, all three types of gas hydrate are potentially stable. Application of 38 kHz imagery to detect significant gas bubble trains in the water column has been unsuccessful. The apparent lack of gas hydrate at the MC 885 site may relate to insufficient hydrocarbon gas flux (Fig. 9) or to brine poisoning. Small volumes of gas and relatively low concentrations of oil occur in sediment.

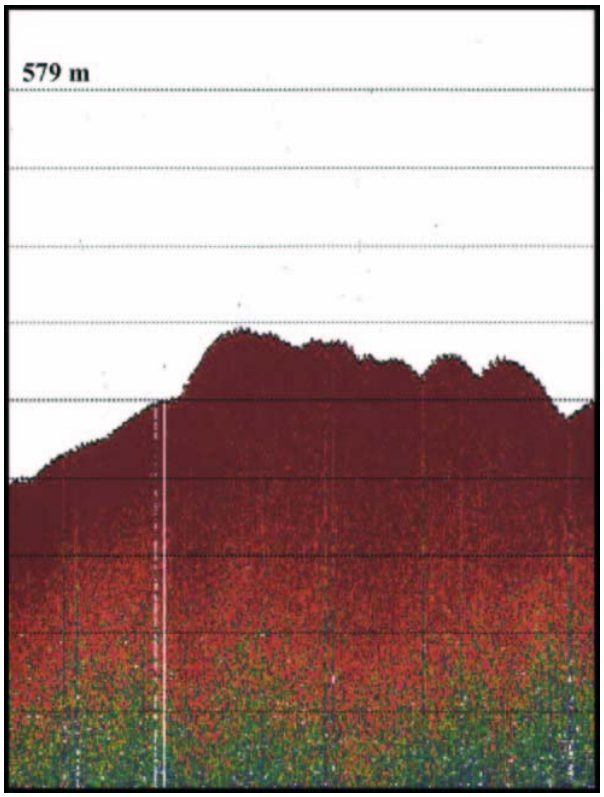

Figure 9. The 38 kHz imagery of MC 885 with no gas vents resolved.

4. Geologic occurrence: The host sediment is largely hemipelagic clay with no sand. Authigenic carbonate rock is present in unusually high abundance as is shell hash of chemosynthetic bivalves. Salinity may vary widely.
5. Gas venting: Fluid flux from the deep subsurface is slow according to the classification of Roberts and Carney (1997). Because the area is not mineralized by carbonate depleted in ^{13}C, it may represent a relict seep site active in the near geologic past, perhaps during the Pleistocene.
6. Ecology: The MC 885 is highly mineralized and gorgonians and coral are quite common. The site has a complex chemosynthetic community with some bacterial mats (*Beggiatoa*), tube worms and mussels, but the area is dissimilar to the classic chemosynthetic communities associated with gas hydrate.
7. JSL samples: During JSL dives in 2002 (4408, 4409) samples of sediment were recovered intact from the sea floor using push-cores (<30 cm). Authigenic carbonate rock samples were also collected.

Viosca Knoll 826

1. The VK 826 site contains no gas hydrate: The VK 826 is a large diameter mineralized sea floor mound over shallow salt where hemipelagic mud partially covers abundant authigenic carbonate rock at ~29° 09.6' N and 88° 01.3' W. The authigenic carbonate rock covers a dome-shaped feature on the sea floor related to the crest of an underlying salt mass. Water depth of JSL dives is between ~ 448 meters at the crest of the dome and ~560 meters on the flank of the dome. A water temperature of 9.6° C was recorded during JSL dive 4410.
2. Method of discovery: The first identification of the site was on the basis of a sea floor bathymetric high and as a geophysical anomaly near a sub-commercial oil discovery (unpublished data) followed by dredging of chemosynthetic fauna. The early findings led to further study by research submersible because of its unique biology.
3. Gas Hydrate stability: Free gas is present at the VK 826 site but no gas hydrate has been proven to occur there. Application of 38 kHz imagery to detect significant gas bubble trains in the water column has been unsuccessful. The apparent lack of gas hydrate is found at the site may be partially attributed to insufficient hydrocarbon gas flux but much of the site is too shallow and warm for structure II gas hydrate to be stable. Small volumes of free gas and low concentrations of oil occur in sediment.
4. Geologic occurrence: Geologic structure is determined by an underlying salt body and long-term seepage of hydrocarbons that resulting in a “cap rock” of authigenic carbonate rock depleted in ^{13}C. Authigenic carbonate rock is present in unusually high abundance. Shell hash from chemosynthetic bivalves is commonly noted. Salinity appears normal. The site is similar to the GC 140 area (see Roberts and Carney, 1997) where massive carbonate is found as a relic of much more active seepage in the geologic past.
5. Gas venting: Fluid flux from the deep subsurface is slow according to the classification of Roberts and Carney (1997). Because the area is highly

mineralized by carbonate depleted in ^{13}C, the area may represent a relict seep site active in the near geologic past. Dead bivalves and much shell hash are noted, perhaps indicating episodic and localized hydrocarbon venting in the recent past.

6. Ecology: Gorgonians and deep-water corals (including black coral) are common along with various bivalves and other organisms. The VK 826 site displays some bacterial mats (*Beggiatoa*), tube worms and mussels but the tube worms appear poorly developed. Overall, the site is dissimilar to the classic hydrate-related chemosynthetic communities at GC 234, GC 232, and GC 185.
7. JSL samples: During JSL dives in 2002 (4410, 4411), samples of mud sediment were recovered intact from the sea floor using push-cores (<30 cm). Authigenic carbonate rock samples were also collected.

GEOCHEMISTRY OF VENT GAS, GAS HYDRATE, AND SEDIMENT GAS

Molecular Properties

A vent is defined as a point orifice of fluid flow where water, gas, and oil enter the water column from the sea floor at a detectable rate which sometimes may be so rapid as to affect sea floor geology and create large mud volcanoes. It is necessary to analyze the molecular and isotopic compositions of vent gas because it is the starting material from which gas hydrate crystallizes. Much gas bypasses the sediment. Gas that is held in sediment is rapidly altered by microbial activity to allow development of the unique chemosynthetic communities of the Gulf of Mexico slope (e.g. Sassen et al., 2001b; Sassen et al., 2004)).

From the sphere of the JSL research submersible, vent gas appears as bubble trains of hydrocarbon gas that issue from the sea floor to the water column. Some vents have relatively low slow flux rates and are only detectable by careful visual observation of the sea floor for evidence of small bubble trains issuing from the sea floor to the water column. Other vents have flow rates that are orders of magnitude higher and are quite obvious during observation from the JSL. Some intermediate to high-flux vents may be documented by 38 kHz imagery of the sea floor and water column.

The molecular properties of the vent gas associated with gas hydrate (see Data Appendix) are basically similar at GC 232, GC 234, and MC 118. In all cases, the vent gas is>90% methane (C_1). Ethane (C_2) is next most abundant, followed by propane (C_3), the butanes (*i*-C_4 and *n*-C_4), and the pentanes (*i*-C_5 and *n*-C_5 and some neo-pentane). The relative abundance of the vent gas molecules simply decreases with increasing carbon number as is commonly noted in subsurface reservoirs of thermogenic gas of oil fields (e.g. Sassen et al., 2001b).

The molecular properties of samples collected during the 2002 JSL cruise reflects the narrow choice of sites on the upper Gulf slope within the shallow diving limits of the JSL research submersible (< 1000 meters) in an area where numerous oil fields have been discovered (Figure 1). The gas found venting to the water column in association with gas hydrate is oil-related and directly correlates with, for example, the subsurface reservoir

gas of Jolliet Field in Green Canyon (Sassen et al., 2001b). If the vent gas has not leaked directly from reservoirs, it has migrated directly from subsurface conduits of the subsurface petroleum system. Data on one vent gas sample from MC 118 appear unreliable because of contamination with gas hydrate fragments during collection at the sea floor.

Molecular Fractionation during Gas Hydrate Crystallization from Vent Gas

The molecular properties of vent gas and the dominantly structure II gas hydrate that crystallizes from the vent gas differ greatly because of molecular fractionation (Sloan, 1998). For example, structure II gas hydrate preferentially encloses ethane, propane, and butanes from vent gas within its crystal structure (Fig. 10). On this basis, the relative abundance of methane in gas hydrate decreases in structure II gas hydrate relative to the vent gas from which it crystallized. In the gas hydrates collected from GC 234, GC 232, and MC 118 methane is the single most abundant molecule, followed by either propane or ethane, and then by isobutane which are the normal hydrocarbon constituents of structure II gas hydrate. However, none of the gas hydrate collected during the 2002 JSL cruise displays the ideal composition of pure "structure II" hydrate. The most obvious anomaly is that propane does not always show greater relative abundance than ethane. In addition, all the gas hydrate contains *n*-butane and some pentanes, molecules that are too large for inclusion in the cages of structure II gas hydrate. The anomalous compositions of Gulf of Mexico slope gas hydrate have been recently explained. X-ray diffraction shows that the typical Gulf of Mexico hydrate is a physical mixture of different crystal structures, explaining the observed molecular compositions of gas hydrate.

Isotopes Fingerprint Vent Gas to Associated Gas Hydrate

Methane gas from the Gulf of Mexico slope shows a wide range of isotopic properties from pure thermogenic methane to pure biogenic methane. The "heaviest" methane thus far measured in the Gulf slope has a $\delta^{13}C$ of -30.1‰ indicating a deep thermogenic origin, whereas the "lightest methane thus far analyzed has a $\delta^{13}C$ of -116.5‰ (Sassen et al, 2002). The mean $\delta^{13}C$ of methane in the Gulf slope (n = 160) is -74.0‰. One key observation is that the C_2-C_5 hydrocarbon gases and oil are commonly associated with methane, even when the methane is strongly depleted in ^{13}C. The best explanation is that methane has different thermogenic and biogenic sources, mixing occurs during migration from depth, and microbial activity impacts isotopic properties either by methane oxidation or via methanogenesis (Sassen et al., 2003).

The $\delta^{13}C$ of methane from vent gas and gas hydrate from individual sites are essentially the same, generally showing differences of 1‰ or less. This is because there is no isotopic fractionation during gas hydrate crystallization (see Sassen et al, 2004 and references therein). For example, the $\delta^{13}C$ of methane of vent gas from GC 234 varies between -48.5‰ to -48.4‰ whereas that of closely associated gas hydrate is -48.0‰ (Fig. 10). At GC 232, the $\delta^{13}C$ of methane of vent gas from varies between -42.8‰ to -43.0‰. Methane of closely associated gas hydrate has $\delta^{13}C$ of -42.7‰. Similarly, at MC 118 the $\delta^{13}C$ of methane of vent gas is -45.7‰ whereas that of closely associated gas

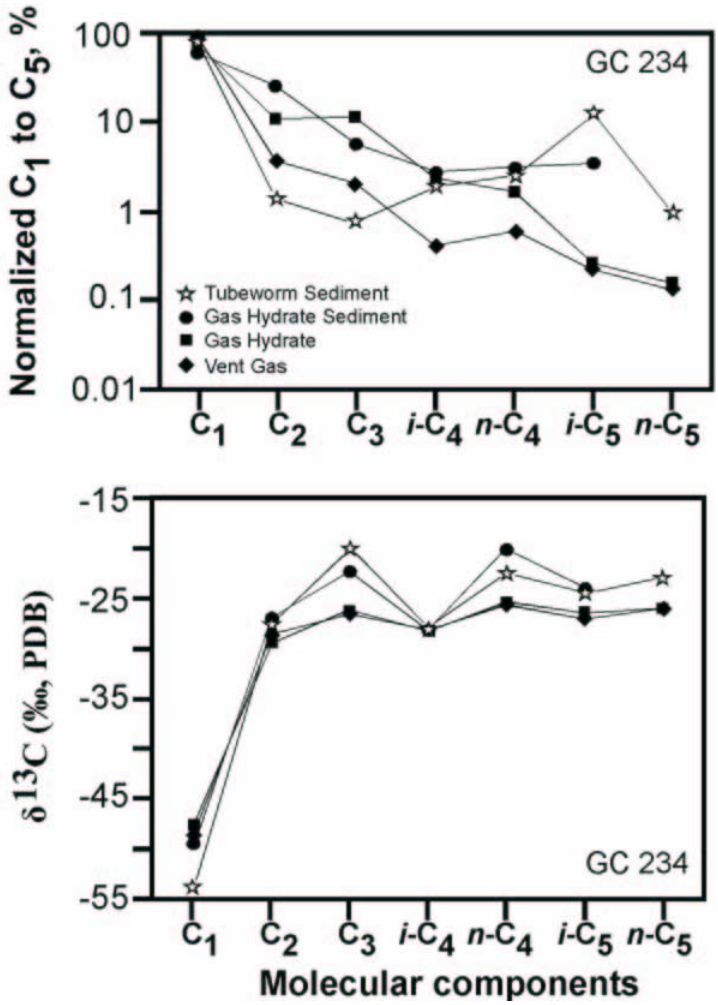

Figure 10. Summary diagrams of molecular and isotopic data from GC 234. Data from Sassen et al. 2004.

hydrate is -45.8‰. The similarity of the hydrogen isotopic properties (δD) of methane at each site establishes a correlation between vent gas and associated gas hydrate. Lastly, the $\delta^{13}C$ of vent gas and hydrate of ethane and propane are so similar as to show a conclusive correlation. The isotopic data provides powerful evidence that at each study site, gas hydrate crystallizes from the adjacent vent gas. Moreover, once held in the crystal structure of gas hydrate, hydrocarbon gases appear protected from microbial oxidation, preserving important geochemical data (Sassen et al., 2001e).

All of the hydrocarbon gases from GC 234, GC 232, and MC 118 are of thermogenic sources, and were formed at great depth and high temperatures from thermally mature source rocks for oil. None of the vent gases encountered on the 2002 JSL cruise contain significant biogenic methane. This is not representative of the Gulf as a whole. There

are many seeps and vents of fossil biogenic methane, as well as mixtures of biogenic and thermogenic gas in vents in the deep subsurface (see Sassen et al., 2003).

Bacterial oxidation of free hydrocarbon gas in hydrate-associated sediments

Free hydrocarbon gas in sediment is rapidly destroyed by bacterial oxidation that is coupled with reduction of sulfate to yield the H_2S common at many gas hydrate sites. To monitor the fate of hydrocarbons in sediment, canned sediment samples from GC 234, GC 232, and from MC 118 were subjected to analysis of C_1-C_5 hydrocarbons by gas chromatography (see Data Appendix). Concentrations of C_1-C_5 hydrocarbons show a wide range but are often relatively high at all study sites with gas hydrate. Indeed, concentrations of gas are often so high as to indicate that small nodules of gas hydrate were frequently sampled along with the sediment. For example Core 1 (0-10 cm depth) from dive 4404 to GC 233 shows a headspace gas composition of 992,393 ppm. In the Gulf slope, any value >10 ppm is considered to be anomalous.

Isotopic data suggest methane is the most rapidly oxidized free hydrocarbon gas in hydrate-associated sediment. Much of the free vent methane in sediment samples has been bacterially oxidized and replaced by biogenic methane via methanogenesis. For example, the $\delta^{13}C$ of methane of vent gas from GC 232 varies between -42.8‰ to -43.0‰. In contrast, the $\delta^{13}C$ of free methane gas from hydrate-associated sediment of GC 232 collected during dives 4401 and 4403/4404 varies between -57.5‰ to -85.9‰ in sediment samples. Isotopically-light CO_2 is present is the same samples, as light as -44.3‰. The best explanation for the relatively light methane in sediment at GC 232 is bacterial reduction of CO_2 (methanogenesis) to form biogenic methane that mixes with residual thermogenic vent methane. Thus, the biogeochemistry of methane at gas hydrate sites appears extremely complex with multiple sources and bacterial processes that affect isotopic properties of the methane.
Samples of free gas show selective preservation of ethane whereas propane, butanes and some pentanes are greatly decreased in abundance, which is indicative of rapid bacterial oxidation of free hydrocarbon gases in sediment (Sassen et al., 2004).

BIODEGRADATION OF CRUDE OIL

Gas chromatography is an objective method to estimate the concentration of crude oil hydrocarbons in hydrate-associated sediment and to characterize the degree of crude oil alteration by biodegradation. The C_{15}+ gas chromatography of sediment samples from the gas hydrate sites of GC 234, GC 232, and MC 118 are similar in terms of gross characteristics and all show anomalous concentrations of crude oil (see Data Appendix). The thermogenic gas hydrate sites are thus unambiguously associated with crude oil which probably also plays a role as a carbon source for chemosynthetic communities and provides some variable fraction of the carbonate-carbon for authigenic carbonate rock.

All samples of hydrate-associated sediment show highly anomalous concentrations of crude oil, which vents with gas from the deep subsurface to the study sites. The mean

concentration of crude oil (UCM) in random sediment samples from across the Gulf slope is < 10 ppm (Sassen et al., 1999a). However, most sediment samples from the gas hydrate sites of GC 234, GC 232, and MC 118 smelled of crude oil, and in many cases free oil was visible filling fractures in sediment as the samples were preserved at sea. One section from a push-core collected on GC 234 (JSL dive 4407) was characterized by visible oil-staining and total UCM concentration is 57,885 ppm. To better communicate this concentration, nearly 6% of the dry sediment is oil by weight. Similarly, a core from GC 232 (JSL dive 4401) was visibly oily and the concentration of UCM is 25,729 ppm, about 2.5% of the core by weight. The MC 118 site is similar with much oil staining. One push core from MC 118 (JSL dive 4415) contained 23,048 ppm of UCM, about 2.3% of total sediment weight.

The saturated hydrocarbons of crude oil from hydrate-associated sediment from GC 234, GC 232, and MC 118 are all highly biodegraded, which is generally characteristic of gas hydrate sites with chemosynthetic communities across the Gulf of Mexico slope. The original *n*-alkanes and isoprenoids present in unaltered crude oil from the sub-surface have been destroyed, leaving an elevated chromatographic baseline called the Unresolved Complex Mixture (UCM). An example of highly biodegraded oil is shown in Figure 11.

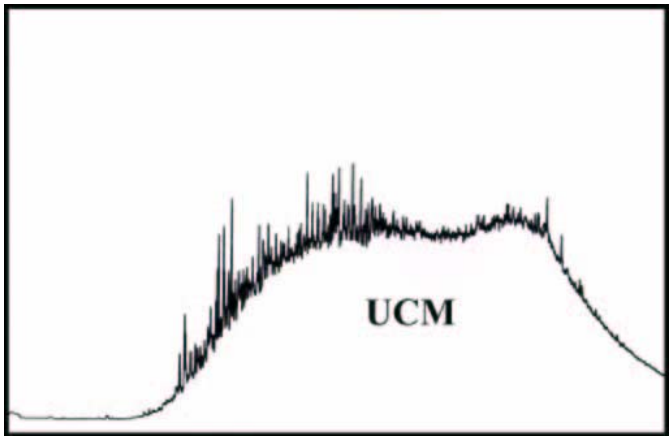

Figure 11. Typical C_{15+} gas chromatogram of crude oil from GC 234 showing advanced alteration from microbial oxidation.

ISOTOPIC PROPERTIES OF AUTHIGENIC CARBONATE ROCK

Microbial oxidation of crude oil is associated with bacterial sulfate reduction in hydrate-associated sediment from GC 234, GC 232, and MC 118. The most important products of these linked bacterial processes are CO_2 from hydrocarbon oxidation and H_2S from bacterial sulfate reduction. The effect of bacterial sulfate reduction is to shift alkalinity in sediment pore water, favoring precipitation of authigenic carbonate rock (e.g. Roberts and Aharon, 1994; Roberts and Carney, 1997; Aharon and Fu, 2000). Authigenic carbonate rock precipitates rapidly, forming massive pavements, slabs, crusts, nodules and cements. The process occurs within mud, not in the water column, but the carbonate rock often encloses the skeletal material from the numerous species of bivalves such as mussels and clams that are abundant in hydrate-associated chemosynthetic communities.

Visual examination of authigenic carbonate rock from hydrate-associated sediment often shows disarticulated bivalves and shell hash which complicates interpretation of $\delta^{13}C$ results (see Data Appendix). This is because the carbon from hydrocarbon oxidation in authigenic carbonate rock is strongly depleted in ^{13}C whereas the carbon skeletal material from bivalves and other calcareous organisms is characterized by $\delta^{13}C$ approximating that of normal marine carbonate. Most samples from the present study are a physical mixture of authigenic carbonate and calcareous skeletal material from chemosynthetic communities.

Ten (10) separate samples of authigenic carbonate rock from GC 234 were subjected to multiple determinations of $\delta^{13}C$ and the results averaged (see Data Appendix). The range of $\delta^{13}C$ from GC 234 is from -18.44‰ to -27.26‰. Six (7) samples from GC 232 showed a range of $\delta^{13}C$ from -15.12‰ to -20.15‰. The range of $\delta^{13}C$ values is similar to that measured using three (3) samples collected during JSL dive 4429 at the similar GC 185 gas hydrate site where authigenic carbonate rock is also abundant. The range of carbonate $\delta^{13}C$ at GC 185 is -22.38‰ to -22.73‰.

In contrast, the $\delta^{13}C$ values of three (3) samples of authigenic carbonate rock from the GC 233 Brine Pool site from JSL dives later in 2002 is from -35.02‰ to -32.65‰, values that are only marginally lighter than at the gas hydrate sites where thermogenic methane and crude oil dominate as carbon sources to authigenic carbonate rock. At GC 233, biogenic methane ($\delta^{13}C$ = ~ -60‰) vents to the water column and is the main source of hydrocarbon-carbon at the site. Thus, there is only a tenuous relationship between hydrocarbon types and $\delta^{13}C$ of carbonate carbon of authigenic carbonate rock other than to note that they are strongly depleted in ^{13}C relative to normal marine carbonate-carbon. There are multiple sources including methane, other hydrocarbon gases, oil, and skeletal material from bivalves and other organisms.

SITES LACKING GAS HYDRATE

The 2002 JSL cruise allowed characterization and collection of samples from a number of sites on the Gulf of Mexico slope at which no gas hydrate has been found. It appears that a combination of factors may prevent the crystallization of gas hydrate. Contrary to a superficial interpretation of thermodynamics and the phase rule, free gas is abundant within the GHSZ of the Gulf. This is most obvious when a push-core is acquired or a rock is turned over using the mechanical arm of the JSL research submarine. Mechanical disturbance of the sediment frequently allows release of copious gas bubbles to the water column where it may immediately form “hydrate snow” that slowly floats upwards in the water column. The question to be asked is why does free gas exist within the GHSZ even though excess water is present?

Although the VK 826 and MC 885 sites display obvious geophysical anomalies, no gas hydrate is present. The apparent lack of gas hydrate at the VK 826 and MC 885 sites may be partially attributed to insufficient hydrocarbon gas flux but the carbonate-rich sites are too shallow and warm for structure I or II gas hydrate to be stable. In addition,

brines are present at both sites that are likely to retard gas hydrate crystallization. The MC 709 is a major geophysical anomaly and may or may not contain any gas hydrate although there are areas with intermediate hydrocarbon flux within the GHSZ. The main reason for the lack of abundant gas hydrate at MC 709 may be brine poisoning. Additional research to explain why gas hydrate fails to crystallize in abundance at sites such MC 709 is justified. As noted earlier, >160 gas seeps in the Gulf of Mexico appear to lack gas hydrate (Sassen et al., 2002) so the question is worth answering.

CONCLUSIONS: IMPLICATIONS TO GAS HYDRATE STABILITY AND MONITORING

It has been uncritically generalized that decomposition of gas hydrate is an important process in nature at this point in geologic time. However, there is no geochemical evidence to support that contention in the Gulf of Mexico. If gas is observed venting from over buried gas hydrate, it is sometimes simply assumed that the vent gas is from decomposition of gas hydrate. However, there are few if any proven examples of geologically significant vent gas derived from gas hydrate decomposition. None are proven in the Gulf of Mexico slope.

Vent gas is better interpreted as the starting material that gives rise to large accumulations of gas hydrate that are at present slowly increasing in size (Sassen et al., 2001b, c). Free gas is constantly migrating from depth and venting to the water column at all studied gas hydrate sites. The end-member gas is either thermogenic C_1 to C_5 hydrocarbons with oil (Sassen et al., 2001b) or is fossil biogenic methane (Sassen et al., 2003). Thermogenic gas hydrate (structure II) contains C_1-C_5 hydrocarbon gases and generally occurs at water depths >500 meters under typical conditions in the Gulf. Under typical conditions in the Gulf slope, methane hydrate (structure I) occurs widely at water depths >650 meters.

It should be emphasized that the composition of vent gas from all sites thus far studied in the Gulf of Mexico slope is consistent with gas hydrate stability and slow accumulation in sediments over recent geologic time (Sassen et al., 2001e). If gas decomposition of gas hydrate is important, then vent gas would show a molecular distribution enriched in structure II gas hydrate-forming hydrocarbon gases. Vent gas from decomposition of structure II hydrate would show enrichment in ethane, propane, and isobutane. This molecular distribution is not observed, providing strong evidence that gas hydrate is not decomposing at a significant rate at typical gas hydrate sites thus far studied in the Gulf of Mexico slope. Instead, there is evidence at GC 185 that vent gas is preferentially "stripped" of hydrate-forming molecules (ethane, propane, isobutane) during migration to gas hydrate sites (Sassen et al., 2001b). Thus, the molecular properties of vent gas are consistent with a great subsurface thickness of gas hydrate beneath the sea floor sites.

The geochemistry of vent gas supports models of the sub-surface depth and morphology of individual gas hydrate accumulations in the Gulf (Milkov and Sassen, 2003). The single largest gas hydrate accumulation in the Gulf of Mexico slope may be beneath the

shallow structure II gas hydrate so widespread in Atwater Valley 425 at ~1,930 meters water depth. The thickness of the gas hydrate vein-fillings in mud at the AT 425 site is suggested to be >1 kilometer. It is suggested that future study of gas hydrate as a potential alternative source of energy concentrate on the sites predicted to have the largest subsurface volumes of hydrocarbon gas that is concentrated as gas hydrate. Some decomposition of exposed or extremely shallow gas hydrate occurs but deeply buried gas hydrate is thought to be stable in the Gulf of Mexico slope over long spans of time. The models of gas hydrate stability in the Gulf of Mexico by Milkov et al. (2000) are widely accepted. There is an effect on hydrate stability predicted from changes in sea water temperature. It should be emphasized that the sediment has insulating properties, and changes of temperature in the water column are rapidly attenuated with depth in sediment (Milkov et al, 2000).

Models suggest that gas hydrate is unstable only when exposed at the sea floor or at depths in sediment of less ~2 meters in sediment (Fig. 12). Field observations are consistent with the model that exposed or shallow gas hydrate is affected by changes in the temperature of sea water. The irregular surface of the sea floor at gas hydrate sites is partly the result of sediment deformation caused by cyclical gas hydrate crystallization and decomposition in only a thin layer nearest the sea floor. Thus, seismic evidence of gas hydrate instability is most likely to be observed in the top few meters nearest the sea floor whereas deeper sediment show little or no evidence of change on any short time scale. Moreover, speculations linking gas hydrate decomposition to significant geologic changes such as massive slope failures must be critically examined in the light of geochemical data.

The 2002 JSL study sites with vent gas and outcropping gas hydrate are all similar. The GC 234, GC 232, and MC 118 sites are representative of all other discoveries of gas hydrate thus far made at the sea floor of the Gulf of Mexico slope. Subsurface migration over shallow salt and along faults focuses gas migration to specific sites at the sea floor that are connected to great depth in the sediment section. The known sea floor gas hydrate sites are each characterized by excess hydrocarbon gas that vents from the sea floor and enters the water column. Oil may coat the interiors of gas bubbles contributing to the natural oil slicks observed on the sea surface in association with many gas hydrate sites (Sassen et al., 2001b). The flux of vent gas at hydrate sites is extremely anomalous and can be detected by 38 kHz imagery of the sea floor and water column. A combination of shallow seismic data and 38 kHz imagery may prove to be the most effective tool for gas hydrate exploration in the Gulf of Mexico slope.

Lastly, many seep and vent sites with abundant hydrocarbon gases lack gas hydrate in the Gulf of Mexico slope even though they are in the Gas Hydrate Stability Zone. Seismic amplitudes merely indicate seeps or artifacts that resemble seeps. Although VK 826 and MC 885 display obvious geophysical anomalies, no gas hydrate is present. The apparent lack of gas hydrate at the VK 826 and MC 885 sites may be partially attributed to insufficient hydrocarbon gas flux but the carbonate-rich sites are too shallow and warm for structure I or II gas hydrate to be stable. In addition, brines are present at both sites

that are likely to retard gas hydrate crystallization. The MC 709 is a major geophysical anomaly and may or may not contain any gas hydrate although there are areas with intermediate hydrocarbon flux within the GHSZ. The main reason for the lack of abundant gas hydrate at MC 709 appears to be brine poisoning.

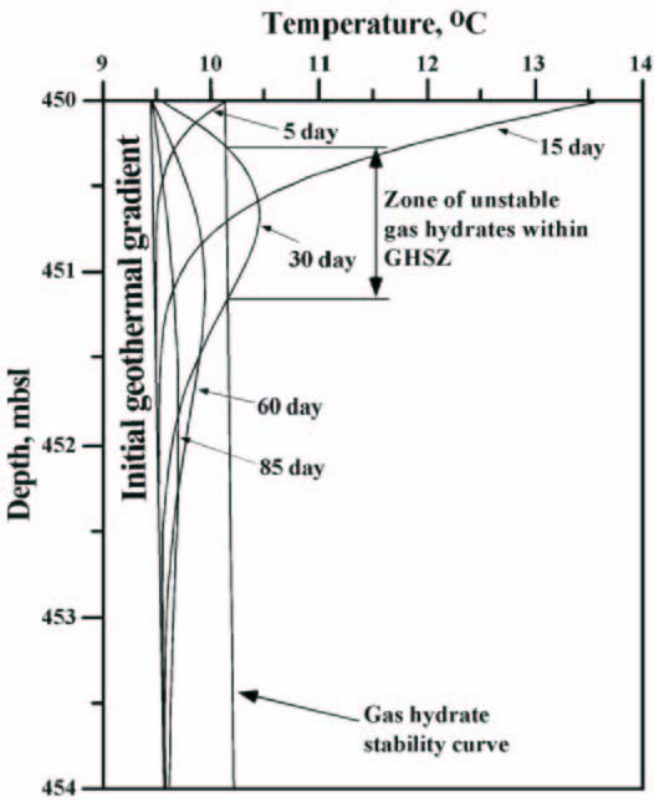

Figure 12. Gas hydrate stability curve showing that, at 450 m water depth, a warm eddy current may only cause thin-skin decomposition of gas hydrate. Exposed or shallow gas hydrate may be affected, but deeper gas hydrate (> 2 m in sediment) is thought to be largely insulated from transient temperature excursions. Diagram from Milkov et al. (2000).

REFERENCES

Aharon, P., and B. Fu (2000) Microbial sulfate reduction rates and sulfur and oxygen isotope fractionations at oil and gas seeps in deepwater Gulf of Mexico. Geochimica et Cosmochimica Acta 64, 233-246.

Fisher, C.R., I.R. MacDonald, R. Sassen, C.M. Young, S.A. Macko, S. Hourdez, R.S. Carney, S. Joye, and E. McMullin (2000) Methane ice worms: *Hesiocaeca methanicola* colonizing fossil fuel reserves: Naturwissenschaften, 87, 184-187.

Fu, B. and P. Aharon (1998) Sources of hydrocarbon-rich fluids advecting on the sea floor in the northern Gulf of Mexico. Gulf Coast Association of Geological Societies Transactions 48, 73-82.

Galloway, W.E., P.E. Ganey-Curry., X. Li, and R.T. Buffler (2000). Cenozoic depositional history of the Gulf of Mexico Basin. American Association of Petroleum Geologists Bulletin 84: 1743-1774.

Kvenvolden, K.A. (1993) Gas hydrates - geological perspective and global change. Reviews of Geophysics, 31. 173-187.

Kvenvolden, K.A. (1995) A review of the geochemistry of methane in natural gas hydrate. Organic Geochemistry, 23. 997-1008.

MacDonald, I.R., G.S. Boland, J.S., Baker, J.M., Brooks, M.C. Kennicutt, II and R.R. Bidigare (1989) Gulf of Mexico hydrocarbon seep communities II. Spatial distribution of seep organisms and hydrocarbons at Bush Hill. Marine Biology, 101. 235-247.

MacDonald, I.R., J.F. Reilly Jr., S.E. Best, R. Venkataramaiah, R. Sassen, J. Amos and N.L. Guinasso, Jr., (1996). A remote-sensing inventory of active oil seeps and chemosynthetic communities in the northern Gulf of Mexico. In: D. Schumacher and M.A. Abrams (Editors), Hydrocarbon migration and its near-surface expression. AAPG Memoir 66, pp. 27-37.

Milkov, A.V. and R. Sassen (2003) Preliminary assessment of resources and economic potential of individual gas hydrate accumulations in the Gulf of Mexico continental slope: Marine and Petroleum Geology. 20, 111-128.

Milkov, A.V. and R. Sassen (2002) Economic geology of offshore gas hydrate accumulations and provinces. Marine and Petroleum Geology 19: 1-11.

Milkov, A.V. and R. Sassen, (2001) Estimate of gas hydrate resource, northwestern Gulf of Mexico continental slope. Marine Geology, 179: 71-83.

Milkov, A.V., and R. Sassen (2000) Thickness of the gas hydrate stability zone, Gulf of Mexico continental slope: Marine and Petroleum Geology, 17, 981-991.

Milkov, A.V., R. Sassen, I. Novikova, and E. Mikhailov (2000) Gas hydrates at minimum stability water depths in the Gulf of Mexico: Significance to geohazard assessment: Transactions Gulf Coast Association of Geological Societies.50, 217-224.

Roberts, H.H., and R. S. Carney (1997) Evidence of episodic fluid, gas, and sediment venting on the northern Gulf of Mexico slope. Economic Geology 92, 863-879.

Roberts, H.H. and P. Aharon, (1994) Hydrocarbon-derived buildups of the northern Gulf of Mexico: A review of submersible investigations. Geo-Marine Letters, 14: 135-148.

Roberts, H.H. and R. Carney, R. (1997) Evidence of episodic fluid, gas, and sediment venting on the northern Gulf of Mexico slope. Economic Geology, 92: 863-879.

Salvador, A. (1987). Late Triassic-Jurassic paleogeography and origin of Gulf of Mexico

basin. American Association of Petroleum Geologists Bulletin 71: 419-451.

Sassen, R., H. H., Roberts, R. Carney, A. V. Milkov, D. A. DeFreitas, B. Lanoil, and C. Zhang (2004) Free hydrocarbon gas, gas hydrate, and authigenic minerals in chemosynthetic communities of the northern Gulf of Mexico continental slope: relation to microbial processes: Chemical Geology v. 205, Issues 3-4, p. 195-217.

Sassen, R., A.V. Milkov, E. Ozgul, H.H. Roberts, J. Hunt, M.A. Beeunas, J. Chanton, S.T. Sweet, and D. A. DeFreitas (2003) Gas venting and subsurface charge in the Green Canyon area, Gulf of Mexico continental slope: evidence of a deep bacterial methane source? Organic Geochemistry. 34, 1555-1464.

Sassen, R., A.V. Milkov, D.A. DeFreitas, and S.T. Sweet (2002) Molecular and isotopic properties of high-flux gas seeps, northwestern Gulf of Mexico: AAPG Annual Meeting, Abstracts, v. 11, p. A. 155.

Sassen, R., S.T. Sweet, A.V. Milkov, D.A. DeFreitas, and M.C. Kennicutt II (2001a) Thermogenic vent gas and gas hydrate in the Gulf of Mexico slope: Is gas hydrate decomposition significant? : Geology, v. 29, p. 107-110.

Sassen, R., S. L. Losh, L. Cathles III, H. H. Roberts, J. K. Whelan, A.V. Milkov, S. T. Sweet, and D.A. DeFreitas (2001b) Massive vein-filling gas hydrate: relation to ongoing gas migration from the deep subsurface in the Gulf of Mexico: Marine and Petroleum Geology, v. 18, p. 551-560.

Sassen, R., S.T. Sweet, A.V. Milkov, D.A. DeFreitas and M.C. Kennicutt II (2001c) Stability of thermogenic gas hydrate in the Gulf of Mexico: constraints on models of climate change. In: C.K. Paull and W.P. Dillon (Editors), Natural Gas Hydrates: Occurrence, Distribution, and Detection. American Geophysical Union, Washington D.C., pp.131-143.

Sassen, R., S.T. Sweet, D.A. DeFreitas, J.A. Morelos, and A.V. Milkov (2001d). Gas hydrate and crude oil from the Mississippi Fan Foldbelt, downdip Gulf of Mexico salt basin: significance to petroleum system. Organic Geochemistry 32:999-1008.

Sassen, R., S.T. Sweet, A.V. Milkov, D.A. DeFreitas, and M.C. Kennicutt II (2001e). Thermogenic vent gas and gas hydrate in the Gulf of Mexico slope: Is gas hydrate decomposition significant? Geology 29: 107-110.

Sassen, R., S.T. Sweet, A.V. Milkov, D.A. DeFreitas, G.G. Salata, and E.C. McDade, E (1999a) Geology and geochemistry of gas hydrates, central Gulf of Mexico continental slope. Gulf Coast Association of Geological Societies Transactions 49: 462-468.
Sassen, R., S. Joye, S.T. Sweet, D.A. DeFreitas, A.V. Milkov, and I.R. MacDonald (1999b). Thermogenic gas hydrates and hydrocarbon gases in complex chemosynthetic communities, Gulf of Mexico continental slope. Organic Geochemistry 30: 485-497.

Sassen, R. and I.R. MacDonald (1997) Hydrocarbons of experimental and natural gas hydrates, Gulf of Mexico continental slope. Organic Geochemistry 26, 289-293.

Sassen, R., I.R. MacDonald, A.G. Requejo, N.L. Guinasso, Jr, M.C. Kennicutt II, S.T. Sweet, and J.M. Brooks (1994) Organic geochemistry of sediments from chemosynthetic communities, Gulf of Mexico slope: Geo-Marine Letters 14, 110-119.

Sassen, R., H.H. Roberts, P.A. Aharon, A., J. Larkin, E.W. Chinn and R. Carney (1993) Chemosynthetic bacterial mats at cold hydrocarbon seeps, Gulf of Mexico continental slope. Organic Geochemistry 20: 77-89.

Sloan, E.D., 1998. Clathrate hydrates of natural gases, (2nd edition). New York, Dekker, 705 p.

Valentine, D.L. and W.S. Reeburgh (2000) New perspectives on anaerobic methane oxidation. Environmental Microbiology, 2 (5). 477-484.

Worrall, D.M. and Snelson, S. (1989) Evolution of the northern Gulf of Mexico with emphasis on Cenozoic growth faulting and the role of salt: In A.W. Bally and E.R. Palmer (Editors), The geology of North America – An overview: Boulder, Colorado, Geological Society of America, v. A, 97-138.

Zhang, C.L., Y. Li, J.D. Wall, J.D., L. Larsen, R. Sassen, Y. Huang, Y. Wang, A Peacock, D.C. White, J. Horita,. and D.R. Cole (2002) Lipid and carbon isotopic evidence of methane-oxidizing and sulfate-reducing bacteria in association with gas hydrates from the Gulf of Mexico. Geology 30 (3), 239-242.

BIBLIOGRAPHY

Brooks, J. M., M.C. Kennicutt II, R.R. Fay, T.J. McDonald, and R. Sassen (1984) Thermogenic gas hydrates in the Gulf of Mexico. Science 225: 409-411.

Brooks, J.M., H.B. Cox, W.B. Bryant, M.C. Kennicutt II, R.G. Mann, and T.J. McDonald, T.J. (1986) Association of gas hydrates and oil seepage in the Gulf of Mexico. Organic Geochemistry 10: 221-234.

Carney, R.S. (1994) Consideration of the oasis analogy for chemosynthetic communities at Gulf of Mexico hydrocarbon vents. Geo-Marine Letters 14: 149-159.

Cook, D. and P. D'Onfro (1991) Jolliet Field thrust structure and stratigraphy, Green Canyon Block 184, offshore Louisiana. Gulf Coast Association of Geological Societies Transactions 41, 100-121.

Coleman, D. D., J.B. Risatti, and M. Schoel (1981) Fractionation of carbon and hydrogen isotopes by methane oxidizing bacteria. Geochimica et Cosmochimica Acta 45, 1033-1037.

Fisher, C.R., I. Urcuyo, M.A. Simpkins, and E. Nix (1997) Life in the slow lane: growth and longevity of cold-seep vestimentiferans. Marine Ecology 18, 83-94.

Julian, D., F. Gaill, E. Wood, A.J. Arp, A.J., and C.R. Fisher (1999) Roots as a site of hydrogen sulfide uptake in the hydrocarbon seep vestimentiferan *Lammellibrachia* sp. Journal of Experimental Biology 202, 2245-2257.

Ginsburg, G.D. and V.A. Soloviev, (1998) Submarine gas hydrates. St. Petersburg, VNIIOkeangeologia, 216 p.

Kennicutt, M.C., II, J.M. Brooks, and G.J. Denoux (1988) Leakage of deep, reservoired petroleum to the near surface of the Gulf of Mexico continental slope. Marine Chemistry 24, 39-59.

Kvenvolden, K.A., 1999. Potential effects of gas hydrate on human welfare: Proceedings National Academy of Sciences, USA. 96, 3420-3426.

Lanoil, B. R. Sassen, M.T. LaDuc, S.T., Sweetand K.H. Nealson (2001) Bacteria and Archaea physically associated with Gulf of Mexico gas hydrates. Applied and Environmental Microbiology 67, 5143-5153.

MacDonald, I.R., N.L. Guinasso, Jr., R. Sassen, J.M. Brooks, L. Lee, and K.T. Scott, (1994) Gas hydrate that breaches the sea floor on the continental slope of the Gulf of Mexico. Geology 22, 699-702.

Ripmeester, J.A., J.S. Tse, J.S., C.I. Ratliffe, C.I. and B.M. Powell (1987) A new clathrate structure. Nature 325, 135-136.

Roberts, H.H., W.J. Wiseman, Jr., J. Hooper, and G.D. Humphrey (1999) Surficial gas hydrates of the Louisiana continental slope – Initial results of direct observations and in situ data collection. Offshore Technology Conference, Houston, Texas, OTC 10770, 259-272.

Roberts, H.H., R. Sassen, and A.V. Milkov (2001) Seafloor expression of fluid and gas expulsion from deep petroleum systems, continental slope of the northern Gulf of Mexico. Gulf Coast Society SEPM Foundation 21st Annual Research Conference, pp. 407-421.

Sassen, R., J.M. Brooks, I.R. MacDonald, M.C. Kennicutt II, N.L. Guinasso, Jr., and A.G. Requejo (1994) Association of oil seeps and chemosynthetic communities with oil discoveries, upper continental slope, Gulf of Mexico. Gulf Coast Association of Geological Societies Transactions 44, 349-355.

Sassen, R., I.R. MacDonald, N.L. Guinasso, Jr., S. Joye, A.G. Requejo, S.T. Sweet, J.. Alcala-Herrera, D.A. DeFreitas,. and D.R. Schink (1998) Bacterial methane oxidation in sea floor gas hydrate. Significance to life in extreme environments: Geology 26, 289-293.

Sassen, R., S.T. Sweet, D.A. DeFreitas, and A.V. Milkov (2000) Exclusion of isopentane during crystallization of structure II gas hydrate in sea floor sediment, Gulf of Mexico. Organic Geochemistry 31, 1257-1262.

Udachin, K.A. and J.R. Ripmeester (1999) A complex clathrate showing bimodal guest hydration. Nature, 397, 420-423.

ACRONYMS AND ABBREVIATIONS

C_1 = methane
C_2 = ethane
C_3 = propane
C_4 = butanes
C_5 = pentanes
CO_2 = carbon dioxide
H_2S = hydrogen sulfide
PDB = PeeDee Belemnite standard used in carbon isotope measurements
JSL = Johnson Sea Link research submersible
GHSZ = Gas Hydrate Stability Zone
AT = Atwater Valley protraction area of Gulf of Mexico
GC = Green Canyon =
VK = Viosca Knoll
MC = Mississippi Canyon

LIST OF GRAPHICS

Figure 1. Map showing locations of main study sites of the Gulf slope with gas hydrate (GC 234, GC 232, and MC 118) within a region of has hydrate occurrences, seeps with chemosynthetic communities, and subsurface accumulations of oil and gas. Other study sites used as control sites without gas hydrate are also shown (MC 709, MC 885, VK 826). Hydrate map modified from Sassen et al. (2001a) and sites of chemosynthetic communities from MacDonald et al. (1996).

Figure 2. A conceptualized north-south cross-section of central Gulf slope from the shelf to the abyssal plain is shown. Numerous geologically young basins formed by salt withdrawal pierce the slope salt thrust. The drainage areas of recently mature Mesozoic source rocks are deeply buried beneath the allochthonous salt. Fluids migrate upward through holes in the salt thrust (arrows). Within basins, salt and related faults provide conduits for vertical migration of fluids to reservoirs and to the seafloor. Hydrocarbon vents and seeps are focused by the structure near the rims of salt withdrawal basins. Modified from Milkov and Sassen (2001).

Figure 3. Features of a typical gas hydrate mound (~ 2 m across) with gas vents and nearby chemosynthetic community of tubeworms (Sassen et al.,1999b).

Figure 4. Photographs of tube worms and seep mussels from chemosynthetic

communities are shown.

Figure 5. Summary diagram of the microbially-mediated carbon and sulfur cycles associated with hydrate-related chemosynthetic communities. These basic biogeochemical processes are generalized to occur at many other hydrocarbon vent, seep, gas hydrate, and chemosynthetic community sites globally.

Figure 6. Photograph of structure II gas hydrate on a freshly exposed fault surface at GC 234. Massive vein-fillings of gas hydrate are separated by deformed hemipelagic mud, and the base of the exposure is under cut by flow of free gas. Note scale bar. Photograph by C.F. Fisher.

Figure 7. The 38 kHz image shows rapid gas venting to the water column from the GC 234 site.

Figure 8. The 38 kHz imagery shows gas venting to the water column from the sea floor at GC 232.

Figure 9. The 38 kHz imagery of MC 885 with no gas vents resolved.

Figure 10. Summary diagrams of molecular and isotopic data from GC 234. Data from Sassen et al. 2004.

Figure 11. Typical C_{15+} gas chromatogram of crude oil from GC 234 showing advanced alteration from microbial oxidation.

Figure 12. Gas hydrate stability curve showing that, at 450 m water depth, a warm eddy current may only cause thin-skin decomposition of gas hydrate. Exposed or shallow gas hydrate may be affected, but deeper gas hydrate (> 2 m in sediment) is thought to be largely insulated from transient temperature excursions. Diagram from Milkov et al. (2000).

Appendix

Johnson Sea Link 2002
C1 to C5 Analysis

Sample Description	Methane (ppm)	Ethane (ppm)	Ethylene (ppm)	Propane (ppm)	Propylene (ppm)	i-Butane (ppm)	n-Butane (ppm)	Neo-Pentane (ppm)	i-Pentane (ppm)	n-Pentane (ppm)	Total C1 - C5 (ppm)
CARNEY YEAR 6	61162.9	111.0	0.8	3.3	1.1	7.7	7.8	0.0	0.0	0.0	61294.5
GC 232 4401 Core 3 Top	4036.5	131.8	1.7	2.3	0.4	8.5	8.4	14.9	84.5	0.3	4289.5
GC 232 4401 Core 3 Bottom	30268.4	340.1	0.9	13.8	0.2	134.9	26.2	45.0	1010.6	5.3	31845.5
GC 232 4401 Core 5 Top	4769.0	111.2	1.0	2.7	0.4	7.8	7.9	0.0	1.0	0.0	4901.2
GC 232 4401 Core 5 Middle	3746.0	119.4	1.1	2.4	0.6	7.7	7.8	0.0	0.2	0.5	3885.6
GC 232 4401 Core 5 Bottom	1226.1	120.0	1.4	2.4	0.8	7.8	8.5	0.0	0.7	0.9	1368.6
GC 232 4401 Core 6 Top	34914.1	815.7	1.6	296.0	0.5	1139.5	135.0	113.1	207.2	162.1	37784.9
GC 232 4401 Core 4 Small Can	68.8	108.8	1.0	0.9	0.4	7.6	7.7	0.0	0.1	0.2	195.4
GC 232 4403 Core 1	67937.9	2400.8	1.1	757.1	0.5	521.8	330.4	127.3	34.0	15.8	72126.7
GC 232 4403 Core 2	222081.3	7418.8	1.2	578.0	0.6	223.3	347.6	184.6	651.8	11.3	231498.5
GC 232 4403 Core 3 Top	108242.5	2690.3	2.7	513.7	1.0	166.9	41.9	15.0	36.1	0.2	111710.5
GC 232 4403 Core 5 Top	21726.4	111.6	7.1	42.6	1.2	8.2	8.1	0.0	1.0	0.1	21906.4
GC 232 4401 Core 6 Bottom	40751.4	266.9	2.4	162.9	0.0	407.4	105.2	21.8	161.7	64.5	41944.3
GC 232 4403 Core 5 Bottom	5909.7	127.1	5.7	42.8	1.1	7.7	7.8	0.0	0.8	0.1	6102.7
GC 232 4404 Gas Hydrate	703729.6	61542.3	0.0	66085.3	0.0	13125.1	9669.7	137.0	4502.2	4197.1	862988.2
GC 232 Dive 4404 hydrate-Decomposed in lab	481047.1	57794.9	0.0	84731.2	0.0	16273.7	3732.4	0.0	56.3	0.0	643635.6
GC 232 4404 Core 1 Top	898763.7	29043.4	0.0	6899.3	0.0	3567.2	23789.1	129.3	17357.6	12843.2	992392.9
GC 232 4404 Core 1 Bottom	505663.7	15284.5	0.2	21039.8	0.0	11570.2	45711.5	140.1	23388.3	20262.7	643061.1
GC 234 4406 Gas Hydrate	782079.6	16986.5	0.0	31929.1	0.0	29990.2	23056.5	464.3	8448.0	6522.1	899476.2
GC 234 Dive 4406 hydrate-Decomposed in lab	480906.6	52649.3	0.0	79056.1	0.0	16502.0	5197.3	41.3	363.8	54.2	634770.6
GC 234 4407 Core 2 Bottom Small Can	738068.7	11477.7	13.9	13161.3	0.9	21369.8	1322.4	685.8	4189.6	0.0	790290.1
MC 885 4409 Core 1	3634.1	111.0	3.9	43.5	0.4	9.8	8.4	0.0	2.7	0.3	3814.2
VK 826 4410 Core 1	99.3	108.8	3.1	41.9	0.7	7.9	7.9	0.0	0.5	0.4	270.6
MC 709 4412 Core 1 Top	46376.6	4562.6	0.0	1890.5	0.0	408.4	317.2	0.0	37.9	11.2	53604.3
MC 709 4412 Core 1 Bottom	37.3	108.7	0.8	41.6	0.5	7.5	7.7	0.0	0.1	0.4	204.7
MC 709 4413 Core 4 Top	146820.8	5139.7	0.6	2631.4	0.4	665.6	142.0	12.7	185.5	13.8	155612.4
MC 709 4413 Core 4 Bottom	306198.7	9004.7	0.0	4322.6	0.0	1361.2	619.8	14.1	182.2	16.9	321720.2
MC 709 4413 Bucket 6	532795.1	9500.9	0.0	1990.3	0.0	997.0	0.0	8.4	207.4	0.0	545499.0
MC 118 4414 Bucket 8	611532.7	13354.0	0.0	526.0	0.0	1045.6	167.0	136.2	135.5	16.2	626913.3
MC 118 4414 Core 3	264059.6	4689.4	0.3	2380.3	2.5	1341.4	398.9	138.1	377.3	81.0	273468.8
MC 118 4415 Core 5 Top	183404.7	11407.9	0.2	23421.4	0.6	33486.0	7382.3	20.6	0.0	115.2	259238.9

Johnson Sea Link 2002
C1 to C5 Analysis

Sample Description	Methane (ppm)	Ethane (ppm)	Ethylene (ppm)	Propane (ppm)	Propylene (ppm)	i-Butane (ppm)	n-Butane (ppm)	Neo-Pentane (ppm)	i-Pentane (ppm)	n-Pentane (ppm)	Total C1 - C5 (ppm)
MC 118 4415 Core 5 Bottom	202352.3	19747.0	0.0	37530.0	0.0	33710.5	11457.5	379.1	3127.8	136.6	308440.9
GC 234 4424 Core 1	179103.2	7508.1	0.6	2056.1	0.0	825.2	8.9	153.7	621.0	0.0	190276.9
GC 234 4424 Core 2	27878.9	4441.0	1.4	1655.5	1.0	321.1	8.6	0.0	1.8	0.3	34309.7
GC 234 4424 Core 5	407639.2	11853.8	0.7	3165.5	0.0	2436.3	17973.3	0.0	8538.8	5964.8	457572.2
GC 233 4425 Core 2	592.0	116.5	0.9	3.3	0.3	8.5	0.0	0.0	2.5	0.5	724.5
GC 233 4425 Core 4	18701.7	139.2	1.4	2.1	0.4	8.2	0.0	0.0	0.7	0.1	18853.9
GC 233 4425 Core 5	414450.2	13372.3	0.7	1207.2	0.0	4664.3	18.0	290.5	5015.4	0.0	439018.5
GC 233 4425 Mussel Bed 1	536502.2	5348.0	1.1	305.9	0.3	23.8	0.0	5.0	22.3	0.2	542208.9
GC 233 4427 Core 1 Top	615.8	107.9	0.8	0.7	0.4	7.7	7.5	3.4	0.0	0.0	744.2
GC 233 4427 Core 1 Bottom 1 mL	704.8	108.4	1.1	0.8	0.6	7.7	7.4	0.0	0.0	0.0	830.8
GC 232 4428 Core 1	67531.6	1751.3	2.9	92.0	0.9	2079.0	0.0	183.2	1481.4	0.0	73122.3
GC 232 4428 Core 5	114106.3	1581.1	6.6	3.7	0.7	7.8	0.0	0.0	0.0	0.0	115706.3
Dive 4428 Core 6	103161.4	2145.3	2.8	1217.1	1.1	1813.8	0.0	591.6	1327.0	12.8	110272.9
GC 185 4429 Bush Hill near Carbonate Roc	2306.2	110.0	2.7	42.2	0.7	7.9	6.7	6.0	0.3	0.2	2482.8
Dive 4431	346916.5	18548.9	1.4	26232.9	0.0	21752.1	10062.6	472.2	9738.7	3412.1	437137.4
Dive 4432	296.7	110.8	6.2	45.0	0.4	11.5	9.7	3.6	4.6	1.3	489.9
Dive 4438	81039.7	2803.3	0.0	1762.2	0.0	2184.6	2887.1	137.4	22605.1	2526.0	115945.5

Johnson Sealink 2002
C1 to C5 Analysis

Sample Description	Methane (norm %)	Ethane (norm %)	Ethylene (norm %)	Propane (norm %)	Propylene (norm %)	i-Butane (norm %)	n-Butane (norm %)	Neo-Pentane (norm %)	i-Pentane (norm %)	n-Pentane (norm %)	Total C1 - C5 (norm %)
CARNEY YEAR 6	99.785	0.181	0.001	0.005	0.002	0.013	0.013	0.000	0.000	0.000	100.000
GC 232 4401 Core 3 Top	94.103	3.073	0.039	0.055	0.010	0.197	0.197	0.347	1.971	0.008	100.000
GC 232 4401 Core 3 Bottom	95.048	1.068	0.003	0.043	0.001	0.424	0.082	0.141	3.174	0.017	100.000
GC 232 4401 Core 5 Top	97.303	2.270	0.021	0.055	0.009	0.159	0.161	0.000	0.021	0.000	100.000
GC 232 4401 Core 5 Middle	96.407	3.073	0.028	0.062	0.015	0.197	0.201	0.000	0.004	0.012	100.000
GC 232 4401 Core 5 Bottom	89.588	8.764	0.106	0.178	0.056	0.568	0.622	0.000	0.052	0.065	100.000
GC 232 4401 Core 6 Top	92.402	2.159	0.004	0.784	0.001	3.016	0.357	0.299	0.548	0.429	100.000
GC 232 4401 Core 4 Small Can	35.193	55.678	0.500	0.465	0.219	3.866	3.951	0.000	0.045	0.083	100.000
GC 232 4403 Core 1	94.192	3.329	0.002	1.050	0.001	0.723	0.458	0.177	0.047	0.022	100.000
GC 232 4403 Core 2	95.932	3.205	0.001	0.250	0.000	0.096	0.150	0.080	0.282	0.005	100.000
GC 232 4403 Core 3 Top	96.896	2.408	0.002	0.460	0.001	0.149	0.038	0.013	0.032	0.000	100.000
GC 232 4403 Core 5 Top	99.178	0.510	0.033	0.195	0.005	0.038	0.037	0.000	0.005	0.000	100.000
GC 232 4401 Core 6 Bottom	97.156	0.636	0.006	0.388	0.000	0.971	0.251	0.052	0.386	0.154	100.000
GC 232 4403 Core 5 Bottom	96.838	2.082	0.094	0.701	0.017	0.125	0.128	0.000	0.014	0.001	100.000
GC 232 4404 Gas Hydrate	81.546	7.131	0.000	7.658	0.000	1.521	1.120	0.016	0.522	0.486	100.000
GC 232 Dive 4404 hydrate-Decomposed in lab	74.739	8.979	0.000	13.164	0.000	2.528	0.580	0.000	0.009	0.000	100.000
GC 232 4404 Core 1 Top	90.565	2.927	0.000	0.695	0.000	0.359	2.397	0.013	1.749	1.294	100.000
GC 232 4404 Core 1 Bottom	78.634	2.377	0.000	3.272	0.000	1.799	7.108	0.022	3.637	3.151	100.000
GC 234 4406 Gas Hydrate	86.948	1.888	0.000	3.550	0.000	3.334	2.563	0.052	0.939	0.725	100.000
GC 234 Dive 4406 hydrate-Decomposed in lab	75.761	8.294	0.000	12.454	0.000	2.600	0.819	0.007	0.057	0.009	100.000
GC 234 4407 Core 2 Bottom Small Can	93.392	1.452	0.002	1.665	0.000	2.704	0.167	0.087	0.530	0.000	100.000
MC 885 4409 Core 1	95.278	2.910	0.103	1.140	0.011	0.257	0.221	0.000	0.071	0.008	100.000
VK 826 4410 Core 1	36.700	40.195	1.140	15.500	0.272	2.938	2.930	0.000	0.178	0.148	100.000
MC 709 4412 Core 1 Top	86.516	8.512	0.000	3.527	0.000	0.762	0.592	0.000	0.071	0.021	100.000
MC 709 4412 Core 1 Bottom	18.225	53.091	0.402	20.308	0.247	3.669	3.781	0.000	0.070	0.207	100.000
MC 709 4413 Core 4 Top	94.350	3.303	0.000	1.691	0.000	0.428	0.091	0.008	0.119	0.009	100.000
MC 709 4413 Core 4 Bottom	95.175	2.799	0.000	1.344	0.000	0.423	0.193	0.004	0.057	0.005	100.000
MC 709 4413 Bucket 6	97.671	1.742	0.000	0.365	0.000	0.183	0.000	0.002	0.038	0.000	100.000
MC 118 4414 Bucket 8	97.547	2.130	0.000	0.084	0.000	0.167	0.027	0.022	0.022	0.003	100.000
MC 118 4414 Core 3	96.559	1.715	0.000	0.870	0.001	0.491	0.146	0.050	0.138	0.030	100.000
MC 118 4415 Core 5 Top	70.747	4.401	0.000	9.035	0.000	12.917	2.848	0.008	0.000	0.044	100.000

Johnson Sealink 2002
C1 to C5 Analysis

Sample Description	Methane (norm %)	Ethane (norm %)	Ethylene (norm %)	Propane (norm %)	Propylene (norm %)	i-Butane (norm %)	n-Butane (norm %)	Neo-Pentane (norm %)	i-Pentane (norm %)	n-Pentane (norm %)	Total C1 - C5 (norm %)
MC 118 4415 Core 5 Bottom	65.605	6.402	0.000	12.168	0.000	10.929	3.715	0.123	1.014	0.044	100.000
GC 234 4424 Core 1	94.128	3.946	0.000	1.081	0.000	0.434	0.005	0.081	0.326	0.000	100.000
GC 234 4424 Core 2	81.256	12.944	0.004	4.825	0.003	0.936	0.025	0.000	0.005	0.001	100.000
GC 234 4424 Core 5	89.087	2.591	0.000	0.692	0.000	0.532	3.928	0.000	1.866	1.304	100.000
GC 234 4425 Core 2	81.719	16.081	0.121	0.449	0.043	1.175	0.000	0.000	0.350	0.062	100.000
GC 234 4425 Core 4	99.193	0.738	0.008	0.011	0.002	0.043	0.000	0.000	0.004	0.001	100.000
GC 234 4425 Core 5	94.404	3.046	0.000	0.275	0.000	1.062	0.004	0.066	1.142	0.000	100.000
GC 234 4425 Mussel Bed 1	98.948	0.986	0.000	0.056	0.000	0.004	0.000	0.001	0.004	0.000	100.000
GC 233 4427 Core 1 Top	82.747	14.499	0.108	0.100	0.050	1.034	1.001	0.459	0.000	0.000	100.000
GC 233 4427 Core 1 Bottom 1 mL	84.838	13.050	0.131	0.100	0.066	0.924	0.889	0.000	0.000	0.000	100.000
GC 232 4428 Core 1	92.354	2.395	0.004	0.126	0.001	2.843	0.000	0.251	2.026	0.000	100.000
GC 232 4428 Core 5	98.617	1.366	0.006	0.003	0.001	0.007	0.000	0.000	0.000	0.000	100.000
Dive 4428 Core 6	93.551	1.945	0.002	1.104	0.001	1.645	0.000	0.536	1.203	0.012	100.000
GC 185 4429 Bush Hill near Carbonate Roc	92.885	4.432	0.108	1.700	0.028	0.319	0.268	0.241	0.012	0.007	100.000
Dive 4431	79.361	4.243	0.000	6.001	0.000	4.976	2.302	0.108	2.228	0.781	100.000
Dive 4432	60.564	22.620	1.273	9.177	0.081	2.352	1.987	0.743	0.945	0.257	100.000
Dive 4438	69.895	2.418	0.000	1.520	0.000	1.884	2.490	0.119	19.496	2.179	100.000

Johnson Sealink 2002
Vent Gas and Gas Hydrate
C1 to C5 Analysis

Sample Description	Methane (%)	Ethane (%)	Propane (%)	i-Butane (%)	n-Butane (%)	Neo-Pentane (%)	i-Pentane (%)	n-Pentane (%)	Total C1 - C5 (%)
4403 GC232 "L"	82.27	2.51	0.30	0.08	0.22	0.02	0.07	0.05	85.52
4403 GC232 "R"	86.83	2.76	0.32	0.08	0.24	0.02	0.08	0.05	90.38
Dive 4404	90.03	3.54	0.89	0.18	0.35	0.02	0.13	0.07	95.22
Dive 4405	84.04	3.10	0.81	0.17	0.30	0.02	0.10	0.06	88.59
Dive 4406	94.78	3.53	1.37	0.27	0.38	0.02	0.11	0.07	100.53
Dive 4407	88.67	3.03	1.10	0.23	0.37	0.02	0.11	0.07	93.61
Dive 4414	90.48	2.95	1.31	0.29	0.36	0.02	0.12	0.08	95.61
Dive 4415	88.91	2.93	1.36	0.34	0.41	0.02	0.16	0.09	94.21
Dive 4415 HYDRATE	90.76	2.30	0.47	0.12	0.28	0.02	0.09	0.06	94.10
Dive 4427	43.88	0.92	0.25	0.10	0.10	0.03	0.04	0.04	45.34
Dive 4428	94.96	3.05	1.19	0.42	0.46	0.01	0.19	0.11	100.39
Dive 4430	95.86	2.71	0.43	0.09	0.35	0.01	0.12	0.08	99.65
Dive 4431	93.94	3.56	1.40	0.24	0.41	0.01	0.12	0.08	99.75
Dive 4432	83.76	2.73	0.85	0.16	0.34	0.01	0.11	0.08	88.03
Dive 4438	94.68	3.69	1.50	0.26	0.44	0.01	0.13	0.10	100.80

Johnson Sealink 2002
Vent Gas and Gas Hydrate
C1 to C5 Analysis

Sample Description	Methane (norm %)	Ethane (norm %)	Propane (norm %)	i-Butane (norm %)	n-Butane (norm %)	Neo-Pentane (norm %)	i-Pentane (norm %)	n-Pentane (norm %)	Total C1 - C5 (norm %)
4403 GC232 "L"	96.20	2.94	0.35	0.09	0.26	0.02	0.09	0.06	100.00
4403 GC232 "R"	96.07	3.05	0.35	0.09	0.27	0.02	0.09	0.06	100.00
Dive 4404	94.55	3.72	0.94	0.19	0.37	0.02	0.14	0.08	100.00
Dive 4405	94.86	3.50	0.92	0.19	0.34	0.02	0.11	0.07	100.00
Dive 4406	94.28	3.51	1.36	0.27	0.38	0.02	0.11	0.07	100.00
Dive 4407	94.73	3.23	1.18	0.24	0.40	0.02	0.12	0.08	100.00
Dive 4414	94.63	3.09	1.37	0.31	0.38	0.02	0.13	0.08	100.00
Dive 4415	94.38	3.11	1.44	0.36	0.43	0.02	0.17	0.10	100.00
Dive 4415 HYDRATE	96.46	2.44	0.50	0.13	0.29	0.02	0.10	0.06	100.00
Dive 4427	96.77	2.02	0.54	0.22	0.22	0.06	0.08	0.08	100.00
Dive 4428	94.59	3.04	1.18	0.42	0.45	0.01	0.19	0.11	100.00
Dive 4430	96.20	2.72	0.43	0.09	0.35	0.01	0.12	0.08	100.00
Dive 4431	94.17	3.57	1.40	0.24	0.41	0.01	0.12	0.08	100.00
Dive 4432	95.14	3.10	0.97	0.18	0.39	0.01	0.12	0.09	100.00
Dive 4438	93.93	3.66	1.49	0.26	0.44	0.01	0.13	0.10	100.00

Dive	Core	Position	Injection, micro-L	Split ratio	C1	CO2	Comments
4401	3	Bottom	250	1:10	-57.28	-35.87	
4401	5	Middle	250	1:10	not enough gas	not enough gas	
4401	5	Middle	1000	1:10	-88.02	not enough gas	
4401	6	Top	250	1:10	too much gas	-39.59	
4401	6	Top	50	1:10	too much gas	-39.65	
4401	6	Top	25	1;100	-57.51	not enough gas	
4401	6		250	1:10	-85.93	-39.06	
4403	1		250	1:10	-46.25	-13.31	
4403	3	Top	250	1:10	-59.97	-31.4	ethane: -23.89
4403	5	Top	250	1:10	-82.06	-41.21	
4403	5	Bottom	200	1:10	-92.1	-44.34	
4409	1		250	1:10	-64.56	-43.57	
4412	1	Top	250	1:10	-56.62	-31.96	
4424	2		200	1:10	-64.46	-24.87	
4425	2		250	1:10	not enough gas	not enough gas	
4425	2		500	1:10	not enough gas	-37.14	
4425	2		1000	1:10	-86.68	-36.87	
4425	4		250	1:10	-54.68	-28.87	
4425	Mussel bed		1000	1:10	too much gas	too much gas	
4425	Mussel bed		500	1:10	too much gas	too much gas	
4425	Mussel bed		250	1:10	-72.45	-46.47	
4425	Mussel bed		250	1:10	-71.42	-46.99	
4427	1	Top	100	1:10	not enough gas	-20.17	
4427	1	Top	1000	1:10	-103.08	-20.37	
4427	1	Bottom	250	1:10	not enough gas	-13.88	
4427	1	Bottom	1000	1:10	-123.15	-15.17	
4428	5		250	1:10	-55.71	-38.79	
4429			250	1:10	not enough gas	-27.89	
4429			1000	1:10	-95.71	-28.53	
Carney			250	1:10	-89.64	too much gas	CO2>>C1
Carney			100	1:10	-88.94	too much gas	CO2>>C1
Carney			30	1:10	-89.24	too much gas	CO2>>C1
Carney			25	1;100	not enough gas	-17.42	CO2>>C1

Sample Location	Dive #	Sample Type	$\delta^{13}C$ C_1	$\delta^{13}C$ C_1	Avg $\delta^{13}C_1$	δD C_1	δD C_1	Avg δD	$\delta^{13}C$ C_2	$\delta^{13}C$ C_2	Avg $\delta^{13}C_2$	$\delta^{13}C$ C_3	$\delta^{13}C$ C_3	Avg $\delta^{13}C_3$	$\delta^{13}C$ i-C_4	$\delta^{13}C$ CO_2	$\delta^{13}C$ CO_2	Avg $\delta^{13}CO_2$
GC 232	4403	Vent Gas (left)	-43.0	-43.1	-43.1	-177	-180	-178.5	-26.4	-26.5	-26.5	-23.7		-23.7				
GC 232	4403	Vent Gas (right)	-42.9	-43.1	-43.0	-181		-181	-26.2		-26.2	-23.4		-23.4				
GC 232	4404	Vent Gas	-43.0	-43.1	-43.1	-181	-181	-181	-26.2	-26.1	-26.2	-23.3		-23.3				
GC 232	4404	Hydrate	-42.7	-42.6	-42.7	-176	-177	-176.5	-27.6	-27.5	-27.6	-24.4	-24.4	-24.4				
GC 232	4405	Vent Gas	-42.8		-42.8	-182	-182	-182	-26.2		-26.2	-23.3		-23.3				
GC 234	4406	Vent Gas	-48.4	-48.2	-48.3	-185	-186	-185.5	-27.3		-27.3	-23.8		-23.8		+15.9		+15.9
GC 234	4406	Hydrate	-48.0	-47.9	-48.0	-183		-183	-27.7		-27.7	-24.7		-24.7	-25.6			
GC 234	4407	Vent Gas	-48.5	-48.6	-48.6	-185		-185	-27.2		-27.2	-24.0		-24.0		+15.7		+15.7
MC 118	4414	Vent Gas	-45.7	-45.8	-45.8	-163	-164	-163.5	-27.0	-27.1	-27.1	-24.4	-24.5	-24.5		+21.2		+21.2
MC 118	4415	Vent Gas	-45.7	-45.6	-45.7	-162		-162	-26.8		-26.8	-24.1		-24.1		+21.5	+21.5	+21.5
MC 118	4415	Hydrate (a)	-45.8	-45.6	-45.7	-163	-162	-162.5	-26.8	-26.7	-26.8	-24.0	-24.1	-24.1		+17.7	+17.8	+17.75

JSL Sealink 2002
Gas Chromatographic Data

File #	Description	UCM<23 (ppm)	UCM>23 (ppm)	Total UCM (ppm)
L52820	GC 232, Dive 4401	4174	4832	9006
L52821	GC 233, Dive 4425	2725	4592	7317
L52822	GC 185, Dive 4429	2269	6491	8761
L52823	GC 234, Dive 4434	389	860	1249
L52824	GC 234, Dive 4435	554	1071	1625
L52825	GC 234, Dive 4436	410	785	1195
L52826	GC 232, Dive 4437	912	1696	2608
L52827	GC 232, Dive 4403	1480	2999	4479
L52828	MC 709, Dive 4412	280	164	445
L52829	MC 118, Dive 4414	3847	3624	7471
L52830	CARNEY YEAR 6	9321	3660	12982
L52831	GC 232 4401 Core 3 Top	6761	8372	15133
L52832	GC 232 4401 Core 3 Bottom	6860	11351	18211
L52833	GC 232 4401 Core 5 Top	4932	7483	12415
L52834	GC 232 4401 Core 5 Middle	9560	11125	20684
L52835	GC 232 4401 Core 5 Bottom	11798	13931	25729
L52836	GC 232 4401 Core 6 Top	7490	9184	16674
L52837	GC 232 4401 Core 4 Small	3184	6192	9375
L52838	GC 232 4403 Core 1	1836	4940	6776
L52839	GC 232 4403 Core 2	8370	8371	16741
L52840	GC 232 4403 Core 3 Top	3355	6098	9453
L52841	GC 232 4403 Core 5 Top	4541	7626	12166
L52842	GC 232 4401 Core 6 Bottom	7627	13454	21081
L52843	GC 232 4403 Core 5 Bottom	11227	14889	26117
L52844	GC 232 4404 Gas Hydrate	1772	2694	4465
L52845	GC 232 4404 Core 1 Top	5363	19838	25201
L52846	GC 232 4404 Core 1 Bottom	7267	8551	15819
L52847	GC 234 4406 Gas Hydrate	7917	10739	18656
L52848	GC 234 4407 Core 2 Bottom	12282	45573	57855
L52849	MC 885 4409 Core 1	14	31	46
L52850	VK 826 4410 Core 1	71	64	136
L52851	MC 709 4412 Core 1 Top	491	1383	1874
L52852	MC 709 4412 Core 1 Bottom	46	359	404
L52853	MC 709 4413 Core 4 Top	43	163	206
L52854	MC 709 4413 Core 4 Bottom	28	71	99
L52855	MC 709 4413 Bucket 6	133	352	485
L52856	MC 118 4414 Bucket 8	3115	6404	9519
L52857	MC 118 4414 Core 3	10230	8591	18820
L52858	MC 118 4415 Core 5 Top	11068	11979	23048
L52859	MC 118 4415 Core 5 Bottom	5056	9916	14972
L52860	GC 234 4424 Core 1	4910	7705	12616
L52861	GC 234 4424 Core 2	7591	1644	9235
L52862	GC 234 4424 Core 5	14987	17334	32321
L52863	GC 233 4425 Core 2	3019	8663	11682
L52864	GC 233 4425 Core 4	3349	13034	16383
L52865	BLANK	13	20	33
L52866	GC 233 4425 Mussel Bed 1	1116	3956	5072
L52867	GC 233 4427 Core 1 Top	166	326	492
L52868	GC 233 4427 Core 1 Bottom	175	338	513
L52869	GC 232 4428 Core 1	11727	11491	23218
L52870	GC 232 4428 Core 5	3544	5332	8876
L52871	Dive 4428 Core 6	8906	8018	16924
L52871	Dive 4428 Core 6	8133	6836	14969
L52872	GC 185 4429 Bush Hill nea	3373	8516	11890
L52873	Dive 4431	9106	10576	19682
L52874	Dive 4432	2503	2986	5489
L52875	Dive 4438	1350	3142	4491

File : C:\HPCHEM\1\DATA\B1402AL\L52866.D
Operator : STS&CRS
Acquired : 18 Feb 2003 21:10 using AcqMethod AL5212N4.M
Instrument : M8 GC-589
Sample Name: GC 233 4425 Mussel Bed 1
Misc Info : A1402
Vial Number: 11

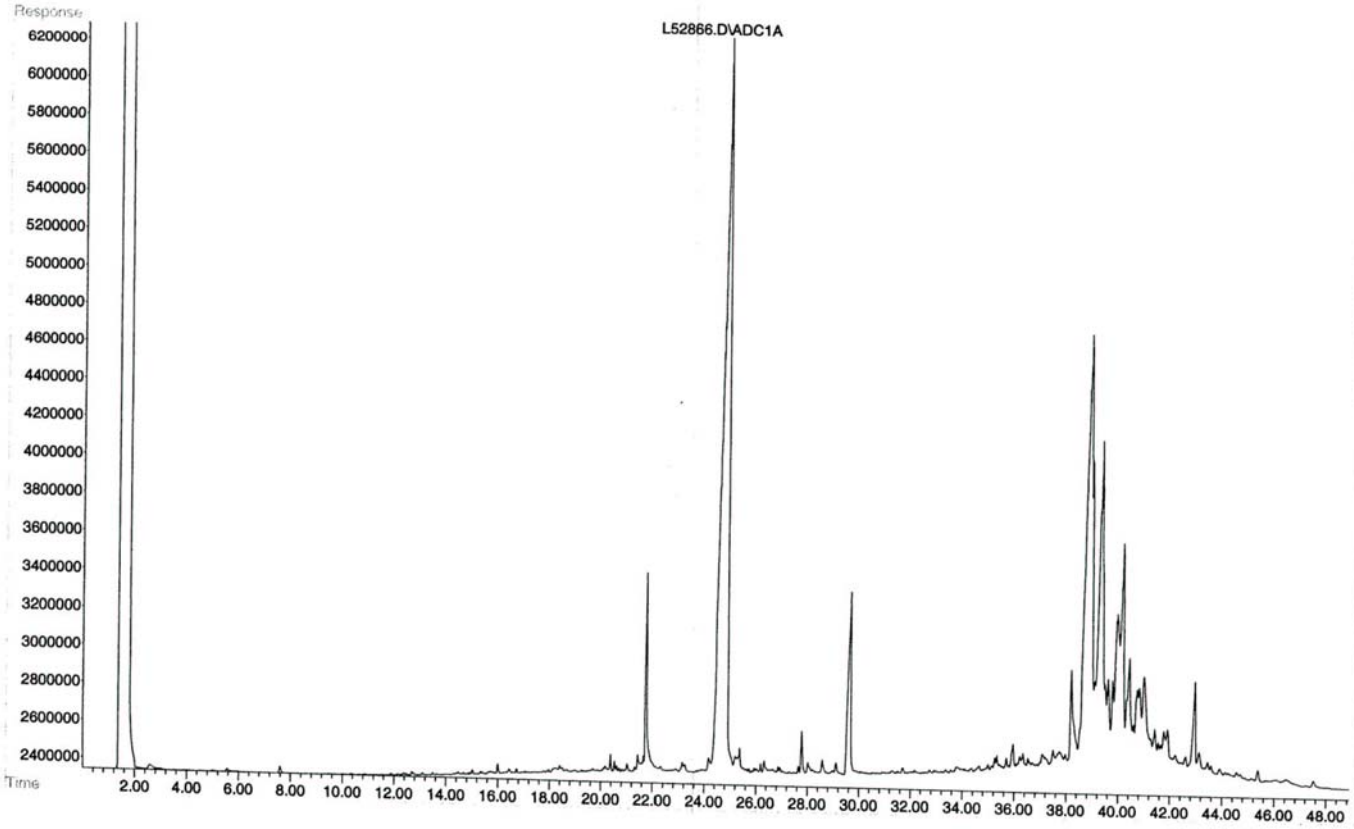

File : C:\HPCHEM\1\DATA\A1401AL\L52830.D
Operator : STS&CRS
Acquired : 16 Feb 2003 10:53 using AcqMethod AL5212N4.M
Instrument : M8 GC-589
Sample Name: CARNEY YEAR 6
Misc Info : A1400
Vial Number: 27

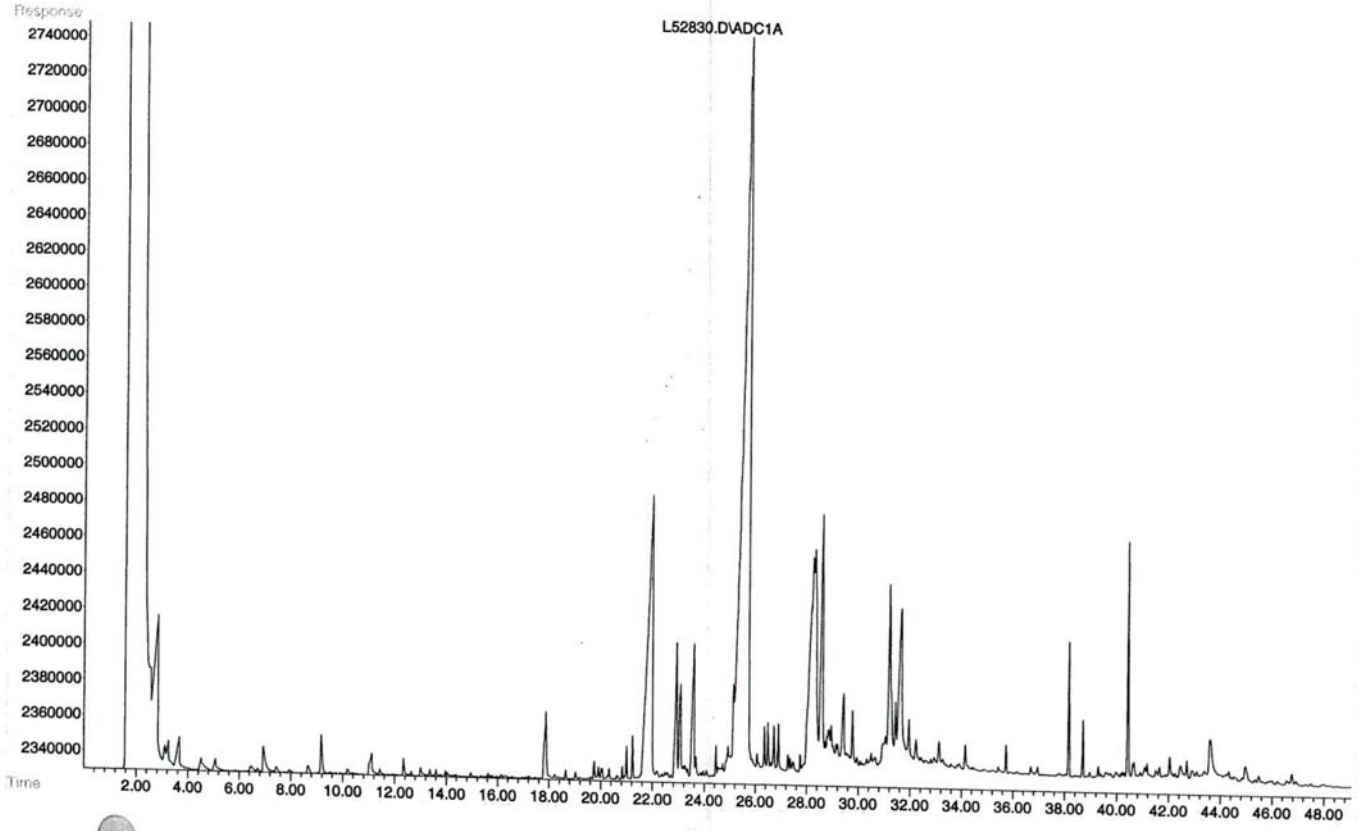

```
File        : C:\HPCHEM\1\DATA\A1402AL\L52867.D
Operator    : STS&CRS
Acquired    : 13 Feb 2003   9:49     using AcqMethod AL5212N4.M
Instrument :   M8 GC-589
Sample Name: GC 233 4427 Core 1 Top
Misc Info   : A1402
Vial Number: 20
```

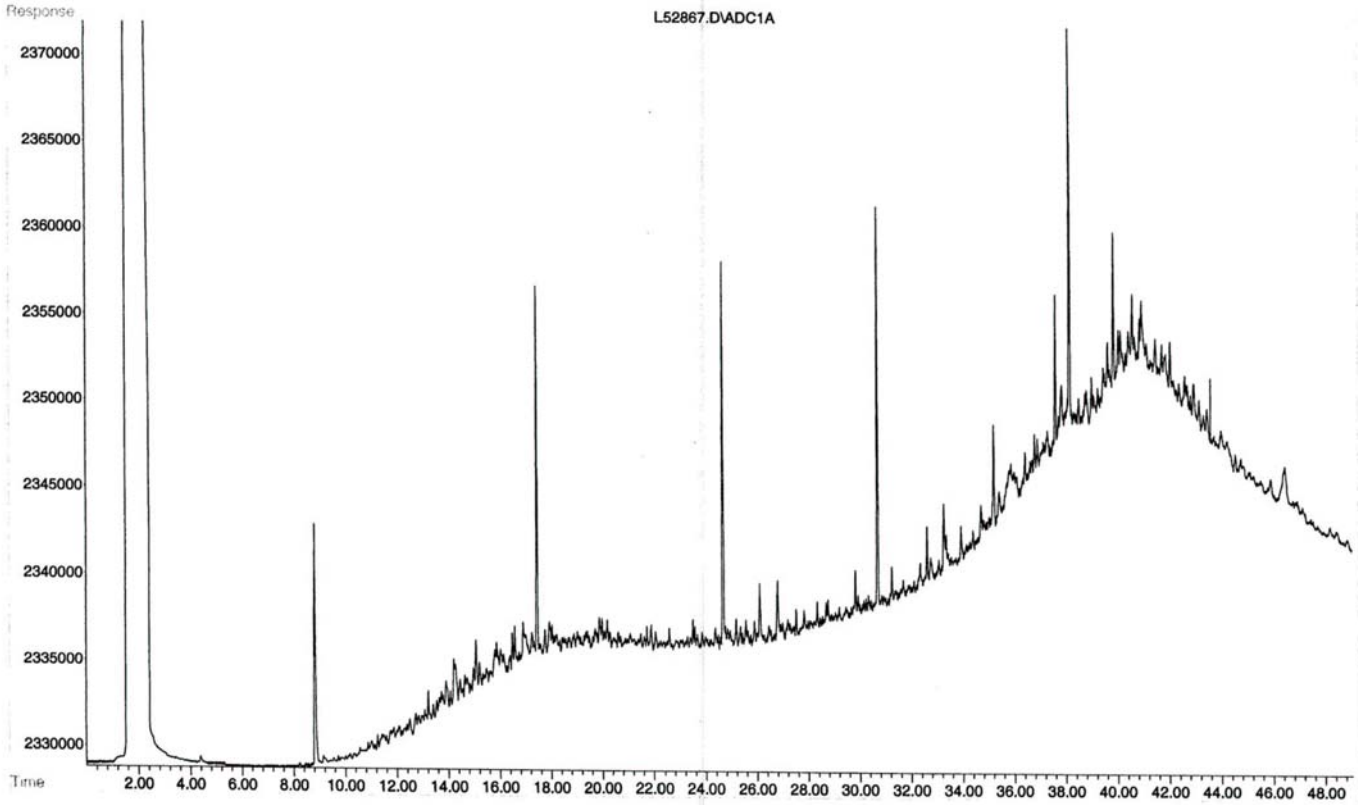

File : C:\HPCHEM\1\DATA\A1400AL\L52821.D
Operator : STS&CRS
Acquired : 11 Feb 2003 17:16 using AcqMethod AL5212N4.M
Instrument : M8 GC-589
Sample Name: GC 233, Dive 4425
Misc Info : A1400
Vial Number: 8

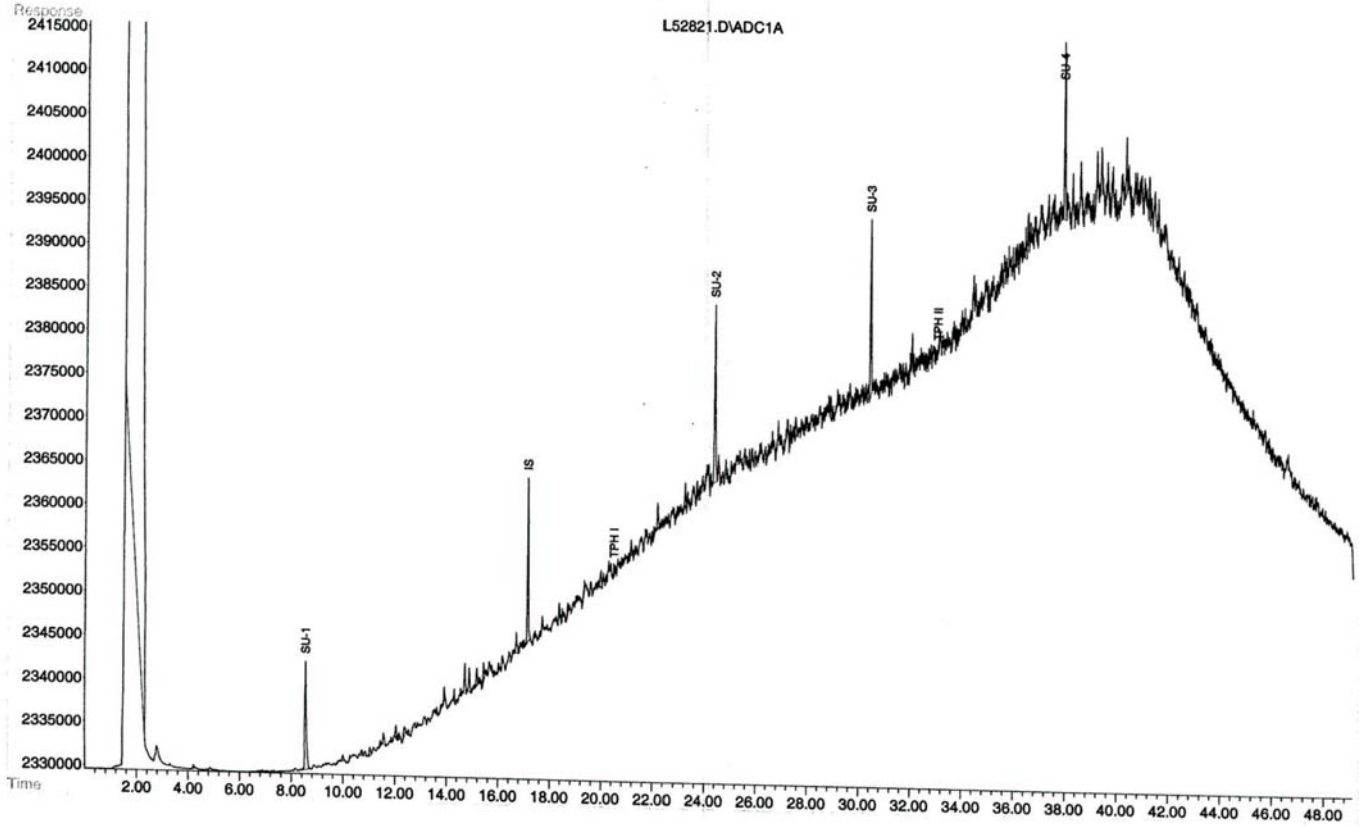

File : C:\HPCHEM\1\DATA\A1400AL\L52822.D
Operator : STS&CRS
Acquired : 11 Feb 2003 18:15 using AcqMethod AL5212N4.M
Instrument : M8 GC-589
Sample Name: GC 185, Dive 4429
Misc Info : A1400
Vial Number: 9

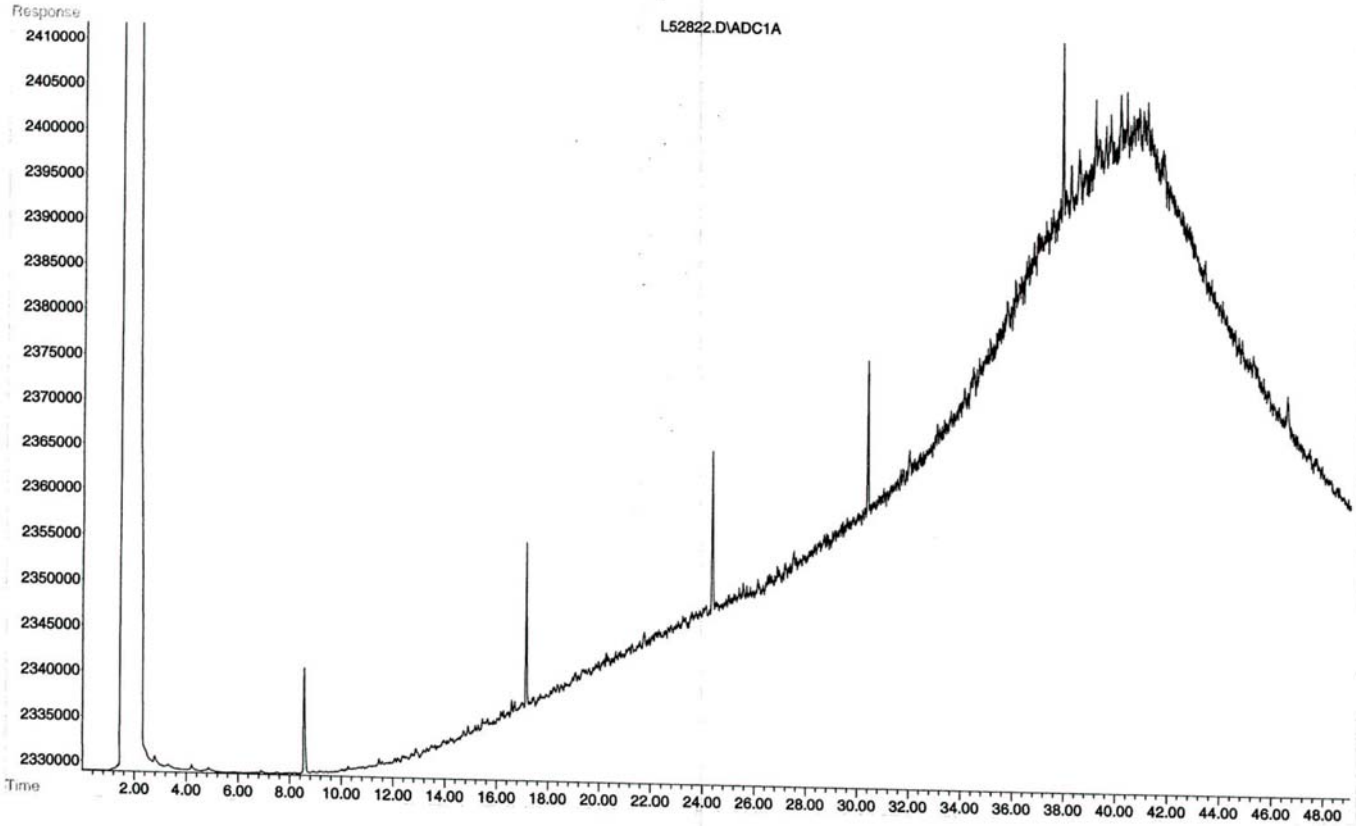

File : C:\HPCHEM\1\DATA\A1400AL\L52823.D
Operator : STS&CRS
Acquired : 11 Feb 2003 19:14 using AcqMethod AL5212N4.M
Instrument : M8 GC-589
Sample Name: GC 234, Dive 4434
Misc Info : A1400
Vial Number: 10

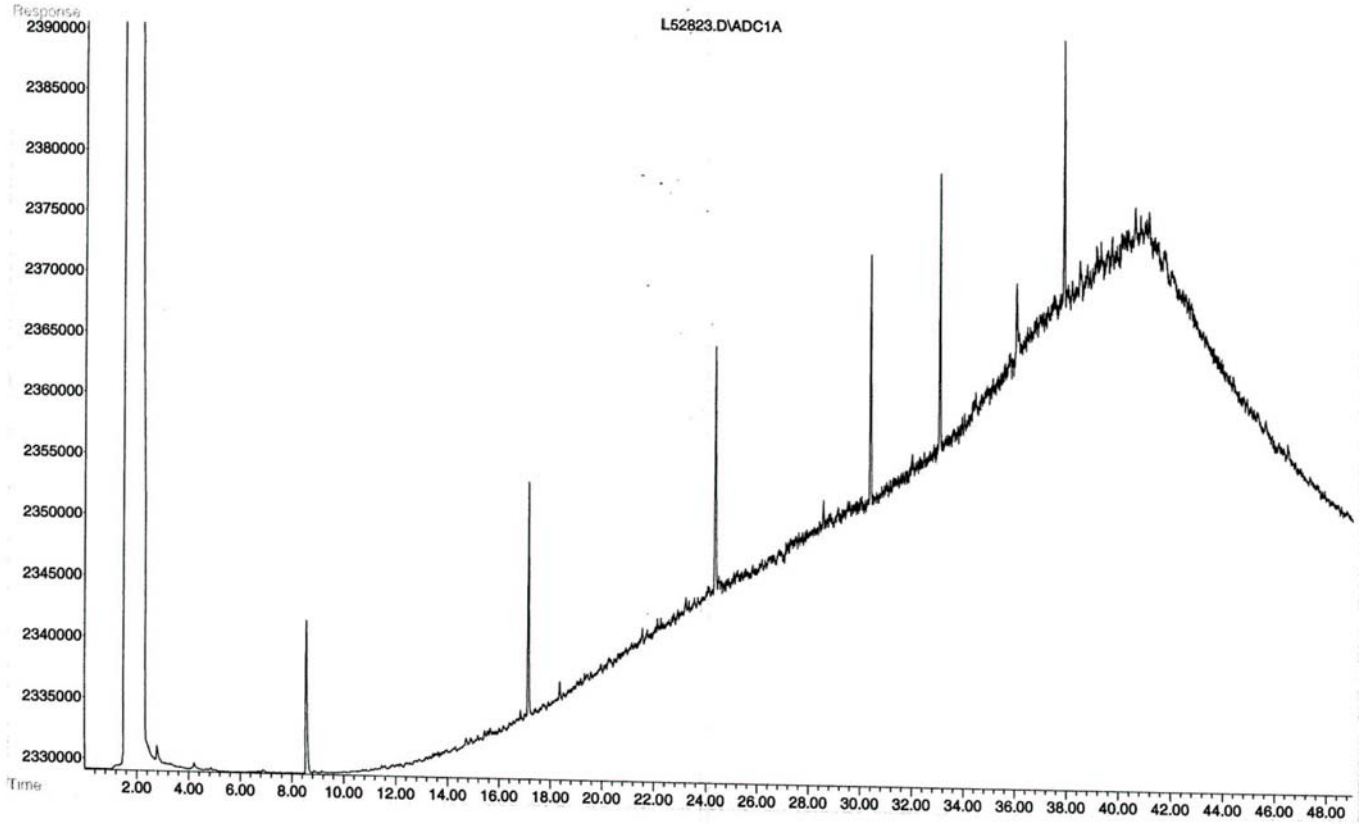

```
File        : C:\HPCHEM\1\DATA\A1400AL\L52824.D
Operator    : STS&CRS
Acquired    : 11 Feb 2003  20:13     using AcqMethod AL5212N4.M
Instrument  :   M8 GC-589
Sample Name: GC 234, Dive 4435
Misc Info   : A1400
Vial Number: 11
```

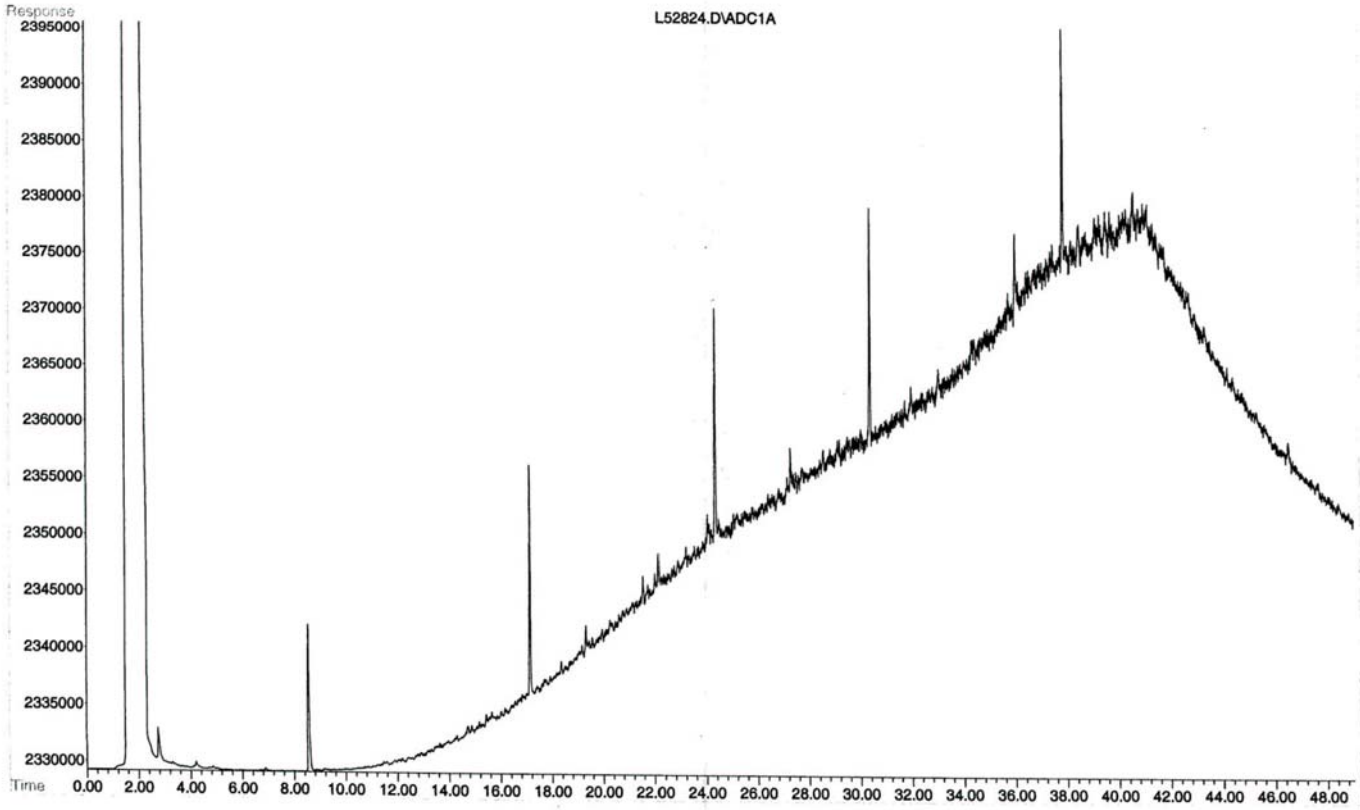

File : C:\HPCHEM\1\DATA\A1400AL\L52825.D
Operator : STS&CRS
Acquired : 11 Feb 2003 21:11 using AcqMethod AL5212N4.M
Instrument : M8 GC-589
Sample Name: GC 234, Dive 4436
Misc Info : A1400
Vial Number: 12

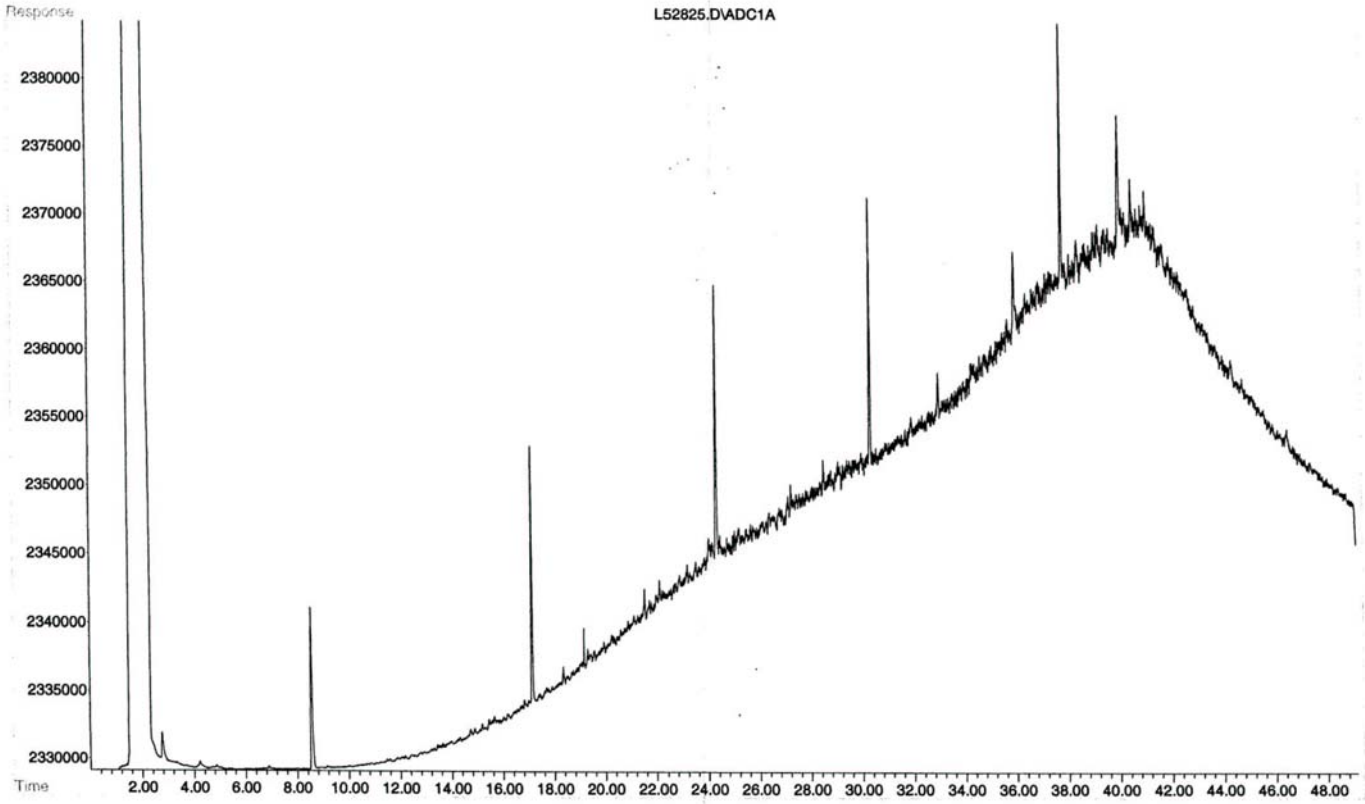

File : C:\HPCHEM\1\DATA\A1400AL\L52826.D
Operator : STS&CRS
Acquired : 11 Feb 2003 22:10 using AcqMethod AL5212N4.M
Instrument : M8 GC-589
Sample Name: GC 232, Dive 4437
Misc Info : A1400
Vial Number: 13

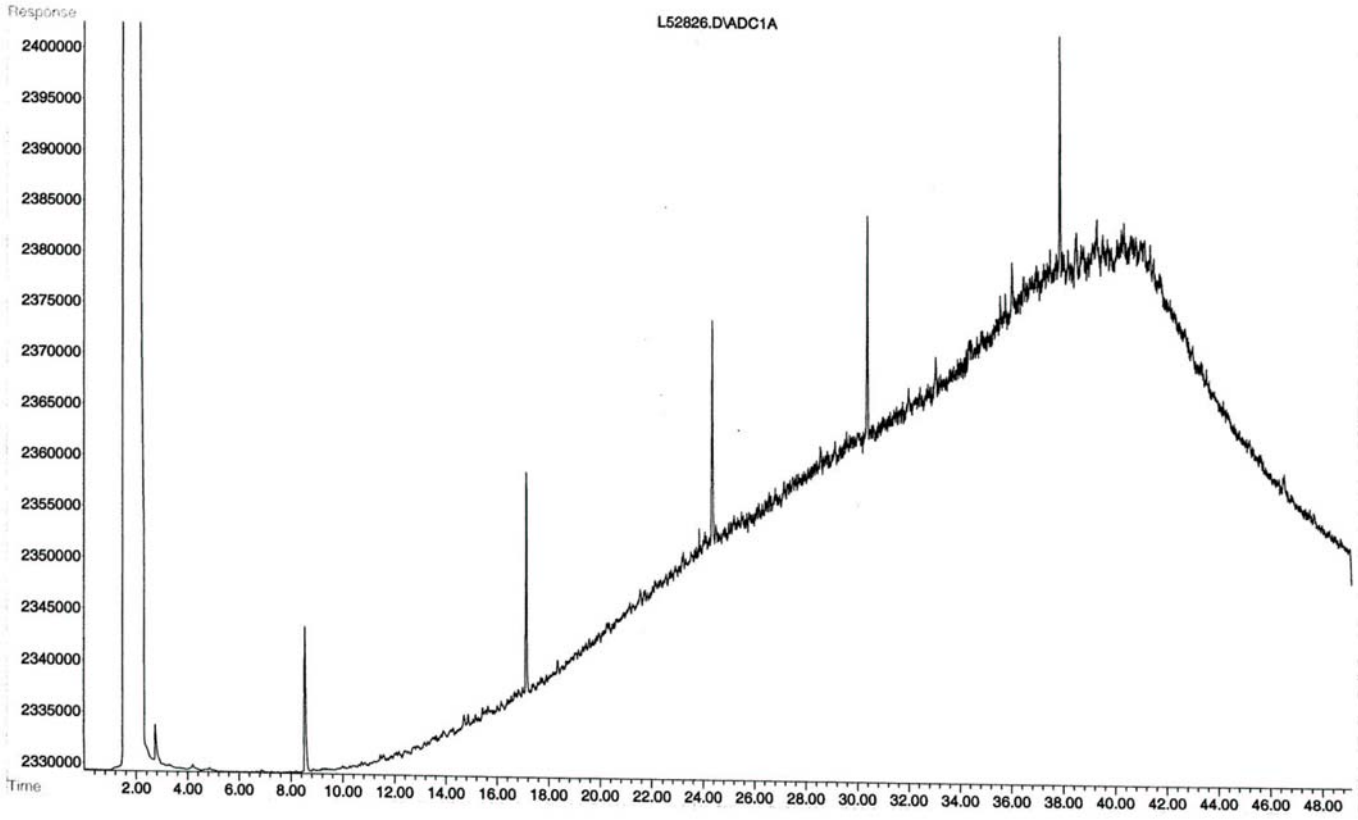

```
File        : C:\HPCHEM\1\DATA\A1400AL\L52827.D
Operator    : STS&CRS
Acquired    : 12 Feb 2003  00:08     using AcqMethod AL5212N4.M
Instrument  :   M8 GC-589
Sample Name: GC 232, Dive 4403
Misc Info   : A1400
Vial Number: 15
```

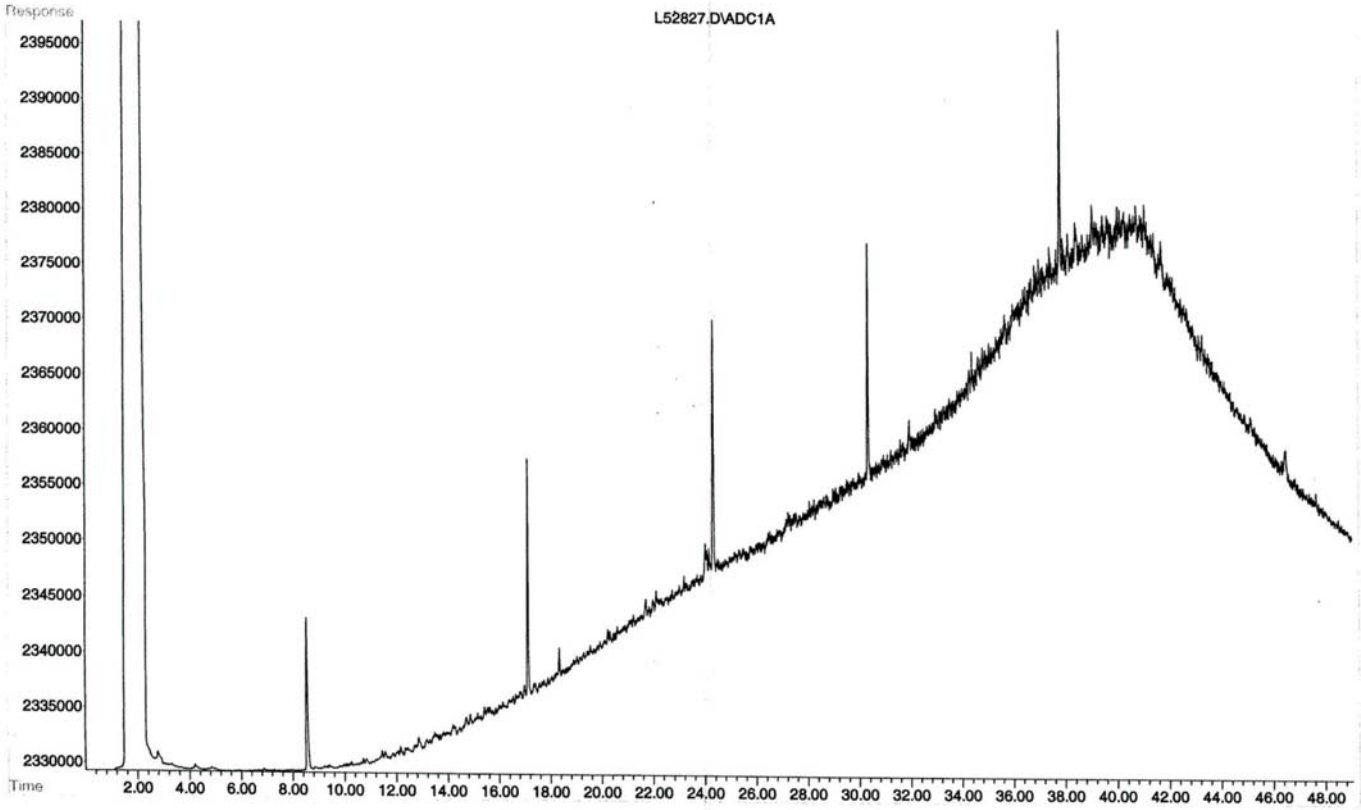

File : C:\HPCHEM\1\DATA\A1400AL\L52828.D
Operator : STS&CRS
Acquired : 12 Feb 2003 1:07 using AcqMethod AL5212N4.M
Instrument : M8 GC-589
Sample Name: MC 709, Dive 4412
Misc Info : A1400
Vial Number: 16

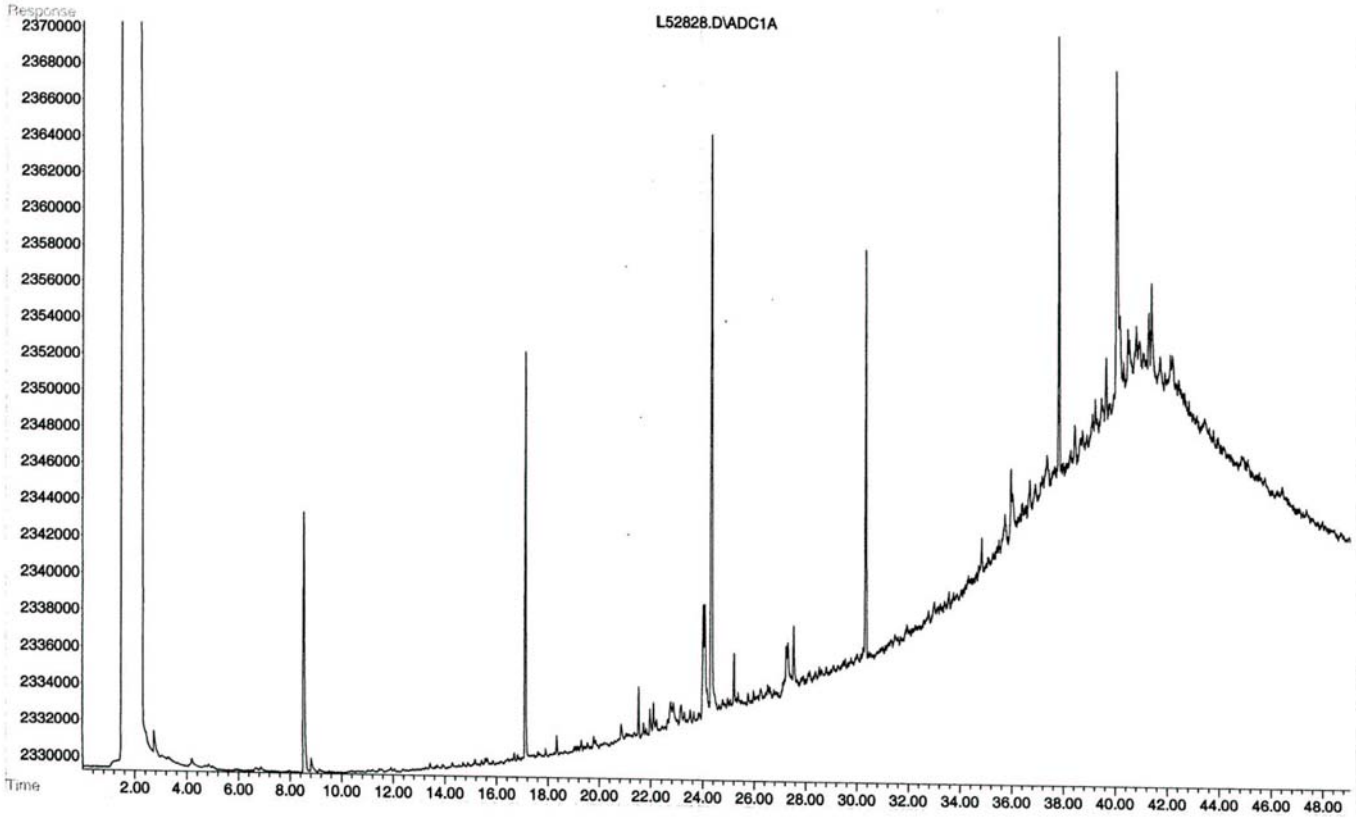

File : C:\HPCHEM\1\DATA\A1400AL\L52829.D
Operator : STS&CRS
Acquired : 12 Feb 2003 2:06 using AcqMethod AL5212N4.M
Instrument : M8 GC-589
Sample Name: MC 118, Dive 4414
Misc Info : A1400
Vial Number: 17

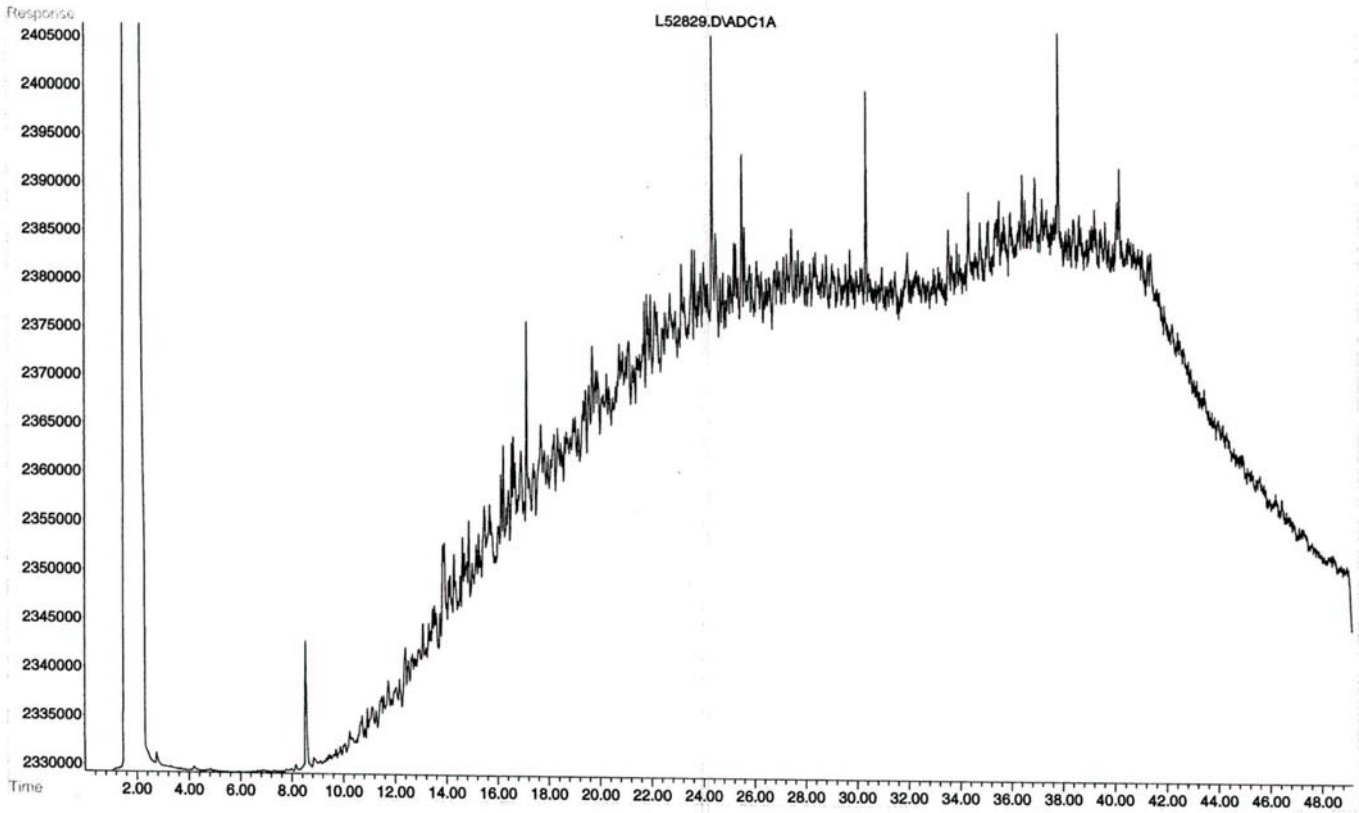

File : C:\HPCHEM\1\DATA\A1400AL\L52831.D
Operator : STS&CRS
Acquired : 12 Feb 2003 4:03 using AcqMethod AL5212N4.M
Instrument : M8 GC-589
Sample Name: GC 232 4401 Core 3 Top
Misc Info : A1400
Vial Number: 19

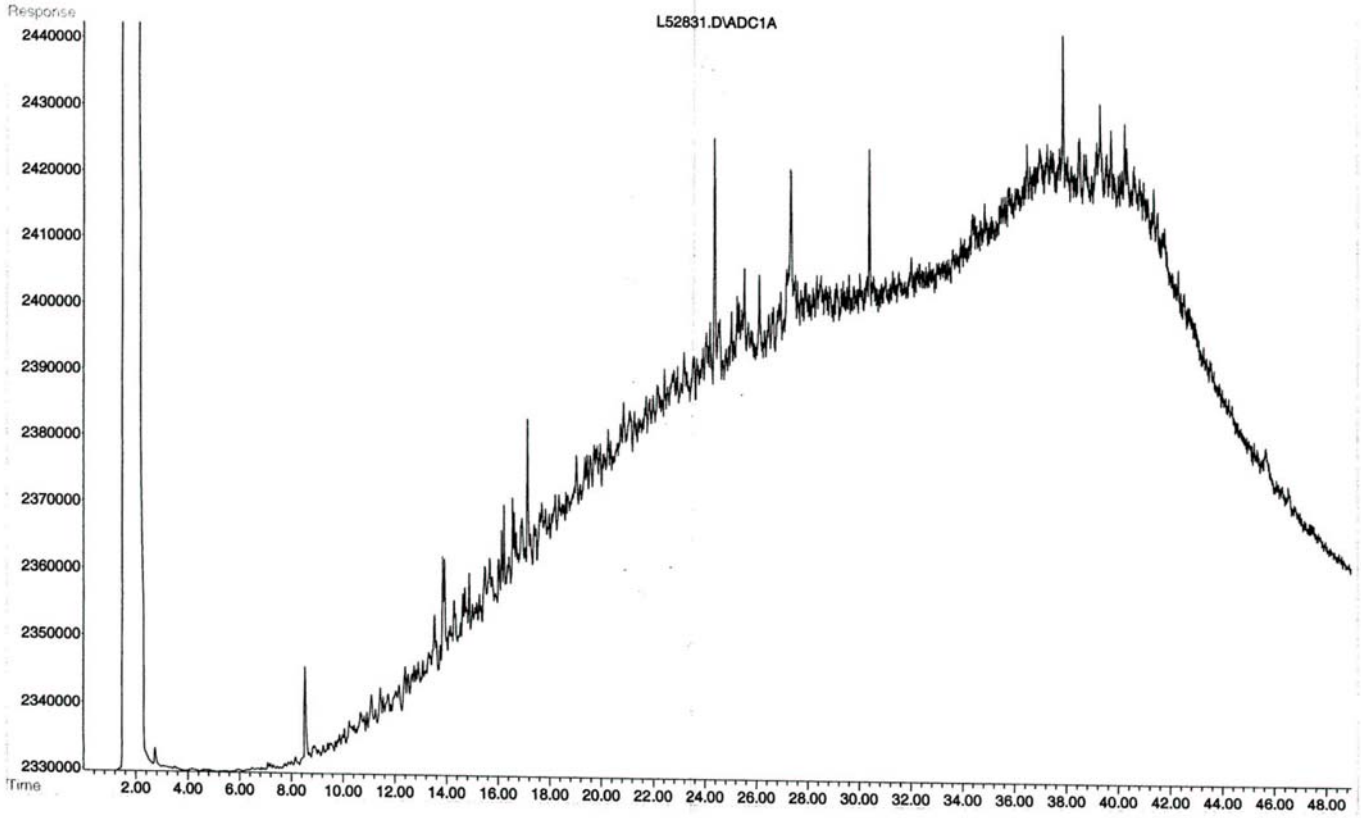

File : C:\HPCHEM\1\DATA\A1400AL\L52832.D
Operator : STS&CRS
Acquired : 12 Feb 2003 5:02 using AcqMethod AL5212N4.M
Instrument : M8 GC-589
Sample Name: GC 232 4401 Core 3 Bottom
Misc Info : A1400
Vial Number: 20

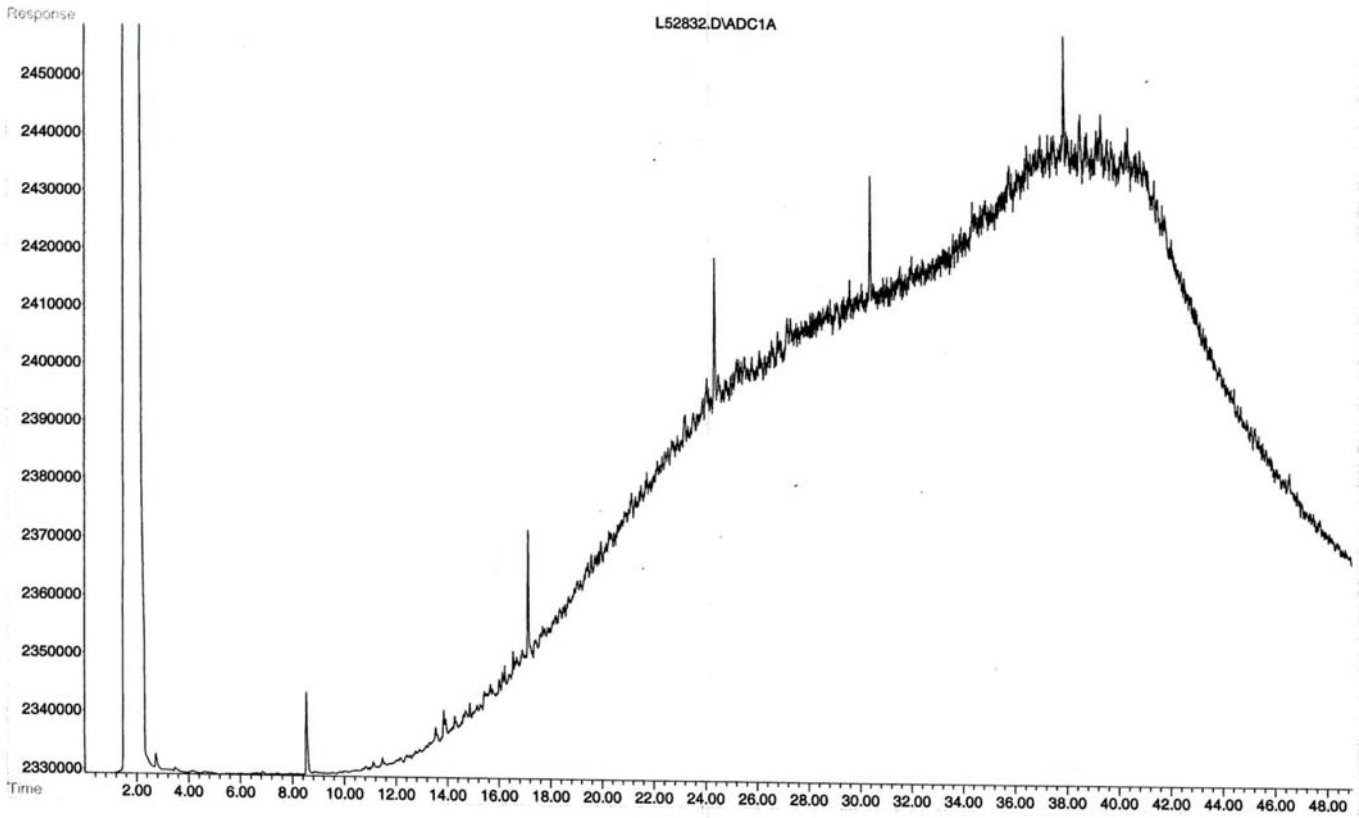

File : C:\HPCHEM\1\DATA\A1400AL\L52833.D
Operator : STS&CRS
Acquired : 12 Feb 2003 6:01 using AcqMethod AL5212N4.M
Instrument : M8 GC-589
Sample Name: GC 232 4401 Core 5 Top
Misc Info : A1400
Vial Number: 21

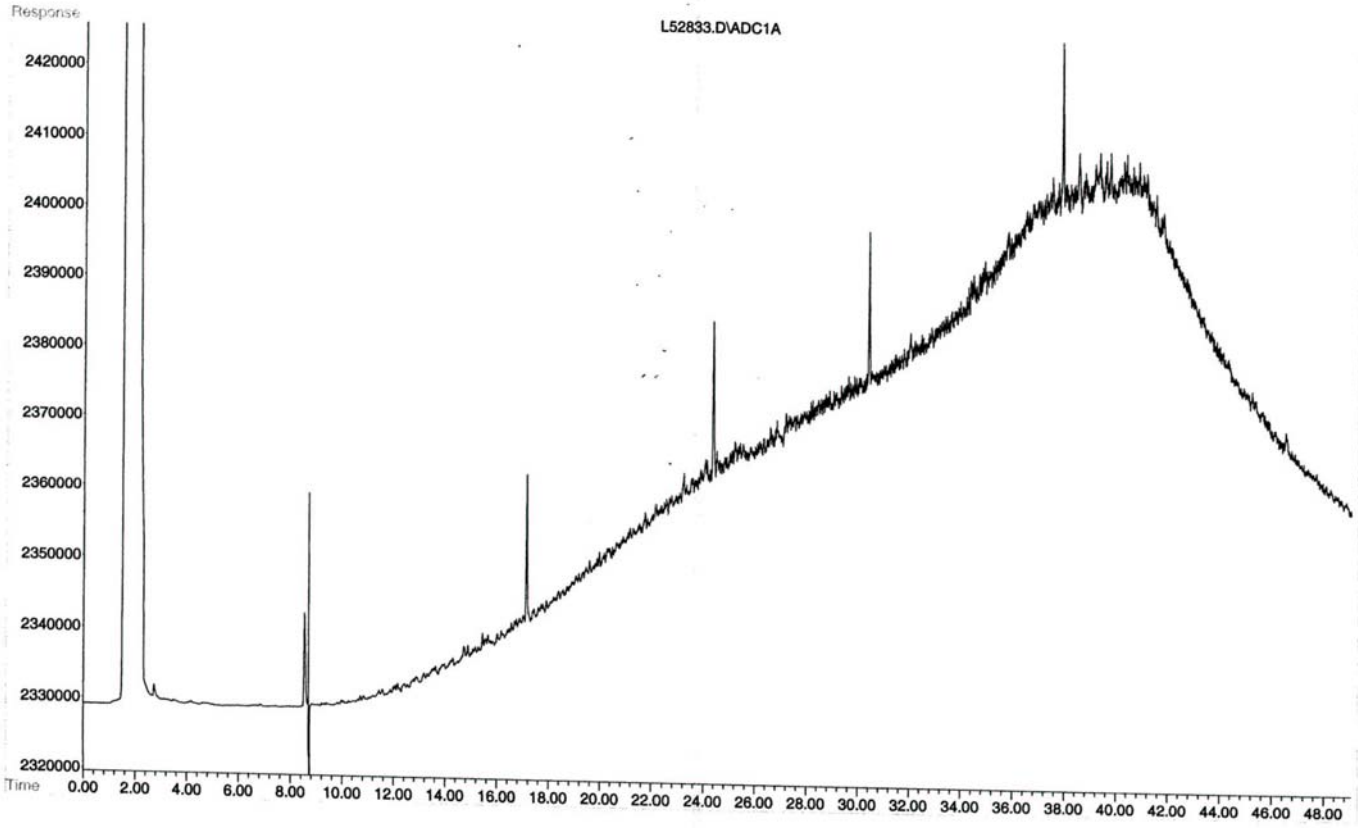

File : C:\HPCHEM\1\DATA\A1400AL\L52834.D
Operator : STS&CRS
Acquired : 12 Feb 2003 7:00 using AcqMethod AL5212N4.M
Instrument : M8 GC-589
Sample Name: GC 232 4401 Core 5 Middle
Misc Info : A1400
Vial Number: 22

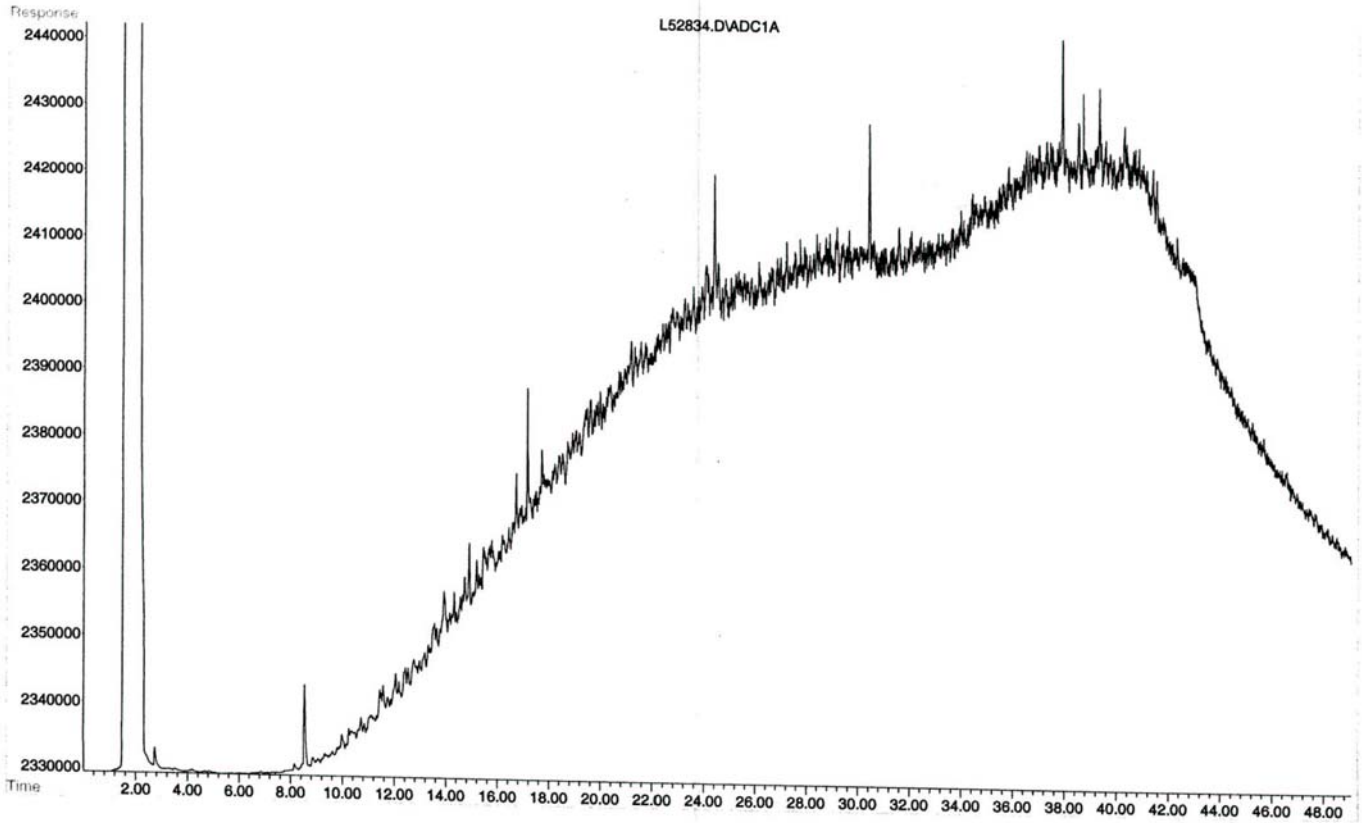

File : C:\HPCHEM\1\DATA\A1400AL\L52835.D
Operator : STS&CRS
Acquired : 12 Feb 2003 7:59 using AcqMethod AL5212N4.M
Instrument : M8 GC-589
Sample Name: GC 232 4401 Core 5 Bottom
Misc Info : A1400
Vial Number: 23

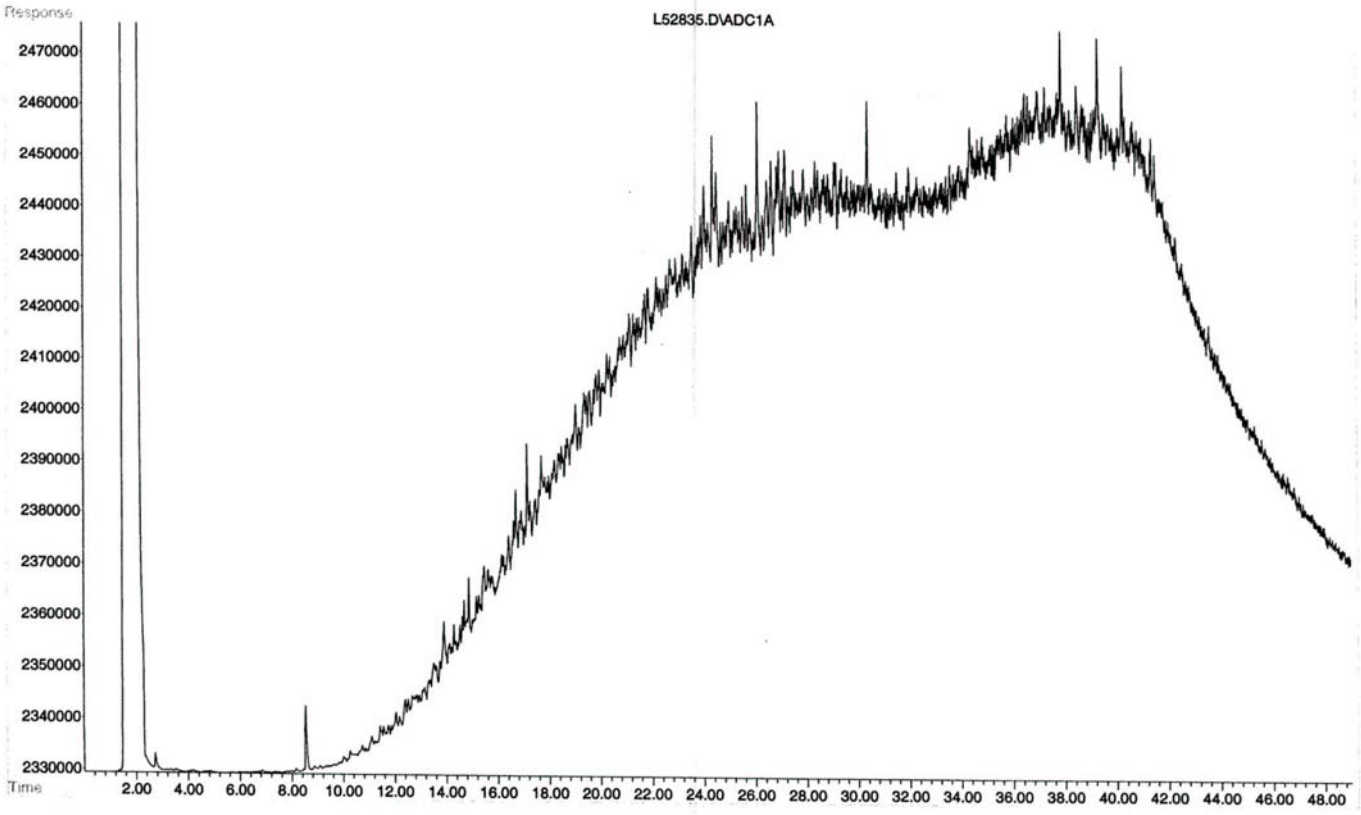

File : C:\HPCHEM\1\DATA\A1400AL\L52836.D
Operator : STS&CRS
Acquired : 12 Feb 2003 9:57 using AcqMethod AL5212N4.M
Instrument : M8 GC-589
Sample Name: GC 232 4401 Core 6 Top
Misc Info : A1400
Vial Number: 25

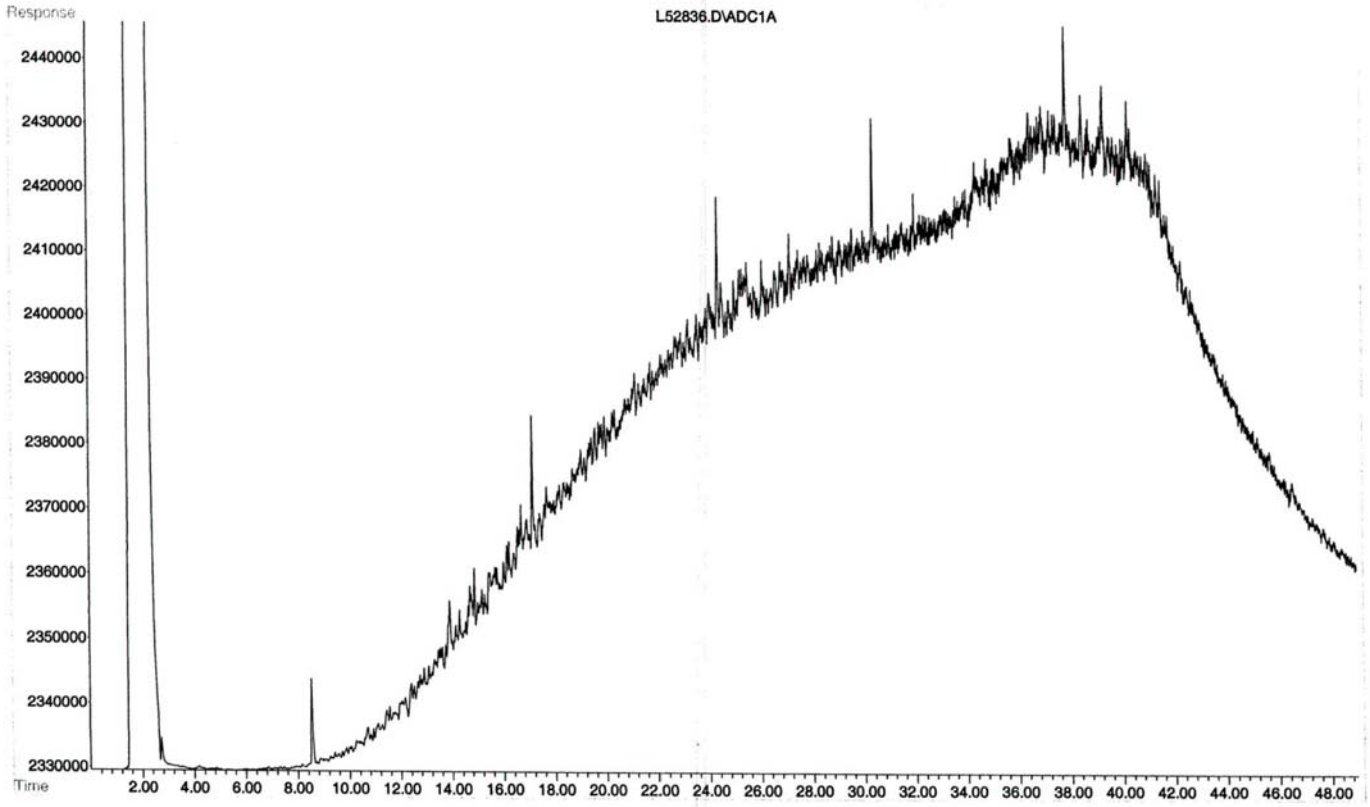

File : C:\HPCHEM\1\DATA\A1400AL\L52837.D
Operator : STS&CRS
Acquired : 12 Feb 2003 10:55 using AcqMethod AL5212N4.M
Instrument : M8 GC-589
Sample Name: GC 232 4401 Core 4 Small
Misc Info : A1400
Vial Number: 26

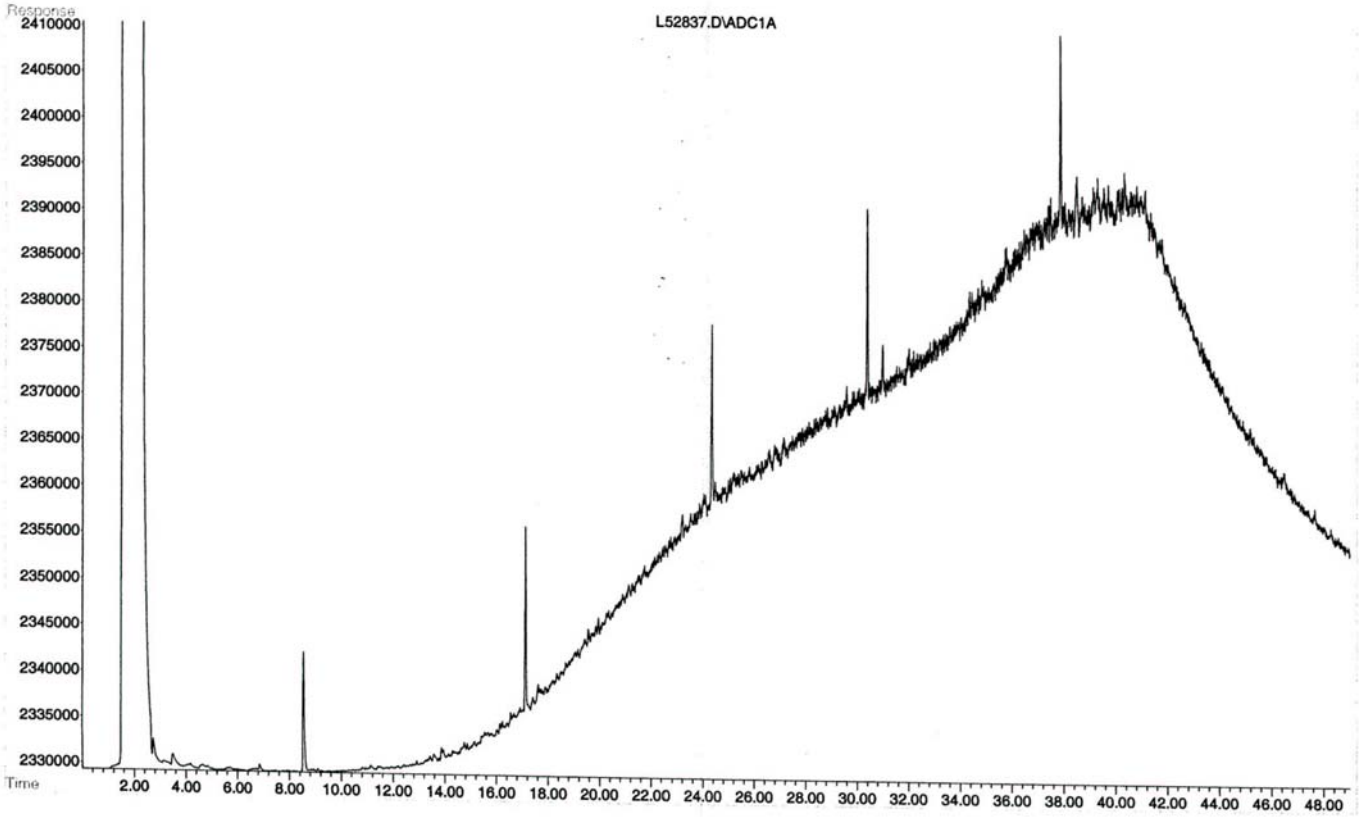

File : C:\HPCHEM\1\DATA\B1402AL\L52838.D
Operator : STS&CRS
Acquired : 18 Feb 2003 22:09 using AcqMethod AL5212N4.M
Instrument : M8 GC-589
Sample Name: GC 232 4403 Core 1
Misc Info : A1401
Vial Number: 12

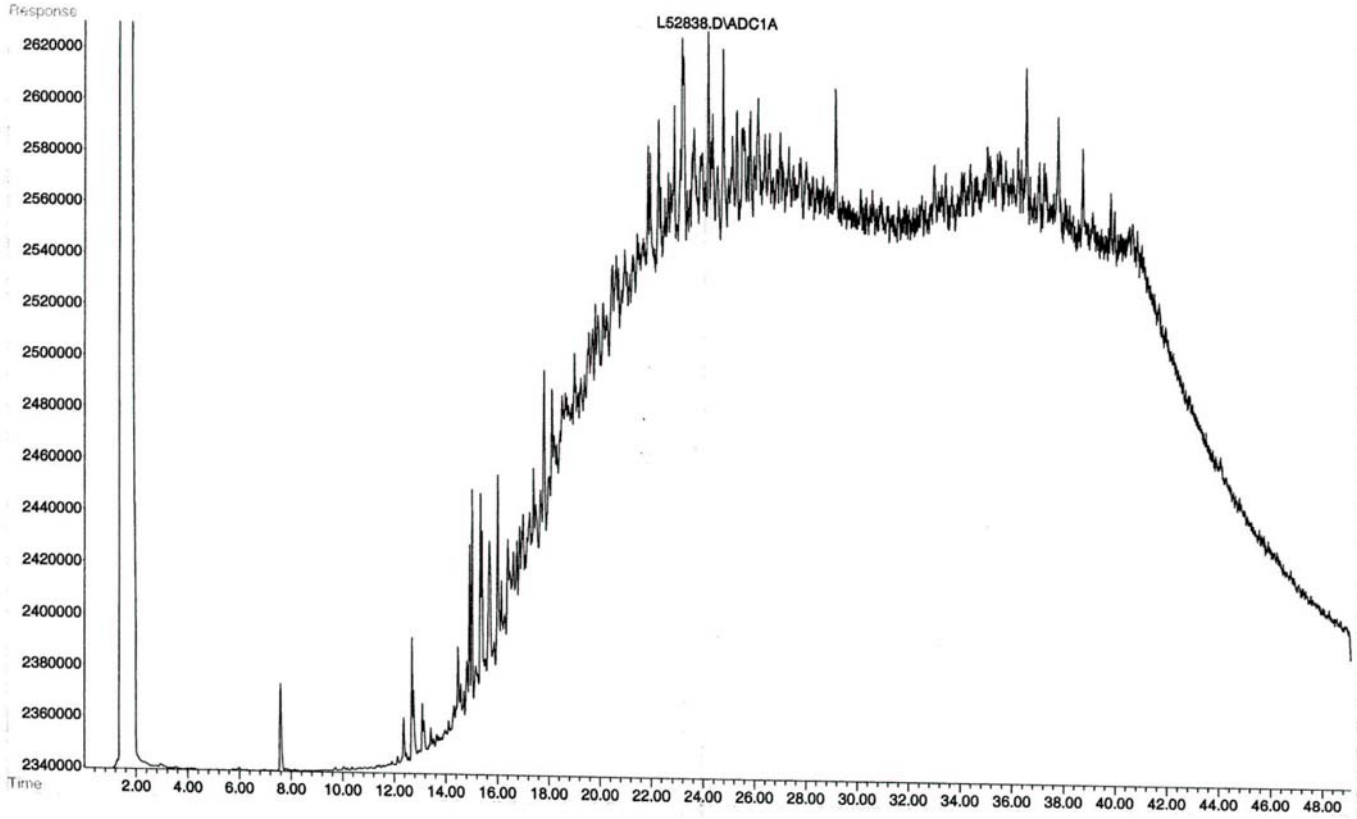

File : C:\HPCHEM\1\DATA\A1401AL\L52839.D
Operator : STS&CRS
Acquired : 15 Feb 2003 16:18 using AcqMethod AL5212N4.M
Instrument : M8 GC-589
Sample Name: GC 232 4403 Core 2
Misc Info : A1401
Vial Number: 8

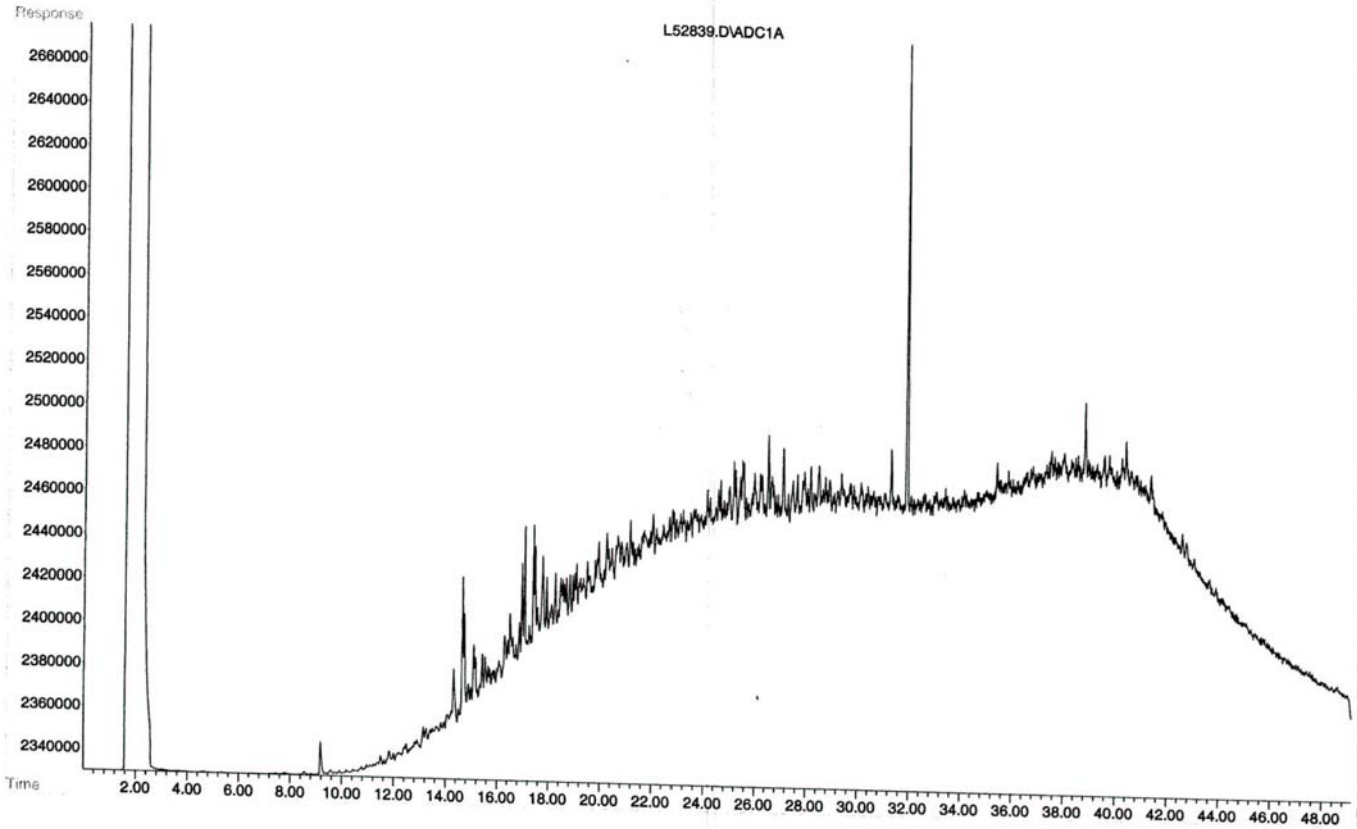

File : C:\HPCHEM\1\DATA\A1401AL\L52840.D
Operator : STS&CRS
Acquired : 15 Feb 2003 17:17 using AcqMethod AL5212N4.M
Instrument : M8 GC-589
Sample Name: GC 232 4403 Core 3 Top
Misc Info : A1401
Vial Number: 9

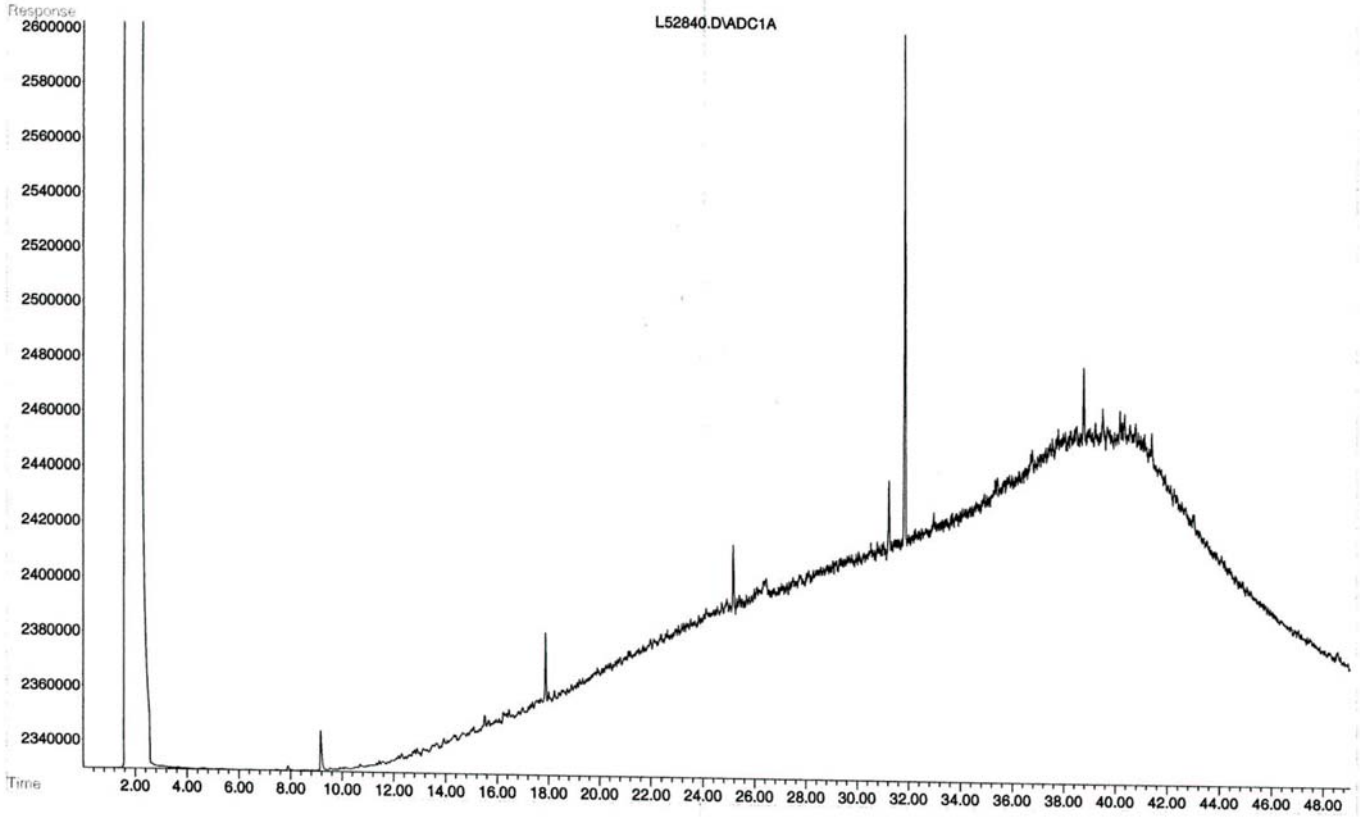

File : C:\HPCHEM\1\DATA\A1401AL\L52841.D
Operator : STS&CRS
Acquired : 15 Feb 2003 18:15 using AcqMethod AL5212N4.M
Instrument : M8 GC-589
Sample Name: GC 232 4403 Core 5 Top
Misc Info : A1401
Vial Number: 10

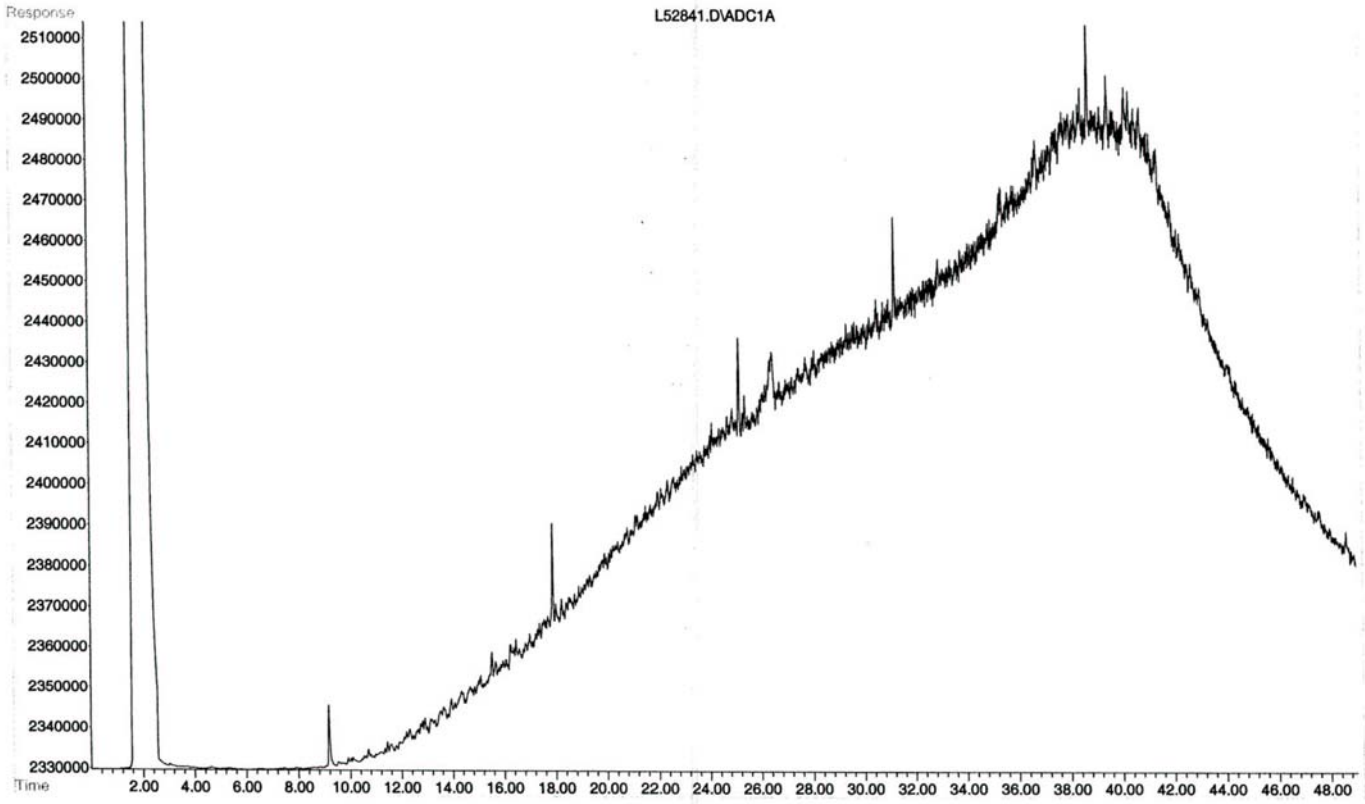

File : C:\HPCHEM\1\DATA\A1401AL\L52842.D
Operator : STS&CRS
Acquired : 15 Feb 2003 19:14 using AcqMethod AL5212N4.M
Instrument : M8 GC-589
Sample Name: GC 232 4401 Core 6 Bottom
Misc Info : A1401
Vial Number: 11

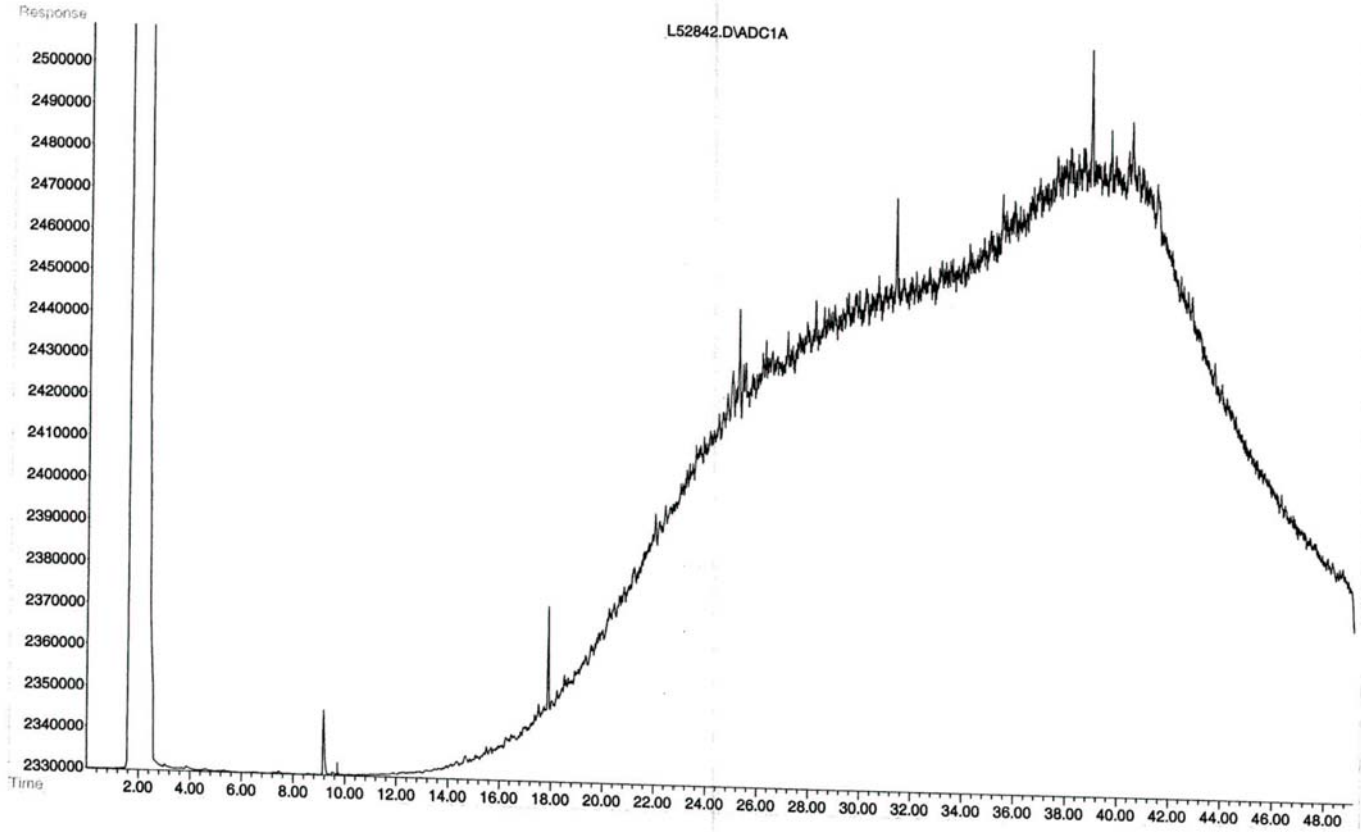

File : C:\HPCHEM\1\DATA\A1401AL\L52843.D
Operator : STS&CRS
Acquired : 15 Feb 2003 20:13 using AcqMethod AL5212N4.M
Instrument : M8 GC-589
Sample Name: GC 232 4403 Core 5 Bottom
Misc Info : A1401
Vial Number: 12

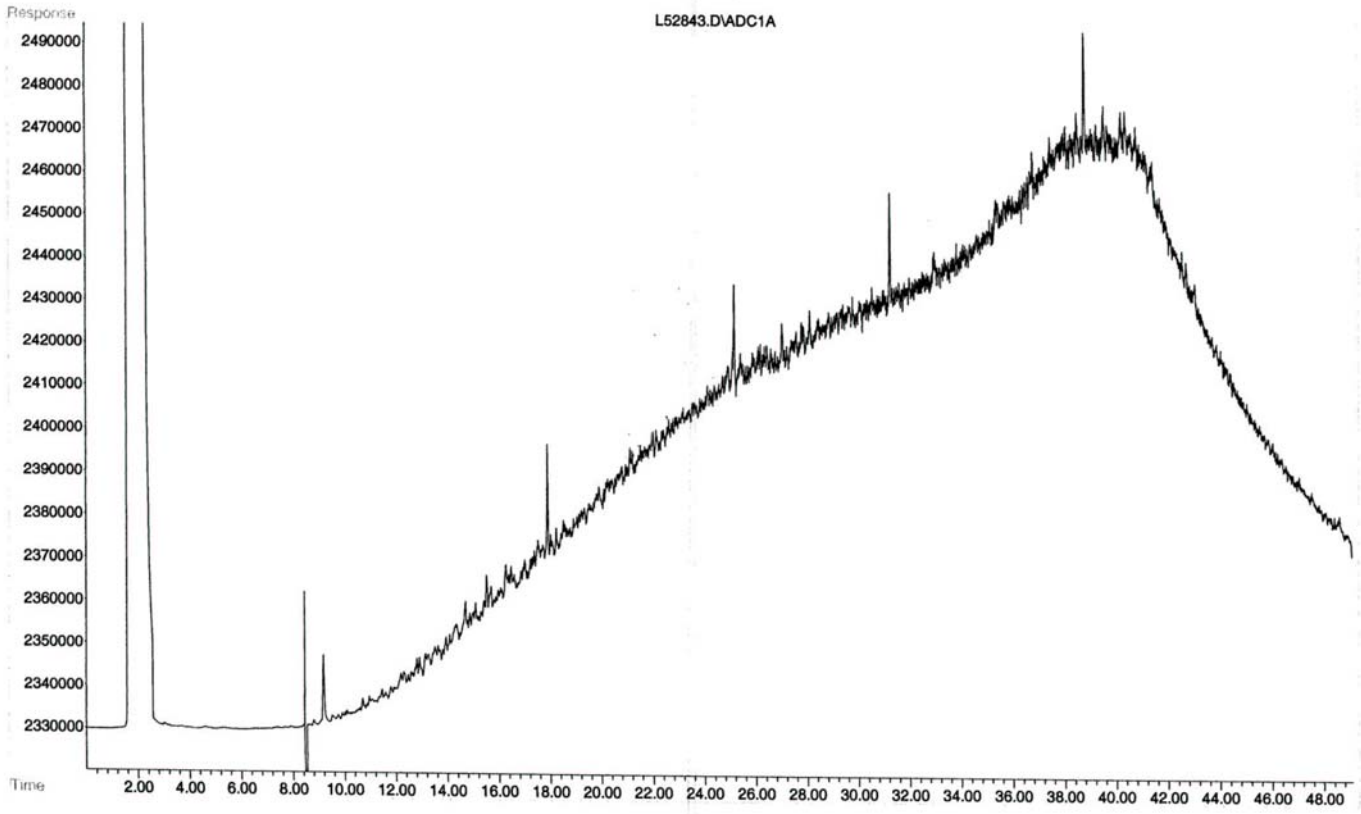

File : C:\HPCHEM\1\DATA\A1401AL\L52844.D
Operator : STS&CRS
Acquired : 15 Feb 2003 21:11 using AcqMethod AL5212N4.M
Instrument : M8 GC-589
Sample Name: GC 232 4404 Gas Hydrate
Misc Info : A1401
Vial Number: 13

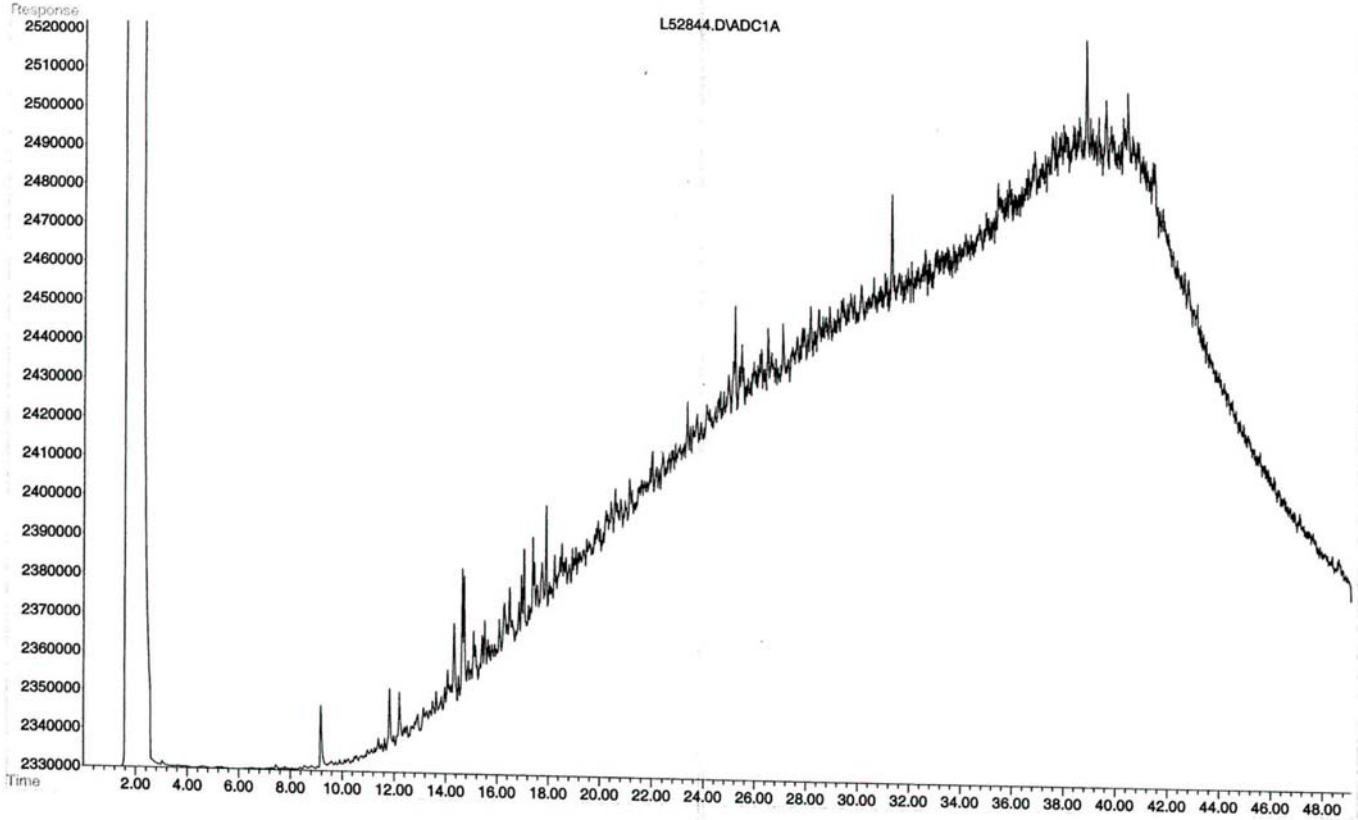

File : C:\HPCHEM\1\DATA\B1402AL\L52845.D
Operator : STS&CRS
Acquired : 18 Feb 2003 23:08 using AcqMethod AL5212N4.M
Instrument : M8 GC-589
Sample Name: GC 232 4404 Core 1 Top
Misc Info : A1401
Vial Number: 13

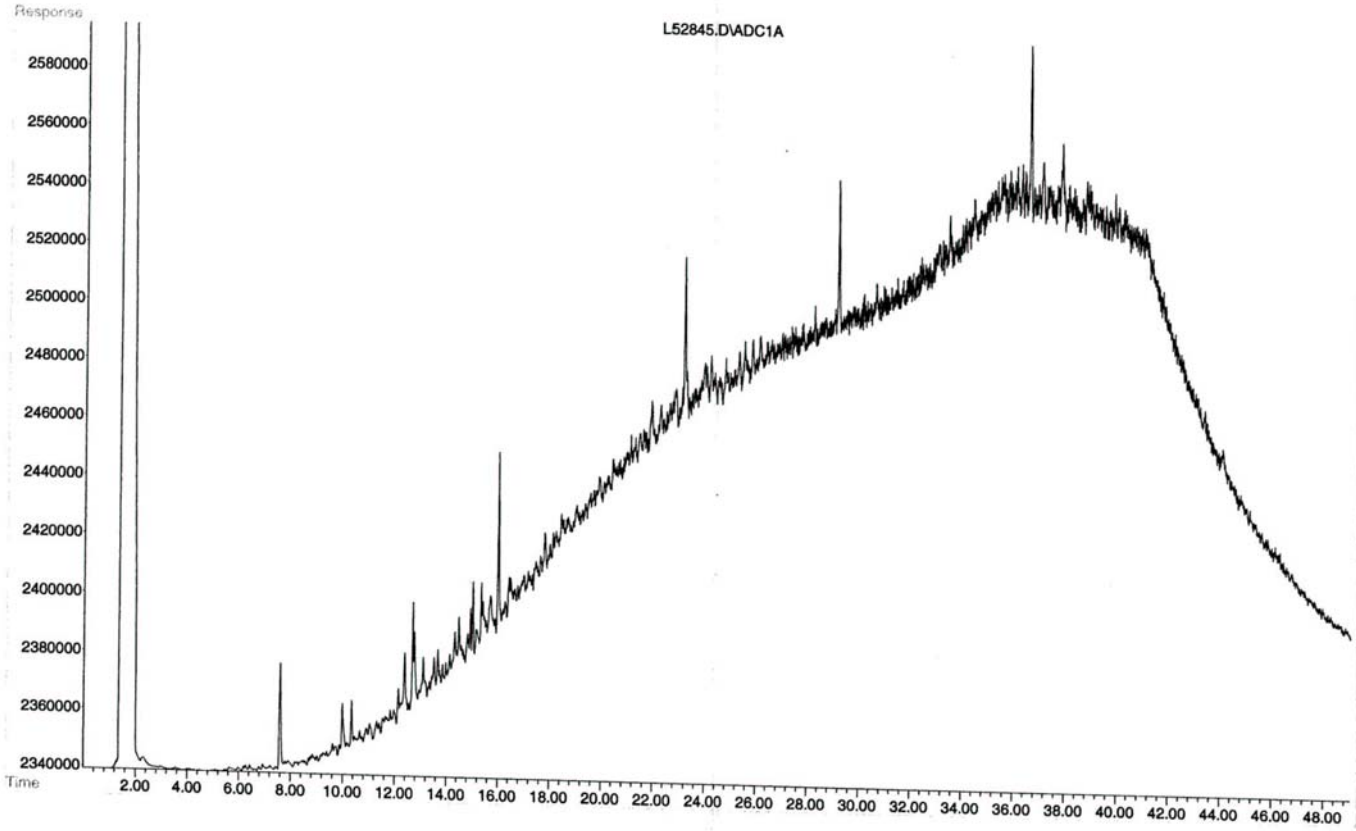

File : C:\HPCHEM\1\DATA\A1401AL\L52846.D
Operator : STS&CRS
Acquired : 16 Feb 2003 00:07 using AcqMethod AL5212N4.M
Instrument : M8 GC-589
Sample Name: GC 232 4404 Core 1 Bottom
Misc Info : A1401
Vial Number: 16

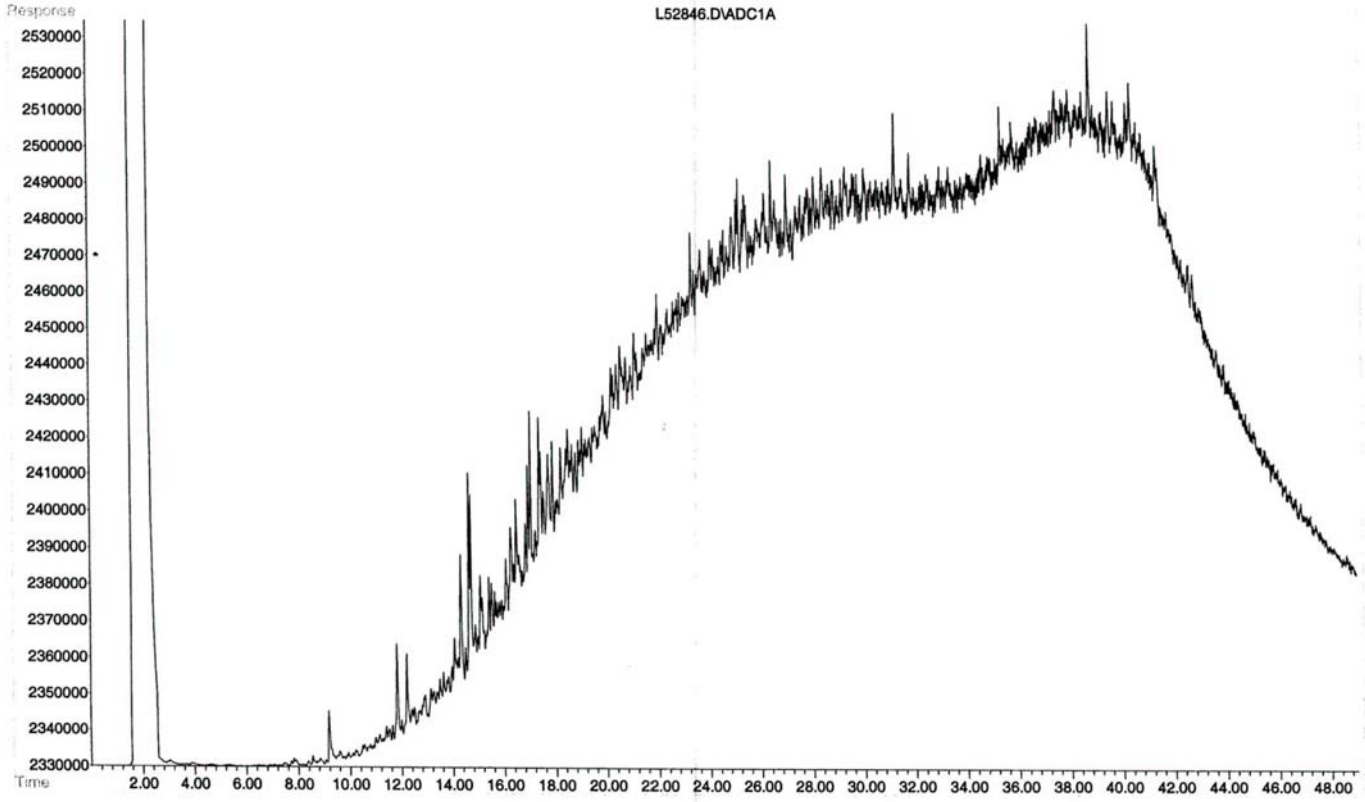

File : C:\HPCHEM\1\DATA\A1401AL\L52847.D
Operator : STS&CRS
Acquired : 16 Feb 2003 1:06 using AcqMethod AL5212N4.M
Instrument : M8 GC-589
Sample Name: GC 234 4406 Gas Hydrate
Misc Info : A1401
Vial Number: 17

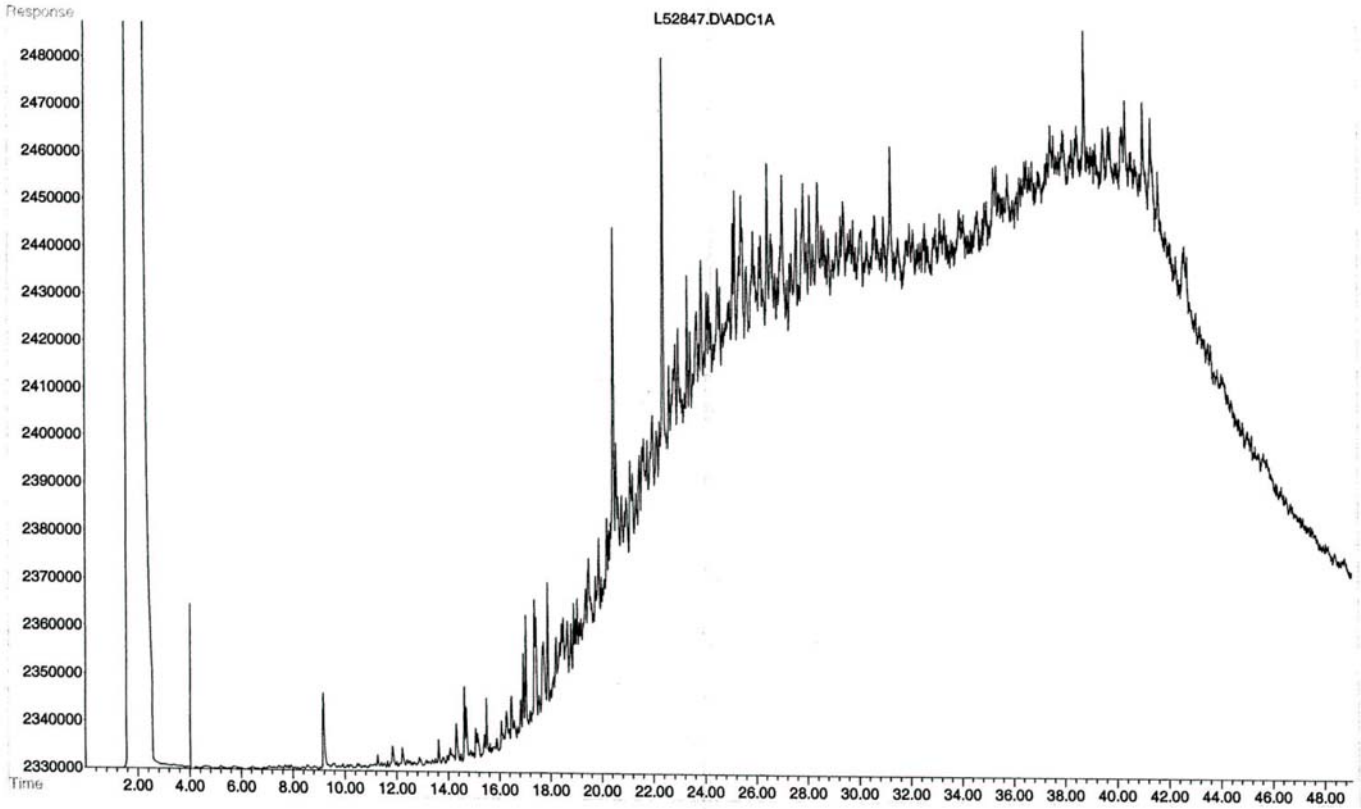

File : C:\HPCHEM\1\DATA\B1402AL\L52848.D
Operator : STS&CRS
Acquired : 19 Feb 2003 00:07 using AcqMethod AL5212N4.M
Instrument : M8 GC-589
Sample Name: GC 234 4407 Core 2 Bottom
Misc Info : A1401
Vial Number: 14

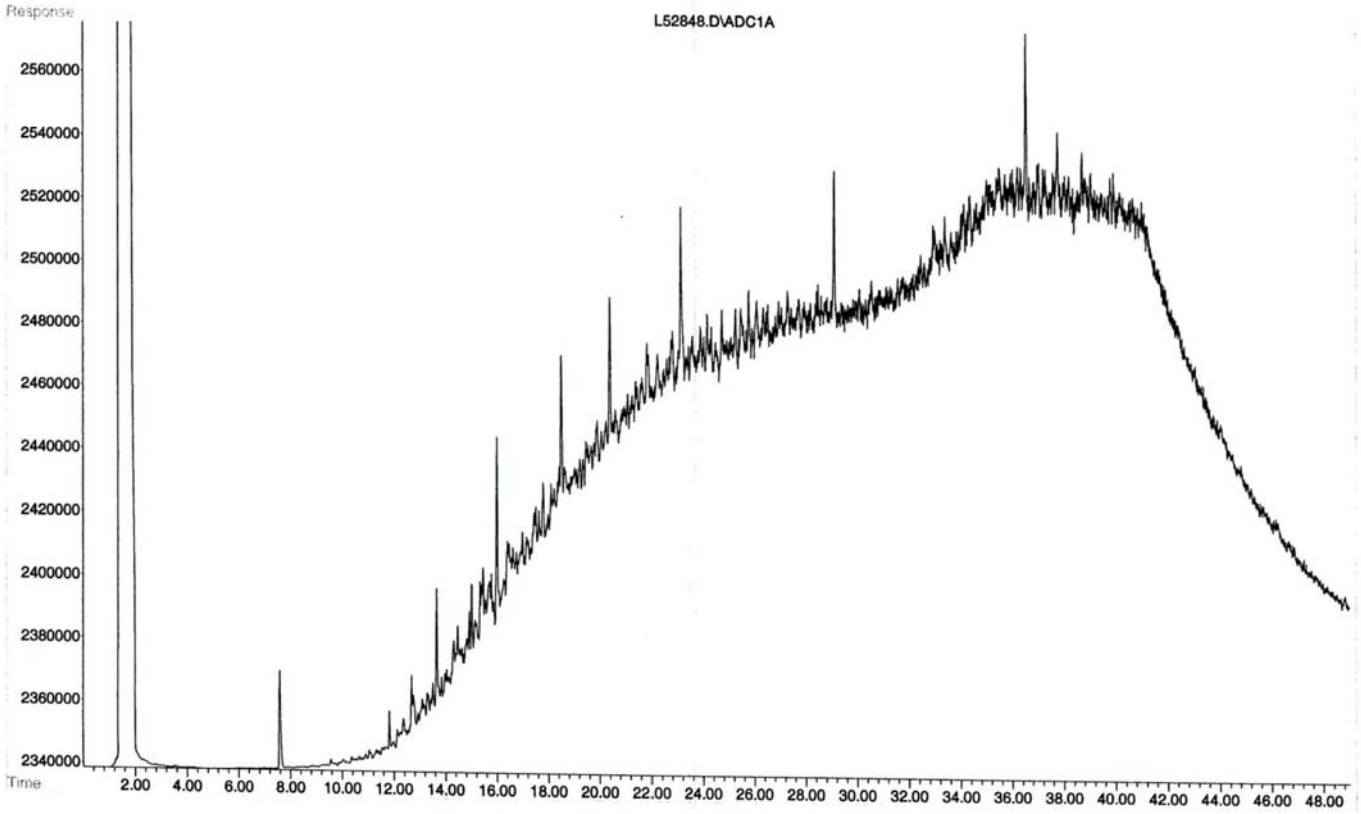

File : C:\HPCHEM\1\DATA\A1401AL\L52849.D
Operator : STS&CRS
Acquired : 16 Feb 2003 3:03 using AcqMethod AL5212N4.M
Instrument : M8 GC-589
Sample Name: MC 885 4409 Core 1
Misc Info : A1401
Vial Number: 19

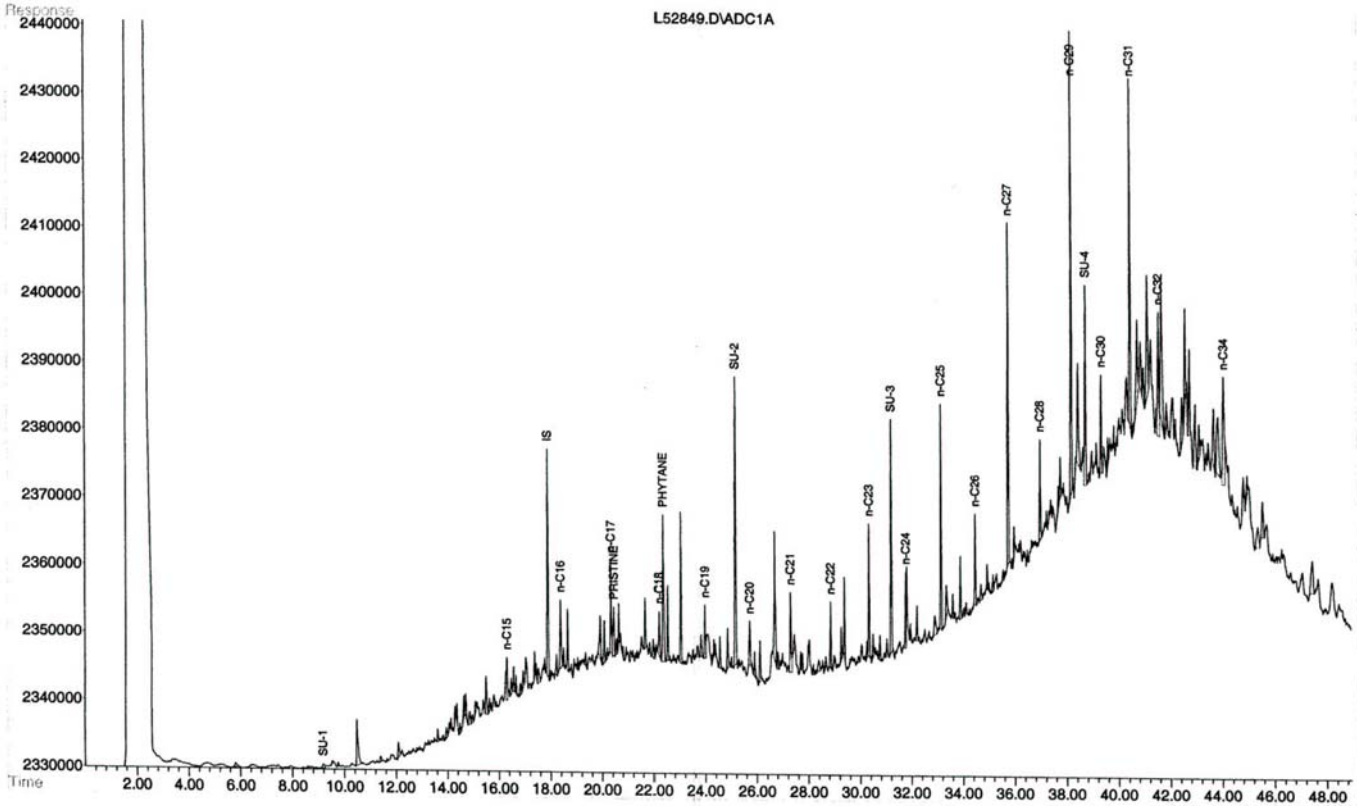

File : C:\HPCHEM\1\DATA\B1402AL\L52851.D
Operator : STS&CRS
Acquired : 18 Feb 2003 14:17 using AcqMethod AL5212N4.M
Instrument : M8 GC-589
Sample Name: MC 709 4412 Core 1 Top
Misc Info : A1402
Vial Number: 4

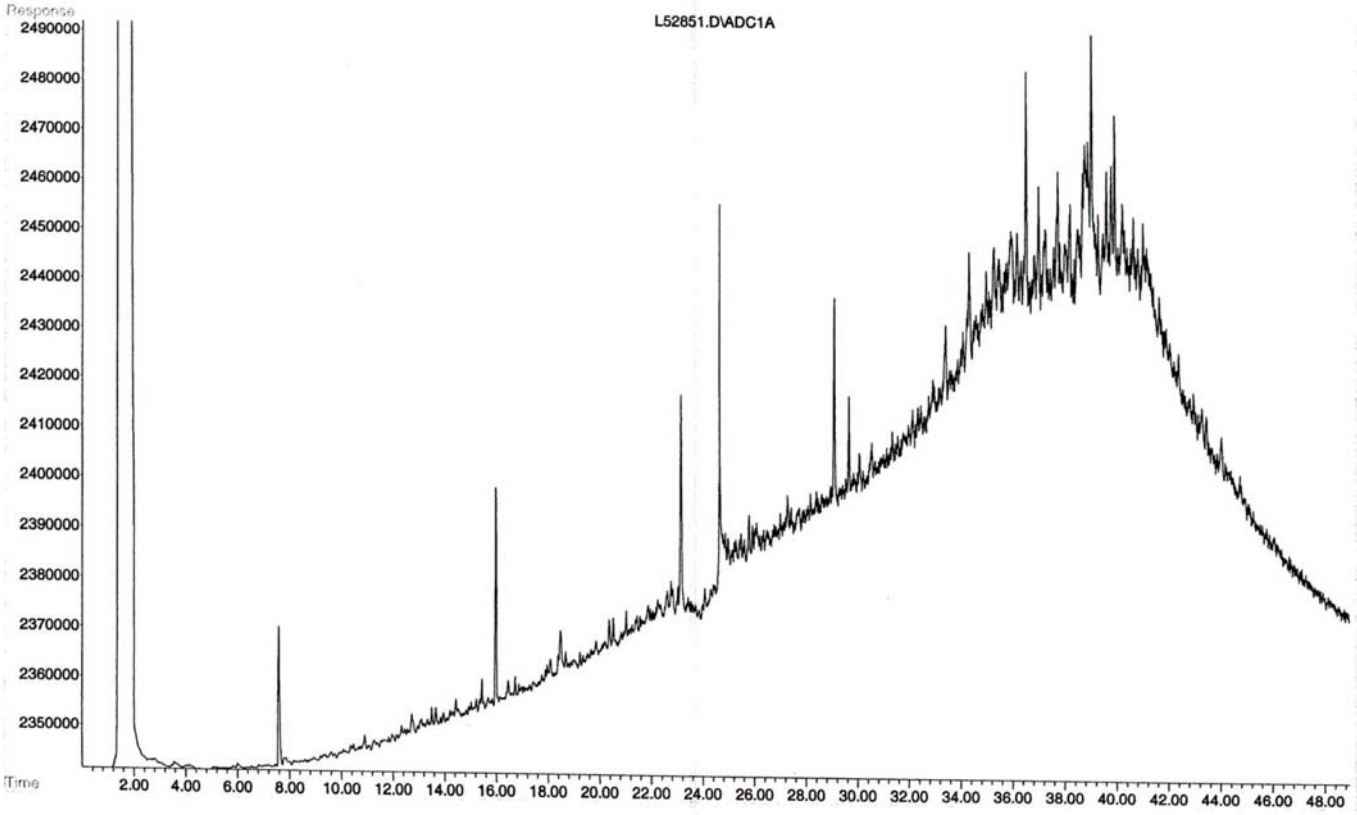

File : C:\HPCHEM\1\DATA\A1401AL\L52850.D
Operator : STS&CRS
Acquired : 16 Feb 2003 4:02 using AcqMethod AL5212N4.M
Instrument : M8 GC-589
Sample Name: VK 826 4410 Core 1
Misc Info : A1401
Vial Number: 20

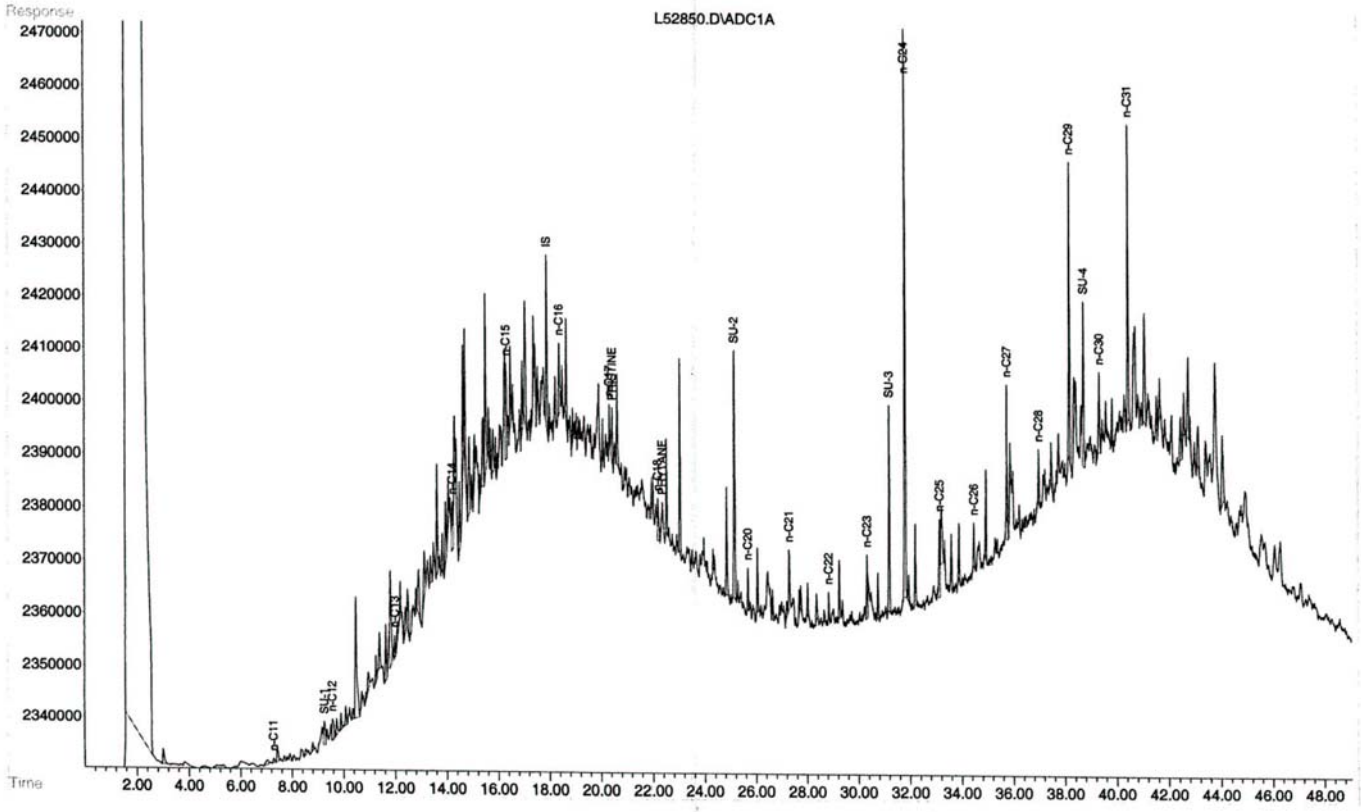

File : C:\HPCHEM\1\DATA\A1401AL\L52852.D
Operator : STS&CRS
Acquired : 16 Feb 2003 5:01 using AcqMethod AL5212N4.M
Instrument : M8 GC-589
Sample Name: MC 709 4412 Core 1 Bottom
Misc Info : A1401
Vial Number: 21

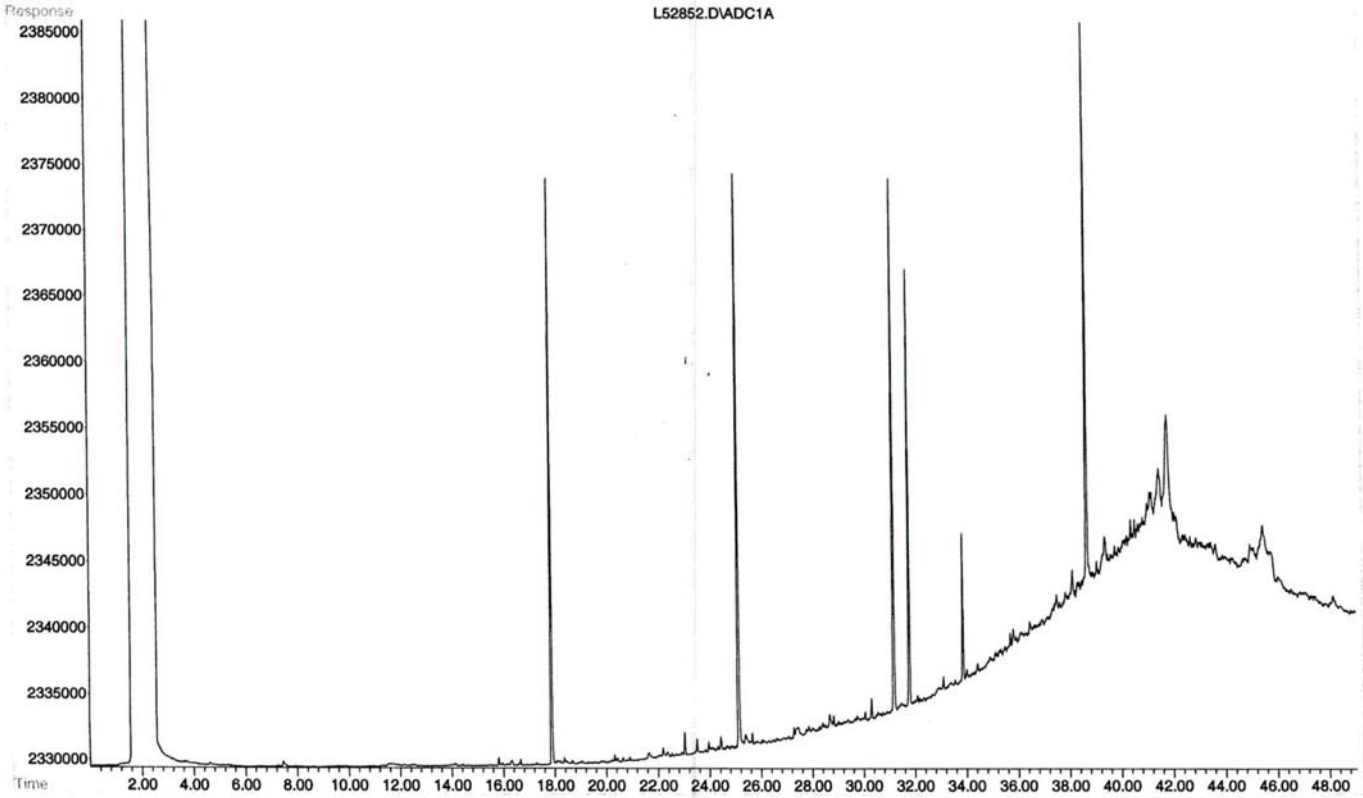

File : C:\HPCHEM\1\DATA\A1401AL\L52853.D
Operator : STS&CRS
Acquired : 16 Feb 2003 5:59 using AcqMethod AL5212N4.M
Instrument : M8 GC-589
Sample Name: MC 709 4413 Core 4 Top
Misc Info : A1401
Vial Number: 22

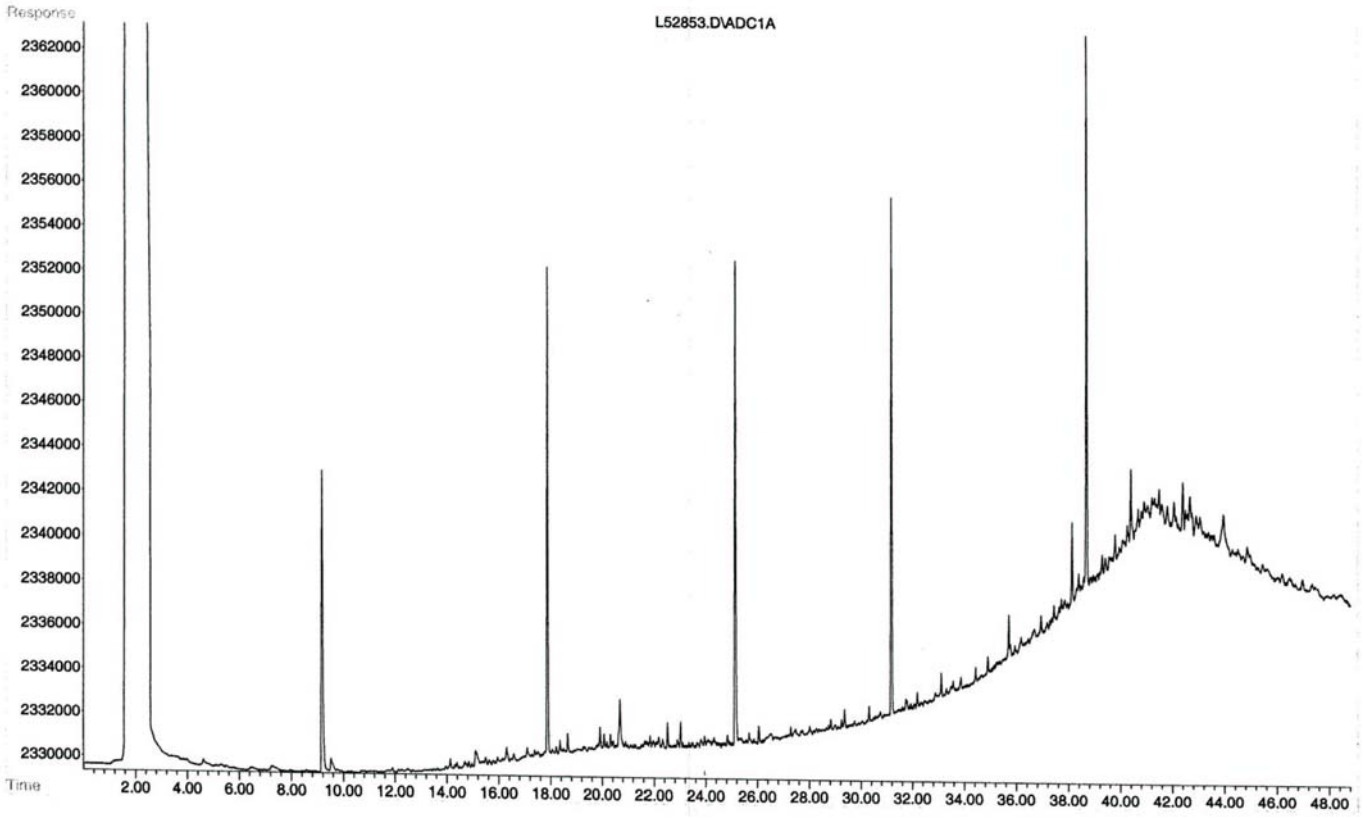

File : C:\HPCHEM\1\DATA\A1401AL\L52854.D
Operator : STS&CRS
Acquired : 16 Feb 2003 6:58 using AcqMethod AL5212N4.M
Instrument : M8 GC-589
Sample Name: MC 709 4413 Core 4 Bottom
Misc Info : A1401
Vial Number: 23

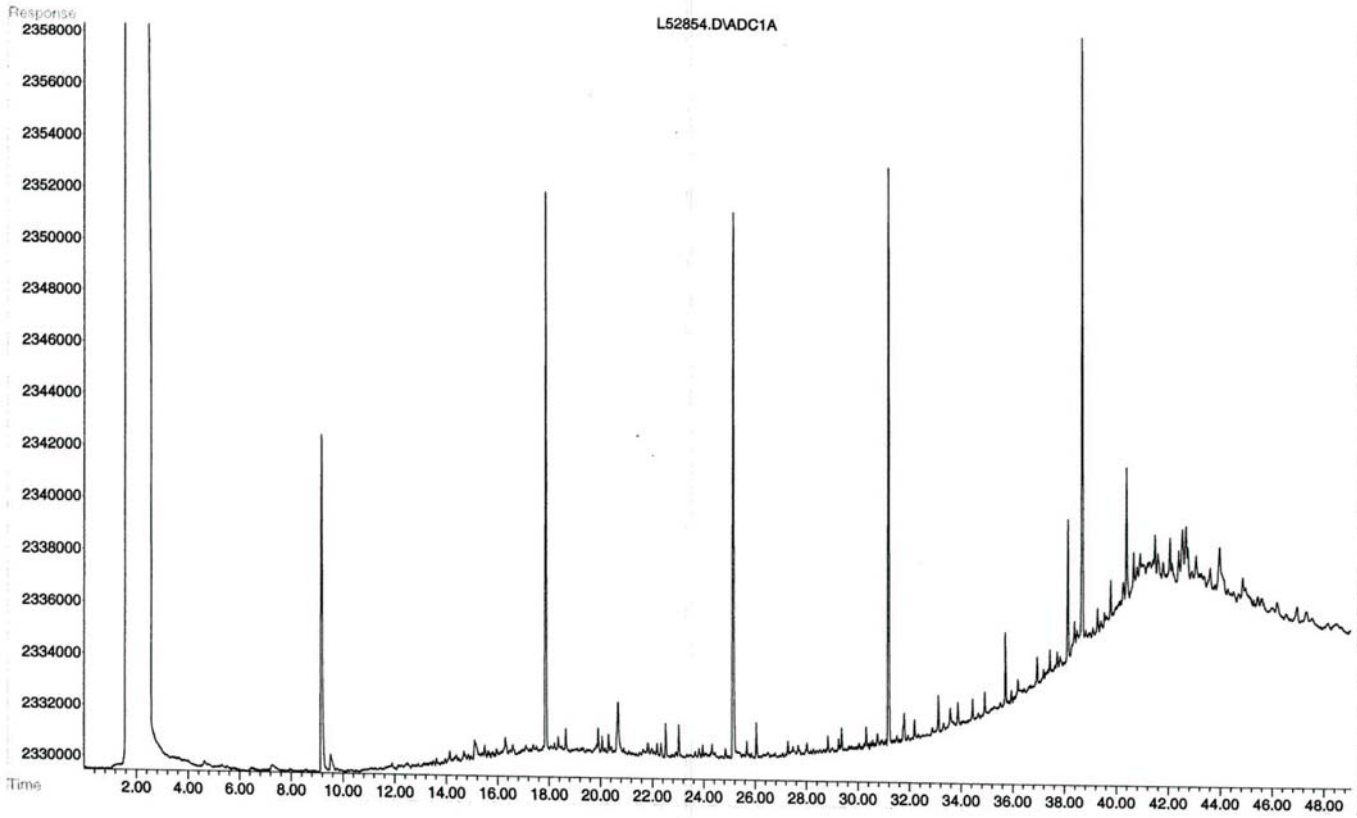

```
File        : C:\HPCHEM\1\DATA\A1401AL\L52855.D
Operator    : STS&CRS
Acquired    : 16 Feb 2003   7:57     using AcqMethod AL5212N4.M
Instrument :   M8 GC-589
Sample Name: MC 709 4413 Bucket 6
Misc Info   : A1401
Vial Number: 24
```

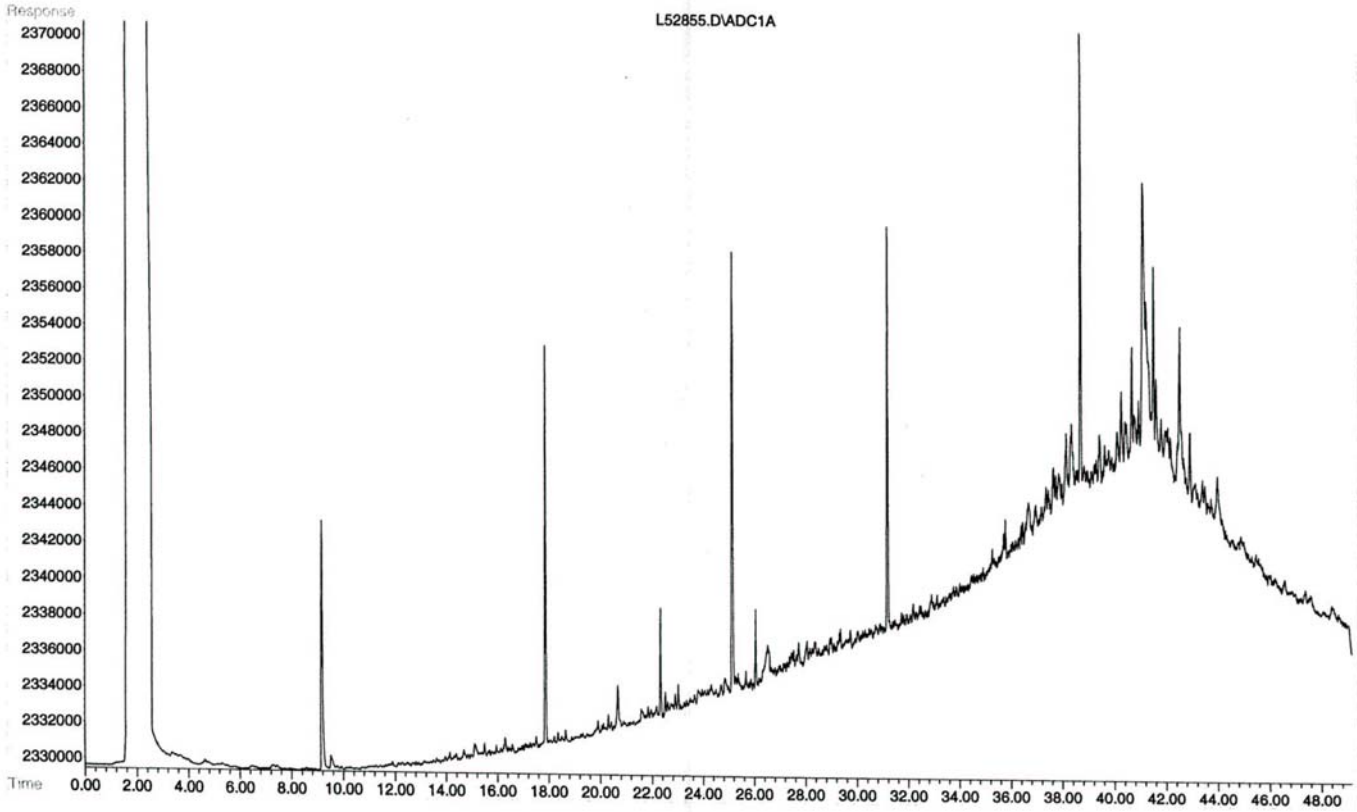

File : C:\HPCHEM\1\DATA\B1402AL\L52856.D
Operator : STS&CRS
Acquired : 18 Feb 2003 15:16 using AcqMethod AL5212N4.M
Instrument : M8 GC-589
Sample Name: MC 118 4414 Bucket 8
Misc Info : A1402
Vial Number: 5

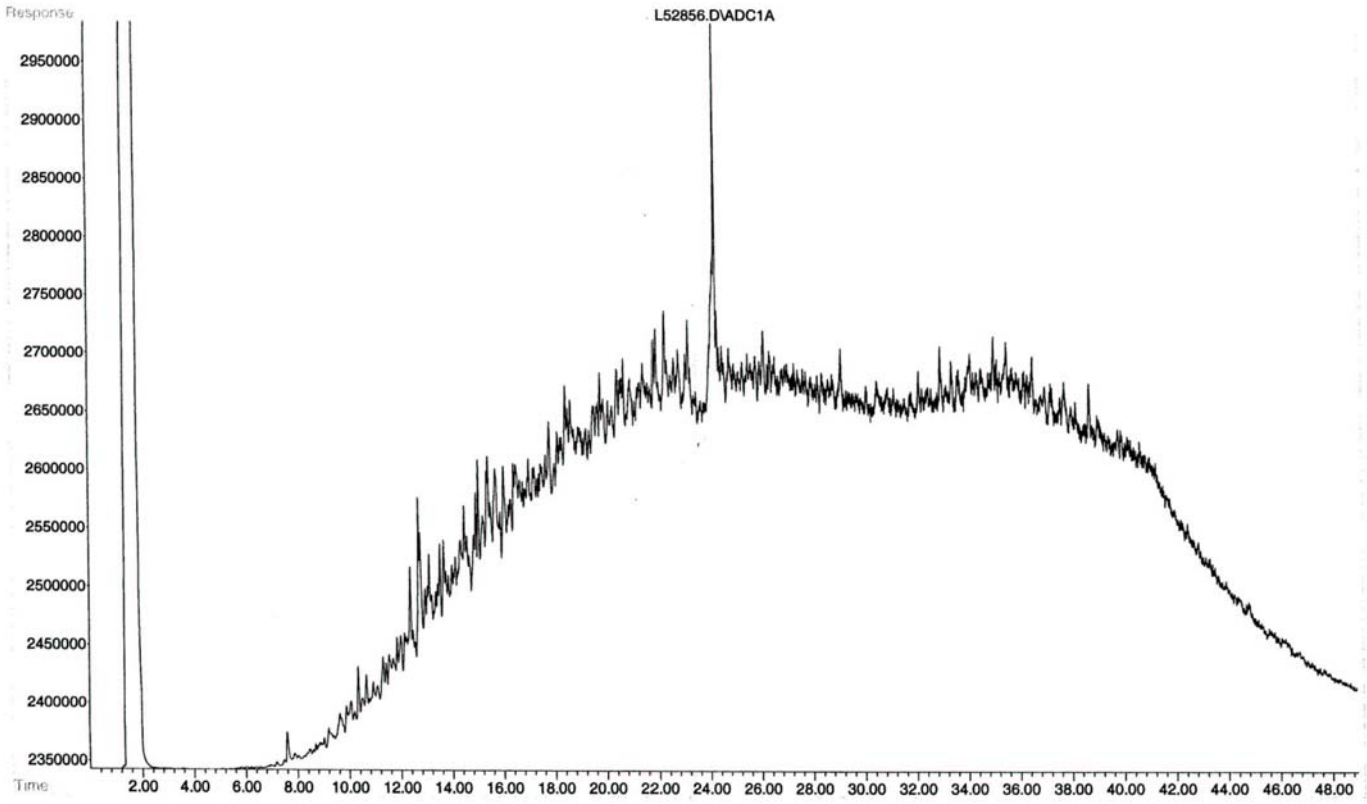

File : C:\HPCHEM\1\DATA\A1401AL\L52857.D
Operator : STS&CRS
Acquired : 16 Feb 2003 12:50 using AcqMethod AL5212N4.M
Instrument : M8 GC-589
Sample Name: MC 118 4414 Core 3
Misc Info : A1402
Vial Number: 29

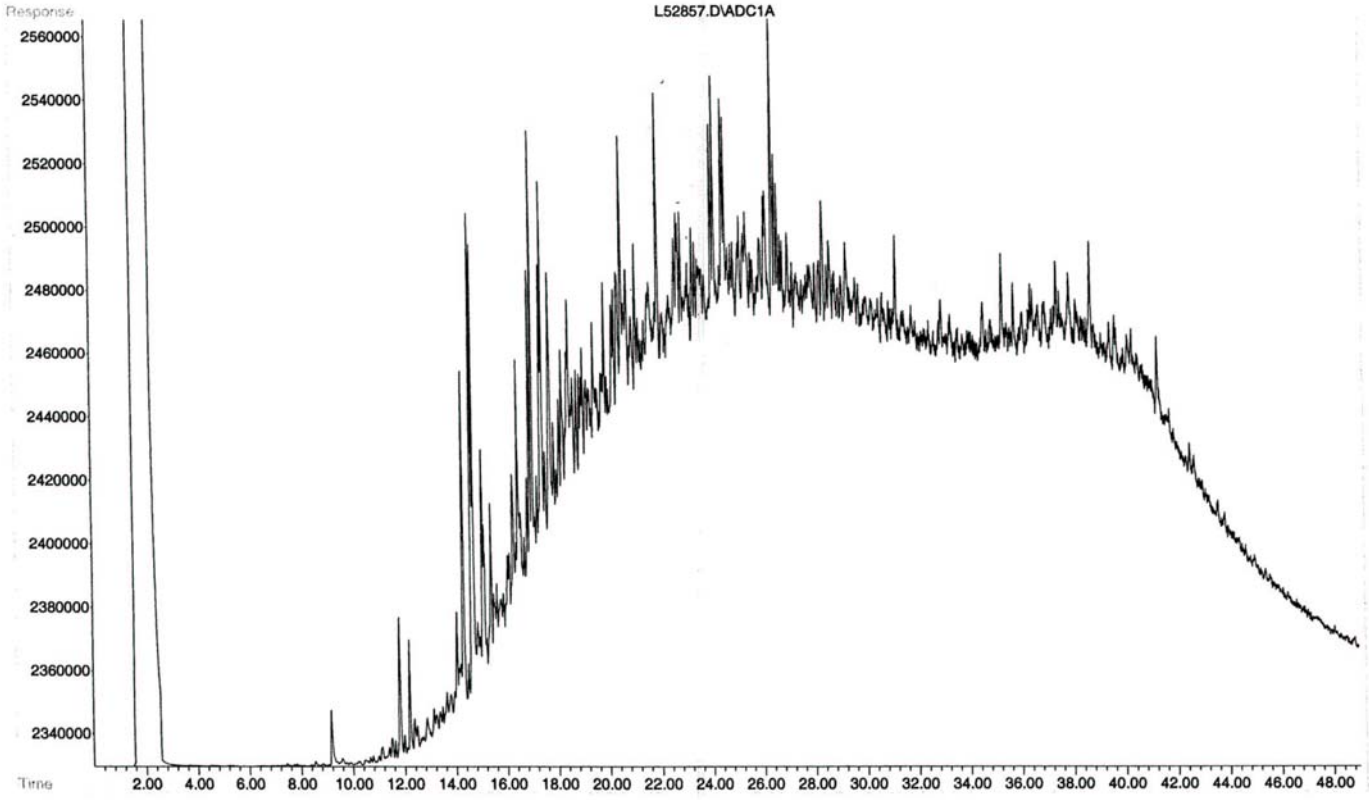

File : C:\HPCHEM\1\DATA\A1401AL\L52858.D
Operator : STS&CRS
Acquired : 16 Feb 2003 13:48 using AcqMethod AL5212N4.M
Instrument : M8 GC-589
Sample Name: MC 118 4415 Core 5 Top
Misc Info : A1402
Vial Number: 30

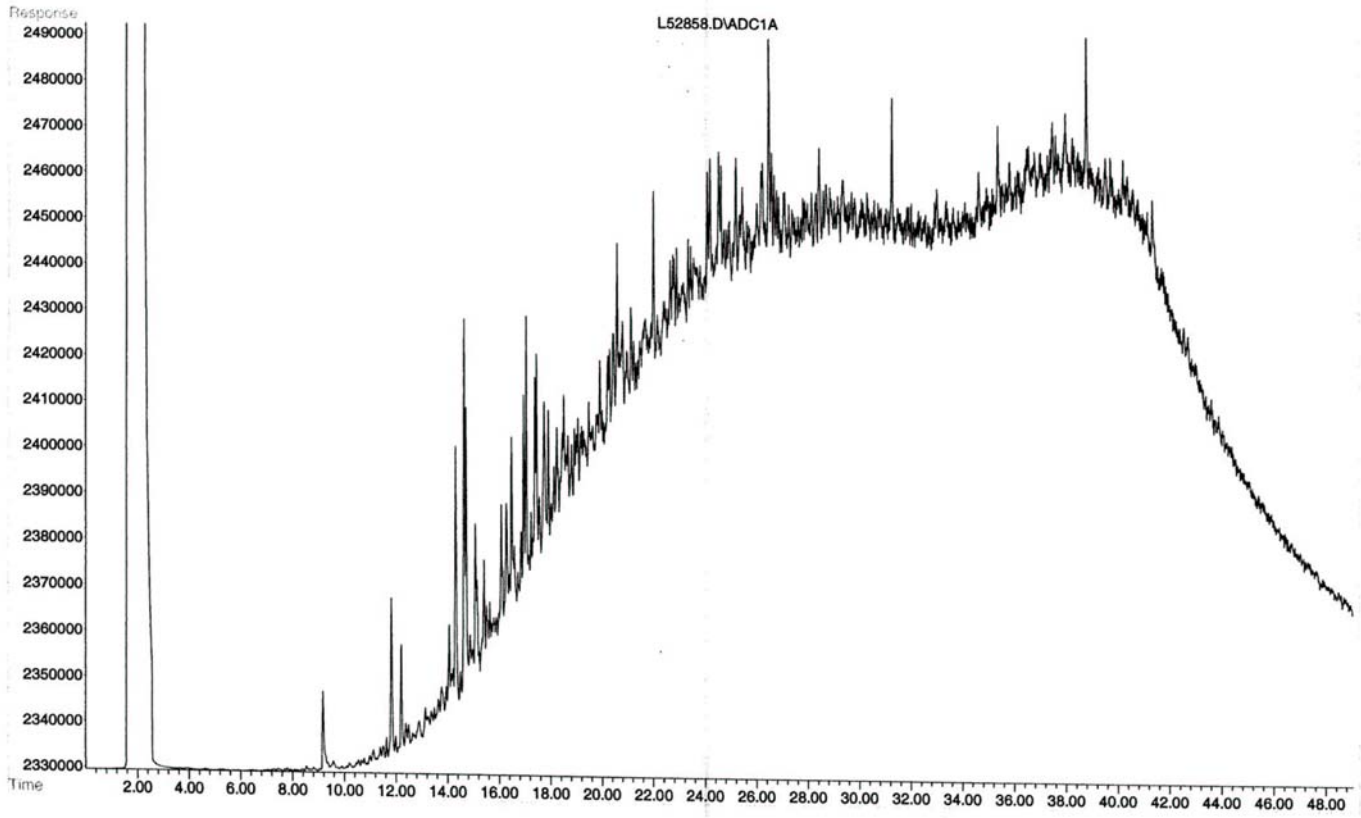

File : C:\HPCHEM\1\DATA\B1402AL\L52859.D
Operator : STS&CRS
Acquired : 18 Feb 2003 16:15 using AcqMethod AL5212N4.M
Instrument : M8 GC-589
Sample Name: MC 118 4415 Core 5 Bottom
Misc Info : A1402
Vial Number: 6

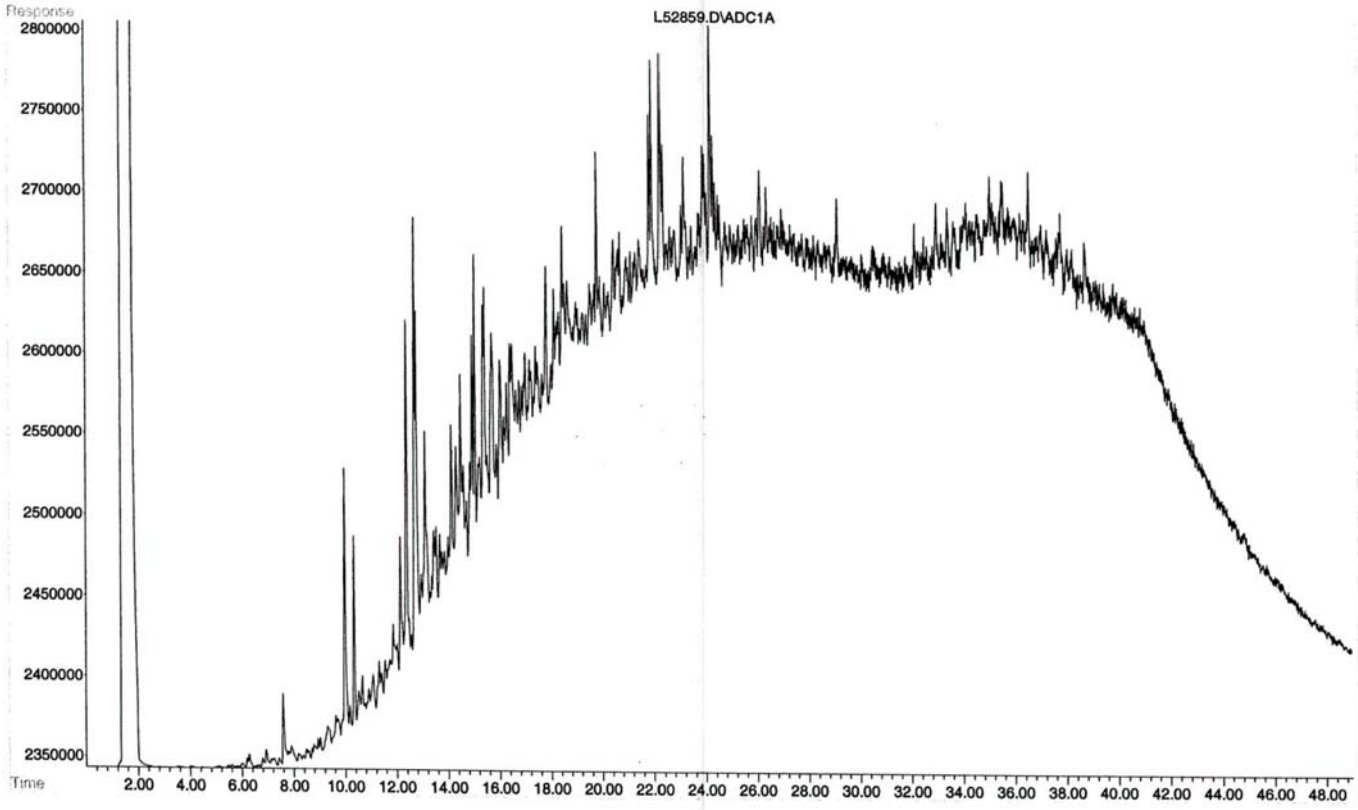

File : C:\HPCHEM\1\DATA\B1402AL\L52860.D
Operator : STS&CRS
Acquired : 18 Feb 2003 17:14 using AcqMethod AL5212N4.M
Instrument : M8 GC-589
Sample Name: GC 234 4424 Core 1
Misc Info : A1402
Vial Number: 7

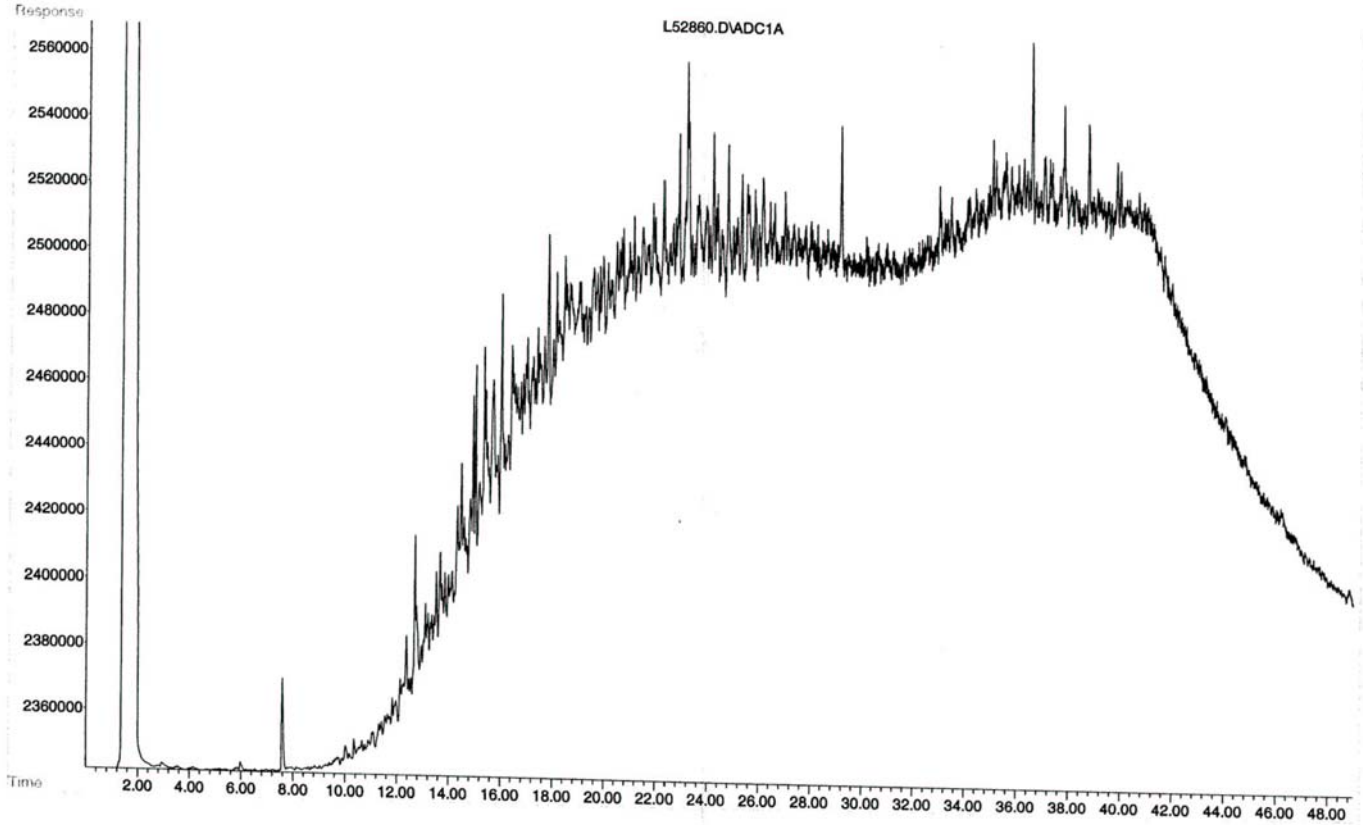

File : C:\HPCHEM\1\DATA\B1402AL\L52861.D
Operator : STS&CRS
Acquired : 18 Feb 2003 18:13 using AcqMethod AL5212N4.M
Instrument : M8 GC-589
Sample Name: GC 234 4424 Core 2
Misc Info : A1402
Vial Number: 8

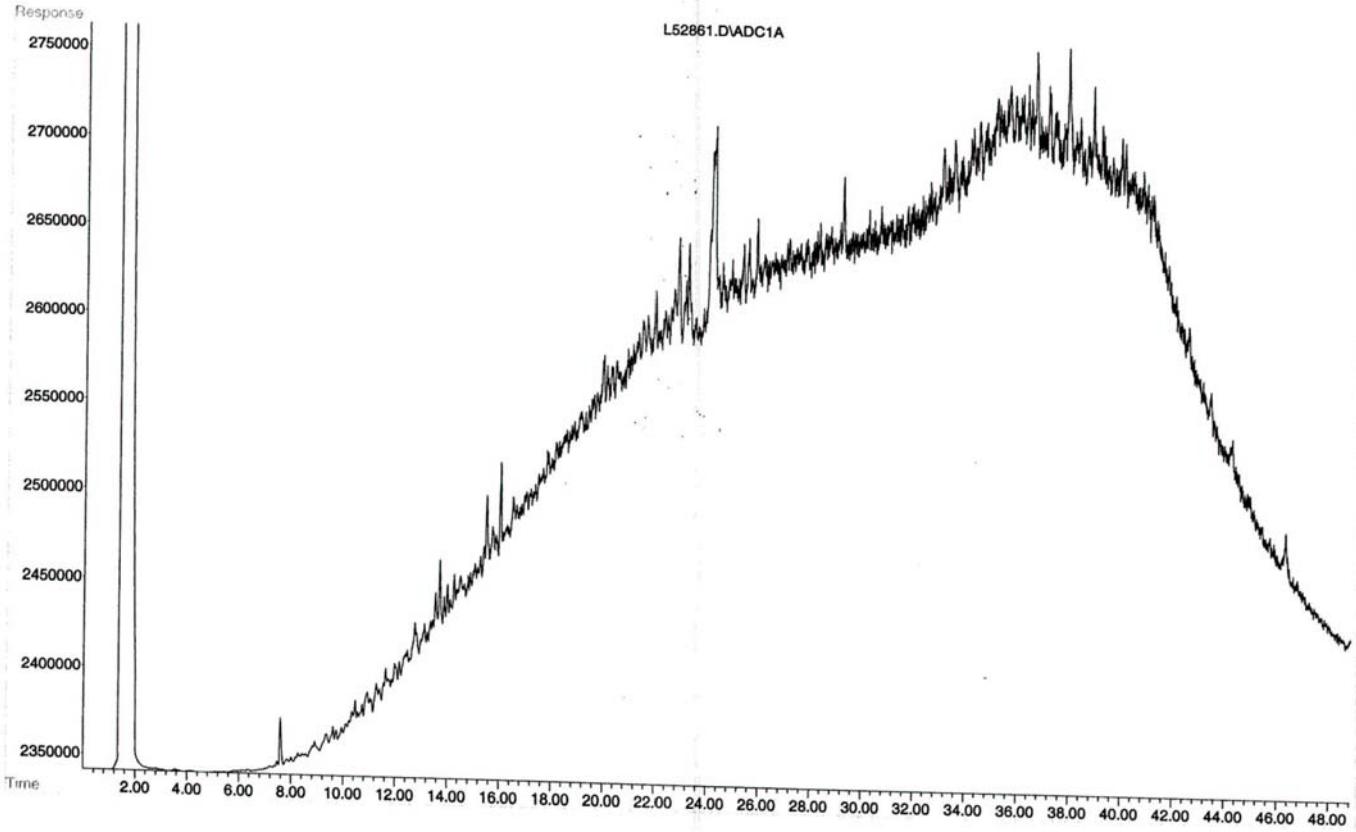

File : C:\HPCHEM\1\DATA\A1401AL\L52862.D
Operator : STS&CRS
Acquired : 16 Feb 2003 14:47 using AcqMethod AL5212N4.M
Instrument : M8 GC-589
Sample Name: GC 234 4424 Core 5
Misc Info : A1402
Vial Number: 31

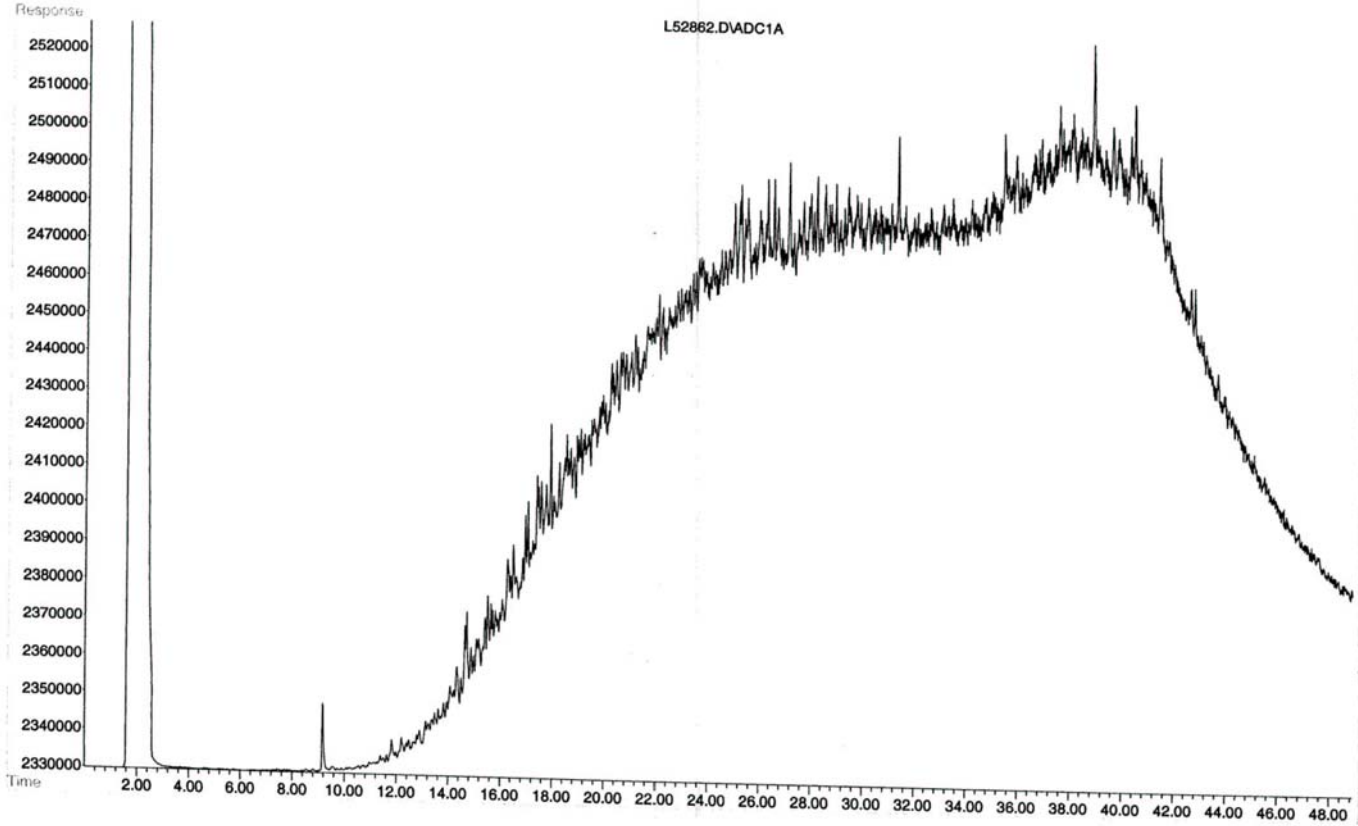

File : C:\HPCHEM\1\DATA\B1402AL\L52863.D
Operator : STS&CRS
Acquired : 18 Feb 2003 19:12 using AcqMethod AL5212N4.M
Instrument : M8 GC-589
Sample Name: GC 233 4425 Core 2
Misc Info : A1402
Vial Number: 9

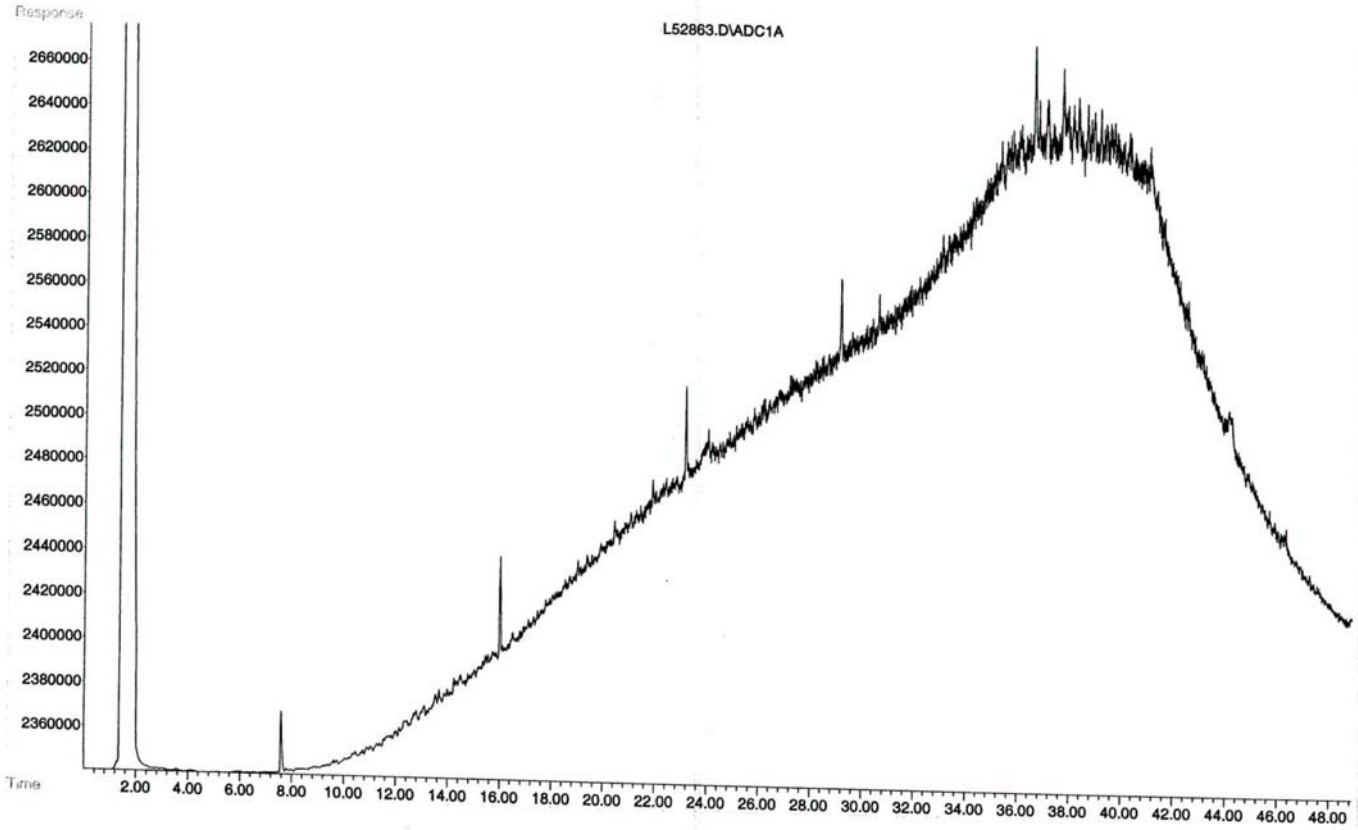

File : C:\HPCHEM\1\DATA\A1401AL\L52868.D
Operator : STS&CRS
Acquired : 16 Feb 2003 15:46 using AcqMethod AL5212N4.M
Instrument : M8 GC-589
Sample Name: GC 233 4427 Core 1 Bottom
Misc Info : A1402
Vial Number: 32

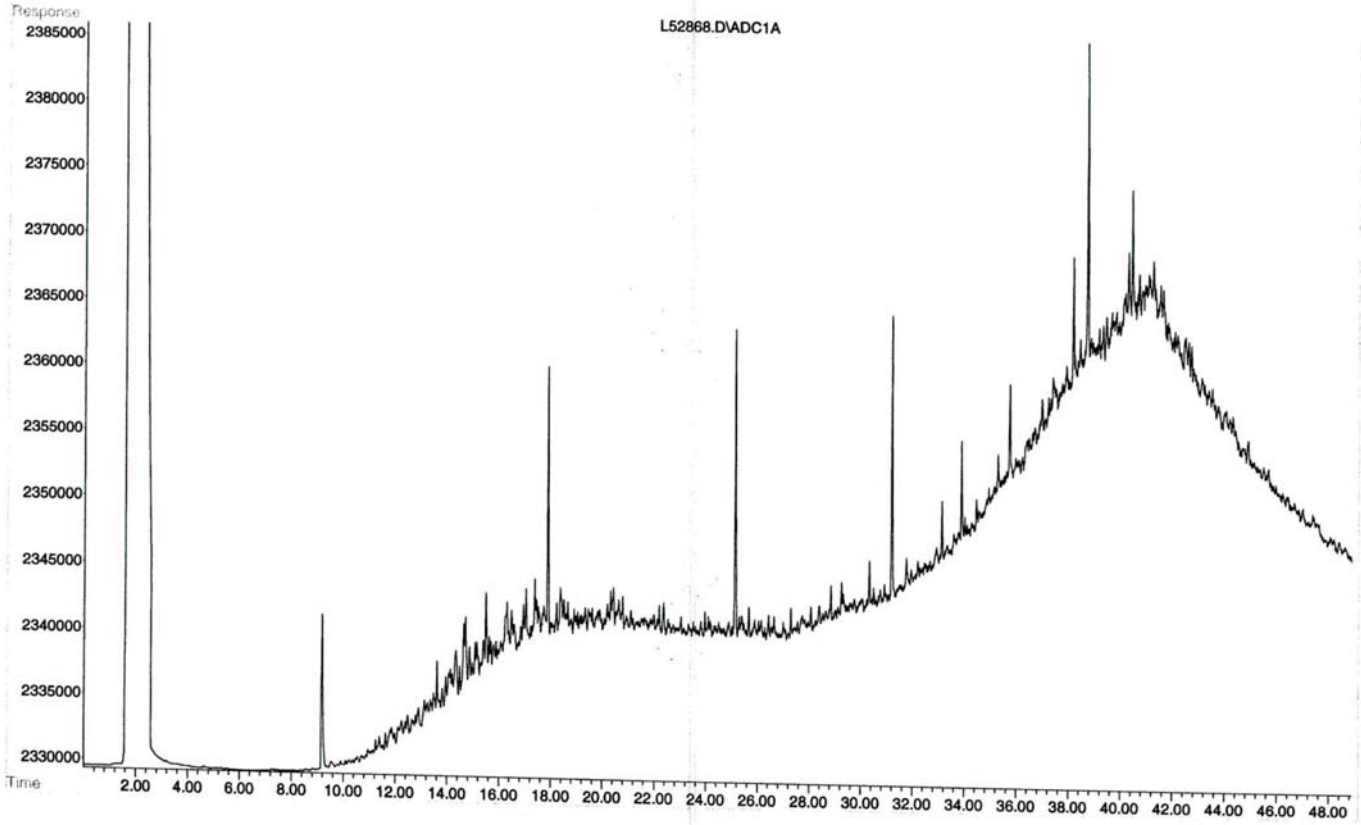

File : C:\HPCHEM\1\DATA\B1402AL\L52864.D
Operator : STS&CRS
Acquired : 18 Feb 2003 20:11 using AcqMethod AL5212N4.M
Instrument : M8 GC-589
Sample Name: GC 233 4425 Core 4
Misc Info : A1402
Vial Number: 10

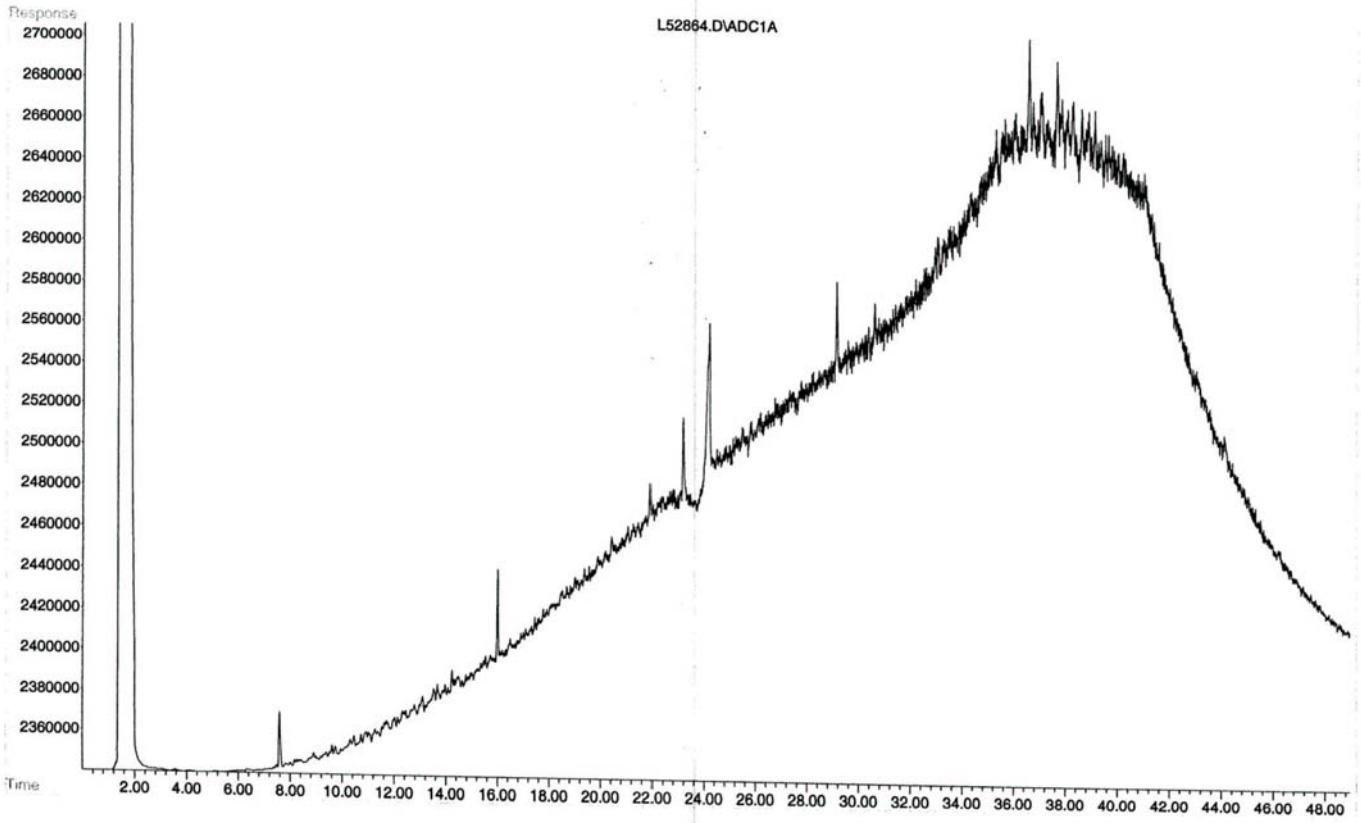

File : C:\HPCHEM\1\DATA\A1400AL\L52820.D
Operator : STS&CRS
Acquired : 11 Feb 2003 16:17 using AcqMethod AL5212N4.M
Instrument : M8 GC-589
Sample Name: GC 232, Dive 4401
Misc Info : A1400
Vial Number: 7

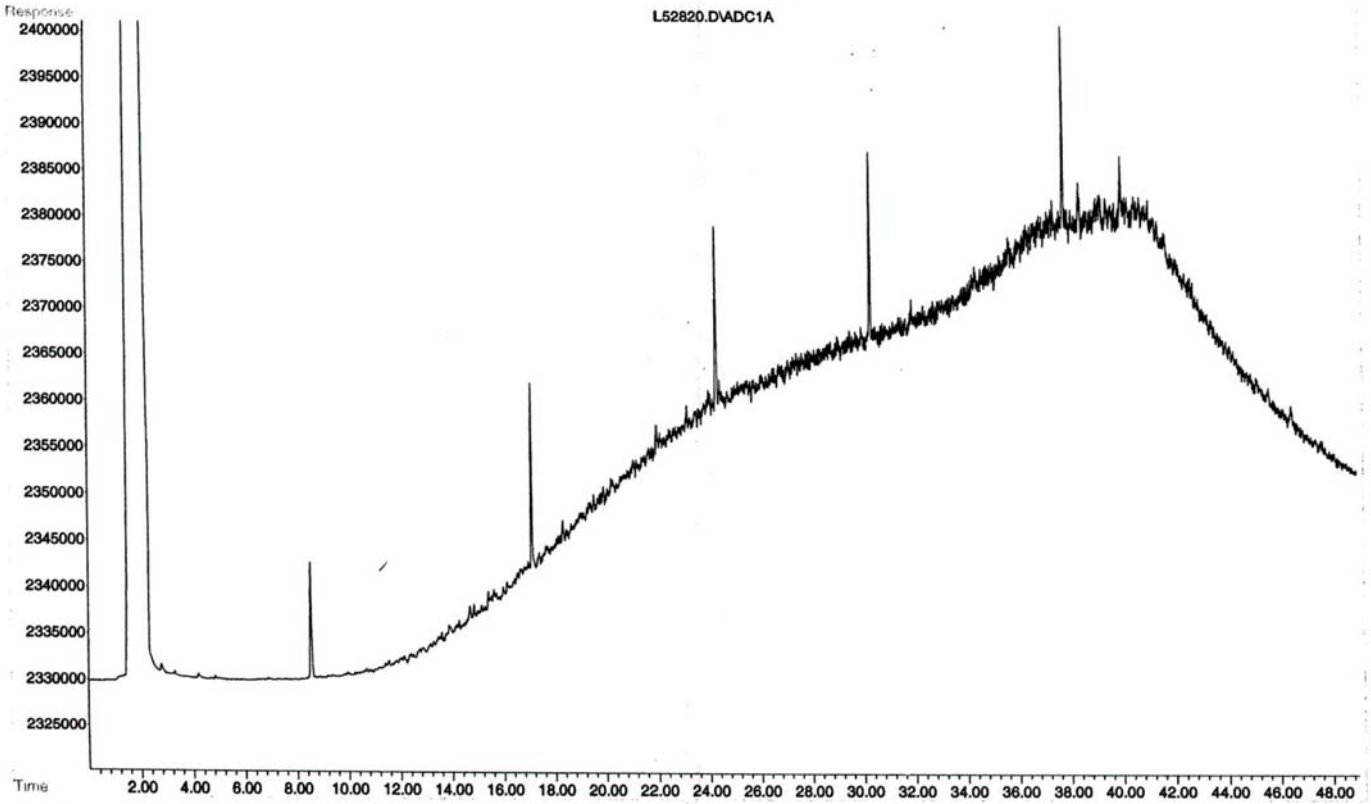

File : C:\HPCHEM\1\DATA\A1401AL\L52869.D
Operator : STS&CRS
Acquired : 16 Feb 2003 16:44 using AcqMethod AL5212N4.M
Instrument : M8 GC-589
Sample Name: GC 232 4428 Core 1
Misc Info : A1402
Vial Number: 33

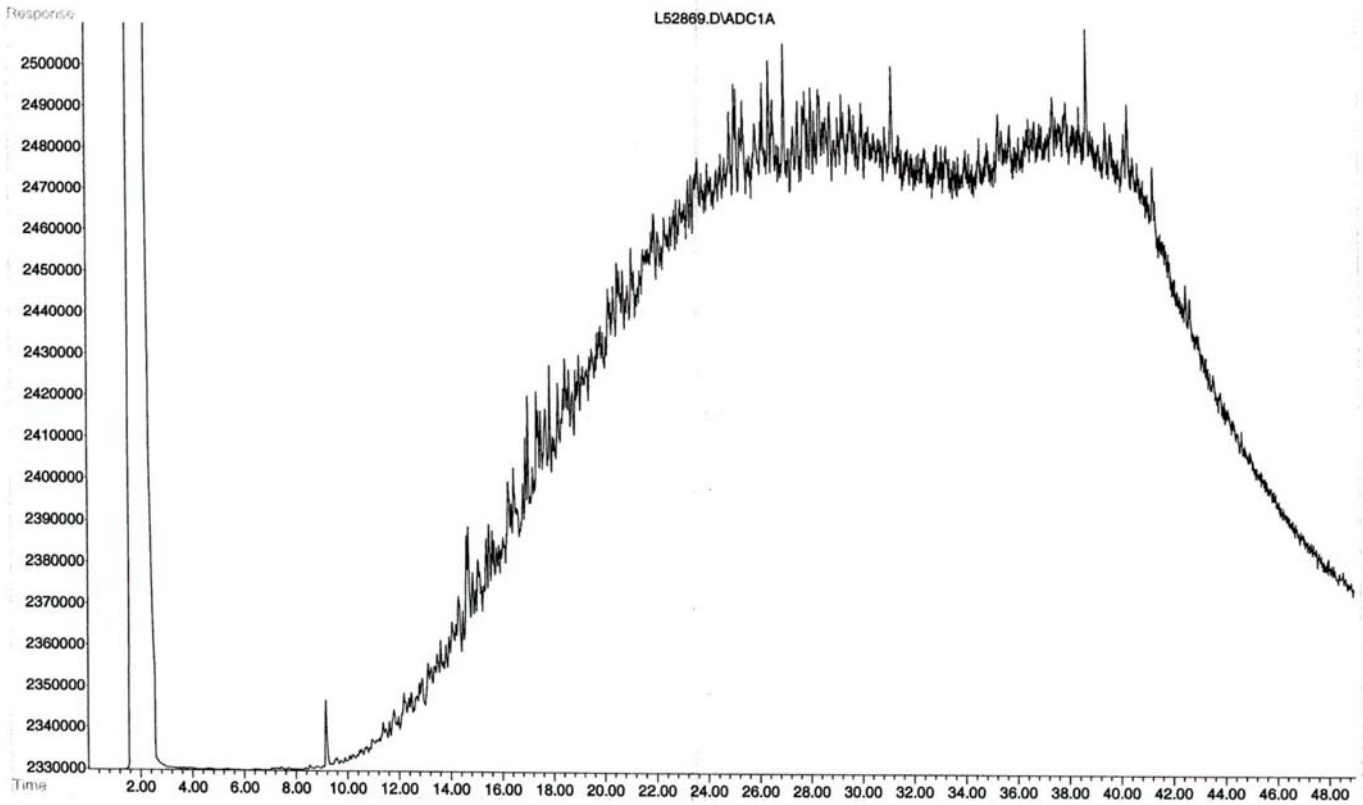

File : C:\HPCHEM\1\DATA\A1402AL\L52870.D
Operator : STS&CRS
Acquired : 13 Feb 2003 12:46 using AcqMethod AL5212N4.M
Instrument : M8 GC-589
Sample Name: GC 232 4428 Core 5
Misc Info : A1402
Vial Number: 23

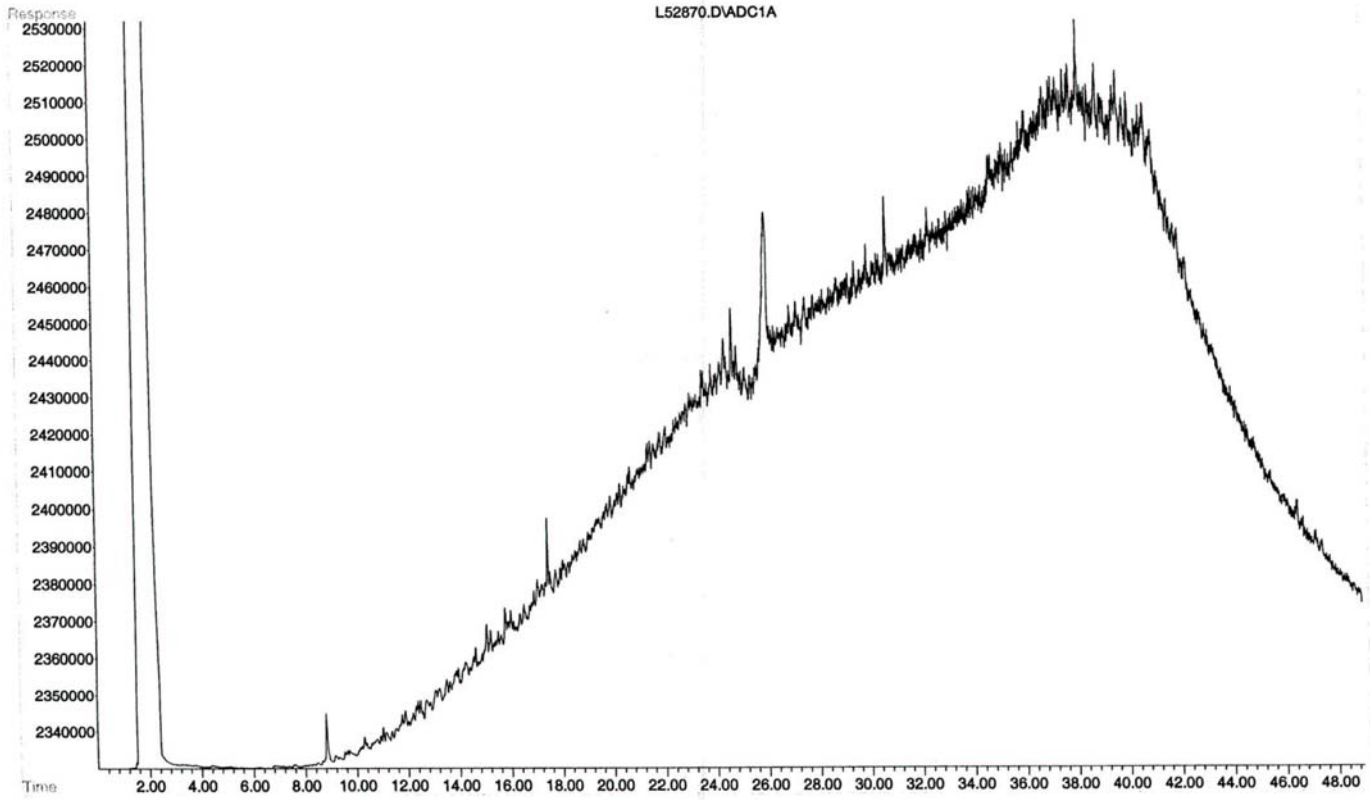

File : C:\HPCHEM\1\DATA\A1401AL\L52871.D
Operator : STS&CRS
Acquired : 16 Feb 2003 17:43 using AcqMethod AL5212N4.M
Instrument : M8 GC-589
Sample Name: Dive 4428 Core 6
Misc Info : A1402
Vial Number: 34

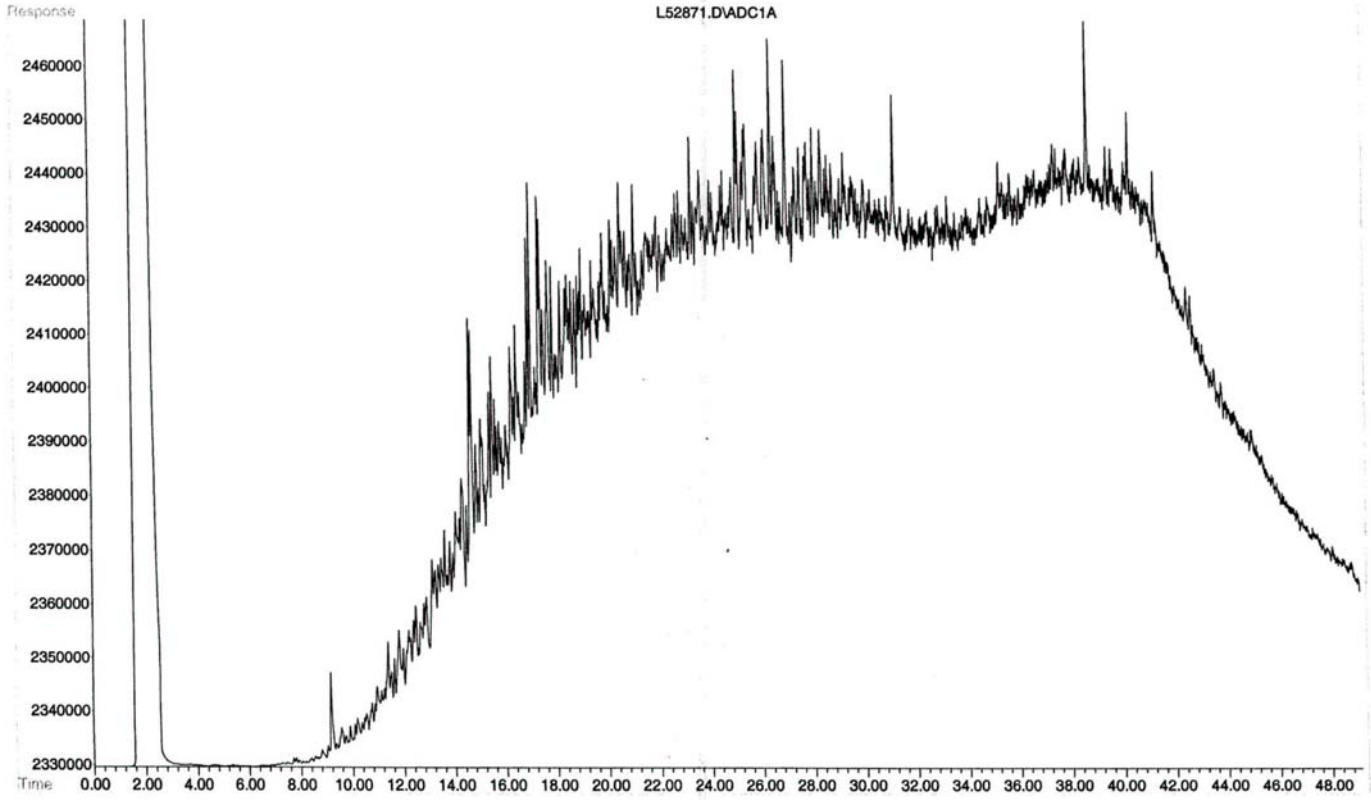

File : C:\HPCHEM\1\DATA\A1402AL\L52872.D
Operator : STS&CRS
Acquired : 13 Feb 2003 15:43 using AcqMethod AL5212N4.M
Instrument : M8 GC-589
Sample Name: GC 185 4429 Bush Hill nea
Misc Info : A1402
Vial Number: 26

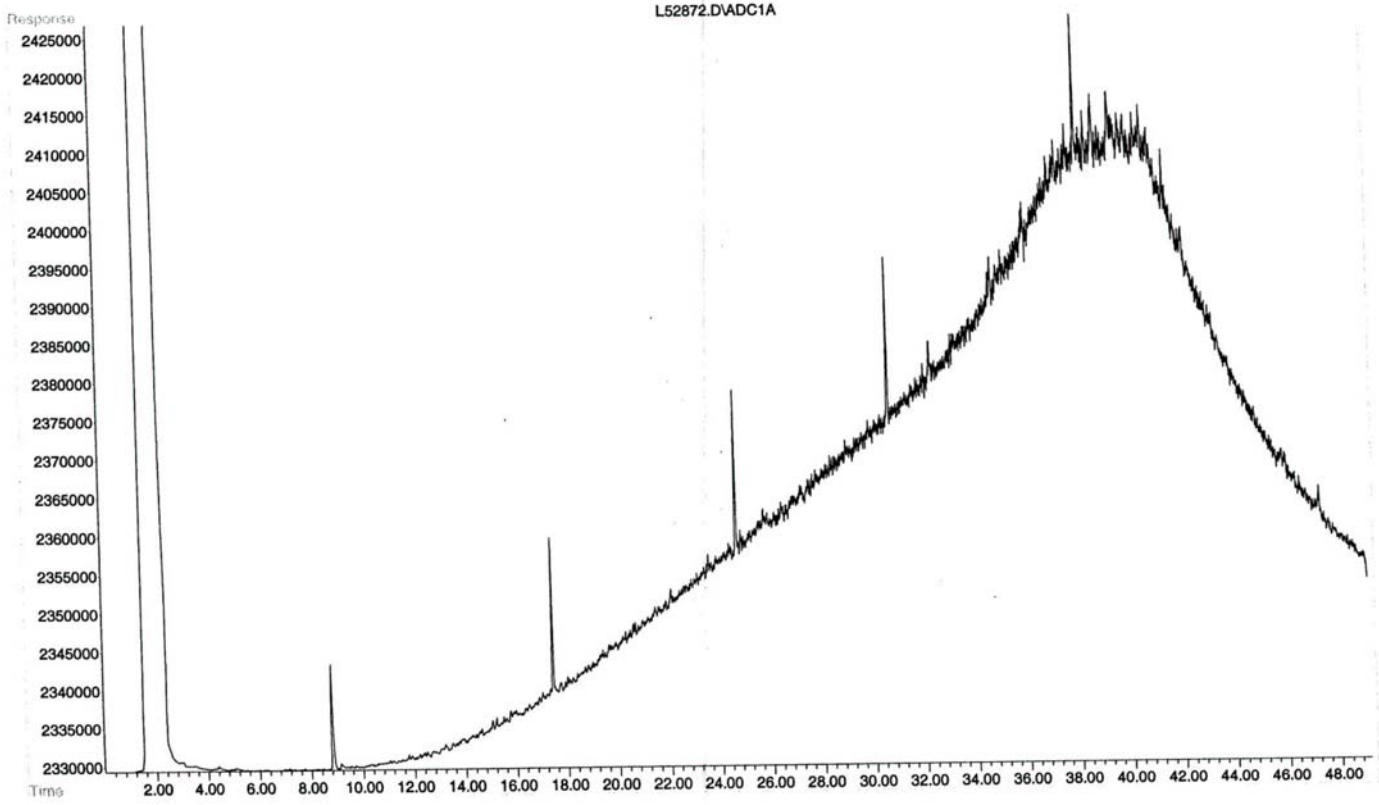

File : C:\HPCHEM\1\DATA\A1402AL\L52873.D
Operator : STS&CRS
Acquired : 13 Feb 2003 16:42 using AcqMethod AL5212N4.M
Instrument : M8 GC-589
Sample Name: Dive 4431
Misc Info : A1402
Vial Number: 27

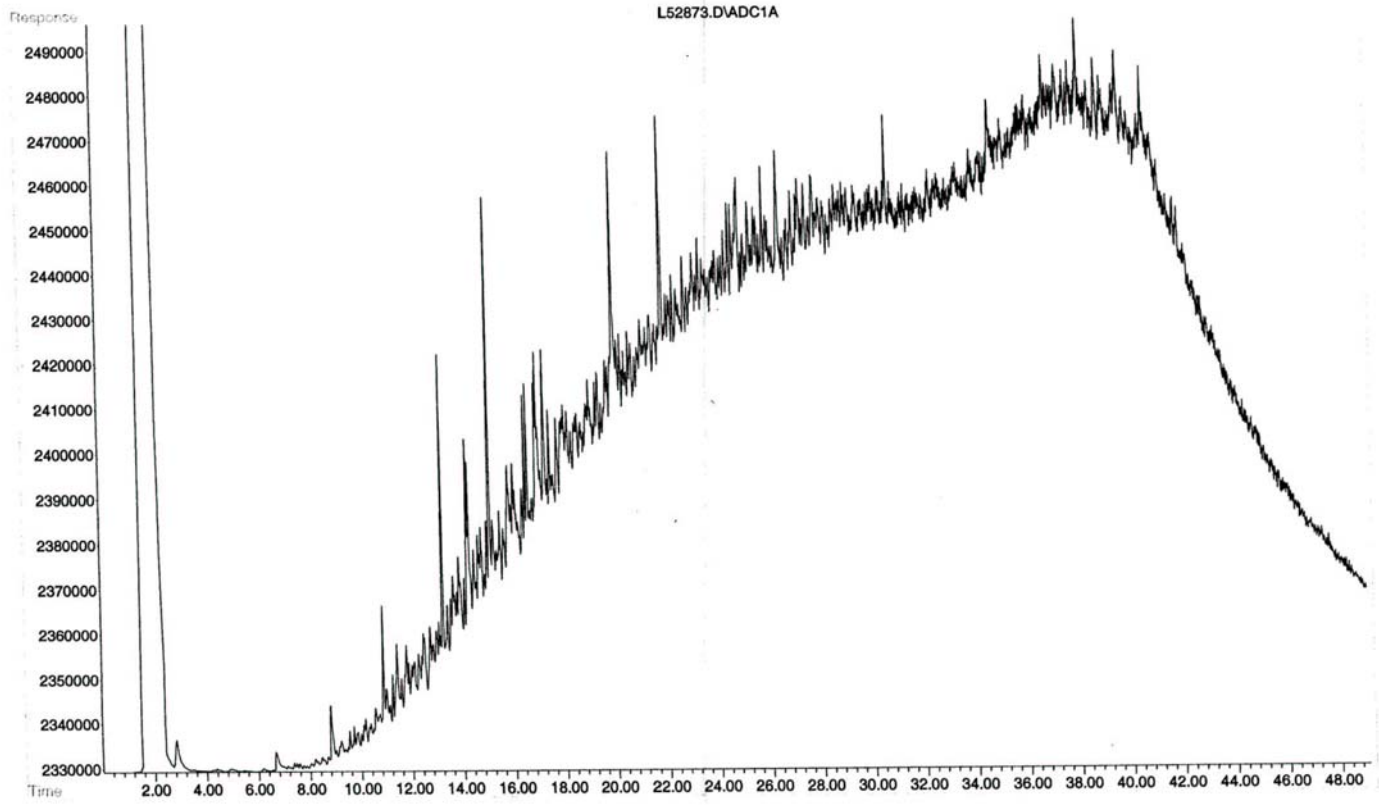

File : C:\HPCHEM\1\DATA\A1402AL\L52874.D
Operator : STS&CRS
Acquired : 13 Feb 2003 17:41 using AcqMethod AL5212N4.M
Instrument : M8 GC-589
Sample Name: Dive 4432
Misc Info : A1402
Vial Number: 28

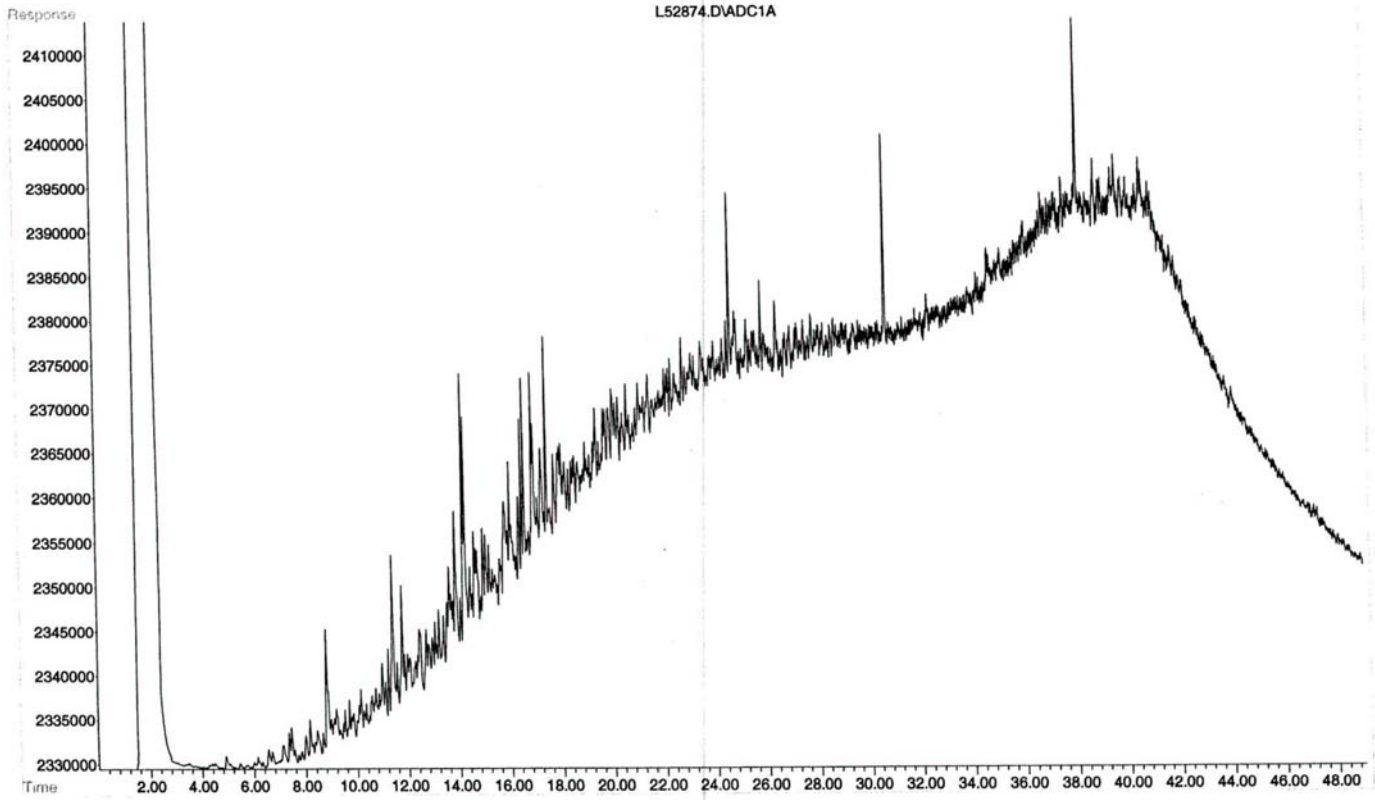

File : C:\HPCHEM\1\DATA\A1402AL\L52875.D
Operator : STS&CRS
Acquired : 13 Feb 2003 18:40 using AcqMethod AL5212N4.M
Instrument : M8 GC-589
Sample Name: Dive 4438
Misc Info : A1402
Vial Number: 29

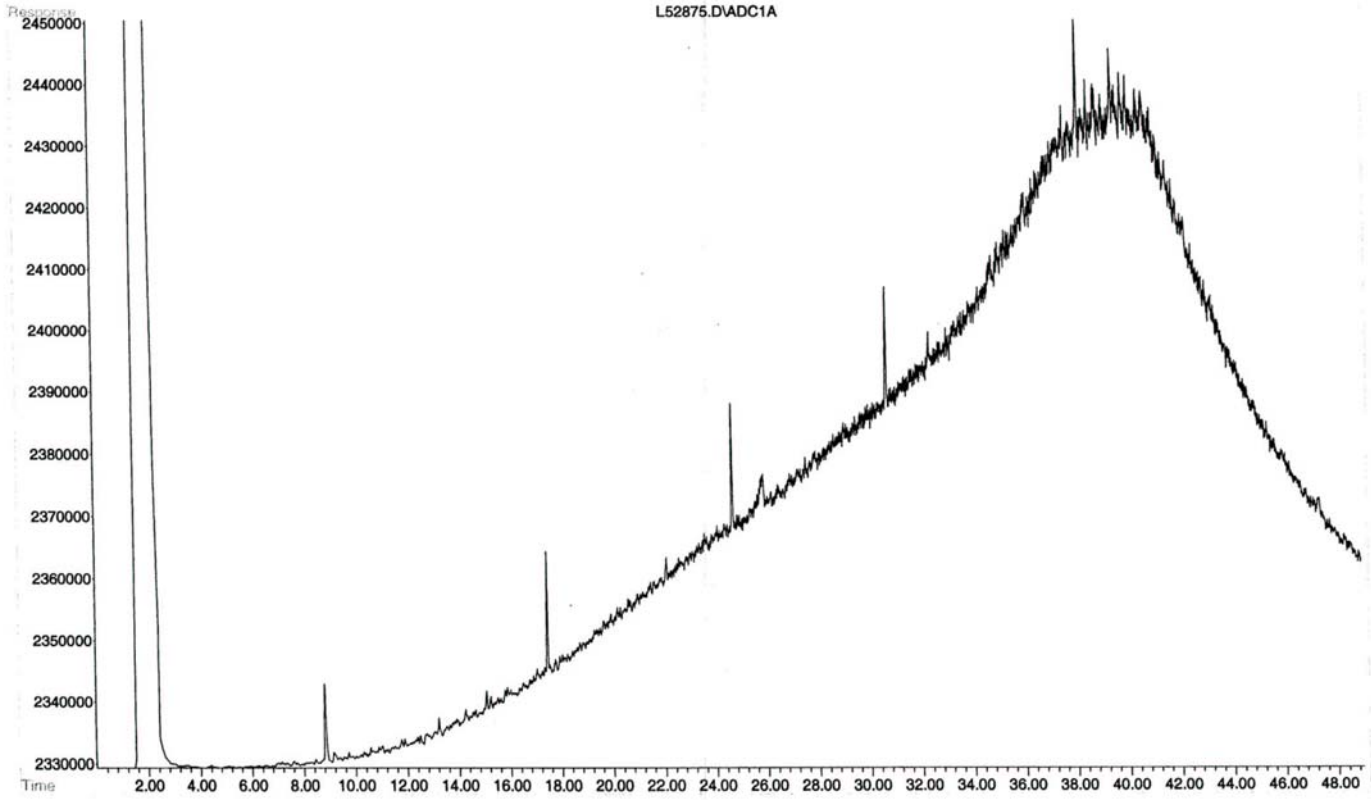

File : C:\HPCHEM\1\DATA\B1402AL\W00976.D
Operator : STS&CRS
Acquired : 18 Feb 2003 12:19 using AcqMethod AL5212N4.M
Instrument : M8 GC-589
Sample Name: STD OIL 2000
Misc Info : A1402
Vial Number: 2

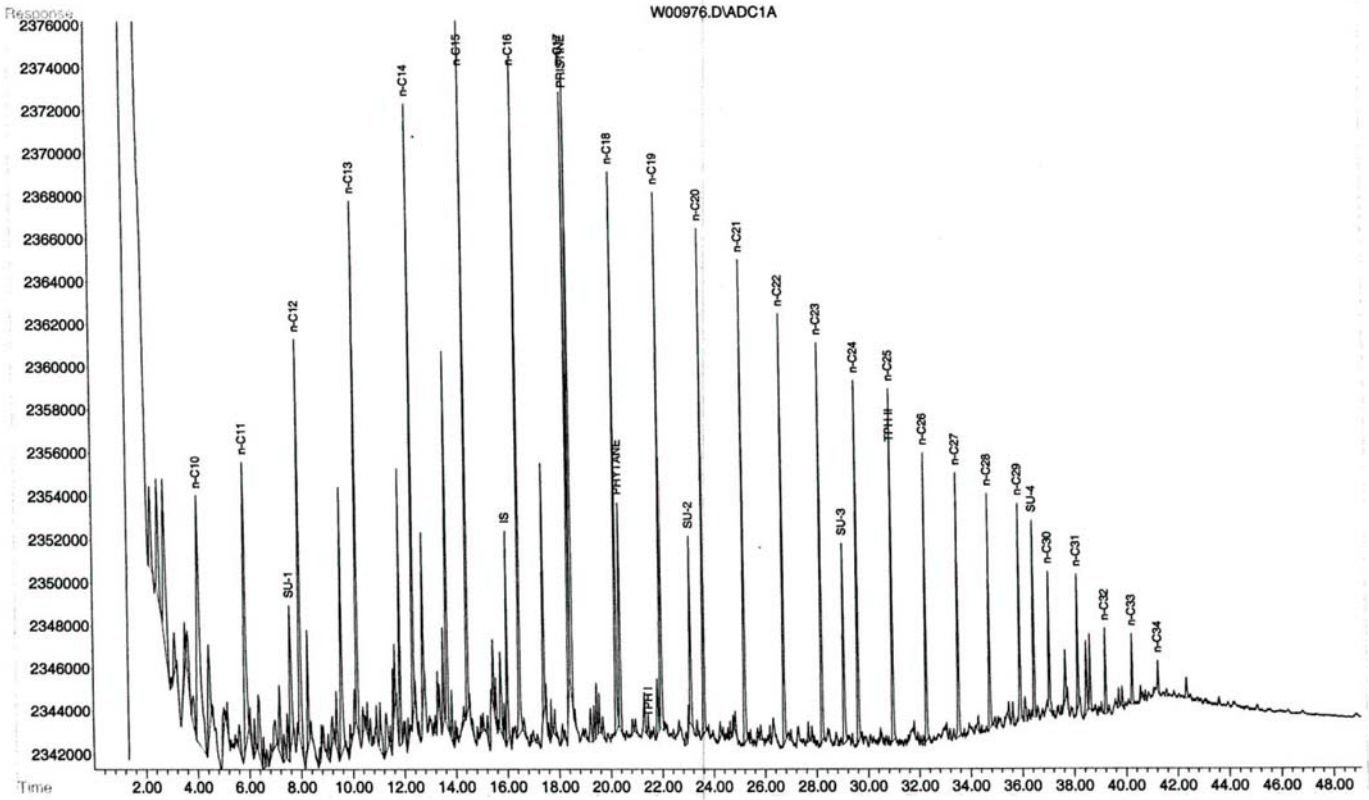

File : C:\HPCHEM\1\DATA\A1400AL\W00957.D
Operator : STS&CRS
Acquired : 11 Feb 2003 11:23 using AcqMethod AL5212N4.M
Instrument : M8 GC-589
Sample Name: STD OIL 2000
Misc Info : A1400
Vial Number: 2

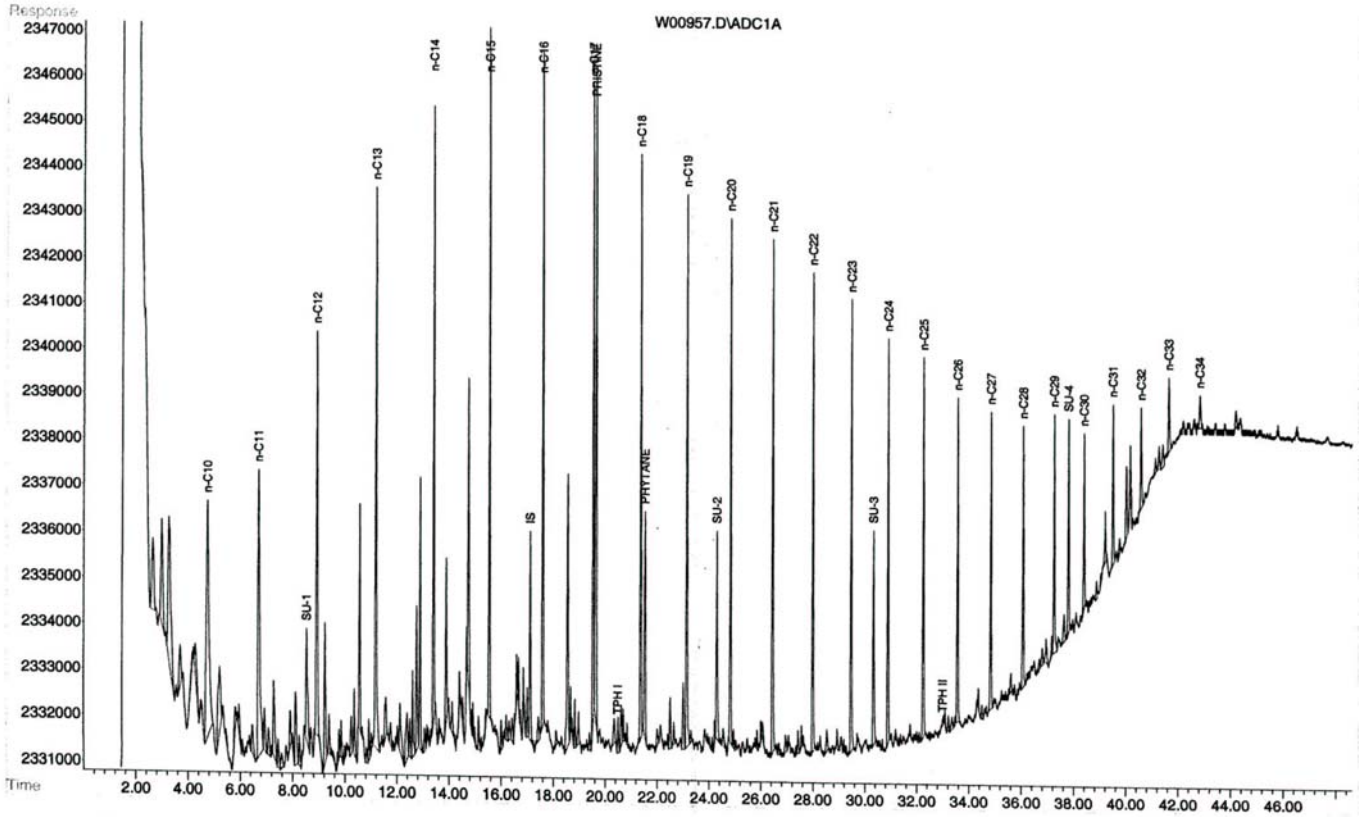

File : C:\HPCHEM\1\DATA\A1401AL\W00967.D
Operator : STS&CRS
Acquired : 15 Feb 2003 10:26 using AcqMethod AL5212N4.M
Instrument : M8 GC-589
Sample Name: STD OIL 2000
Misc Info : A1401
Vial Number: 2

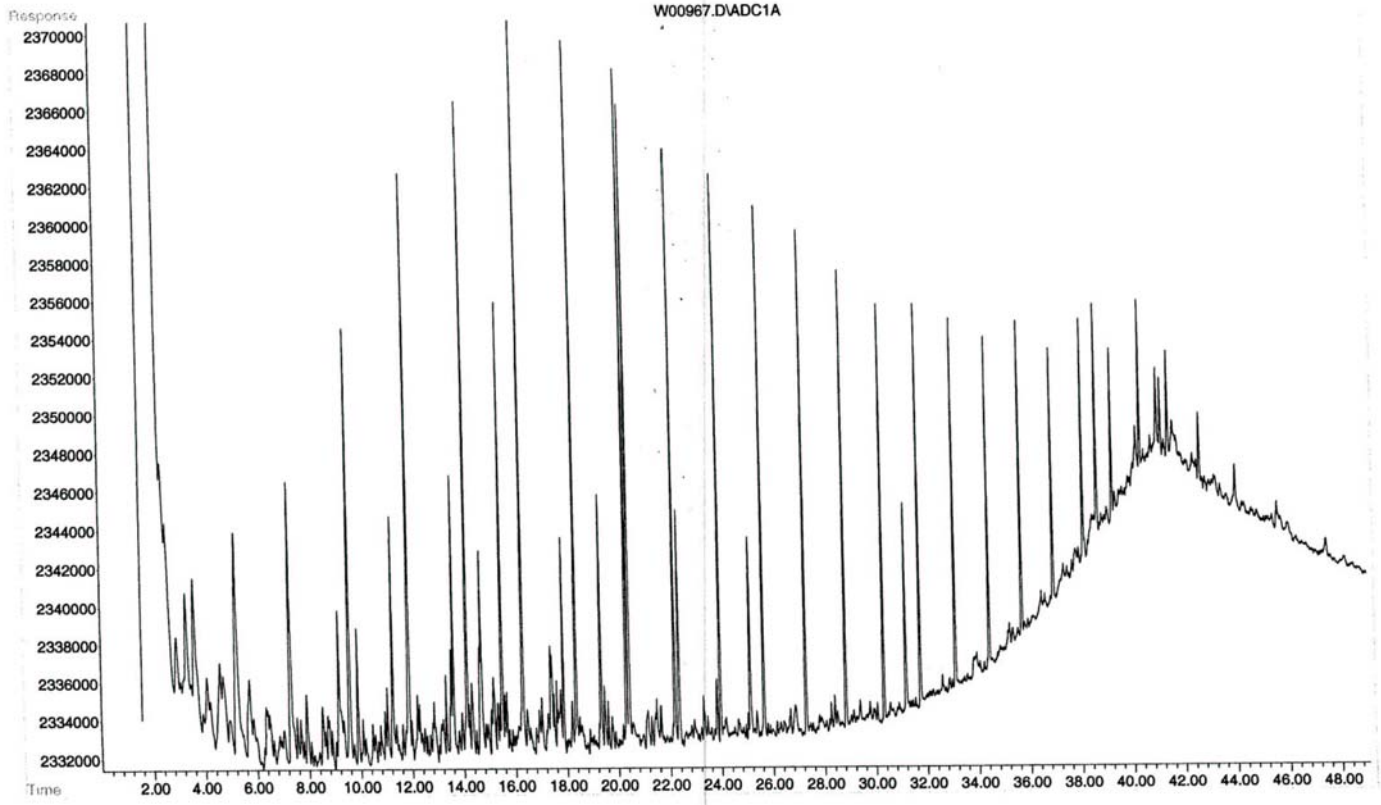

Isotope Data for Carbonate Samples

Sample Location	Dive #	$\delta^{13}C$	$\delta^{13}C$	$\delta^{13}C$	Average $\delta^{13}C$	$\delta^{18}O$	$\delta^{18}O$	$\delta^{18}O$	Average $\delta^{18}O$
GC 234	4434	-26.30	-26.73		-26.52	2.89	3.07		2.98
MC 709	4412	-26.61	-27.06		-26.84	3.88	3.80		3.84
MC 709	4413	-14.67	-12.59		-13.63	3.40	3.36		3.38
MC 709	4413	-29.33	-30.36	-28.64	-29.44	3.71	3.55	3.49	3.58
MC 709	4413	-27.33	-28.08		-27.71	4.33	4.08		4.21
MC 709	4413	-29.73	-27.96		-28.85	4.33	4.28		4.31
MC 709	4413	-34.29	-34.78		-34.54	3.94	3.91		3.93
MC 709	4413	-27.36	-26.10	-26.61	-26.69	4.30	4.49	3.95	4.25
GC 232	4401	-16.02	-15.39		-15.71	3.13	3.24		3.19
GC 232	4401	-16.42	-17.12		-16.77	3.57	3.59		3.58
GC 232	4401	-15.30	-14.94		-15.12	3.50	3.42		3.46
GC 233	4425	-32.46	-32.72		-32.59	4.29	4.23		4.26
GC 233	4425	-32.64	-32.24	-33.06	-32.65	4.22	4.30	4.15	4.22
GC 233	4425	-35.31	-34.72		-35.02	3.98	3.71		3.85
GC 185	4429	-22.58	-22.18		-22.38	3.34	3.32		3.33
GC 185	4429	-22.42	-23.03		-22.73	3.20	3.29		3.25
GC 185	4429	-22.19	-22.56		-22.38	3.20	3.42		3.31
GC 234	4434	-27.09	-26.77	-26.94	-26.93	3.27	3.39	3.40	3.35
GC 234	4434	-27.26	-26.81		-27.04	3.24	3.48		3.36
GC 234	4434	-26.64	-26.68		-26.66	3.26	3.50		3.38
GC 234	4435	-24.18	-25.94		-25.06	3.97	4.20		4.09
GC 234	4435	-21.13	-21.50		-21.32	3.94	4.26		4.10
GC 234	4435	-18.53	-19.34	-18.44	-18.77	3.91	4.08	4.35	4.11
GC 234	4436	-21.62	-21.87		-21.75	4.09	4.15		4.12
GC 234	4436	-20.82	-20.58		-20.70	4.27	3.99		4.13
GC 234	4436	-21.81	-21.83		-21.82	3.94	3.79		3.87
GC 232	4437	-19.49	-19.12		-19.31	3.78	3.58		3.68
GC 232	4437	-20.63	-20.16	-19.66	-20.15	3.49	3.48	3.64	3.54
GC 232	4437	-19.09	-18.24		-18.67	3.55	3.62		3.59

Dive Log

(1)

LOUISIANA STATE UNIVERSITY

SUBMERSIBLE DIVE LOG

Dive Number: 4401 Date: 29May02 AM

Location: GC 232 hydrate site

Time: start 8:03:27

end left bottom 11:00

Maximum Depth: 1870 ft (feet or meters)

Personnel: Roger Sassen, Craig Caddigan, Tom McGee, Hugo Marrero

Mission/Dive Objective: Sample muds and fauna near gashydrate exposures and gas vents

Photographs: Hand held camera Sub-mounted camera

Roll #

Frame #'s Many

Video: Tape # 2

Sampling (type) push cores, suction, grab

Mapping n/a

Equipment emplacement (type) n/a

Other

Comments - If sampling was done or equipment emplaced, please give a brief description including: how many samples/pieces of equipment, type, depth(s), etc.

See attached

Dive 4401 GC 232 (2)

1. Acquired water samples every 200 ft from surface to bottom for Jeff Chandler.
bottom = 1870.1 ft, 7.59 °C, Salinity = 34.93 ‰
Current 0.1 knot FIX 3

2. Collected small intact tube worm bush with roots and attached carbonate hold fasts, crab
1869' 7.55 °C 34.93 ‰ salinity
Archived tube worms, roots, carbonate, crab for molecular and isotopic analyses.
FIX. 4.

3. crossed irregular sea floor. FIX 5. Sampled white-gray bacterial mat at 0850.
oil and gas bubbles vented from the sea floor when disturbed. Core 1 used for geotechnical analysis.

4. Hydrate Site #1. outcropping in hummocky area. Large gas and oil-laden bubbles when sediment disturbed. FIX 7.
Used grab to fill Bucket 8 with ~~calcareous~~ calcite cemented sediment. 0907.
Hydrate is white thin vein fillings and massive oil-stained orange vein fillings with gas vents. Used suction to crumble mud in bucket 10. Calcite-cemented sediment

(3)

5. 0928. Took 4 push cores in line from hydrate outcrop to tube worm bass

FIX 8 1865 ft

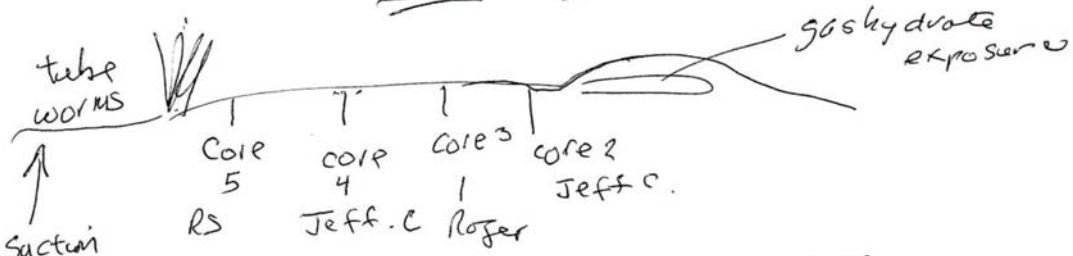

Suction Sediment bucket 9
Calcite-cemented sediment, nodules.
0935

Short core penetration ~ 20 cm.

6. Explored. 0950 nearby hydrate site #2. Thin white veins, thick deformed orange veins, odd carbonate nodules. Took Push core #6. FIX 9 immediately in front of hydrate mass.

7. Passed huge carbonate rock large colonies of tube worms, odd gas vents FIX 10

8. Sampled carbonate slabs FIX, 11–12

9. Spoted gas hydrate over 3. FIX 13 Took core 6 near hydrate.

To left.

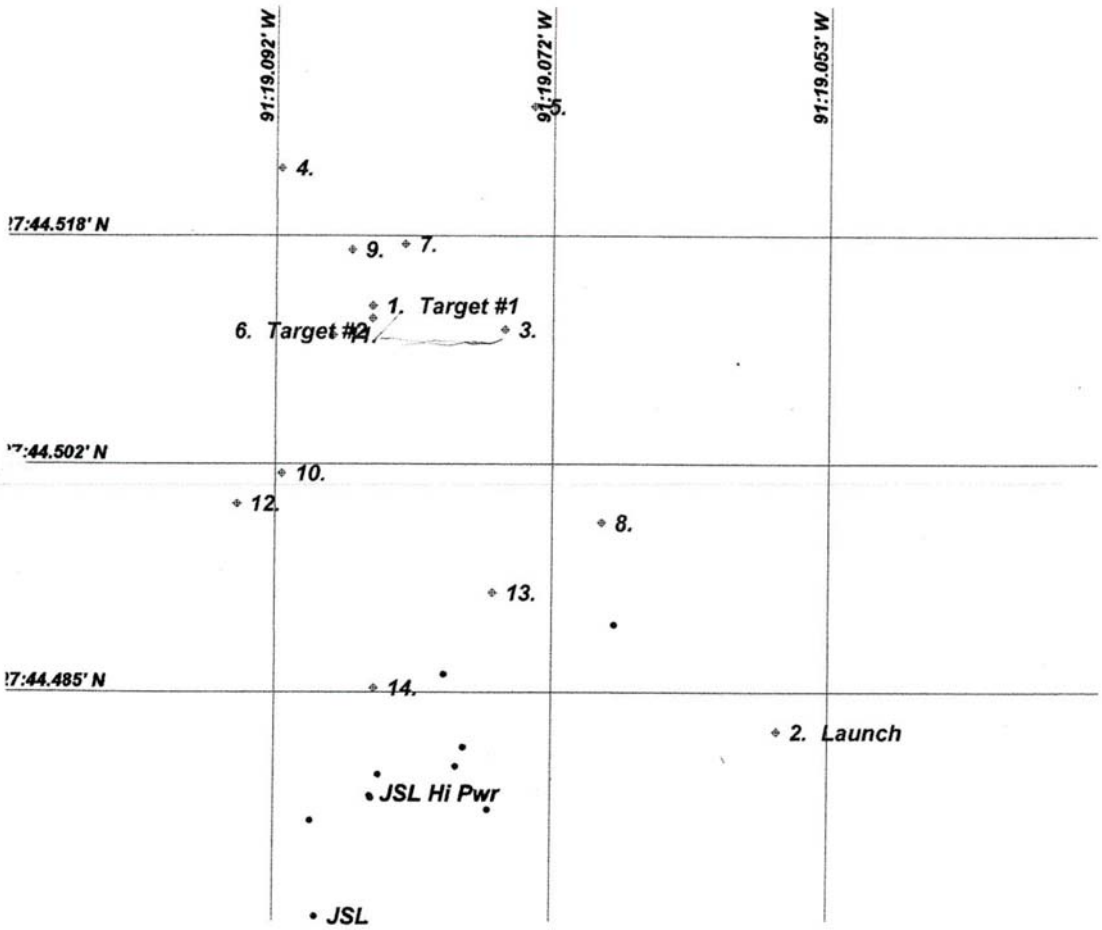
91:19.092' W
91:19.072' W
91:19.053' W
5.
4.
7:44.518' N
9.
7.
1. Target #1
6. Target #2
3.
7:44.502' N
10.
12.
8.
13.
7:44.485' N
14.
2. Launch
JSL Hi Pwr
JSL

ORE Interenational. IPS: WayPoint Report 5/29/2002 11:04:47

C:\Program Files\ORE\1-4401

RVSJ 2 & JSL 1-4401

1. Ship 7:52:57 N 27:44.5129 W 91:19.0851 0 ft Target #1
2. Ship 8:03:27 N 27:44.4825 W 91:19.0562 0 ft Launch
3. Target [1] 8:31:02 N 27:44.5112 W 91:19.0757 1870 ft On Bottom -Water Sample
4. Target [1] 8:36:25 N 27:44.5227 W 91:19.0916 1869 ft Tube Worm Samples
5. Target [1] 8:50:35 N 27:44.5271 W 91:19.0737 1871 ft Bacterial Sample tube #1
6. User 8:54:59 N 27:44.5120 W 91:19.0851 1871 ft Target # 2
7. Target [1] 9:07:30 N 27:44.5173 W 91:19.0828 1866 ft Exposed Hydrate
8. Target [1] 9:28:02 N 27:44.4974 W 91:19.0687 1865 ft 4-push cores
9. Target [1] 9:58:35 N 27:44.5169 W 91:19.0866 1865 ft Exposed Hydrate-# 6 Push Core
10. Target [1] 10:17:07 N 27:44.5009 W 91:19.0915 1867 ft Large Area of Tube Worms
11. Target [1] 10:26:35 N 27:44.5108 W 91:19.0879 1867 ft Small Rocks
12. Target [1] 10:46:10 N 27:44.4987 W 91:19.0947 1870 ft Exposed Tube Worms & Rock
13. Target [1] 10:51:30 N 27:44.4924 W 91:19.0765 1868 ft Large Exposed Hydrate & Worms
14. Target [1] 11:00:00 N 27:44.4856 W 91:19.0849 1867 ft Leaving Bottom

LOUISIANA STATE UNIVERSITY

SUBMERSIBLE DIVE LOG

Dive Number: 4402 & 4403 (4402 ABORTED)

Date: 29 May 2002

Location: GC 232

Time:		DIVE #4402	DIVE #4403
	start	15:34	16:03
	end	15:45	19:26

Maximum Depth: 1871 FEET (feet or meters)

Personnel: CRAIG CAMPBELL, DAN McCONNELL } sphere HUGO MARRERO, MARK BRAUSSE

Mission/Dive Objective: PUSH CORES ON TRANSECT FROM GAS HYDRATE outcrop, and from TUBE WORM colony. Sample BACTERIAL MATS and MUSSELS

Photographs:	Hand held camera	Sub-mounted camera
Roll # / Frame #'s	~10 frames	~10-15 frames

Video: Tape # 3 TAPES

Sampling (type) PUSH CORES, SUCTION, GRAB

Mapping none

Equipment emplacement (type) none

Other

Comments - If sampling was done or equipment emplaced, please give a brief description including: how many samples/pieces of equipment, type, depth(s), etc.

JSL 4402-
ABORTED DUE TO BUCKET implosion, AT ABOUT 300 ft.
CAUSED JAM ON BUCKET platform.
RECOVERED SUB- REPAIRED BUCKET PLATFORM JAM

JSL 4403
5/29/02

Fix 3 (3) BOTTOM 1871' - UNEVEN SEAFLOOR. TUBEWORM BUSHES COVER MOST of surface - spaced ABOUT 2 TO 10 ft APART PATCHES of white bacterial MATS COVER ground BETWEEN TUBE WORM BUSHES.

Fix 4 (4) Exposed gas HYDRATE, LOOKS yellowish. IS AT BASE OF MOUND. MOUND IS ABOUT 2 ft HIGH. HAS ROUNDED BUT IRREGULAR SHAPE. MASS OF GAS HYDRATE CROPPING OUT AT BASE OF MOUND is ABOUT 1.5 x 6 inches.

Fix 5 (7) BEGIN PUSH CORE TRANSECT AWAY FROM GAS HYDRATE OUTCROP. PUSHCORE #1 ABOUT 2 FT TO LEFT of gas HYDRATE OUTCROP. PUSH CORE #2 ABOUT 4 FT TO LEFT OF PUSH CORE #1. PUSH CORE #3 ABOUT 4 FT TO LEFT OF PUSH CORE #2. Oil seep OBSERVED AT PUSH CORE #3

Fix 8. BUSHES OF TUBE WORMS COVER A HYDRATE MOUND - GAS HYDRATE CROPS OUT AT BASE OF MOUND. ABOUT 15 ft TO Right OF PUSHCORES 1, 2, and 3

PUSH CORE SAMPLES ON TRANSECT 120° FROM TUBE WORM BUSH.

Fix 9 GAS SAMPLE. 1862' GAS HYDRATE VENT APPEARS TO COME FROM HOLE IN GAS HYDRATE MASS. BURPED TUBE. SET GAS CATCH TUBE OVER VENT. Small sporadic BUBBLES. ABORTED BECAUSE GAS BUBBLES TOO few.

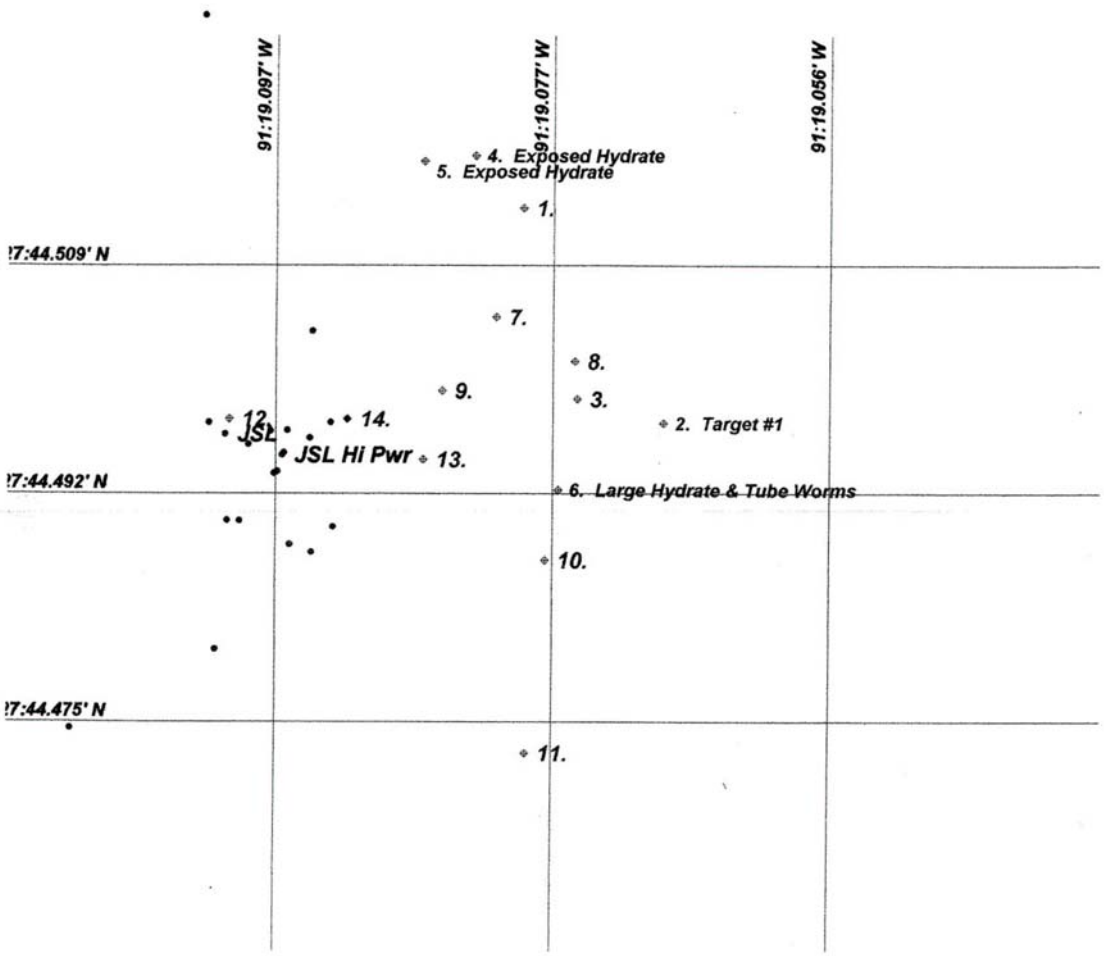
91:19.097' W
91:19.077' W
91:19.056' W
4. Exposed Hydrate
5. Exposed Hydrate
1.
7:44.509' N
7.
8.
9.
3.
12.
14.
2. Target #1
JSL
JSL Hi Pwr
13.
7:44.492' N
6. Large Hydrate & Tube Worms
10.
7:44.475' N
11.

Fix 10. 1866' SAMPLED WHITE BACTERICAL MAT and RED BACTERIAL MAT.

BUCKET #10 - WHITE BACTERICAL MAT

Fix 11 BUCKET #12 - RED BACTERICAL MAT

BUCKET #11 - RED BACTERICAL MAT ABOUT 1ft DIAMETER

Fix 11 is ~~at~~ RED BACTERICAL MAT FOUND IN TRANSIT TO FIND GAS VENT.

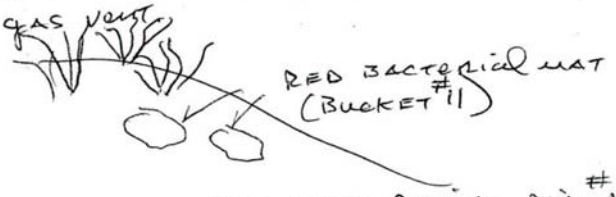

IN TRANSIT TO GAS VENT FOUND DURING DIVE #4401
FLEW OVER GAS HYDRATE MASS FOUND DURING #4401
LOOKING AROUND FOR VENTS.

Fix 12 1867'

GRABBED MUSSELS - PUT IN BUCKET #2
(SOME MAY HAVE spilled OVER TO BUCKET #9)

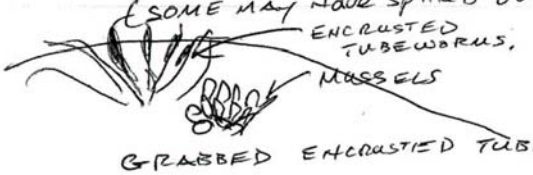

GRABBED ENCRUSTED TUBEWORMS PUT IN BASKET.

Fix 13 1867'ft

GAS SAMPLE TUBE TO PILOT'S RIGHT (BEHIND BASKET) WAS FIRST SAMPLE.

FOUND SMALL VENT AT BASE of TUBEWORM colony. GAS HYDRATE CROPPING OUT AT SEAFLOOR. FILLED TUBE WITH GAS SAMPLE. FILLED SECOND GAS SAMPLE FROM SAME VENT. THIS SECOND SAMPLE IN TUBE TO PILOT'S LEFT. MUSSELS GROWING AT BASE OF OUTCROPPING GAS HYDRATE. TUBE WORMS BUSHES ALL AROUND AREA.

Fix 14 LEAVING BOTTOM.

GAS OBSERVED COMING FROM all PUSH CORES especially from PUSH CORES 1, 2, and 3.

ORE Interenational. IPS: WayPoint Report 5/29/2002 19:06:09

C:\Program Files\ORE\1-4403_trk

RVSJ 2 & JSL Hi Pwr

1. Ship 16:03:13 N 27:44.5134 W 91:19.0792 0 ft Launch
2. User 16:06:29 N 27:44.4974 W 91:19.0687 0 ft Target #1
3. Target [1] 16:30:41 N 27:44.4992 W 91:19.0751 1871 ft On Bottom
4. Target [1] 9:07:30 N 27:44.5173 W 91:19.0828 1866 ft Exposed Hydrate
5. Target [1] 9:58:35 N 27:44.5169 W 91:19.0866 1865 ft Exposed Hydrate-# 6 Push Core
6. Target [1] 10:51:30 N 27:44.4924 W 91:19.0765 1868 ft Large Exposed Hydrate & Worms
7. Target [1] 16:59:46 N 27:44.5053 W 91:19.0812 1865 ft Punch Core #1,2,3
8. Target [1] 17:09:22 N 27:44.5020 W 91:19.0753 1865 ft Punch Cores #4,5,6
9. Target [1] 17:22:18 N 27:44.4998 W 91:19.0852 1862 ft Gas Sample
10. Target [1] 17:33:22 N 27:44.4872 W 91:19.0775 1866 ft Bacterial Mat - grab sample
11. Target [1] 17:54:01 N 27:44.4728 W 91:19.0789 1870 ft Suction Sample Bacterial Mat
12. Target [1] 18:18:57 N 27:44.4977 W 91:19.1010 1867 ft grabbing mussels and tubeworm
13. Target [1] 18:42:09 N 27:44.4947 W 91:19.0866 1867 ft Gas sample
14. Target [1] 19:03:29 N 27:44.4977 W 91:19.0922 1867 ft Leaving Bottom

LOUISIANA STATE UNIVERSITY

SUBMERSIBLE DIVE LOG

Dive Number: 4404 Date: May 30, 2002

Location: GC 232 hydrate site

Time: start 8:16 am - launch

end 11:51 am - on seasurface

Maximum Depth: 1870 (feet or meters)

Personnel: Alexei Milkov Tylez
Don Libezatore

Mission/Dive Objective: Sample gas and gas hydrate

Photographs:	Hand held camera	Sub-mounted camera
Roll #	~ 15 shots (digital)	~60 shots
Frame #'s		

Video: Tape # 3

Sampling (type) push cores, suction, grab, gas samples, gas hydrate samples

Mapping n/a

Equipment emplacement (type) n/a

Other

Comments - If sampling was done or equipment emplaced, please give a brief description including: how many samples/pieces of equipment, type, depth(s), etc.

See attached

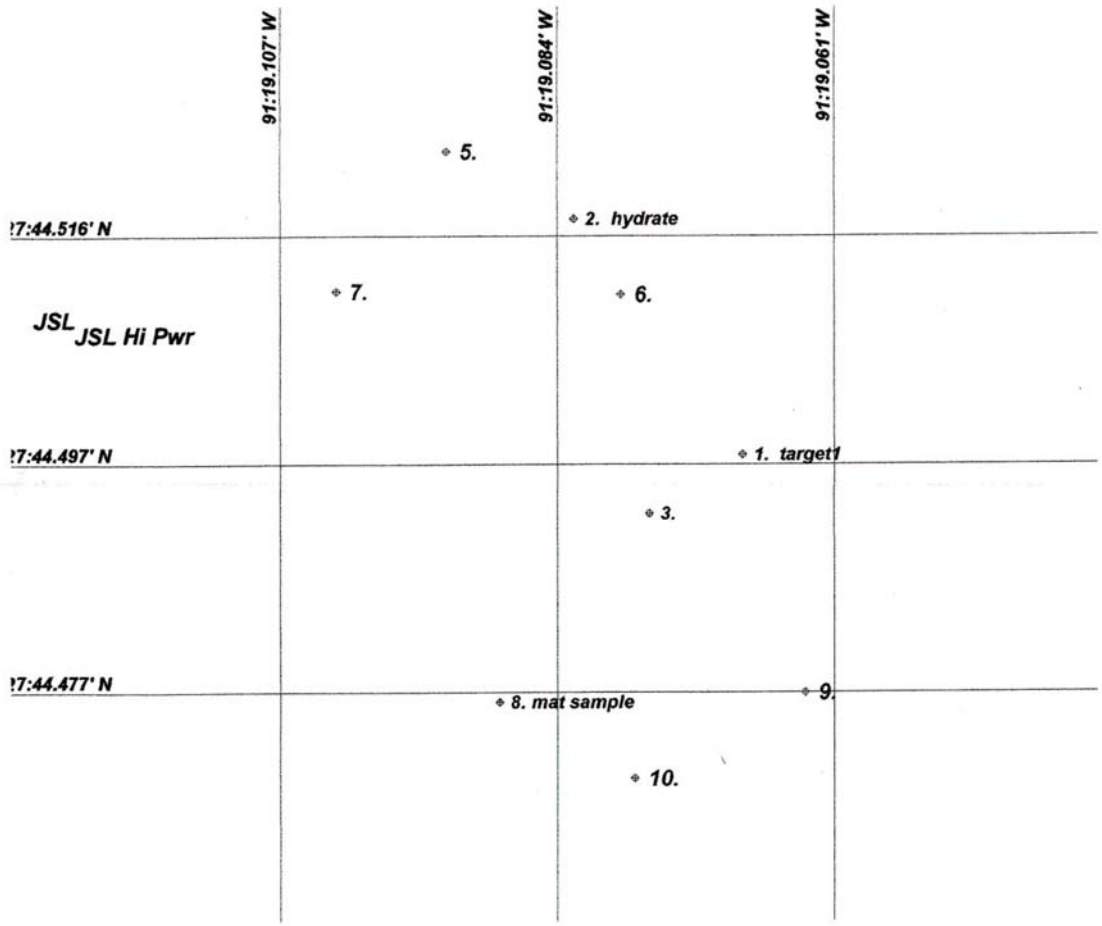
91:19.107' W
91:19.084' W
91:19.061' W
5.
2. hydrate
?7:44.516' N
7.
6.
JSL
JSL Hi Pwr
?7:44.497' N
1. target1
3.
?7:44.477' N
8. mat sample
9.
10.

ORE Interenational. IPS: WayPoint Report 5/30/2002 11:46:34

C:\Program Files\ORE\1-4404_trk

RVSJ 2 & JSL 1-4404

1. User 16:06:29 N 27:44.4974 W 91:19.0687 0 ft Target #1
2. Target [1] 9:07:30 N 27:44.5173 W 91:19.0828 1866 ft Exposed Hydrate
3. Target [1] 10:51:30 N 27:44.4924 W 91:19.0765 1868 ft Large Exposed Hydrate & Worms
4. Ship 8:18:21 N 27:44.4904 W 91:19.0068 0 ft launch
5. Target [1] 8:47:05 N 27:44.5230 W 91:19.0936 1866 ft on bottom
6. Target [1] 8:57:08 N 27:44.5109 W 91:19.0789 0 ft shooting photos
7. Target [1] 10:22:50 N 27:44.5112 W 91:19.1028 0 ft Push core
8. Target [1] 10:50:50 N 27:44.4765 W 91:19.0891 0 ft sample orange mat
9. Target [1] 10:56:46 N 27:44.4773 W 91:19.0634 1865 ft Grab Sample
10. Target [1] 11:08:46 N 27:44.4701 W 91:19.0777 1866 ft push core and sample tube worm

Dive 4404 GC 232 (2)

1) Collected water samples for Jeff (Chandon) every 200 feet from surface to bottom. At seafloor: 8:47 am, T = 7.4 °C, D = 1866.4, S = 34.94

2) 8:50 Went through a mound ~2 m high covered with individual bush hills

3) Fix #6 Exposed gas hydrate (gh) mound ~0.5 m long, 0.4 m wide. Gas bubble trains coming from 3 or 4 individual small vents. Gas hydrate is orange on the exposed surface (it's white on fresh surface). Gh is located inside a depression (~1.2 m long, ~0.5 m wide). Gh is outcropping at one side of the depression, the other side is partly covered with sediment and partly exposed. The preliminary interpretation is that a half of the original mound broken and floated away (Fig.1)

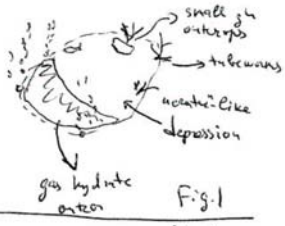

Fig.1

Another gas hydrate outcrop is ~1.5-2 m away (Fig.2). Gas is coming out from the second outcrop too, but is much less abundant and episodic. The preliminary interpretation is that the entire area represents a "hydrate" ridge (~20 m long, ~5 m wide, but the dimensions are hard to identify from the sub).

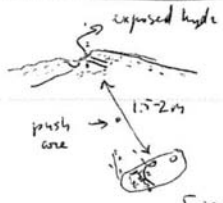

Fig.2

4) 9:05 Taking gas samples D = 1866.4, T = 7.39, S = 34.92
Gas bubbles are relatively small (~0.5 cm), do not change in size when go up (~2 m vic
continuous flow, no oil droplets. When we took a first sample, we broke some hydr
and it went up. The first sample was dumped (reverse the tube) because we did not
and hydrate inside the tube. Got a new gas sample in presumably clean tube. Gas
bubbles appear not rounded, but rather oval (⬭). Gas sample was finally collec
at 9:20 am, the tube (~3.5 in diam) has a gas/water interface right below the
white cap (~2 in high gas column).

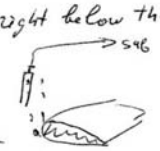

Gas hydrate mound has some tubeworms inside, but not much, and only individuums, not bushes. Pilot noticed some oil droplets coming out the sediment.

5) 9:30 Took ~20 still shots of the mound with bubbles.

6) 9:33 Start getting a hydrate sample. Took a large piece (~50 cm?) in the arm (no chipper), put it in the sampler, one piece of the gh went down into

the sampler. Tryed to put in second piece, but lost it, the piece floated away. Used the chipper to push the first piece inside. Tryed to put the lead on, did not succeed first time. Cleaned the surface of the sampler (pump, reverse pump (wash)). Tryed to put the lead on again - successful. Sample is taken at 10:05.

7) 10:00 Took a push core right between two gh mounds in a depression. The core went out easily, no hard material. Push core #1. Close look at second gh outcrop indicates that ice worms are present inside the gh. We took ~12 pictures. Ice worms are 0.5 in long, 10-15 species in orange gas hydrate. We sucked some ice worms into <u>bucket #5</u> (suction sample) at 10:15 am <u>Push core #1</u> is taken between two outcrops of gh, next to small individual tubeworms. Oil and gas vent up from the hole made by the push core. Bubbling stoped when we got the core up. It was <u>Fix # 7</u>

8) 10:35 Going to explore around the mound. See white bacterial mats and individual tubeworm bushes. Worms do not live on mats, only on clean brown seafloor. TW <u>bact. mat</u> TW

9) 10:40 Found a little (~20 cm across) orange (red, rose) bacterial mat. Took ~10 shots Thick mat (several mm). Collected suction sample in <u>Bucket # 7</u> (Fix # 8) Depth 1867.3

10) 10:55 Depth = 1865 Took 3 grab samples next to tubeworm bush. Fix # 9

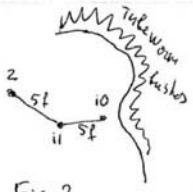

Fig. 3

<u>Bucket # 10</u> is right next to the TW bush

<u>Bucket # 11</u> is ~5 feet from # 10 further from TW

<u>Bucket # 12</u> is another ~5 feet from # 11 (Fig. 3)

11) 11:08 Depth 1866, Fix 10, Taking push core for geotechnical analysis between two TW hills

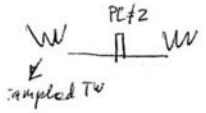

Fig. 4

<u>Push core # 2</u> is taken near TWs, poor slow penetration, apparently there is something hard in sediments (Fix # 10)

12) 11:15 Took tubeworms next to the push core (~1m apart), put them in the front bucket (Fig. 4)

13) 11:30 Going up. Gas is coming out <u>push core # 1</u>

14) 11:51 - Sea surface !!!

LOUISIANA STATE UNIVERSITY

SUBMERSIBLE DIVE LOG

Dive Number: 4405 Date: 5/30/02

Location: GC 232

Time: start 3:48 pm (began descent)

end 6:59 pm (left bottom)

Maximum Depth: 1868 ft (feet or meters)

Personnel: Don / Laura front

/ Jeff back

Mission/Dive Objective: To deploy porewater sampler, collect 3 cores, gas sample + grab bacteria mat sediments in grabber.

Photographs: Hand held camera Sub-mounted camera

Roll #

Frame #'s ~5 pics..

Video: Tape # 3 tapes

Sampling (type) porewater + sediment.

Mapping

Equipment emplacement (type)

Other

Comments - If sampling was done or equipment emplaced, please give a brief description including: how many samples/pieces of equipment, type, depth(s), etc.

During Descent @ 3:48pm.

Saw jellys at ~300ft deep, a shark about 2ft long was seen near bottom.

Saw bottom ~1840 ft

Hydrate mound visited (~~at 1. exposed~~ was hydrate outcropping very near (we could see it from the sub) the outcropping where ice worms were found on dive 4405. fix 5

Found spot to set probe in mud. Deployed probe - it sank to the bottom of tubing ~ 2 cm above the PVC lip. Values triggered at 4:33 pm. At 5:03, ~~the probe~~ ~~and~~ was put back in quiver + valves closed ~~at 5:03pm~~. Don used the side of the scooper to close 20 values. Need to make tubing longer so the probe can be turned. It took ~ 20 min to close values. fix 6

fix 7 Core #4 taken next to probe - not much there

Core #3 taken ~ 2 ft from probe - nice size core.

At 5:40pm, gas sample was taken above hydrate outcropping. While we were sitting on bottom looking at bubble streams, new ones kept forming - it was quite a site... how does one get a gas flux here?! Secured gas sampler at 5:50pm.

Put rock sitting right next to hydrate mound in bucket #2. It looks like light grey w/ lots of holes - maybe lithification around tube worms - Harry R. said.

While sampling for rock, we bumped the hydrate outcrop + it moved - very unstable. gas/oil streams coming from all over. Some constant flow, some spiradic others had little bits of oil coming out.

Core #2 taken in hydrate crevas. Actually cored the hydrate! We didn't want this though. Shaked out hydrate + cored about 2 feet off hyd. mound. Nice core.

Had some time to kill - let's get some bacterial mats! Found some white mats, took scoop + put in bucket #4.

Found a rock outcropping + took a chunk off - bucket #6. Also took scoop of seds next to rock outcrop b/c lots of shells. - bucket #8. (fix 8)

Found large rock + put in basket - it had shells, tubeworms + maybe some coral on it.

Bucket #10 was filled w/ orange bacterial mat found on way to see clam beds. (fix 9)

Dive ended at 6:59 pm @ 1867 ft. (fix 10)

While ascending, core #2 bubbed like mad, core #3 began to degas at the surface + the probe didn't bubble - it looked great!

see back for map.

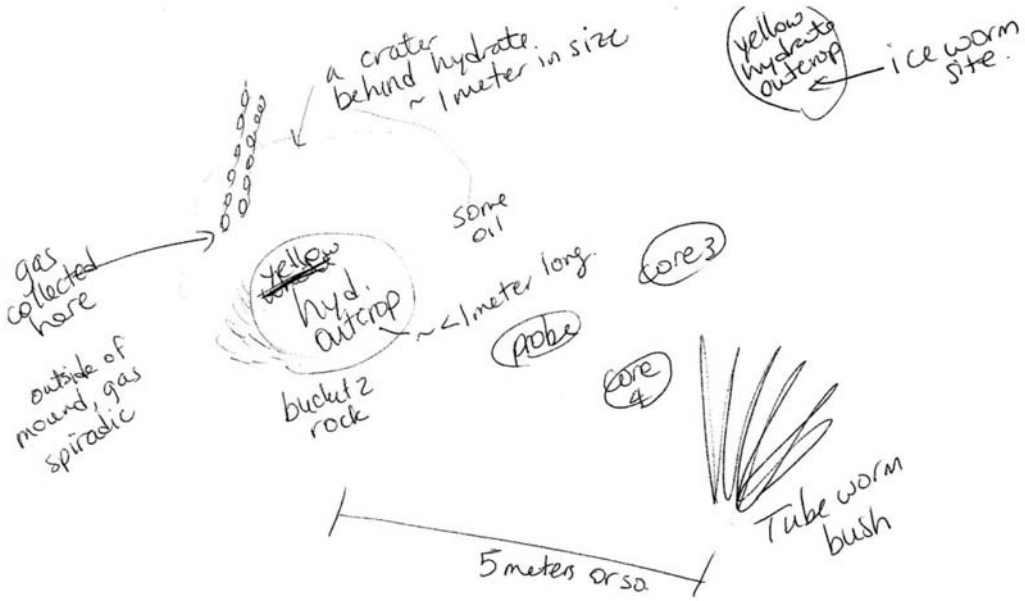
a crater behind hydrate ~ 1 meter in size
yellow hydrate outcrop
ice worm site.
some oil
gas collected here
yellow hyd. outcrop
~<1 meter long
core 3
probe
core 4
outside of mound, gas spiradic
bucket 2 rock
Tube worm bush
5 meters or so

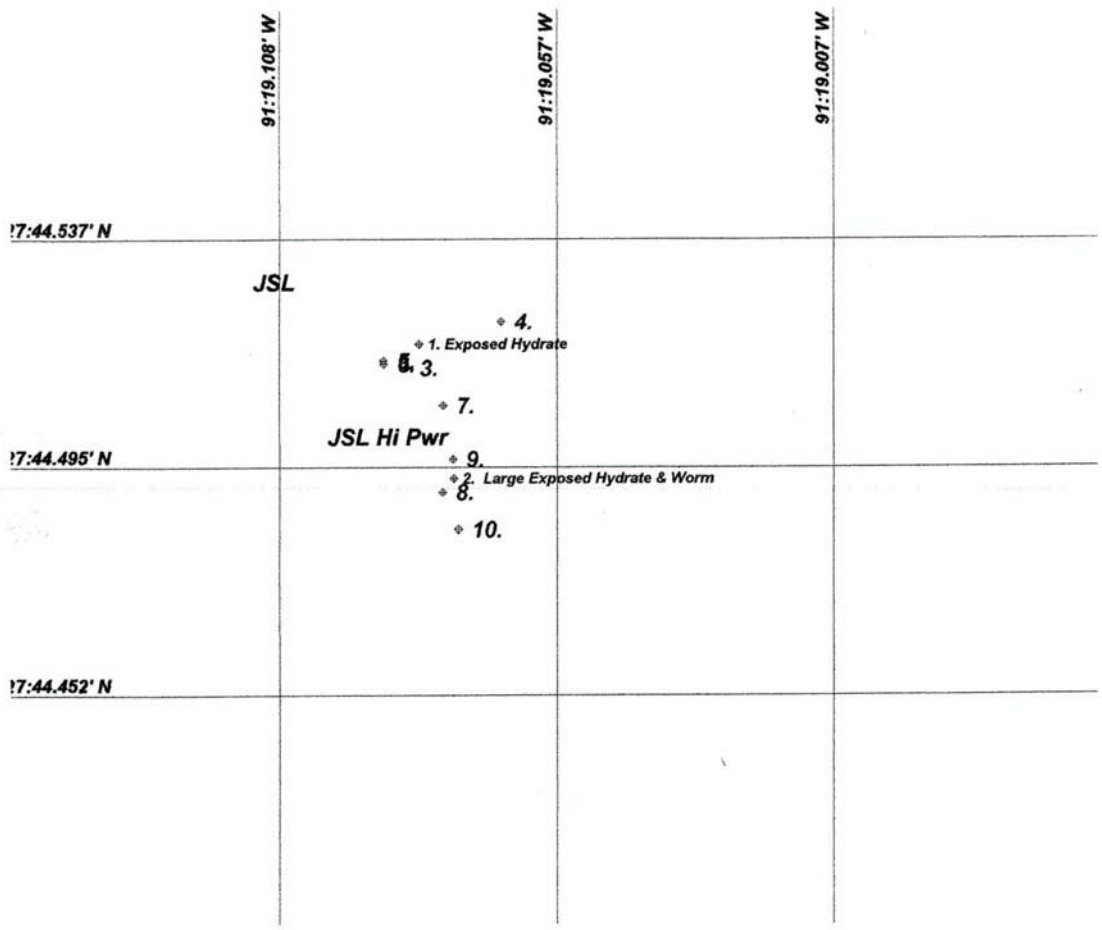
91:19.108' W
91:19.057' W
91:19.007' W
?7:44.537' N
JSL
4.
1. Exposed Hydrate
6.
3.
7.
JSL Hi Pwr
?7:44.495' N
9.
2. Large Exposed Hydrate & Worm
8.
10.
?7:44.452' N

ORE Interenational. IPS: WayPoint Report 5/30/2002 19:09:09

C:\Program Files\ORE\1-4405

RVSJ 2 & JSL 1-4405

1. Target [1] 9:07:30 N 27:44.5173 W 91:19.0828 1866 ft Exposed Hydrate
2. Target [1] 10:51:30 N 27:44.4924 W 91:19.0765 1868 ft Large Exposed Hydrate & Worms
3. User 15:49:23 N 27:44.5129 W 91:19.0851 1864 ft Target 1
4. Ship 15:49:56 N 27:44.5214 W 91:19.0677 1855 ft Launch
5. Target [1] 16:21:01 N 27:44.5142 W 91:19.0893 1862 ft On Bottom
6. Target [1] 16:26:23 N 27:44.5136 W 91:19.0893 1867 ft Deploy water probe
7. Target [1] 17:18:48 N 27:44.5059 W 91:19.0784 1867 ft Punch core
8. Target [1] 18:31:17 N 27:44.4899 W 91:19.0785 1864 ft scoop and rock sample
9. Target [1] 18:44:12 N 27:44.4960 W 91:19.0766 1864 ft sample orange mat
10. Target [1] 18:55:08 N 27:44.4830 W 91:19.0756 1867 ft leaving bottom

LOUISIANA STATE UNIVERSITY

SUBMERSIBLE DIVE LOG

Dive Number: 4406 Date: 31 May 02

Location: GC 234

Time: start 8:01 AM

end 11:48 Surface

Maximum Depth: (feet or meters)

Personnel: Roger Sassen Kelly Peeler

Dan Boggess Hugo Marrero

Mission/Dive Objective: hydrate, gas, sediment

Photographs: Hand held camera Sub-mounted camera

Roll #
Frame #'s ~~only a~~ only a few 35 mm

Video: Tape # 1 and 2 (#3 malfunctioned)

Sampling (type) pressure bomb/chipper + gas sampler

Mapping n/a

Equipment emplacement (type) n/a

Other n/a

Comments - If sampling was done or equipment emplaced, please give a brief description including: how many samples/pieces of equipment, type, depth(s), etc.

see next sheets

ORE Interenational. IPS: WayPoint Report 5/31/2002 11:48:25

C:\Program Files\ORE\1-4406

Dive #4406 Green Canyon ~~#243~~ 234 31 May 02

1. Ship 8:01:17 N 27:44.7543 W 91:13.3406 0 ft Launch
2. User 8:12:56 N 27:44.7700 W 91:13.3400 1746 ft Target 1
3. Target [1] 8:32:30 N 27:44.7422 W 91:13.4194 0 ft Bottom Report
4. Target [1] 8:37:50 N 27:44.7766 W 91:13.3613 0 ft Org. Mat Sample
5. Target [1] 9:02:07 N 27:44.7587 W 91:13.3101 0 ft Gas Sample & Hydrate
6. Target [2] 11:18:56 N 27:44.7448 W 91:13.3201 0 ft Leaving Bottom 1777ft.
7. Target [1] 11:44:48 N 27:44.7797 W 91:13.4166 0 ft Surfaced

GC 234 Dive 4406
31 May 02

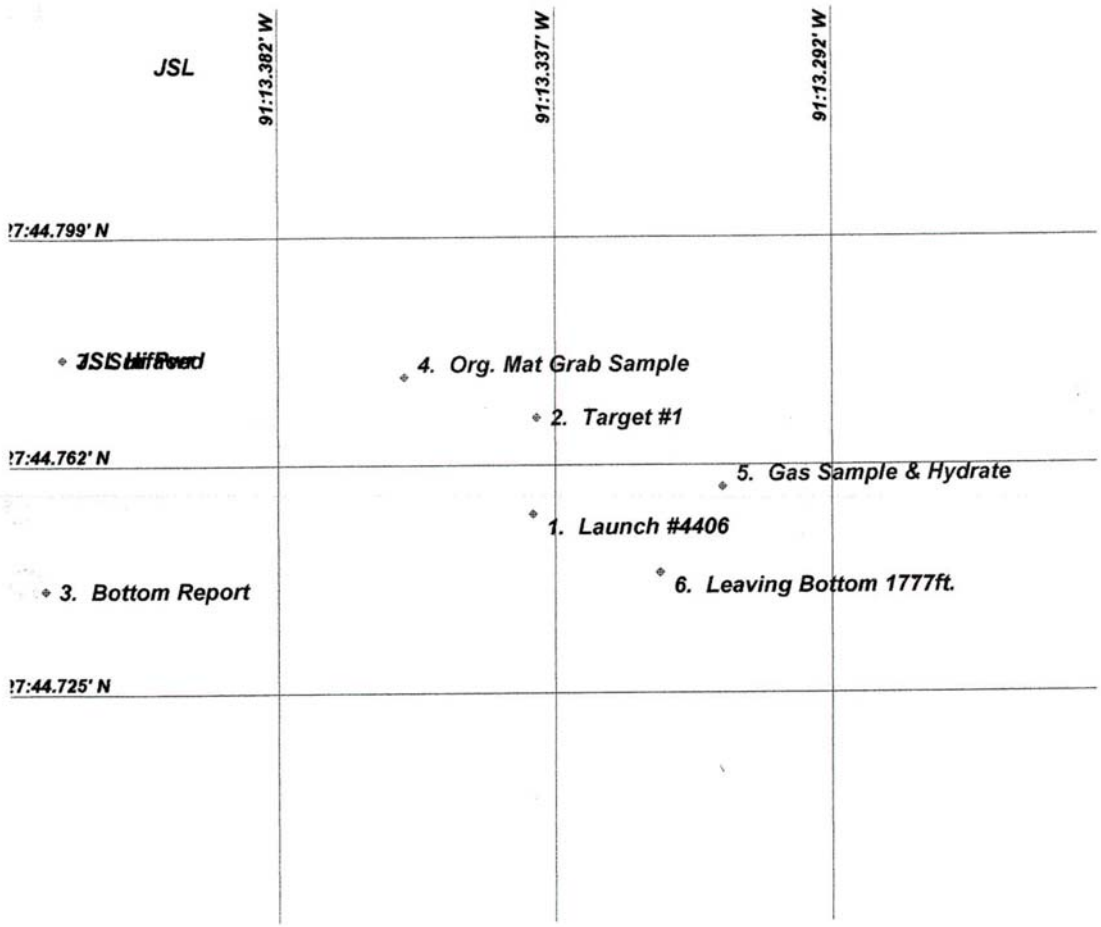

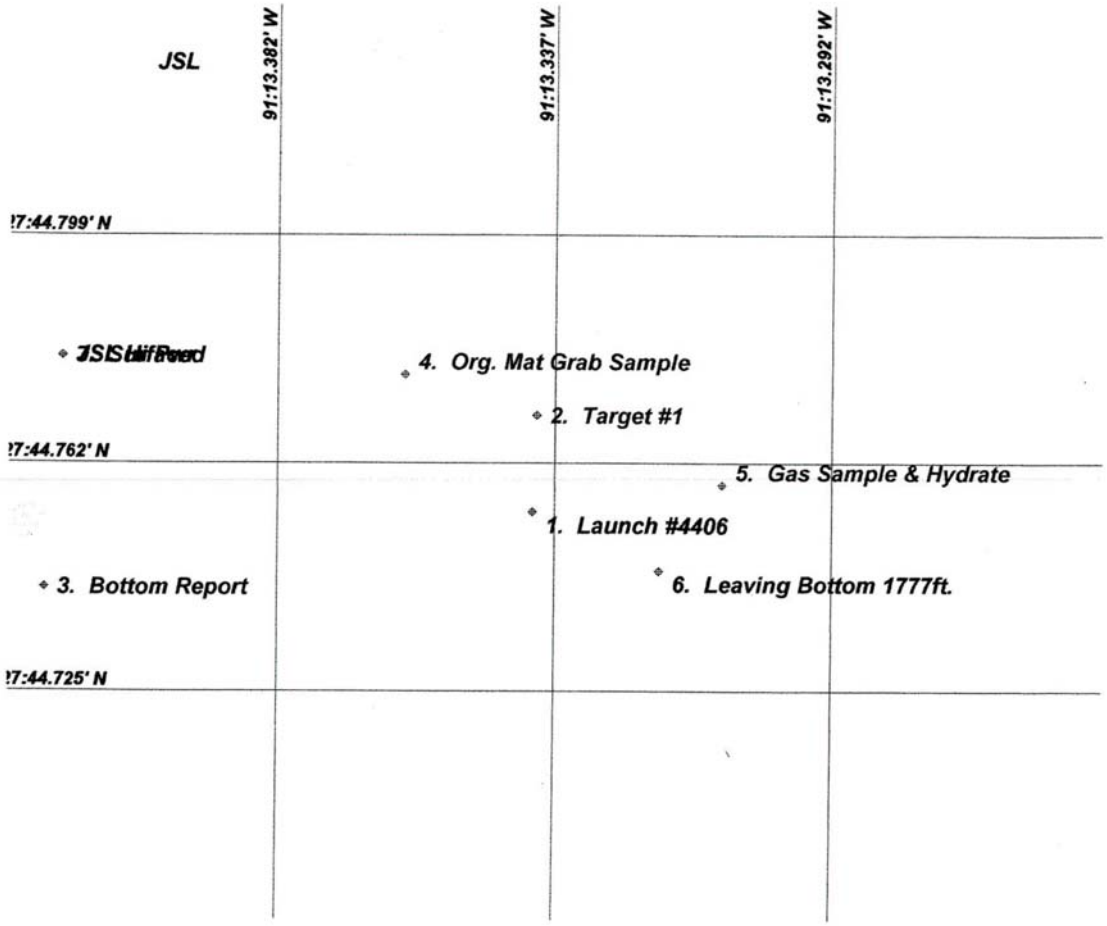
JSL
91:13.382' W
91:13.337' W
91:13.292' W
!7:44.799' N
4. Org. Mat Grab Sample
2. Target #1
!7:44.762' N
5. Gas Sample & Hydrate
1. Launch #4406
3. Bottom Report
6. Leaving Bottom 1777ft.
!7:44.725' N

ORE Interenational. IPS: WayPoint Report 5/31/2002 11:48:15

C:\Program Files\ORE\1-4406

Dive #4406 Green Canyon #243

1. Ship 8:01:17 N 27:44.7543 W 91:13.3406 0 ft Launch
2. User 8:12:56 N 27:44.7700 W 91:13.3400 1746 ft Target 1
3. Target [1] 8:32:30 N 27:44.7422 W 91:13.4194 0 ft Bottom Report
4. Target [1] 8:37:50 N 27:44.7766 W 91:13.3613 0 ft Org. Mat Sample
5. Target [1] 9:02:07 N 27:44.7587 W 91:13.3101 0 ft Gas Sample & Hydrate
6. Target [2] 11:18:56 N 27:44.7448 W 91:13.3201 0 ft Leaving Bottom 1777ft.
7. Target [1] 11:44:48 N 27:44.7797 W 91:13.4166 0 ft Surfaced

4406 GC234 Recon dive

1. took water samples for J. Chatonon way down and on bottom at 1714 ft.

2. observed gorgonians, carbonate rock, small white mats, burrows, tracks, oil 0830 photographs.

3. Grab sample orange mat at 0835-0840 Bucket 8 - 1762 ft.

4. main hydrate site at 0850, 1778 ft

5. Aquired ventgas sample with 0.1 m of bottom. Grew gas hydrate in tube.

6. After great struggle, obtained multiple samples of gas hydrate from outcrop. See Harry's note book for precise site description.

7. found "ice worm" with hydrate + "unknown" worm species.

PS 31 May 02

LOUISIANA STATE UNIVERSITY

SUBMERSIBLE DIVE LOG

Dive Number: 4407 Date: 5/31/02

Location: Green Canyon 234

Time: start 1603

end ?

Maximum Depth: (feet or meters)

Personnel: Dan + Jeff Chanton

Hugo + Howard Mendoutz

Mission/Dive Objective: 6 cores on a transect away from hydrate
Obtain mat, deploy ion pump, sample carbonate,
collect water sample profile, deploy ion pump

Photographs: Hand held camera Sub-mounted camera
took ~ 15 pictures

Roll #
Frame #'s

Video: Tape # 1, 2 + 3

Sampling (type) cores, mat, water, rocks

Mapping no

Equipment emplacement (type) ion pump pore water sampler

Other

Comments - If sampling was done or equipment emplaced, please give a brief description including: how many samples/pieces of equipment, type, depth(s), etc.

see next page

4407 Cont

Fix #1

16^{38} MAT SAMPLING orange MAT to BAG #9
SAMPLER stuck – wouldnt open

Fixed SAMPLER

16^{58} fix #2 suctioned orange mat into Bag #9
seemed to work very well
several still frames of mat taken with
subs camera (still camera)

1722 fix #3 just off to left of hydrate mound
5 ft to left of it 1777m depth
MARKER "RI" on bottom
collected tube cores #1 + 2. 10cm veneer of
sediment over rock or hydrate ice

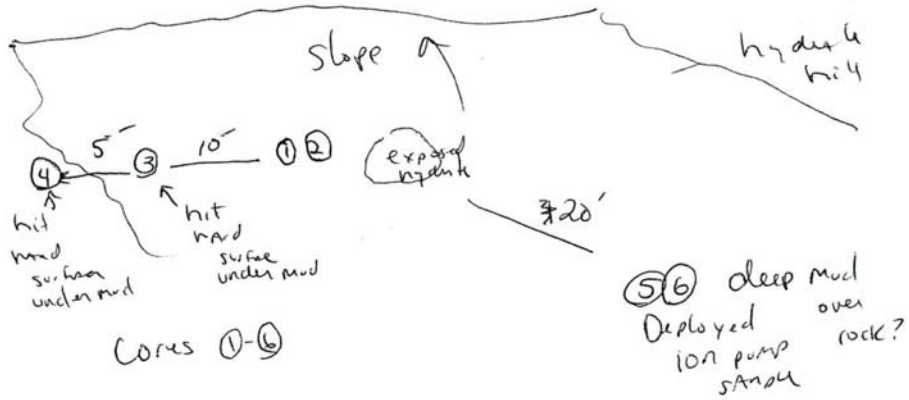

18^{15} 1776m collected gas sample
SAME site

18^{22} Rock sample to Bucket #12

Over

Fix

1768m Bucket 11 large mesh screen sample
mat blew away

1768 ft
1827 pm – Rock sample from sparse tube worm area
to basket (Big Rock)

1830 Another try at mat – no go

1761 ft Fix
Basket #11 got more orange mat
sample

lots globs of floating oil.

ORE Interenational. IPS: WayPoint Report 5/31/2002 19:01:21

C:\Program Files\ORE\1-4407

Dive # 4407 Green Canyon # 234

1. Ship 16:06:17 N 27:44.7614 W 91:13.3365 0 ft Launch #4407
2. User 17:01:07 N 27:44.7906 W 91:13.3467 0 ft Bottom
3. User 17:01:47 N 27:44.7700 W 91:13.3400 0 ft Target #1
4. Target [1] 17:02:35 N 27:44.7882 W 91:13.3426 0 ft Red Mat Sample 1759ft.
5. Target [1] 17:21:31 N 27:44.7531 W 91:13.3119 1777 ft punch core near hydrate
6. Target [1] 17:50:23 N 27:44.7563 W 91:13.3078 1784 ft punch core #5
7. Target [1] 18:27:11 N 27:44.7723 W 91:13.3104 0 ft Rock Sample
8. Target [1] 18:59:34 N 27:44.7341 W 91:13.3003 0 ft Leaving Bottom

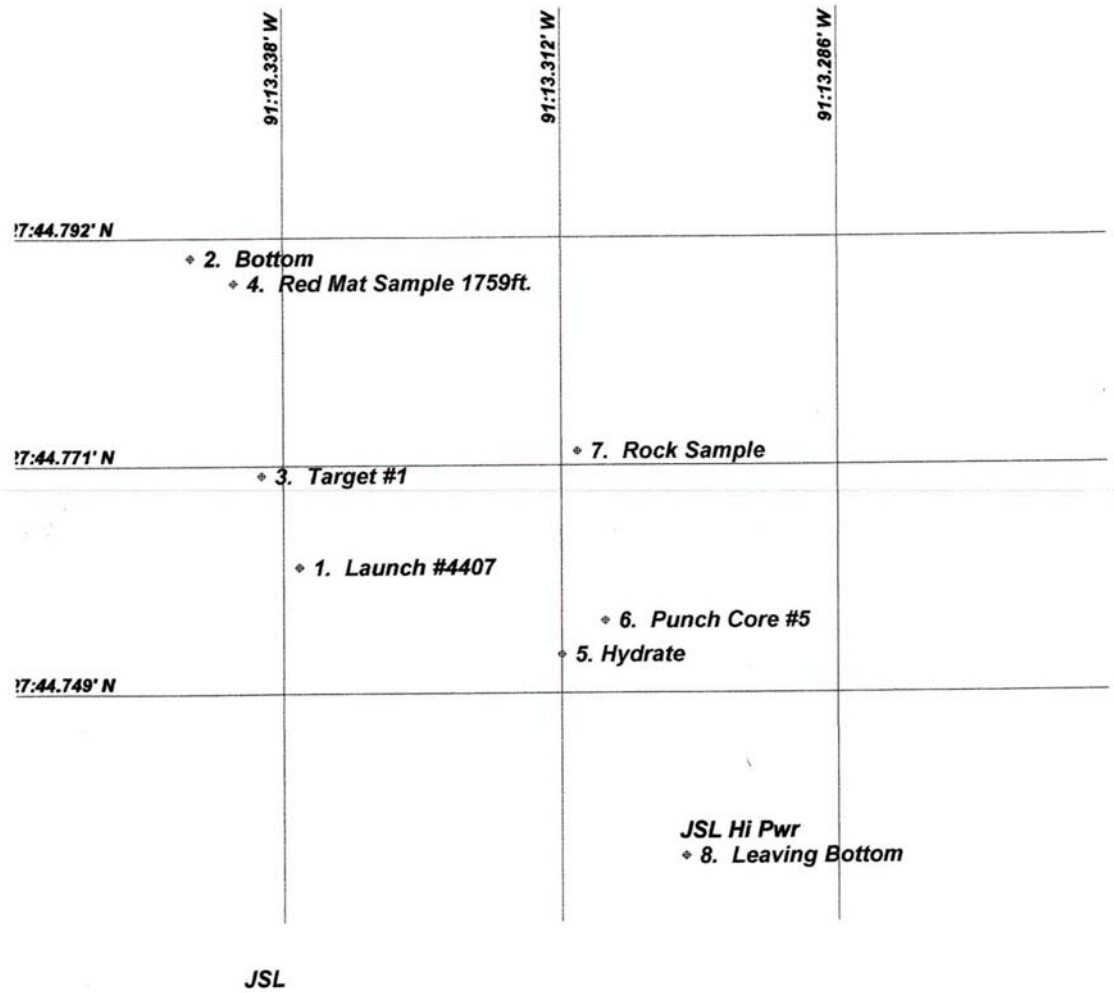
91:13.338' W
91:13.312' W
91:13.286' W
!7:44.792' N
2. Bottom
4. Red Mat Sample 1759ft.
!7:44.771' N
7. Rock Sample
3. Target #1
1. Launch #4407
6. Punch Core #5
5. Hydrate
!7:44.749' N
JSL Hi Pwr
8. Leaving Bottom
JSL

LOUISIANA STATE UNIVERSITY

SUBMERSIBLE DIVE LOG

Dive Number: 4408 Date: 6/1/02

Location: MC 885 "JAKE" site

Time: 8:03:56 start

11:40:12 end

Maximum Depth: 2160' (feet or meters)

Personnel: Dick Fillon, Barry Kohl, Craig Caddigan, Frank Palumbo

Mission/Dive Objective:

Photographs: Hand held camera Sub-mounted camera

35 mm ~ 20 exposures

Roll #

Frame #'s

Video: Tape #

Sampling (type) Push cores (4) + Grab samples (2) plus + (1 failed attempt)

Mapping —

Equipment emplacement (type)

Other – Searched for thermistor probe deployed in 1998 — unsuccessful!

Comments - If sampling was done or equipment emplaced, please give a brief description including: how many samples/pieces of equipment, type, depth(s), etc.

one push core failed due to hard substrate obtained grab sample at that location.

08:32h on bottom - WD: 2160 ft. - soft burrowed bottom
with 0.4 knot current from 030°
08:34h Fix#7 (ON BOTTOM)
08:47h push core #1 (Tube #6) - full penetration
08:55h same bottom type 2124 ft. - new course 020°
rare starfish, brittle star, small octopus - 08:56h.
08:58h changed course to correct lateral drift
08:59h digital camera shots.
09:00h sub-35mm camera shots
* 09:18h first gorgonians w/ brittle stars seen -
bottom still flat - but gorgonians suggest
09:17h Fix#8 shallowly underlain by hard substrate.
09:21h → push core #2 (Tube #5) 2079 ft.
09:25 gorgonians @ 2077 ft. on rim of dip
09:27 climbing out of dip - 35mm shots.
09:30 Calyptogena shell hash @ 2055 ft.
crossing series of ridges topped w/ Gorgonians

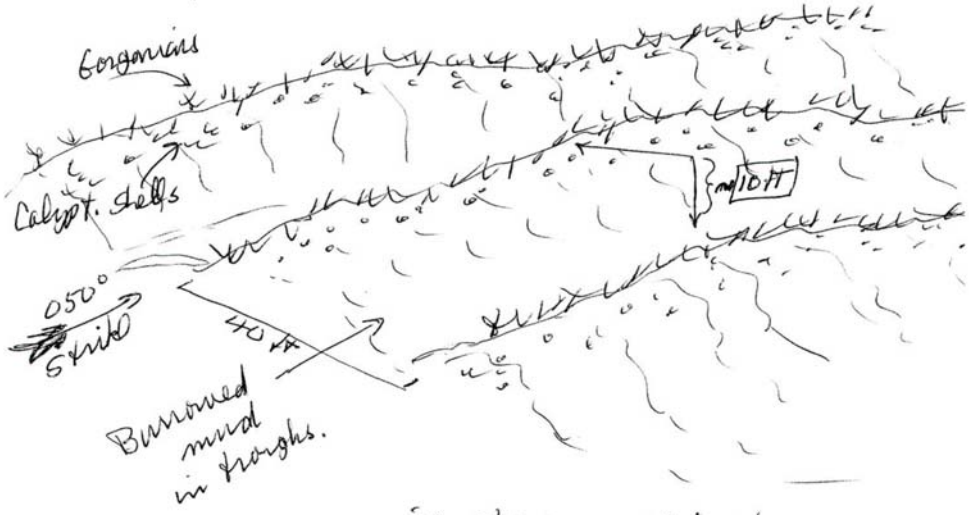

09:39h changed videotape - put in tape 2.

09:53 Fix #9 push core #3 (Tube #4)

09:45 – Steep-sided mound w/ tube worms + Acesta – outcropping carbonate.

09:47 – bearing change. to 025° @ 2045 ft.

push core 09:55h – aborted due to lack of penetration caused by hard substrate.

09:58 – Grab sample #1 (bucket #4) @ 2038 ft.

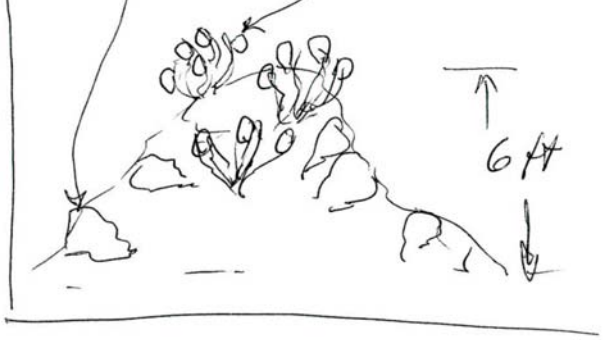

Consistent shell hash (Calyptogena)

10:00h underway after grab sample

10:04h Acesta attached to small rocks outcrop

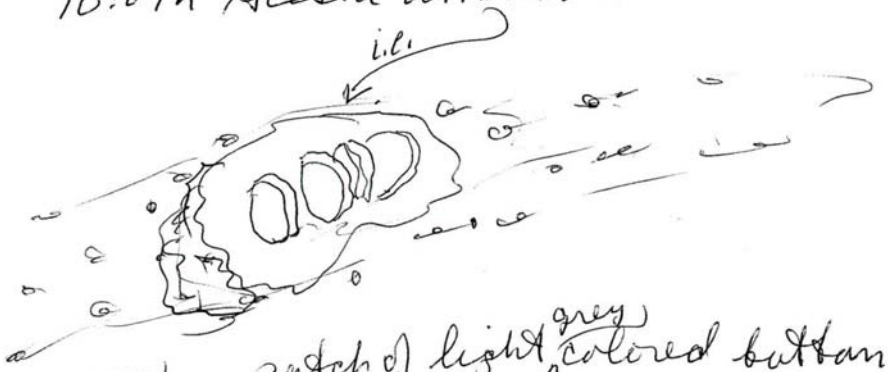

10:14h – patch of light grey colored bottom – possible shallowly buried hydrate @ 2066 ft. – ~6 ft x 3 ft

10:15h – featureless mud bottom w/ rock marks furrows – digital camera shots.

10:24:55h FIX#10 [illegible]
10:24h Pushcore #4 (Tube#4) full penetration
@10:25:23h @ 2065.3ft. 6.8°C.

10:29h underway on new course 150°
still shell hash distributed patchily over bottom.

10:27h 35mm photos

10:33h shell hash out starboard port

10:34h Rare patchy Gorgonians

10:37h Acesta on tube worms

10:40h Gorgonians on rock, shell hash w/ large gaping Calyptogenas - dead but in growth position - @ 2048ft.

10:45h Featureless bottom

10:50:55h FIX#12 - Pushcore.

10:52h Push core #5 (Tube #3) full penetration
2/3 recovery. @ 2075ft.

10:52h featureless bottom <10% burrowed

10:55h underway due north (000°)

11:01h mud bottom w/ burrows @ 2071ft.

11:09h featureless mud bottom - Grab sample #2
(Bucket #6)

11:10:12h FIX#13

11:11h leave bottom.

ORE Interenational. IPS: WayPoint Report 6/1/2002 11:16:19

C:\Program Files\ORE\1-4408_trk

RVSJ 2 & JSL I Dive 4408

1. User 7:23:48 N 28:04.0830 W 89:43.3170 2140 ft SOL
2. User 7:24:10 N 28:04.0062 W 89:43.1667 2140 ft WP 1
3. User 7:24:41 N 28:03.9670 W 89:42.7500 2140 ft WP 2
4. User 7:25:01 N 28:03.9500 W 89:42.5170 2140 ft WP 3
5. User 7:25:23 N 28:03.7000 W 89:42.4000 2140 ft EOL
6. User 8:03:56 N 28:04.0497 W 89:43.2765 0 ft Launch
7. User 8:34:00 N 28:04.0403 W 89:43.3787 2160 ft Bottom fix
8. Target [1] 9:17:51 N 28:03.9712 W 89:43.0429 2080 ft Long push core PC 2
9. Target [1] 9:53:19 N 28:03.9611 W 89:42.7557 2037 ft Long push core PC 3 (aborted) GS 1
10. Target [1] 10:24:55 N 28:03.9564 W 89:42.5319 2066 ft Push core #4 PC 4
11. User 10:47:45 N 28:03.7699 W 89:42.3825 0 ft Change hdg to 200 deg
12. Target [1] 10:50:55 N 28:03.6664 W 89:42.4005 2075 ft Push core #3 PC 5
13. User 11:10:12 N 28:03.7227 W 89:42.4090 2063 ft Grab sample - leaving bottom GS 2

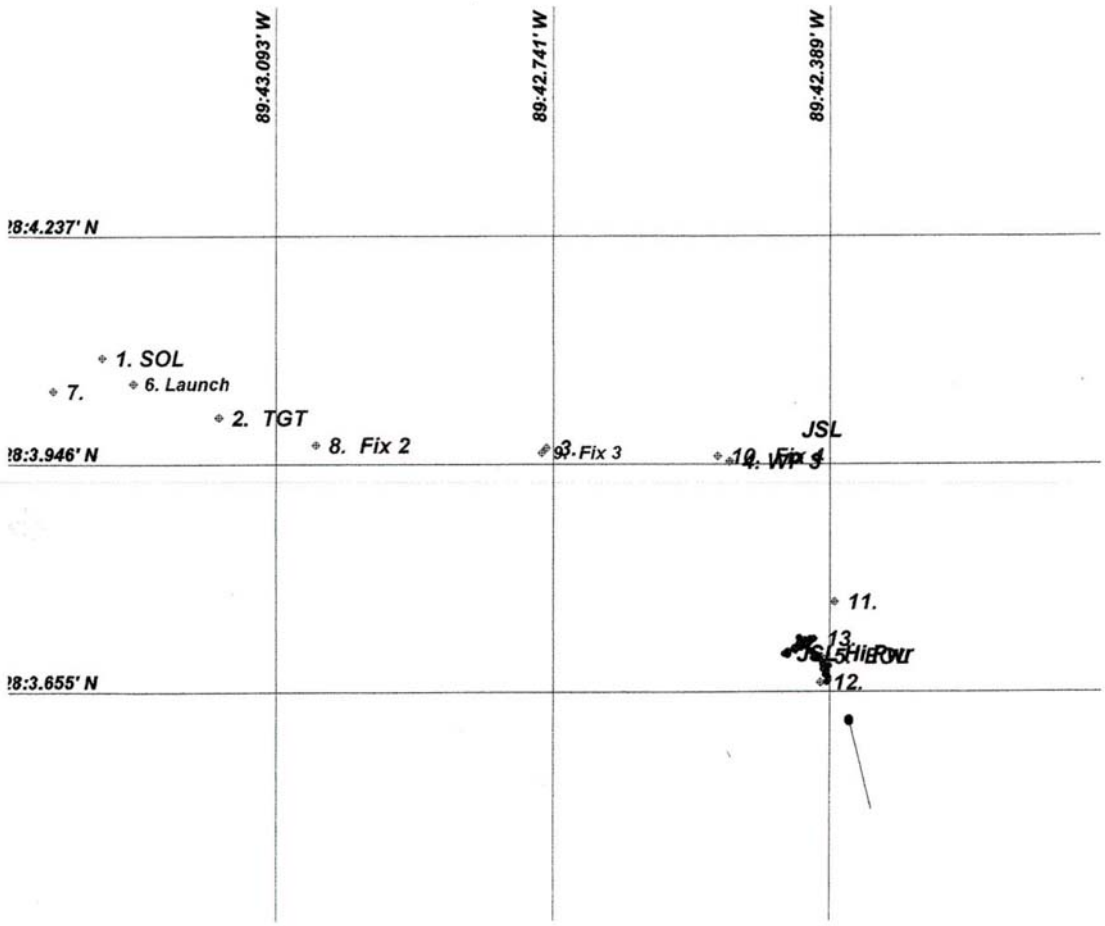
89:43.093' W
89:42.741' W
89:42.389' W
28:4.237' N
28:3.946' N
28:3.655' N
1. SOL
6. Launch
7.
2. TGT
8. Fix 2
3. Fix 3
JSL
11.
13.
12.

LOUISIANA STATE UNIVERSITY

SUBMERSIBLE DIVE LOG

Dive Number: 4409 Date: 6/1/02

Location: MC 885

Time: start 1540

end 1801

Maximum Depth: 2104' (feet or meters)

Personnel: Pilot GREG Bob Woolsey, Forward Sci. Obs.

Aft Obs. Frank Tyler Hodges, Aft Sci. Obs

Mission/Dive Objective:

Photographs: Hand held camera Sub-mounted camera

Roll #

Frame #'s

Video: Tape # 1 ROLL (#4409)

Sampling (type) Cores (5) ; Clam 1 (acesta) ; Gorgonians (3)

Mapping

Equipment emplacement (type) Recovered Thermister Probe

Other

Comments - If sampling was done or equipment emplaced, please give a brief description including: how many samples/pieces of equipment, type, depth(s), etc.

Sample Stops:

No. 1: one Core #3 ; 1 large Gorgonian ; 1 clam ; Map pt. 9

No. 2: Cores #1 & #4 ; 1 med size Gorgonian + rock hold fast ; Map Pt. #10

No. 3: Core #5 ; Map Pt. #13

No. 4: Core #6 ; Gorgonian + rock hold fast (small) ; Map Pt. #16

JSL DIVE 4409
Date: 6/1/02
Forward: Woolsey
Aft: Hodges

Time	Discription
1514	Commense Dive
1608	on bottom, dpt. -2087.5', t-6.82° sal. 34.89
	Bottom cond's - Mud, ~~flat~~ flat to undulating, bioturbated, surface with burrows and mounds, 10 to 20 per sq. meter: Type A
1611	Commense Traverse C-060°
1614	CC-150°, dpt 2088', T 6.82° Bottom-Type A
1618	C 150°, dpt. 2068', Bottom type A
1623	CC 155°, dpt. 2070', t 6.81°, Bottom type A
1624	Bottom - type A with lone small rock (auth. carb.) with gorgonian; dpt. 2064', t 6.82°
1630	Bottom - type A with numerous carbonat rocks, (.15 x .5 m, long axis) with attached gorgonians! Type B - New bottom type designation
	Sample Stop #1 samples: 1) large gorgonian with hold fast rock; 2) large accesta clam (with bissel attachment to base of rock - torn loose in sampling); 3) Push core in mud, #3
1640	Depart Stop #1, resume traverse; bottom, type A C 155°
1644	Bottom type A with patches of clam shell hash, no visable live clams; dpt. 2067'
1646	CC 220°; Bottom type A + shell hash

1647 - Bottom type B + clam sh. hash

1648 - cc 330°

1649 - way pt. #1, Bottom type A; dpt. 2063'

1651 - cc 150°

1703 - Bottom type A, but steeper slopes ~5-10°; decended to 2104' lowest point

1705 - Bottom type A with lone gorgonian

1708 - On top of gentle rise, dpt 2052', t 6.80°

1711 - Bottom type A + scattered, small gorgonians (no visable rock hold fast), clam sh. hash, dpt 2049'

1716 - New bottom type; ridges and runnels, smooth mud surfaces, bioturbate as in type A with clam shell hash and gorgonians / carb. rock hold fast, ridge & runnel relief, 5 to 10', orientation - open crescentric to SE; dpt 2040'. New bottom type designated Type C

1720 - Sample Stop #2; dpt. 2040, t 6.81°, bottom of runnel
Samples: 1) push core (short) #1 (Hit burried rock on first attempt - made full core second attempt) - mud
2) push core (long) #4 - full core - mud
3) gorgonian (med.) + rock hold fast + egg cases

1730 - Depart Stop #2, resume traverse, c 150°; dpt 2046'; t 6.81'
Bottom type C

1734 cc 220°, large tenaphore ~.3-.5 m, bottom type A + occaisional gorgonians

1736 Bottom type C, ridge segment orientation NW-SE

1740 cc 195°

1742 Bottom type A, dpt 2058'

1744 Bottom type C, (NW-SE), dpt. 2060'

1747 Sample Stop #3, top of ridge: sample, one push core #5 full core, mud; dpt 2064'

1750 Dept. stop #3, resume traverse; c 195°

1754 Bottom type A + occaisional gorgonians & clam sh. hash dpt. 2068, T 6.86°, Sal. 34.90; cc 150°

(OVER)

1758 Bottom type C; Advised in vicinity of Thermister station, commence search

1804 Sample Stop #4; dpt. 2061.3' - Top of ridge
Samples: 1) push core #6 (long) - first attempt encountered rock below mud surface - relocated ~10', second attempt successful - full core, mud
2) gorgonian (small) + rock held fast

1812 Sampling operation complete, resume search for Thermister, ∠ 280°

1845 Found Thermister on ridge top, dpt. 2061.5

1831 Thermister Probe safely onboard, departing bottom: Dive Complete

ORE Interenational. IPS: WayPoint Report 6/1/2002 18:35:06

C:\Program Files\ORE\1-4409_trk_wpt

RVSJ 2 & JSL 1 dive 4409, 1928 ft squares

1. User 12:47:10 N 28:04.7000 W 89:42.8330 2100 ft SOL
2. User 12:47:30 N 28:04.4170 W 89:42.8000 2100 ft WP 1
3. User 12:47:56 N 28:03.9670 W 89:42.7500 2100 ft WP 2
4. User 12:48:19 N 28:03.7061 W 89:42.8664 2100 ft WP 3
5. User 12:48:40 N 28:03.5670 W 89:43.0500 2100 ft EOL
6. Target [1] 15:40:05 N 28:04.5120 W 89:43.3480 0 ft Launch
7. Target [1] 16:08:44 N 28:04.6908 W 89:42.8598 2087 ft On Bottom
8. Target [1] 16:23:54 N 28:04.5735 W 89:42.7919 2068 ft Bottom Small Outcroppings
9. Target [1] 16:29:21 N 28:04.4861 W 89:42.7767 2066 ft Gorgonians & Punch Core #3
10. Target [1] 17:27:28 N 28:03.9825 W 89:42.7463 0 ft Push core #1 & #4 & rock
11. Target [1] 17:36:03 N 28:03.9060 W 89:42.7587 2052 ft Gorgonians & shell hash
12. Target [1] 17:40:11 N 28:03.8602 W 89:42.8101 0 ft New hdg 195 deg
13. Target [1] 17:46:05 N 28:03.7866 W 89:42.8436 2064 ft Push core #5
14. Target [1] 17:53:20 N 28:03.7607 W 89:42.8731 2064 ft Change hdg to 170 deg
15. Target [1] 17:55:36 N 28:03.7231 W 89:42.8782 0 ft Change hdg to 160 deg
16. Target [1] 18:05:22 N 28:03.7116 W 89:42.8518 2061 ft ~~Tried~~ push core #6
17. Target [1] 18:23:59 N 28:03.6917 W 89:42.8765 2052 ft Thermistor
18. Target [1] 18:28:39 N 28:03.6863 W 89:42.8649 0 ft Leaving Bottom

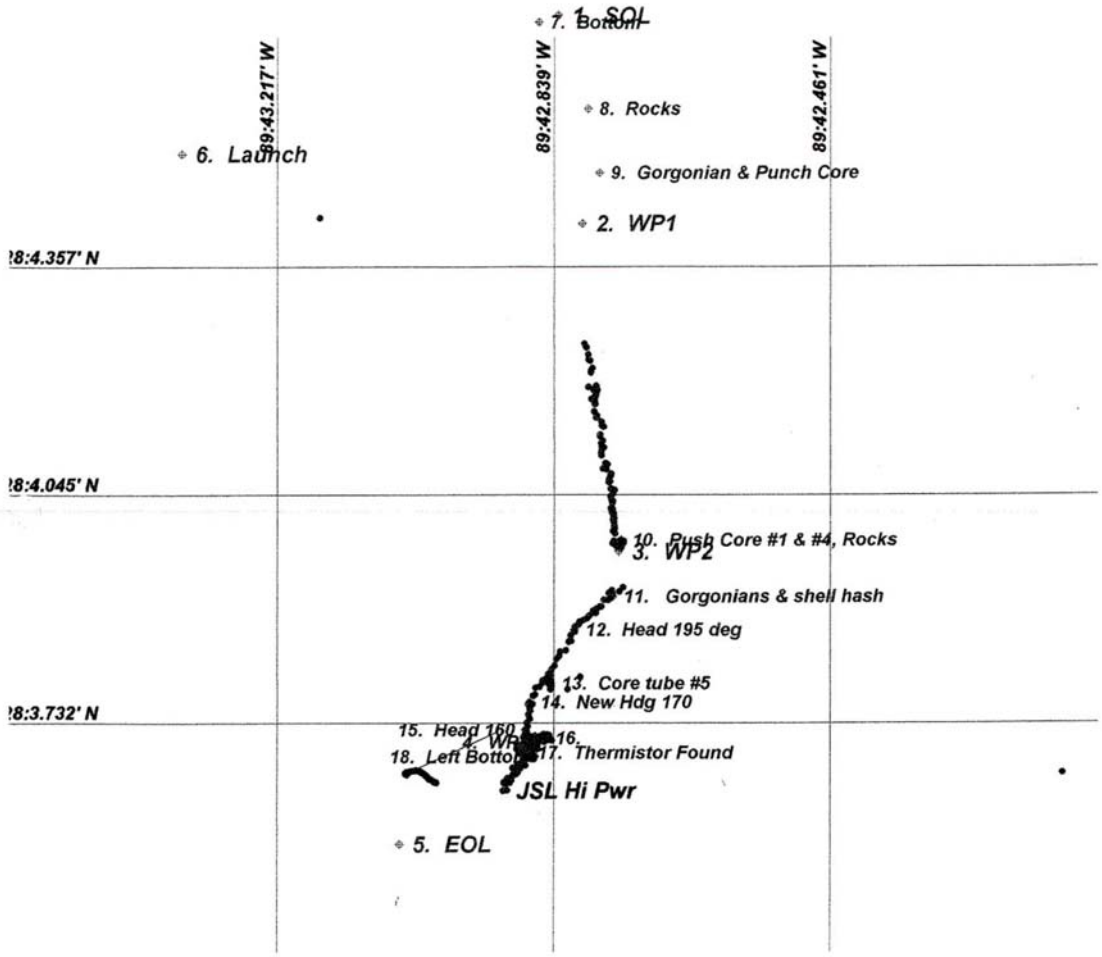
7. Bottom
1. SOL
89:43.217' W
89:42.839' W
89:42.461' W
8. Rocks
6. Launch
9. Gorgonian & Punch Core
2. WP1
8:4.357' N
8:4.045' N
10. Push Core #1 & #4, Rocks
3. WP2
11. Gorgonians & shell hash
12. Head 195 deg
13. Core tube #5
14. New Hdg 170
8:3.732' N
15. Head 160
16.
17. Thermistor Found
18. Left Bottom
JSL Hi Pwr
5. EOL

ORE Interenational. IPS: WayPoint Report 6/1/2002 18:44:38

C:\Program Files\ORE\1-4409_trk_wpt

RVSJ 2 & JSL 1 dive 4409, 1899 ft squares

1. User 12:47:10 N 28:04.7000 W 89:42.8330 2100 ft SOL
2. User 12:47:30 N 28:04.4170 W 89:42.8000 2100 ft WP 1
3. User 12:47:56 N 28:03.9670 W 89:42.7500 2100 ft WP 2
4. User 12:48:19 N 28:03.7061 W 89:42.8664 2100 ft WP 3
5. User 12:48:40 N 28:03.5670 W 89:43.0500 2100 ft EOL
6. Target [1] 15:40:05 N 28:04.5120 W 89:43.3480 0 ft Launch
7. Target [1] 16:08:44 N 28:04.6908 W 89:42.8598 2087 ft On Bottom
8. Target [1] 16:23:54 N 28:04.5735 W 89:42.7919 2068 ft Bottom Small Outcroppings
9. Target [1] 16:29:21 N 28:04.4861 W 89:42.7767 2066 ft Gorgonians & Punch Core
10. Target [1] 17:27:28 N 28:03.9825 W 89:42.7463 0 ft Push core #1 & #4 & rock
11. Target [1] 17:36:03 N 28:03.9060 W 89:42.7587 2052 ft Gorgonians & shell hash
12. Target [1] 17:40:11 N 28:03.8602 W 89:42.8101 0 ft New hdg 195 deg
13. Target [1] 17:46:05 N 28:03.7866 W 89:42.8436 2064 ft Push core #5
14. Target [1] 17:53:20 N 28:03.7607 W 89:42.8731 2064 ft Change hdg to 170 deg
15. Target [1] 17:55:36 N 28:03.7231 W 89:42.8782 0 ft Change hdg to 160 deg
16. Target [1] 18:05:22 N 28:03.7116 W 89:42.8518 2061 ft Tried push core (2nd attempt successful - core #6)
17. Target [1] 18:23:59 N 28:03.6917 W 89:42.8765 2052 ft Thermistor
18. Target [1] 18:28:39 N 28:03.6863 W 89:42.8649 0 ft Leaving Bottom

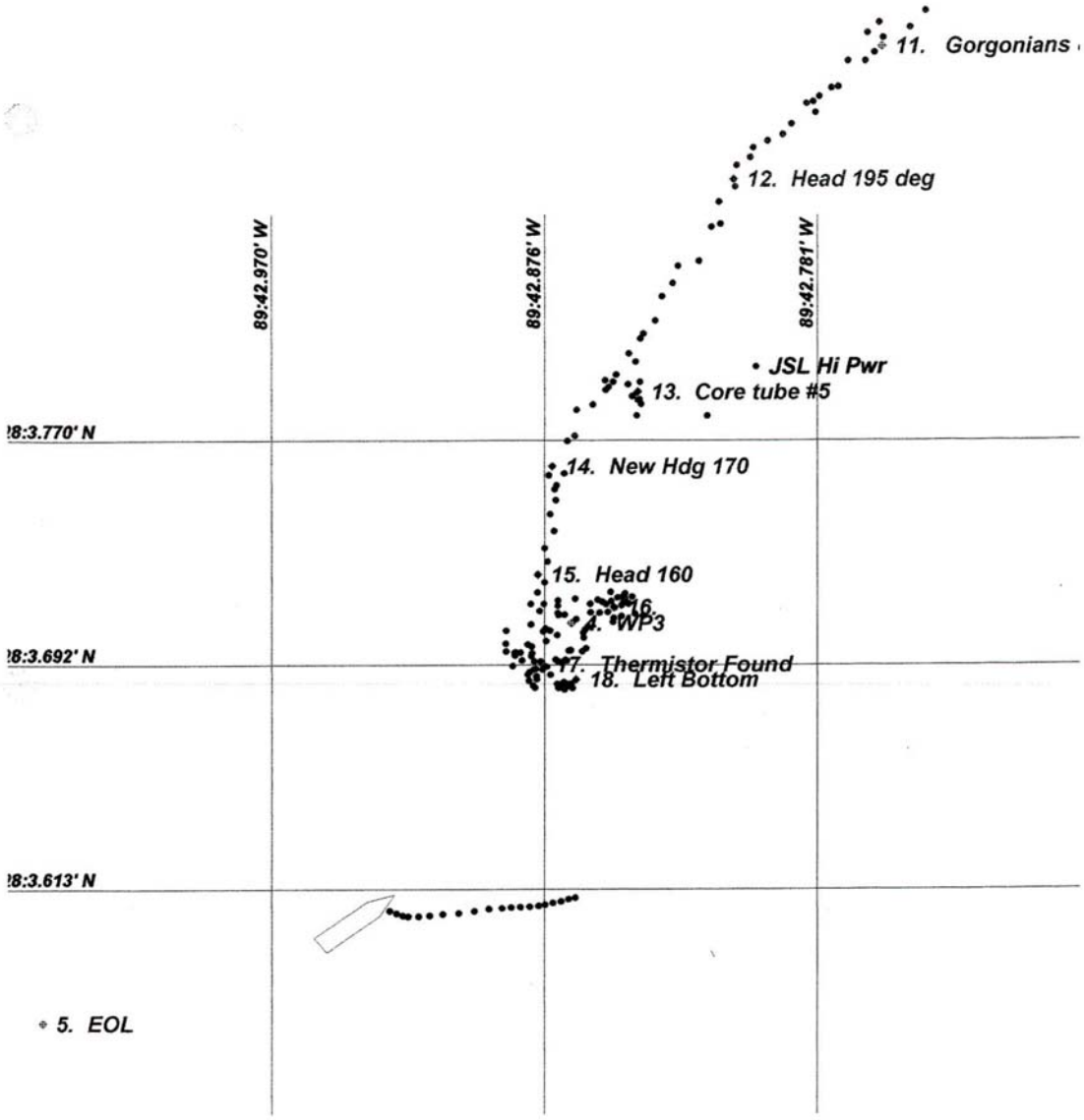
11. Gorgonians
12. Head 195 deg
89:42.970' W
89:42.876' W
89:42.781' W
JSL Hi Pwr
13. Core tube #5
8:3.770' N
14. New Hdg 170
15. Head 160
16.
4. WP3
8:3.692' N
17. Thermistor Found
18. Left Bottom
8:3.613' N
5. EOL

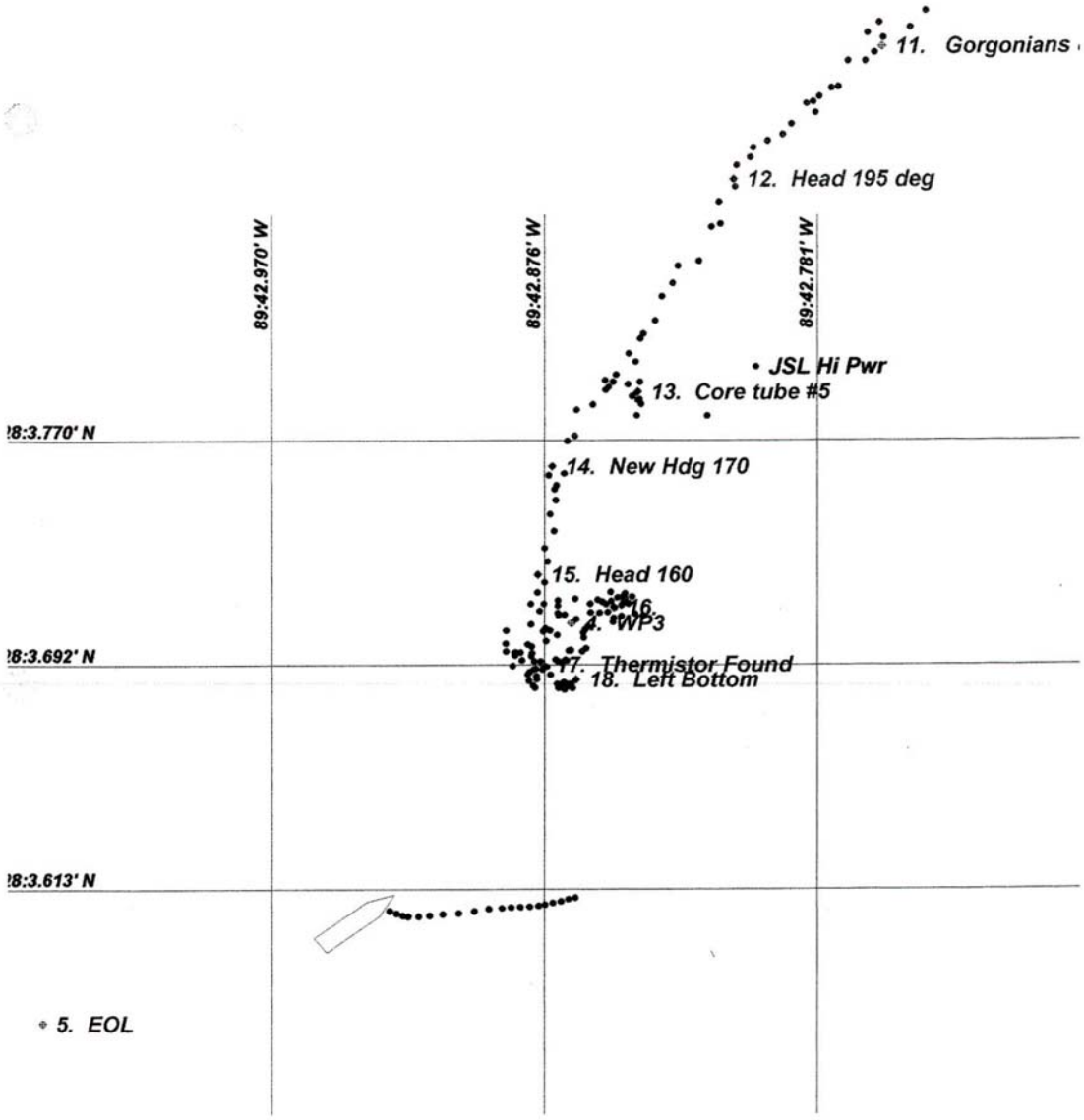
11. Gorgonians
12. Head 195 deg
89:42.970' W
89:42.876' W
89:42.781' W
JSL Hi Pwr
13. Core tube #5
8:3.770' N
14. New Hdg 170
15. Head 160
16.
4. WP3
8:3.692' N
17. Thermistor Found
18. Left Bottom
8:3.613' N
5. EOL

LOUISIANA STATE UNIVERSITY

SUBMERSIBLE DIVE LOG

Dive Number: JSL 4410 Date: 6/20/02

Location: Viosca Knoll Blk. 826

Time: start 0800

end 1115 (leave bottom)

Maximum Depth: 1834 ft (crater) (feet or meters)
1466 ft. (crest of dome)

Personnel: H. Roberts (forward) Don Liberatore (Pilot)

Training dive

Mission/Dive Objective: Explore the top of the VK826 dome

Photographs: Hand held camera Sub-mounted camera

Roll # Shot a number of 35 mm
Frame #'s frames (dive started with 4410 sign on film)

Video: Tape # Shot 3 video tapes.

Sampling (type) Rock samples, clams, Acesta

Mapping (Don caught 2 fish, one in basket and one in claw)

Equipment emplacement (type)

Other None

Comments - If sampling was done or equipment emplaced, please give a brief description including: how many samples/pieces of equipment, type, depth(s), etc.

Touchdown

Temperature: 9.6°C current: 0.1-.2 kts from 090°
Salinity 35.15 ‰

Dive started with lots of clay-sized sediment in the water column to a depth of about 400-500 feet. It was very clear by a depth of 800'. We touched down at a depth of 1585' and proceeded to the south to explore the circular hole (vent?) north of the VK 826 mound. Going into the crater-like depression side slopes got up to 60°-70°, but nothing was found at the bottom. It was covered with hemipelagic sediment with no characteristics of a brine or gas seep. A push core was taken in the bottom (Push Core #6). The slopes in and out of this depression are impressive.

As we topped the ridge to the south of the circular depression, the bottom changed from featureless hemipelagic mud to lithified clasts, gorgonians, sponges, and Lophophyllia "bushes." The flanks of the overall mound-like feature at the VK826 are covered with coral colonies. A sample was taken in Bucket #2.

The dominant characteristic of the dome top is carbonate lithification. Crusts, clasts, mounds, ledges, and pavements are all present. A sample of carbonate with sponges (white) on surface was collected in Bucket #4.

Structure of the dome top seems to be a series of concentrically arranged ridges all of which are lithified. Bacterial mats and tube worms are present in the fractures like GC140. Acestes were collected for Barry (no notches). These clams were associated with the corals, but didn't see any on tube worms.

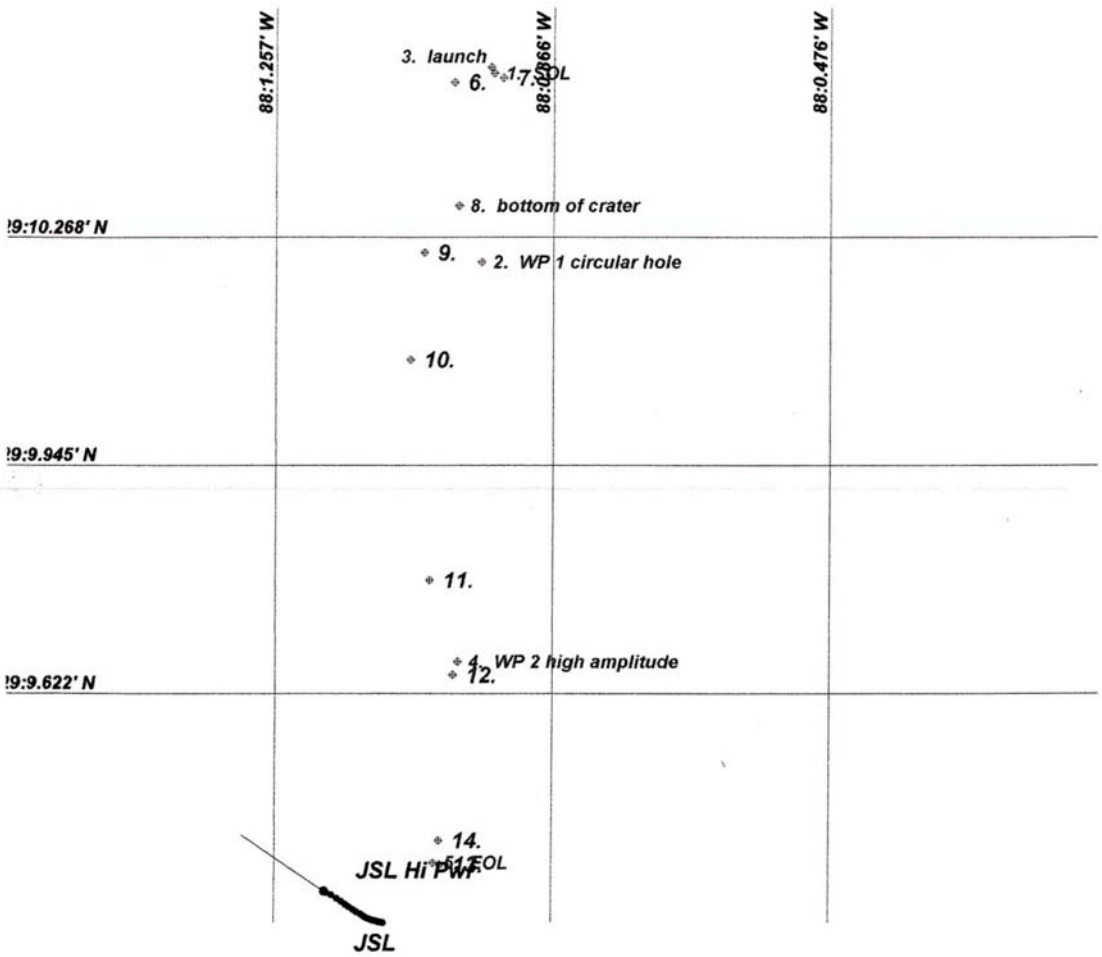
88:1.257' W
88:0.866' W
88:0.476' W
3. launch
6.
17. EOL
8. bottom of crater
!9:10.268' N
9.
2. WP 1 circular hole
10.
!9:9.945' N
11.
4. WP 2 high amplitude
12.
!9:9.622' N
14.
51. EOL
JSL Hi PWR
JSL

ORE Interenational. IPS: WayPoint Report 6/2/2002 11:37:33

C:\Program Files\ORE\1-4410

RVSJ 2 & JSL 1-4410

1. Ship 7:56:27 N 29:10.5000 W 88:00.9500 0 ft SOL
2. User 7:59:28 N 29:10.2330 W 88:00.9670 0 ft WP 1 Circular hole
3. Ship 8:00:41 N 29:10.5088 W 88:00.9544 0 ft Launch
4. User 8:08:01 N 29:09.6670 W 88:01.0000 0 ft WP 2 High Amplitude
5. User 8:08:32 N 29:09.3830 W 88:01.0330 0 ft EOL
6. Target [1] 8:25:11 N 29:10.4874 W 88:01.0064 1581 ft On Bottom
7. Target [1] 8:30:29 N 29:10.4937 W 88:00.9372 1581 ft Sub starts Xsect
8. Target [1] 8:58:15 N 29:10.3128 W 88:00.9993 1832 ft Bottom of Crater
9. Target [1] 9:25:52 N 29:10.2464 W 88:01.0481 1637 ft Top of Crater
10. Target [1] 9:38:48 N 29:10.0951 W 88:01.0672 1573 ft Ridge
11. Target [1] 9:56:59 N 29:09.7827 W 88:01.0395 1532 ft coral
12. Target [1] 10:15:32 N 29:09.6482 W 88:01.0060 1466 ft rock sample
13. Target [1] 10:59:19 N 29:09.3803 W 88:01.0239 1643 ft sampling clams
14. Target [1] 11:15:16 N 29:09.4147 W 88:01.0255 1565 ft Leaving Bottom

LOUISIANA STATE UNIVERSITY

SUBMERSIBLE DIVE LOG

Dive Number: 4411 Date: 6/2/02

Location: Viosca Knoll Block 826

Time: start 1530

end 1840

Maximum Depth: 1,708 ft (feet or meters)

Personnel: Sphere Don/Barry Kohl Rear Hugo/Marc Brausse

Mission/Dive Objective: Ground truth/calibrate seismic amplitudes Sampled for Geochem and microgates. Sample near hydrates if found.

Photographs: Hand held camera Sub-mounted camera

Roll #
Frame #'s took 35mm photos X

Video: Tape # 3 tapes

Sampling (type) Grab samples (3); Push cores (3)

Mapping ——

Equipment emplacement (type) None

Other

Comments - If sampling was done or equipment emplaced, please give a brief description including: how many samples/pieces of equipment, type, depth(s), etc.

3 Grab samples taken & 3 push cores.

Fix 6 on bottom, mud with small burrows, depth 1708.4'
1600 hrs took 2 push cores. (at same location)
PC1-4411 (tube #1) short core } 60% recovery
PC2-4411 (tube #2) long core

1607 hrs to 1622 hrs featureless bottom w/ small burrows, common shrimp, 150 gpd

1627 hrs – small gorgonian, 20 ft visibility

1635-40 hrs – octopus and "six gilled" shark which cross in front of sub. Small tubeworm bush at base of rock. Gorgonians on rock outcrops. WD = 1,684 ft. Areas between rock shelly lucinid shell hash.

Fix 7 1,654 ft depth Took rock sample for Harry.
R1-4411
1645 hrs

Fix 8 1,560 ft Carbonate with gorgonians and black coral.
1657 hrs mix of scattered carbonate and dead shell (lucinid)
to 1706

Fix 9 1,495 WD Large slabs of carbonate approximately 1 ft thick
1710 hrs Polygonal in shape with 4-6" cracks between slabs
Coral thickets (Lophelia), some tube worms poorly developed.

Detailed Video of site showing vertical relationships of carbonate, shell and tubeworms. One tubeworm with blue sponge.

1715-1730 hrs Featureless bottom with shells covered by mud.
(Water depth at 1717 hrs was 1466'; 1721 hrs = 1451 (approx. top of dome)

Fix 10 WD = 1480'
1730 hrs Took grab sample to determine composition of sediment
GS1-4411 in bucket #9

Battery box impression at WD = 1484.5 from previous transect (4410)

Fix 11 1750 hrs — Push core PC3-4411 taken at bottom of furrow between ridges (60% recovery). WD = 1,517'
Bottom featureless with soft mud. w/ common urchins and various soft bodied invertebrates

Fix 12 1801 hrs — Grab sample GS2-4411 (bucket #10). Water depth 1,640'. Sampled in furrow between high areas.

1814 hrs — going up rise

Fix 13 1835 hrs — WD = 1,702' Grab sample GS3-4411 (bucket #11). Soft sediment with burrows. Very fine clay.

Fix 14 1840 hrs — Leaving bottom. WD = 1,702'

General Comments/Notes:

- no evidence of gas hydrates, gassy sediment, mud volcanoes
- tubeworm bushes, that were seen at some areas, were only poorly developed
- slopes over entire area seemed to be "relatively steep" for submarine slopes
- strong currents
- shells appear to be dead, no current fauna-activity, no veining (→ "dieing area")

6/2/02 3 of 3

VK 826

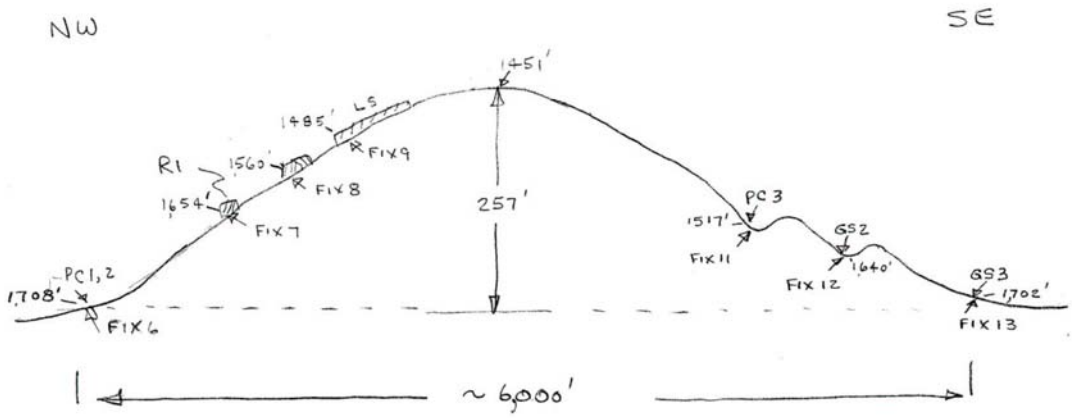

Diagram of traverse across VK 826.

ORE Interenational. IPS: WayPoint Report

6/2/2002 18:48:15

RVSJ 2 & JSL 1-4411

1. Ship 13:47:28 N 29:09.7670 W 88:01.9170 0 ft SOL
2. User 13:50:04 N 29:09.7330 W 88:01.6670 0 ft WP 1 anomaly 1
3. User 13:51:42 N 29:09.6170 W 88:01.0330 0 ft WP 2 center
4. User 13:52:21 N 29:09.4670 W 88:00.1330 0 ft EOL
5. User 15:32:00 N 29:09.7557 W 88:01.8910 0 ft Launch
6. Target [1] 16:00:36 N 29:09.7528 W 88:01.9246 1708 ft On Bottom
7. Target [1] 16:46:07 N 29:09.6671 W 88:01.3772 1654 ft Rock Sample
8. Target [1] 16:57:11 N 29:09.6497 W 88:01.2705 1560 ft Large Black Carbonate & Coral
9. Target [1] 17:10:31 N 29:09.6290 W 88:01.1307 1485 ft Taking Video
10. Target [1] 17:30:44 N 29:09.6108 W 88:00.9784 1480 ft grab sample
11. User 17:50:41 N 29:09.6006 W 88:00.8949 1517 ft Push Core # 3
12. Target [1] 18:01:15 N 29:09.5929 W 88:00.7415 1640 ft Grab Sample
13. Target [1] 18:35:02 N 29:09.5233 W 88:00.3467 1702 ft Grab Sample
14. Target [1] 18:40:54 N 29:09.5257 W 88:00.3417 1702 ft Leaving Bottom

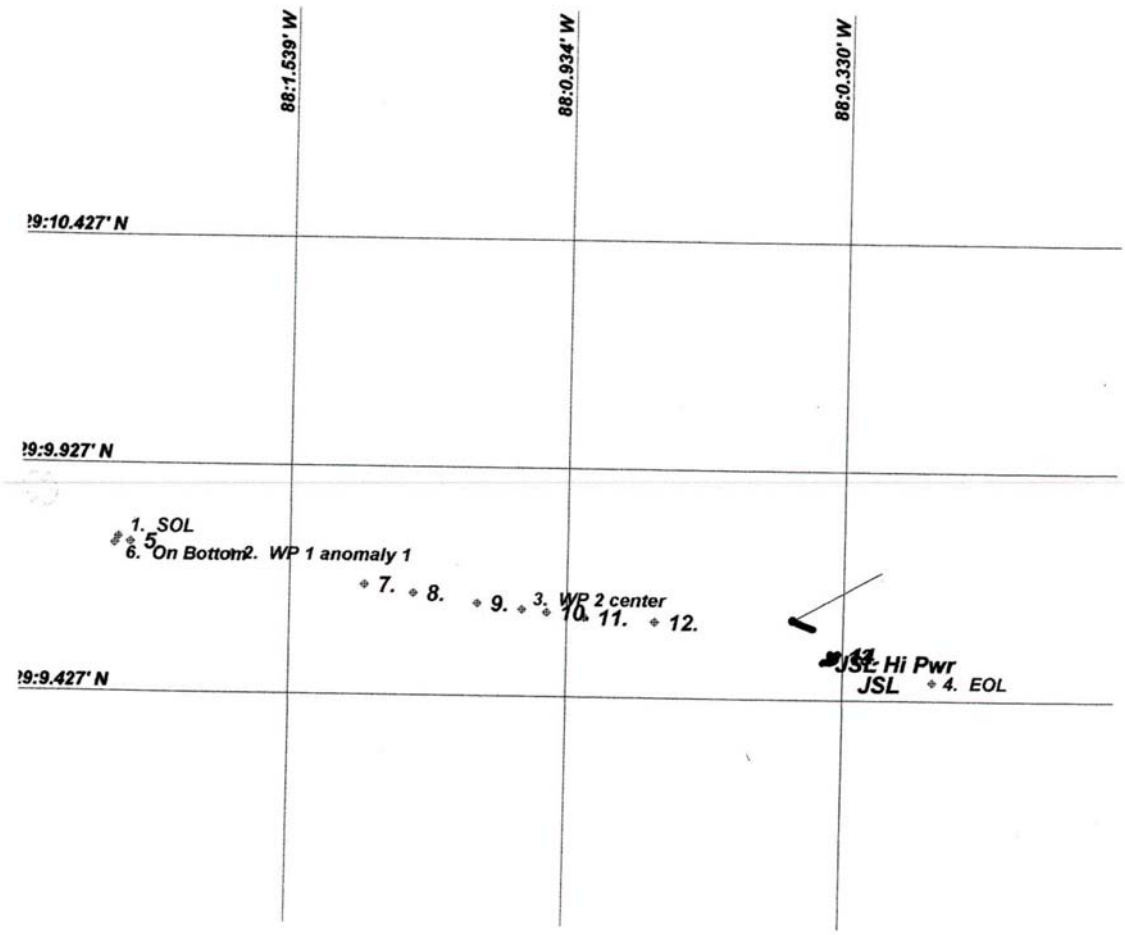
88:1.539' W
88:0.934' W
88:0.330' W
29:10.427' N
29:9.927' N
29:9.427' N
1. SOL
5.
6. On Bottom
2. WP 1 anomaly 1
7.
8.
9.
3. WP 2 center
10.
11.
12.
JSL Hi Pwr
JSL
4. EOL

1¼ mi

LOUISIANA STATE UNIVERSITY

SUBMERSIBLE DIVE LOG

Dive Number: 4412 Date: 3 June 02

Location: Miss. Canyon Block 709

Time: start 0755 hrs. launch
end 1105 hrs. left bottom

Maximum Depth: 2322 ft (feet or ~~meters~~)

Personnel: Sassen/Bogsess Chanton/Frank

Mission/Dive Objective:

Photographs:	Hand held camera	Sub-mounted camera
Roll #		
Frame #'s		#30

Video: Tape # 1, 2, 3 (partial)

Sampling (type) push core, grab, suction

Mapping

Equipment emplacement (type)

Other

Comments - If sampling was done or equipment emplaced, please give a brief description including: how many samples/pieces of equipment, type, depth(s), etc.

4412/MC709 RS ①

1. acquired water samples on the way down, and on bottom. time ~ 0830 6.85°C, 35.15 salinity.
2. observed brown burrowed ~~[illegible]~~ mud, shell fragments, and low visibility from suspended sediment.
3. ~ 0835 observed carbonate rock, quite isolated.
4. ~ 0840 shell hash, starfish, small white to gray bacterial mats, scattered.
5. ~ 0844 started seeing large shallow depressions (craters) up to 10's of meters across. Many holothurians.
6. ~~0910~~ Long transit of burrowed brown mud, continued murkiness from suspended clay. Isolated sea fans. ~~[illegible]~~ Failed to acquire Core 1 for geotech at 2223 ft, 7.35°C, 34.90 salinity. took water sample # 288.
7. 0910. Used Core #2 for geotech in typical brown burrowed mud. Good penetration and recovery. Most of sediment was fine-grained/gray.
8. 0918 More brown mud, isolated tiny mats, perhaps diffuse gas seepage
9. 0920 Used grab to sample mussels and sediment on upper outside rim of shallow crater. Fix. 10. Dark anoxic sediment in bucket 12.
10. Found black rivulet ~~with~~ originating from a small orifice upslope (0920) Brine rivulet has been incised into brown mud. Mussels on edges of incised channel. Used Core #1 for geochem. Short ~~[illegible]~~ recovery (~ 10cm) 6.87°C, 34.90 Sal., 2226 ft depth. Gas and oil entered water column in minor volumes. Black sediment canned.

RS (2)

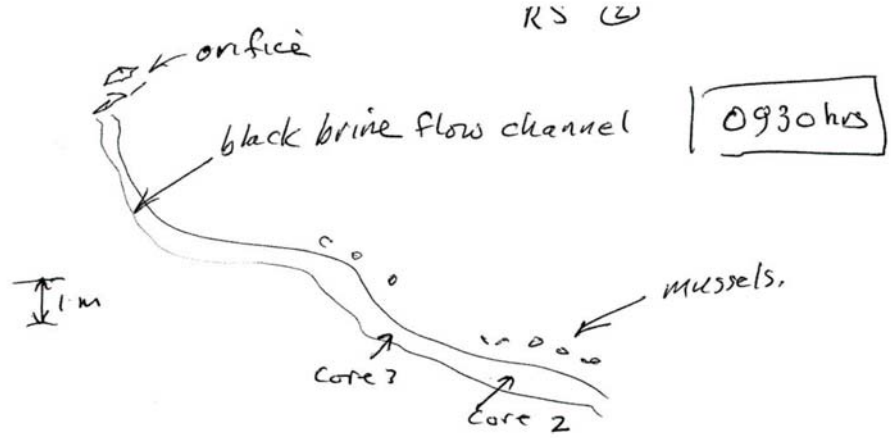

11. acquired Core 3 for chemistry. Short penetration in floor of brine channel. Black sediment. No bubbles (0930 hrs).

12. long stretches of brown surfaced burrowed mud, poor visibility, many shallows near circular dormant craters

13 1020 hrs. observed nice circular hole, 30 m across at 2280 ft. Still murky.

14. 1040. Saw smaller craters, area largely flat. 2285 ft 6.5 °C

15. 1045 max depth of 2322 ft.

16. 1055 Acquired core #4 for geotech purposes. Representative of large area. Good penetration and recovery.
2329 ft 6.3 °C 34.88 sal.

17. . left bottom at 1105 hrs.

ORE Interenational. IPS: WayPoint Report 6/3/2002 11:07:16

C:\Program Files\ORE\1-4412_trk_trk

RVSJ 2 & JSL 1-4412

1. User 8:46:09 N 28:13.8670 W 89:42.4670 2262 ft SOL
2. User 8:48:34 N 28:13.6670 W 89:42.2170 2262 ft WP1
3. Ship 8:49:14 N 28:13.8469 W 89:42.4109 2254 ft Mud volcano
4. User 8:50:41 N 28:13.8633 W 89:42.4378 2262 ft Bottom report
5. User 9:01:09 N 28:13.8670 W 89:42.4670 2262 ft SOL
6. Target [1] 9:02:54 N 28:13.7296 W 89:42.3210 2223 ft Punch core 1
7. User 9:57:25 N 28:13.5330 W 89:42.0500 2262 ft WP 2
8. User 9:58:03 N 28:13.3170 W 89:41.7830 2262 ft WP 3
9. User 9:58:20 N 28:13.0670 W 89:41.4670 2262 ft EOL
10. User 9:38:00 N 28:13.6011 W 89:42.1661 2232 ft mussels and mats
11. User 9:53:00 N 28:13.6050 W 89:42.1433 2225 ft mussels and clams
12. Target [1] 11:01:11 N 28:13.0739 W 89:41.4570 2329 ft punch core

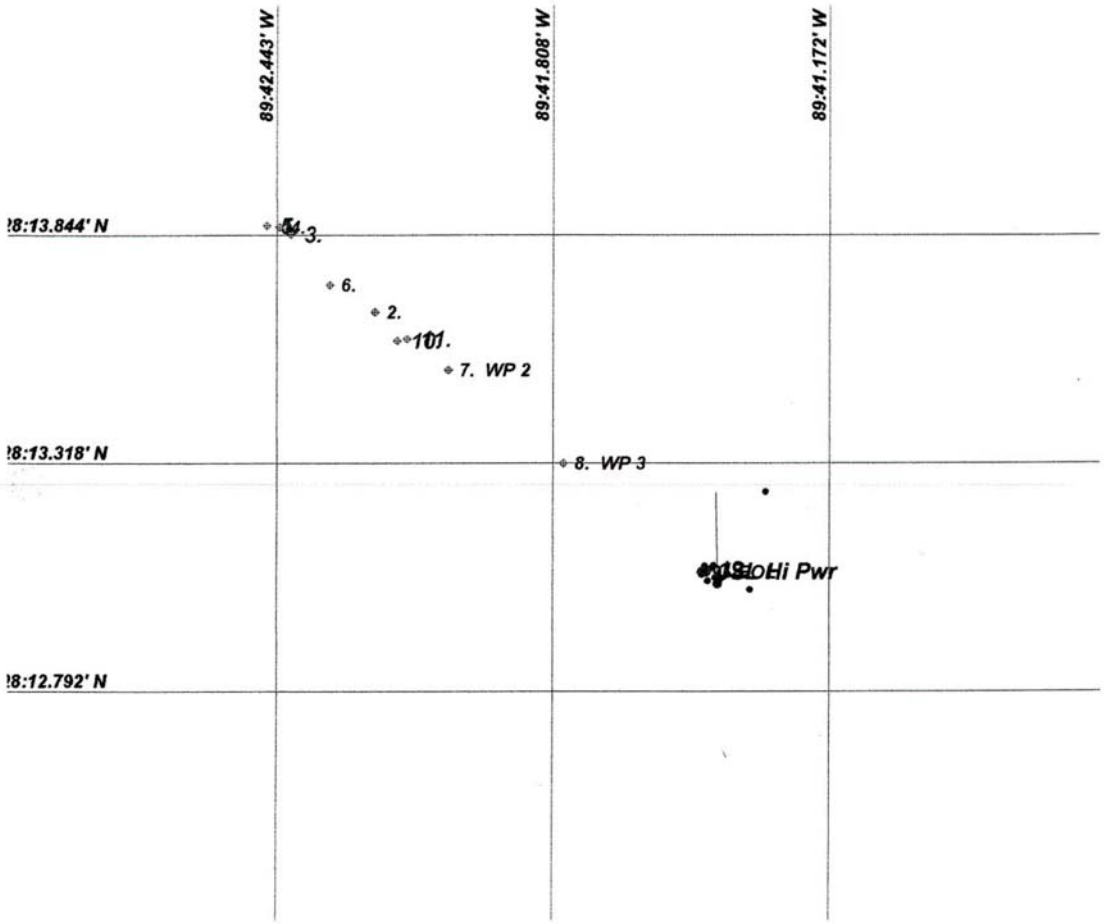
89:42.443' W
89:41.808' W
89:41.172' W
8:13.844' N
3.
6.
2.
101.
7. WP 2
8:13.318' N
8. WP 3
Hi Pwr
8:12.792' N

-SC DIVE 4412

6/3/02 ~ 2240 ft

Front: Sassen MC709

Aft: Chanton 0855 hrs

PS

air bubble behavior

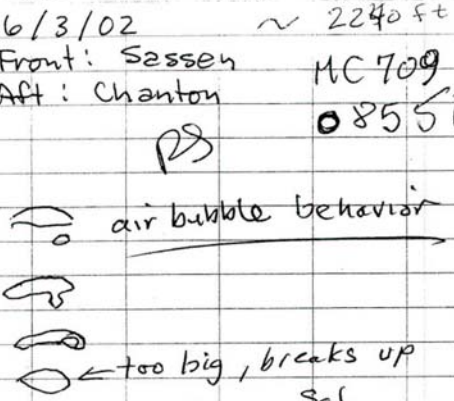

	T	Sal.
1100 ft	10.57°C	35.32
1200	9.35	35.13
1300	9.18	35.10
1400	9.00	35.07
1600	8.28	35.02
1800	8.03	34.97
1900	7.96	34.97
2000	7.86	34.95
2100	7.71	34.95
2200	7.54	34.93

bottom 0825 2260.3

6.85°C, 35.15

brown mud - very murky - sheets, tiny mats, many very small burrows

2262, 5.99°C, 34.89

report at 0830

0835 carbonate rock, sorted

0837 fish picture

2254 ft 5.99°C 34.99

0840 shell hash, starfish, mats

0844 large shallow depression
Sea mats on edge
visibility increasing
many holothurians.

846 [crest a slope
many small isolated
white Beggiatoa mats
dropping off
- more mats
mounds old mud volcano
circular craters
in deep 2223 ft
many holothurians

0848 many craters
old, filled, mounded

0940 -
more active holes are
flooded with shell
hash

2211 ft course 0950
Sea fans / shell patches

pendi core 0900 hours
grey-white mat in
craters surrounded by ridge/
tips with gorgonians
Core #1 2223 ft T 7.35°
34.90

Took water sample
288
a bandicoring attempt
because of poor visibility.

0910 -
geotech. Tube #2
2232 ft.
core went in all the way - good
reddish gray mud

Core 2 – [illegible]

mostly brown/gray
some darker reducing areas.
0915 core acquired

0918 crossing areas mud, dull
odd gorgonian, rare
carbonate, thin sheet
bass

areas of diffuse gas
seepage – no bubbles

shallow craters 0920
dull, brown mud,
odd gorgonian

* 0920 mussels mussels on
-0930 upper inside rim of
shallow craters FIX 10

0935 – Garden cove
mussels, debris, brine
2225 ft no gas bubbles
arise from disturbed area.
sample

~~Jeff~~ Core 1 – long core on
Roger
black rivulet depression
from brine flow erosion
6.87°C 34.90
2226.0 ft
full penetration, oil
gas/oil coming up.

Core 3 – Jeff shot
penetration
0950 grab mussels,
dark reducing mud.
bucket ?
second bucket

0958 – [illegible]

pick works

Holothurians ~~[illegible]~~

mussels, mud.

1010 2257 ft 7.05 °C

34.90

big carbonate rocks

photo 10:110

– BORING –

2268 ft fix

1017 same mud –

key areas are isolated by

featureless plains

big areas

Circular hole,

1020 30 meters across

2280 ft

still moving

1030 2259 6.71

34.89

featureless

Then big hole

30 mm across

1035 nothing!

1040 shallow craters.

small vent

1040 ?

more shallow craters

2285 ft

1045

6.5 °C

2.50C ft 1050

deep

2307

2322 Max depth

1050 geotech one
in representative
area

Core #4 Geotech
2329 st 6.30°C
34.88 sal

Good penetration
gray mud

2330 st

st
bottom
at 1105' m

LOUISIANA STATE UNIVERSITY

SUBMERSIBLE DIVE LOG

Dive Number: JSL 4413 Date:

Location: Miss. Canyon Blk 709

Time: start

end

Maximum Depth: (feet or meters)

Personnel:

Mission/Dive Objective:

Photographs:	Hand held camera	Sub-mounted camera
Roll #		
Frame #'s		
Video: Tape #		
Sampling (type)		
Mapping		
Equipment emplacement (type)		
Other		

Comments - If sampling was done or equipment emplaced, please give a brief description including: how many samples/pieces of equipment, type, depth(s), etc.

ORE Interenational. IPS: W

ORE Interenational. IPS: W

RVSJ 2 & JSL 1 dive 4413

1. User 15:32:21 N 28:13.6670
2. Ship 15:38:52 N 28:13.6669
3. Target [1] 16:16:07 N 28:13.6
4. Target [1] 16:30:00 N 28:13.6
5. User 17:41:08 N 28:13.6400
6. Target [1] 17:57:02 N 28:13.6
7. Target [1] 18:08:50 N 28:13.6
8. Target [1] 18:24:31 N 28:13.6
9. Target [1] 18:47:35 N 28:13.6

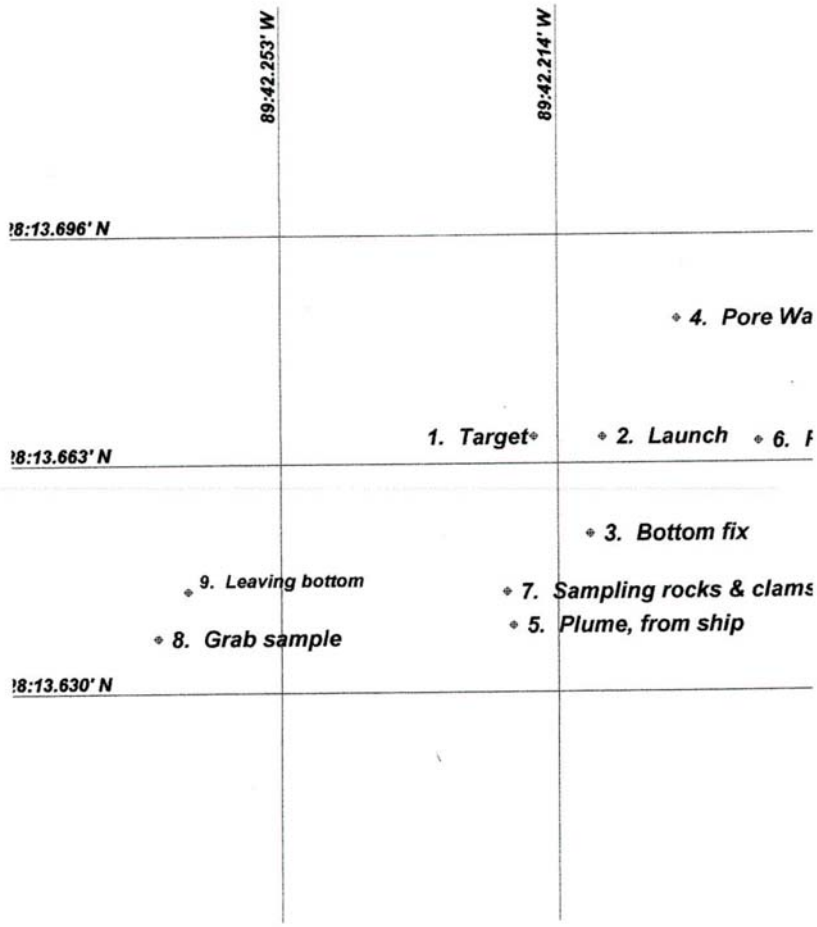

LOUISIANA STATE UNIVERSITY

SUBMERSIBLE DIVE LOG

Dive Number: JSL DIVE 4414 Date:

Location: Miss. Canyon Blk. 118

Time: start

end

Maximum Depth: (feet or meters)

Personnel:

Mission/Dive Objective:

Photographs:	Hand held camera	Sub-mounted camera
Roll # Frame #'s		
Video: Tape #		
Sampling (type)		
Mapping		
Equipment emplacement (type)		
Other		

Comments - If sampling was done or equipment emplaced, please give a brief description including: how many samples/pieces of equipment, type, depth(s), etc.

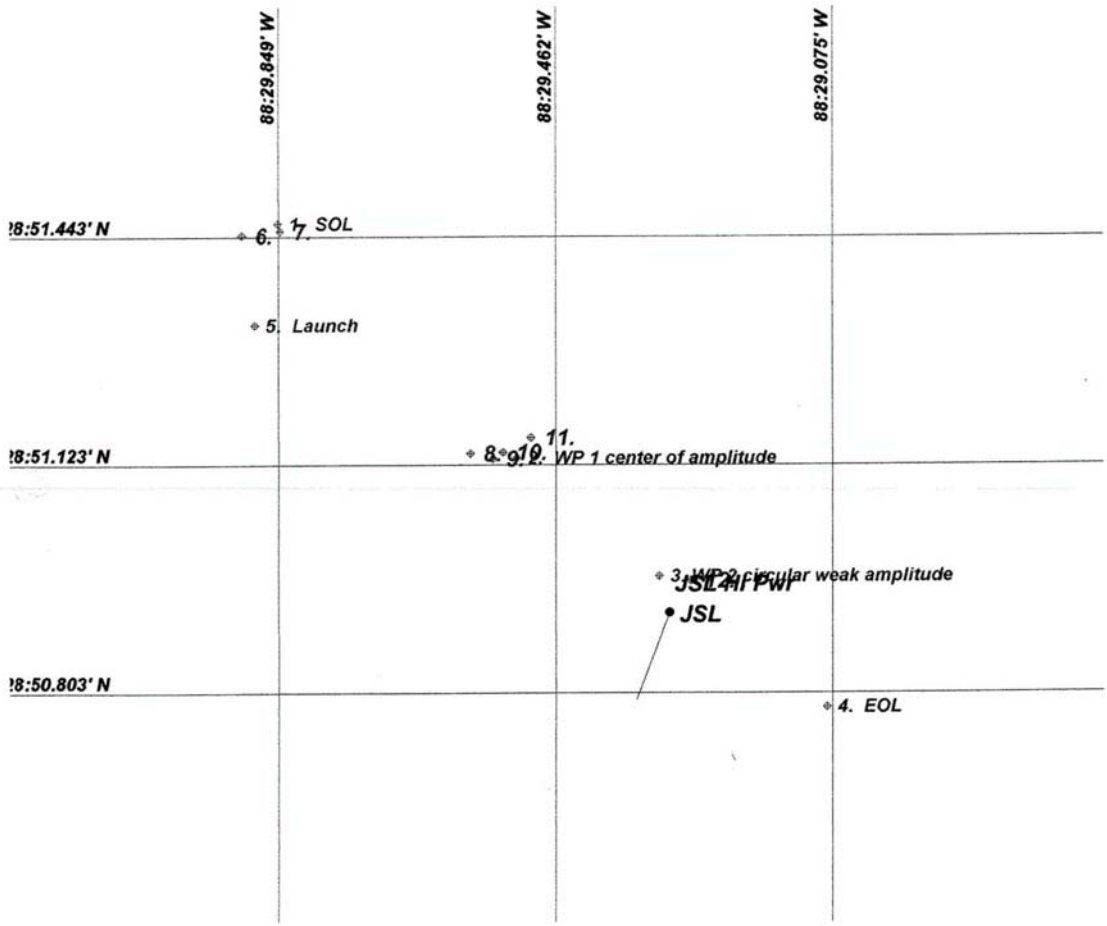
88:29.849' W
88:29.462' W
88:29.075' W
28:51.443' N
6.
1.
7.
SOL
5. Launch
28:51.123' N
11.
8.
9.
10.
WP 1 center of amplitude
3. WP 2 circular weak amplitude
JSL4HrPwr
JSL
28:50.803' N
4. EOL

ORE Interenational. IPS: WayPoint Report 6/4/2002 10:56:32

C:\Program Files\ORE\1-4414

RVSJ 2 & JSL 1-4414

1. User 7:52:55 N 28:51.4624 W 88:29.8500 0 ft SOL
2. User 7:54:08 N 28:51.1330 W 88:29.5170 0 ft WP 1 center of amplitude
3. User 7:55:20 N 28:50.9670 W 88:29.3170 0 ft WP 2 circular weak amp.
4. User 7:55:52 N 28:50.7830 W 88:29.0830 0 ft EOL
5. Ship 7:58:20 N 28:51.3198 W 88:29.8819 0 ft Launch
6. Target [1] 8:39:50 N 28:51.4457 W 88:29.9005 2869 ft On Bottom
7. Target [1] 8:46:35 N 28:51.4516 W 88:29.8469 2873 ft Start of Xsect
8. Target [1] 9:16:11 N 28:51.1394 W 88:29.5820 2898 ft Grab Sample
9. Target [1] 9:30:35 N 28:51.1319 W 88:29.5502 2912 ft punch core
10. Target [1] 9:38:26 N 28:51.1409 W 88:29.5361 2915 ft gas seep & hydrate
11. Target [1] 10:14:03 N 28:51.1615 W 88:29.4967 2898 ft Push core thru bacterial matt
12. Target [2] 10:49:07 N 28:50.9608 W 88:29.2729 2970 ft Leaving Bottom

LOUISIANA STATE UNIVERSITY

SUBMERSIBLE DIVE LOG

Dive Number: Date:

Location:

Time: start

end

Maximum Depth: (feet or meters)

Personnel:

Mission/Dive Objective:

Photographs:	Hand held camera	Sub-mounted camera
Roll # Frame #'s		
Video: Tape #		
Sampling (type)		
Mapping		
Equipment emplacement (type)		
Other		

Comments - If sampling was done or equipment emplaced, please give a brief description including: how many samples/pieces of equipment, type, depth(s), etc.

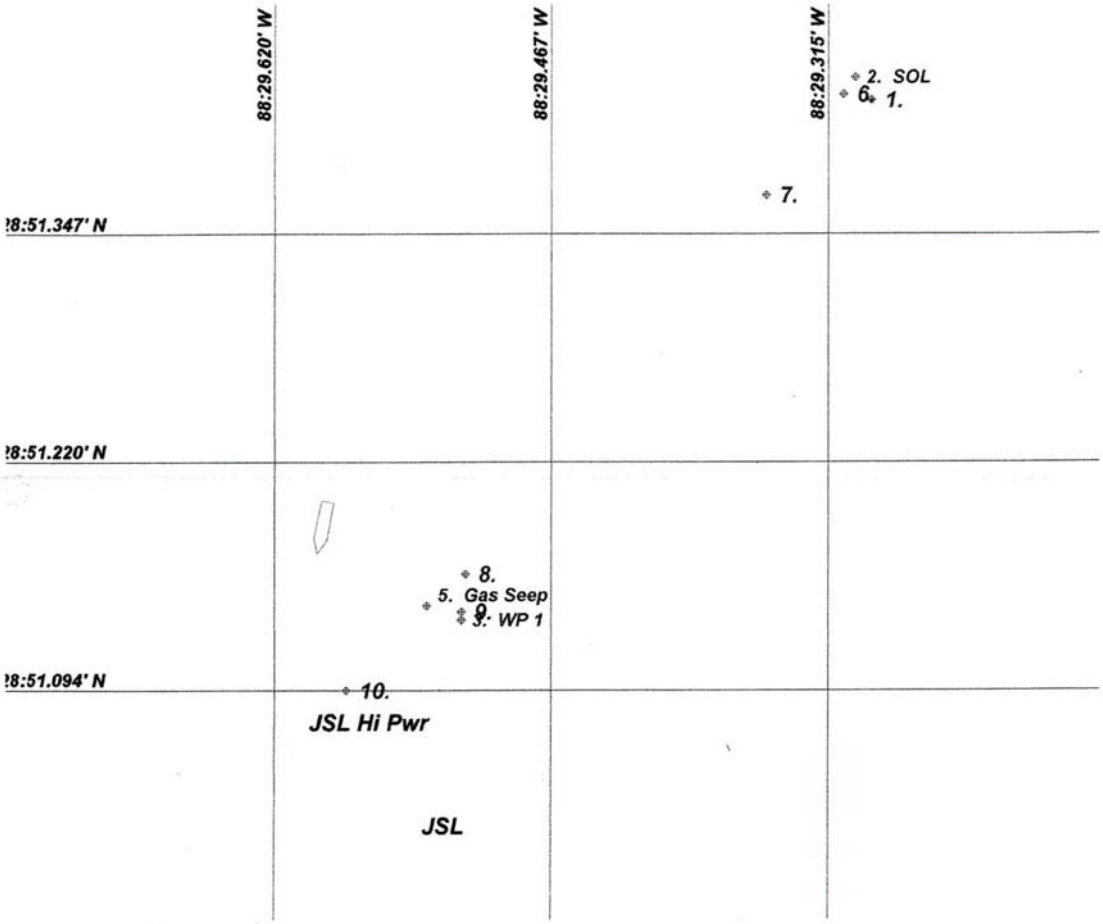
88:29.620' W
88:29.467' W
88:29.315' W
2. SOL
6.
1.
7.
28:51.347' N
28:51.220' N
8.
5. Gas Seep
9.
3. WP 1
28:51.094' N
10.
JSL Hi Pwr
JSL

ORE Interenational. IPS: WayPoint Report 6/4/2002 18:35:14

C:\Program Files\ORE\1-4415

RVSJ 2 & JSL1-4415

1. Ship 15:29:19 N 28:51.4204 W 88:29.2909 0 ft Launch
2. User 15:32:35 N 28:51.4330 W 88:29.3000 0 ft SOL
3. User 15:33:39 N 28:51.1330 W 88:29.5170 0 ft WP 1
4. User 15:56:20 N 28:50.7670 W 88:29.7830 0 ft EOL
5. User 16:04:10 N 28:51.1409 W 88:29.5361 0 ft Gas Seep
6. Target [1] 16:09:07 N 28:51.4235 W 88:29.3064 2907 ft On Bottom
7. Target [1] 16:17:32 N 28:51.3682 W 88:29.3491 2903 ft Grab Sample
8. Target [1] 16:40:52 N 28:51.1585 W 88:29.5148 2895 ft Crater
9. Target [1] 16:44:51 N 28:51.1377 W 88:29.5170 2908 ft Alot of gas & oil
10. Target [1] 18:30:00 N 28:51.0942 W 88:29.5805 2926 ft Push Cores / Leaving Bottom

Communications Log
Johnson Sea Link Submersible 2002 Cruise

Friday, May 17:

Load at Gulfport, cold front blew through. Stayed at the dock Sat. and Sun.

Sunday, May 19:

Depart Gulfport and steamed overnight to be on station at VK 826.

Monday, May 20:

Too rough to dive. By 2:00pm, decided to return to Gulfport to repair lower deck A/C unit and ship's freezer. Departed Gulfport at 11:30 pm for VK 826.

Tuesday, May 21:

Hove to all day on VK 826. Still too rough to dive.

Wednesday, May 22:

Hove to all day. Decided to abort the site and head west in search of better weather. Ran west overnight.

Thursday, May 23:

Hove to at MC 885 all day.

Friday, May 24:

MC 885, Dive 4392

Crew: Front, Craig Caddigan, Mike Smith
Rear, Frank Lombardo, Susan Childs

Purpose: Survey traverse and find and recover thermistor.

Attempted to dive, but had to abort due to weather. Hove to all day, and decided to run west to GC 185 (Bush Hill). Arrived at Bush Hill, attempted to trip acoustic release on current meter array. Did not release.

Saturday, May 25:

GC 185, Dive 4393

Crew: Front, Craig Caddigan, Harry Roberts
Rear, Frank Lombardo, Eric Guilbeau

Purpose: Free current meter, collect bubbleometers, deploy rabbit chow.

7:58 Boom out
8:01 Launch
8:02 Permission to dive, problem with a contact in the sub. Depth 250 ft.
8:08 Resurface, recovered sub. Water in a breaker tripped it.
8:13 Recovered sub and began repairs.

GC 185, Dive 4394

Same crew.
Same purpose.

9:23 Boom out
9:25 Launch
9:26 Permission to dive. Launch at 27-46.8031N 91-30.3743W
9:30 Returning to surface. An alarm was getting louder.
9:36 Surface, repaired sub.

GC 185, Dive 4394

Same crew, same purpose.

15:56 Launch, permission to dive 27-46.8652N 91-30.4087W
16:09 Depth 1000 ft.
16:19 Near bottom, mooring 20 ft. in front of sub.
16:22 On bottom. Depth 1793 ft., 0.1 kt. of current from W, Temp. 7.40
Released mooring.

GC 185, Dive 4394 (cont.)
16:24 Mooring on the way up.
16:27 Deploy a bucket of rabbit chow at 27-46.0931N 91-30.4081W
16:30 Heading due West
16:32 Current meter array on the surface.
16:34 Deployed bucket #2 on bearing of 345 (no fix) approx. 27-46.9437N 91-30.4550W.
16:37 Within 50 ft. of the numbers, searching for instruments.
16:38 Instruments in sight
16:40 Will deploy bucket #1 just North of where Harry's gear was, Just down from Junk yard, Depth 1783 ft.
16:49 At the first funnel, trying to get the can off the side.
17:00 Can is in the basket, but can't close the lid, will try to fit the funnel on top.
17:10 Funnel onboard, moving away from the time lapse camera.
17:16 Don't know how the funnel will ride. Request permission to leave bottom. Must go back and look at something.
17:20 By Ian McDonald's time lapse camera, looking at thermistors. Will take water samples.
17:23 Depth 1772 ft., Permission to leave bottom. 27-46.9763N 91-30.4724W.
17:47 Done with water samples at 2000 ft. Permission to surface.
17:51 On surface.

GC 185, Dive 4395

Crew: Front, Craig Caddigan, Harry Roberts
Rear, Frank Lombardo, Duofu Chen

Purpose: Retrieve gear and conduct acoustics experiments (night dive)

20:38 Launch, permission to dive, 27-46.9850N 91-30.4715W
20:50 Showing bottom at 1800 ft. on ship.
20:53 Range 100 ft. bearing 174 degrees to landing site.
20:55 Ship showing bottom at 1775 ft.
20:57 Target at 100 ft. at 165 degrees.
21:00 Bottom in sight

GC 185, Dive 4395 (cont.)

21:01 On bottom, 1780 ft., Temp. 7.33, visibility 45 to 50 ft., 0.1 kt. Of current from due North. Next to Ian's cameras, getting video at 27-46.9530N 91-30.4178W.

21:19 Got the other funnel on board, will go back and do some video.

21:31 Depth 1763 ft., took video, request permission to leave bottom 27-46.9529N 91-30.4865W

21:55 On surface.

Sunday, May 26

GC 185, Dive 4396

Crew: Front, Don Liberatore, Harry Roberts
Rear, Hugo Marrero, Rex Poling

Purpose: Locate and retrieve tripod and thermistor string, Target mud vent, and shoot stills of the bottom.

07:03 Launch and permission to dive 27-46.0511N 91-30.3480W
07:04 Ship showing bottom at 1858 ft.
07:15 Range to target 459 ft. at 339 degrees.
07:16 Range 600 ft. at 340 degrees.
07:17 Ship showing bottom at 1852 ft.
07:19 Ship showing bottom at 1844 ft., sub at 1200 ft.
07:22 Range 350 ft. at 325 degrees, sub at 1400 ft.
07:29 Sub depth 1800 ft.
07:30 Range 400 ft., bearing 345 degrees.
07:31 Bottom in sight.
07:34 Range 150 ft., Bearing 350 degrees.
07:36 Range 100 ft., Bearing 290 degrees.
07:37 Sighted bacterial mat, probably coming into mud vent site.
07:41 Range 90 ft., Bearing 120 degrees. Unable to locate site.
07:46 Range 150 ft., Bearing 350 degrees, Unable to locate site.
07:49 Currently searching for site, bottom (from ship) 1862 ft.
07:54 Range 250 ft., Bearing 040 degrees, searching for site.
07:55 Sub underway at 040 degrees.
07:59 At the mud vent.

GC 185, Dive 4396 (cont.)

08:02 Found something on mud vent, probably old thermistor. Harry confirms this is the thermistor.

08:03 Sub depth 1876 ft.

08:06 See the ADCP, do not see the auger with the thermistor string.

08:09 Sitting at the tripod, Depth 1878 ft., Temp. 7.14, Visibility 25 ft., Current 0.1 kt. at 090 degrees.

08:11 Will move around and look for the auger and come back and retrieve the tripod.

08:24 Unable to locate the auger and thermistor, heading back to retrieve the doppler current meter from tripod.

08:31 Unable to lift instruments, will back off and try again. T-handle at top is broken off (Harry doesn't remember that problem during deployment. At 27-46.1579N 91-30.4132W.

08:40 Unable to dislodge doppler instrument, Regrouping and waiting for sediment to clear.

08:45 Trying to tip the tripod and get the doppler exposed for easier access.

08:58 Tried pulling on it and still unable to dislodge it, waiting for sediment to settle.

09:18 Grabbed the doppler and blew the ballast tanks, failed to dislodge. Standing by.

09:27 Leaving the mud vent site and heading for Bush Hill site.

09:29 Underway due east, depth 1880 ft., taking water samples at 27-46.1970N 91-30.3672W

09:31 Changed course to north, following mud flow to investigate.

09:33 New vent observed at 1873 ft., 27-46.1975 N 91-30.3589W

09:35 At top of the vent, observing bubble stream. Top at 1875 ft.

09:43 Permission to leave bottom at depth 1875 ft.

09:44 Leaving bottom at 27-46.2018N 91-30.3587W

10:08 On surface.

GC 238, Dive 4397

Crew: Front, Don Liberatore, Mike Smith
Rear, Hugo Marrero, Charles Billups

Purpose: Survey Traverse 1 and record observations. If time permits, collect two push cores and 1 carbonate sample.

GC 238, Dive 4397 (cont.)

13:19 Launch, permission to dive at 27-44.3886N 91-03.0461W. Punch cores are OK.

13:21 Ship showing bottom at 2276 ft.

13:24 Depth 295 ft., going through murky layer of sediment laden water.

13:36 Range 700 ft. Bearing 280 degrees.

13:42 Ship showing bottom at 2325 ft.

13:45 Sub at 2000 ft. and descending

13:49 Sub at 2200 ft., ship shows bottom at 2335 ft.

13:52 Bottom in sight.

13:53 On bottom, depth 2343 ft., Temp. 6.23, Visibility 35-40 ft., current 0.1 kt. at 300 degrees, 27-44.4453N 91-03.0470W

13:56 WP1 range 950 ft., bearing 140 degrees.

13:58 Underway at 140 degrees.

14:00 Coming up on slight slope at 4 to 5 degrees, on way to WP1.

14:06 Range 250 ft., bearing 110 degrees to WP1. Depth 2294 ft., Lots of bacterial mats, mounds, shells (mussels and clams). Most shells observed are dead, possibly active area at one time. Seeing chemo biota.

14:08 27-44.3441N 91-03.0025W, traveling to WP1.

14:14 Sending sub to WP2, Range 400 ft. bearing 270 degrees.

14:15 More shells, big depressions, smooth bottom, no bacterial mats present.

14:16 Dan instructs sub to stand by, checking on incorrect bearing of 270 degrees.

14:17 WP2 is at 450 ft., bearing of 150 degrees.

14:18 Sub at 2276 ft., ship showing 2273 ft.

14:21 New heading of 175 degrees, depth 2274 ft. Big craters with bacterial mats at the base, approximately 3m across.

14:23 Changing bottom, more bacterial mats, anemones, mussels.

14:24 Depth 2274 ft., anemones only on slope sides.

14:27 New heading of 150 degrees, depth at 2278 ft.

14:30 On way to WP3, Range 750 ft., bearing 140 degrees.

14:32 Change in bottom, hundreds of starfish, small shallow depressions, occasional hard bottom. Depth 2283 ft. 21-44.1256N 91-02.8683W

14:35 Depth 2282 ft., "Starfish City".

14:36 Back in larger depression, no starfish.

14:37 Investigating location of bacterial mat for punch core sample.

GC 238, Dive 4397 (cont.)

14:44 Due east to WP3, Depth 2290 ft., taking punch core in bacterial mat at 27-44.0516N 91-02.8310W

14:49 Soft sediment, push core went in and came out half full, underway due east.

14:50 Range 200 ft. to WP3.

14:51 090 degrees, underway due east.

14:52 Crossing over small furrow 1 to 1.5 ft. across running N-S.

14:54 Course change, bearing 140 degrees, range 1300 ft.

14:56 Depth 2310 ft., underway at 140 degrees to EOL.

14:57 Headed downslope

15:02 Depth 2390 ft., changing video tapes, 27-43.9884N 91-02.6707W

15:07 Course change to due S.

15:11 At EOL. Depth 2415 ft., bottom is smooth and homogeneous, no mats.

15:16 Shooting video of starfish.

15:17 Depth 2417 ft., request permission to leave bottom, 27-43.8256N 91-02.6217W.

15:40 On surface.

GC 238, Dive 4398

Crew: Front, Don Liberatore, Susan Child
Rear, Hugo Marrero, Bob Hardage

Purpose: Survey and photodocument Traverse 2

19:03 Launch, permission to dive, 27-43.9001N 91-02.8074W

19:08 Going through a layer of murky water at 300 ft., looks like sediment in the water column.

19:16 Depth 1000 ft.

19:21 Target range 300 ft., bearing 220 degrees, getting underway.

19:26 Drop straight down, depth 1770 ft.

19:32 Depth 2200 ft.

19:37 On bottom, depth 2389 ft., 27-43.9072N 91-02.8360W

19:48 Going upslope

19:50 Course change to 355 degrees, range 350 ft.

19:51 Small craters with bacterial mats, depth 2310 ft.

GC 238, Dive 4398 (cont.)

19:57 Bigger craters with some rock, will take sample, also clams and mussels, took push core and grab sample 27-44.0266N 91-02.8252W

20:11 Completed push core, some hard substrate, will look around for several minutes.

20:15 Came across battery box tracks, get underway at 005 degrees, range 1800 ft., depth 2280 ft.

20:17 Huge chunk of coral about 4 ft. across, will sample 27-44.0772N 91-02.8232W

20:26 Back underway, small piece of coral in the basket, course 005 degrees, range 1700 ft.

20:28 back in big field of starfish

20:31 Two more big mounds of coral, all dead.

20:38 Out of area of depressions and mats, now even seafloor 27-44.2089N 91-02.8226W

20:43 Depth 2295 ft. Changing video tapes, 27-44.2635N 91-02.7774W

20:44 Feature in the bottom like a tow fish or cable drug across, runs N-S.

20:46 Change course to 330 degrees.

20:56 Waypoint 2, change course to 230 degrees, range 1060 ft., overshot WP2, course change 27-44.4021N 91-02.8822W. Depth 2372 ft.

21:06 Change course to 230 degrees, 27-44.3691N 91-03.0352W

21:10 Course change to due S., crossing over battery box tracks again.

21:11 Big depressions with bacterial mats, depth 2294 ft., 27-44.3671N 91-03.0629W

21:15 Back on line, course change to 260 degrees, range 1600 ft. 27-44.3039N 91-03.0455W

21:24 Depth 2297 ft., shallow depressions with bacterial mats. 27-44.2969N 91-03.1792W. course change to 240 degrees, range 800 ft., fix 27-44.2701N 91-03.3665W, depth 2280 ft., taking water sample, permission to leave bottom.

21:43 depth 2288 ft.

22:12 On surface.

Monday, May 27

GC 257, Dive 4399

Crew: Front, Dan Boggess, Bill Shedd

GC 257, Dive 4399 (cont.)
Rear, Frank Lombardo, Melissa Lobegeier

Purpose: Survey and photodocument 8200 ft. Traverse, depressional seafloor.

07:58 Launch and permission to dive. Ship shows depth of 2887 ft. 27-42.403N 90-07.223W
08:25 Depth 2000 ft., ship shows bottom at 2914 ft.
08:25 Underway at 271 degrees, range 700 ft.
08:32 On the numbers, drop straight down, bottom shows at 2880 ft.
08:39 Bottom in sight.
08:42 On bottom, depth 2894 ft., Temp 5.42, visibility 35-40 ft., current less than 0.1 kt. from 010 degrees. 27-42.443N 90-07.272W, bottom soft muddy, small deep slope craters, but mostly soft mud.
08:45 Bearing 050 degrees, range 1400 ft.
08:48 Fairly sharp ridge line in sight.
08:48 Fix 27-42.473N 90-07.166W, taking video of ridge and associated bottom.
08:51 Flat spot at depth of 2895 ft.
08:53 Depth 2910 ft., steep drop off, terracing down at 60 degree angle. Heading of 050 degrees, ridge lines running perpendicular, 5 to 8 m wide.
08:55 Leveled off, same soft sediment with some shell hash, depth 2933 ft.
08:56 Mussel shell clumps along heading.
08:58 Depth 2928 ft., gentle slope.
08:59 Depth 2926 ft., small bacterial mat.
09:00 More small bacterial mats.
09:02 Visibility 30-35 ft., turbidit increasing and decreasing, fog-like, possible proximity to mud vent, within 140 ft. of WP1.
09:03 Depth 2915 ft., very gentle slope, very smooth bottom, no big mounds or large depressions.
09:05 Depth 2911 ft., taking punch core sample within 40 ft. of WP1, trying to find vent, following flow back to vent, found a big lake , got fathometer trace showing plume in water column, 27-42.609N 90-06.997 W.
09:12 Depth 2910 ft., gas coming up, also sediment. Visibility low and slight increase in currents. Bubbles are about a mm in diameter.

GC 257, Dive 4399 (cont.)

09:21 Could not tell where flow is originating, no visibility and not enough current.

09:22 Course 055 degrees, range 900 ft. to WP2. Back at flow and trying to take samples again, Harry says to take grab sample. Sample in bucket 12. 27-42.609N 90-06.997W (sample lost over the side.)

09:30 Have grab sample and underway.

09:32 More flows, smooth, new looking flows, several inches thick. Taking still shots.

09:33 Bill thinks they are at the vent site, 27-42.648N 90-07.006W, now heading to WP2.

09:42 Pock marks, observing loose scattering of mussels and clams, not much relief.

09:45 Coming up on ridge line, carbonate structures, mussels. 27-42.692N 90-06.860W, within 100 ft. of WP2.

09:49 Very steep upslope, within 80 ft. of WP2.

09:50 Following slope up, then head on new course of 190 degrees.

09:51 Depth 2938 ft., heading to top of slope and took punch core, will send S (190 degrees) at top of slope.

10:01 Depth 2911 ft., came up on terrace, seems to be the top, heading 190 degrees, 27-42.716N 90-06.797W

10:03 Depth 2925 ft., Coming up on drop off of about 25 ft.

10:05 Depth 2941 ft., Slight drop off, WP2.

10:14 Depth 2934 ft., Taking another mat sample (push core), need to go 045 to 050 degrees, get underway, no more samples.

10:17 Depth 2942 ft., Getting underway.

10:19 Coming up on very steep slope, very soft bottom.

10:22 Depth 2919 ft., near top of slope (15 degree slope).

10:25 Depth 2912 ft., Large depression about 1m across, 600 ft. due E from WP2.

10:30 Depth 2898 ft., All stop, coming up on a slight slope, changing course to 260 degrees, range 1000 ft., 27-42.720N 90-06.691W

10:32 underway at 260 degrees.

10:34 Depth 2905 ft., passing large crater about 3m diameter, very round.

10:39 Depth 2925 ft., now on downslope, observed small mats along the terrace. Slightly north of previous transect.

10:42 Depth 2938 ft., observed carbonate structure, will grab carbonate sample, 27-42.715N 90-06.855W. Could not get basket to close, had to abandon grab sample of carbonate.

GC 257, Dive 4399 (cont.)

11:00 Regrouping and plan to get underway at 260 degrees. Observed gorgonians.

11:02 Depth 2923 ft., observing mussels and clams.

11:08 Depth 2912 ft., observing area of possible old flows, heading 260 degrees, flow is at least 50 ft., unable to find the end.

11:10 Reach the edge of the flow field, approximately 120 ft. wide.

11:13 Battery getting weak on sub. Will transect at least 5 minutes. Harry-probably 200 ft. from site, 500 ft. west of WP1.

11:15 Depth 2920 ft., Now on mussels and clams, appear to be alive.

11:22 Depth 2930 ft., Mounds, about 1.5 m across, small craters.

11:24 Very soft mounds, like mud vents.

11:26 Depth 2915 ft., 10-15 degree upslope.

11:27 70 degree slope about 40 ft. tall, instructions to look for carbonates.

11:28 Depth 2873 ft., At top of slope, no carbonate. End of transect, leaving bottom. 27-42.607N 90-07.207W

12:08 On surface.

EW 1001, Dive 4400

Crew: Front, Dan Boggess, Larry Cathles
Rear, Trainee Jimmy Nelson, Frank Lombardo

Purpose: Run transect, collect carbonates and push cores.

16:34 Launch and permission to dive. 27-57.644N 90-23.477W, Ship shows bottom at 1770 ft.

16:40 Bearing 270 degrees, range 450 ft., bottom showing at 1775 ft.

16:50 Depth 1000 ft., bottom showing at 1760 ft.

16:55 Bearing 270 degrees, range 150 ft.

16:58 Dropping straight down.

17:05 Bottom in sight.

17:07 On bottom, depth 1794 ft., temp. 7.73, visibility 35-40 ft., current 0.1 kt. from N. 27-57.686N 90-23.538W Light sediment covering bottom.

17:09 Bearing 320 degrees, range 1600 ft., getting underway to WP1.

17:13 45-50 degree slope about 25 ft. high, 27-57.731N 90-23.574W, depth 1790 ft.

EW 1001, Dive 4400 (cont.)

17:15 Depth 1740 ft., on top of feature.

17:17 Depth 1720 ft., another slope, 55-60 degrees, 27-57.744N 90-23.593W

17:24 Depth 1693 ft., continuing on gentle upslope.

17:26 Depth 1689 ft., Going over beggiatoa mat.

17:27 Bearing 295 degrees, range 325 ft.

17:30 Depth 1683 ft., going over area with gorgonians, with encrusting sponges and small beggiatoa mats. Took sample of beggiatoa 27-57.925N 90-23.780W, 300 ft. to WP1.

17:39 Bearing 156 degrees, range 350 ft. underway to WP1.

17:41 Depth 1675 ft., Could be going over gas vent, suspended particles look like they are coming from the east.

17:42 Depth 1675 ft., Turning easterly to hunt for origin of suspended sediments.

17:48 Depth 1679 ft., Change course to 060 degrees, range 2100 ft. to WP1. 27-57.8888N 90-23.7754W

18:01 Depth 1729 ft. Noticed gentle downslope.

18:03 Depth 1741 ft., Change video tape 27-57.994N 90-23.6032W, heading 065 degrees and getting underway.

18:04 Beggiatoa and small tube worms.

18:07 Depth 1758 ft. Sampling a beggiatoa mat (bucket sample) 27-58.0014N 90-23.5835W, 0.3 kt. Current at 090 degrees.

18:18 Sample finished, underway at 070 degrees..

18:22 Depth 1758 ft., Going up a 30 degree slope, 750 ft. from WP2.

18:27 Observed light sediment plume as approaching a ridge, 650 ft. from WP2.

18:29 Depth 1718 ft., Top of small ridge and is starting downslope 27-58.0309N 90-23.5211W, bearing 070 degrees, range 600 ft.

18:36 Change course to 030 degrees, at WP2, 27-58.0273N 90-23.4440W.

18:37 Depth 1715 ft., heading 030.

18:39 Depth 1710 ft., Sub stopped, getting course to WP3.

18:40 Bearing 110 degrees, range 1500 ft. to WP3.

18:41 Depth 1704 ft., Came up on old mud vent, coming up on slope of mud volcano.

18:45 Depth 1701 ft., Taking grab sample of mud, same coordinates (active area on fathometer image).

18:49 Good scoop in Bucket #5, underway on 110 degrees.

EW 1001, Dive 4400 (cont.)

19:03 Depth 1735 ft., Changing tape in video camera, 27-58.0267N 90-23.3011W

19:06 heading 110

19:13 Depth 1748 ft., Large mat of beggiatoa, white and yellow deposits as well, extensive, goes at least 30 ft. to N, new heading 160 degrees, range 180 ft.

19:15 Underway heading 160

19:17 Depth 1729 ft., New heading of 040 degrees, 27-57.9503N 90-23.1674W

19:23 Course correction 029 degrees.

19:31 Passed over cable trench perpendicular to sub track.

19:33 Depth 1757 ft., Stopped at EOL, 27-58.1166N 90-23.0572W, going over more beggiatoa, no significant relief, soft silty sediment cover over sticky sand. Heading 200 degrees upslope.

19:44 Depth 1726 ft., stop, permission to leave bottom.

19:44 Depth 1729 ft., leaving bottom, 27-58.0423N 90-23.0430W

18:15 On surface.

Tuesday, May 28

Port day at Fourchon to change scientific crews.

Wednesday, May 29

GC 232, Dive 4401

Crew: Front, Craig Caddigan, Roger Sassen
Rear, Hugo Marrero, Tom McGee

Purpose: Locate, videotape and sample hydrates, take cores in the area.

08:03 Launch and permission to dive, 27-44.4825N 91-19.0562W.

08:28 Bottom in sight.

08:30 On bottom, Depth 1870 ft., Temp. 7.6, Visibility 30-40 ft., 0.1 to 0.2 kts. Current, mud bottom with white bacterial mats, taking water sample. 27-44.5112N 91-19.0757W, within 70 ft. of target.

08:34 Heading 310 degrees.

GC 232, Dive 4401 (cont.)

08:36 Depth 1869 ft., Stopping to take tube worm samples, 27-44.5227N 91-19.0916W

08:39 Getting back underway.

08:40 Range 80 ft., due S

08:42 Course change to 130 degrees.

08:42 Lost main control box that controls camera, arc lamp, pilots box, etc. Check main connector on back of pilots box.

08:45 Bottom connection loose, tightened it and all came back.

08:48 Depth 1868 ft., small tube worm bushes and bacterial mats.

08:50 Setting down to sample bacterial mat, punch core #1, 27-44.5721N 91-19.0737W.

08:54 Back underway.

08:55 Heading NE of site and searching

08:56 100 ft. N of target

09:06 Good plume, 075 degrees about 200 ft. away.

09:07 Good sized piece of exposed hydrate, depth 1866 ft., 27-44.5173N 91-19.0828W.

09:12 Taking sample, gas escaping from bottom of hydrates, tried to take sample but hundreds of small pieces broke off.

09:23 Took grab sample with tube worms in it.

09:26 Moved left of hydrate, will take 4 punch cores, depth 1865 ft., tubes #2,3,4&5. 27-44.4974N 90-19.0687W

09:37 Will now do suction sample.

09:58 Another exposed hydrate sample about 15 ft. from the other, depth 1865 ft., doing last punch core. 27-44.5165N 91-19.0866W. Pin came out of bucket, cannot rotate anymore.

10:03 Finished with push cores and will cruise around and look for more hydrates.

10:11 Hydrates just downhill from landing, did small circle, will get underway at 310 degrees to see what else is there.

10:17 Large area of tubeworms, appears to have exposed carbonate, depth 1867 ft. 27-44.5009N 91-19.0915W.

10:26 Setting down to take couple of small rocks. 27-44.5108N 91-19.0879W.

10:29 Back underway.

10:46 Fix #12 27-44.4907N 91-19.0457W, depth 1870 ft., exposed carbonate and tube worms, carbonate sampled.

GC 232, Dive 4401 (cont.)
10:52 Fix #13 27-44.4924N 91-19.0765W, depth 1868 ft., exposed gas hydrates with tube worms and mussels.
10:57 Permission to leave bottom. 27-44.4856N 91-19.0849W.
11:23 On surface.

GC 232, Dive 4402

Crew: Front, Craig Caddigan, Dan McConnell
Rear, Hugo Marrero, Mark Brausse

Purpose: Push cores, grab samples, and gas samples adjacent to hydrates.

15:34 Launch and permission to dive. 27-44.5190N 91-19.0066W
15:37 Sounded like a bucket imploded at about 150 ft.
15:40 Abort dive to repair bucket. Depth 300 ft.
15:43 180 ft., permission to surface.
15:45 On surface, repaired imploded bucket.

GC 232, Dive 4403

Crew: same

Purpose: same

16:03 Launch and Permission to dive. 27-44.5134N 91-19.0792W.
16:21 Bearing 150 degrees, range 400 ft., depth now 1000 ft.
16:21 Range 100 ft., bearing 130 degrees, depth now 1600 ft.
16:26 Bottom in sight.
16:30 On bottom, depth 1871 ft., Temp. 7.71, Visibility 30-35 ft., current 0.1 kt. from 310 degrees, 27-44.4992N 91-19.0751W, target 60 ft. at 180 degrees.
16:39 Range 150 ft., bearing 110 degrees.
16:46 Range 250 ft., bearing 340 degrees to 1st hydrate mound.
16:56 At hydrate mound. Will go behind to punch cores with tubes #1, 2, and 3.
16:59 Sitting on slope of hydrate mound, will take 3 punch cores in that location. 27-44.5053N 91-19.0812W.

GC 232, Dive 4403 (cont.)

17:02 GPS down.

17:07 Finished with punch cores #1, 2, and 3. Will now move over and take the other 3.

17:08 GPS back on line.

17:08 Will take the other 3 punch cores on back side of tube worm patch. Mud bottom with a little bacteria, will space cores about 3 ft. apart.

17:17 Will go to the other side for a gas sample.

17:22 25 ft. from the vent this morning, still bubbling a little. Will try for a gas sample. Depth 1862 ft. 27-44.4998N 91-19.0852W

17:30 Abort gas sampling because gas is coming out too slowly.

17:31 Bearing 130 degrees to WP6, large exposed hydrate mound.

17:33 Fix 10, small bacterial mats. Getting 2 grab samples. Depth 1866 ft. White and orange bacterial mats.

17:52 Left bacterial mat site to look for gas vent.

17:54 Suction sample of bacterial mat. Depth 1870 ft., 21-44.4728N 91-19.0789W.

17:58 Back underway.

18:00 Bearing 010 degrees, range 190 ft. to hydrates and mussels.

18:03 Change course to 310 degrees.

18:07 Change course to due N.

18:18 Depth 1867 ft., mussels and tube worms with encrustations, will sample each. 27-44.4977N 91-19.1010W.

18:36 On back side of the hydrate mound found this morning. Will try for a gas sample. 27-44.4947N 91-19.0866W.

18:56 Definitely at the hydrates found this morning, gas coming out but not as much.

19:02 Depth 1867 ft., Permission to leave bottom. 27-44.4977N 91-19.0922W.

19:24 Depth 200 ft., permission to surface.

19:26 On surface.

Thursday, May 30

GC 232, Dive 4404

Crew: Front, Don Liberatore, Alexi Milkov
Rear, Frank Lombardo, Tyler Hodges

GC232, Dive 4404 (cont.)
Purpose: Collect hydrate samples, cores, grab samples and water samples.

08:16 Launch and permission to dive. 27-44.4904N 91-19.0068W
08:19 Weird caution light on both videos, "Caution C31". Took the tape out and put it back in and fixed the problem.
08:36 Get underway bearing 330 degrees, range 180 ft.
08:40 Change course to 030 degrees.
08:43 All stop, go straight down.
08:45 Bottom in sight.
08:47 On bottom, depth 1866 ft., Temp. 7.4, Visibility 30-35 ft., current 0.1 kt. at 035 degrees. 27-44.5230N 91-19.0936W
08:48 Bearing 140 degrees, range 80 ft. to hydrates.
08:50 Sandy area with tube worm bushes, will scout around.
08:53 Coming up on exposed hydrate, will take still shots for a few minutes.
08:56 Hydrates. 27-44.5109N 91-19.0789W
09:01 Seeing fogging in camera (condensation on the lens).
09:03 Emptied air from the gas sampler, going in to collect gas sample.
09:22 Got a gas sample. Will take more still shots.
09:31 Shot still shots all around the mound. Will settle in and try to break a piece of hydrate off to put in pressure bomb.
09:41 Broke off a big piece of hydrate. Stayed in. Waiting for silt to clear to put the lid on.
09:49 Can't get the lid all the way down. Last quarter inch won't go. Will take the lid off and try to vacuum the threads and try again.
10:02 Think they have the lid down, will proceed.
10:10 Moved over to a small depression. Have iceworms in the hydrates. Will attempt to sample ice worms with the suction and take photos.
10:19 Tried to sample iceworms. Broke off a piece and got it in bucket #5. Don't know if we got a worm or not.
10:21 Getting in position to take push core between 2 hydrate sites. Depth 1865 ft. 27-44.5112N 91-19.1028W.
10:32 Question for Roger: 1st site from yesterday, would you like to break off a big chunk and bring it up in the basket? Leave it alone or try to bring it up? Leave it alone in case we need another sample.
10:35 Bearing 180 degrees, range 100 ft. to other hydrate zone. May be able to break off a piece there.

GC 232, Dive 4404 (cont.)

10:38 Found an orange bacterial mat. Will stop and take a suction sample. Depth 1867 ft., Also took photos and video. 27-44.4765N 91-19.0891W.

10:47 Want push cores or suction samples? Harry – take suction sample, push cores are for Jeff.

10:51 Quite a bit of sponge. Will get another sample. Depth 1865 ft., 27-44.4773N 91-19.0634W

10:59 Take 2nd push core by the tube worm bush.

11:08 Will take push core and grab sample of tube worms. Depth 1866 ft., 27-44.4701N 91-19.0777W

11:21 Got samples. Now looking for orange bacterial mat for one more suction sample.

11:29 Time to wrap it up.

11:30 Depth 1862 ft., permission to leave bottom.

11:50 On surface.

GC 232, Dive 4405

Crew: Front, Don Liberatore, Laura Laham
Rear, Frank Lombardo, Jeff Chanton

Purpose: Collect pore water samples, and other samples.

15:49 Launch, permission to dive. 130 ft. from station, depth showing 1855 ft. 27-44.5214N 91-19.0677W

16:09 Bearing 210 degrees, range 130 ft.

16:15 Bearing 090 degrees, range 280 ft. Getting underway to E.

16:17 Bottom in sight.

16:19 Getting close to target. Tube worm bushes in sight.

16:21 On bottom at target site, depth 1862 ft., Temp. 7.77, Visibility 30-35 ft., current 0 to 0.1 kt. at 140 degrees. 27-44.5142N 91-19.0893W

16:26 At exposed hydrates. Going to deploy the pore water sampler. Fix 6: 27-44.5136N 91-19.0893W Depth 1867 ft.

16:29 One of the valves is closed, putting it into the bottom.

16:31 Sampler is in the bottom. Seafloor is very soft.

16:33 Got sampler triggered, waiting for 30 minutes.

17:00 Two minutes to go. Then they will take the pore water sampler out of the soft soil. When the sampler is on the sub, will trigger the valves.

GC 232, Dive 4405 (cont.)
17:02 Pick up probe and sampler.
17:06 Got sampler on sub.
17:18 Closed all valves. Took push core #4 right next to pore water sampler location. Fix 7 27-44.5059N 91-19.0784W Depth 1867 ft.
17:29 Second push core taken next to first one. Moving in to take another sample near bubble stream.
17:41 Collecting a gas sample in the same location as the 2nd push core.
17:50 Grab sample of sediment above the gas hydrate.
18:06 Took push core next to the hydrate mound. Shook the push core to get the sample out.
18:12 Took third push core at the same location (redid the previous one).
18:21 Took scoop sample, moving on bearing 140 degrees, range 90 ft. Target location is large exposed hydrate.
18:29 Picked up rock sample at depth of 1864 ft., could not find hydrate mound. Range 40 ft. to exposed hydrates.
18:31 Picked up scoop sample, Fix 8 27-44.4899N 91-19.0785W, depth 1864 ft.
18:41 Sword fish in sight.
18:44 Fix 9 27-44.4960N 91-19.0766W, depth 1864 ft., took scoop sample of orange material.
18:52 Still have not found second hydrate mound, time to wrap dive up.
18:56 Permission to leave bottom, depth 1867 ft.
19:16 Depth 200 ft., permission to surface.
19:18 On surface.

Friday, May 31

GC 234, Dive 4406

Crew: Front, Dan Boggess, Roger Sassen
Rear, Hugo Marrero, Kelley Peeler

Purpose: Take hydrate samples, cores, and grab samples.

08:01 Launch and permission to dive. 27-44.7543N 91-13.3406W
08:16 Bottom showing at 1730 ft., get underway due S for 200 ft.
08:23 Adjust heading to 200 degrees.
08:25 Change course to 100 degrees.

GC 234, Dive 4406 (cont.)

08:28 Bottom in sight.

08:31 On bottom, depth 1711 ft., Temp. 8.66, visibility 40-45 ft., current 0.1 kt. from 070 degrees. 27-44.7422N 91-13.4194W. Bearing 090 degrees, range 400 ft.

08:37 Area with lots of tube worms, will sit down and take grab sample of orange mat, bucket #8, depth 1762 ft. 27-44.7766N 91-13.3613W

08:45 Done with sample. Underway due E.

08:47 At marker "TX", small float to left, depth 1772 ft.

09:00 Moving toward marker "V", depth 1778 ft. Think they found hydrate.

09:01 Will try for a gas sample, 27-44.7587N 91-13.3101W.

09:57 took gas sample, getting hydrate sample.

10:36 Dropped chipper off platform, recovering it and still trying to get hydrate sample.

11:02 Still trying to get hydrate sample, got some pieces, depth 1778 ft.

11:10 Directed to wrap up operation.

11:17 Permission to leave bottom.

11:18 Left bottom, 27-44.7448N 91-13.3201W

11:43 Depth 200 ft., permission to surface.

11:45 On surface.

GC 234, Dive 4407

Crew: Front, Dan Boggess, Jeff Chanton
Rear, Hugo Marrero, Howard Manlovitz

Purpose: Observe hydrates, take video and stills, take push cores and grab samples.

16:06 Launch and permission to dive. 27-44.7614N 91-13.3365W

16:23 Course change to 050 degrees, range 400 ft.

16:25 Stop, drop straight down, bottom showing at 1735 ft.

16:31 Bottom in sight.

16:34 On bottom, depth 1756 ft., Temp. 8.1, Visibility 35-40 ft., current 0 to 0.1 kt. from 130 degrees. Fix 27-44.7906N 91-13.3467W. Landed in tube worms, no markers, will look around.

16:35 Found Marker "T2"

GC 234, Dive 4407 (cont.)

16:37 Depth 1763 ft., will sample orange mat, will do mesh bag #9 first, then screen.

16:38 Platform is stuck. Bucket #9 is the one stuck under the funnel. Will forget that spot and try to find hydrate mound.

16:50 Moving, using gas sampler to push down on lid of bucket. Worked, and platform will rotate again.

16:56 Taking suction sample of red mat into fine mesh bucket, Fix 27-44.7882N 91-13.3426W.

17:12 At 1767 ft., at marker "A1", also at marker "TX" again. Should be on hydrate.

17:16 Went straight over a tub worm bush at "TX", has flat tile with "12" on it, upslope are 2 floats, perhaps near hydrates.

17:17 Moving in on hydrates now at marker "B".

17:20 Taking tube #1 push core. Depth 1777 ft., 5 ft. from hydrate mound. Fix 27-44.7531N 91-13.3119W.

17:30 Take cores 1 & 2 on side of hydrate mound. Take core 3 to left of tube worm bush about 10 ft. away.

17:37 Tube core 4 will be taken there also (about 15 ft. to west of core 3 location).

17:47 Depth 1784 ft., Taking push core 5 downslope from thermistor site. Fix 6: 27-44.7661N 91-13.2936W.

18:02 Have Ion pump device deployed, going back to collect mussels.

18:03 Back on mussel bed, same place they took the gas sample this morning. Will take another gas sample.

18:15 Done at hydrate mound, depth 1776 ft. Will now go look for rocks for Harry.

18:24 Depth 1768 ft., Put one piece of rock in bucket #12, will try to suction bacterial mat in Bucket 11, which has mesh. Didn't work out.

18:26 Will grab another rock. Fix 27-44.7723N 91-13.3104W. Rock is in the basket, will try for another bacterial mat.

18:29 Depth 1771 ft., Found orange bacterial mat, will attempt to sample.

18:35 Moved over a ridge. Will try to sample another orange bacterial mat.

18:42 Have bacterial mat sampled.

18:57 Depth 1792 ft., Request permission to leave bottom (no fix available).

19:15 Permission to surface.

19:15 Surface in sight, surface clear.

19:17 On surface.

Saturday, June 1

MC 885, Dive 4408

Crew: Front, Craig Caddigan, Dick Fillon
Rear, Frank Palumbo, Barry Kohl

Purpose: Survey preselected traverse, collect still shots, video and samples.

08:01 Launch and permission to dive. Fix 28-04.0497N 89-43.2765W
08:26 Course 085 degrees, range 200 ft. Depth showing 1800 ft.
08:32 Bottom in sight.
08:34 On bottom. Depth 2160 ft., Temp 6.79, visibility 20-30 ft., current 0,4 kt. from 030 degrees. Fix 1: 28-04.0403N 89-43.3787W. Core sample 1.
08:40 Head on course 100 degrees. Bottom is basically mud. 100 degrees is taking sub diagonally up a gentle slope.
08:50 Depth 2134 ft., Bottom is the same.
08:56 New heading of 040 degrees, depth 2117 ft., bottom is the same.
08:59 At WP1, All stop, look for thermistor.
09:07 New heading of 100 degrees to WP2.
09:11 Underway at 100 degrees, bottom is the same.
09:15 Depth 2100 ft.
09:17 Depth 2080 ft., Starting to see rocks with crinoids.
09:19 Took long push core, Fix 2: 28-03.9712N 89-43.0429W Punch core #5.
09:20 Just lost forward horizontal thruster.
09:26 Coming to small drop off, one big boulder there with coral on it. Going down, then back up again.
09:28 Area of small rocks and small gorgonians, depth 2065 ft.
09:30 Going over a series of ridges, current up to 0.5 kts.
09:31 Back over clean mud bottom.
09:31 Lots of shell hash with gorgonians.
09:32 New heading of 070 degrees.
09:39 Change to video tape #2.

MC 885, Dive 4408 (cont.)
09:40 Tube worms with clams on top.
09:46 New heading of 035 degrees.
09:47 Underway at 025 degrees.
09:49 Bottom covered with dead clams.
09:52 All stop. Took long punch core. Fix 3: 28-03.9611N 89-42.7557W. Depth 2037 ft. Be advised forward horizontal is coming on by itself. Punch core only penetrated 2 or 3 inches, took grab sample.
09:59 New course of 080 degrees, range 1000 ft.
10:07 Next time clams are seen, take sample.
10:08 Came across fiberglass pole sticking out of bottom.
10:09 Starting to see series of small ridges.
10:11 New heading of 060 degrees.
10:14 New heading of 035 degrees.
10:21 WP3 is due N range 100 ft.
10:23 On WP3, depth 2066 ft., clean bottom with some shell hash. Took punch core #4. Fix 4: 28-03.9564N 89-42.5319W.
10:28 New heading of 150 degrees to EOL.
10:33 New heading of 120 degrees (current set)
10:38 Changing to video tape #3.
10:42 Be advised, sub going sideways more than forward.
10:46 New heading of 200 degrees.
10:49 WP due N about 100 ft.
10:50 Stop and take punch core.
10:50 Depth 2575 ft., clean mud bottom, punch core #3, Fix 5: 28-03.664N 89-42.4005W.
10:55 Head back to WP 3, due N.
11:01 Getting swept up slope.
MC 885, Dive 4408 (cont.)
11:02 Go up slope, about 330 degrees.
11:04 At top of slope, depth 2061 ft., turning to head back into current.
11:08 Bottom is featureless mud with burrows.
11:09 Will take grab sample. Fix 6: 28-03.7227N 89-42.4090W, Depth 2063 ft.
11:10 Request permission to leave bottom. Total distance covered 6493 ft.
11:36 On surface.

MC 885, Dive 4409

Crew: Front, Craig Caddigan, Bob Woolsey
Rear, Frank Palumbo, Tyler Hodges

Purpose: Survey traverse 2 and sample, take stills and video.

15:40 Lunch and permission to dive. Fix 1: 28-04.5120N 89-43.3480W
15:57 Start heading on course of 320 degrees.
16:01 New heading of due N, bottom showing at 2060 ft.
16:04 New heading of 020 degrees.
16:06 Bottom in sight, new heading of 060 degrees.
16:08 On bottom, depth 2087 ft., Temp. 6.82, visibility 20-25 ft., current 0.3 to 0.4 kts. at 030 degrees. Fix 2: 28-04.6908N 89-42.8598W Same bottom as this morning, flat muddy bottom. Underway at 060 degrees.
16:13 New heading of 150, SOL.
16:17 Depth 2068 ft., bottom is the same.
16:22 New heading of 155 degrees.
16:23 Came across first outcropping of rocks with gorgonians on them, Fix 3: 28-04.5735N 89-42.7919W.
16:26 Bottom featureless again, depth 2063 ft.
16:28 Coming into more gorgonians, will sample. Fix 4: 28-04.4861N 89-42.7767W.
16:36 Got sample of small rock with egg sacks on it, will take punch core. Depth 2055 ft.
16:39 Back underway at 155 degrees.
16:44 Depth 2067 ft. Crossed small rocks, then barren bottom, starting to see shell hash.
16:45 New heading of 220 degrees, range about 100 ft.
16:46 Small rocks with shell hash.
16:48 Near WP1, heading of 150 degrees to WP2.
16:57 Depth 2056 ft., Barren bottom, gently rolling up and down maybe 10 ft.
17:01 Came down a slope to 2104 ft., now going back up.
17:07 Depth 2056 ft. On clean bottom.
17:11 Depth 2049 ft. Getting back into shell hash.
17:13 Shell hash getting thicker, also occasionally seeing gorgonians.

MC 885, Dive 4409 (cont.)

17:16 Shell has thicker, depth 2041 ft. Will do 1 long push core and 1 short push core. Fix 5: 28-03.9911N 89-42.7551W

17:22 Punch core 1, punch core 4. Sent to WP3 on bearing of 200 degrees, range 1700 ft.

17:32 Small gorgonians, rocks, and shell hash.

17:40 Going slightly upslope. Depth 2057 ft. Have now left shell covered bottom and now on burrowed mud.

17:44 Back in shell covered bottom, rocks, and gorgonians. Going back upslope.

17:46 Depth 2064 ft. Top of a little ridge, took punch core #5.

17:49 Have punch core and getting underway bearing 195 degrees.

17:52 Change course to 170 degrees.

17:55 Change course to 160 degrees.

17:57 Change course to 090 degrees.

18:01 Near WP3. Take long push core.

18:03 Setting down, depth 2061 ft., sitting atop a silt covered rock formation. Fix 6: 28-03.7116N 89-42.8518W.

18:11 Got core, had to move slightly.

18:11 Proceed approximately 80 ft. at 280 degrees.

18:12 Course change, 50 ft. due south.

18:15 Course change 110 degrees.

18:23 Looking around for thermistor, heading 110 degrees.

18:24 Found the thermistor. Fix 7: 28-03.6917N 89-42.8765W, Depth 2052 ft., Taking video and will recover thermistor.

18:30 Have thermistor on platform, won't go in the basket.

18:54 Permission to surface.

18:56 Surface in sight, surface clear.

18:57 On surface.

Sunday, June 2

VK 826, Dive 4410

Crew: Front, Don Liberatore, Harry Roberts
Rear, Hugo Marrero and trainee Curt Patterson

Purpose: Survey traverse 1, take stills, video and samples.

VK 826, Dive 4410 (cont.)

08:00 Launch and permission to dive. Fix 1: 29-10.5088N 88-00.9544W, bottom showing at 1599 ft.

08:03 Going through layer of turbid water, coming up on depth of 200 ft.

08:14 Get underway at 060 degrees.

08:19 Course change to 080 degrees, range 400 ft. Depth showing at 1400 ft.

08:22 Bottom in sight.

08:25 On bottom, depth 1581 ft., Temp 9.67, visibility 25-30 ft., current 0.2 kts. at 090 degrees. Fix 2: 29-10.4874N 88-00.0064W. Bottom flat, soft sediment, and lots of small fish.

08:29 At SOL, new course of 170 degrees, range 1600 ft.

08:33 Came over a ridge, now heading down slope.

08:37 Depth 1600 ft., Slope increasing, no difference in bottom type.

08:40 Depth 1640 ft., Looks like slope is 30 degrees or more.

08:41 Bottom starting to flatten out, same type, mud.

08:42 Continues on down. Will follow. Appears course of 230 degrees.

08:43 Course of 220 degrees, depth 1700 ft.

08:45 Request estimated depth of hole. Appears to be 1800 to 1850 ft. deep. At 1728 and still going down.

08:46 Depth 1750 ft.

08:48 Still going down, now at 1775 ft.

08:56 At 1838 ft., not flat but slight slope, waiting for sediment to clear. Fix 4: 29-10.3128N 88-00.9993W

08:59 Bottom looks flat.

09:07 Motored around a bit, depth 1837 ft., will take punch core #6. WP2 is at course of 170 degrees, range 4000 ft.

09:15 Found a gorgonian with a clam growing on it.

09:22 Depth 1700 ft.

09:26 Depth 1637 ft., looks like top of the slope. Fix 5: 29-10.2464N 88-01.0481W. Bottom change, harder with gorgonians, anomenes, etc.

09:27 Down slope slightly, back into soft sediment.

09:31 Working back up a shallow slope.

09:39 Leveled out at 1580 ft.

09:40 Ridge with gorgonians and small rock.

09:41 Depth 1573 ft., Fix 6: 29-10.0951N 88-01.0672W, back underway at 170 degrees.

09:43 Lost tilt function on video, still have pan.

VK 826, Dive 4410 (cont.)

09:44 More of hard bottom with gorgonians.

09:47 Going back upslope.

09:50 Course change to 150 degrees, range 1400 ft. At the top of a little hill, depth 1590 ft.

09:51 Series of ridges, couple of meters high with shell hash, etc.

09:52 Lot of shell hash, mostly dead stuff.

09:56 Coming across Lophelia coral, depth 1532 ft., (photo of fathometer plume) Fix 7: 28-09.7827N 88-01.0395W. Large field of lophelia.

09:58 Depth 1538 ft. Will sample coral.

10:02 Back underway on course of 150 degrees.

10:03 Course change to 165 degrees, range 700 ft.

10:06 Getting out of coral area and into broken bottom with shell hash.

10:07 Hard bottom, broken material and shell hash.

10:08 Just spotted 1st tube worms, course change to 145 degrees.

10:10 Up a mound of thick coral, carbonate mound.

10:11 Course change to 120 degrees, range 180 ft. to WP2.

10:15 New course of 040 degrees, 80 ft. Will stop and grab rock sample. Fix 8: 29-09.6482N 88-01.0060W. Got rock sample, will continue on 030 degrees 120 ft.

10:24 At WP2, bearing 185 degrees, range 1800 ft. to EOL. Depth 1465 ft.

10:39 Back into coral field, depth 1529 ft., course change to 160 degrees.

10:42 Depth 1546 ft., will take scoop sample of clams and little sediment.

10:51 Very rocky bottom, coral and gorgonians.

10:54 Depth 1580 ft., down slope at a steep angle.

10:56 At EOL, will mosey around and look for something interesting.

10:58 See a few clams on coral, will take samples. Fix 9: 29-09.3803N 88-01.0239W, tilt now working again.

11:07 Got 2 clams, heading upslope, depth 1526 ft.

11:14 Depth 1565 ft., permission to leave bottom. Fix 29-09.4147N 88-01.0255W.

11:33 Surface in sight, surface clear.

11:34 On surface

VK 826, Dive 4411

Crew: Front, Don Liberatore, Barry Kohl
Rear, Hugo Marrero, Mark Brausse

Purpose: Survey traverse 2, take stills, video and samples, get 2 background cores for Jeff.

15:32 Launch and permission to dive. 29-09.7557N 88-01.8910W
15:58 Bottom in sight.
15:58 On bottom, depth 1708 ft., Temp. 8.80, visibility 25-30 ft., current 0.1 kt.
16:02 Instructed to take 2 background push cores for Jeff.
16:05 Have push core #1.
16:08 Have push core #2. Bearing 100 degrees, range 1400 ft. to WP1. Bottom is featureless soft sediment with pock marks. Fix 6: 29-09.7528N 88-01.9246W
16:21 Course change to 090 degrees, range 400 ft. Featureless, small pock marks. (Moderately high amplitude on map)
16:23 Different bottom type, shells, but not hard bottom.
16:24 Depth 1696 ft., on hard bottom with gorgonians (corresponds to high amplitude on map). At WP 1, ridge with some tubeworms.
16:26 Course 100 degrees, range 3500 ft. to WP2.
16:27 Flat mud bottom, depth 1700 ft.
16:31 Huge shark spotted, trying to get video.
16:34 Chasing shark, coming on hard bottom and gorgonians.
16:35 Rock outcrop, depth 1708 ft., gorgonians and tubeworms.
16:36 Bigger bushes of tubeworms. Depth 1703 ft.
16:37 Over small ridges, rough outcrop.
16:39 Over soft bottom.
16:39 Small patches of hard bottom among flat sand.
16:41 Depth 1684 ft., Bottom change upslope and shell hash.
16:43 Crossing isopods, a lot more than before.
16:44 Depth 1661 ft., rocky bottom.
16:44 Going to find rock sample.
16:46 Rock sample at depth of 1654 ft., Fix 7: 29-09.6671N 88-01.3772W.
16:47 Bearing 100 degrees. Shark following.
16:49 No sign of gas or any hydrate so far.
16:52 Depth 1600 ft., Gorgonians, sponges and more hard ground.

VK 826, Dive 4411 (cont.)

16:53 Slope about 20 degrees, lophilia more dominant.

16:57 Large carbonate structures, depth 1560 ft., many gorgonians and black coral. Fix 8: 29-09.6497N 88-01.2705 W.

17:04 Transition to deep soft sediment, depth 1519 ft.

17:06 Back in coral area, depth 1487 ft.

17:07 Carbonate structure under lophelia bushes, lots of shell hash among boulders.

17:08 Horizontal slabs of carbonate rock (corresponds to high ampltude). 600 ft. west on line from WP 2

17:10 Coral, tubeworms, stopping to take video. Fix 9: 29-09.6290N 88-01.1307W.

17:15 Back underway at 100 degrees.

17:19 Course 090 degrees, 0.4 to 0.5 kts. of current.

17:24 Depth 1453 ft., now going downslope.

17:25 Now at WP 2, new course 100 degrees, range 5000 ft.

17:27 Softer bottom with shell hash, depth 1474 ft.

17:28 Depth 1480 ft., going back upslope.

17:29 On top of ridge, now going back downslope, depth 1474 ft.

17:30 Depth 1480 ft., grab sample. Fix 10: 29-09.6108N 88-00.9787W

17:35 Now have grab sample.

17:37 Back underway.

17:38 Seeing battery track marks, depth 1479 ft., 0.6 kts of current at 100 degrees, going against sub.

17:45 Stopping to take push core, Fix 11 29-09.6006N 88-00.8949W, push core tube #3. Depth 1517 ft.

17:55 Depth 1565 ft., downslope, sharp break downslope.

17:57 Urchins, smooth sediment bottom, depth 1600 ft.

18:00 Flat bottom with anemones, depth 1638 ft. Stopping for grab sample at depth of 1640 ft.

18:17 Heading downslope, depth 1587 ft.

18:20 Arrived at bottom of slope, depth 1660 ft.

18:32 Bottom a little more local relief.

18:34 Area looks disturbed (perhaps anchor drag). Will take grab sample in flat area at depth of 1702 ft.

18:41 Grab sample (Fix 13) acquired, and leaving bottom. 29-09.5233N 88-00.3467W

Monday, June 3

MC 709 Dive 4412

Crew: Front, Dan Boggess, Roger Sassen
Rear, Frank Lombardo, Jeff Chanton

Purpose: Survey Traverse 1, take stills, video and samples, and select site for pore water sample.

07:58 Launch, permission to dive.
08:21 Get underway at 330 degrees.
08:24 Change course to 300 degrees, range 400 ft.
08:27 Bottom in sight.
08:31 On bottom, depth 2262 ft., Temp. 5.99, visibility 25 ft., current 0.1 kt. at 220 degrees. Soft brown pock marked mud. New course of 275 degrees to SOL.
08:34 All stop. At SOL, get underway at 140 degrees, range 1800 ft. to WP 1. Fix 28-13.8670N 89-42.4670W.
08:38 Across wide drag marks, 3 ft. wide, not very deep.
08:39 Soft mud bottom with pock marks, up shallow slope. Depth 2254 ft.
08:41 Light shell hash and bacterial mats.
08:48 Edge of depression, old mud volcano. Has shell hash and bacterial mats. Fix 28-13.8469N 89-42.4109W.
08:53 Another wide track mark, 1m wide, 0.5m deep, crossing perpendicular to sub track., back into regular pock marked mud.
08:56 Small terrace about 2 m wide, another about 10 m. wide, heading down, depth 2213 ft.
08:56 Fix (ship) 28-13.82N 89-42.44 W(tracking problems, fix from ship).
09:02 Punch core sample of bacterial mat in tube #1, Fix 28-13.7296N 89-42.3210W, depth 2223 ft.
09:09 Forget punch core, silted in. no visibility, back underway at 140 degrees.
09:12 Course change, heading 040 degrees (tracking now working). Setting down for core, push core tube #2. Depth 2232 ft., Fix 9: 28-13.6284N 89-42.2415W
09:17 Getting underway course 035 degrees.

MC 709, Dive 4412 (cont.)

09:20 New course of 130 degrees, range 1200 ft.

09:28 Found small depression, will try to sample mussels and bacterial mat. Fix 10: 28-13.6011N 89-42.1661W, depth 2232 ft.

09:38 Suction sample of clams and mussels, Fix 11: 28-13.6050N 89-42.1433W, depth 2225 ft. (Photo of fathometer – oil seep).

09:53 Two push cores, short push Core (#3), also taking a carbonate sample. The two initial push cores were long ones, no numbers given. No carbonate sample taken.

09:58 Underway bearing 140 degrees.

10:00 Pockmarks, bacterial mats, and scattered shells (can't get fix).

10:03 Underway at 150 degrees, stopped to sample holothurian, but encouraged to get back underway. (Photo of plume on fathometer).

10:12 At WP 2, Course 125 degrees, range 700 ft. to WP 3.

10:18 Going downhill, depth 2269 ft., change course to 115 degrees.

10:20 Coming over the edge of a large circular depression about 30 m in diameter., shell hash and possibly a brine pool, depth 2280 ft.

10:28 Change course to 100 degrees.

10:30 At WP 3, new course of 130 degrees, range 2255 ft. to EOL.

10:31 Bottom small pock marked fine mud, shallow upslope, depth 2258 ft.

10:33 Coming over a big hole with steep sides, 30 m diameter and 5 m deep.

10:41 Depression between 2 ridges, now slight upslope of about 15 degrees, every 15 or 20 m are small depressions with nothing inside.

10:44 Depth 2267 ft., small mud vent.

10:49 Course change to 115 degrees.

10:52 Depth 2292 ft., been on a shallow downslope.

10:54 Depth 2302 ft., on 15 degree downslope. Change course to 090 degrees.

10:56 At bottom of slope, depth 2332 ft.

10:58 All stop, geotechnical punch core, depth 2329 ft., Fix 28-13.0739N 89-41.4570W.

11:03 Lost up and down on arm.

11:05 Permission to leave bottom.

11:38 On surface.

MC 709, Dive 4413

Crew: Front, Dan Boggess, Harry Roberts.
Rear, Frank Lombardo, Laura Laham

Purpose: Find vent site, install and retrieve pore water sampler, survey and take stills, video, grab samples and push cores. Will launch at WP 1 on Traverse 1 and search for vent.

15:38 Launch, permission to dive. Fix 1: 28-13.6669N 89-42.2072W
15:43 Murky layer at about 250 ft.
15:53 Get underway at 075 degrees.
15:56 Change course to 060 degrees.
15:58 Lot of turbidity in water at 1400 ft.
16:00 Change course to 030 degrees.
16:04 Drop straight down.
16:11 Bottom in sight.
16:14 On bottom, depth 2231 ft., Temp. 6.85, visibility 30-35 ft., current 0.2 kt. from N, Fix 2: 28-13.6530N 89-42.2089W Landed at brine seeps. Punch core tube #4.
16:25 Got punch core, heading of at 030 degrees.
16:29 Haven't found seep site, found tube worms, mussels, depth 2329 ft., Deploying pore water sampler.
16:39 Tripped handles, closed 1st. Sitting for 28 more minutes.
17:07 30 seconds to go, will move in, pick up pore water sampler and bring back on board. Fix 4: 28-13.6837N 89-42.1965W
17:22 Have sampler back on board, closing valves.
17:34 Got scoop of sediment in bucket #3, will head off into current (330 degrees), will take punch core sample. (Plume on fathometer, but appears to be sub and not seep, took photo), Fix 28-13.64N 89-42.22W.
17:41 Heading to plume, 300 ft. at 200 degrees.
17:56 Depth 2228 ft., stopped to sample carbonate rock, Fix 28-13.6661N 89-42.1850W. Did not sample.
18:00 Bearing 225 degrees, range 140 ft. to plume.
18:03 On site, will look around.
18:08 Sample rocks and clams, fix 28-13.6448N 89-42.2209W, depth 2230 ft.

MC 709, Dive 4413 (cont.)

18:24 Will stop and take grab samples of mussels and clams, depth 2232 ft., fix 28-13.6531N 89-42.2707W

18:45 Time to wrap it up, attempting to sample rock.

18:47 Depth 2231 ft., request permission to leave bottom, fix 28-13.6540N 89-42.2664W

19:13 Permission to surface.

19:15 Surface in sight, surface clear.

19:16 On surface.

Tuesday, June 4

MC 118, Dive 4414

Crew: Front, Craig Caddigan, Harry Roberts
Rear, Hugh Marrero, Tyler Hodges

Purpose: Survey Traverse 1, sample.

07:57 Launch, permission to dive. Fix 1: 28-51.3198N 88-29.8819W

08:04 Going through layer of turbid water at 400 ft.

08:11 Get underway at 340 degrees.

08:22 Course change to 030 degrees, range 650 ft.

08:29 Course change to 040 degrees, range 260 ft. Bottom showing at 2200 ft.

08:31 Course change to due N, range 180 ft.

08:34 Drop straight down, within 50 ft.

08:38 Bottom in sight

08:39 On bottom, depth 2869 ft., Temp. 5.74, visibility 20-25 ft., current 0.3 to 0.4 kts. at 050 degrees. Fix 2: 28-51.4457N 88-29.9005W.

08:40 Get underway on course of 080 degrees, range 300 ft. to SOL. Bottom is featureless mud with creature depressions

08:46 At SOL, Depth 2873 ft., same bottom, much suspended sediment in water column, get underway at 140 degrees, Fix 3: 28-51.4516N 88-29.8469W.

08:55 Depth 2885 ft., bottom same.

09:03 Depth 2915 ft., down slight slope, visibility worse (15 to 20 ft.), course change to 120 degrees, range 1300 ft.

09:09 Course change to 100 degrees.

MC 118, Dive 4414 (cont.)
11:27 Surface in sight, surface clear.
11:27 On surface.

MC 118, Dive 4415

Crew: Front, Craig Caddigan, Harry Roberts
Rear, Hugo Marrero, Howard Manlovitz

Purpose: Will start at EOL and proceed to WP 1 (amplitude), then search for vent site. Won't try for EOL.

15:29 Launch, permission to dive. Fix 1: 28:51.2402N 88-29.2909W
15:45 Get underway at 330 degrees, range 300 ft.
15:51 Drop straight down.
16:07 Bottom in sight.
16:08 On bottom, depth 2907 ft., Temp. 5.75, visibility 15-20 ft., current 0.2 to 0.3 kts. at 080 degrees. Fix 28-51.4325N 88-29.3064W. Get underway at 200 degrees, range 2000 ft. Lost pan and tilt on camera. Seeing clams and bacterial mat.
16:14 Got camera back.
16:17 Depth 2903 ft., will stop for grab sample. Bottom is plain mud. Fix 28-51.3682N 88-29.3491W. Sample in Bucket #9.
16:22 Back underway at 200 degrees.
16:25 Back in plain old mud, depth 2908 ft.
16:30 Depth 2908 ft., Starting to see a few clam shells.
16:38 Depth 2899 ft., Some clam shells and small bacterial mats.
16:39 Just passed over site that looks like they worked this morning.
16:40 Starting to see small rocks.
16:40 Depth 2895 ft., Fix 28-51.1585N 88-29.5148W, going down into a crater.
16:45 Depth 2908 ft., found gas vent with hydrates and a lot of oil. Will take sample. Fix 28-51.1377N 88-29.5170W.
16:59 Got gas sample. Trying to get hydrate sample. Tough to break.
17:04 Repositioned and kicked up a bunch of silt. Will sit a wait for it to clear.
17:17 Unable to get hydrate sample. Got one small piece in jaws, but couldn't get it into container.
17:23 Lost arm. Shutting down to see if breakers kick back in.

MC 118, Dive 4414 (cont.)

09:12 Depth 2914 ft., bottom same.

09:13 Course change to due E (090).

09:14 Starting to see a few dead shells, starting up slope slightly, depth 2900 ft.

09:15 Starting to see a few small rocks, depth 2898 ft., will take sample. Fix 4: 28-51.1394N 88-29.5820W. Grab sample in bucket #4.

09:19 Getting back underway at 090 degrees.

09:20 will follow up slope, about 080 degrees.

09:21 Just over a small rise, now dropping back down (photo of plume on fathometer).

09:24 At bottom of the feature, more shell hash.

09:24 Will set down for punch core, depth 2912 ft., Fix 5: 28-51.1319N 88-29.5502W. 2 punch cores and 1 grab sample. Oil coming out of bottom of 2nd punch core.

09:37 Found small crater, gas seep with hydrates in the side at depth of 2915 ft. Fix 5: 28-51.1409N 88-29.5361W. Will attempt to sample gas. (Photo of fathometer).

09:55 Gas sample successful, also got punch core and small rock, will look around for more hydrates.

09:56 Lost camera, lights out, green light blinking. No pan and tilt.

10:00 Got camera back.

10:02 Depth 2902 ft., stop for gorgonian and rock sample.

10:13 Range 200 feet, bearing 200 degrees to middle of anomaly.

10:14 Depth 2898 ft., taking push core through bacterial mat. Fix 7: 28-51.1615N 88-29.4769W.

10:21 Course 130 degrees, range 1500 ft. to WP 2.

10:28 Depth 2922 ft., out of shell hash and back onto mud bottom.

10:30 Course change to 120 degrees, range 900 ft. depth 2932 ft., visibility 15-20 ft.

10:36 Course change to 110 degrees, range 400 ft.

10:38 Course change to 090 degrees.

10:40 Stopping at 2968 ft. to collect sea cucumber.

10:41 Back underway at 070 degrees, range 300 ft.

10:43 Depth 2974 ft., starting upslope.

10:47 At WP 2, circular weak amplitude, depth 2970 ft., fix 28-50.9608N 88-29.2729W

10:48 Permission to leave bottom.

11:25 Permission to surface, depth 175 ft.

MC 118, Dive 4415 (cont.)

17:28 Got arm back.

17:41 Lost arm again, waiting to reset breakers.

18:09 Got lid on and valve closed, will take grab sample and rock sample.

18:13 Course 195 degrees, 100 ft. from WP 1, bearing 210 degrees. 2800 ft. to EOL, getting underway.

18:17 Depth 2910 ft., sea fans and gorgonians.

18:20 Will take 2 punch cores. Time to wrap it up. Depth 2926 ft., fix 28-51.0942N 88-29.5805W.

18:29 Permission to leave bottom.

Task 4: Heat Flow and Temperature Studies at Bush Hill and other Hydrate Sites using the Submersible, Johnson Sea Link

Final Report

Principle Investigators:
James Brooks, TDI-Brooks International, Inc.
Ian MacDonald and Bernie Bernard, Geochemical and Environmental Research Group,
Texas A&M University, College Station, Texas, 77845

DOE Award DE-FC26-00NT40920

ABSTRACT

Natural gas hydrates occur on the sea floor of the Gulf of Mexico in outcropping mounds that also contain other minerals, such as carbonates, that have been precipitated by microbial activity. Temperature probes were inserted in one such mound and in the mud nearby by researchers from Texas A&M University and TDI-Brooks International, Inc. Each probe contained two recording thermistors, one at the top to measure water temperature and one at the bottom to measure temperature in the sea-floor hydrate or mud. Measurements and time-lapse photos were taken over about 11 months. Preliminary results of the experiment:

- show no dramatic changes in the size or shape of the mound or in the amount of gas being vented.
- Include mean temperatures of 7.87^{o}C in the water and 7.81^{o}C in both hydrate and mud.
- Temperatures in hydrate and mud lag behind water temperatures.

TABLE OF CONTENTS

TITLE PAGE
ABSTRACT
TABLE OF CONTENTS
GRAPHICAL MATERIALS
INTRODUCTION
EXECUTIVE SUMMARY
EXPERIMENTAL
RESULTS AND DISCUSSION
CONCLUSION
REFERENCES
ACRONYMS/ABBREVIATIONS

GRAPHICAL MATERIALS

Figure 4-1. Temperature in a hydrate mound
Figure 4-2. Temperature measurements
Figure 4-3. Fathometer image of gas seep
Figure 4-4. Device for measuring gas from seeps
Figure 4-5. Temperature and gas activity during passage of Loop Eddy
Figure 4-6. Graph of temperature data from Thermistor Probe #1
Figure 4-7. Graph of temperature data from Thermistor Probe #2
Figure 4-8. Short thermistor probe.
Figure 4-9. Long probe prior to deployment on Sea Link.
Figure 4-10. Thermistor probe deployment at GC 234

INTRODUCTION

Natural gas hydrates occur on the sea floor of the Gulf of Mexico in outcropping mounds that also contain other minerals, such as carbonates, that have been precipitated by microbial activity. Temperature probes inserted into such mounds have been used to collect data that can help define the extent of the hydrate stability zone (HSZ). This study was designed to explore locations and shifts in the HSZ at several sites of documented hydrate occurrence in the northern Gulf of Mexico. Measurements and time-lapse photos were taken over about 11

months. Further analysis is expected to advance efforts to model and understand the thermal response (i.e. thermal conductivity) of exposed hydrate deposits.

Gas activity also has been observed, acoustically, by depth sounders mounted on surface vessels and by current meters located on the sea floor. Warm-water eddies detach from the principal current in the Gulf of Mexico, the Loop Current, and drift westward along the Louisiana-Texas continental slope causing increases in bottom-water temperature that have been observed to coincide with increases in gas activity.

EXECUTIVE SUMMARY

Natural gas hydrates occur on the sea floor of the Gulf of Mexico in outcropping mounds that also contain other minerals, such as carbonates, that have been precipitated by microbial activity. Temperature probes were inserted in one such mound (fig.4-1) and in the mud nearby by researchers from Texas A&M University and TDI-Brooks International, Inc. Each probe contained two recording thermistors, one at the top to measure water temperature and one at the bottom to measure temperature in the sea-floor hydrate or mud. Measurements and time-lapse photos were taken over about 11 months. The temperature measurements are presented graphically in fig.4-2. Preliminary results of the experiment are:

1) Photos show no dramatic changes in the size or shape of the mound or in the amount of gas being vented.
2) Mean temperatures were 7.87^{o}C in the water and 7.81^{o}C in both hydrate and mud.
3) Temperatures in hydrate and mud lag behind water temperatures.

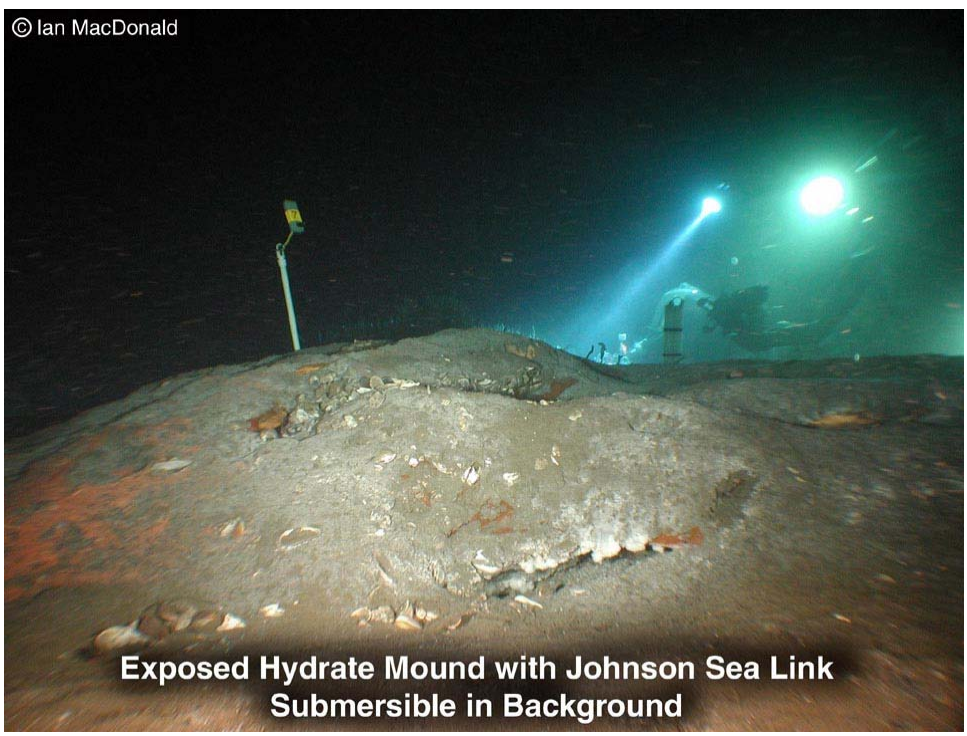

Figure 4-1. Temperature probe in a hydrate mound.

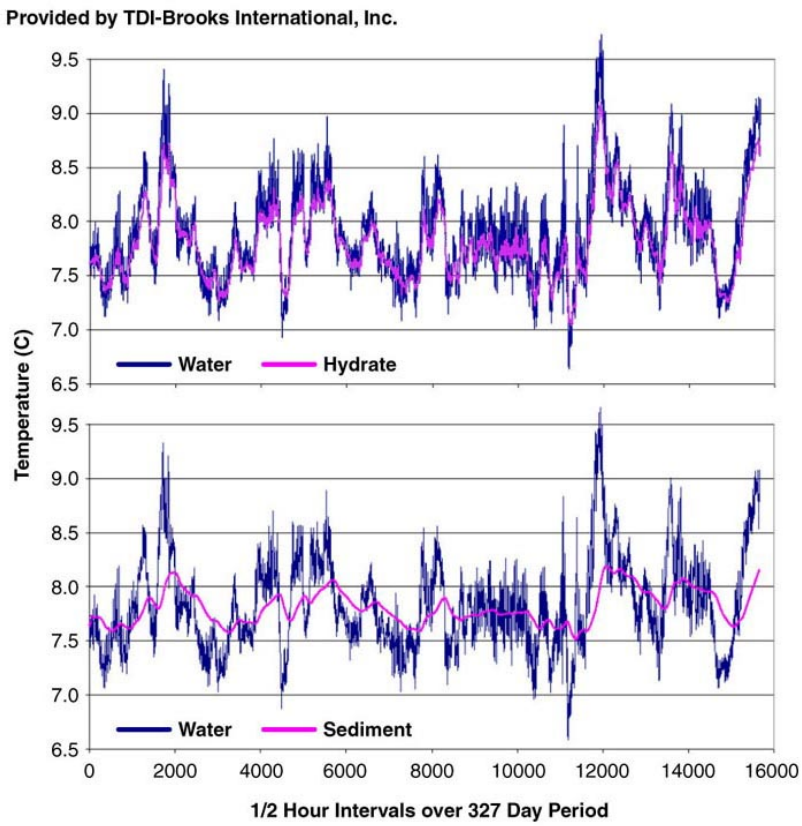

Figure 4-2. Temperature measurements from hydrate mound

Further analysis is expected to advance efforts to model and understand the thermal response (i.e. thermal conductivity) of exposed hydrate deposits.

Gas activity also has been observed acoustically by depth sounders mounted on surface vessels (fig.4-3) and by current meters located on the sea floor (fig.4-4). Warm-water eddies detach from the principal current in the Gulf of Mexico, the Loop Current, and drift westward along the Louisiana-Texas continental slope. These cause increases in bottom-water temperature that have been observed to coincide with increases in gas activity (fig.4-5).

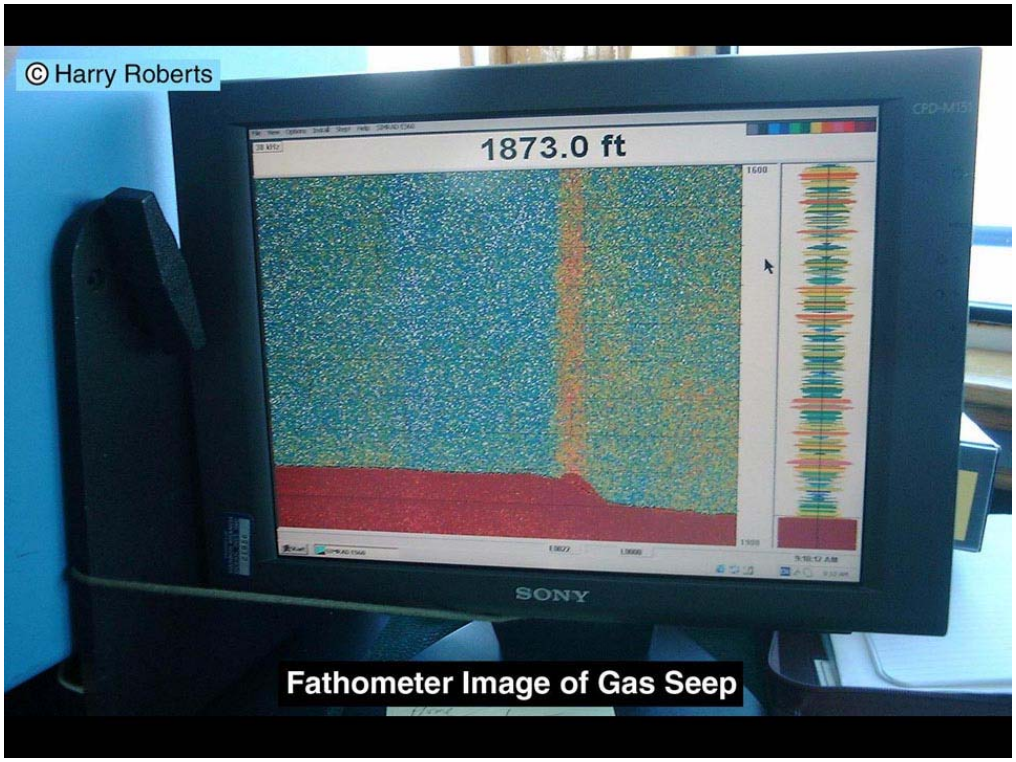

Figure 4-3. Fathometer image of gas seep

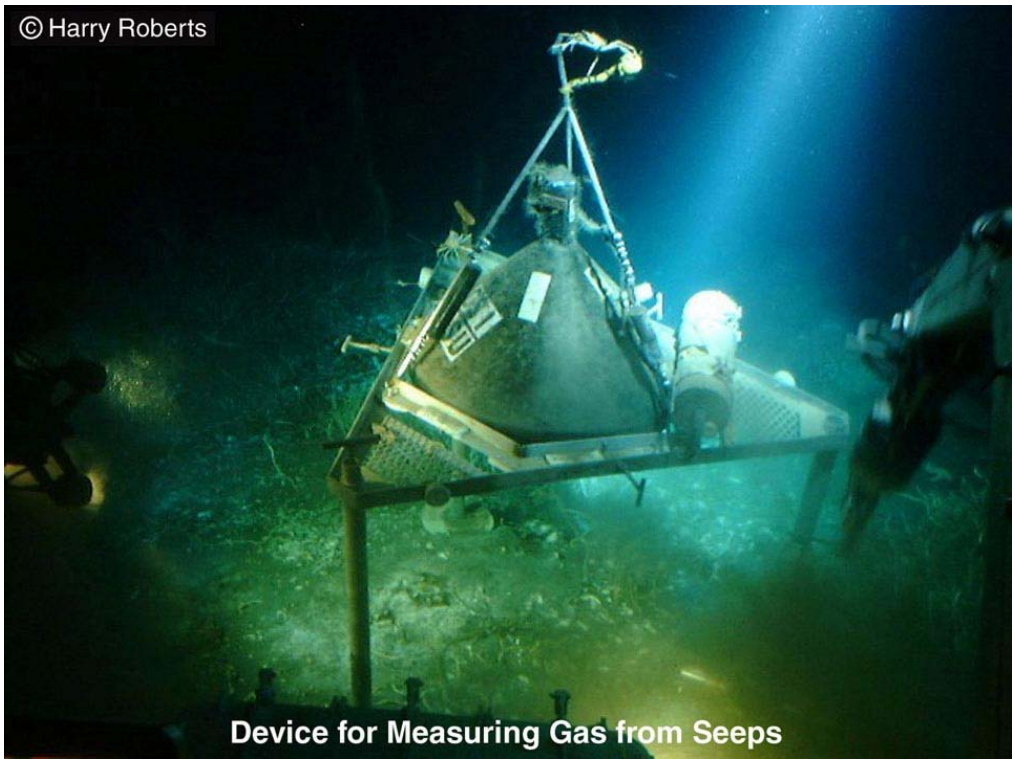

Figure 4-4. Device for measuring gas from seeps

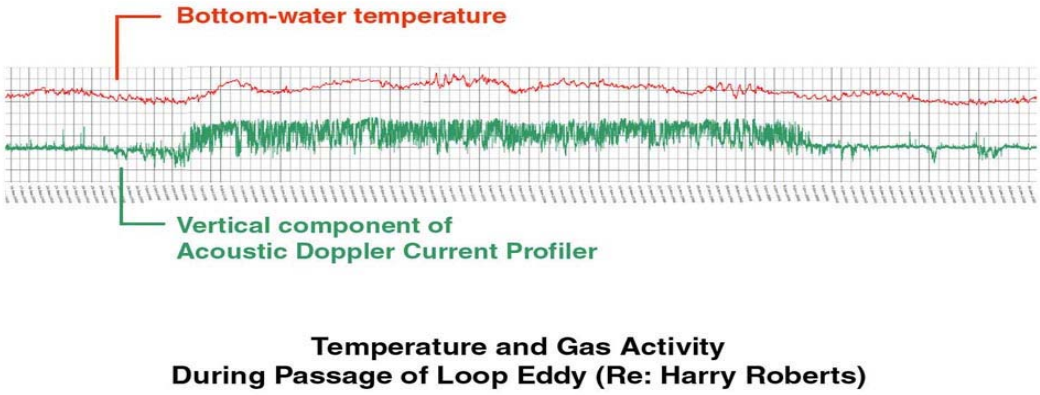

Figure 4-5. Temperature and gas activity During passage of Loop Eddy

EXPERIMENTAL

OVERVIEW OF TEMPERATURE LOGGER DEPLOYMENTS/RECOVERIES AT "BUSH HILL" ON 6-14 JUNE CRUISE

Sixteen (16) Antares temperature loggers (thermistors) were previously deployed in July 2001 at "Bush Hill" and at GC-233/234 using the Johnson SEA-LINK during dives funded to Dr. Ian MacDonald. Eight (8) temperature loggers were placed in four (4) short PVC probes (each of which could hold two thermistors) which were placed in hydrate or sediment. Two (2) of these hydrate probes were placed on "Bush Hill" and two (2) were placed in GC-233 hydrate areas. The remaining eight (8) were placed in two longer probes and inserted into a brine pool, but only four of these will be recoverable due to a mishap during deployment.

This report describes the recovery of the two (2) sets of probes from "Bush Hill" and the deployment of two new probes during this 6-14 June cruise. Additional probes were recovered and re-deployed on a subsequent SEA-LINK cruise on 1-22 July 2002.

Thermistor Probes 1 and 2 were recovered from Bush Hill (GC-185) during Dive #4416, and temperature data from Antares data loggers #33, 34, 41 and 42 was removed and downloaded. 15,693 data points were collected over the period of deployment from 7/16/01 to 6/8/02, with a sampling frequency of 30 minutes. Probe 1 had been placed in hydrate, with thermistor #33 buried 7-cm into a hydrate drill hole and thermistor #34 exposed to the water (**Fig. 4-6**). Probe 2 was positioned so that thermistor #42 was buried in 49 cm of sediment and thermistor #41 was exposed to the water (**Fig. 4-7**).

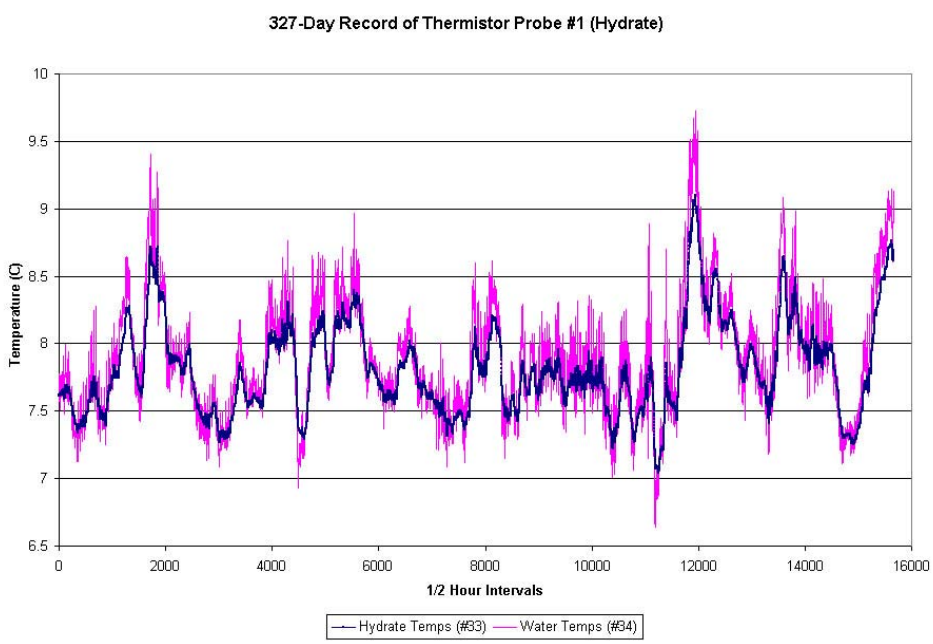

Fig. 4-6. Graph of temperature data from Thermistor Probe 1.

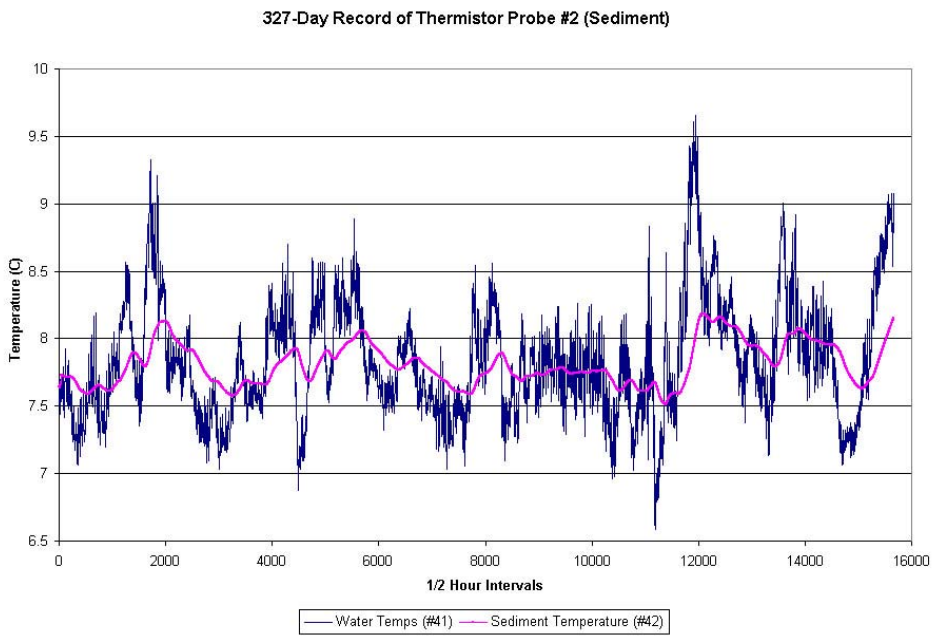

Fig. 4-7. Graph of temperature data from Thermistor Probe 2.

The thermistors were recovered in good condition, except for one which had some corrosion on the case. The batteries were still holding charge, but as they had been running for nearly a full year it was decided that replacing them would be prudent.

Five (5) new data loggers were provided for redeployment during the 6-14 June SEA-LINK cruise. The thermistors were #88, 89, 91, 102 and 103. During an inspection of the thermistors and a check of the setup, #103 stopped working. It was able to record data and be recognized by the download cradle, but after the date/time was reset it suddenly deactivated and was unresponsive after that. The other loggers worked perfectly. They were calibrated during Dive #4416 by activating them to sample once a second and placing them in a bucket attached to the submersible.

Probes 7 and 8 (of the same design as Probes 1 and 2) were deployed during Dive #4419 on 6/9/02. Probe 7 contained thermistors #88 (bottom) and 89 (top), and Probe 8 contained thermistors #91 (bottom) and 102 (top). The loggers were started at 06:00 on 6/9/02, sampling every 70 seconds for 1,242 hours (the maximum allowed by the internal memory), lasting until 8/1/02 at 00:00. The Johnson SEA-LINK submersible placed the probes in two new holes in the same hydrate mound that Probe 1 had been deployed in previously. Probe 7 was inserted 8 cm into the drill hole, but Probe 8 was only able to penetrate about 6 cm into the second hole. Probe 8 was later removed from that hole during Dive #4421 on 6/11/02 and redeployed 16 cm deep in sediment adjacent to an active methane and oil bubble stream. These probes will be recovered during the July 2002 SEA-LINK cruise and will provide a short-term, high-frequency sample to accompany the long-term, low frequency data obtained from the 2001 thermistor deployment.

FIELD REPORT JOHNSON SEALINK CRUISE 2001

During the JSL 2001 LEXEN cruise we deployed a total of 16 ANTARES High Resolution Temperature Data Loggers, or thermistors, on the sea floor in the Gulf of Mexico. These are titanium-cased cylindrical temperature sensors, 185 mm long, 120 g in weight, with an internal 3 V DC battery. The main body of the thermistor is 15 mm in diameter, and the sensor is at the tip of a 20 mm long x 1 mm diameter projection, which extends out of the center of one end. They are pressure rated up to 9000 psi and have a measuring range of -20°C to 50°C (-4 F to 122 F), with +/- 0.1°C accuracy. The internal memory can hold up to 65000 data points, and the sampling interval is programmable using an ANTARES type 1855 Datalogger Programming Station and ANTARES WinTemp software. The programming station connects to a PC through a RS232 port, using a null modem cable, and holds the thermistor in a springloaded clamp. Galvanic coupling between the thermistor and the station allows both programming and data readout.

All 16 thermistors that were brought on the cruise (numbered 33 through 48) were calibrated by sending them down on Dive #4306 in bucket #3 on the submarine. They were activated at 07:00 on 7/4/01, collecting temperature data every 10 seconds for 5 hours. Data was collected on the return of the submarine and placed in an Excel spreadsheet. The data was interpreted using preset calibration files from ANTARES, and analyzed using S-Plus 2000 software. The calibration files for thermistors 45 and 48 were corrupted, so new ones were made using an old calibration file for thermistor 31 as a template. Each thermistor's temperature data was plotted against temperature data from another thermistor using a linear least squares fit, using thermistors that would be deployed together in a probe. A linear regression was then performed to calculate the standard error. The linear coefficients ranged from 0.9923 to 1.021 and the standard error varied from 0.0005 to 0.0017. The mean linear coefficient was 1.003, and the mean standard deviation was 0.001. (See attached data)

Each individual thermistor was placed inside a probe constructed of a hollow tube of Schedule 40 PVC. There were six probes constructed, in two configurations: four hydrate/sediment probes which were shorter, containing only two thermistors (Figure 4-8), and two longer brine pool probes which held four thermistors each (Figure 4-9). The short probes were about 55 cm long, with a 45 cm shaft and a T-pipe threaded onto the end. One thermistor was in the bottom of the tube, held in by a beveled plug on the bottom and a 1/4" nylon bolt threaded through the pipe above the other end of the thermistor. The tip of the temperature sensor fit into a hole in the plug and projected about 1 mm beyond the surface of the cap. The thermistor on top was also held up by a bolt, and extended through the T-pipe, with a spacer of plastic tubing between the edge of the thermistor and the small hole in the top, through which the sensor tip protruded about 1 mm. A plastic float covered with a strip of reflective tape was attached to the T-pipe end of the probe with a short length of polypropylene line.

All of the thermistor deployments during the JSL 2001 LEXEN cruise are summarized in Table 1. The short probes were labeled one through four, and deployed on the sea floor. These probes were designed to be pushed into the sediment by the robotic arm of the submarine, or inserted into the drill holes left in the hydrate surface after collecting hydrate samples. This will allow temperature readings to be collected from the interior of the hydrate or sediment, and simultaneous readings to be taken from the ambient seawater. Probes #3 (containing thermistors 46 and 47) and #4 (containing thermistors 35 and 36) were activated at 05:00 on 7/6/01, sampling every 30 minutes for 32,500 hours (the maximum number of data points). They were deployed at the GC 234 site on 7/6/01 during Dive #4310. Probe #3 was wedged about 10 cm into a hydrate drill hole, while Probe #4 was thrust about 49 cm into the sediment, up to the bottom of the T-pipe (see Figure 4-10).

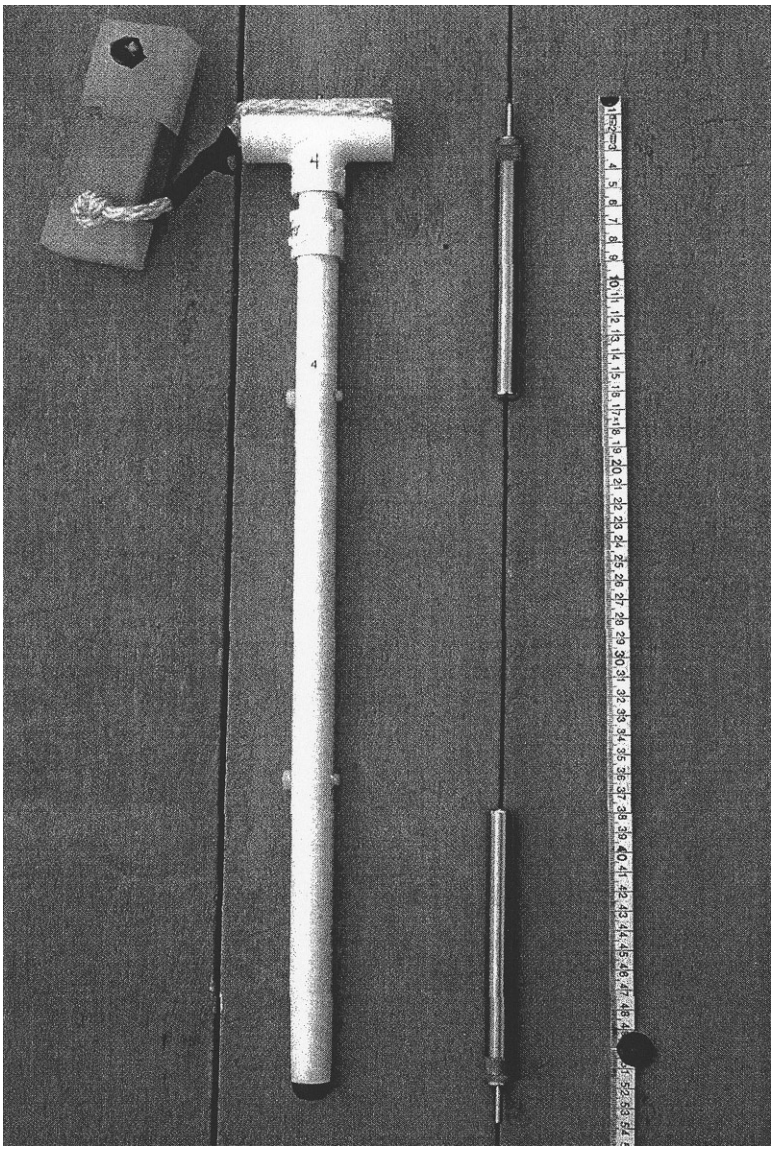

Figure 4-8. Short thermistor probe. From left: Assembled PVC probe, two thermistors showing relative position in probe, and meter scale.

Probes #1 (containing thermistors 33 and 34) and #2 (containing thermistors 41 and 42) were activated on 7/16/01 at 13:40, sampling every 30 minutes for 32,500 hours. Dive #4325 planted them on the seafloor at Bush Hill, but both thermistors were in hydrate drill holes. Dive #4327 repositioned Thermistor #2 so that it was pushed fully into the sediment next to the hydrate mound.

The probes intended for the brine pool were constructed of three individual PVC pipes, joined by slightly larger diameter pipe, which was glued with PVC cement and bolted together. Fully assembled, the probes were about 1.385 meters long. The first long probe constructed, Probe #5, had thermistor #45 at the bottom extending through the beveled plug and braced by a nylon bolt. Thermistor #44 was in the middle section, which was open to the water through a T-connector, which joined that section of PVC pipe to the bottom segment. The top section,

which had the beveled plug facing upwards, contained thermistor #43. A plastic spring-loaded handle was clamped to the top section, and a length of rope attached to a yellow plastic float ball on one end and a 25 lb. weight attached to the other end, was fed through it. Thermistor #48 was attached to the float. The weight was screwed to a wooden plate in order to prevent it from sinking into the mud bottom of the brine pool. When the submarine's arm closed on the handle, it could let out more slack on the line and move the probe up and down in relation to the weight. This way Probe #5 could be deployed in the brine pool at a certain depth and measure the temperature below the brine surface, at the brine/seawater interface, at the ambient water level, and at the level of the float. The thermistors were all activated at 01:20 on 7/9/01 and set to record a sample every 30 minutes for 32,500 hours. Probe #5 was deployed during Dive #4319 on 7/14/01. Unfortunately, the slope of the brine pool edge was steeper than anticipated: when released, the probe slid below the brine entirely, and is too deeply submerged in the pool to be retrieved.

Probe #6 was constructed to replace #5, and it had a similar design. Thermistor #40 was at the bottom, and thermistor #38 was in the middle segment, extending into a T-connector. However, the top section is constructed like the smaller probes, with the beveled plug facing downwards and a T-pipe on top. Thermistor #37 extended through the plug into another T-connector, and thermistor #39 extended through the T on top, with a plastic tubing spacer keeping only 1 mm of the sensor tip protruding beyond the probe surface. Another spring-loaded handle was attached to the top section. In order to prevent this probe from meeting a fate similar to that of #5, two 25 lb. weights were attached to the bottom plate to better anchor it, and a longer rope was strung between the float and the weights. The thermistors were activated at 14:40 on 7/14/01, sampling every 30 minutes for 32,500 hours. This probe was deployed successfully during Dive #4321, but it is in a shallow area of the brine pool and thus not recording the full range of temperatures anticipated. Only thermistor #40 is submerged in the brine.

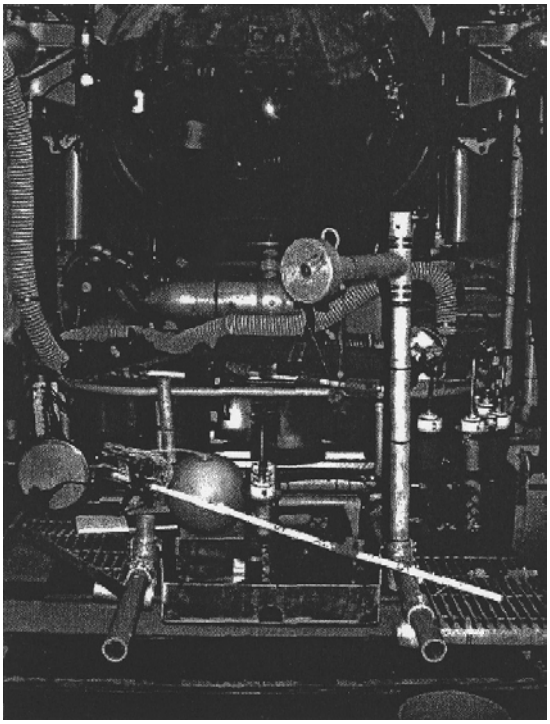

Figure 4-9. Long probe prior to deployment on Sea Link.

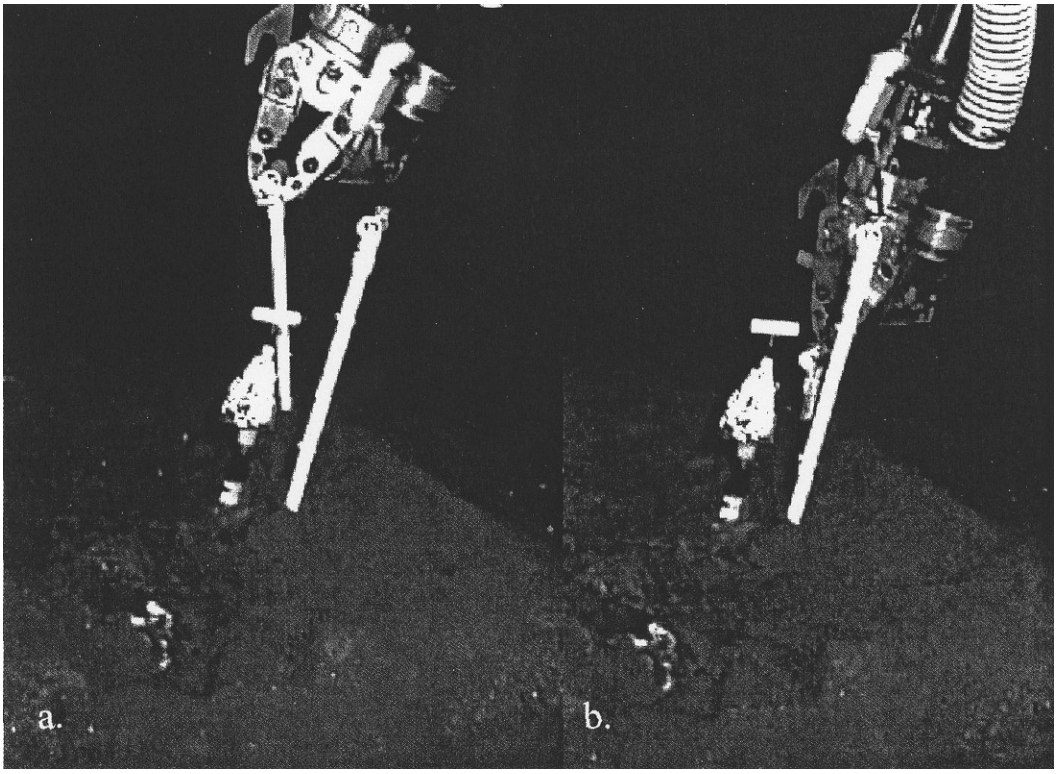

Figure 4-10a. Thermistor probe deployment at GC 234. Probe #3 is in the foreground, in a hydrate drill hole, Probe #4 is being pushed into the sediment by the robotic arm. Figure 4-10b shows the final position of Probe #4. An agar plug is shown in the left foreground.

Table 1. Summary of thermistors deployed during Johnson Sea Link 2001 Cruise

Probe Deployment Site	Probe Number	Length of Probe	Thermistor Number	Location in Probe	Date/Time of Activation	Sampling Rate	Dive #, Date of Deployment
Bush Hill, hydrate	**1**	short, 55 cm	33	Bottom, in hydrate	7/16/01, 13:40	30 min.	#4325, 7/16/01
Bush Hill, hydrate	**1**	short, 55 cm	34	Top, in seawater	7/16/01, 13:40	30 min.	#4325, 7/16/01
Bush Hill, sediment	2	short, 55 cm	41	Top, in seawater	7/16/01, 13:40	30 min.	#4325, 7/16/01, repositioned 7/17/01, #4327
Bush Hill, sediment	2	short, 55 cm	42	Bottom, in sediment	7/16/01, 13:40	30 min.	#4325, 7/16/01, repositioned 7/17/01, #4327
GC 234, hydrate	**3**	short, 55 cm	46	Top, in seawater	7/6/01, 05:00	30 min.	#4310, 7/6/01
GC 234, hydrate	**3**	short, 55 cm	47	Bottom, in hydrate	7/6/01, 05:00	30 min.	#4310, 7/6/01
GC 234, sediment	4	short, 55 cm	35	Top, in seawater	7/6/01, 05:00	30 min.	#4310, 7/6/01
GC 234, sediment	4	short, 55 cm	36	Bottom, in sediment	7/6/01, 05:00	30 min.	#4310, 7/6/01
Brine Pool - unrecoverable	**5**	long, 138.5 cm	43	Top	7/9/01, 01:20	30 min.	#4319, 7/14/01
Brine Pool - unrecoverable	**5**	long, 138.5 cm	44	Middle	7/9/01, 01:20	30 min.	#4319, 7/14/01
Brine Pool - unrecoverable	**5**	long, 138.5 cm	45	Bottom	7/9/01, 01:20	30 min.	#4319, 7/14/01
Brine Pool - unrecoverable	**5**	long, 138.5 cm	48	Float	7/9/01, 01:20	30 min.	#4319, 7/14/01
Brine Pool	6	long, 138.5 cm	37	Middle-top	7/14/01, 14:40	30 min.	#4321, 7/15/01
Brine Pool	6	long, 138.5 cm	38	Middle-bottom	7/14/01, 14:40	30 min.	#4321, 7/15/01
Brine Pool	6	long, 138.5 cm	39	Top, in seawater	7/14/01, 14:40	30 min.	#4321, 7/15/01
Brine Pool	6	long, 138.5 cm	40	Bottom, in brine	7/14/01, 14:40	30 min.	#4321, 7/15/01

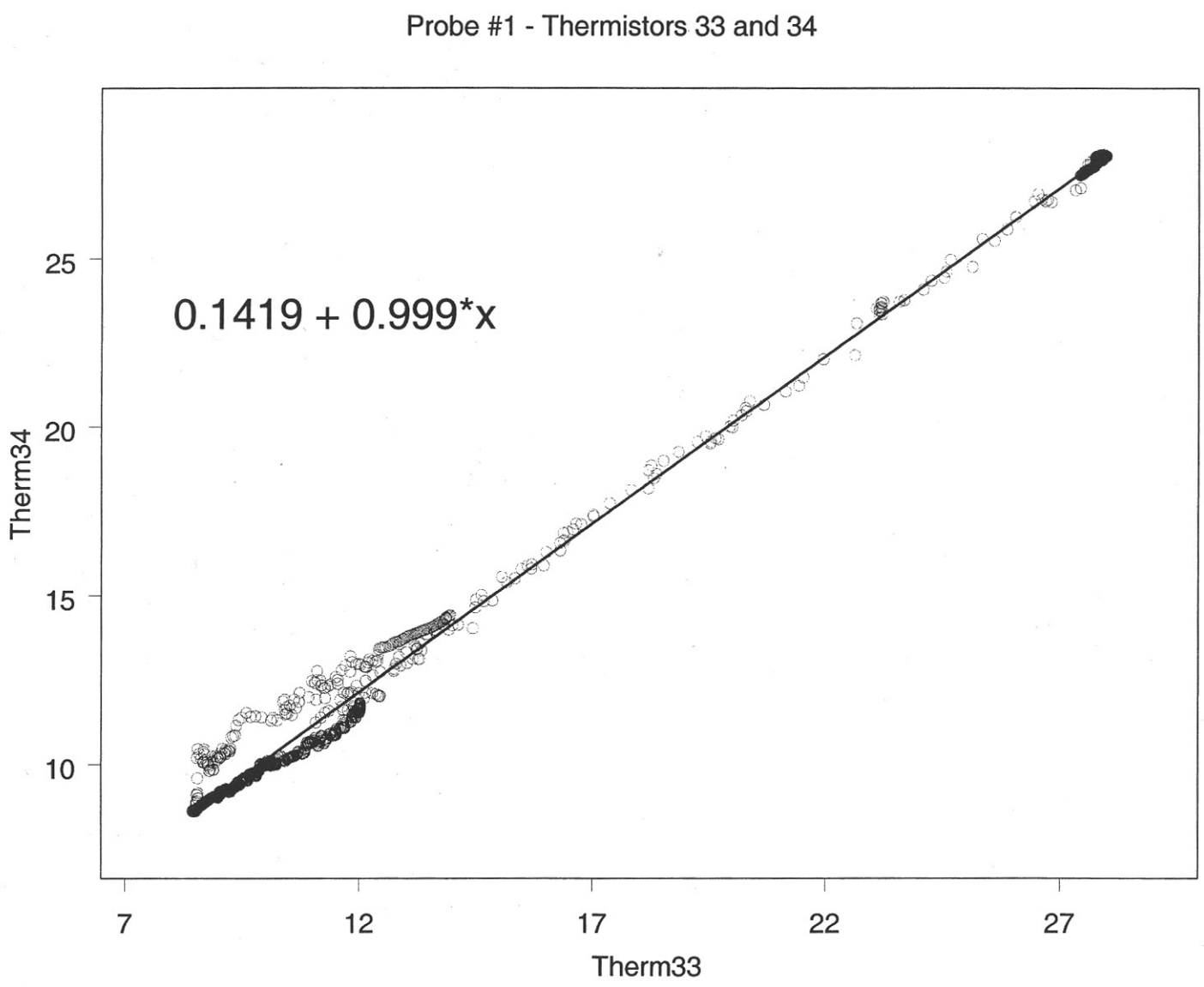
Probe #1 - Thermistors 33 and 34
0.1419 + 0.999*x
Therm34
25
20
15
10
7
12
17
22
27
Therm33

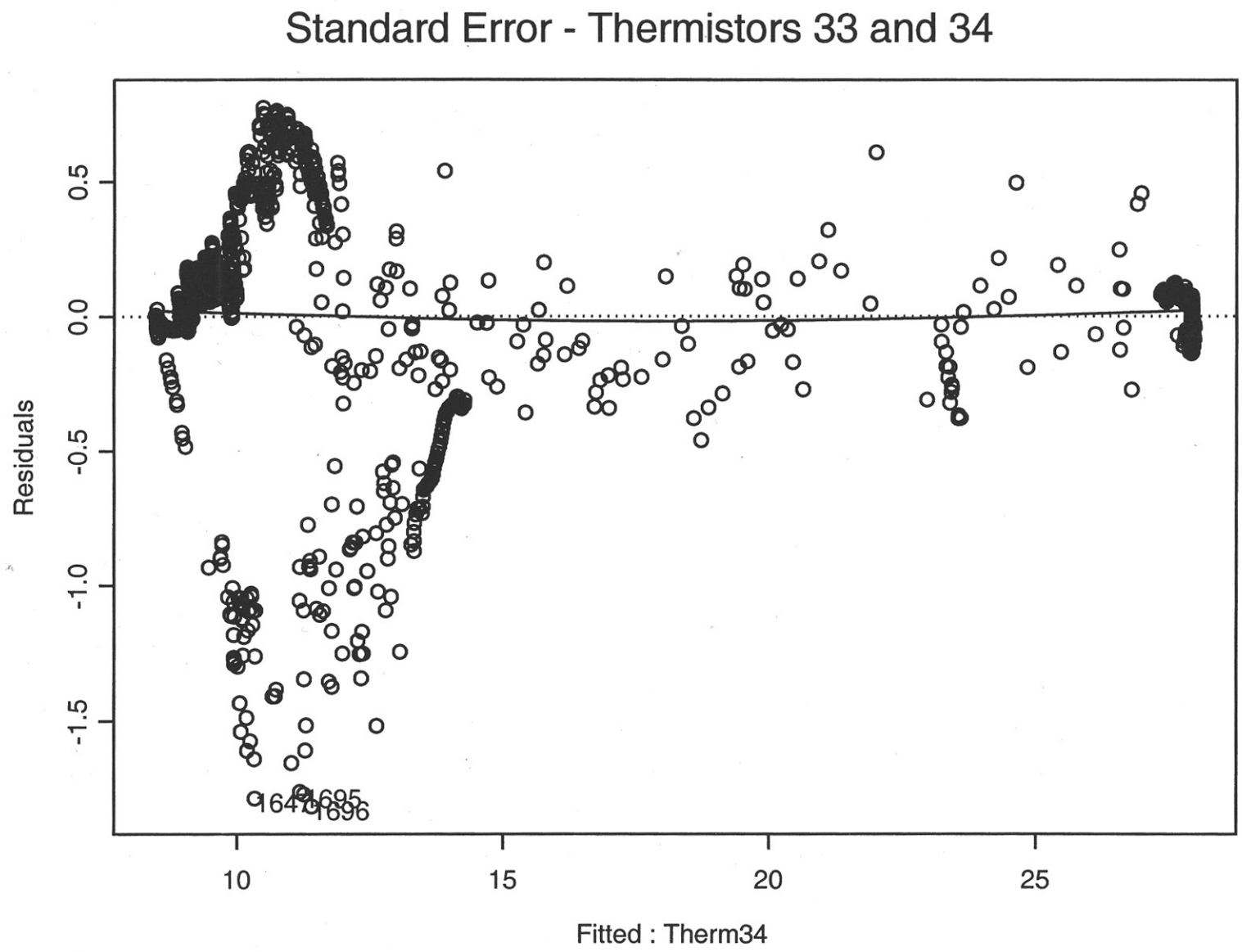
Standard Error - Thermistors 33 and 34
Residuals
0.5
0.0
-0.5
-1.0
-1.5
1647
1695
1696
10
15
20
25
Fitted : Therm34

```
      *** Linear Model ***

Call: lm(formula = Therm33 ~ Therm34, data = ThermistorCalibrationData,
na.action =
      na.exclude)
Residuals:
    Min       1Q  Median     3Q    Max
 -1.814 -0.04917 0.01692 0.109 0.7734

Coefficients:
                Value Std. Error   t value  Pr(>|t|)
(Intercept)   -0.1115    0.0184    -6.0583    0.0000
    Therm34    0.9991    0.0010   958.4521    0.0000

Residual standard error: 0.362 on 1797 degrees of freedom
Multiple R-Squared: 0.998
F-statistic: 918600 on 1 and 1797 degrees of freedom, the p-value is 0
```

Thermistor 34 = 0.1419 + 0.999*Thermistor 33

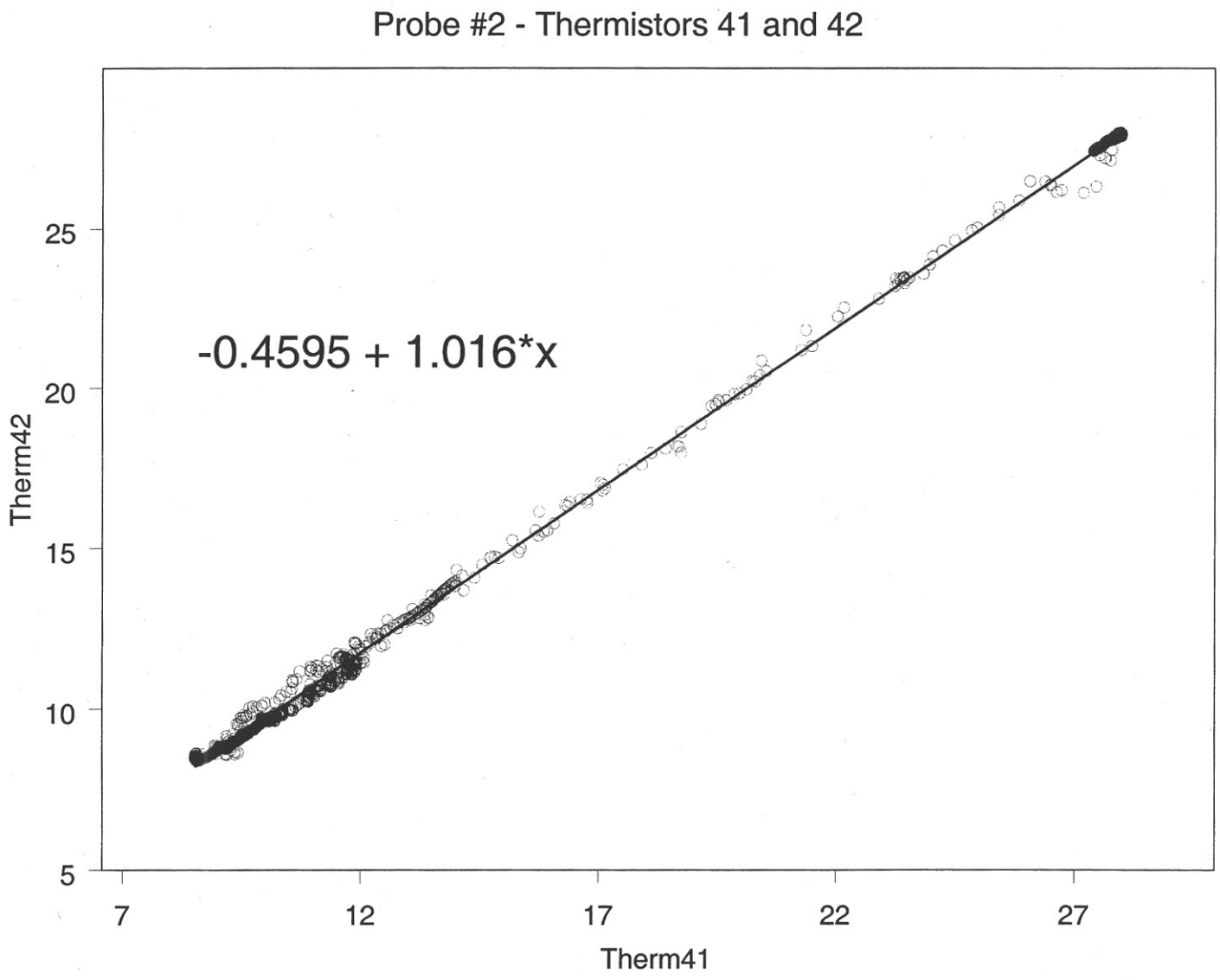
Probe #2 - Thermistors 41 and 42
-0.4595 + 1.016*x
Therm42
Therm41
5
10
15
20
25
7
12
17
22
27

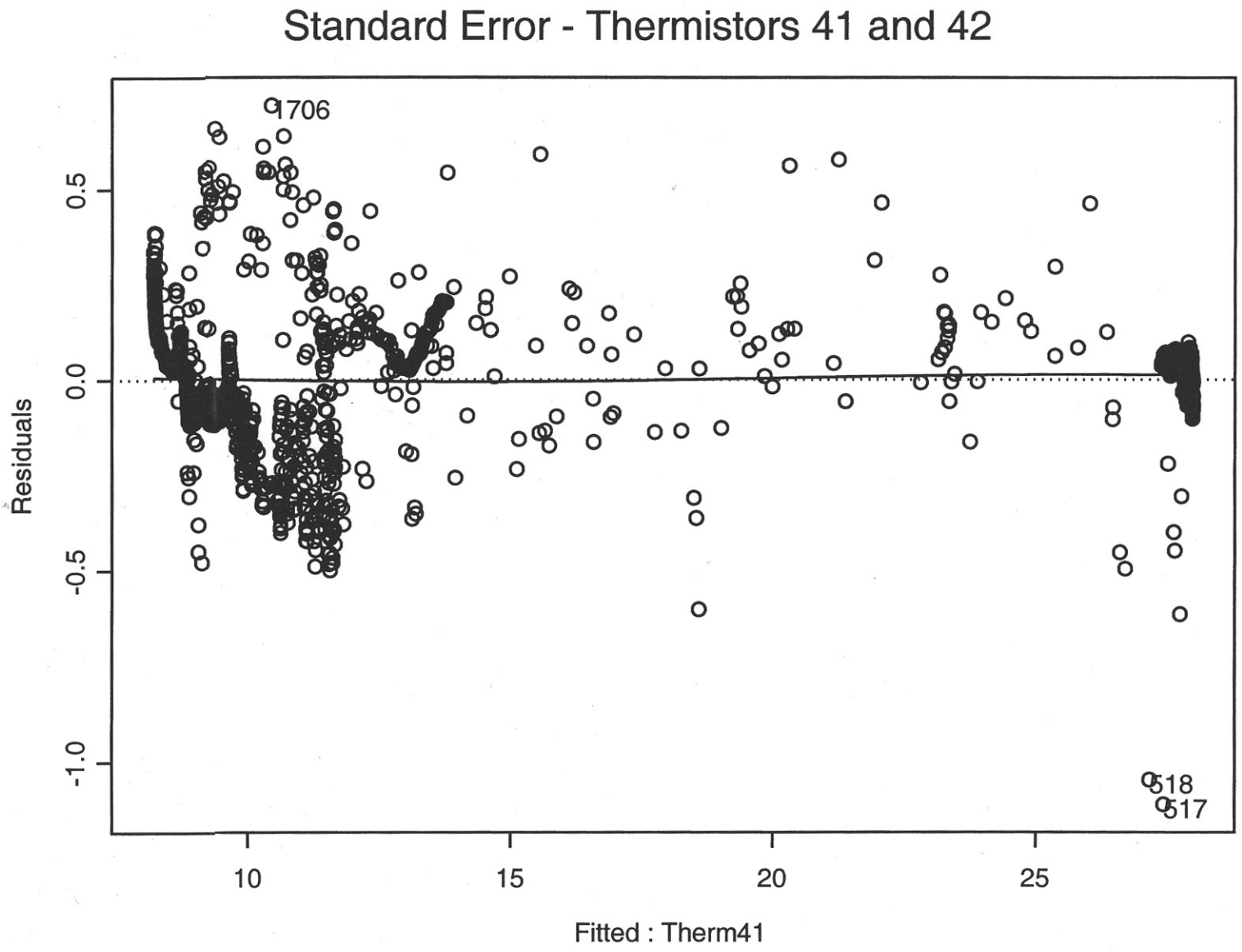
Standard Error - Thermistors 41 and 42
1706
518
517
0.5
0.0
-0.5
-1.0
Residuals
10
15
20
25
Fitted : Therm41

```
      *** Linear Model ***

Call: lm(formula = Therm42 ~ Therm41, data = ThermistorCalibrationData,
na.action =
      na.exclude)
Residuals:
    Min       1Q  Median      3Q    Max
 -1.111 -0.07473 0.01917 0.06744 0.7194

Coefficients:
                 Value Std. Error    t value   Pr(>|t|)
(Intercept)    -0.4595     0.0084   -54.6075     0.0000
    Therm41     1.0163     0.0005  2125.4770     0.0000

Residual standard error: 0.1656 on 1797 degrees of freedom
Multiple R-Squared: 0.9996
F-statistic: 4518000 on 1 and 1797 degrees of freedom, the p-value is 0
```

Thermistor 42 = -0.4595 + 1.016* Thermistor 41

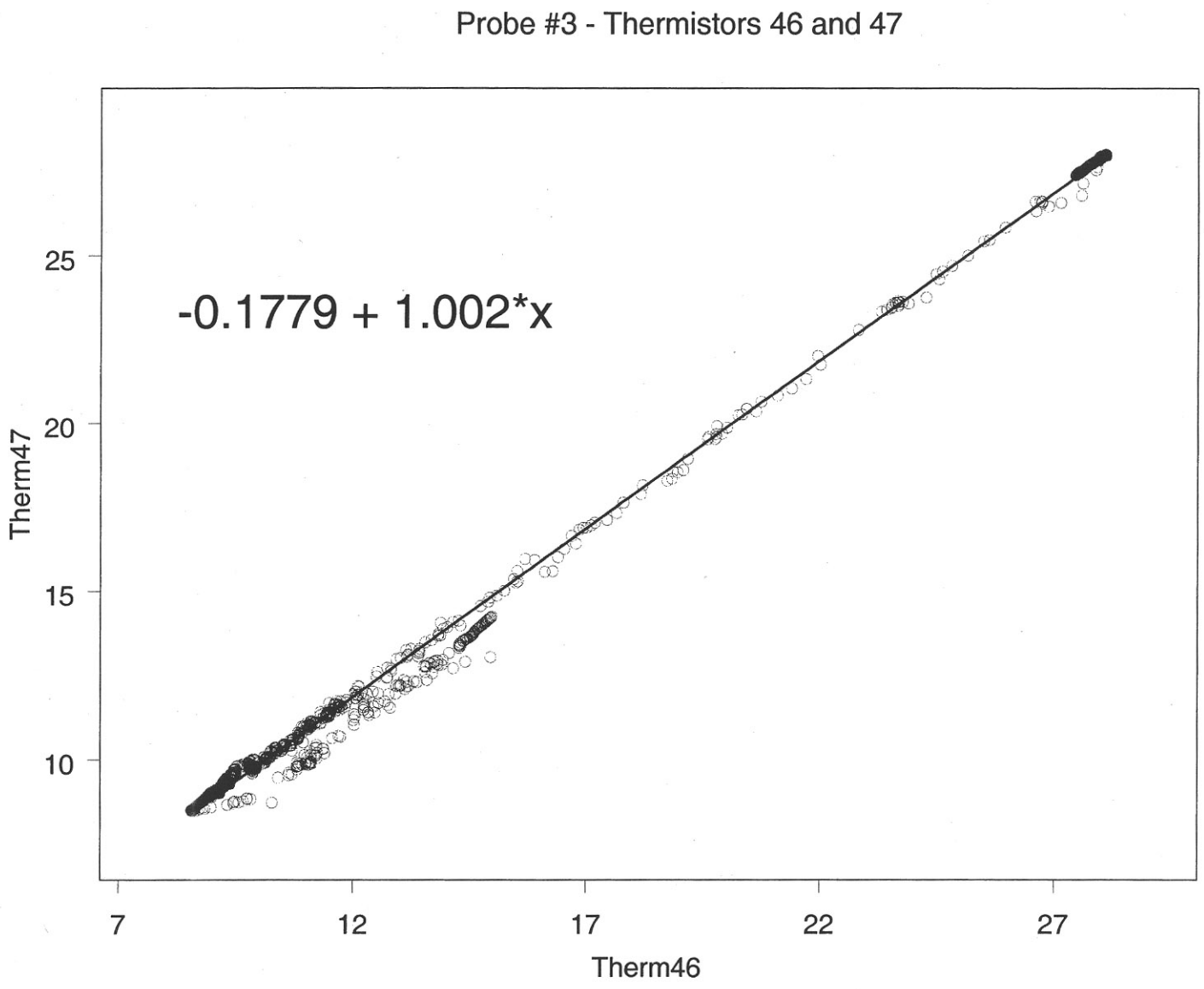
Probe #3 - Thermistors 46 and 47
-0.1779 + 1.002*x
Therm47
Therm46
25
20
15
10
7
12
17
22
27

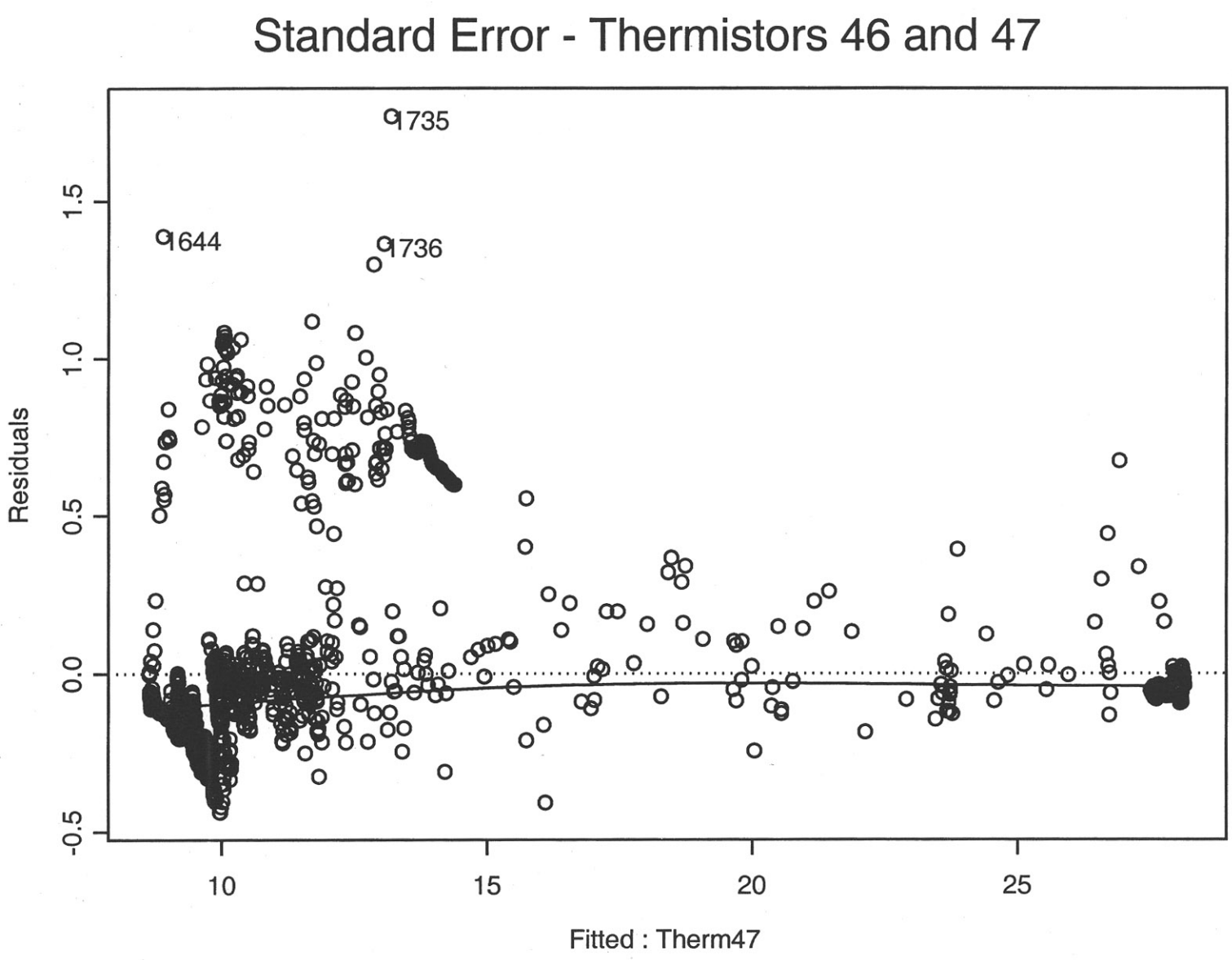
Standard Error - Thermistors 46 and 47
1735
1644
1736
1.5
1.0
0.5
0.0
-0.5
Residuals
10
15
20
25
Fitted : Therm47

```
      *** Linear Model ***

Call: lm(formula = Therm46 ~ Therm47, data = ThermistorCalibrationData,
na.action =
      na.exclude)
Residuals:
     Min      1Q   Median      3Q   Max
 -0.4374 -0.1202 -0.05541 -0.0235 1.768

Coefficients:
                Value Std. Error   t value  Pr(>|t|)
(Intercept)    0.1943    0.0136    14.2956    0.0000
    Therm47    0.9966    0.0008  1287.4252    0.0000

Residual standard error: 0.2704 on 1797 degrees of freedom
Multiple R-Squared: 0.9989
F-statistic: 1657000 on 1 and 1797 degrees of freedom, the p-value is 0
```

Thermistor 47 = -0.1779 + 1.002*Thermistor 46

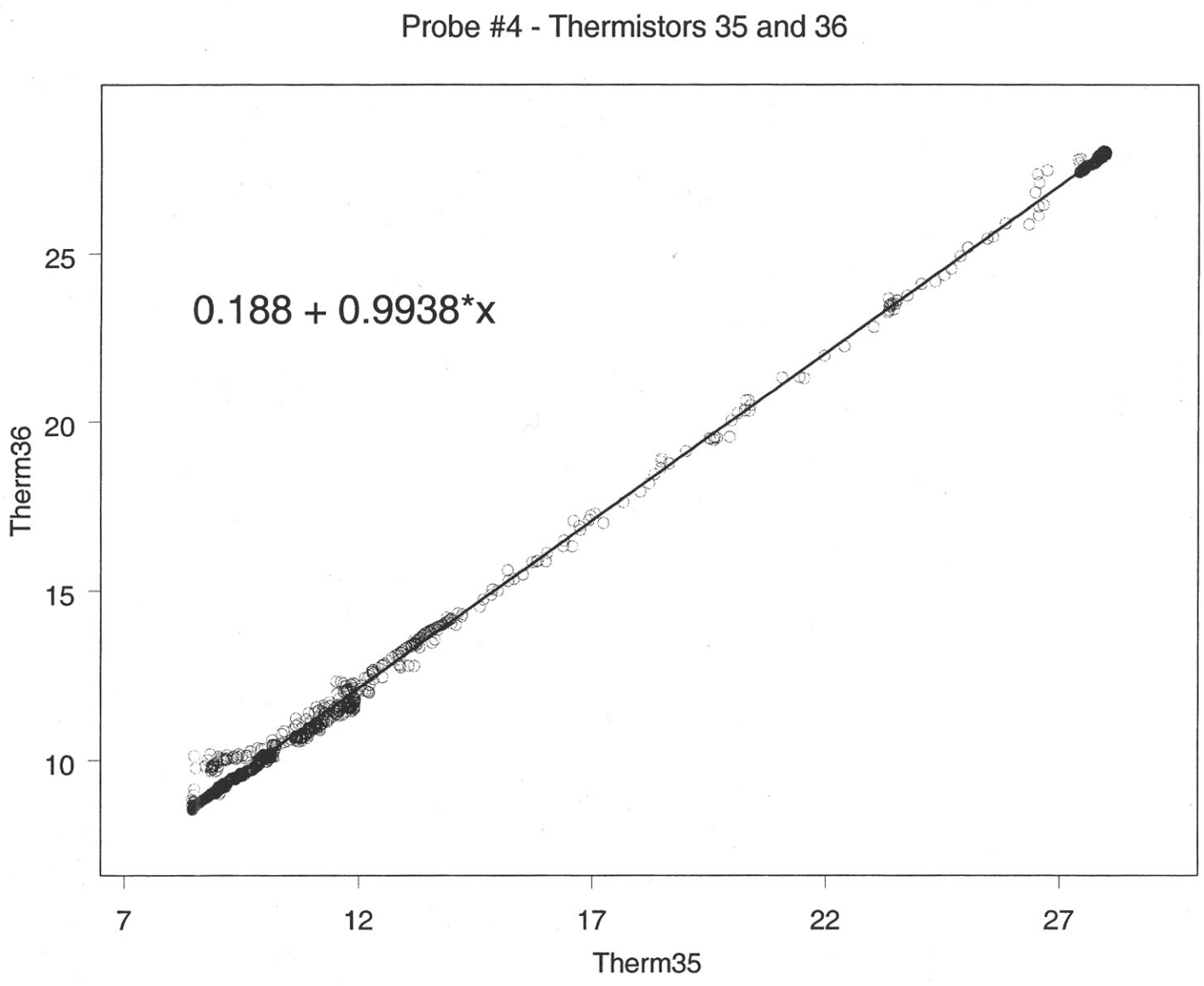
Probe #4 - Thermistors 35 and 36
0.188 + 0.9938*x
Therm36
Therm35
25
20
15
10
7
12
17
22
27

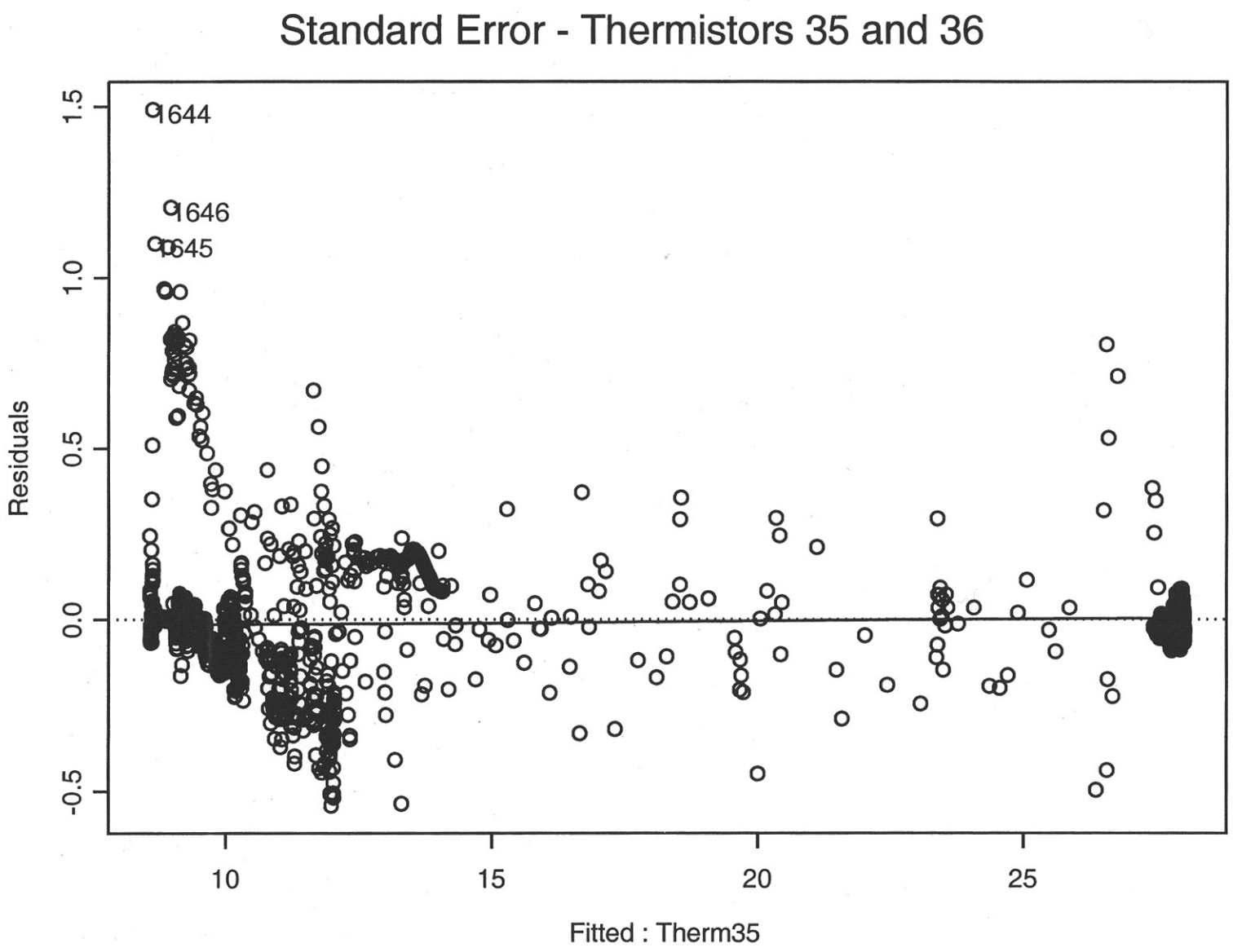
Standard Error - Thermistors 35 and 36
1644
1646
1645
1.5
1.0
0.5
0.0
-0.5
Residuals
10
15
20
25
Fitted : Therm35

```
      *** Linear Model ***

Call: lm(formula = Therm36 ~ Therm35, data = ThermistorCalibrationData,
na.action =
      na.exclude)
Residuals:
     Min       1Q      Median      3Q   Max
 -0.5412 -0.05419 -0.00005447 0.03447 1.491

Coefficients:
                Value Std. Error   t value  Pr(>|t|)
(Intercept)    0.1880    0.0089    21.2304    0.0000
    Therm35    0.9938    0.0005  1970.2619    0.0000

Residual standard error: 0.1759 on 1797 degrees of freedom
Multiple R-Squared: 0.9995
F-statistic: 3882000 on 1 and 1797 degrees of freedom, the p-value is 0
```

Thermistor 36 = 0.188 + 0.9938* Thermistor 35

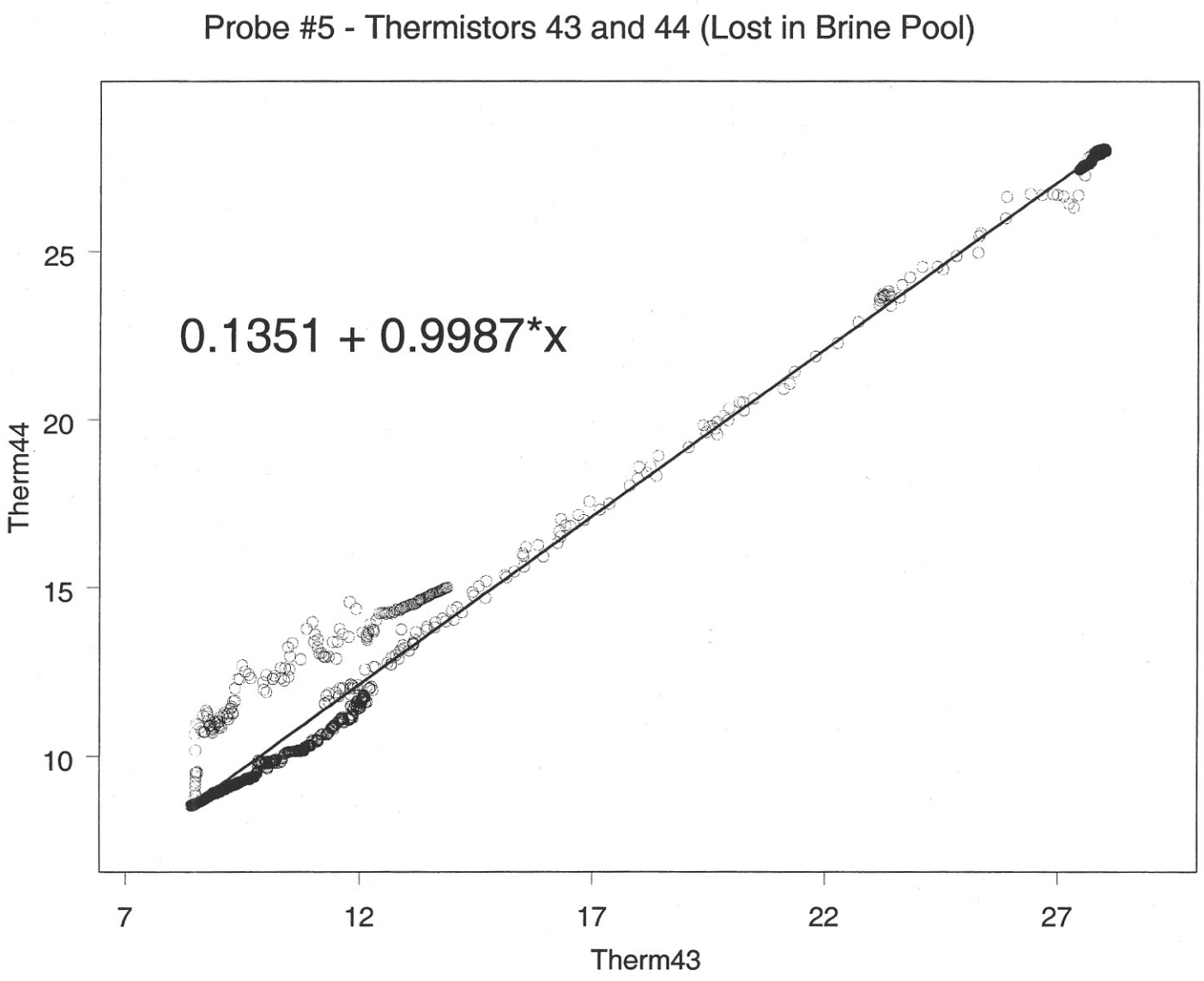
Probe #5 - Thermistors 43 and 44 (Lost in Brine Pool)
0.1351 + 0.9987*x
Therm44
Therm43
25
20
15
10
7
12
17
22
27

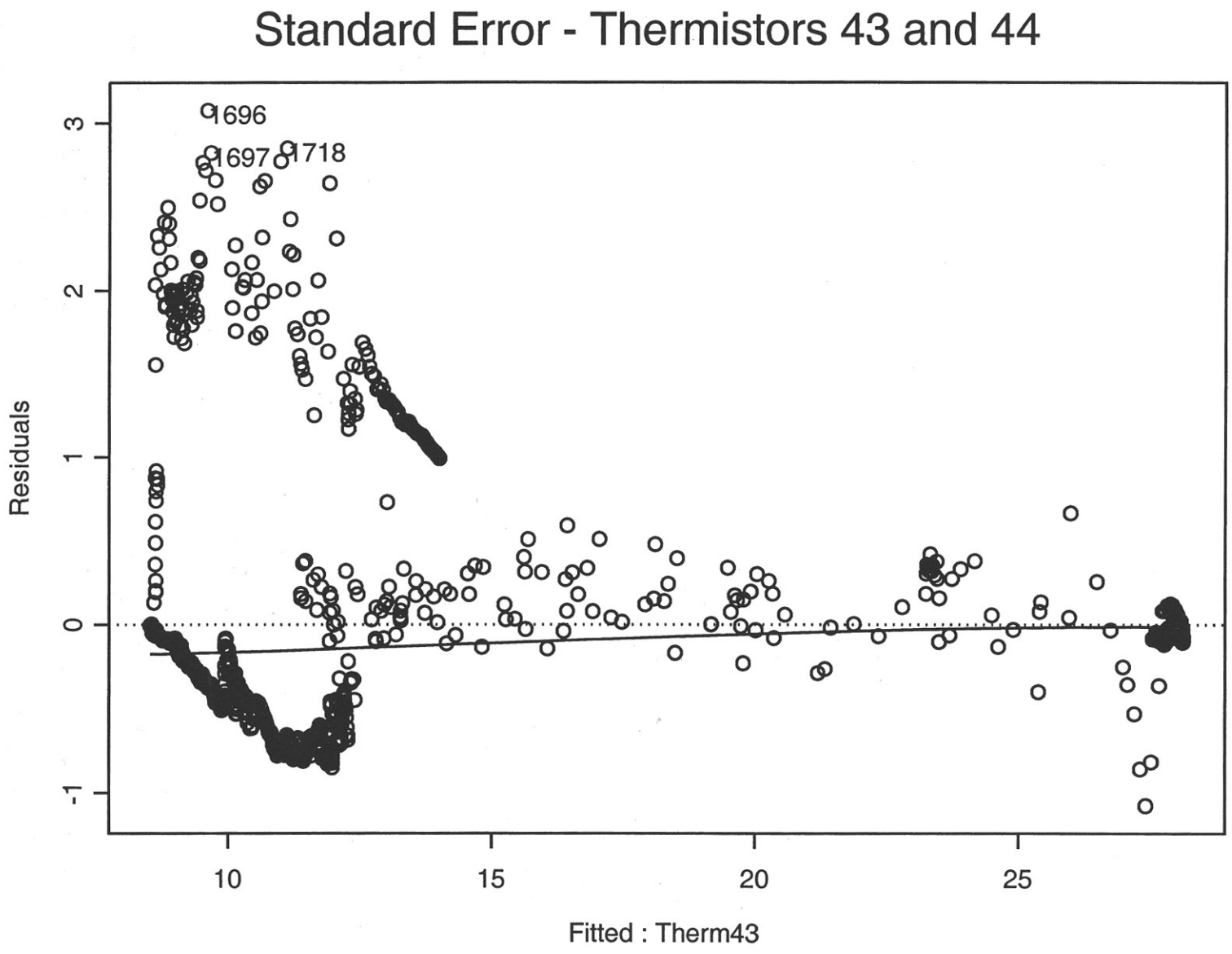
Standard Error - Thermistors 43 and 44
1696
1697
1718
Residuals
3
2
1
0
-1
10
15
20
25
Fitted : Therm43

```
      *** Linear Model ***

Call: lm(formula = Therm44 ~ Therm43, data = ThermistorCalibrationData,
na.action =
      na.exclude)
Residuals:
    Min      1Q   Median        3Q   Max
 -1.075 -0.265 -0.08311 -0.001328 3.077

Coefficients:
                Value Std. Error  t value Pr(>|t|)
(Intercept)    0.1351   0.0304     4.4462   0.0000
    Therm43    0.9987   0.0017   576.4508   0.0000

Residual standard error: 0.6037 on 1797 degrees of freedom
Multiple R-Squared: 0.9946
F-statistic: 332300 on 1 and 1797 degrees of freedom, the p-value is 0
```

Thermistor 44 = 0.1351 + 0.9987* Thermistor 43

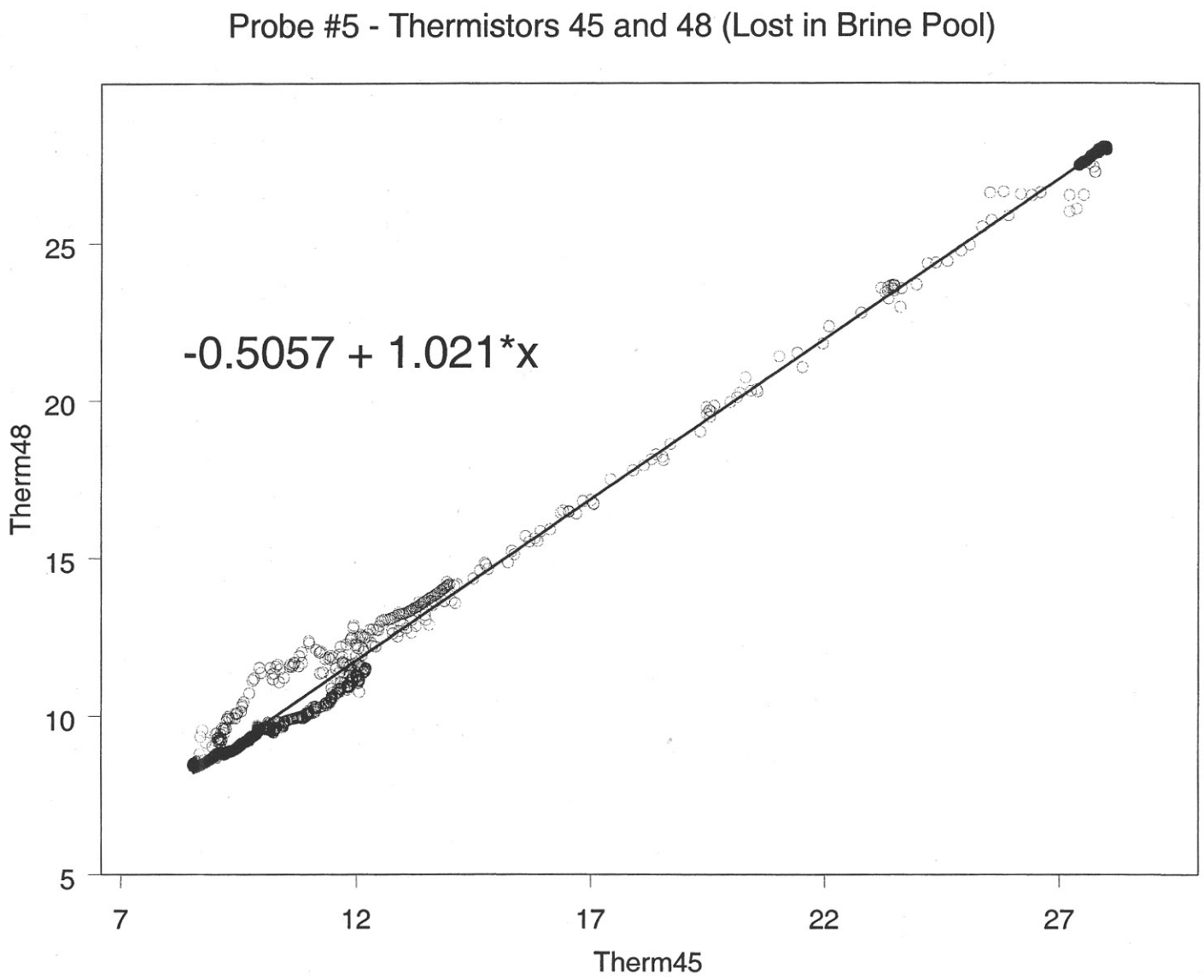
Probe #5 - Thermistors 45 and 48 (Lost in Brine Pool)
-0.5057 + 1.021*x
Therm48
Therm45
5
10
15
20
25
7
12
17
22
27

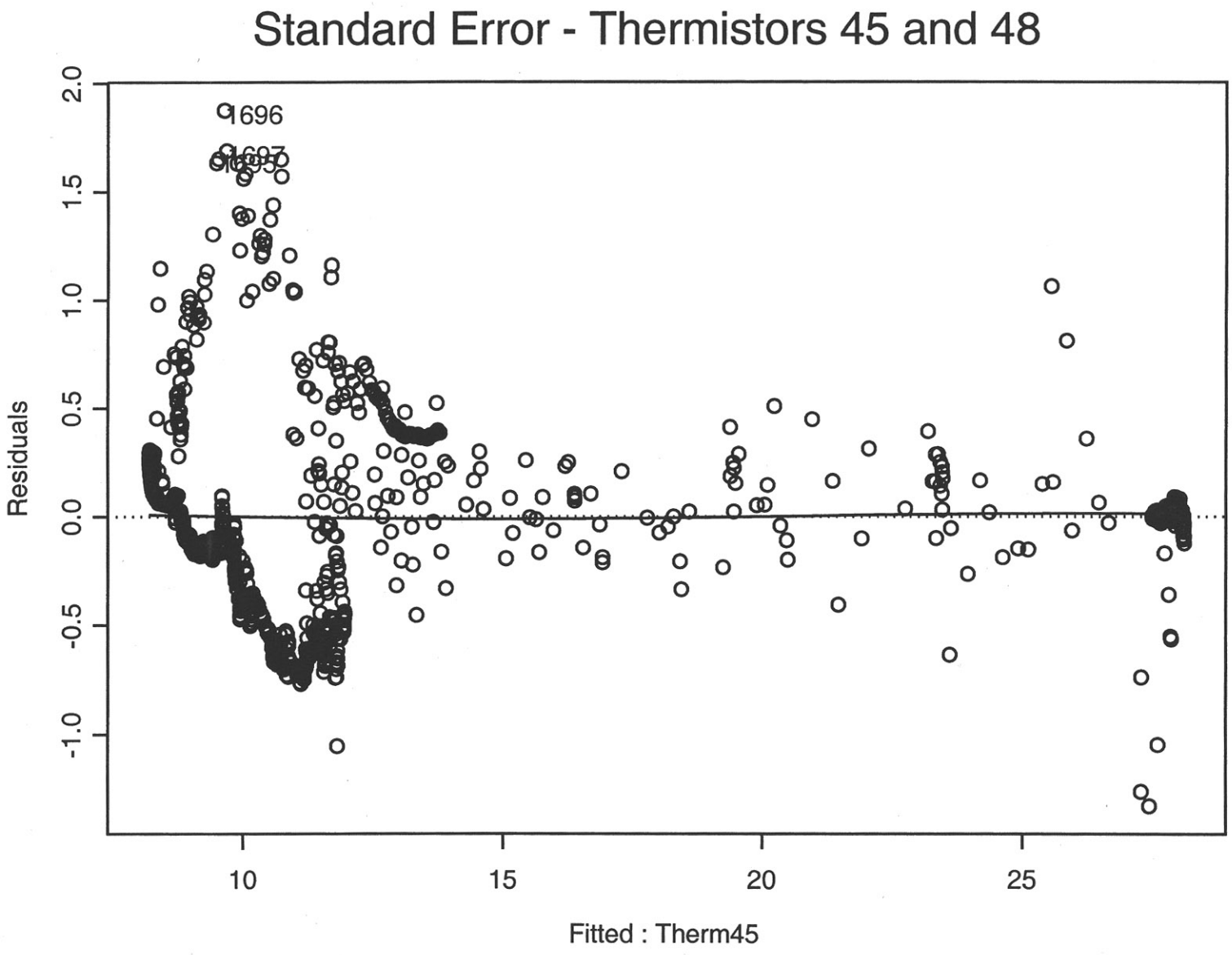
Standard Error - Thermistors 45 and 48
Residuals
2.0
1.5
1.0
0.5
0.0
-0.5
-1.0
1696
10
15
20
25
Fitted : Therm45

```
      *** Linear Model ***

Call: lm(formula = Therm48 ~ Therm45, data = ThermistorCalibrationData,
na.action =
      na.exclude)
Residuals:
    Min      1Q  Median      3Q   Max
 -1.329 -0.1289 0.01746 0.07936 1.876

Coefficients:
                 Value Std. Error    t value   Pr(>|t|)
(Intercept)    -0.5057     0.0171   -29.6144     0.0000
    Therm45     1.0212     0.0010  1051.6676     0.0000

Residual standard error: 0.336 on 1797 degrees of freedom
Multiple R-Squared: 0.9984
F-statistic: 1106000 on 1 and 1797 degrees of freedom, the p-value is 0
```

Thermistor 48 = -0.5057 + 1.021* Thermistor 45

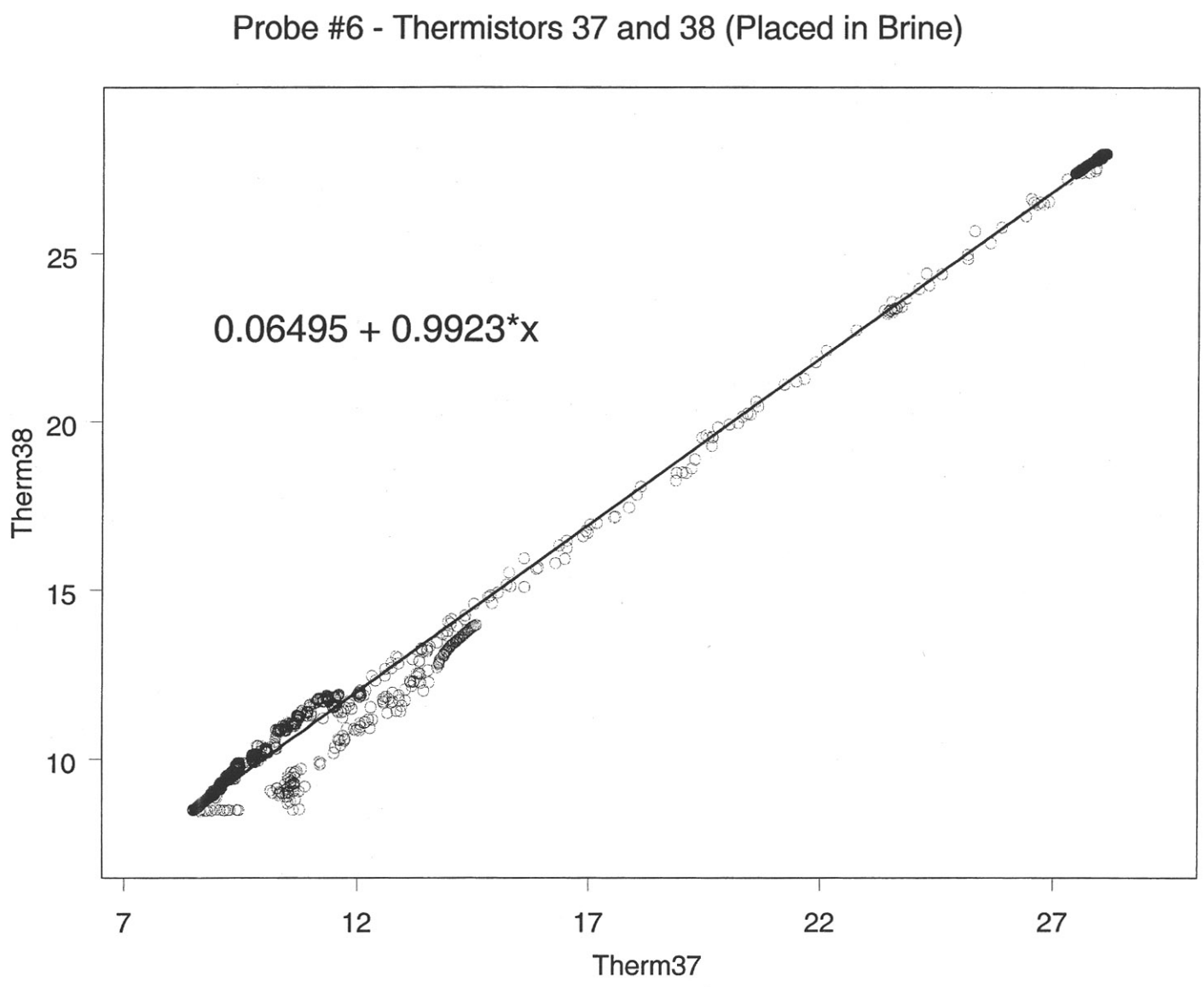
Probe #6 - Thermistors 37 and 38 (Placed in Brine)
0.06495 + 0.9923*x
Therm38
Therm37
25
20
15
10
7
12
17
22
27

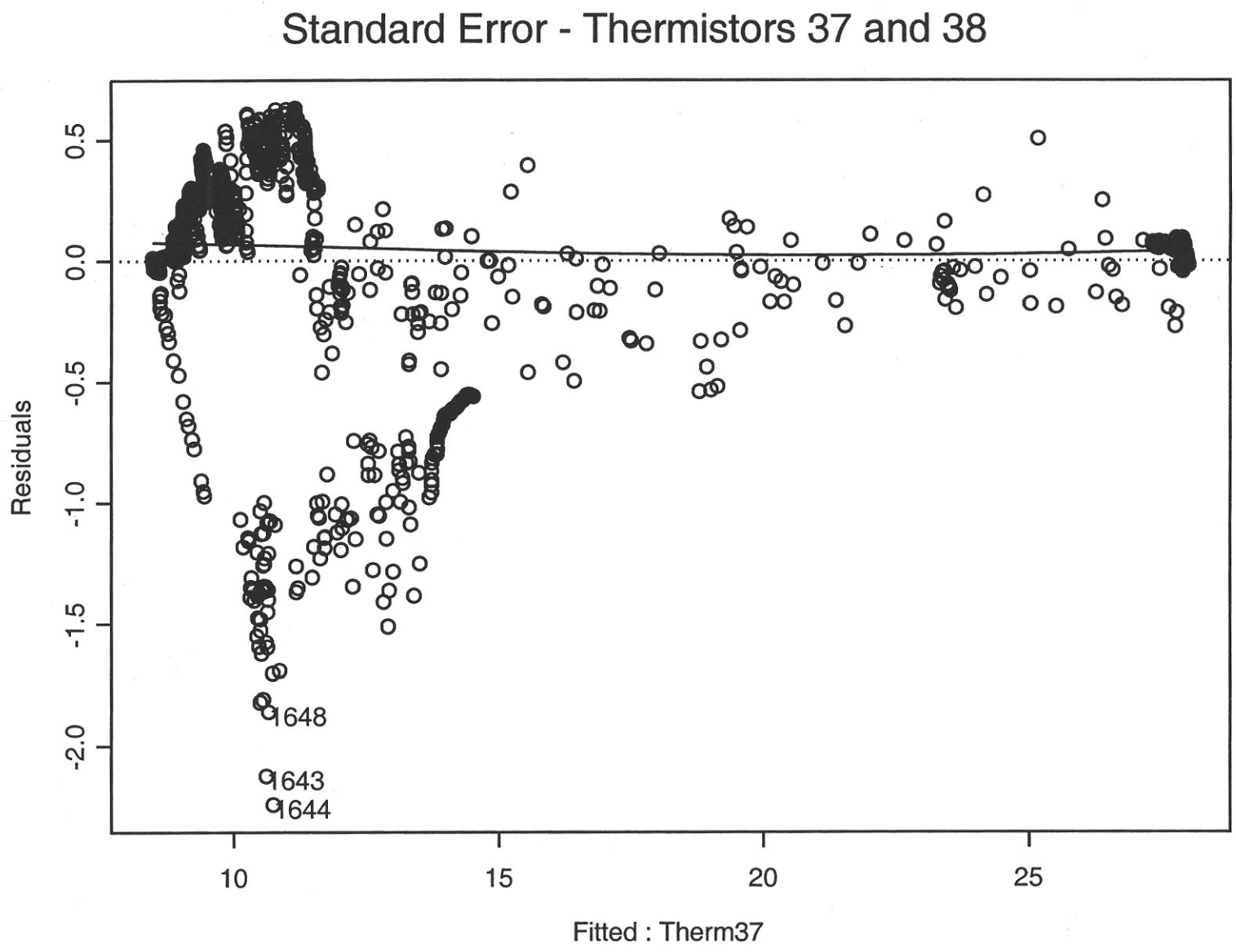
Standard Error - Thermistors 37 and 38
Residuals
0.5
0.0
-0.5
-1.0
-1.5
-2.0
1648
1643
1644
10
15
20
25
Fitted : Therm37

```
      *** Linear Model ***

Call: lm(formula = Therm38 ~ Therm37, data = ThermistorCalibrationData,
na.action =
      na.exclude)
Residuals:
    Min       1Q  Median     3Q    Max
 -2.242 -0.00358 0.04901 0.1446 0.6303

Coefficients:
               Value Std. Error  t value Pr(>|t|)
(Intercept)   0.0650   0.0190     3.4149   0.0007
    Therm37   0.9923   0.0011   919.5900   0.0000

Residual standard error: 0.3775 on 1797 degrees of freedom
Multiple R-Squared: 0.9979
F-statistic: 845600 on 1 and 1797 degrees of freedom, the p-value is 0
```

Thermistor 38 = 0.06495 + 0.9923* Thermistor 37

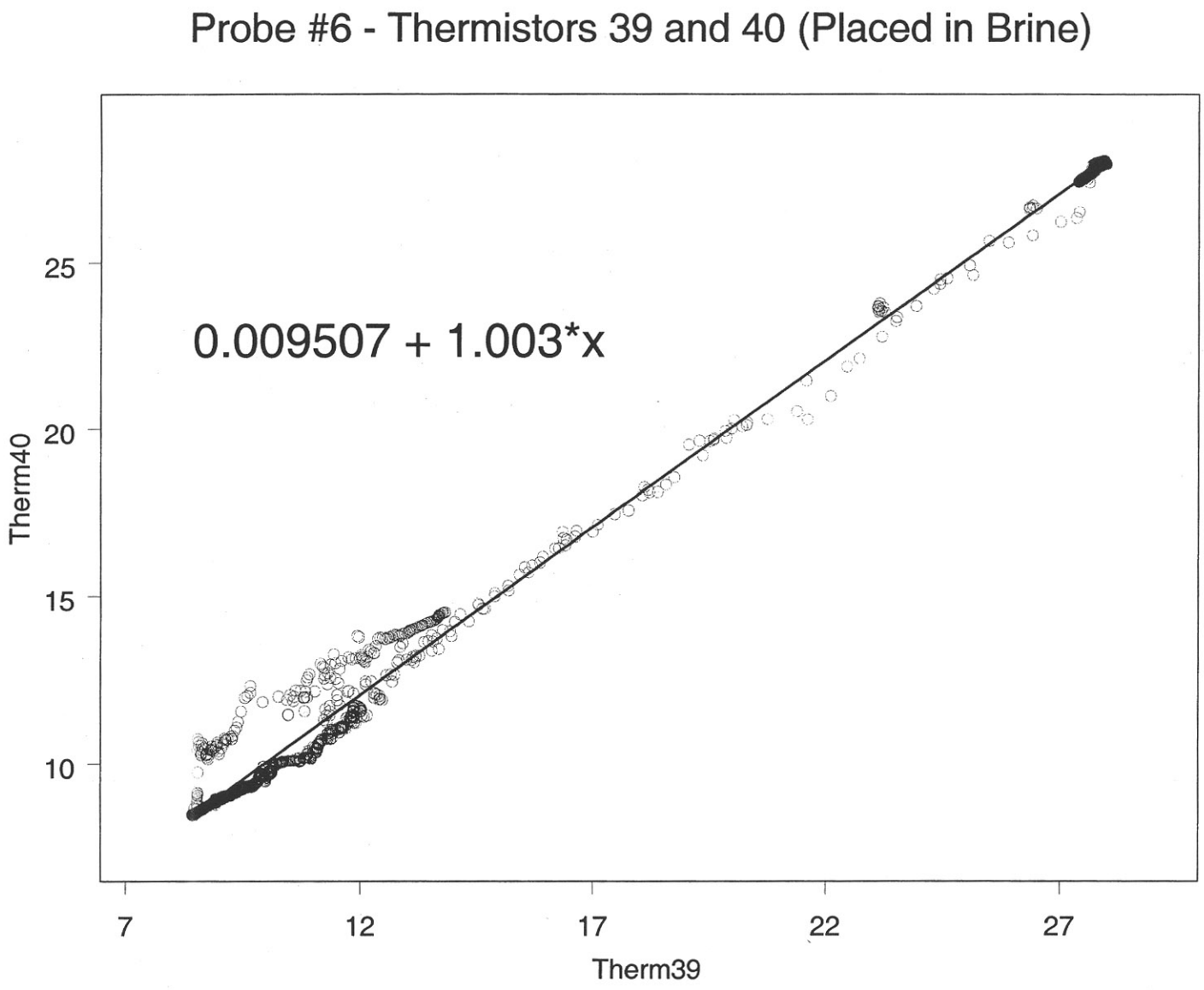
Probe #6 - Thermistors 39 and 40 (Placed in Brine)
0.009507 + 1.003*x
Therm40
Therm39
25
20
15
10
7
12
17
22
27

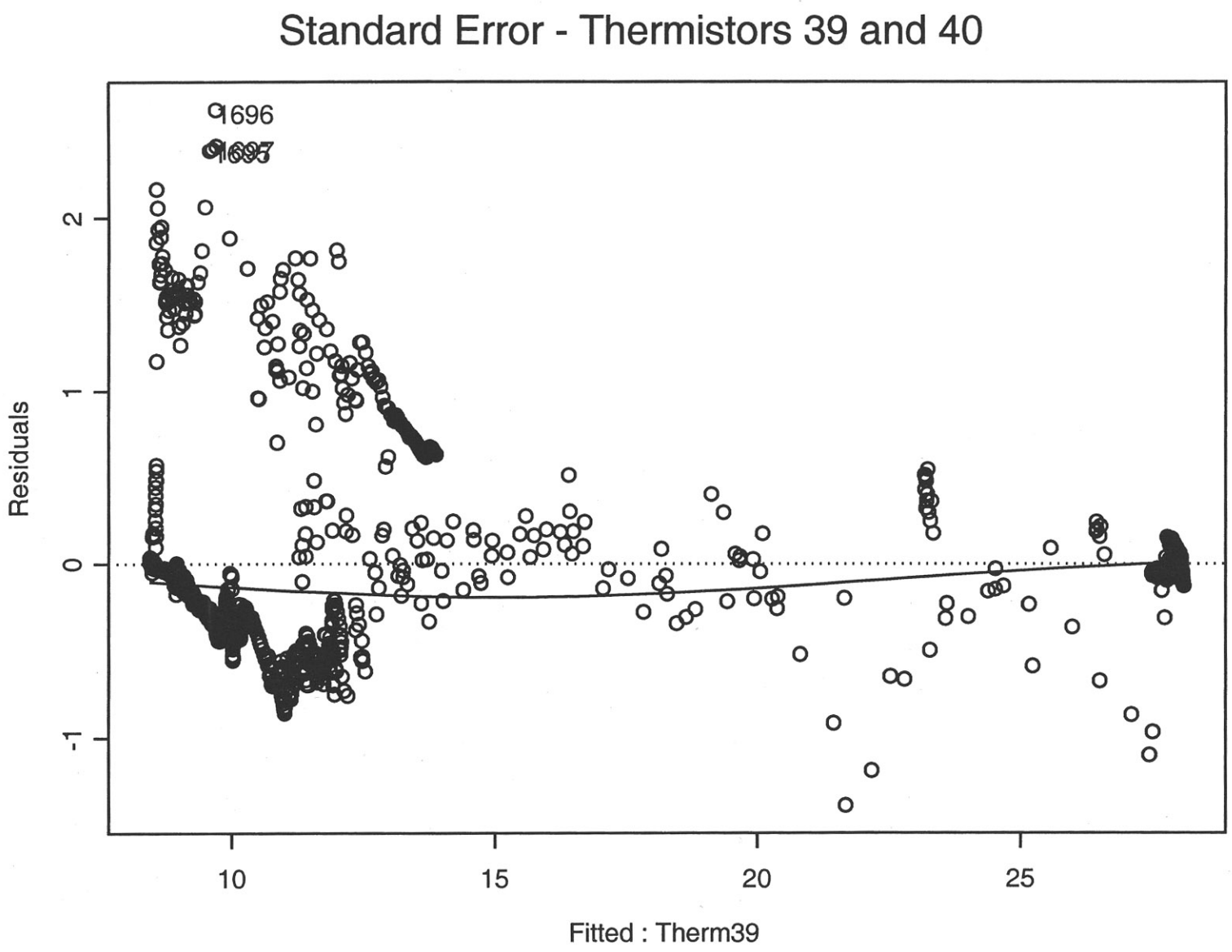
Standard Error - Thermistors 39 and 40
1696
1697
1695
Residuals
2
1
0
-1
10
15
20
25
Fitted : Therm39

```
      *** Linear Model ***

Call: lm(formula = Therm40 ~ Therm39, data = ThermistorCalibrationData,
na.action =
      na.exclude)
Residuals:
    Min      1Q   Median      3Q   Max
 -1.387 -0.1983 -0.04565 0.02206 2.622

Coefficients:
               Value Std. Error  t value Pr(>|t|)
(Intercept)   0.0095   0.0233     0.4089   0.6827
    Therm39   1.0029   0.0013   754.6330   0.0000

Residual standard error: 0.4635 on 1797 degrees of freedom
Multiple R-Squared: 0.9969
F-statistic: 569500 on 1 and 1797 degrees of freedom, the p-value is 0
```

Thermistor 40 = 0.009507 + 1.003* Thermistor 39

Task 5: Gas Hydrate Formation and Decomposition in Ocean Sediments
Laboratory Experiments with Hydrated Sediments

Final Report
March 2003

Principal Investigator: R. E. Rogers

DOE Award DE-FC26-00NT40920

Mississippi State University
Box 9595
Swalm School of Chemical Engineering
Mississippi State, MS 39762

ABSTRACT

Gas hydrate induction times and formation rates in seawater-saturated sand/clay packs are catalyzed in the laboratory by a few ppm of biosurfactants. To determine if biosurfactants are indigenous to sediments near Gulf of Mexico gas-hydrates, such sediment samples were analyzed for catalytic effects on hydrate formation. This work addressed some relationships of biosurfactants, sand, and clays with gas hydrate formation rates, induction times, and form (dispersed, nodular, stratified, massive), relating these factors to gas hydrate occurrence in GOM sediments.

Included are two electron microscope views of the tube walls of a tube worm and of a biopolymer on the surface of sand.

TABLE OF CONTENTS

Abstract .....
Table of Contents .....
List of Figures .....
Executive Summary .....
I. Introduction .....
Statement of Theory and Definitions.....
Biosurfactant Effects on Induction Times .....
Biosurfactant Effects on Formation Rates .....
Experimental Method …….....
II. Results and Discussion .....
Electron Microscope Photographs .....
Evaluation of Gulf of Mexico Sediments Near Gas Hydrates..
III. Conclusions .....
Nomenclature .....
References .....

LIST OF FIGURES

Figure 1 Photomicrograph Emulsan on Sand
Figure 2 Photomicrograph Tube Worm's Tube Wall
Figure 3 Relative Formation Rates with GOM Sediments
Figure 4 Particle Size Distribution Sediment Samples

EXECUTIVE SUMMARY

Evaluation was continued of biosurfactant effects on gas hydrate formation.

Although the biopolymer Emulsan does not form micelles, it promotes gas hydrate formation on bentonite surfaces. Emulsan does not promote hydrate formation on sand surfaces. Apparently, the large Emulsan polymer uncoils to spread over the bentonite surface, orienting hydrophilic and hydrophobic groups to associate hydrocarbon gases in nucleation centers on the polymer. A photomicrograph suggests that the orientation is not favorable if Emulsan spreads over a sand surface.

GOM sediment samples from hydrate mounds showed a correlation of hydrate formation rate with particle size of the media. Additional extensive tests are needed to determine if biosurfactants adsorb on GOM sediment surfaces in sufficient quantities to catalyze gas hydrate formation.

GOM sediments, tube worms, and commercially-available biosurfactants were analyzed during the report period to determine effects on seafloor gas hydrates.

I. INTRODUCTION

While searching for a surfactant to retard gas hydrate formation, Bishnoi first reported a catalytic effect of some surfactants on gas hydrate formation (1). Zhong and Rogers (2) first reported not only the catalytic effect of some anionic surfactants on hydrate formation but the additional facilitation of self-packing hydrates on metal surfaces as they form and complete reaction of interstitial water. These properties have been incorporated into a conceptual design of a large gas-storage facility (3), and DOE is currently sponsoring a scale-up of the design for industrial gas storage.

Vysniauskas and Bishnoi developed Equation 1 with data taken from a chilled, hydrocarbon-gas and water, stirred system. The vigorous stirring continually renewed the gas-water interfacial boundary to prevent hydrate barrier films from developing (4).

$$r = Aa_S \exp(-\Delta E_a / RT) \exp(-a / \Delta T^b) P^\gamma \quad \text{.....} \quad (1)$$

Significantly, Equation (1) was found to also apply to a non-stirred, anionic-surfactant water solution in which the hydrates migrate and adsorb on the surface of a metal at the water-gas interface (2). The migration of forming hydrate crystals clears the water surface of any hydrate film and gives about the same rate of formation as when vigorously stirred. Whether by mechanical stirring or by crystal migration, the reacting surface is kept clear of a barrier film; mass transfer is not a rate-limiting factor in either case.

The results of the synthetic surfactants on the gas storage process suggested a study of the effect of biosurfactants on hydrate formation in sea floors. There, water-borne microbes, in order to feed on the organic matter in ocean-floor sediments, would be expected to produce biosurfactants to make that insoluble matter accessible. Consequently, those biosurfactants could catalyze gas hydrate formation. Results of our investigation address the possibility.

Statement of Theory and Definitions. In the gas storage process, the surfactant's catalytic effect on gas hydrate formation is caused by the formation of surfactant micelles. The sodium dodecyl sulfate (SDS) anionic surfactant used in the gas storage process forms a micelle. The 12-carbon alkyl groups form a spherical micelle that solubilizes hydrocarbon gases (5). Water associates around the periphery of the micelle in close proximity to the solubilized gas. Thus, micelles act as nucleation sites for hydrate crystals. The threshold concentration of surfactant to form micelles occurs at the critical micellar concentration (CMC), and this CMC is traditionally measured by surface tension at ambient conditions. Because CMC is difficult to determine by surface tension at hydrate-forming conditions, hydrate induction time has been developed as a precise means of that measurement (2). For a rhamnolipid surface-active agent in distilled water, the CMC was found to decrease by a factor of about 11.2 from ambient conditions to hydrate conditions.

The hydrocarbon-gas-laden micelles are evenly distributed throughout the water. Therefore, crystallization can commence in the water subsurface. The buoyancy of the developing hydrate crystal moves it through the bulk of the free water to the liquid-gas interface, and the affinity of the surfactant to the cold metal surface facilitates movement of surfactant and attached hydrate crystal to adsorb on the metal surface (2).

This interesting laboratory phenomenon with synthetic surfactants could be important in the formation of gas hydrates in ocean sediments, where microbial action is reported to be prolific in the vicinity of gas hydrates in the Gulf of Mexico.

Biosurfactants fall into five classifications: (1) hydroxylated and crosslinked fatty acids, (2) polysaccharide-lipid complexes or polymers, (3) glycolipids, (4) lipoproteins-lipopeptides, and (5) phospholipids (6; 7). They are named according to their hydrophilic groups:

carboxylates, saccharides, glycoproteins, peptides and phosphates (7). The common hydrophobic group is the long-chain fatty acid. Samples that are available commercially from each of the five classifications were used in the experimentation.

Consequently, laboratory tests were made under the subject DOE grant and reported in the previous year's Final Report. A summary of these results is as follows.

Biosurfactant Effects on Induction Times. Surfactin, a lipoprotein-lipopeptide classification, in the presence of bentonite reduced the induction time drastically, shortening the time for hydrate initiation by 71% from the control in which no biosurfactant was present. Rhamnolipid, a glycolipid, also reduced induction time substantially, decreasing it about 58% from the bentonite control; the fatty acid exhibited a similar influence. Phospholipids and polysaccharide-lipid complexes (Emulsan and Snomax) reduced the induction times 20% to 44% from the bentonite control

With kaolin present instead of bentonite, some different reactions occur. Rhamnolipid has the greatest positive effect, reducing the time by about 66% over the kaolin control. With fatty acid in the presence of kaolin, no hydrates formed. These results indicate that biosurfactant can determine the residence time required for hydrates to form from a gas migrating through the hydrate zone of the ocean floor, and that the induction time is affected by the biosurfactant and specific sand, bentonite, or kaolin surface present.

Biosurfactant Effects on Formation Rates. Although in the absence of a biosurfactant, kaolin reduces hydrate formation rates compared to when bentonite is present, kaolin further reduces hydrate formation rate in the presence of Surfactin, phospholipids, Snomax, and Emulsan. An exceptional effect was observed in the case of rhamnolipid. A 16-fold increase of rate occurred when rhamnolipid solution was saturating the pack that included kaolin. With bentonite in the pack, the Surfactin biosurfactant increased hydrate formation rate about 4-fold, but kaolin-Surfactin interaction suppressed the rate increase.

Our tests also indicate that only small amounts of biosurfactant may be necessary to affect gas hydrate formation in the sea floor. The CMC of rhamnolipid in seawater at hydrate conditions was determined to be only 13 ppm for the 25% active rhamnolipid sample used in the tests.

Experimental Method. To meet the objectives of the experimental work, it was necessary to compare hydrate formation rates of samples containing the various biosurfactants and to observe visually any specificity the biosurfactants exhibited toward solid surfaces as evidenced by gas hydrate formation appearances.

The experimental apparatus was designed to allow determining induction times and gas-occlusion rates, parameters that define gas hydrate formation rates. Also, the apparatus was designed to allow visual observation of hydrate formation.

Stainless steel test cells were provided with pressure transducer, RTD temperature sensors, and visual access. One means of visual access was a two-inch thick, four-inch diameter quartz viewing port in the top of a test cell. The second visual access came from two sapphire-sealed viewing ports that allowed borescope image capture and fiber-optic light entry. Samples were placed in the test cells, test cells were placed in a cold environment, and temperature-time-pressure recorded with an Omega data-acquisition system.

An induction time for the system was defined as the time to cool the sample from the equilibrium temperature to hydrate initiation. Hydrate initiation was indicated by pressure drop at constant temperature. The equilibrium pressure-temperature curve for the given gas composition was calculated using the CSMHYD program (24). Because beginning pressure-temperature combination before cooldown and rate of cooldown were maintained constant, relative values of induction times for all runs could be made.

In order to calculate the rate of hydrate formation, the Peng-Robinson equation of state was used to determine moles of gas occluded into hydrates from a known constant cell volume and recorded pressure/temperature. Temperature-pressure-time data were collected every 20 seconds.

Gulf of Mexico seawater was used in all experimental runs. A natural gas of 90.0% methane, 6.0% ethane, and 4.0% propane was used for all runs. Combinations of sand, bentonite or kaolin were used for the porous media.

II. RESULTS AND DISCUSSION

Electron Microscope Photographs. Emulsan was found to catalyze gas hydrate formation in porous media, especially in the presence of bentonite. To help understand the mechanism, consider some of the properties of Emulsan, bentonite, and sand that might account for different reactions.

Emulsan is a bioemulsifier originating from the *Acinetobacter calcoaceticus* oil-degrading bacterium, and falls within the biosurfactant general classification of polysaccharide-lipid complexes. The biopolymer's molecular weight is approximately 980,000. As a polyanionic heteropolysaccharide bioemulsifier, it is effective in removing and emulsifying oil films (16; 17; 18; 19). Despite not significantly lowering surface tension, it is a powerful oil-in-water emulsion stabilizer- the large molecule covers the surface of the suspended oil drop to prevent coalescence. Emulsan does not form micelles, however, its separate hydrophobic-hydrophilic moieties could serve to unite the water and the host hydrocarbon to promote hydrate formation.

Sand has a negatively charged surface, whereas the bentonite has positive sodium ions situated at the edge of the clay platelet (a platelet consists of three layers ordered as silicon tetrahedra, aluminum octahedra and silicon tetrahedra), and in the accessible area between bentonite platelets positive sodium ions connect the negatively-charged platelets. One might expect, therefore, that the anionic biosurfactants would attach to the positive sites of bentonite but be repulsed, to some extent, from the sand surfaces. This anticipated result is verified with gas hydrate experiments where hydrates are usually catalyzed on the bentonite surfaces in the presence of biosurfactants.

Although Emulsan does not form micelles, its large molecules help bring the hydrocarbon gases and water to a common hydrate nucleation site. Ordinarily, this long-stranded biopolymer might resemble a tangled thread, yet it has been characterized as unfolding to orient hydrophobic groups on an oil-drop surface while positioning its hydrophilic groups into the surrounding water. Probably, the molecule unfolds and spreads on the bentonite surface in a similar manner to facilitate hydrate formation.

In Figure 1 is a photograph from an electron microscope showing the surface of a sand particle after being exposed to an Emulsan-water solution. Seen on the sand surface are some crystals of salt and a fibrous web of a partial coating that is probably Emulsan. It is possible that unfolding and spreading of the Emulsan polymers occur on the sand as well as the bentonite, but the orientation of hydrophobic-hydrophilic groups on the sand is such to not promote hydrate formation.

In Figure 2 is a photograph from an electron microscope showing the surface of a tube worm taken from near a gas hydrate mound in the Gulf of Mexico. Note the fibrous nature of the walls of the tube where one column is broken to reveal a panel-like mass. Hydrates would not form on the tube worm mass in the laboratory.

Evaluation of Gulf of Mexico Sediments Near Gas Hydrates. In the only reported analysis of sediments around or in gas hydrate mounds in the Gulf of Mexico to identify bacteria, the parent microbes that produce Surfactin and rhamnolipid were found by Lanoil, et al, (15). It is

significant that the biosurfactants of these two bacteria gave the most pronounced effects on gas hydrate formation in the laboratory tests reported here.

Four samples of sediments from gas hydrate fields in the northern Gulf of Mexico were analyzed for any associated catalysis effects on gas hydrates. In each case the dried sediments were mixed with sand to restructure a porous media sample containing 10% of the sediments. The mixture was reconstituted with seawater from the Gulf of Mexico, and hydrate formation rates calculated from laboratory data.

The results were compared to two control tests where one test included only sand and the second control included the sand saturated with 1000 ppm rhamnolipid in seawater. The relative formation rates are presented in Figure 3. Two of the samples indicated no effect on gas hydrate formation (Samples 4234A and 4236), whereas two samples (4234B and 2904) indicated an increased formation rate. The control with rhamnolipid biosurfactant surpassed all samples with a high formation rate of hydrates. The sediment samples were analyzed for particle size distributions and percentages of sand, silt, and clays. In Figure 4 is shown the percentage in each sediment of particles with sizes >1 mm. A correlation is suggested by comparing Figures 4 and 3; higher hydrate formation rates occurred with those sediments composed of larger particles.

III. CONCLUSIONS

Biosurfactants must fall into one of five classifications. By testing commercially available samples from each of the five classifications, some notable effects on gas hydrate formation in seawater-biosurfactant saturated sand/clay packs resulted. Hydrate induction times and formation rates were generally enhanced by the biosurfactants, and in many cases (especially rhamnolipid and Surfactin) the enhancements were very large. The fatty acid retarded (bentonite) or prevented (kaolin) hydrate formation, the only classification that did so. The biosurfactant effect may occur even at low concentrations; for example, the CMC of rhamnolipid was reduced to 13 ppm at hydrate-forming conditions.

Investigations on GOM sediment samples show a correlation of hydrate formation rate with sediment particle size; higher rates are associated with larger particle sizes.

Analysis of tube worms from around GOM hydrate mounds showed hydrates would not form on the tube surfaces. Photomicrographs of the tube walls showed a very fibrous structure.

Emulsan biopolymer is indicated to spread over bentonite surfaces in such a way as to help concentrate hydrocarbon gases for hydrate nucleation.

NOMENCLATURE

ΔT = degree of supercooling below equilibrium
T = absolute temperature of system
P = pressure of system
γ = overall order of reaction with respect to pressure
a,b = constants
A = lumped pre-exponential constant
a_s = surface area of gas-water interface
ΔE_a = activation energy for hydrate formation
R = universal gas constant

REFERENCES

1. Kalogerakis, N., Jamaluddin, A.K.M., Dholabhai, P.D., & Bishnoi, P.R. (1993). "Effect of surfactants on hydrate formation kinetics", SPE 25188, SPE *International Symposium on Oilfield Chemistry*, New Orleans.
2. Zhong, Y., & Rogers, R.E. (2000). "Surfactant effects on gas hydrate formation", *Chem. Eng. Sci*. 55, 4175.
3. Rogers, R.E. (1999). "Natural gas hydrates storage project, phase II. Conceptual design and economic study", Final report. DOE Contract DE-AC26-97FT33203, U.S. Department of Energy.
4. Vysniauskas, A., & Bishnoi, P.R. (1983). "A kinetic study of methane hydrate formation", *Chemical Engineering Science* 38, 1061.
5. MacKerell, A.D. (1995). "Molecular dynamics simulation analysis of a sodium dodecyl sulfate micelle in aqueous solution: decreased fluidity of the micelle hydrocarbon interior", *J. Phys. Chem.* 99, 1846.
6. Kosaric, N. (1992). "Biosurfactants in industry", *Pure and Appl.Chem*. 64, 1731.
7. Fujii, T. (1998). "Biodetergents", In *New Products and Applications in Surfactant Technology*, (D.R. Karsa, ed.), Sheffield Academic Press, Sheffield, England. 88.
8. Rosenberg, E. (1986). "Microbial surfactants", *CRC Crit. Rev. Biotech* 3, 109.
9. Thangamani, S., & Shreve, G.S. (1994). "Effect of anionic biosurfactant on hexadecane partitioning in multiphase systems", *Environ. Sci. Technol.* 28, 1993.
10. Herman, D.C., Artiola, J.F. & Miller, R.M. (1995). "Removal of cadmium, lead, and zinc from soil by a rhamnolipid biosurfactant", *Environ. Sci. & Technol.* 29, 2280.
11. Churchill, S.A., Griffin, R.A., Jones, L.P., & Churchill, P.F. (1995). "Biodegradation and bioremediation", *JournalEnviron. Qual*. 24, 19.
12. Banat, I.M. (1995). "Biosurfactants production and possible uses in microbial enhanced oil recovery and oil pollution remediation: a review", *Bioresource Technology* 51, 1.
13. Bai, G., Brusseau, M.L., & Miller, R.M. (1997). "Influenceof a rhamnolipid biosurfactant on the transport of bacteria through a sandy soil", *Appl. Environ. Microbiol*. 63, 1866.
14. Champion, J.T., Gilkey, J.C., Lamparski, H.,Retterer, J., & Miller, R.M. (1995). "Electron microscopy of rhamnolipid (biosurfactant) morphology: effects of pH, cadmium, and octadecane", *J. Colloid Interface Sci.* 170, 569.
15. Lanoil, B.D., Sassen, R. La Duc, M.T., Sweet, S.T., & Nealson, K.H. (2001). *Appl. Environ. Microbiol*. 67, 5143.
16. Jones-Meehan, J., Beard, M., & Hind, J. (1995). "In-situ maintenance of oil/water separators", Final report CDNSWC/CODE 634, prepared for A. Lardis, Annapolis, MD.
17. Gutnick, D.L. (1987). "The Emulsan polymer: perspectives on a microbial capsule as an industrial product", In *Biopolymers,* John Wiley & Sons: New York. S223
18. Cohen, Y., & Rosenberg, E., eds. (1989). "Microbial mats: physiological ecology of benthic microbial communities", *American Society for Microbiology*, Washington, D.C.
19. Rosenberg, E. (1993). "Microbial diversity as a source of useful biopolymers", *J. Ind. Microbiol*. 11, 131.
20. Goodnow, R.A., Harrison, M.D., Morris, J.D., Sweeting, K.B., & Laduca,R.J. (1990). "Fate of ice nucleation- active *Pseudomonas syringae* strains in alpine soils and waters and in synthetic snow samples", *Appl. Environ. Microbiol*. 56, 2223.
21. Amende, B. & Gordon, J. (1999). Literature and analyses reports on Snomax. York Snow, Inc., Victor, NY.

22. Nakano, M.M., Marahiel, M.A. & Zuber,P. (1988). "Identification of a genetic locus required for biosynthesis of the lipopeptide antibiotic Surfactin in *Bacillus subtilis", J. Bacteriology* 170, 5662.
23. Genzyme Pharmaceuticals (2001). "Synthetic lipids", *Product Data Sheet*. Cambridge, MA. pharmaceuticals@genzyme.com.
24. Sloan, E.D., Jr., (1990). *Natural Hydrates of Natural Gases*, Marcel Dekker, Inc., New York, N.Y. 550.

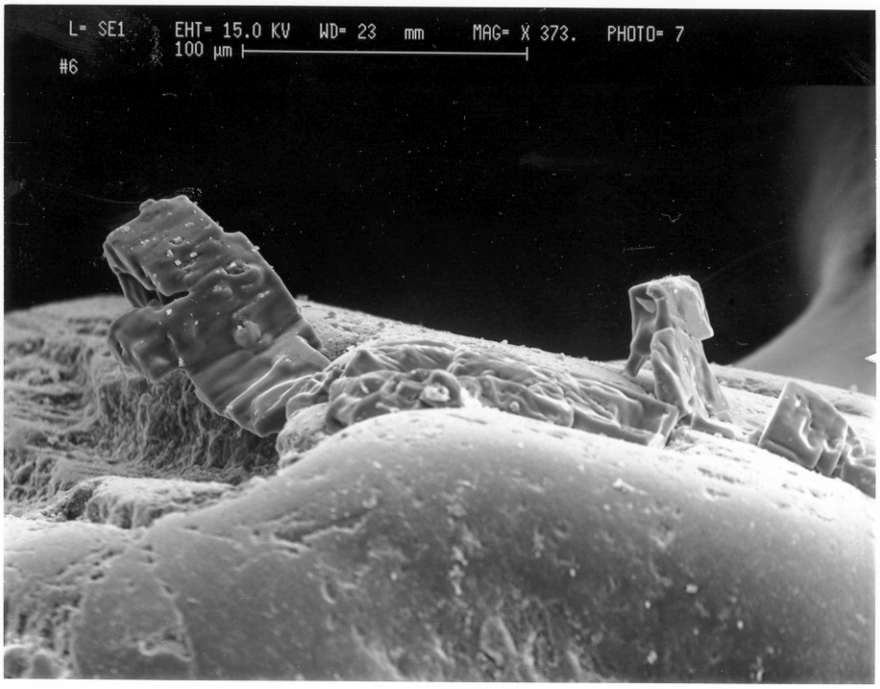

Figure 1. Photomicrograph Emulsan on Sand

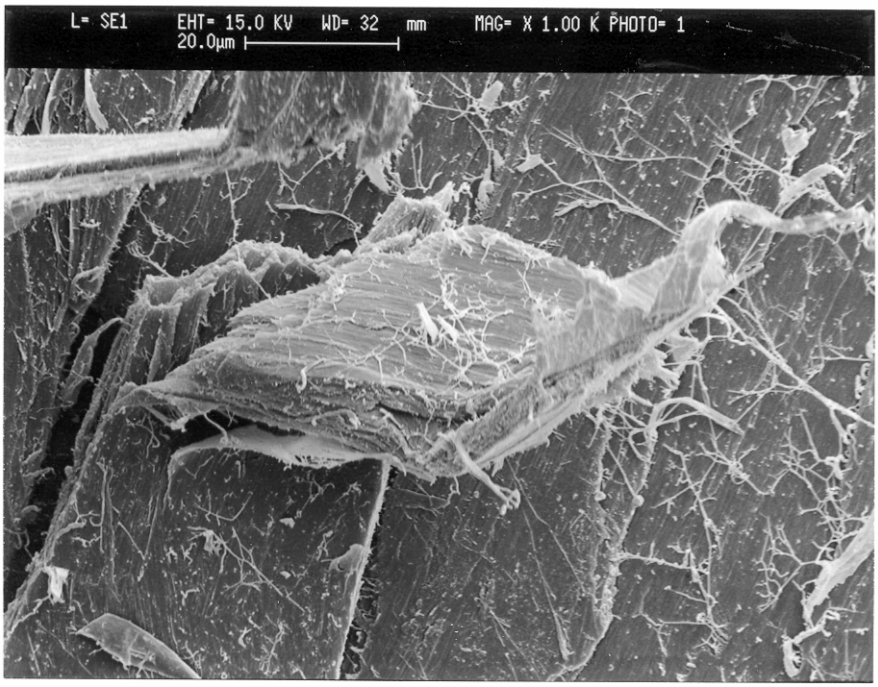

Figure 2. Photomicrograph Tube Worm's Tube Wall

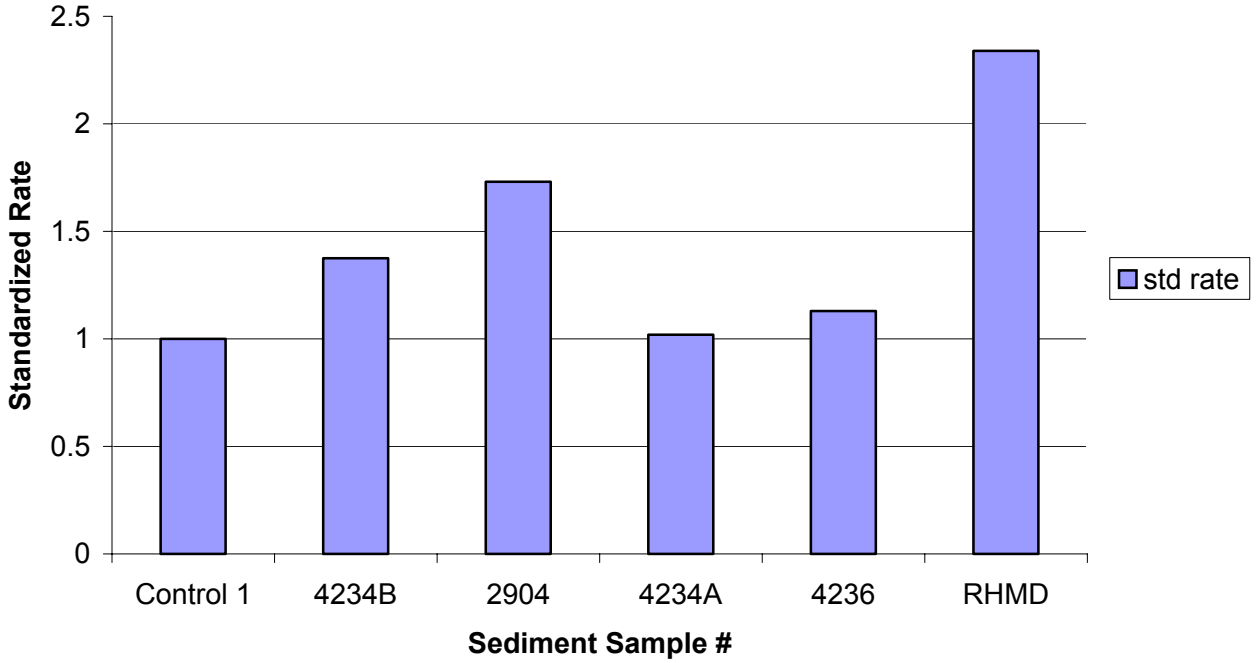

Figure 3. Relative Formation Rates with GOM Sediments.

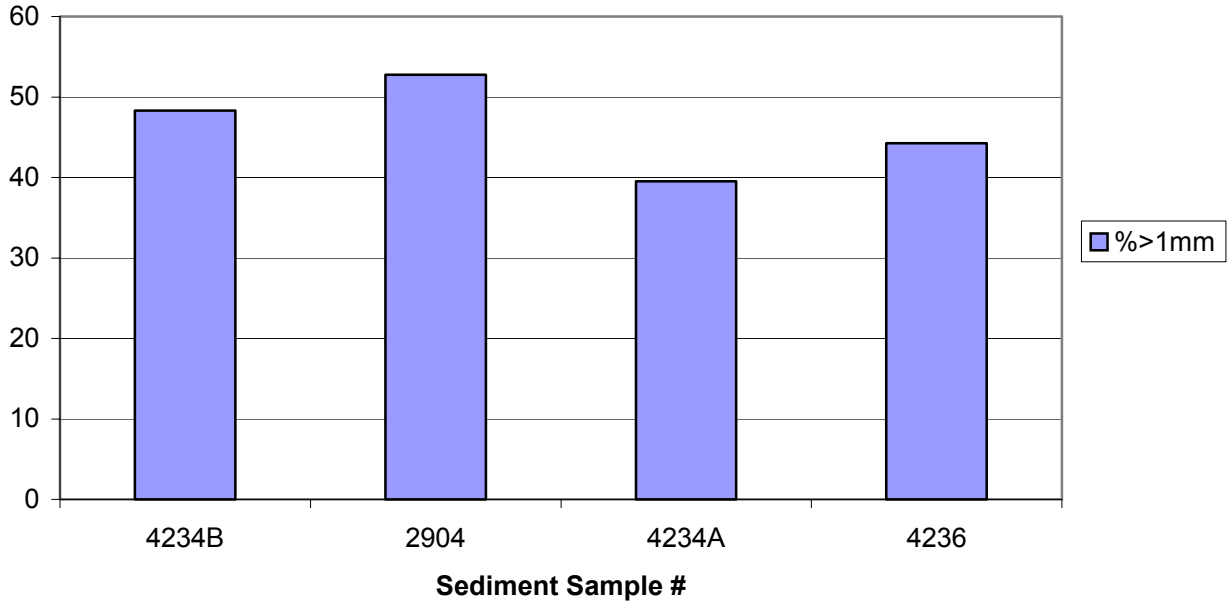

Figure 4. Particle Size Distribution of Sediment Samples.

Title: Subcontract to University of Mississippi: Gas Hydrates - Organic Geochemistry
Type of Report: Final
Reporting Period Start Date: July 1, 2003
Reporting Period End Data: September 30, 2003
Principal Author: Jean Whelan
Date Report Issued: December 30, 2003
DoE Award Number: DE-FC26-00NT40920
Submitting Institution: Woods Hole Oceanographic Instititution, Woods Hole, MA 02543

Abstract

Result to date are described in building and deploying an in situ methane sensor to explore for and characterize ocean bottom methane seeps associated with gas hydrates and subsurface petroleum accumulations. A Raman detector has been built and tested and, to date, found not to possess the required sensitivity for this task except in areas of large scale gas venting. Initial tests on the commercially available METs sensor have not been promising to date, although sea trials in March off Victoria B. C. will be used to field test the most recent version of the instrument. Because of these limitations. Work was begun to build an underwater mass spectrometer for this purpose. The advantages of this instrument, the present state of technology, and a possible design are described. Sources of initial funding obtained for this work are described along with proposals still pending. Work has begun on building the MS instrument.

New analytical procedures for characterizing biodegraded seep oils from both the Gulf of Mexico surface seep and hydrate oils and Santa Barbara Coal Oil Point seep oils are described. The most promising technique in two dimensional gas chromatography (2DGC) which rapidly gives quantitative data on individual oil components. This is a very large breakthrough since these oils were previously not very useful for quantitative analyses. These results may allow better coupling of surface seep geochemical data with subsurface reservoir data so that seep geochemistry could become a much better exploration tool than has previously been possible.

Table of Contents

Abstract
List of Figures and Tables
Introduction
Executive summary
Experimental
Results and Discussion
- Progress in development of in situ continuous methane sensor
  - Progress on Raman Sensor and testing of METs sensor
  - Initiation of development on oceanic in situ mass spec sensor
- Measurement of hydrocarbons in biodegraded oils: Gulf of Mexico
- Measurement of hydrocarbons in biodegraded oils; Santa Barbara, Coal Oil Point Seep oils

Conclusions
References
List of acronyms and abbreviations
Appendices
- I) Progress report submitted to NOAA on development of methane sensor
- II) Proposal submitted to Woods Hole Oceanographic Institution for Green Technology Award (funded). A Deep Diving Mass Spectrometer for Ocean Exploration of Gas Seeps and Pollution Monitoring
- III) Report: Hydrocarbon distributions from extant petroleum seep sites and associated gas hydrate deposits in sea water and ocean floor sediments from Santa Barbara and Gulf of Mexico, Jean K. Whelan and Lorraine B. Eglinton

Figures and Tables

Fig 1- Gulf of Mexico hydrate- gas seep overview
Table 1 - Typical methane concentrations in various oceanic seeps and concentration ranges available from various instruments

Introduction

Natural oil and gas seep zones associated with seafloor gas hydrate zones in the Gulf of Mexico show very large variations in a number of chemical species associated with venting over very small distances. This natural variability will present major problems for appropriate siting of a monitoring station to follow gas venting as it relates to resource evaluation and hydrate formation and destruction over time. The major accomplishments of our research group in addressing this problem has been two-fold this year:

1) development of a suitable methods for in situ measurements of methane and other light hydrocarbon concentrations issuing from active vents and

2) development of methods for relating biodegraded oils found in hydrates and seeps to both their parent oils and to the degree that they have been affected by various alteration processes, including biodegradation, water washing, and gas washing.

The longer term goal of the project is to integrate these measurements with geophysical data to determine the amounts and compositions of subsurface hydrates and hydrocarbon in reservoirs for use both as an exploration tool and as means of quantitating the amounts of gas either trapped or flowing through the complex sedimentary hydrate-gas flow network (Fig 1).

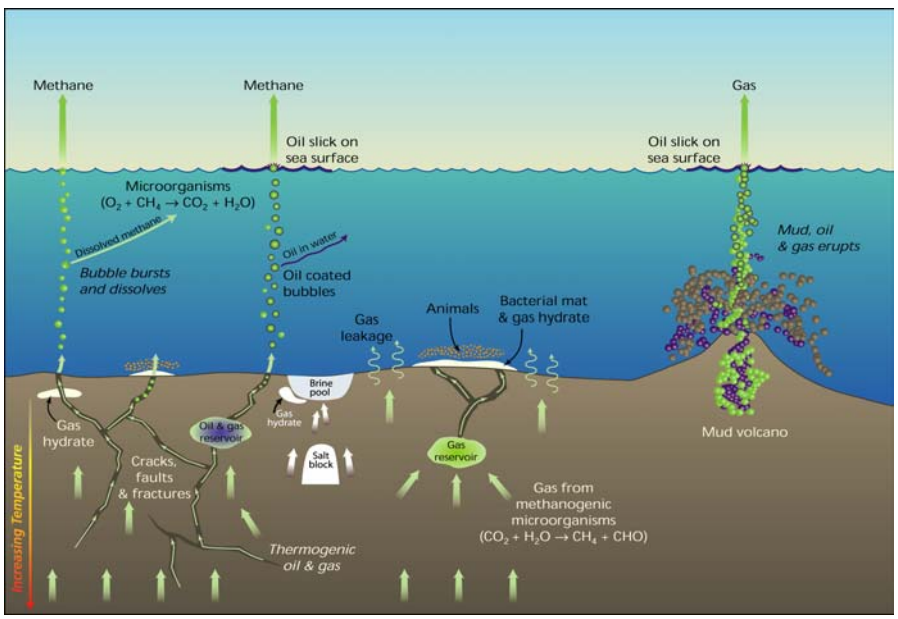

Figure 1: Summary of all gas seep related processes observed in Green Canyon area in the northern Gulf of Mexico (location shown in Fig 1)**.** The processes shown include thermogenic oil and deeper gas generation (to the left) and biogenic methane generation (to the right). Gas from either source migrates upward either rapidly through faults and fractures or more slowly by diffusion through sediments into overlying oil and gas reservoirs. Most of the gas bypasses the reservoirs and continues its upward migration to the sediment water interface where it can form gas (methane) hydrate deposits (shown in white) or can be vented into the overlying water column. If methane concentrations do not reach saturation, the gas in the dissolved phase is largely biodegraded to carbon dioxide in the water column. When methane reaches saturation in sea water, gas bubbles form and migrate upward. Oil can coat the bubbles and be delivered into a sea surface oil slick (see Leifer et al., this volume). If bubbles survive to within 100m of the surface, methane can be vented to the atmosphere. Chemosynthetic communities of

animals, shown with pink dots, tend to congregate on surfaces of gas hydrates and within bacterial mats near surface sediment gas seeps.

The geochemical data to be collected in the initial field study proposed here and from the longer term monitoring station measurements will provide basic information needed to assess the resource potential of seafloor gas hydrates in the Gulf of Mexico. These data address three basic questions: 1) rate of formation and long term stability of the hydrates; 2) their rate of destruction via interaction with the surrounding biological communities which are probably dependent on hydrocarbons as a food source; and 3) rates of hydrate formation and destruction from gas seeping upward from depth and venting into the overlying water column. The specific long term measurements to be carried out, if they prove useful in this initial field work, include changes in salinity, temperature, methane, fluorescence (related to amount of oil and microorganisms), and possibly pH, turbidity, and sulfate. All of these parameters relate directly or indirectly to either gas hydrate stability or to the biogeochemistry of gas hydrates and seeping gas. In addition, discrete water samples must be collected periodically to monitor changes in gas compositions and isotopes.

This initial data and the longer term continuous measurements from the monitoring station will answer several basic questions regarding seafloor gas hydrates in the Gulf of Mexico which are important in assessing their long-term resource potential:

What are the effects of long term venting of gases and fluids from depth on seafloor hydrate formation and destruction? Are these gas hydrates a relatively fixed and reliable resource, which can be produced? Or do they represent only a localized and ephemeral phenomenon dependent on the degree of localized gas flux and the related degrees of microbial cycling of sulfur and carbon?

How much of gas from the hydrates or from the gases venting through them might actually be available as a future potential resource?

How does the very dynamic biogeochemistry and presence of sulfur within and around the hydrate zone affect the resource potential of methane from hydrates? How localized is gas venting from or through hydrates and how is it affected by the biological processes? How does gas venting interact with microbial processes of methane production versus utilization, sulfate reduction versus sulfur oxidation? What other microbial processes are operating and how do they affect methane resource potential from the surface gas hydrates?

Seafloor hydrates recovered during the Aug 2000 cruise had a strong disagreeable odor caused by sulfur compounds. What is the chemical form of the sulfur and does it affect the economic viability of seafloor hydrates as a potential fuel source?

If the upward flow of gas is on-going and hydrates are continuously being formed and destroyed, then seafloor hydrates might be a self-renewing energy source and any disruption caused by their seafloor mining might be minimal.

Can gas hydrates be mined from the seafloor with minimal disruption of the biogeochemistry of animals and organisms dependent on them?

Executive summary

Natural oil and gas seep zones associated with seafloor gas hydrate zones in the Gulf of Mexico show very large variations in a number of chemical species associated with venting over very small distances. This natural variability will present major problems for appropriate siting of a monitoring station to follow gas venting as it relates to resource evaluation and hydrate formation and destruction over time. The major accomplishments of our research group in addressing this problem has been two-fold this year:

1) development of a suitable methods for in situ measurements of methane and other light hydrocarbon concentrations issuing from active vents and

2) development of methods for relating biodegraded oils found in hydrates and seeps to both their parent oils and to the degree that they have been affected by various alteration processes, including biodegradation, water washing, and gas washing.

The longer term goal of the project is to integrate these measurements with geophysical data to determine the amounts and compositions of subsurface hydrates and hydrocarbon in reservoirs for use both as an exploration tool and as means of quantitating the amounts of gas either trapped or flowing through the complex sedimentary hydrate-gas flow network

The geochemical data to be collected in the initial field study proposed here and from the longer term monitoring station measurements will provide basic information needed to assess the resource potential of seafloor gas hydrates in the Gulf of Mexico. These data address three basic questions: 1) rate of formation and long term stability of the hydrates; 2) their rate of destruction via interaction with the surrounding biological communities which are probably dependent on hydrocarbons as a food source; and 3) rates of hydrate formation and destruction from gas seeping upward from depth and venting into the overlying water column.

Progress in development o reliable in situ methane sensor:

Raman Sensor and testing of METs sensor Funding was obtained from NOAA to build a combined METs-Raman methane sensor which would have the wide dynamic range for in situ methane measurements needed to characterize natural ocean floor methane vent features. We proposed to build a dual detection methane sensing system utilizing a Raman spectrometer for monitoring higher methane concentrations near the venting plume (micromolar to millimolar methane concentrations) and a CAPSUMs METS sensor for the lower methane concentrations further away from the plume. The original concept was that the Raman spectrometer would be used to protect the METS sensor from over saturation by triggering a shut off of the METS detector window whenever high methane concentrations are encountered.

To date, intial tests of the METs sensor have not been promising, although new field trials are planned for Feb 2004 using a newly designed instrument.

Mass Spectral methane detector It came to our attention this year that an underwater mass spectromether might be the ideal instrument for our purposes. Funding and personnel have been obtained to start building and testing such an instrument. Details of the project and initial design of the instrument are described in the results and discussion section and in Appendix 2.

Experimental - See experimental sections in Appendices I, II, and III

Results and discussion

Progress in development of in situ continuous methane sensor

Progress on Raman Sensor and testing of METs sensor

The main purpose of our research this year is to develop an oceanic in situ methane measurement device which can be used both for exploration and characterization of gas hydrate deposits. At the present time, no system exists which can continuously monitor methane over the very wide dynamic range encountered around ocean floor methane vent features. Existing technologies have, so far, proven to be ill suited to sense and monitor methane dissolved in waters around these vent features.

In this work, with the bulk of the money coming from NOAA we proposed to build a dual detection methane sensing system utilizing a Raman spectrometer for monitoring higher methane concentrations near the venting plume (micromolar to millimolar methane concentrations) and a CAPSUMs METS sensor for the lower methane concentrations further away from the plume. The original concept was that the Raman spectrometer would be used to protect the METS sensor from over saturation by triggering a shut off of the METS detector window whenever high methane concentrations are encountered.

The research to date is described in Appendix 1 which is a annual report submitted to NOAA, who is funding this part of our research, on progress up to September of 2003. The technical data needed to address the scientific problem above are: How methane much and where is methane associated with gas hydrates venting from bottom seeps into the water column? How fast is the venting? What are the temporal and spatial variabilities of methane venting from ocean floor? Data in hand prior to this project show changes in methane concentration of several orders of magnitude (uM to nM, Table 1) over small distances (a few meters) in the vicinity of gas hydrates and their associated gas seeps. These initial discrete methane measures showed the need for continuous in-situ profiling of methane by a technique having very large dynamic range and a relatively rapid response time (a few seconds). These constraints ruled out most common methane measurement techniques and required an instrument having a high sensitivity, wide dynamic range, and a rapid response time to handle large spatial and temporal variations expected during long or short time-series monitoring of seeps.

Table 1: Typical methane concentrations in various water bodies and typical sensitivities of various methane measuring techniques (2ppm=3nM).

Gulf of Mexico:	Methane concentration
Surface waters	100ppm=150nM=0.15uM
mid-depth waters	180-700 ppm = 0.27-1.05 uM
Bottom waters- near seep	average: 4-10uM
- mid water directly over seep	0.1 to 0.7 uM
pore waters at seep	0.5 to 40 uM
pore waters away from seep	<0.5 uM
methane saturation values, 600m	60mM=60,000uM
Open Ocean	Methane Concentration
Bubbles venting from gas plume	>60mM = >60,000 uM
A few meters from plume	40 uM
In plume as it spreads out into ocean	10 to 100 nM = 0.01 to O.1 uM
Oceanic background levels	1-3 nM or less = 0.001 to 0.003 uM
Sensitivities, methane measuring devices	
Current Raman spectrometer	1mM = 1000 uM
projected -modified Ramen spectrometer (minimum modification)	25 to 100 uM
Further instrument modification - projected estimate of maximum sensitivity	0.25-1uM
Gas Chromatograph (GC) - FID detector, surface detection with gas stripping on deck of ship	all oceanic levels including background
Commercially available METs methane sensor	5-10 nM = 0.005 to 0.01 uM

.

Our proposed solution was to combine a Raman sensor which has a wide dynamic range and rapid response time, but low sensitivity (10s of uM) with a METS sensor, a commercially available detector utilizing membrane absorption and chemical reaction of methane. Previous researchers have found this instrument to have a low dynamic range and sluggish response time (minutes) but high sensitivity (nM). Raman spectroscopy meets all technical requirements except for sensitivity (existing Welldog instrument: about 100 uM; estimated that this can be increased to 100nM or better with more sophisticated spectrometer)

The commercially available (METS) sensor has smaller dynamic range, but theoretically higher sensitivity. Based on previous work with an instrument borrowed from Bob Lamontagne and co-workers at the Naval Research Laboratory, the METS sensor detects low methane concentrations (nM to uM) but oversaturates and becomes inoperable at higher methane concentrations. This process is reversible by bringing the METs back on deck and flushing the membrane with nitrogen. Thus, the METs insrument appeared to have a number of limitations for our work. In addition, no reliable laboratory or field calibrations of the instrument were available at the time our work started.

The first task in this project has been to evaluate and test both the Raman and METs sensors in our laboratories to determine for ourselves their suitablity for this project. Our progress to date shows that:

1) The Raman detector looks very promising and may be much more sensitive that we originally anticipated and

2) The METs sensor doesn't look very promising in work so far. However, the manufacturer of the instrument will be working with us in ship-board testing of a new version of the sensor in February of this year. This will give us a definitive test of the technology as well as a comparison between laboratory and in situ methane measurements. The older METs instruments used so far have not performed very well in these tests.

Progress on Raman Spectometer Initial tests with the existing Welldog instrument indicated that an upgraded Raman may be much more sensitive than we originally predicted and may ultimately produce usable methane signals for concentrations as low as 10s to 100s of nM, or almost open ocean background methane levels. The results shown in Figs 1-5 of Appendix 1 were all carried out on the existing Welldog instrument which is much less sensitive than our upgraded spectrometer will be. Work has started on the upgraded Raman spectrometer, but has been delayed because the initial instrument had to be returned to the manufacturer because it did not meet the contracted specifications. We are aiming for a new upgraded (more sensitive) instrument to be ready for its first (shallow water) oceanic tests in Saanich Inlet, B.C. in Feb of 2004 (water depth: 300 m). On that cruise, we plan to compare in situ methane measurements from the Raman and from the METs sensor with laboratory measurements on discrete water samples from the same zone. An ancillary benefit of using the Raman spectrometer in this project is its potential ability to detect and measure other seep-related organic compounds along with methane possibly including: dimethylsulfide, higher alkanes and aromatic hydrocarbons, alcohols, carboxylic acids, amines, carbon dioxide, etc. Some examples from laboratory analyses to date are shown in Appendix 1.

Initiation of development on oceanic in situ mass spec sensor

The in situ Raman Spectrometer technology above looks very promising for higher methane concentrations around seeps in active seep areas of the Gulf of Mexico, but may not ever have the sensitivity needed to detect the lower concentrations of methane from deeper water seeps both in the open ocean and in the deep water Gulf of Mexico (range: 100- a few nM). Conversations between Dr Michael Whiticar, myself and Dr. Rich Camilli, who recently received his Ph.D. in Civil Engineering from MIT, made us aware that underwater mass spectrometry might be the best possibility to solve this problem. Recent conversations with scientists at both the University of South Florida (Bob Byrne) and at MIT (Rich Camilli) indicate that the underwater mass spectrometer part of such an instrument is already technologically possible. Both groups have carried out successful intial tests of various types of spectrometers and obtained in situ measurements of pollutant organics in shallow waters (aromatic compounds). Some very preliminary work was also carried out on fixed and hydrocarbon gas analysis in coastal waters to maximum depths of about 100ft. Discussions to date indicate that the main technological problem to going deeper is designing a suitable inlet system. Rich Camilli who built the MIT underwater spectrometer as part of his doctoral thesis is currently applying for a Postdoctoral Scholar award at Woods Hole. (His chances seem very good - he wrote most of the text for the successful Green Technology Award and the pending NOAA proposals described below). In the meantime, he has been appointed as a Guest Investigator at WHOI working in the laboratories of Jean Whelan in the Marine Chemistry and Geochemistry Department and Dr Hanu Singh, a WHOI scientist in the Applied Ocean Physics and Engineering Department. Jean Whelan and Rich Camilli have just received a Green Technology Award from the Woods Hole Oceanographic Institution to build the initial stages of the instrument. Rich Camilli, Jean Whelan, and Mike Whiticar have also applied for funding from the NOAA Ocean Exploration program for this project. A description of the instrument proposed

and progress so far can be found in Appendix II. We are aiming to carry out initial shallow water sea trials of the instrument at the University of Victoria in the fall of 2004.

Abstract We propose to build and test an in-situ mass spectrometer suitable for continuous monitoring of methane, gases, and low molecular weight organic compounds including pollutants in the ocean and which can operate to at least several hundred meters water depth. This instrument is intended to be a prototype for a future instrument capable of operation at all ocean depths. The scientific motivation for this project is development of a sensitive and versatile in situ monitoring instrument for gases and volatile organic compounds vented from oceanic "cold" seeps associated with methane hydrate deposits. The resulting data will be used along with geophysical data to distinguish between two different models of methane hydrate formation and maintenance - a "stable methane hydrate" model where the hydrate deposit has a relatively long lifetime versus a "steady state" model where methane is continuously streaming upward to form the bottom and is continuously being lost from the top of the hydrate deposit. The mass spectrometer will also serve as an exploration tool for exploration for new thermal and biogenic methane gas seeps in the oceean floor. These can be associated with hydrothermal vent sites and areas of discharge of land-based run-off as well as cold seeps. In situ mass spectrometry would compliment data from our in situ Raman spectrometer (currently being built with NOAA funding-University of Mississippi funding) in characterization of the fluid discharge from all three types of ocean floor vent sites. Alternatively the instrument can be used in shallower waters to unobtrusively monitor a variety of organic compounds in coastal waters impacted by urban runoff, shipping lanes, and point sources of ground water discharge to the ocean.

Description of proposed mass spectrometer (summarized from Appendix II). We propose to develop and deploy a versatile and rugged submersible mass spectrometer, for operation aboard a variety of oceanographic platforms. This new analytical instrument will be capable of real-time, continuous, in-situ, high-resolution measurements of dissolved gases, particularly methane, and volatile organic compounds in the ocean and will be able to operate to at least several hundred meters water depth. Funds from this project will be used as seed money to develop a similar deep water instrument for operation to full ocean depths.

In our laboratory, the instrument will be used to find and monitor methane seeps associated with ocean floor gas hydrate deposits. An abundance of recent evidence has shown that methane venting through small faults and fractures in the seafloor occurs in many locations worldwide and is important to the biology, chemistry, and geology of the ocean. Also, methane is a greenhouse gas. Even though the seafloor gas venting occurs primarily through localized fractures, the volume of methane involved may be substantial enough to contribute to global warming. However, no systematic exploration strategy currently exists for finding these generally very localized methane vents on the ocean floor. Furthermore, it is difficult to obtain reliable measurements of the gas concentrations or fluxes involved because venting tends to be very heterogenous and episodic. Methane concentrations commonly vary over several orders of magnitude within a few meters of the vent; reliable data on amounts as well as molecular and isotopic compositions involved cannot be obtained on samples brought to the surface and allowed to degas. Therefore, it is currently almost impossible to measure quantitatively how the venting methane interacts with the complex biological communities, gas hydrates, and bubble streams flowing around and through the hydrates.

The underwater mass spectrometer will be capable of monitoring oceanic in situ concentrations of both the high methane concentrations near venting plumes (micromolar to tens of millimolar methane concentration) to the lower methane concentrations (as little as 0.01 to 0.02 uM) typically found in moving away even a few meters away from the plume. The high sensitivity is important for finding new vents and monitoring the effects of methane in moving

away from the vent site. This work will compliment that currently in progress under a NOAA funded project to build an underwater Raman spectrometer. Laboratory and pressure tank tests so far have shown the Raman instrument to be suitable for the higher but not the lower methane concentrations found at hydrate associated vents. Additional work on this NOAA project has conclusively shown that the commercially available METS sensor possesses a number of technical problems making it unsuitable for this work.

Mass spectrometry is by far the most sensitive and versatile analytical technique available for identifying and quantifying a large variety of organic compounds likely to be found in the ocean in various settings. For some compounds, such as aromatic hydrocarbons typical of petroleum seeps and low molecular weight functionalized organics typical of various types of microorganisms (e.g. methane, acetic acid, carbon dioxide, hydrogen sulfide and alkyl sulfides from anaerobic bacteria in sediments), organic signatures are very diagnostic of the type of chemosynthetic organisms supported by these ocean floor seeps. These ocean floor gas and liquid venting sites have been described in many areas around the world in a number of deep sea environments for which this mass spectrometer is intended, including 1) natural gas and oil seeps ("cold seeps"); 2) hydrothermal vent sites; and 3) areas of discharge of land-based run-off.

Despite the advantages of in-situ mass spectrometry, to date only two submersible mass spectrometer designs have been deployed which are limited to operational depths of less that tens of meters. One of these was designed and built by Rich Camilli who will be involved in this project (Fig 2, Appendix 2). Our instrument is intended to be compact and fully self-contained, permitting continuous in situ measurements aboard platforms including ship-borne rosettes, ROVs such as the Jason vehicle, and various AUVs. It will function as a low power, ruggedized system that can be deployed in harsh environments with a mass range from 1-300AMU, sensitivity of 10-100 ppb for most volatile chemicals, and a time response on the order of tens of seconds.

Measurement of hydrocarbons in biodegraded oils: Gulf of Mexico and Santa Barbara, Coal Oil Point Seep oils

Experimental

Analysis of Gulf of Mexico seep oils both from waters, sediments and from hydrate melt waters were carried out using the procedures described in Appendix 3. The waters did not contain sufficient hydrocarbon concentrations to warrant further analysis. Results here are for the Gulf of Mexico sediment and hydrate seep oils collected on the Aug 2000 cruise. For comparison to other seep oils where gas hydrates are not involved, three sediment samples and three water samples containing oil globules from seep sites the Santa Barbara Coal Oil Point seep were also analyzed as described in Appendix III.

Univerally, hydrocarbons in seawater samples contained only trace amounts of oil and could not be analyzed except for one Gulf of Mexico sample where trace amounts of mono-aromatic steroids could be seen. Because large water volumes would have to be extracted, further analysis of oils in waters was not undertaken.

The sediment and hydrate extracts commonly produced some resolved GC peaks on top of a very large unresolved complex mixture of compounds

Conclusions

Both Areas Initial results with 2D GC show that this may be the ideal method for characterizing biodegraded seep and reservoir oils. Extensive series of resolvable cyclic and

branched alkanes are present in both the Gulf of Mexico and Santa Barbara seep oils which remain hidden in the UCM or unresolved complex mixture of most GC methods. This compound class, rather than much higher molecular weight compounds, appear to comprise the bulk of the oil in both areas and were previous unanalyzable. The method also provides quanitative data on the amounts of individual compound present and so my allow us to gain a quantitative measure of the relative extent of various oil alteration processes in both areas, water washing versus gas washing versus biodegradation.

Santa Barbara Based on loss of *n*-alkanes, modification of steranes, an emerging series of 25-norhopanes the Santa Barbara samples have been heavily biodegradation (rank 6) based on the biodegradation rank of Peters and Moldowan (1993). The degree of biodegradation changed little over the sampled area within the sediment extract and the globules. This may indicate rapid replenishment of hydrocarbon material and possibly a high degree of biodegration within the reservoired oils feeding the seep.

Fluids in the Santa Barbara seep site are rich in hydrocarbons consistent with petroleum sourced from the Monterey formation. This correlates with other seep oils found up and down the West coast. The oils are severly biodegraded. Biodegradation may have occurred subsurface in reservoirs or migration conduits cool enough o support biodegradation. Distinguishing biodegradation in reservoirs versus that in the water column requires further investigation but identification of suites of sulfur containing compounds may hold the key

Gulf of Mexico Initial results suggest that the seep oils and underlying reservoir oils are identical in terms of source and maturity, based biomarker and aromatic hydrocarbon analyses. If this observation holds up to further scrutiny, then we will be able to use these seep oils as a proxie for the underlying oils. In contrast, the n- and branched alkanes are almost completely degraded in the seep oils.

The Gulf of Mexico oils appear to be much less extensively biodegraded than the Santa Barbara oils.

List of acronyms and abbreviations

C1-C3 light hydrocarbon methane, ethane, and propane having one to three carbon atoms
13C the isotope of carbon having an atomic weight of 13 mass units. Delta 13 C measurements are expressed as the enrichment of 13C versus 12C in comparison to a standard.
DoE Department of Energy
GC gas chromatography
2D GC See figure 8 - The separated material in the initially resolved individual GC peaks is subjected to a 2nd rapid GC analysis.
GC-IRMS gas chromatography-isotope ration mass spectroscopy
GC185 Green Canyon Block 185 in the Gulf of Mexico - location of seep site on August 2000 cruise
WHOI Woods Hole Oceanographic Institution
CH4 methane
m meters
METs Brand name for commercially available methane sensor
uM micromolar = micromoles of methane per liter of water
mM millimolar = thousandths of a mole per liter of water
ft feet
ppm parts per million
MIT Massachusetts Institute of Technology
Raman A technique utilizing the infrared absorption range to identify individual organic compounds
Coal Oil Point location of a persistent oil seep in shallow water in the Santa Barbara Channel
MS mass spectrometer

Appendices

I) Progress report submitted to NOAA on development of methane sensor

From: Jean Whelan, Woods Hole Oceanographic Institution

Date: September 23, 2003

Associates: John Pope, Well Dog Inc, Laramie, Wy

Mike Whiticar, University of Victoria, B.C., Canada

Background and Introduction

Gas hydrate deposits are thought to represent one of the largest carbon reservoirs on earth based on interpretations of seismic data (Kvenvolden, 1988, 1993). Understanding the biology and geochemistry as well as the geology of the seafloor surrounding gas hydrate deposits is crucial to understanding where and how these important deposits form as well as

how they might be exploited commercially. Biogeochemical processes strongly influence rates of both formation and destruction of hydrates (Grabowski et al., 2003).

Gas hydrate are commonly associated with seafloor methane gas venting. It is currently unclear how much of this methane comes from dissociation of the hydrate versus how much is flowing up from depth in a continuous steady state hydrate formation/destruction process.

The purpose of our research is to develop an oceanic in situ methane measurement device which can be used both for exploration and characterization of gas hydrate deposits. At the present time, no system exists which can continuously monitor methane over the very wide dynamic range encountered around ocean floor methane vent features. Existing technologies are ill suited to sense and monitor methane dissolved in waters around these vent features.

In this work, we proposed to build a dual detection methane sensing system utilizing a Raman spectrometer for monitoring higher methane concentrations near the venting plume (micromolar to millimolar methane concentrations) and a CAPSUMs METS sensor for the lower methane concentrations further away from the plume. The original concept was that the Raman spectrometer would be used to protect the METS sensor from over saturation by triggering a shut off of the METS detector window whenever high methane concentrations are encountered.

Progress to date

The technical data needed to address the scientific problem above are: How methane much and where is methane associated with gas hydrates venting from bottom seeps into the water column? How fast is the venting? What are the temporal and spatial variabilities of methane venting from ocean floor? Data in hand prior to this project show changes in methane concentration of several orders of magnitude (uM to nM) over small distances (a few meters) in the vicinity of gas hydrates and their associated gas seeps. These initial discrete methane measures showed the need for continuous in-situ profiling of methane by a technique having very large dynamic range and a relatively rapid response time (a few seconds). These constraints ruled out most common methane measurement techniques and required an instrument having a high sensitivity, wide dynamic range, and a rapid response time to handle large spatial and temporal variations expected during long or short time-series monitoring of seeps.

Our proposed solution was to combine a Raman sensor which has a wide dynamic range and rapid response time, but low sensitivity (10s of uM) with a METS sensor, a commercially available detector utilizing membrane absorption and chemical reaction of methane. Previous researchers have found this instrument to have a low dynamic range and sluggish response time (minutes) but high sensitivity (nM). Raman spectroscopy meets all technical requirements except for sensitivity (existing Welldog instrument: about 100 uM; estimated that this can be increased to 100nM or better with more sophisticated spectrometer)

The commercially available (METS) sensor has smaller dynamic range, but theoretically higher sensitivity. Based on previous work with an instrument borrowed from Bob Lamontagne and co-workers at the Naval Research Laboratory, the METS sensor detects low methane concentrations (nM to uM) but oversaturates and becomes inoperaable at higher methane concentrations. This process is reversible by bringing the METs back on deck and flushing the membrane with nitrogen. Thus, the METs insrument appeared to have a number of limitations for our work. In addition, no reliable laboratory or field calibrations of the instrument were available at the time our work started.

The first task in this project has been to evaluate and test both the Raman and METs sensors in our laboratories to determine for ourselves their suitablity for this project. Our progress to date shows that:

1) The Raman detector looks very promising and may be much more sensitive that we originally anticipated and

2) The METs sensor doesn't look very promising in work so far.

Progress on Raman Spectometer Initial tests with the existing Welldog instrument indicated that an upgraded Raman may be much more sensitive than we originally predicted and may ultimately produce usable methane signals for concentrations as low as 10s to 100s of nM, or almost open ocean background methane levels. The results shown in Figs 1-5 were all carried out on the existing Welldog instrument which is much less sensitive than our upgraded spectrometer will be. Figures 1-3 shows laboratory data for methane dissolved in seawater. Figures 1 shows the methane signal in water and how it responds to progressively lower methane concentrations. Figure 2 shows that the response of the instrument is very linear over a wide concentration range. Comparison of Figures 3 and 4 suggest that it may be possible to utilize the second derivative of the Raman methane signal to minimize the problem of overlap between the methane and the much stronger water peaks which is apparent in Fig 3.

Work has started on the upgraded Raman spectrometer, but has been delayed because the initial instrument had to be returned to the manufacturer because it did not meet the contracted specifications. A new instrument has been ordered. It is expected that the new upgraded (more sensitive) instrument will be ready for its first (shallow water) oceanic tests in Saanich Inlet, B.C. in Nov (water depth: 300 m). On that cruise, we plan to compare in situ methane measurements from the Raman with laboratory measurements on discrete water samples from the same zone.

An ancillary benefit of using the Raman spectrometer in this project is its potential ability to detect and measure other seep-related organic compounds along with methane possibly including: dimethylsulfide, higher alkanes and aromatic hydrocarbons, alcohols, carboxylic acids, amines, carbon dioxide, etc. Some examples from laboratory analyses to date are shown in Fig 5

Progress on METs sensor Initial tests of the Naval Research laboratory METs sensor at the University of Victoria by Mike Whiticar and co-workers have not been promising. The METs detects small concentrations of methane. However, there there is little correspondence between the METs readings and the actual concentrations. Also, the recovery of the sensor after introduction of methane is very slow - it took 80 minutes for methane to flush from the membrane in one test.

However, the scientists associated with the French company which makes the instrument believes that these problems are caused by our use of an older instrument. Therefore, Michell Mason, president of the company builds and sells the METS, is traveling to the University of Victory to work with Mike Whiticar on deploying the newer version of the instrument on gas seeps around Vancouver Isand within the next few months. Dr Mason's time and the instrument are donated for this test; we are allocating NOAA funds for reimbursement for his travel.

Exploration of other possibilities - Mass Spectroscopy In the meantime, Jean Whelan and Mike Whiticar are also exploring the feasibility of using an underwater mass spectrometer as an in situ methane sensor. Recent conversations with scientists at both the University of South Florida (Bob Byrne) and at MIT (Rich Camilli) indicate that the underwater mass spectrometer part of such an instrument is already technologically possible. Both groups have carried out successful intial tests of various types of spectrometers and obtained in situ measurements of pollutant organics in shallow waters (aromatic compounds). Some very preliminary work was also carried out on fixed and hydrocarbon gas analysis in coastal waters to maximum depths of about 100ft.

Discussions to date indicate that the main technological problem to going deeper is designing a suitable inlet system. Rich Camilli who built the MIT underwater spectrometer as part of his doctoral thesis is currently applying for a Postdoctoral Scholar award at Woods Hole. If he is successful, he will go to work building a new instrument suitable for deeper water work.

Jean Whelan and Mike Whiticar are currently seeking funding from the NOAA Ocean Exploration program to support the needed instrument parts for this project.

Future plans:

A proposal has just been submitted to the DoE gas hydrate program through the University of Mississippi to install in situ water column geochemical methane and CTD sensors on the seafloor northern Gulf of Mexico. Seafloor fluid and gas venting associated with surface and subsurface gas hydrates will be monitored as part of the Gulf of Mexico Research Consortium to use the combined geophysical and geochemical data from the monitoring station are to determine processes controlling hydrate growth and dissociation.

The Woods Hole part of the project is to measure continuous in situ bottom water geochemical data (in situ methane and CTD measurements of salinity, temperature, pressure, fluorescence, and turbidity) to look for changes associated with the gas hydrate. Our overall approach utilizes the observation that most gas hydrates in the Gulf of Mexico and in many other areas world wide are also associated with significant upward gas flow though faults and fractures into overlying sediments, waters, and possibly the atmosphere (e.g., Brooks et al, 1987, Roberts and Carney, 1997, Whelan et al 1998; Kvenvolden and Lorenson, 2001, and Sassen et al, 2001,).

Two different hypotheses currently exist for the origin of this seeping gas:

1) the gas comes from a deeper source, either thermogenic or biogenic, and forms a hydrate deposit whenever high enough pressures and low enough temperatures are present for hydrate formation to occur. In this scenario, the hydrate is viewed as a capacitor in a very dynamic methane flow system (Zatsepina, et al, 1997; Dickens, et al, 1997; Sassen et al, 2001; and Cathles et al, 2002;

2) methane to form hydrates is derived from upward diffusion of local in-situ sediment sources of biogenic methane produced by anaerobic methanogenic bacteria so that hydrate amounts and lifetimes of the methane hydrate deposit can be estimated from in situ porewater profiles of methane and sulfate (as being done by I. MacDonald and M. Kastner in this research using procedures of Xu and Ruppel, 1999, Ruppel, 2000, and Valentine et al., 2001).

In scenario 2, the hydrate and associated seeping gas are primarily a function of the relative rates of hydrate replenishment via upward methane diffusion from the sediments below and hydrate decomposition due to interactions with warmer water column temperatures above . Recent temperature data from the MacDonald/Kastner group on several Gulf of Mexico surface gas hydrate deposits is consistent with scenario 2, but does not explain the vigorous gas evolution through fractures in the hydrates which is commonly observed around these deposits. Furthermore, recent modeling of the GC185 hydrate deposit by Cathles and co-workers at Cornell, based on a thermogenic gas source from underlying sediments, indicates that only 10 percent of the upward flowing gas is trapped in the hydrate while 90 percent is vented to the overlying water column and the atmosphere.

These two scenarios of methane hydrate formation and maintenance are very different; knowing which is correct significantly impacts the amount and concentration of methane ultimately recoverable from any particular hydrate deposit. In the overall DoE UMiss research program, both scenarios are being investigated: scenario 2 by the MacDonald/Kastner group and Scenario 1 by the Whelan/Chanton group. Although more research is needed, our previous work strongly suggests much more heterogeneous and pervasive upward gas flow in the Gulf of Mexico than is available from only the diffusive methane flow (Whelan, 1997, Whelan et al, 1998; Sassen et al. 2001, Cathles, et al., 2002 ; Roberts and Carney, 1997). The seafloor proposed geochemical monitoring combined with the geophysics would provide the quantitative geochemical data needed to distinguish the two scenarios and could be used

together with the geophysical data to provide a general method for using surface data for detection and characterization underlying gas hydrate deposits.

References

Brooks, J.M., M.C. Kennicutt II, C.R. Fisher, S.A. Macko, K. Cole, J.J. Childress, R.R. Bidegare, and R.D. Vetter (1987) Deep-sea hydrocarbon seep communities: Evidence for energy and nutritional carbon sources, Science, v. 238, pp 1138-1142.

Cathles, L.M.; Dofu, C.; Roberts, H.H. (2002) Estimation of the hydrate gas content of the Bush Hill vent site, Green Canyon Block 185, Gulf of Mexico, (abstract) AAPG Bull, abstracts of annual meeting in Houston, Tx, March 2002, AAPG Bull, vol. 86.

Dickens, G.R., Castillo, M.M., and Walker. J.C.G., 1997, A blast of gas in the latest Paleocene: simulating first-order effects of massive dissociation of oceanic methane hydrate, *Geology, 25*:259-262

Grabowski, K., R. Rogers, J.Chanton, J.Whelan, P. Sobecky, 2002. Summary Report - Session II, Biological Influence on Hydrate Formation Stability, Content and Lattice Saturation. International Gas Hydrate Meeting, Washington, DC, November 2002

Kvenvolden, K.A. (1988) Methane hydrate - a major reservoir of carbon in the shallow geosphere? Chem Geol., v.71, pp 41-51.

Kvenvolden, K.A. (1993) Gas Hydrates-Geological perspective and global change. Reviews of Geophysics, v.31, pp 173-187.

Kvenvolden, K.A. and T.D. Lorenson (2001) Attention Turns to Naturally Occurring Methane Seepage (2001), EoS, v. 82, No. 4, p.457

Roberts, H.H. and R.S. Carney (1997) Evidence of episodic fluid, gas, and sediment venting on the Northern Gulf of Mexico Continental Slope. Economic Geology.

Ruppel, Carolyn (2000) Natural gas hydrates in oceanic and permafrost environments, Kluwer Academic Publishers, pp .

Sassen, R., S. Losh, L. Cahtles, H. Roberts, J.K. Whelan, A.V. Milkov, S.T. Sweet, and D.A. deFreitas (2001). Massive vein-filling gas hydrate: Relation to ongoing gas migration from the deep subsurface in the Gulf of Mexico. *Marine and Petroleum Geology*, 18, 551-560.

Valentine, DL. , D.C. Blanton, W.S. Reeburgh and M. Kastner (2001) Water column methane oxidation adjacent to an area of active hydrate dissociation, Eel river Basin. Geochimica Et Cosmochimica Acta, 2001, V 65, N 16, pp. 2633-2640

Whelan, J.K. (1997) The dynamic migration hypothesis, How fast are oil & gas leaking to the ocean floor and replenishing themselves in some reservoirs? Sea Technology, v.38, pp 10-18, September, 1997.

Whelan, J.K., N. Mah, G. Eisheid, R. Chen, X. Wand, H. Roberts, and P Aharon, Gas and Oil Seepage and hydrothermal venting in the ocean bottom – detection by fluorescence. Proceedings of the Marine Technology Society Annual Conference, Nov. 1998, 7 pp:

Xu, W. and C. Ruppel (1999) Predicting the occurrence, distribution, and evolution of methane gas hydrate in porous marine sediments, J. Geophys Res, v.104, pp 5081-5095.

Zatsepina, Olga Y. and Buffett, Bruce A. (1997) Phase equilibrium of gas hydrate; implications for the formation of hydrate in the deep-sea floor, Geophysical Research Letters, v. 24, pp 1567-1570

Figures

Figure 1: Spectrum of methane dissolved in water on WellDog's current Raman spectrometer

Figure 2: Dissolved Methane Calibration in Seawater, Existing Welldog Raman spectrometer

Figure 3: Raman spectra - methane CH stretch used for quantitation and water bands.

Figure 4: Use of 2nd derivative of C-H stretch to increase Raman instrument sensitivity for measurement of methane dissolved in water

Figure 5a: Examples of other chemicals which have been identified and measured with Raman in the laboratory with existing spectrometer

Figure 5b: Raman signature for methanol

Figure 1: Spectrum of methane dissolved in water on WellDog's current Raman spectrometer

Calibration spectra for WellDogÕs RA-1 spectrometer

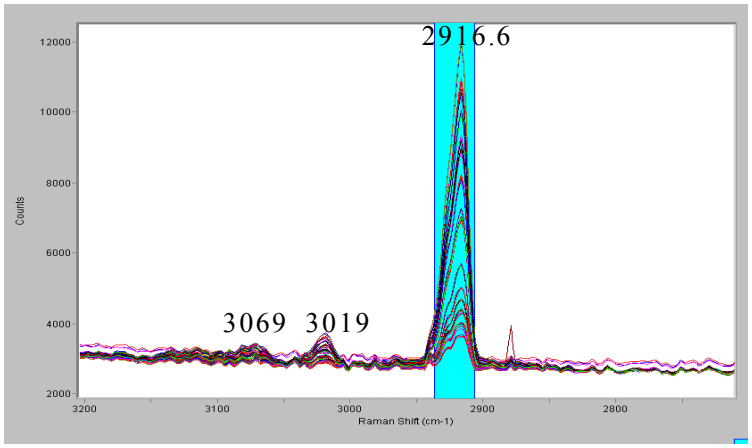

WellDog Inc.

Methane dissolved in water. Each curve represents one measurement At a specific methane concentration.

Figure 2: Dissolved Methane Calibration in Seawater,
Existing Welldog Raman spectrometer

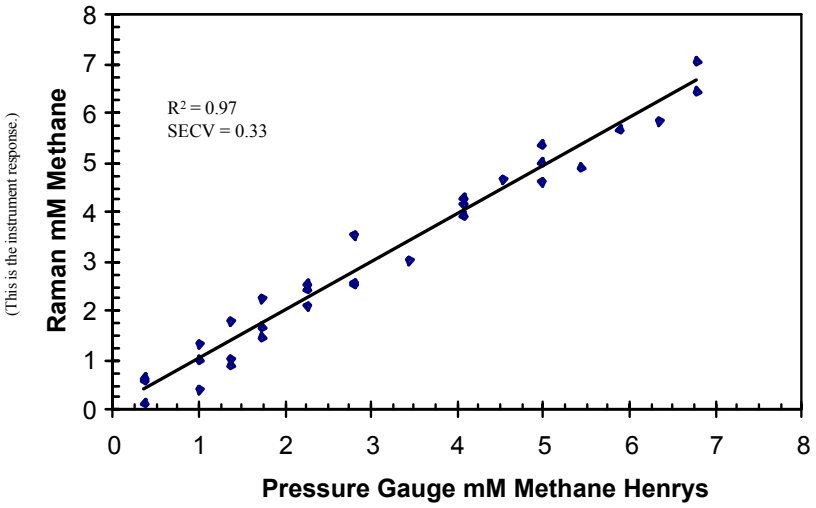

(This is the concentration of methane in the water as determined by the pressure gauge reading and HenryÕs law.)

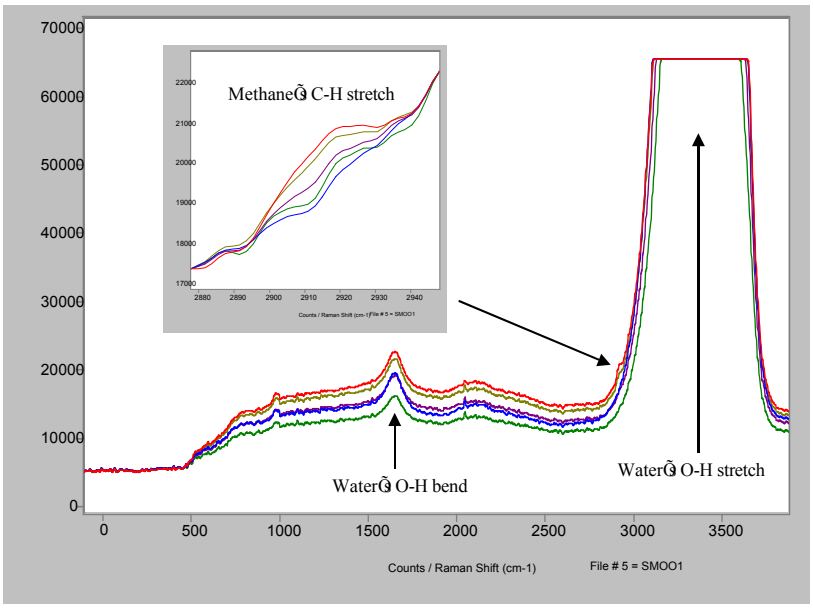

Figure 3: Raman spectra - methane CH stretch used for quantitation and water bands.

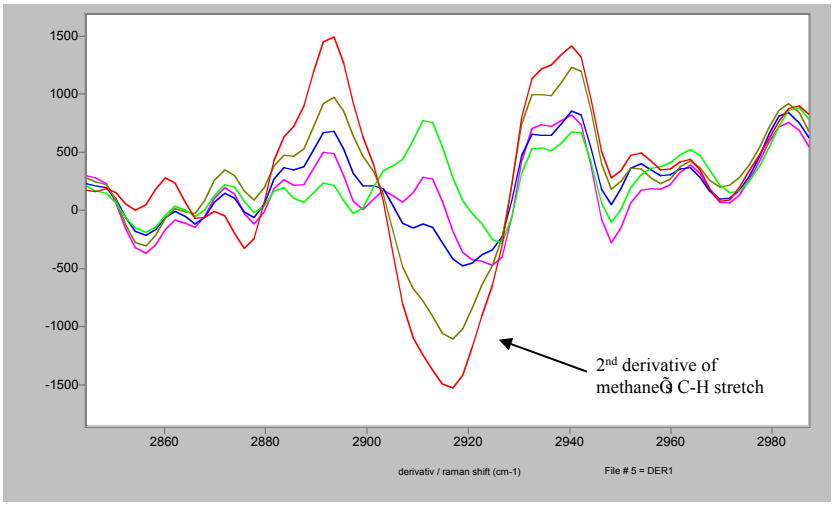

Figure 4: Use of 2nd derivative of C-H stretch to increase Raman instrument sensitivity for measurement of methane dissolved in water

Figure 5a: Examples of other chemicals which have been identified and measured with Raman in the laboratory with existing spectrometer

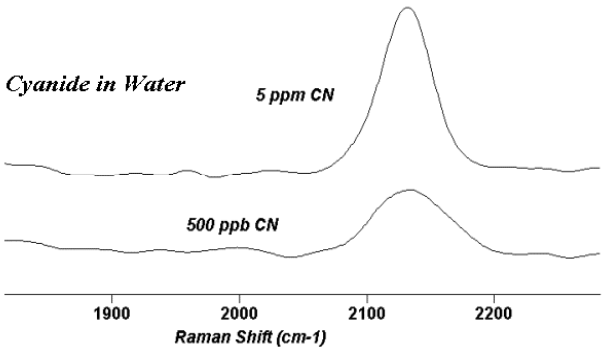

Figure 5b: Raman signature for methanol

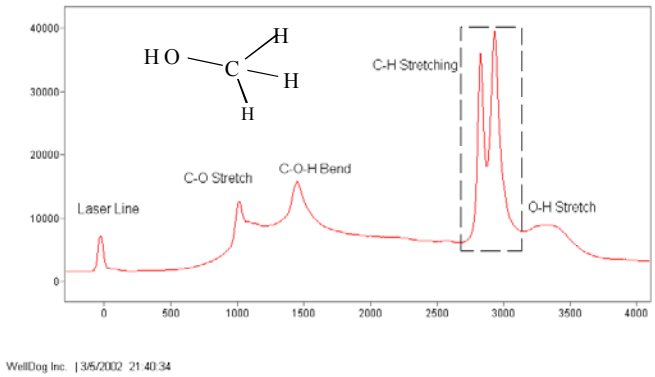

Appendix II: Proposal submitted to Woods Hole Oceanographic Institution for Green Technology Award (funded).

A Deep Diving Mass Spectrometer for Ocean Exploration of Gas Seeps and Pollution Monitoring

Abstract We propose to build and test an in-situ mass spectrometer suitable for continuous monitoring of methane, gases, and low molecular weight organic compounds including pollutants in the ocean and which can operate to at least several hundred meters water depth. This instrument is intended to be a prototype for a future instrument capable of operation at all ocean depths. The scientific motivation for this project is development of a sensitive and versatile in situ monitoring instrument for gases and volatile organic compounds vented from oceanic "cold" seeps associated with methane hydrate deposits. The resulting data will be used along with geophysical data to distinguish between two different models of methane hydrate formation and maintenance - a "stable methane hydrate" model where the hydrate deposit has a relatively long lifetime versus a "steady state" model where methane is continuously streaming upward to form the bottom and is continuously being lost from the top of the hydrate deposit. The mass spectrometer will also serve as an exploration tool for exploration for new thermal and biogenic methane gas seeps in the oceean floor. These can be associated with hydrothermal vent sites and areas of discharge of land-based run-off as well as cold seeps. In situ mass spectrometry would compliment data from our in situ Raman spectrometer (currently being built with NOAA funding-University of Mississippi funding) in characterization of the fluid discharge from all three types of ocean floor vent sites. Alternatively the instrument can be used in shallower waters to unobtrusively monitor a variety of organic compounds in coastal

waters impacted by urban runoff, shipping lanes, and point sources of ground water discharge to the ocean.

Description We propose to develop and deploy a versatile and rugged submersible mass spectrometer, for operation aboard a variety of oceanographic platforms. This new analytical instrument will be capable of real-time, continuous, in-situ, high-resolution measurements of dissolved gases, particularly methane, and volatile organic compounds in the ocean and will be able to operate to at least several hundred meters water depth. Funds from this project will be used as seed money to develop a similar deep water instrument for operation to full ocean depths.

In our laboratory, the instrument will be used to find and monitor methane seeps associated with ocean floor gas hydrate deposits. An abundance of recent evidence has shown that methane venting through small faults and fractures in the seafloor occurs in many locations worldwide and is important to the biology, chemistry, and geology of the ocean. Also, methane is a greenhouse gas. Even though the seafloor gas venting occurs primarily through localized fractures, the volume of methane involved may be substantial enough to contribute to global warming. However, no systematic exploration strategy currently exists for finding these generally very localized methane vents on the ocean floor. Furthermore, it is difficult to obtain reliable measurements of the gas concentrations or fluxes involved because venting tends to be very heterogenous and episodic. Methane concentrations commonly vary over several orders of magnitude within a few meters of the vent; reliable data on amounts as well as molecular and isotopic compositions involved cannot be obtained on samples brought to the surface and allowed to degas (Fig 1). Therefore, it is currently almost impossible to measure quantitatively how the venting methane interacts with the complex biological communities, gas hydrates, and bubble streams flowing around and through the hydrates.

The underwater mass spectrometer will be capable of monitoring oceanic in situ concentrations of both the high methane concentrations near venting plumes (micromolar to tens of millimolar methane concentration) to the lower methane concentrations (as little as 0.01 to 0.02 uM) typically found in moving away even a few meters away from the plume. The high sensitivity is important for finding new vents and monitoring the effects of methane in moving away from the vent site. This work will compliment that currently in progress under a NOAA funded project to build an underwater Raman spectrometer. Laboratory and pressure tank tests so far have shown the Raman instrument to be suitable for the higher but not the lower methane concentrations found at hydrate associated vents. Additional work on this NOAA project has conclusively shown that the commercially available METS sensor possesses a number of technical problems making it unsuitable for this work.

Mass spectrometry is by far the most sensitive and versatile analytical technique available for identifying and quantifying a large variety of organic compounds likely to be found in the ocean in various settings. For some compounds, such as aromatic hydrocarbons typical of petroleum seeps and low molecular weight functionalized organics typical of various types of microorganisms (e.g. methane, acetic acid, carbon dioxide, hydrogen sulfide and alkyl sulfides from anaerobic bacteria in sediments), organic signatures are very diagnostic of the type of chemosynthetic organisms supported by these ocean floor seeps. These ocean floor gas and liquid venting sites have been described in many areas around the world in a number of deep sea environments for which this mass spectrometer is intended, including 1) natural gas and oil seeps ("cold seeps"); 2) hydrothermal vent sites; and 3) areas of discharge of land-based run-off.

Despite the advantages of in-situ mass spectrometry, to date only two submersible mass spectrometer designs have been deployed which are limited to operational depths of less that tens of meters. One of these was designed and built by Rich Camilli who will be involved in this project (Fig 2). Our instrument is intended to be compact and fully self-contained, permitting

continuous in situ measurements aboard platforms including ship-borne rosettes, ROVs such as the Jason vehicle, and various AUVs. It will function as a low power, ruggedized system that can be deployed in harsh environments with a mass range from 1-300AMU, sensitivity of 10-100 ppb for most volatile chemicals, and a time response on the order of tens of seconds.

The two most challenging aspects of long-term underwater mass spectrometry are: 1)vacuum maintenance and 2) sample introduction. To overcome the limited duration and excessive power consumption of standard ultra-high vacuum pumping strategies, while at the same time avoiding the instability of ion pumps [9], we propose to use a miniaturized molecular drag pump in parallel with an ion pump. Initial calculations indicate that this approach will yield a pumping velocity of approximately 40 l/s while requiring approximately 15 watts and will probably greatly extend service intervals between ion pump repair and replacement.

The ultimate limiting factor for sending submersible mass spectrometers to full ocean depths is designing a viable inlet system with the required mechanical strength. The analyte introduction system must be exposed to the ambient hydrostatic pressure in order to allow dissolved substances into the analyzer while simultaneously excluding water in order to preserve the near-perfect vacuum within the analyzer region of the instrument. The instrument will be incorporated within a standard cylindrical metal pressure housing and initially a membrane inlet developed specifically for deep deployment. Calculations indicate that this inlet will permit operation to at least several hundred meters depth, thus enabling investigation of many previously inaccessible environments. We will also explore the possibility of incorporating a capillary inlet which would allow operation to much greater depth.

The computational architecture will utilize a low power, small form factor, PC-104 or μ-controller based embedded computer allowing for real-time data processing. Electronic drift must be minimized for operation over extended timeframes. Furthermore, because the instrument must operate within a dynamic and oftentimes noisy environment, noise filtering techniques need to be incorporated to improve signal to noise ratio. Therefore, a suite of hardware and digital signal processing techniques will be implemented to improve signal quality, including: baseline identification to compensate for electronic artifacts such as detector signal DC offset and baseline drift, bandpass filtering, signal averaging and median filtering to minimize the effects of internal electronic interference, and microphonic vibrational noise.

We intend for the design to be extremely durable, with service intervals on the scale of weeks to months. A modular design will allow for periodic maintenance and component upgrade. For example, the initial analyzer design is a quadrupole type, but can be replaced by more advanced analyzers (i.e. miniature ion trap) as technology progresses. Likewise, variations of the initial inlet system and the embedded computer system will be developed to optimize instrument performance and to make possible real-time autonomous data analysis and adaptive sampling and mapping (5) based on real-time environmental conditions. Adaptive sampling would allow, for example, sample rate to increase whenever high methane concentration gradients were observed. This will require the creation of a type of expert system intelligence that allows the instrument to identify individual ion peaks and to vary its sampling interval in real-time, according to the rate of change of ion signatures; thus helping to avoid the aliasing sometimes associated with uniform temporal or spatial sampling.

Plans for initial deployment: An initial series of deployments are planned for the instrument in areas of known shallow methane seeps (less than 100m), off the coast of British Colombia Canada. These cruises will be conducted in partnership with the Dr Michael Whiticar of University of Victoria in parallel with shipboard methane measurements using standard surface gas stripping and gas chromatograpic procedures. This water column methane data will also be used to calibrate and test the in situ Raman Spectrometer. As development continues, the instrument can be tested in the same way over a deeper water gas hydrate zone (up to 3000m) in the same area and with the same group in cruises to the Cascadia Margin off Oregon and over gas hydrate and seep zones in the Gulf of Mexico which we are currently studying as

part of a collaborative DoE-UMiss funded project to set up one or more Gulf of Mexico gas hydrate monitoring stations.

Plans for seeking future funding and and to leverage these funds. The Green Technology award would be used primarily to pay for instrument parts and to allow Dr Rich Camilli to rapidly begin building the mass spectrometer. Rich, a recent MIT graduate of the Joint Program, is ready to begin building this instrument as a postdoctoral investigator as soon as funding becomes available. His Ph.D. thesis involved building one of the two existing underwater mass spectrometers. He has already written much of the text for this proposal and for a successful NOAA preproposal to the Ocean Exploration Program. Rich has already written much of the text for the full NOAA proposal which will be submitted later this month. All of this work has been carried out along with dealing with a very serious family medical problem in New York. If funded, the full proposal to the NOAA Ocean Exploration program would provide salary support for Rich to come to Woods Hole as a Postdoctoral Investigator. He is also applying for a WHOI Postdoctoral Scholar award.

Additional funds to extend this work to a system capable of operating at all ocean depths will be sought through the NSF Ocean Technology Program which helped to fund a very successful workshop entitled: "The Next Generation of in situ Biological and Chemical Sensors in the Ocean" at Woods Hole last summer. Several working groups at that workshop indicated the urgent need for an in situ oceanic mass spectrometer. The Green Technology Award funds will also provide a match for the on-going Woods Hole funding from the DoE-Univ of Miss-Woods Hole grant to install the Gulf of Mexico gas hydrate monitoring station.

References

5. Smith, C.M., et al. *Feature-based concurrent mapping and localization for autonomous underwater vehicles*. in *Proceedings of IEEE Oceans*. 1997.
6. Delaney, J.R. and A.D. Chave, *NEPTUNE: A fiber-optic 'telescope' to inner space.* Oceanus, 2000. **42**(1): p. 10-11.
7. Short, R.T., et al., *Underwater mass spectrometers for in situ chemical analysis of the hydrosphere.* Journal of the American Society for Mass Spectrometry, 2001. **12**(6): p. 676-682.
8. Camilli, R., *Thesis: Creation and Deployment of the NEREUS Autonomous Underwater Chemical Analyzer and Kemonaut, an Odyssey Class Submarine*, in *Department of Civil and Environmental Engineering*. 2003, Massachusetts Institute of Technology: Cambridge. p. 314.
9. Varian, *Ion Pumps- vacuum products from Varian*. 2001.

Appendix III) Report: Hydrocarbon distributions from extant petroleum seep sites and associated gas hydrate deposits in sea water and ocean floor sediments from Santa Barbara and Gulf of Mexico, Jean K. Whelan and Lorraine B. Eglinton

Experimental

From the Gulf of Mexico, sediment and hydrate seep oils were analyzed together with two sea water samples from the Gulf of Mexico Dive (4208) over a gas hydate ice core , as shown in Figs 1-8.. A number of water samples were also collected which showed no discernable hydrocarbon signal and so are not discussed further. From the Santa Barbara Coal Oil point seep oils, three sediment samples and three water samples containing oil globules were analysed.

Initial screening of the Santa Barbara oil globules was performed on a approximately 10 mg of oil that was separated from the aqueous sample. Total soluble hydrocarbons were extracted by dissolution in 3 sequential 10 mL aliquots of dichloromethane. Extracts were reduced by rotary evaporation and further reduced in a stream of nitrogen. The concentrate was transferred with DCM to 150 l glass inserts and followed by gentle evaporated in a stream of nitrogen to near dryness. The fractions were diluted with 100 l DCM and the insert was placed into 1.5 ml autosampler vial capped and submitted for analysis.

Santa Barbara and Gulf of Mexico seawater samples were extracted using conventional liquid/liquid extraction techniques on 2 L using 3 X 200 mL Dichloromethane. Samples were concentrated by rotary evaporation. Removal of residual water was performed by passing the samples over sodium sulfate. Final concentration was conducted in a stream of nitrogen.

Quantitative analysis of the Santa Barbara sediment samples was performed on a 10 g aliquot of homogenized wet sample, spiked with a recovery standard (d_{50} *n*-tetracosane and d_{12} 2,6-dimethylnaphthalene), was soxhlet extracted for 48 hours in tandem with a spiked blank. Solvent soluble hydrocarbons were fractioned from the wet sediment using 150 mL of an azeotrophic mixture of dichloromethane/methanol (93:7 ‰). The total extracts were reduced by rotary evaporation. The extracts were transferred to 4 mL vials. Total extracts were run through a sodium sulfate funnel for removal of residual water and an activated copper column for removal of elemental sulfur. Micro column chromatography, using 90% activated silica gel, was used to fractionate the extracts in to saturated and aromatic hydrocarbon pools. The fractions were concentrated using rotary evaporation. The concentrate was transferred with DCM to 150 l glass inserts and followed by gentle evaporated in a stream of nitrogen to near dryness. The fractions were diluted with 100 l DCM and the insert was placed into 1.5 ml autosampler vial and submitted for analysis.

Biological marker distributions were obtained using gas chromatography coupled with mass specific detection using the saturated hydrocarbon fraction. A Hewlett Packard (HP) 6890 gas chromatograph fitted with a Restek® DB-5 MS 60 m glass capillary column and connected directly to a HP 5693 mass specific detector was used. After cool on-column injection the gas chromatograph was programmed from 50ºC to 325ºC at a rate of 4ºC/min and held at 325ºC for 20 mins. The mass spectrometer was operated at 70 eV in selected ion monitoring mode. A total of 30 ions characteristics of *n*-alkane, sterane, terpane, aromatic steroid, aromatic hydrocarbons. Full mass spectra (50 – 550 amu) were recorded on the saturated fraction to identify less common biological markers. Compounds were identified by their key fragmentograms based on relative retention times and comparison with published data (*e.g.* Mackenzie 1980, 1981).

Results summary

Seawater

Hydrocarbons in seawater samples were below sensitivity levels except for one Gulf of Mexico sample where trace amounts of mono-aromatic steroids could be seen. Future extraction directly onto a solid phase extraction cartridge of several liters of water might improve resolution.

Sediment extract yields

Santa Barbara Hydrocarbon yields from Soxhlet extracted sediment at the Santa Barbara seep site is 363 mgHC/gdrySed. This decreases to 53 mgHC/gdrySed within a short distance (10 m) away from the seep (not shown). This indicates that hydrocarbons may be washed away from the seep site by ocean currents and gas bubbles and/or the seep site is constrained to a somewhat tight fissure. Similar procedure were used for the Gulf of Mexico sediments affected by oil seepage

Aliphatic (C_{15} +) hydrocarbons and isoprenoids

Santa Barbara The Total ion current (Fig. 11) shows an unresolved complex envelope of hydrocarbons with some partially resolved lighter weight hydrocarbons but no resolvable C_{15} + *n*-alkanes. There are relatively minor amounts of resolved peaks from the TIC from the sample analyzed in scan mode. Even when a diagnostic fragment ion (m/z 57) for *n*-alkanes is extracted the samples are devoid of straight chain saturated hydrocarbons. The isoprenoids pristane and phytane are also absent. The lack of *n*-alkanes and the isoprenoids indicates biodegradation has progressed to at least moderate to heavy based on the biodegradation ranking of Peters and Moldowan (1993). The total ion current from the same seep site sample analyzed in SIM mode is dominated by tri- and monoaromatics steroids and hopanes and dibenzothiophenic compounds (Fig. 16).

Gulf of Mexico sites GC 184 & 234

Similar results were obtained for Gulf of Mexico surface seep oils (Figs 1-3) except that more resolvable GC peaks appear to be present suggesting a lower degree of biodegradation.

Hopanes

Santa Barbara Hopane distributions are similar for the three Santa Barbara samples but show a decrease in abundance with distance from the seep vent. A typical m/z 191 fragmentogram for hopanes is shown in Figure 12. The dominant peak in this fragmentogram is the C_{29} ββ hopane. In unaltered oils the C_{30} ββ hopane is usually prominent. Another unusual feature is the elevated abundances of C_{28} and C_{29} and other tricyclic hydrocarbons together with high abundances of gammacerane and the presence of oleanane. There is also increased amounts of 28,30 bisnorhopane. 25,28,30-trisnorhopane is also observed. This biomarker has been observed in highly anoxic, mostly marine sediments globally (e.g., Grantham et al., 1980; Mello et al., 1988; Requejo et al., 1994). Literature searches indicate that elevated C_{28} and C_{29} tricyclic terpanes is a feature of Californian oils ranging from Coal Oil Point seeps to Santa Cruz seeps and the Guaymas basin (this study, Kvenvolden et al.; Simoniet et al.,) indicating a

common source. Although still open to interpretation, gammacerane in high concentration is often associated with hypersaline depositional conditions (ten Haven et al., 1988; 1989).

The presence of gammacerane, oleanane, elevated 28, 30 bisnorhopane, abundance of sulfur derived hydrocarbons and elevated tricyclic terpanes indicate a source consitstent with those of the Miocene Monterey formation based on published fragmentograms (Peters and Moldowan, 1993). A high abundance of 28,30 bisnorhopane is thought to be due to bacterial mats present in the Monterey formation. The fossilized *Thioploca* bacterial mats may represent a possible source according to Katz and Elrod (1983).

Trace abundances of 2□(CH_3)-hopanes and 3□(CH_3)-hopanes have been tentatively identified from the m/z 205 from the seep site. Although methylhopanes can derive from a variety of prokaryokes Summons et al., (1996) and Collister et al., 1992 suggest the presence of cyanobacteria and or methylotrophic bacteria to account for homologous series of 2□and 3□methylhopanes respectively.

Gulf of Mexico The GCMS mass scans for the hopane biomarkers in the GC234 sediment seep samples are shown in Fig 5. The pattern is almost idential to that found previously for the subsurface GC184 oils, suggesting that biodegradation has affected this fraction only slightly, if at all.

Steranes and aromatic steroids

Santa Barbara Steranes in the Santa Barbara Seep sediment samples have been affected by biodegradation and do not exhibit a distribution normal to reservoired unaltered petroleum. The high abundance of Mono- and triaromatic steroids indicate conversion of steranes due to thermal maturity and resistance to biodegradation processes (Fig 13). Monoaromatic steroids were also found in trace abundances in a water sample from the Gulf of Mexico.

Gulf of Mexico The normal and aromatic sterane mass scans for the GC 234 seep and hydrate oils are shown in Figs 4 and 6 respectively and are very similar to those of the underlying reservoir oils, consistent with a low degree of biodegradation of this fraction.

Aromatic hydrocarbons

Gulf of Mexico All of the aromatic hydrocarbon data is available for Gulf of Mexico seep and hydrate melt water oils. For comparison, extensive set of similar data have been measured for all of the underlying Green Canyon oils as part of a previous project.

Santa Barbara In spite of the high degree of biodegradation, the methyl phenanthrenes are well resolved and should provide a reliable maturation markers for these biodegraded oils. A summary of the various classes of compounds analyzed to date is given below.

<u>Methylphenanthrene</u>

Calculated vitrinite reflectance based on methylphenahtrene index 1 (Radke 19) indicates a fluid maturity of around R_c 1.00 %. Thus, these seep oils are

<u>Naphthalenes</u>

The extracts are devoid of resolvable naphthalenes indicating removal by biodegradtaion.

Dibenzothiophene and methyldibenzothiophenes

m/z 184 and 198 diagnostic of dibenzothiophenes and methyl dibenzothiophenes are noisy. And contain abundant as yet unknown peaks. Based on the m/z 184 sulfur containing compounds are consumed at a faster rate since they are present in only trace abundance 10 m away from the seep site.

Biodegradation

Based on loss of *n*-alkanes, modification of steranes, an emerging series of 25-norhopanes the Santa Barbara samples have been heavily biodegradation (rank 6) based on the biodegradation rank of Peters and Moldowan (1993). The degree of biodegradation changed little over the sampled area within the sediment extract and the globules. This may indicate rapid replenishment of hydrocarbon material.

Conclusions to date

Fluids in the Santa Barbara seep site are rich in hydrocarbons consistent with petroleum sourced from the Monterey formation. This correlates with other seep oils found up and down the West coast. The oils are severly biodegraded. Biodegradation may have occurred subsurface in reservoirs or migration conduits cool enough o support biodegradation. Distinguishing biodegradation in reservoirs versus that in the water column requires further investigation but identification of suites of sulfur containing compounds may hold the key.

References:

Grantham , P.J., Posthuma, J., and DeGroot, K. (1980): Variation and significance of the C27 and C28 triterpane content of a North Sea core and various North Sea crude oils. In: Advanbces in organic geochemistry 1979 (A<G Douglas and J.R Maxwell, eds.) Pergamon Press New York P. 29-38

Mello , M. R., Telnaes, N Gaglionone, P.C, Chicarelli, M. I Brassell, S. C., and Maxwell, J. R (1988b): Organic geochemical characterization of depositional paleoenvironments in Brazilian Marginal basins. Organic Geochemistry, Vol. 13, p. 31-46.

A. G. Requejo[1], R. Sassen[1], M. C. Kennicutt II[1], I. Kvedchuk[2], T. McDonald[1], G. Denoux[1], P. Comet[1] and J. M. Brooks[1] Geochemistry of oils from the northern Timan-Pechora Basin, Russia Organic Geochemistry, Vol. 23 (3) (1995) pp. 205-222

Kvenvolden, K.A., Hostettler, F.D., Rosenbauer, R.W., Lorenson, T.D., Castle, W.T., Sugarman, S., 2002. Hydrocarbons in recent sediment of the Monterey Bay National Marine Sanctuary. Mar. Geol. 181, p.101-113.

Peters and Moldowan (1993): The Biomarker guide, Prentice Hall

ten Haven , De Leuww, J. W Sinninghe Damste, J.S. Schenck, P. A Palmer, S.E and Zumberge, J. E (1988): Application of biological markers in the recognition of

palaeohypersaline environments. IN: Lacustrine Petroleum Source Rocks (A.J. Fleet, K. Kelts and M. R. Talbot eds.) Geological Society Special Publication No 40, P.123-130

ten Haven, H. L., Rohmer, M. Rullkotter, J and Bisserret, P (1989): Tetrahymanol, the most likely precursor of gammacerane occurs ubiquitously in marine sediments. Geochimica et Cosmochimica Acta Vol 53., p. 3073-3079.

Collister , J. W. Summons, R.E Lichtfouse, E. L and Hayes J. M (1992): An isotopic bio-geochemical study of the Green River oil shale. Org. Geochem. 19, 265-276.

Figure 1: Biodegraded oil recovered from surface seep oil, Green Canyon 234, Gulf of Mexico

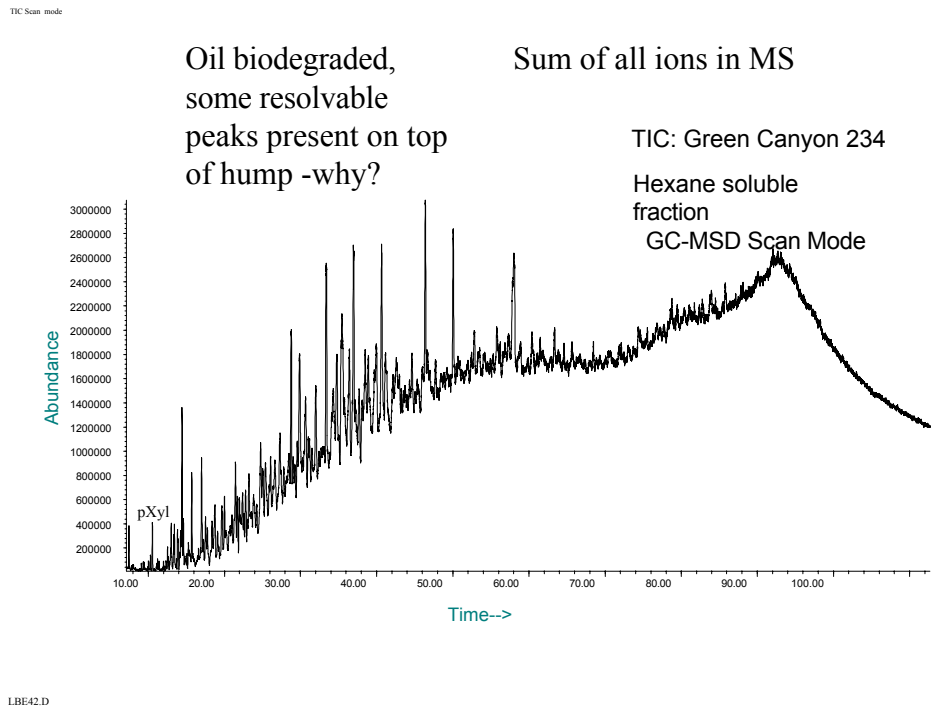

Figure 2: Same as Figure 1, hexane soluble fraction

TIC SIM mode

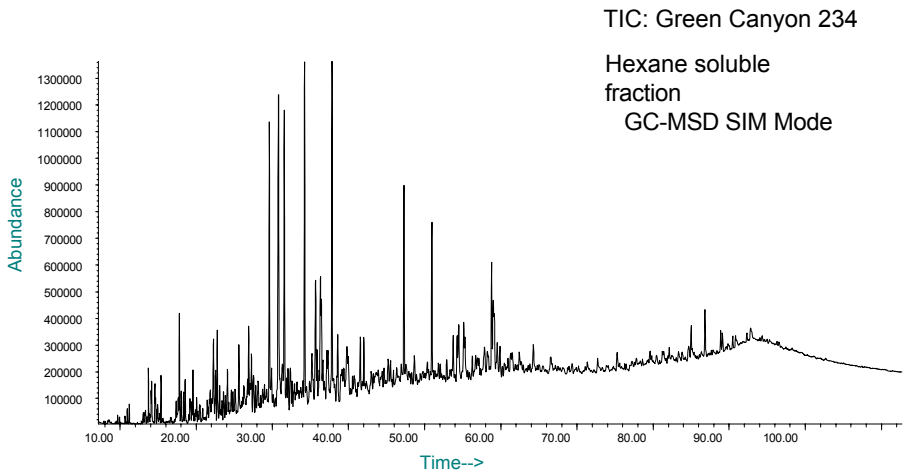

LBE48.D

Figure 3: Same as Figure 1, GCMS scan for alkanes only (mass 57)

57 n-alkanes SIM

Branched, cyclo, &n-alkanes - impies biodegradation hasn't progressed very far

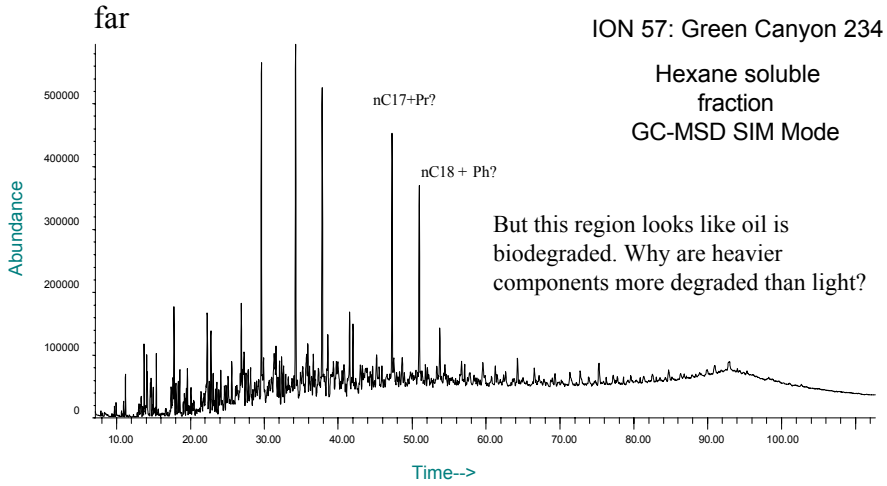

LBE48.D

Figure 4: Biomarkers, steranes, from GCMS - GC234 seep oil, hexane extract

Steranes

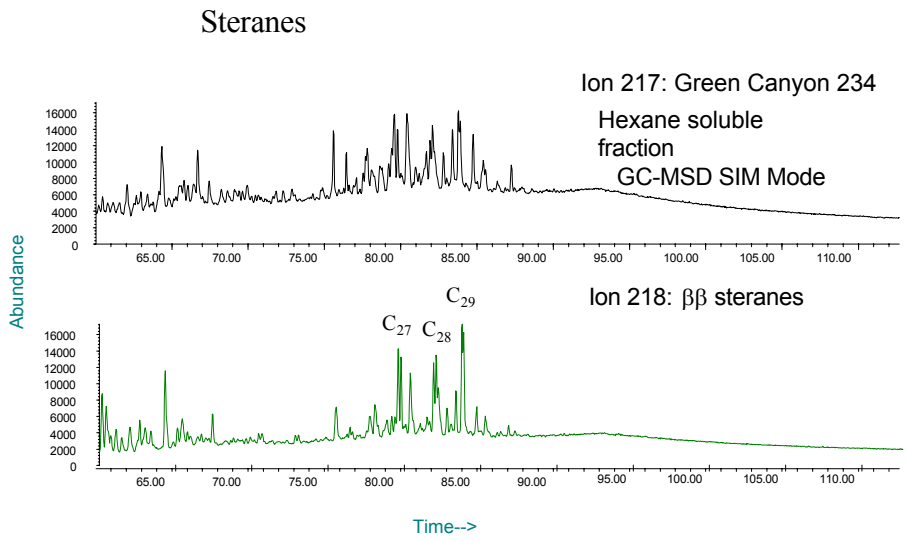

Figure 5: GCMS data, GC234 seep oil, mass scan showing hopanes in biodegraded seep oil

Triterpanes

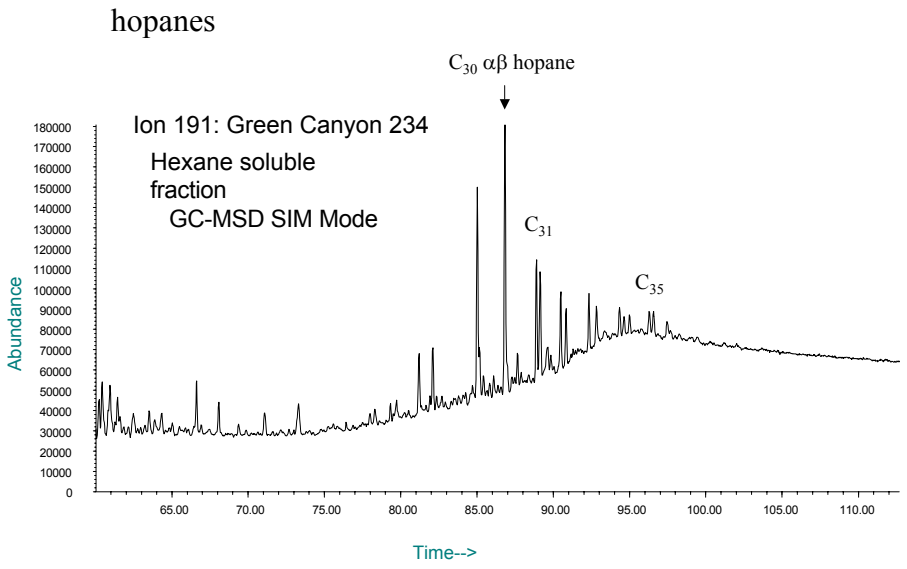

Figure 6: Same as Figure 4, aromatic steranes

Diasteranes

Aromatic Steranes

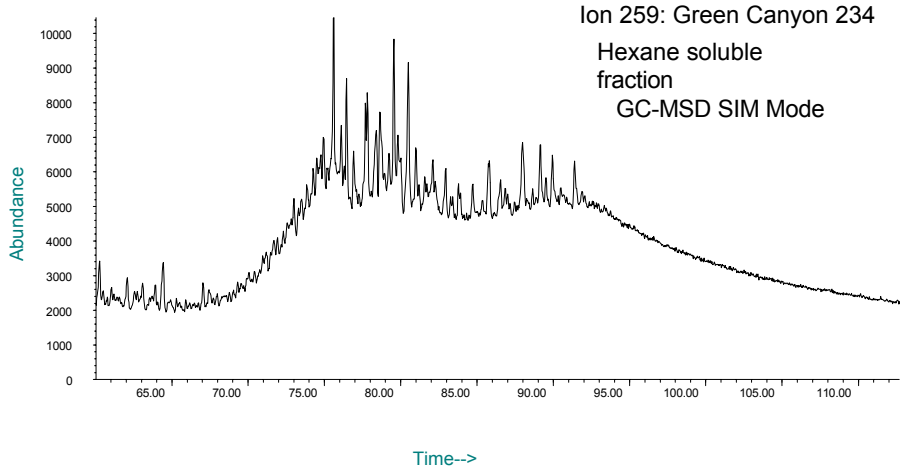

Conclude - Biodegradation not extensive enough to affect steranes and hopanes.

LBE48.D

Figure 7: Same as Figure 4, Sulfur containing aromatic compounds

Benzothiophene/C-4 alkylbenzenes

Sulfur containing aromatics

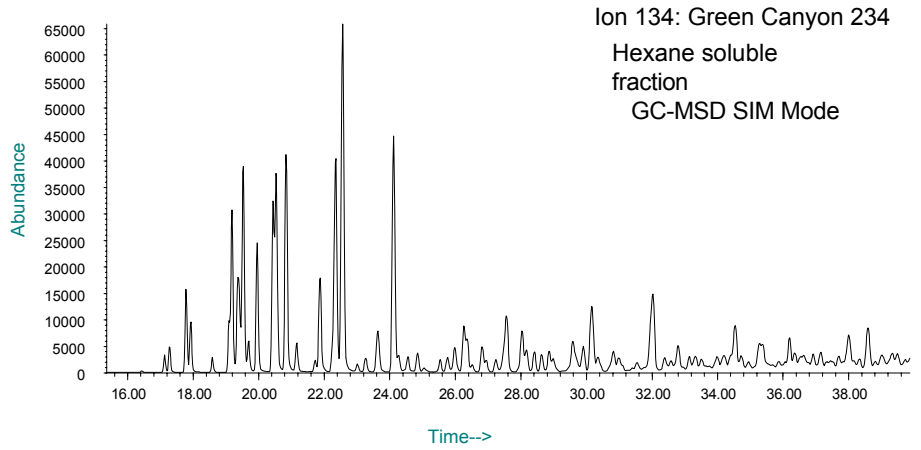

LBE48.D

Figure 8: 2D GC method for resolving compounds under hump in a biodegraded oil (from C. Reddy)

Further analysis of oil under the hump: 2-D gas chromatography (in process)

- The method:

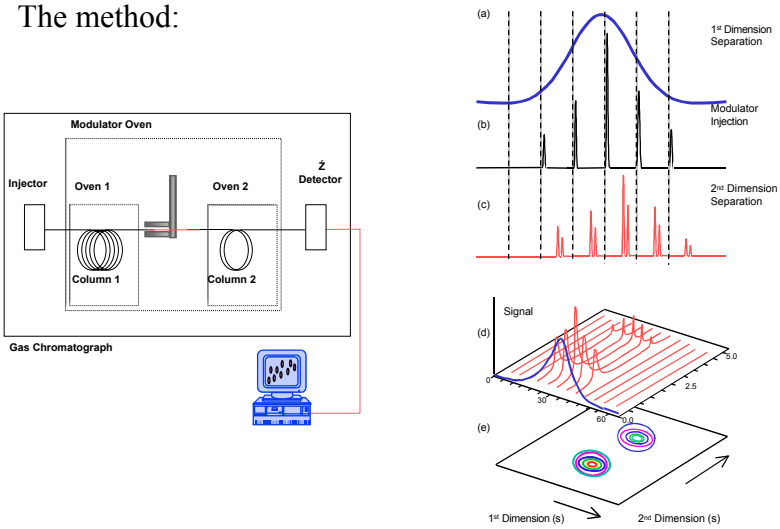

Figure 9: Example of 2D GC technique as applied to oil contaminated sediment and to diesel oil (from Chris Reddy, WHOI)

Two dimensional map from GC-GC showing separation of various compound classes and homologous series in: a) an oil extrated from a contaminated sediment and b) a typical diesel oil. Note the homologous series of n-alkanes at the bottom of each plot. All peaks are identified and quantified using a flame ionization GC detector and a GCMS detector.

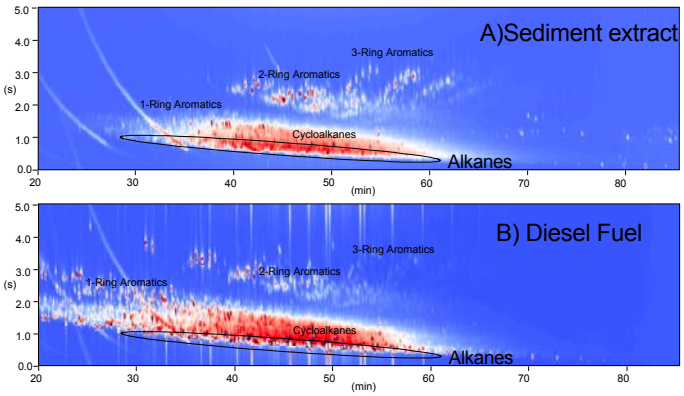

Figure 10: 2D GC, 184 seep oil

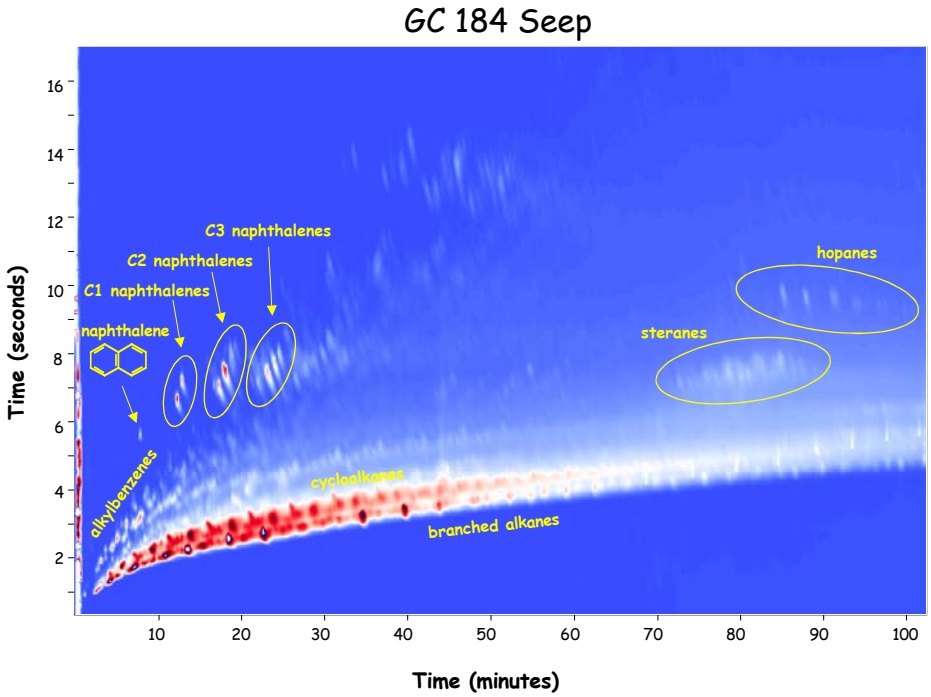

Figure 11: Santa Barbara, Coal Oil Point seep - biodegraded oil, mass scan of biomarker hopanes

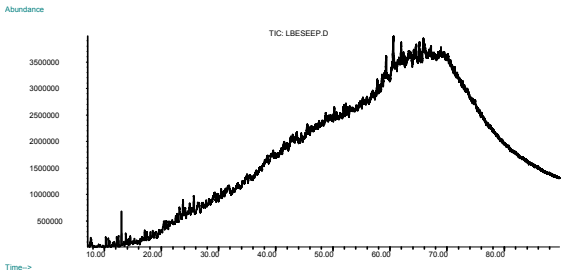

Figure 12: Biomarkers, hopanes, in Santa Barbara Shane tar mound oils

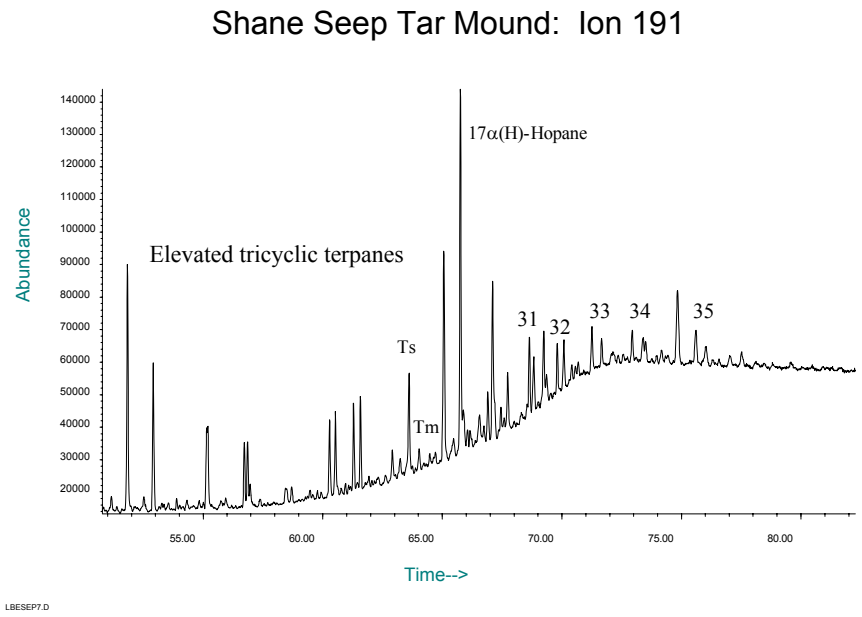

Figure 13: Santa Barbara, Shane Seep tar mounds, aromatic steranes in biodegraded oil

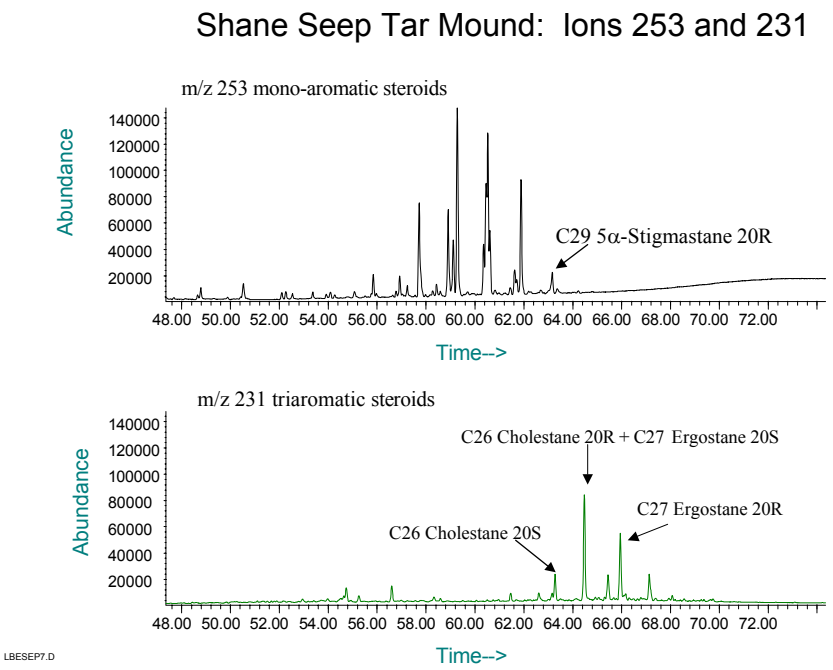

Figure 14: Santa Barbara, Shane Seep Tar mound, methyl phenanthrenes

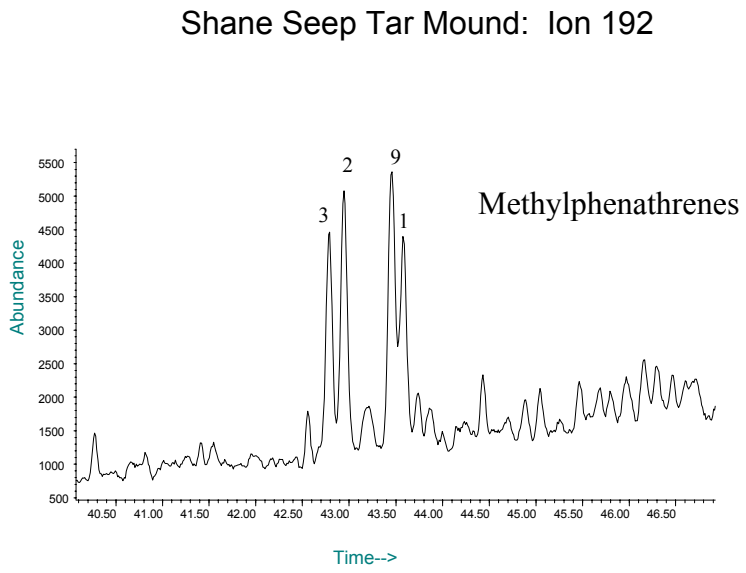

Figure 15: Santa Barbara, Tar mound, total resolvable one dimensional GC peaks in biodegraded oil

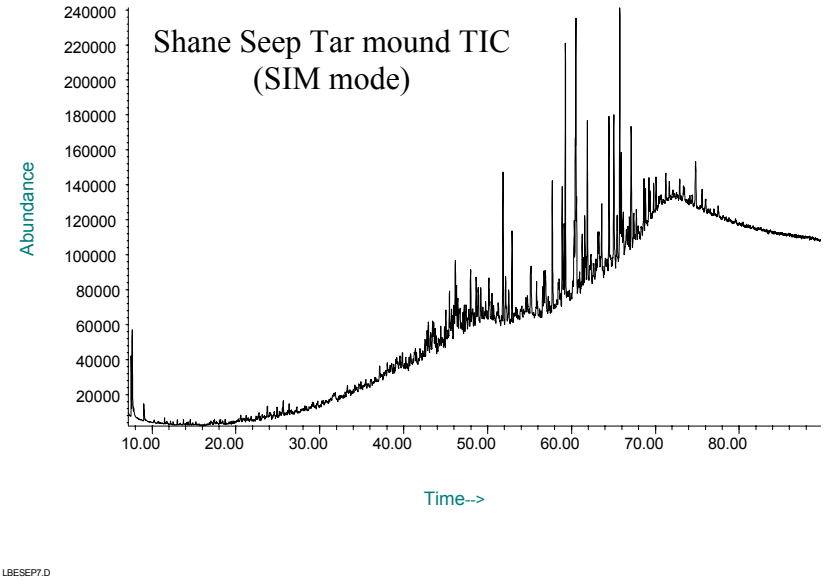

TIC: LBESEP7.D

Figure 16: 2D GC - Santa Barbara, Shane seep tar mound

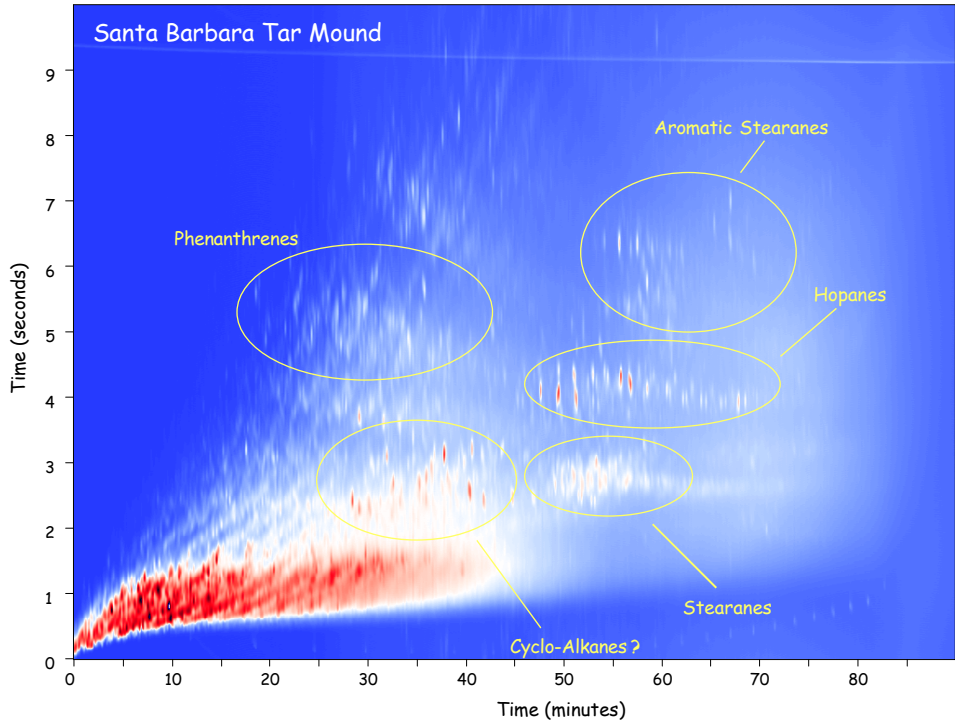

FINAL REPORT

Monitoring biogeochemical processes controlling hydrate formation, decomposition and composition in the Gulf of Mexico

Jeffrey P. Chanton, Department of Oceanography, Florida State University, Tallahassee, Florida 32306-4320. jchanton@mailer.fsu.edu, 850-644-7493.

Christopher S. Martens, Laura L. Lapham, Marine Science Department, University of North. Carolina, Chapel Hill, NC 27599. 919-962-0152. cmartens@email.unc.edu, llapham@email.unc.edu

FINAL Report to the Department of Energy
From the University of Mississippi Gas Hydrate Research Consortium

February 24, 2004

Abstract/ Executive Summary

On the global scale, hydrates need to be included in models of how the biosphere functions. A large portion of the earth's reduced carbon is held within the hydrate reservoir and this reservoir may be more dynamic than is currently thought. Understanding the biology and geochemistry of the seafloor surrounding gas hydrate deposits is crucial to understanding where and how hydrates form. Biological processes and geochemistry strongly influence rates of both formation and destruction of hydrates (Figure 1). Biology and geochemistry play a role in determining the type of hydrate formed and, thus, the specific pressure and temperature conditions where hydrate formation can occur in the subsurface. We need biological and geochemical information to constrain rates of formation and destruction of hydrates (Grabowski et al., 2003)

Accurate geochemistry. For this endeavor, *in situ* concentrations of gases and ions in pore water need to be measured, since samples recovered and brought to the ocean surface without pressurization yield inaccurate results (see below). When measured properly, gas and ion concentrations in pore water can be used to help understand the formation, decomposition and stability of hydrates.

We have developed new tools and techniques for application at the long-term gas hydrate monitoring station. We have constructed an *in situ* pressurized pore water sampler and built and deployed the first osmosampler in the Gulf of Mexico. Modifications to our in situ porewater probe sampler have allowed the collection and determination of accurate dissolved gas concentration and ^{13}C from the seafloor. Comparisons with pressurized and un-pressurized sampling demonstrates the necessity of such a system to collect accurate and meaningful data. Further studies undertaken in summer of 2003 indicate over an order of magnitude greater dissolved gas concentrations with the in situ pressurized sampler relative to traditionally taken samples. The osmosampler will allow long-term data sets to be collected at a single site, and with our design, samples can be recovered at in situ pressures.

We have completed chemical analyses of samples collected on two cruises in the Gulf of Mexico in the summer of 2000 and 2002. Samples from a third cruise from the summer of 2003 are currently being analyzed. These data will be used by Laura Lapham as a portion of her dissertation project. Highlights are described within.

Variability of rates of microbial process is extreme on small spatial scales. Sulfate reduction rates, methane concentrations, total organic carbon, and sulfate depletion all show evidence for extremely high rates of microbial respiration at gas hydrates sites but this respiration is patchy on small scales.

Microbial respiration is not driven only by methane oxidation. There is strong isotopic evidence that oxidation of higher hydrocarbons plays a major role in driving elevated rates of microbial processing in the Gulf of Mexico.

Radiocarbon evidence indicates that hydrocarbon sources are driven by deep reservoirs and there is little evidence for extensive methane production associated with recycling of organic matter fixed on the sea floor via chemosynthetic processes.

Table of Contents

List of Figures and Tables
Introduction
Methods
Results and Discussion
Conclusions
Figures
Tables
References

List of Figures

Figure 1. Conceptual model of methane flux, production and consumption processes that can affect gas hydrate deposits.

Figure 2. In situ porewater probe sampling through a tube worm bush. This figure illustrates the utility of this device in allowing pinpoint sampling of vertical dissolved hydrocarbon sampling on the seafloor.

Figure 3. In situ porewater probe at the base of a gas hydrate mound.

Figure 4. Porewater probe following modification to allow pressurized sample recovery.

Figure 5. Difference in quality of data after modification.

Figure 6. Comparison of methane concentration and isotopic ratio from Probe and traditional cores taken from Cascadia Margin.

Figure 7. Averaged dissolved methane del13C values from the Probe over 50-cm interval.

Figure 8. Example of spatial variability in dissolved gas concentrations.

Figure 9. Example of spatial variability in dissolved sulfate concentrations.

Figure 10. Example of spatial variability in sulfate reduction rates.

Figure 11. Total organic carbon concentrations.

Figure 12. $\delta^{13}C$ isotopic composition of solid phase organic carbon.

Figure 13. Keeling plot analysis of dissolved CO_2 data.

List of Tables

Table 1. Sites visited from three cruises to the Gulf of Mexico.

Table 2. Calculation of substrates supporting microbial respiration from CO_2 isotopic data.

Table 3. $\delta^{3}C$ isotopic composition of cements.

Table 4. Radiocarbon values of methane.

Introduction:

Gas hydrate deposits are important because: a) they represent an enormous potential energy source, b) they present engineering problems for deep water operations, and c) they have been implicated as agents of global climate change, possibly releasing large volumes of methane, a highly efficient green house gas, into the atmosphere thus serving as a positive feedback for warming **(**Kvenvolden, 1988, Kennet et al., 2003). However, the identification of gas hydrates and estimation of their total volume using remotely sensed seismic data is not straight forward. Little data on seabed methane fluxes from dissociation of gas hydrates exist. Furthermore, we do not know the processes that drive gas hydrate dissociation or the effects of methane release to the water column. Gas hydrate dissociation is an important issue for seafloor stability considerations. We need to develop reliable techniques to relate the quantity of gas hydrate deposits to seismic data and to measure the waxing and waning of gas hydrate reservoirs and the rates of and controls on these processes. The Gulf of Mexico is an ideal gas hydrate study site because these unusual frozen gas/water deposits occur exposed at the seafloor at relatively shallow water depths (Brooks et al., 1984; MacDonald et al., 1994; Sassen et al., 1997, 1999a). Therefore, localized areas of gas hydrate can be identified, gas emission monitored, and water column and pore water chemistry responses to external variables measured.

In this project we have undertaken studies and conducted chemical analysis that will aid in the identification of the sources of the reduced compounds fueling hydrate deposits (e.g. Sassen et al., 1999a,b) and investigated the processes controlling hydrate formation and decomposition so that their current state of stability can be assessed. We have measured rates of sulfur cycling to evaluate the role of hydrates in supporting local benthic and water column communities and developed an approach to evaluate the relative contributions of different substrates driving microbial respiration.

A central focus of our research is "How are spatial and temporal variations in hydrate formation, decomposition and composition related to variations in the mechanisms and rates of carbon and sulfur cycling processes in surrounding sediments?"

Scope of work: The project has three parts:

1. To assess spatial and temporal variations in hydrate stability, we have visited 8 hydrate-containing sites in the Gulf of Mexico (Table 1). We have completed chemical analyses of samples collected on a 12-day cruise in the summer of 2000 in collaboration with Dr. R. Coffin and Dr. K. Grabowski of the Naval Research Lab. Samples have also been analyzed from participation on the consortium cruise in 2002. And finally, significant progress has been made on the completion of sample analysis from the summer 2003 cruise. These analyses are complete and will be used by Laura Lapham as a portion of her dissertation project.

2. Mechanisms and rates of carbon and sulfur cycling processes are assessed by the aforementioned chemical analysis and the development of new tools and techniques for application at the long-term gas hydrate monitoring station. We have developed an *in situ* pressurized pore water sampler and deployed the first osmosampler in the Gulf of Mexico. As will be shown below, the quality of data retrieved from our pressurized sampler is much better than what we have seen before. Recent studies undertaken in summer of 2003 indicate over an order of magnitude greater dissolved gas concentrations with the *in situ* pressurized sampler relative to traditionally collected samples.

3. In the summer of 2003, we also visited a site similar to the Gulf of Mexico thermogenic gas hydrate sites off Vancouver Island in the Pacific Ocean to further test the device developed in #2. The *in situ* pore water probe was used to assess the rate of hydrate dissolution (Flux 9 in Figure 1) and this technique will be used on future dives to the Gulf of Mexico sites.

How does our work fit in with consortium?

The focus of the consortium is to establish a long term monitoring station, and to follow a gas hydrate deposit over a long time frame using acoustical and geophysical methods. Geochemistry serves as the ground truth for the geophysics. The central issues which our proposal focuses upon are:

1. Patchiness in seepage and hydrate quantity.
2. Exchange of hydrocarbons, monitoring of hydrate decomposition and formation with an eye toward seafloor stability issues.
3. Identification of the sources of reduced compounds fueling the deposits.

Why is patchiness important? The question is related to the hydrate inventory, its formation and its decomposition. We want to know how a km^2 of seafloor dominated by hydrates works. Our approach is to deploy tools to quantify hydrate growth and decomposition, the processes that affect the hydrocarbons, and pore water parameters that are affected by them. The monitoring station will sense remotely a limited footprint or spatial area. Our work will determine the variability within that footprint. Our consortium needs to know how the temporal changes we observe at the station are related to spatial variability.

Site descriptions:

Samples have been collected during three cruises aboard R/V Seward Johnson II in the summers of 2000, 2002, and 2003 at a reference site and eight hydrate sites.

The reference site (27°44.9'N, 91°16.63'W, 535 m depth) was sampled by collecting a box core over the side of the ship. From the box core, two 5cm x 30cm lexan push cores were taken and immediately stored at *in situ* temperatures of 7°C for later analysis. Sediments were light brown in color and there were no visible disturbances in the cores due to gas expansion or dissociating hydrates. Hydrates are not known to exist in this area.

The hydrate sites were sampled from the submersible Johnson Sea Link. Four of the sites are found in the Green Canyon (GC) Lease Block 185, 234, 233, and 232 and have been described elsewhere (Brooks et al., 1984, Brooks et al., 1985 MacDonald et al., 1994, Roberts et al., 1999; Sassen et al., 1999; Sassen et al., 1998; Sassen et al., 2001; Sassen et al., 1999). Briefly, GC 185 (27°46.9'N, 91°30.4'W, 550-580m depth) and GC 234 (27°44.7'N, 91°13.3'W, 525-560m depth) have exposed hydrates at the sediment water interface, chemosynthetic communities (tube worms, methanotrophic mussels, and clams), seeping gas of low molecular weight hydrocarbons (such as methane, ethane, and propane), and oil associated with the surrounding sediments. GC 233 (27°43.4'N, 91°16.8'W, 640m depth) is a brine pool surrounded by a mussel beach. Mississippi Canyon (MC) is east of the GC sites (28°51.1409'N, 89°29.5361'W, 2915m water depth).

Mississippi Canyon (MC) 709 and 118 (28°51.1409'N, 89°29.5361'W, ~970-m water depth) were visited in 2002. MC 118 is the easternmost hydrate site of all discoveries in the Gulf of Mexico thus far (Sassen, personal communication). MC 118 has chemosynthetic communities but I am unsure if shallow surfacing hydrates exist. Geochemically, the oil and the

gas do not look much different than at a well-studied site, MC 852/853 that is thought to contain more gas hydrate accumulations than any other site in the central Gulf of Mexico ((Sassen et al., 1999)).

Viosca Knoll 826 (29°09.7528'N, 88°01.9246'W, ~570-m water depth) and Garden Banks 425 (27°33.2113'N, 92°32.4463'W, ~625-m water depth) were also visited but information about these sites is still being gathered. An active mud volcano at GC 205 was visited in 2003 that had been discovered by the Navy submersible NR-1 a few years prior. Information on this site is also being gathered.

Methods:

Sampling methods

At the hydrate sites, sediment and pore water samples were collected from the submersible platform by two different methods. The first method collected only pore waters by using an *in situ* pore water extraction device, known as the Probe (Figures 2 and 3). Ideally, for every deployment of the probe, there was a sediment core to compliment. During the 2000 cruise, the probe was not pressure tight so concentrations are a minimum. However, the probe was modified to hold *in situ* pressures for the 2002 and 2003 cruises (Figure 4). Briefly, the submersible's manipulator arm placed the probe tip into the desired sediment and triggered a hydraulic spring that provided the suction to extract pore water through 10 filtered ports along a 50-cm shaft for 30 minutes. For the 2000 cruise, samples were collected in PVC chambers that were open to the outside pressure thereby allowing expansion of the gas during ascent. These chambers collected about 7mL of water. To obtain *in situ* concentrations, the probe was modified with stainless steel chambers and heavy-duty gas tight valves to hold pressures up to a maximum of 4000psi. This modification led to significantly improved results. The sample volume stayed the same as the original design. Once the probe was shipboard, pore waters were collected into gas tight syringes and immediately analyzed for gas concentrations using a gas chromatograph. Remaining pore water was preserved by injecting it into evacuated serum vials and frozen upside down for determination of carbon isotopic ratios at the mass spectrometry labs at UNC and FSU.

The second sampling method collected sediment and pore water with traditional Lexan 30cm push cores. Once onboard ship, cores were sectioned into 2-3 cm sections and pore waters expressed by pressure filtration. Sub-cores of each section were taken to measure sulfate reduction rates (described below). Pore waters were stored cold in 2mL o-ring sealed plastic microcentrifuge tubes. Sediment patties were frozen in plastic bags for determination of total organic carbon concentrations and $\delta^{13}C$.

Analytical methods

Sulfate was measured by diluting 100uL of sample to 10mL with eluent and injecting 1mL into a Dionex Ion Chromatograph. Sample concentrations were determined after running several standards. Dissolved gas samples were analyzed for concentrations of methane, ethane, and propane aboard ship using a Shimadzu Mini-II gas chromatograph equipped with a poropaq Q column. Dissolved gas samples were also analyzed for carbon isotopic signatures using a gas chromatograph-isotope ratio mass spectrometer (GC-IRMS) with a Hewlett-Packard 5890 GC equipped with a Poroplot Q column set at 30°C and a Finnigan Mat IRMS. Low concentration gases were analyzed by pre-concentrating gas aliquots of ~10-30mL in-line with a liquid nitrogen/ethanol slush at approximately -130°C and a column baked at 30°C and then introduced into the GC-IRMS system. Microliter volumes of high concentration gases were

directly injected onto the column to be introduced to the mass spectrometer. Total organic carbon concentrations and isotopes were measured on freeze-dried and ground sediment patties. Approximately 30mg of sample was introduced by flash combustion into a Carlo Erba Elemental Analyzer and resultant carbon dioxide swept into the same IRMS system as described above. Results are presented in the standard d notation, in ‰.

$\delta^{13}C$‰ = [(Rsam/Rstd) – 1] * 1000 where R = $^{13}C/^{12}C$ and Rsam is the sample and Rstd is PDB standard.

Sulfate reduction rate measurements

Briefly, triplicate sub-cores were taken from each section, carefully excluding oxygen with silicone-filled stoppers. They were then injected with approximately 40 KBq ^{35}S-sulfate contained in a 10 μL volume and incubated at 7°C for 24 hours onboard ship. After incubation, sub-cores were extruded into empty 120mL glass serum vials and preserved as a slurry in 5mL of 1.6M zinc sulfate and 1mL of 0.1M sodium sulfide carrier solution. These chemicals stabilized sulfide in the form of insoluble zinc sulfide and stopped biological activity. Samples were then stoppered with blue butyl rubber stoppers and frozen for later determination of biologically produced ^{35}S-sulfide.

Determination of biologically produced ^{35}S-sulfide was measured by a modification of an active distillation/chromium reduction technique, also described in Albert et al. (1995). In short, samples were flushed with oxygen-free nitrogen and then acidified through the septa with 10mL of 2M HCl containing 0.5 M Cr^{2+}, prepared previously by reduction of an anoxic solution of $CrCl_3$ solution in a bed of zinc-mercury amalgam bubbled with nitrogen. Upon acidification and heating (4 minutes at 100°C), labeled and unlabeled hydrogen sulfide was released from the slurry, carried through a glass-wool aerosol trap, and finally precipitated out in a solution of 6mL of 0.5 M zinc acetate in 0.5% iso-butanol. Trap contents were transferred to scintillation vials and an equal volume of Scintiverse II (Fisher Scientific) for counting on a Beckman LS 6800 scintillation spectrometer was added. Counts were corrected for quench from the counting efficiency of an external standard. Sulfate reduction rates were than calculated using the following equation,

$$Sulfatereductionrate(mM/d) = \frac{H_2{}^{35}S * [SO_4{}^{2-}(mM)] * 1.04 * \phi}{{}^{35}SO_4{}^{2-}(added) * incubationtime(d)}$$

Where, $H_2{}^{35}S$ is the amount produced during the incubation time, SO_4^{2-} is the concentration of pore water sulfate measured in the cores, 1.04 is the fractionation factor taken into account when bacteria preferentially take up the lighter sulfur isotope rather than the heavier isotope, ϕ is the porosity of the sediments, $^{35}SO_4^{2-}$ is the amount of labeled sulfate added to the incubations and incubation time is in days.

Results and Discussion:

We have successfully developed an in-situ pore water probe to allow collection and recovery of dissolved gas samples without de-pressurization. This improvement led to the observation of significantly greater concentrations and smoother concentration profiles (Figure 5).

Experiments were conducted in 2003 between traditional coring techniques and the Probe to compare dissolved methane concentrations and isotopes (Figure 6). As expected,

methane concentrations are an order of magnitude lower in the cores than in the Probe. However, there are also slight variations between the methane carbon isotopic composition from the core and Probe pore waters. These variations are being further investigated with the same comparison samples taken from the Gulf of Mexico this past summer 2003.

With the use of the Probe, we were able to look at a spatial survey of methane concentrations and isotopes in the shallow subsurface from eight different locations in the Gulf of Mexico. In the upper 50-cm of the subsurface, methane concentrations increased downcore (Figure 5) and varied widely between sites. For example, we observed great variability at nearby locations at GC-234. Methane concentrations varied by almost two orders of magnitude (Figure 8) between two separate deployments of the Probe taken only several meters from each other. Methane carbon isotopes did not show much variability within a profile (see error bars on Figure 7) but showed some variation over several sites. Most methane showed a thermogenic signature (-48.36±5.27) while the brine pool at GC 233 was biogenic (-64.61±0.10) (Figure 7). Variability was also seen in sulfate concentrations and sulfate reduction rates between sites. Sulfate showed greater depletion at site 4217 and almost no depletion, only a few meters away, at site 4218 (Figure 9). Sulfate reduction rates varied by two orders of magnitude, similar to methane concentrations (Figure 10).

One might suspect from perusal of this data that methane concentrations were driving the elevated rates of sulfate reduction at site 4217 relative to site 4218. However, TOC (total sedimentary organic carbon) was also significantly greater at site 4217 than 4218 (Figure 11). Stable isotope data, indicated that the organic carbon was not methane derived (Figure 12) as it was more like conventional organic matter (low – 20's ‰ rather than methane –48‰). We hypothesize that microbial degradation of petroleum could also be driving the high rates of microbial respiration observed. To evaluate this hypothesis we have examined the $\delta^{13}C$ of dissolved porewater CO_2 and calculated the excess CO_2 over background seawater which is produced by microbial respiration. This approach, called a Keeling plot, plots the reciprocal of the CO_2 concentration versus the $\delta^{13}C$ of dissolved porewater CO_2 and allows us to calculate the isotopic signature of the CO_2 produced by microbial respiration as the y-intercept of the line (Figure 13). The $\delta^{13}C$ of CO_2 produced from microbial respiration is identical to the isotopic composition of the substrates supporting microbial respiration (Lapham et al., 1999; Proctor et al., 2001).

From our Keeling plot approach (Figure 13), we calculate that the $\delta^{13}C$ of organic carbon driving microbial respiration is –36.1‰, a value intermediate between methane and petroleum hydrocarbons. If we assume that the petroleum compounds are –29‰, and the methane we have measured to be –49‰ with a fractionation effect of 1.012, we can calculate that the microbial respiration at this site was 24% supported by methane oxidation while 76% is supported by oil oxidation (Table 2). Analysis of cements (calcified CO_2) collected at a variety of gas hydrate sites are consistent with the hypothesis that methane oxidation alone is not driving microbial respiration at gas hydrate sites (Table 3) as only 1 site (4408) showed unequivocal evidence for methane oxidation.

In collaboration with Dr. Sassen, of Texas A&M University, we recently measured the ^{14}C content of vent gases of both biogenic and thermogenic origin (Table 4; Sassen et al., 2003). The thermogenic gas is the first in the table below as indicated by its $\delta^{13}C$ value of –46.7‰. The two biogenic gases have $\delta^{13}C$ values of –62‰. We tested the hypothesis that the biogenic gases would have some contribution from modern carbon associated with decomposition of recently fixed carbon on the seafloor. Our hypothesis was not consistent with the data. All of the hydrocarbons are of ancient origin.

Conclusions:
Preliminary Conclusions from our first years of funding are:

1. Modifications to our *in situ* porewater probe sampler have allowed the collection and determination of accurate dissolved gas concentration and ^{13}C from the seafloor. Comparisons with pressurized and un-pressurized sampling demonstrates the necessity of such a system to collect accurate and meaningful data. When measured properly, gas and ion concentrations in pore water can be used to help understand the formation, decomposition and stability of hydrates.

2. Variability of rates of microbial process is extreme on small spatial scales. Sulfate reduction rates, methane concentrations, total organic carbon, and sulfate depletion all show evidence for extremely high rates of microbial respiration at gas hydrates sites but this respiration is patchy on small scales.

3. Microbial respiration is not driven only by methane oxidation. There is strong isotopic evidence that oxidation of higher hydrocarbons plays a major role in driving elevated rates of microbial processing.

4. Radiocarbon evidence indicates that hydrocarbon sources are driven by deep reservoirs and there is little evidence for extensive methane production associated with recycling of organic matter fixed on the sea floor via chemosynthetic processes.

Figures:

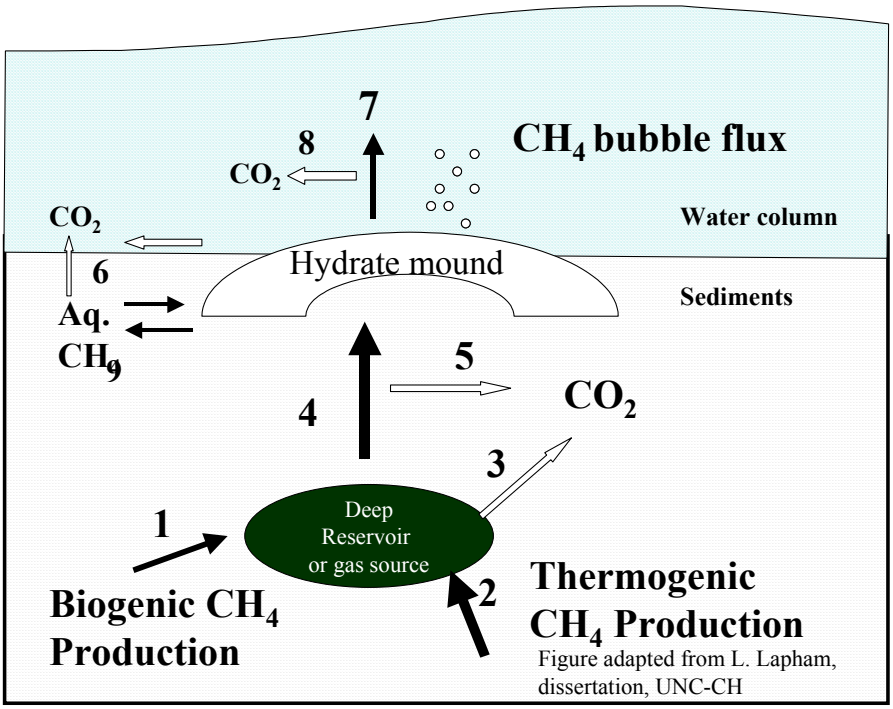

Figure 1 depicts a conceptual model of methane flux, production and consumption that can affect gas hydrate deposits. The deposits considered derive contributions of methane from both biogenic and thermogenic sources. A biogenic hydrate model might simply omit the thermogenic components of this model. Black arrows represent methane flux from a source; open arrows represent microbial methane consumption. Flux 1 is from biogenic methane production, 2 is from thermogenic methane production, 4 represents the flux from a deep reservoir or distributed sources to the surface where it can form hydrates, bubbles or dissolved methane. Flux 7 represents methane flux from either hydrate, pore water, or gas bubbles into the water column where it can enhance secondary production. Fluxes 3, 5, 6 and 8 represent anaerobic and aerobic methane oxidation. Equilibrium and exchange with dissolved methane is also depicted, flux 9. Any bubbles that make it to the top 100-m of the water column can be injected directly into the atmosphere.

Figure 2. The pore water probe can be utilized to sample a variety of discrete environments. In the picture above, a porewater profile below a tube worm bush is being obtained.

Figure 3. Here the probe is deployed by the arm of the Sea Link to collect a discrete sample immediately at the base of a gas hydrate deposit.

Figure 4. The porewater probe following its redesign to allow collection and retrieval of in situ samples at ambient pressure. The probe is resting on a table with the sampling proboscis extending through the deck of the table.

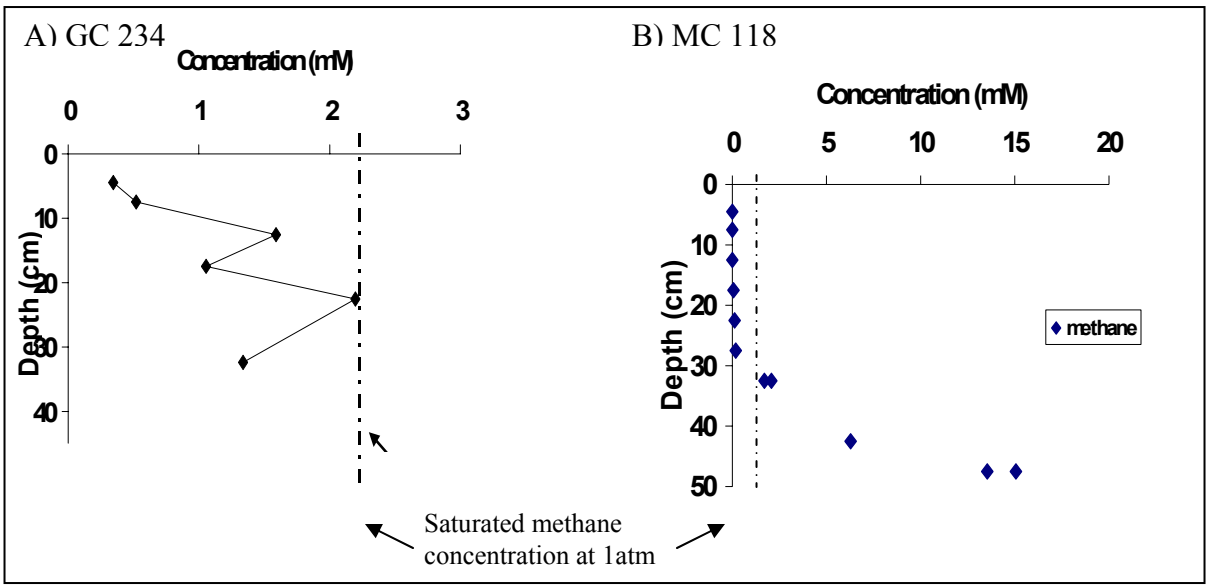

Figure 5. Comparison of in situ pore water gas probe gas analysis on un-pressurized (left) and pressurized (right) pore water sampler. The profile on the left does not exhibit gas concentrations above equilibrium values with 1 atmosphere pressure (dashed line) whereas the right profile does. These results indicate the loss of dissolved gases as the instrument ascended

to the surface. The saw-tooth nature of the profile also may indicate degassing during assent. The right profile reaches concentrations of 15 mM CH_4 and is smooth, exhibiting a convex upward shape consistent with methane oxidation. Modeling exercises will enable us to calculate a rate of methane consumption from this data that would not be possible otherwise. To our knowledge, this profile is the first ever pressurized in situ profile collected from the deep sea.

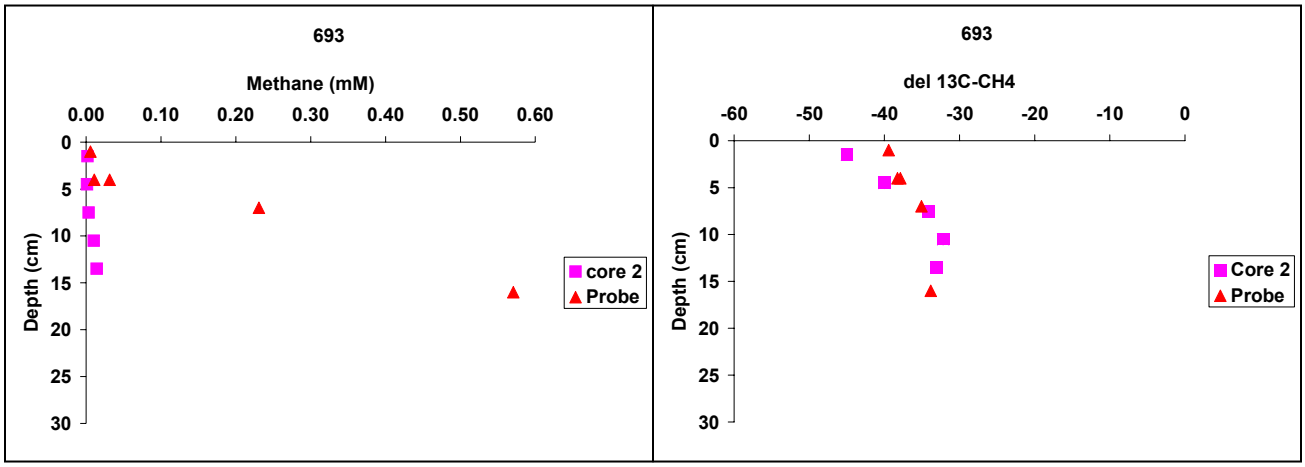

Figure 6. Comparison of methane concentration and isotopic ratio from Probe and traditional cores taken from Cascadia Margin.

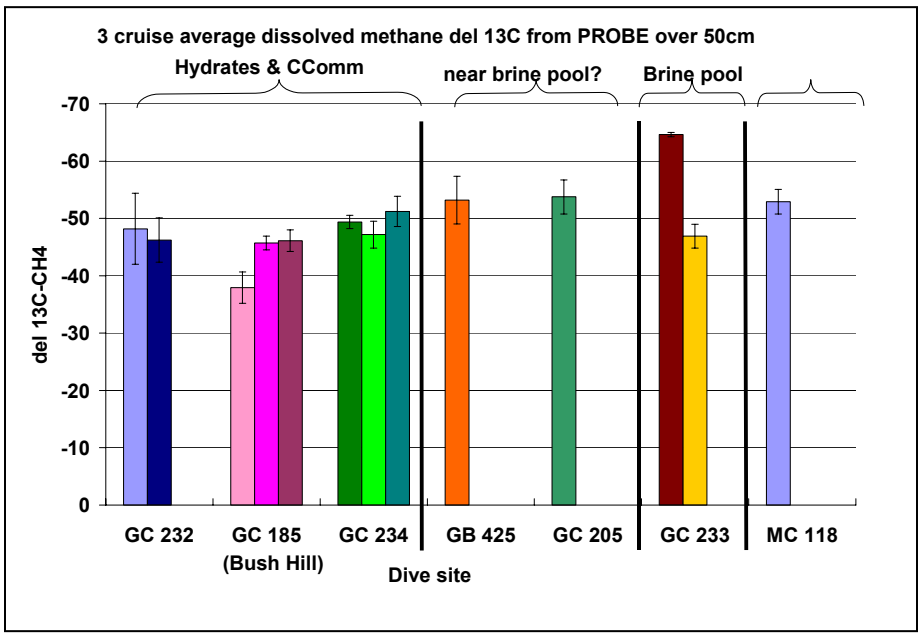

Figure 7. Averaged dissolved methane del13C values from the Probe over 50-cm interval. Error bars signify 1 standard deviation.

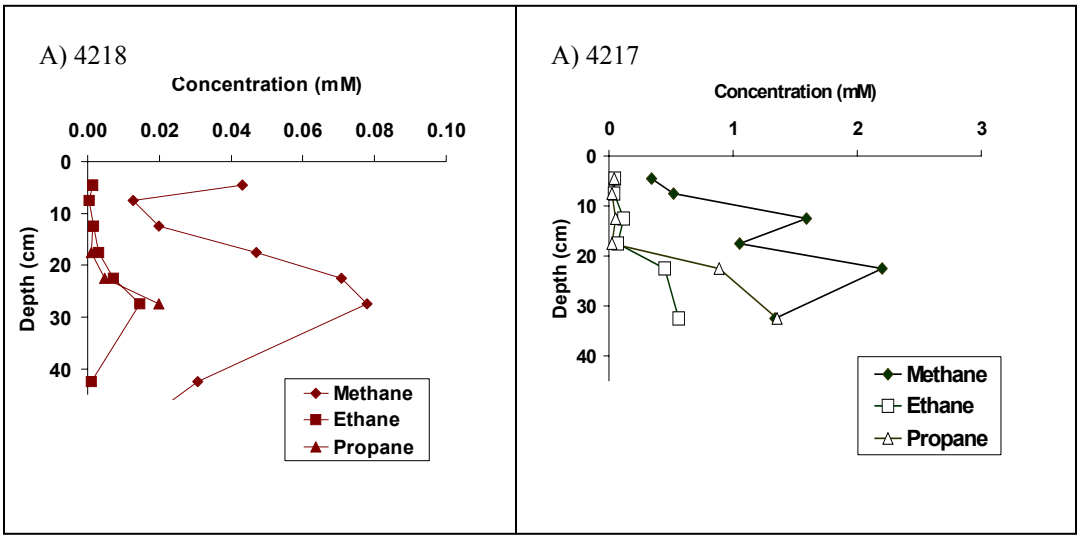

Figure 8. We observed almost two orders of magnitude variability hydrocarbon concentrations in sediments surrounding the gas hydrate deposits. These two sites also showed great variability in sulfate reduction rates (see Figures 9 and 10).

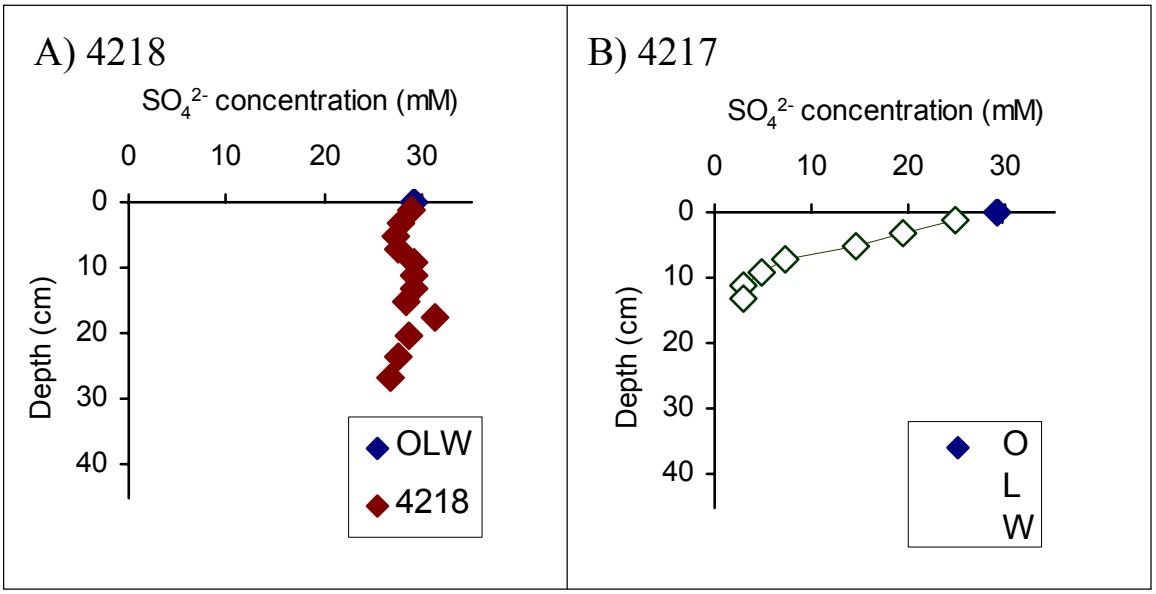

Figure 9. Sulfate depletion is greatest in core 4217,consistent with the higher hydrocarbons measured there and the greater sulfate reduction rates.

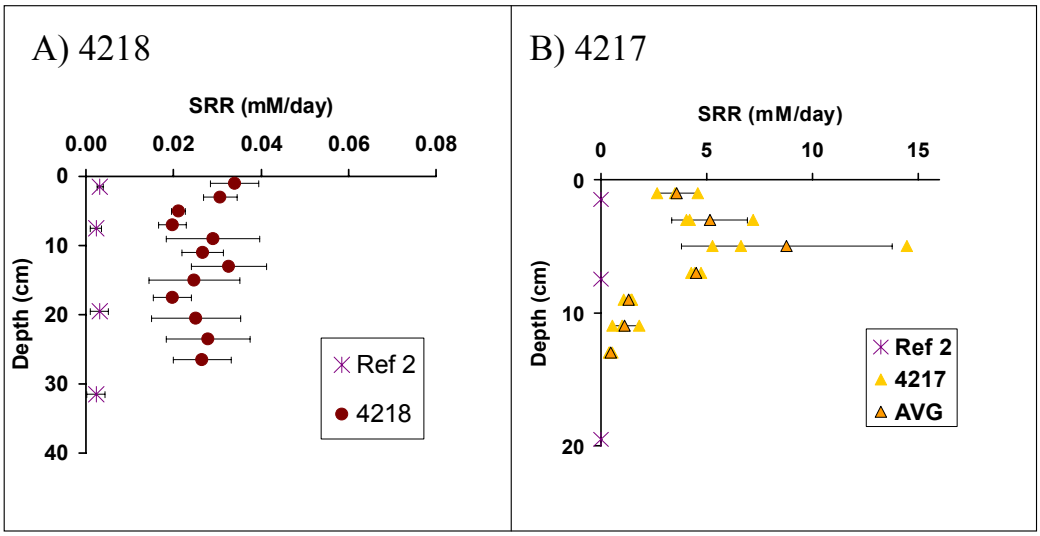

Figure 10. Sulfate reduction rates varied by over two orders of magnitude between the sites. Also shown in the figure are sulfate reduction rates at a reference or background site away from a gas hydrate deposit.

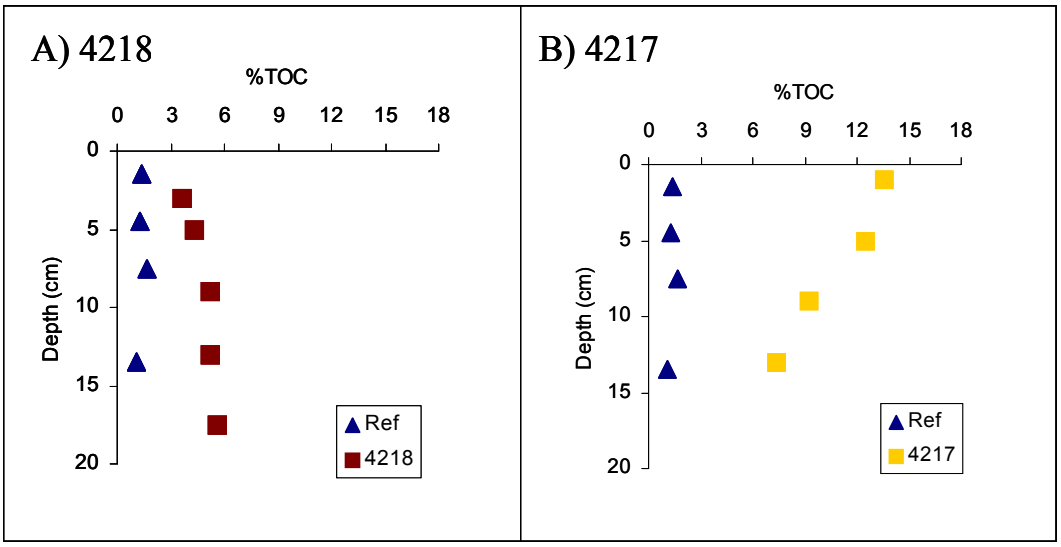

Figure 11. The % organic carbon at the sites discussed above. Similar to methane concentrations and respiration rates, organic carbon concentration was much greater at site 4217.

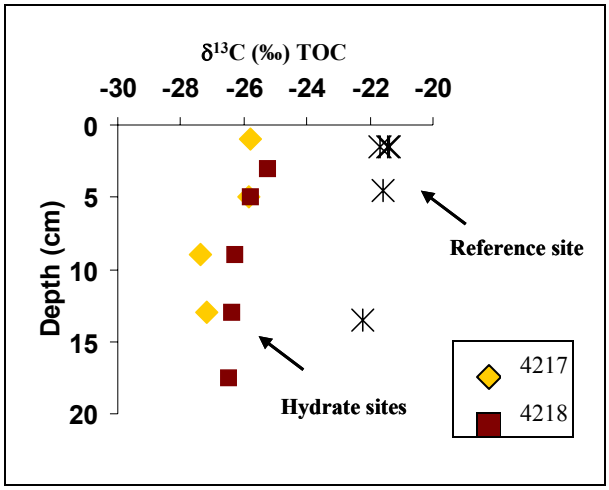

Figure 12. The $\delta^{13}C$ of TOC at the two sites was not different, nor was it clearly derived from methane oxidation. TOC $\delta^{13}C$ was more similar to petroleum values.

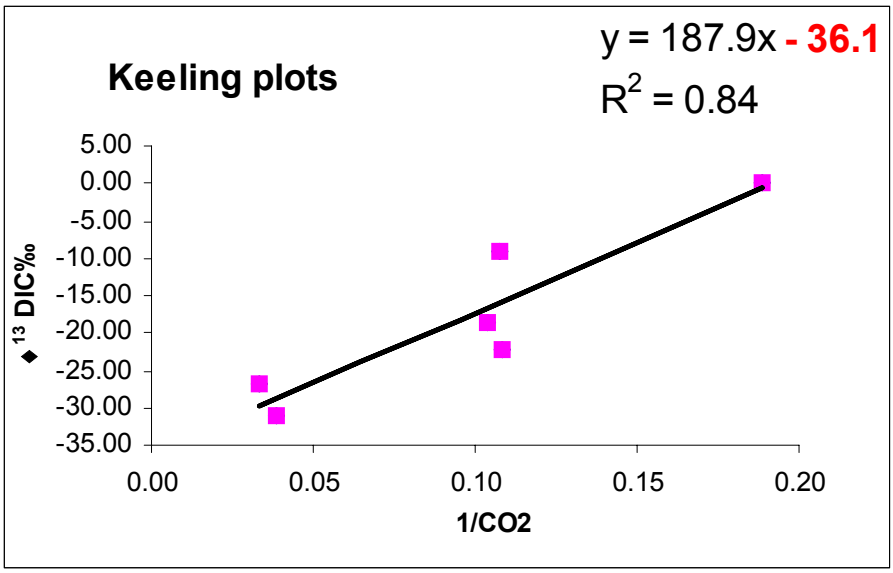

Figure 13. Keeling plot analysis to determine the $\delta^{13}C$ of excess CO_2 in porewater driven by respiration. The intercept of the line fit to the data is the $\delta^{13}C$ of CO_2 in excess over background seawater. This excess CO_2 was supplied by microbial respiration, and reflects the isotopic composition of the substrate utilized by the bacteria (Lapham et al., 1999). This value was used in Table 1, above to determine the relative contributions of the hydrocarbons driving microbial respiration at the gas hydrate sites.

Tables:

Site	# dives	Exposed hydrate	Chemosynthetic communities	# cores	# Probe deployments
GC 185 Bush Hill	10	Y	Y	14	3
GC 233 Brine Pool	2	N	Y	2	2
GC 234	8	Y	?	10	3
GC 232	4	Y	Y	7	2
GC 425	1	?	Y	1	1
GC 205 mud volcano	1	N	N	2	1
Viosca Knoll 826	2	?	?	3	0
Miss Canyon 118	3	?	Y	3	1

Table 1. Sites visited from three cruises to the Gulf of Mexico.

Petroleum or methane oxidation?

- Signature of added DIC = -36.1‰
- Methane source = -47 (α = 1.012) → -59‰
- Oil source = -29‰
- Mass Balance:

$$-59(f) + -29(1-f) = -36.1$$

~24% methane oxidation
~76% petroleum oxidation

Table 2. Calculation of the relative importance of substrates driving microbial respiration from an isotopic balance.

Cement $CaCO_3$ **$\delta^{13}C$ ‰**

Sample ID	**δ13C**
Bucket 3, 709, Miss. Canyon, 4413	-23.8
4405, 5/30/02, Rock	-20.5
4401, 5/29/02, Carbonate	-22.0
4413, Core 6 Rocks from 6-9 cm 6/3/02	-26.8
4403, #6, 27 cm carbonate, 5/29/02	-18.0
GC 232, 4403, core #4, carbonate at 21 cm	-14.6
4401, Core #2, 5/29/02, carbonate	-18.0
4405, 5/30/02	-22.0
4408, 6/1/02 Offshore 65-1	-49.7
4413, 118 Miss. Canyon 6/3/02	-28.6
Gc 234, 4407, 5/31/02 smaller of 2 rocks	-20.4
4413, Miss Canyon, Block 3/6/02, 709, Bucket 9	-28.2

Table 3. $\delta^{13}C$‰ of carbonate cements recovered from gas hydrate sites. With the exception of the sample highlighted in yellow, none of these samples show unequivocal evidence for methane oxidation. The samples highlighted in pink are 13C enriched relative to marine organic matter.

Sample	$\delta^{13}C$‰	AGE yrs	F modern	Fm error	$\Delta^{14}C$
4228-3	-46.7	>52000 (1100)	0.001061	0.0001	-998.9
4232-2	-62.8	48100 (610)	0.00253	0.0002	-997.5
4229 1R	-62.9	45700 (410)	0.003384	0.0002	-996.6

Table 4. Radiocarbon values of methane (modified from Sassen et al., 2003). F modern stands for fraction modern carbon.

References

Aharon, P. and Fu, B. (2000). Microbial sulfate reduction rates and sulfur and oxygen isotope fractionations at oil and gas seeps in deepwater Gulf of Mexico. *Geochim. Cosmochim. Acta,* **64 (2)**, 233-246.

Boetius, A., Ravenschlag, K., Schubert, C.J., Rickert, D., Widdel, F., Gieseke, A., Amann, R., Jorgensen, B.B., Witte, U., and Pfannkuche, O. (2000). A marine microbial consortium apparently mediating anaerobic oxidation of methane. *Nature* **407**, 623-626.

Brooks, J.M., Kennicutt II, M.C., Fay, R.R., McDonald, T.J., and Sassen, R. (1984). Thermogenic gas hydrates in the Gulf of Mexico. *Science* **225**, 409-411.

Chanton, J.P., Martens, C.S., Paull, C., and Coston, J.A. 1993. Sulfur isotope and porewater geochemistry of Florida Escarpment Seep Sediments, *Geochim. Cosmochim . Acta*, 57, 1257-1266.

Chanton, J.P., Martens, C.S., and Paull, C.K. 1991. Control of pore-water chemistry at the base of the Florida Escarpment by processes within the platform. *Nature*, **349,** 229-231.

Cragg B.A., Parkes R.J., Fry J.C., Weightman A.J., Rochelle P.A., and Maxwell J.R. (1996). Bacterial populations and process in sediments containing gas hydrates (ODP Leg 146: Cascadia Margin). *Earth and Planetary Science Letters* **139**, 497-507.

Grabowski, K., R. Rogers, J. Chanton, J. Whelan, P. Sobecky, 2003, Summary Report - Session II, Biological Influence on Hydrate Formation, Stability, Content and Lattice Saturation. International Gas Hydrate Meeting, Washington DC, November, 2003.

Kvenvolden K.A. (1988). Methane hydrate-a major reservoir of carbon in the shallow geosphere? *Chem. Geol*. **71**, 41-51.

Lapham, L., L. Proctor and J. Chanton. 1999. Using Respiration Rates and Stable Carbon Isotopes to Monitor the Biodegradation of Orimulsion by Marine Benthic Bacteria, Environmental Science and Technology, 33, 2033-2039.

MacDonald I.R., Boland G.S., Baker J.S., Brooks J.M., Kennicutt II M.C., and Bidigare R.R. (1989). Gulf of Mexico hydrocarbon seep communities. *Mar. Biol*., **101**, 235-247.

MacDonald I.R., Callender W.R., Burke Jr. R.A., McDonald S.J., and Carney R.S. (1990). Fine-scale distribution of methanotrophic mussels at a Louisiana cold seep. *Prog. Oceanogr.* **24**, 15-24.

MacDonald I.R., Reilly II J.F., Guinasso Jr, N.L., Brooks J.M., Carney R.S., Bryant W.A., and Bright T,J. (1990). Chemosynthetic mussels at a brine-filled pockmark in the northern Gulf of Mexico. *Science* **248**, 1096-1099.

MacDonald I. R. N. L. Guinasso, R. Sassen, J. Brooks, L. Lee, K. Scott. (1994) Gas hydrate that breaches the sea floor on the continental slope of the Gulf of Mexico. Geology 22, 699-702.

Martens, C. S. and R. A. Berner, 1977. Interstitial water chemistry of anoxic Long Island Sound sediments. I. Dissolved gases. *Limnol. Oceanogr. 22*: 10-25.

Martens, C.S., Chanton, J.P., and Paull, C.K. (1991). *Fossil Biogenic methane at the Florida Escarpment. Geology,* **19**, 851-854.

Martens, C.S. (1990) Generation of short chain organic acid anions in hydrothermal altered sediments of Guaymas Basin, Gulf of California. Applied Geochemistry, 5, 71-76.

Martens, C.S., D.B.Albert, and M.J. Alperin. 1999. Stable isotope tracing of methane production and oxidation in the gassy sediments of Eckernforde Bay, German Baltic Sea. *Amer. Journal Science* (Invited paper for R.A. Berner Special Issue) *299:* 589-610.

Paull, C.K., Chanton, J. P., Neumann, A.C., Coston, J.A., and Martens, C.S. (1992). Indicators of methane derived carbonates and chemosynthetic organic carbon deposits: examples from the Florida Escarpment. *Palaios*, **7**, 361-375.

Paull, C.K., Chanton, J.P., Martens, C.S., Fullagar, P.D., Neumann, A.C., and Coston, J.A. (1991). Seawater circulation through the flank of the Florida platform: evidence and implications. *Marine Geology*, **102**, 265-279.

Paull, C.K., Martens, C.S., Chanton, J.P., Neumann, A.C., Coston J., Jull, A.T., and Toolin, L.J. (1989). Fossil methane carbon in living chemosynthetic organisms and young carbonate cements at the Florida Escarpment. *Nature*, **342**, 166-168

Proctor, L.M., E. Toy, L. Lapham and J. Cherrier and J. Chanton. 2001. Enhancement of orimulsion biodegradation through the addition of natural marine carbon substrates. Environmental Science and Technology, 35, 1420-1424

Sassen R., Roberts H.H., Aharon P., Larkin J., Chinn E.W., and Carney R. (1993). Chemosynthetic bacterial mats at cold hydrocarbon seeps, Gulf of Mexico continental slope. *Org. Geochem.*, **20**, 77-89.

Sassen, R. and I.R. MacDonald. (1997). Hydrocarbons of experimental and natural gas hydrates, Gulf of Mexico continental slope. Org. Geochem, 26, 289-293.

Sassen, R., I.R. MacDonald and others. (1998). Bacterial methane oxidation in sea-floor gas hydrate: Significance to life in extreme environments. Geology, 26, 851-854.

Sassen, R., S.T. Sweet, A. Milkov, D. DeFretias, F. Salata, E. McDade. (1999) Geology and geochemistry of gas hydrates, central Gulf of Mexico Continental Slope, Gulf Coast Association of Geological Societies Transactions, vol XLIX, pages 462-468.

Sassen, R. S. Joye, S. Sweet, D. DeFreitas, A. Milkov and I. MacDonald. (1999). Thermogenic gas hydrates and hydrocarbon gases in complex chemosynthetic communities, Gulf of Mexico, continental slope. Organic Geochemistry, 30, 485-497.

Sassen, R. et al., 2003. Gas venting and subsurface change in the Green Canyon area, Gulf of Mexico continental slope: evidence of a deep bacterial methane source? Organic Geochemistry, 34: 1455-1464.

Deep Sea Microbes as Sources of Biomedically-Important Natural Products

Task 8

Final Report
December 2003

Principal Investigator: Marc Slattery

DOE Award DE-FC26-00NT40920

University of Mississippi
National Center for Natural Products Research
University, Mississippi, 38677

Abstract

Extremophile microbes, specifically those from methane hydrate seeps in the Northern Gulf of Mexico, represent a potentially important and novel resource for marine biotechnology. Microbes are known to produce up to one third of all antibiotics on the market today, and deep-sea organisms also produce unusual enzymes that operate under extreme pressures and temperatures. The purpose of this project was to isolate strains of microorganisms from the methane hydrate seep sites, to culture these strains in our labs at the University of Mississippi, and to test broth extracts for unusual biomedical activity.

Table of Contents

Abstract
Introduction
Executive Summary
Experimental
Results and Discussion
Conclusion

Introduction

Recent studies have demonstrated the significance of the marine environment as another resource for the discovery of novel bioactive metabolites (Paul 1992; Attaway & Zaborsky 1993). The oceans encompass approximately 75% of the planet's surface and over 90% of its crust volume, thus conditions represent the extremes of temperature, pressure, and salinity encountered by organisms. To survive, marine organisms have adapted unique metabolic processes, and often metabolites, which are not observed in terrestrial systems (Pietra 199*). Many important biomedical metabolite discoveries have been reported and at least two compounds, Bryostatin 1 and Didemnin B, have advanced to clinical trials as anticancer agents (Flam 1994). Like their terrestrial counterparts, marine microbes (bacteria and fungi) offer the potential of a rich resource of novel chemotherapeutic agents. Nonetheless, relatively few studies have focused on marine microbes; this may be due in part to the complexities involved in the isolation and cultivation of this resource (Fenical 1993; Liberra & Lindequist 1995), or to misidentified metabolite source organisms (Stierle et al. 1988; Faulkner et al. 1994).

The bacteriocidal properties of seawater were recognized by ZoBell and coworkers approximately 50 yrs ago; they subsequently showed that the diverse bacterial communities produced antimicrobial agents. Nonetheless the first marine bacterial metabolite was only recently isolated from a species of *Alteromonas* found on blades of the seagrass *Thalassia* sp. in Puerto Rico (Burkholder et al. 1966). The highly brominated pyrole (**1**), pentabromopseudiline, exhibited impressive in vitro antibiotic activity (MIC's of 0.0063 to 0.2 ug/ml) against Gram-positive bacteria including *Mycobacterium tuberculosis* but was not active in

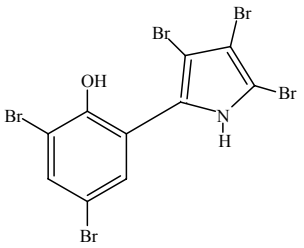

vivo; antitumor properties of this compound have been reported more recently (Laatsch & Pudleiner 1989).

Historically, terrestrial soil samples have yielded many of the antibiotic producing microorganisms (Robbers et al. 1996). Microbes derived from marine sediment samples, which tend to be nutrient-rich, produce a diversity of bioactive compounds as well. For instance, *Streptomyces griseus* from a coastal sediment sample in Japan produced an unusual group of boron-containing antimicrobials: aplasmomycin A (**2**), B (**3**), and C (**4**) (Hotta et al. 1980). These compounds were active against Gram-positive bacteria (MIC's of 0.8 to 3.0 □g/ml), but were particularly effective in vivo against *Plasmodium berghei*, the causal agent of malaria in mice. More recently this strain has been crossed with the species *S. tenjimariensis*, which produces a class of compounds that have strong activity against aminoglycoside-resistant microbes, to produce a strain that yields novel indolizine antibiotics (Yamashita et al. 1985).

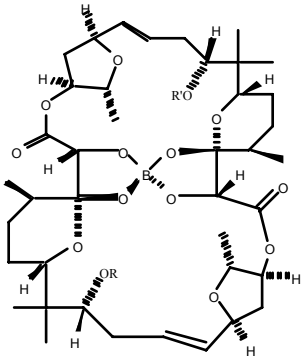

2: R=R'=H
3: R=H, R'=Ac
4: R=R'=Ac

Marine fungi also offer a potential source of bioactive compounds including alkaloids, polyketides, and terpenes. For example, an undescribed species of *Phoma* was isolated from the carapace of the crab *Chionoecetes opilio* which yielded the phomactines A-D; these act as inhibitors of PAF receptor binding (Sugano et al. 1994). The D analog (**5**) exhibited the lowest IC50 (= 0.12uM) of all conformers. In addition, it was discovered that these compounds don't effect the ADP-, arachidonic acid-, or collagen-induced platelet aggregation indicating phomactines represent a new class of potent and specific PAF antagonists.

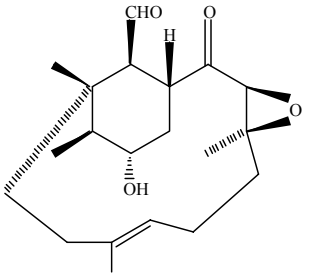

Recent evidence has confirmed the importance of microbial biofilms as settlement cues for invertebrate larvae representing diverse taxonomic affinities (Johnson & Sutton 1994, Keough & Raimondi 1995, Wieczorek et al. 1995). Included among the species which respond to biofilms are several examples of commercially cultured or harvested marine invertebrates (Cameron & Hinegardner 1974, Weiner et al 1985, Pearce & Scheibling 1991, Rodriguez et al 1995, Anderson 1996). Marine biofilms possess physical and chemical characteristics that can influence larval settlement. The presence of bacteria can significantly change the nature of a substrate through alteration of wettability; this can positively or negatively impact various larval settlers (Holmstrom & Kjelleberg 1994). Likewise, bacterial surface domain characteristics can influence cell-cell and cell-surface interactions. The production of exopolysaccharides might promote settlement: 1) by passive entrapment of the larvae, 2) by direct attraction of larvae, and 3) by amplification of inductive metabolites sequestered within the slime layer (Bonar et al. 1986, Szewzyk et al. 1991). Bacteria-derived inductive chemical cues have proven exceptionally difficult to identify although evidence for their existence appears unequivocal. Unknown chemical "factors" have been isolated from *Alteromonas espejiana*, *Vibrio* sp., and *Shewanella colwelliana* (previously *Alteromonas colwelliana* and LST) which induce settlement in a hydrozoan, a scyphozoan, and 2 species of oysters respectively (Neumann 1979, Weiner et al. 1989, Leitz & Wagne 1993). While various neurotransmitters and inorganic compounds can be used by aquaculturists to induce laboratory settlement and metamorphosis of commercially-important marine invertebrates, the compounds are often very costly and use can lead to

significant developmental aberrations and post-settlement mortality (Hadfield 1984, Pawlik 1990, Slattery 1992). Thus the search for natural inducers of larval settlement is still warranted and requisite for cost-effective hatchery reared resources.

Marine microbes have been notoriously difficult to culture despite evidence for vast numbers and species diversity in seawater (Sieburth 1979). Direct enumeration of seawater samples using fluorochrome stains indicate that as much as 99% of the bacteria in any given sample are incapable of forming colonies on traditional media formulations (Daley & Hobbie 1975; Kirchman et al. 1982). These media typically incorporate complex carbon and nitrogen sources at concentrations that are an order of magnitude higher than found in the oligotrophic conditions of the open ocean (*sensu* Valiela 1984). Moreover, the observations that marine bacterial growth can be inhibited by peptone and some amino acids (Buck 1974; Button et al. 1993), and that many marine bacterial species exhibit physiological adaptations to growth in low nutrient conditions (Roszak & Colwell 1987; Ostling et al. 1993), indicate that the successful culture of marine microbes will need to be based on specific low nutrient formulations. Recent high recoveries of viable marine bacteria have utilized pre-dilution of microbes and low nutrient formulations (Schut et al. 1993; Jensen et al. 1996).

Executive Summary

Extremophile microbes, specifically those from methane hydrate seeps in the Northern Gulf of Mexico, represent a potentially important and novel resource for marine biotechnology. Microbes are known to produce up to one third of all antibiotics on the market today, and deep sea organisms also produce unusual enzymes that operate under extreme pressures and temperatures. The purpose of this project was to isolate strains of microorganisms from the methane hydrate seep sites, to culture these strains in our labs at the University of Mississippi, and to test broth extracts for unusual biomedical activity. Our group conducted a broad survey of the microorganisms from the 2002 GOM cruise, and isolated at least 237 strain. During the 2003 GOM cruise, we specifically assessed actinomycetes using selective media and isolated at least 41 strains. Those isolates have been maintained in our culture facility for 3-15 mos (= 1-5 cell line transfers) on specific media developed for this purpose. Approximately 26% of the isolates were cryophilic and 12% had unusual hydrocarbon nutrient requirements suggesting they might contain novel enzymes with biotechnological roles (antifreezes and oil spill remediation, respectively). EtOAc broth extracts yielded a biomedical “hit rate”, in at least one of our antimicrobial screens, of 6% compared to an average of 5% for most of our shallow-water microbial isolate extracts. Preliminary chemical fingerprinting LC/MS data indicate that unusual halogenated compounds may be relatively common amongst these bioactive extracts. Bacteriaphage experiments and further isolation/structure elucidation of the bioactive constituents are ongoing and will form the general outline of a PhD dissertation (T. Hodges; University of Alabama, expected completion 2007).

Experimental

To maximize species diversity, marine microbes will be collected from multiple cores taken at the GOM methane hydrate seep sites. Sites will be chosen based on eco-physiological variability which can have tremendous influence on phenotypic (=chemical compounds)

variation (Harvell et al. 1993; Slattery & Paul in press). For instance, we will collect in the shallow intertidal communities, deeper soft-bottom habitat characteristic of the Gulf Coast and the relatively rare hard-bottom structures, as well as in and outside of run-off plumes (varying in size from the Mississippi River to seasonal streams). Likewise seasonal collections will increase the chances of isolating temporally discrete microbial blooms. It is often difficult to isolate enough microbial cells from seawater samples so these collections will focus only on the benthic microbial fauna. I have had much success in swabbing substrate and/or sediment in situ using clinical culturettes® (Slattery et al. 1995). These can be stored for up to 3-5 days (ie. the approximate time of a collection trip) prior to isolation in the laboratory onto marine agar plates. Isolated strains are then cultured in batch marine broth (alternatively, I have utilized Mueller-Hinton and Sabaroud Dextrose successfully for certain microbe species) on a shaker table at approximate ambient conditions. Subsamples of the monocultures are stored frozen (-80º C), lyophilized, and under oil for subsequent identification or re-isolation of bioactive species.

Marine microbes exhibit much variability in doubling times, however it is my experience that a batch culture (approximately 50 ml broth in a 125 ml flask) usually produces detectable quantities of bioactive compounds within 5-8 days. The broth will be extracted in a separatory funnel using 1:1 methylene chloride/methanol and the resulting lipophilic and hydrophilic fractions will be dried under reduced pressure (Okazaki & Okami 1972). A bioassay guided scheme (see below) will guide subsequent fractionation via column- and high performance liquid chromatography (Still et al. 1978). As the sample becomes progressively purer, NMR can be used to assist in dereplication. Those samples that show the greatest activity and/or potential for development can be re-isolated from fermentation plants (ie., liter+ batch cultures) using the archived microbes and taxonomic identities ascertained with BioLog methodologies. In addition, compound selectivity can be enhanced through the production of novel microbial biotransformation analogs (Clark & Hufford 1991).

Chemo-attractant/repulsive compounds from the batch microbe cultures will be assessed using standard microalgae and invertebrate larval assays (Rittschof et al. 1984; Rittschof et al. 1988; Slattery 1992; Slattery et al. 1995). It is my experience that *Navicula* sp., *Balanus amphitrite*, and *Bugula neritina* represent significant and common fouling organisms on the Gulf Coast; *Crassostrea virginica* represents the most common wild mollusc species along the Southeast Gulf Coast and a potential species for aquaculture. The experimental techniques have been previously described; briefly, cultures of either microalgae, barnacles, bryozoans, or oysters are maintained in the laboratory and subsampled at a stage prior to spawning and/or settlement. Diatoms or larvae are introduced to a container with either control nutrients (Guillard's f/2 for diatoms: Guillard 1983) &/or seawater, or microbe isolated compounds resuspended at natural concentrations in nutrients &/or seawater to assess chemically-mediated settlement cues. These data will have implications either to aquaculture (enhancement) or fouling prevention (inhibition). Moreover, the compounds will be tested in a standard battery of pharmaceutical assays (tumor, protozoal, microbial, opportunistic infection, malarial) established at the National Center for the Development of Natural Products; these assays will determine the practicality of drug development from marine microbial sources.

Results and Discussion

Between August and December of 2002, single strains of bacteria and fungi were isolated from the mixed cultures obtained from gas hydrate sites in the Gulf of Mexico. At least 237 strains of microorganisms, including a number of Streptomyces and fungi, were isolated from the 2002 gas hydrate cruise. The isolated microorganisms were stored on media slants at 4ºC. Now that these microorganisms have been isolated, work has been initiated on small scale broth cultures

and solvent extraction of some of theses microbes. The extracts of these microorganisms will be submitted for biomedical evaluation. We have a number of cellular based biomedical assays at our disposal for the screening of these extracts; these include antibacterial, anticancer, antimalarial, and antifungal bioassays.

	2002	2003
Number of Isolates	237	41
Number of Cryphiles	58	13
Number of Hydrocarbon Metabolizers	27	6
Number Biomedical Hits	3	13

On the August 2003 Gulf of Mexico cruise, our efforts were focused on marine sediment in the vicinity of gas hydrate mounds. We were particularly focusing on isolation of actinomycete species and organisms capable of degrading hydrocarbon mixtures found in crude oil. A variety of cultivation medias were employed for this purpose. Although some colonies have appeared, minimal work has begun on isolation of individual strains. These organisms are being grown near environmental temperatures, and many reproduce slowly under these conditions. Another experiment conducted on the most recent cruise was the collection of sediment for isolation of bacteriophage capable of infecting bacteria collected at similar sites. We are using bacteria collected from the 2002 cruise as indicator strains for bacteriophage infection. bacteriophage have been shown to have important roles in bacterial ecosystems, and are relatively unexplored from these environments.

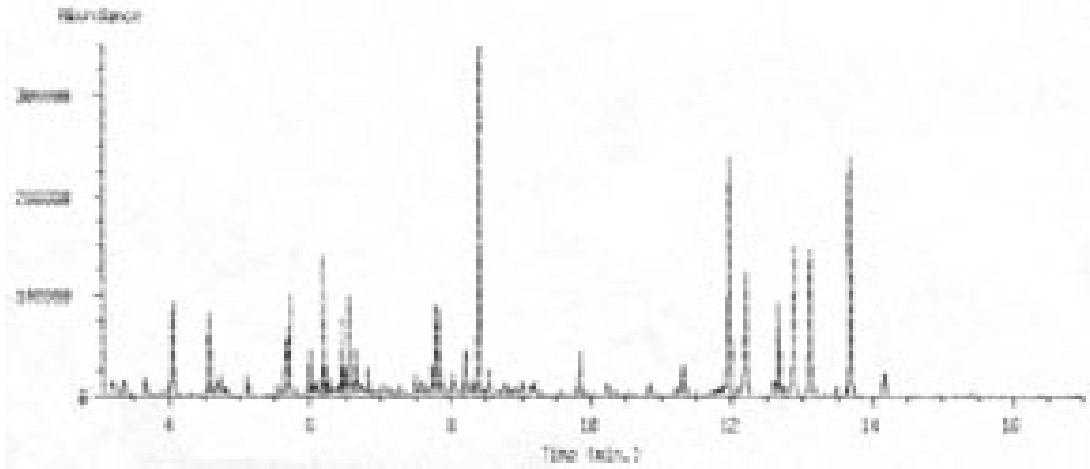

Representative LC/MS fingerprint of marine microbe EtOAc broth extract. Data indicate that several metabolites are produced, and MS peak picks indicate that several of these compounds contain unusual halogenation and probably novel structures.

Conclusion

Our group has isolated several hundred extremophile microbe strains, and has developed culture methods to maintain these strains in the laboratory. Many of these strains appear to be cryophilic (i.e., they cannot adapt to laboratory bench temperatures and only survive at 4°C), and several appear to have unique hydrocarbon requirements probably representative of their adaptation to the methane hydrate seep environment. While the degree of novel biomedical activity was modest, it did overlap with activity levels reported previously by our group from shallow coastal (Florida) and coral reef (Bahamas, Belize, Jamaica, Ponape, Guam, Saipan, Hawaii, and Egypt) ecosystems. Moreover, preliminary LC/MS chemical fingerprinting data indicate that the bioactivity may be due to unique natural products with unusual halogenation patterns. Ongoing research by our group will examine the biotechnological potential for enzymes responsible for hydrocarbon utilization, and the importance of bacteriophages to deep sea microbial communities.

Department of Energy via University of Mississippi
Coperative Agreement DE-FC26-00NT40920
Scripps Institution of Oceanography Microbiology and Geochemistry
Final Report

PI: Douglas H. Bartlett, Professor
Marine Biology Research Division
858-534-5233
dbartlett@ucsd.edu

Co-PI: Miriam Kastner, Professor
Geosciences Research Division
858-534-2065
mkastner@ucsd.edu

Scripps Institution of Oceanography
University of California, San Diego
La Jolla, CA 92093

Abstract:

Funds from this award were used for the partial support of two Staff Research Associates, supplies, flux meters and travel to the University of Mississippi, Oxford for planning meetings.

Microbiological analyses were performed on a sediment core obtained near the monitoring station. DNA was extracted from this material and used to isolate and characterize 16S rRNA bacterial gene sequences, from which inferences were obtained regarding the diversity of microorganisms present . The results indicated a remarkable similarity to *Bacteria* present in other anoxic hydrocarbon seep/hydrate environments examined in other parts of the world. The great majority of the *Bacteria* belonged to the *epsilon- Proteobacteria* cold seep group.

Geochemical analyses were performed on pore fluids from sediment push cores at Bush Hill (BH) and on water column samples at and near the main Bush Hill plume. Pore fluid samples from the cores and CTD water samples were analyzed for the depth distributions of dissolved methane, Cl, Ca, Mg, alkalinity, sulfide, and sulfate concentrations, and for dissolved inorganic carbon (DIC) and methane $\delta^{13}C$ values. The spatial and depth distribution of pore fluid solute concentrations provide information on the subsurface hydrology, and on solute fluxes across the sediment-water interface. The pore fluid chemistry indicates regional sulfate reduction and anaerobic methane oxidation (AMO), particularly intense in and near seeps, the intensity is manifested by the spatial distribution of benthis chemosynthetic communities, and *in situ* methane hydrate formation and authigenic carbonate formation near the sediment-water interface at and in the vicinity of the main BH plume. In the water column, a significant enrichment in $^{13}C\text{-}CH_4$ along isopycnals away from the plume, from the methane source, is observed, indicative of extensive aerobic methanotrophy in the water column. The $\delta^{3}C\text{-}CH_4$ value range from -41 to -49‰ at Bush Hill.

List of Graphical Materials:

Table 1: Similarity of selected Bush Hill 16S RNA sequences with those present at the National Center for Biotechnology Information.

Figure 1: Pore fluid δ^{13}C-DIC (‰) versus Alkalinity (mM) at Bush Hill and GC234.

Figure 2: Water column methane concentrations at and near the methane hydrate mound plume, at Bush Hill.

Introduction:

Microoorganisms are likely to play important roles in the formation, stability and decomposition of gas hydrates and hydrocarbons present in sediment pore fluids. A number of methodologies have been used to characterize the microbial diversity associated with cold seep or gas hydrate environments. These include 16s rRNA gene sequencing (3, 4, 6, 9, 13, 19, 21), lipid stable isotope analyses (9, 23), fluorescent in situ hybridization (4, 20, 23-25), secondary ion mass spectrometry (24, 25), and more recently proteomics (12). An excellent recent review of this topic can be found in a book chapter by Widdel et. al (30).

The results of these studies suggests that anaerobic methane oxidation (AMO) in these settings is frequently accomplished through the activities of methanogen-like archaea belonging to the ANME-1 or ANME-2 groups, in syntrophic association with sulfate-reducing bacteria, typically members of the Desulfosarcinales order. These associations may not always be necessary for AMO as in many cases ANME-1 and ANME-2 archaea are present in monospecific cell aggregates (25). Studies of this biochemical process have been greatly hampered by the lack of cultures of microbes capable of AMO, but laboratory incubation experiments have been performed which support a linkage between AMO and sulfate reduction (8, 22).

At this time relatively few studies have been performed on the microbial diversity associated with the hydrates and hydrocarbon seeps present in the Gulf of Mexico. The Gulf of Mexico hydrate and seep environments are distinct from other regions studied to date by the presence of both thermogenic and biogenic methane, as well as a variety of aliphatic and aromatic hydrocarbons (see for example, (28). Lanoil et. al (13) have reported on bacterial and archaeal diversity associated with thermogenic and biogenic gas hydrates taken from the Gulf of Mexico. Their results indicated moderately high bacterial diversity, but low archaeal diversity, with most of *the Archaea* being closely related to members of the Methanosarcinales. More recently Mills et. al (21) have published on the microbial diversity present on hydrates and associated sediments obtained from two gas hydrate sedimentary systems in the Gulf of Mexico. As with the Lanoil study they also found low archaeal diversity. However, the bacterial diversity in their samples was lower than that of Lanoil. 62% of their clones were most closely related to the *epsilon-Proteobacteria (ε-Proteobacteria),* and *delta-Proteobacteira (δ-Proteobacteria)* were also highly abundant.

In this project we have used culture-independent rRNA sequence analyses to assess the bacterial diversity in a sediment sample in the vicinity of the monitoring station. Our results indicate a large fraction of *ε-Proteobacteria* belonging to a group of clones that has come to be known as the cold seep group (10). We suggest that there is a need for further investigations of the activities of these microbes in anoxic hydrocarbon-bearing sediments.

Seafloor or shallow-buried gas-hydrates, within 10-30 mbsf, have been recovered at Hydrate Ridge and offshore Vancouver, Cascadia, (e.g. Kastner et al., 1998; Suess et al., 1999; Spence et al., 2000; ODP Leg 204 reports). Near seafloor hydrates have also been recovered in the Eel River Basin, northern California (brooks et al. 1991), Okhotsk Sea and Black and Caspian Seas (Kvenvolden et al., 1993). The seafloor occurrence is especially prominent and the Gulf of Mexico, at Bush Hill (e.g. Macdonald et al., 1994).The occurrence of methane hydrate near or at the seafloor indicates active upward advection of methane-rich fluids or of methane gas. The seafloor and shallow buried gas hydrates are the most vulnerable hydrates to global warming. The environmental impact of release of large quantities of methane into the ocean and atmosphere could have important societal and microbiological consequences.

The Bush Hill hydrate mound site has been studied extensively for some time (e.g. MacDonald et al., 1994; Sassen et al., 1998; Aharon and Fu, 2000; and references therein). However, *in situ* temperature monitoring, continuous flux measurements, and the impact of the methane advection into the water column have not been documented as yet.

In this project we focused on documenting the present system that maintains the BH hydrate mound. The main questions we tried to address were: what is the subsurface hydrology, what are the methane and solute fluxes at the hydrate mound, in the vicinity, and at a "background" site; how much of the methane escapes across the seafloor into bottom water; how much of the methane gets oxidized in the water column, thus how much escapes into the atmosphere. Accordingly, we recovered push cores as close to the mound as possible and in the vicinity and regionally, we analyzed the pore fluids for methane, major and minor component concentrations, and for methane and DIC C-isotope ratios; we analyzed the water column samples for methane concentrations and $\delta^{13}C$ values, and deployed flux meters, MOSQUITOs (Multiple Orifice sampler and Quantitative Injection Tracer Observer), at critical sites for long-term continuous monitoring seafloor temperature and sampling fluids and gases. The processing of the flux data are still in progress.

Experimental:

Sediment Collection:

Sediments were recovered with push cores near and in the vicinity of the Bush Hill hydrate mound, as well as regionally, to document "background" properties. At each sediment sampling site a separate push core was recovered for pore fluid chemistry, and a third core for dissolved methane concentration analysis. For microbiology, sediment was obtained from push core #8, obtained during Johnson Sea Link submersible Dive # 4556 (2003), from a water depth of 1772 feet located at N 27deg 46.953', W 91deg 30.4724'. It was in the footprint of our MOSQUITO #1 Osmotic Sampler which was deployed in a mussel field just west of the main Bush Hill hydrate mound. The sediment used for molecular biology was from 5-10 cm below the surface. Authigenic carbonates were as well recovered, but as yet not analyzed.

DNA isolation, PCR amplification, and cloning:

Total nucleic acids were extracted from 1 g of sediment using the Ultraclean Soil DNA Isolation Kit (MO BIO Laboratories, Inc.). Modifications to the standard protocol included bead-beating the sediment for 25 seconds at 4.5m/s (Mo Bio Laboratories), following the extraction with a chloroform: isoamyl alcohol (24:1) clean-up, and precipitating the DNA with 3M sodium oxaloacetate and 2 volumes of 95% ethanol (personal communication, Brian Lanoil). Bacterial 16s rDNA was amplified using primers Eub27F and Eub1492R (7). The PCR conditions used were 40 seconds of denaturation at 94°C, 40 seconds of annealing at 48 ^{o}C, and 2 minutes of elongation at 72 ^{o}C for 25 cycles in an Applied Biosystems GeneAmp PCR System 2700 thermal cycler. Amplification products were cloned into vector pCR2.1 according to the TOPO TA cloning kit instructions (Invitrogen, Carlsbad, Calif).

RFLP analysis and sequencing clone libraries:

The 16s rDNA inserts were amplified using M13 primers. The polymerase chain reaction conditions used were 40 seconds of denaturation at 94 ^{o}C, 40 seconds annealing at 52 ^{o}C, and 2 minutes of elongation at 72 ^{o}C for 30 cycles. The product was digested with *Hae III* restriction endonuclease (New England Biolabs, Beverly, Mass.) at 37 ^{o}C for 2 hours. Banding patterns were grouped according to similarity, and representative members of each pattern group were fully, bidirectionally sequenced using M13 primers by San Diego State University Core Facility.

Pore fluid and water column Analyses:

Pore fluids were recovered by centrifuging subsections of the push cores at *in situ* temperature and under anaerobic conditions. The samples were immediately analyzed for alkalinity and sulfide and sulfate concentrations, and different aliquots were individually pretreated, depending on the component, and appropriately stored for shore-based analyses. For most solutes the pore fluids were analyzed by ICP-OES or ICP-MS. Chloride concentrations were determined by titration with $AgNO_3$, and Sulfate concentrations were also determined by IC. The pore fluid samples for methane and other hydrocarbon analyses, as well as and the water column samples were stored in serum bottles poisoned with mercuric chloride. Concentrations of hydrocarbons were measured by gas chromatography and the $\delta^{13}C$-CH_4 -and-DIC were determined by mass spectrometry. The flux meter data in progress are being analyzed for dye concentrations; the degree of the dye dilution is determined by the fluid flow rate.

Results/Discussion:

The bacterial diversity present in the Bush Hill sediment sample is presented in Table 1. Restriction fragment length polymorphism analysis indicated 6 dominant clone types. However, sequence analysis of representatives of these clones revealed that 4/6 were derived from closely related members of the *ε-Proteobacteria* cold seep group (10). The remaining clones reflected affiliation with the genus *Holophaga* and the order *Desulfosarcinales*. All of the sequences were obtained from *Bacteria* closely related to microbes obtained in other cold-seep marine sediments.

The predominance of the *ε-Proteobacteria* in our sample is quite striking. Related Bacteria are probably best appreciated as members of microbial mats or ectosymbionts of invertebrates in hydrothermal vent environments. For example, similar microbes have been detected in the mucous secretions of the hydrothermal vent polychaete *Paralvinella palmiformis* (1). Culture-dependent and independent methods have resulted in the identification of similar *ε-Proteobacteria* from white tubes of the polychaete *Alvinella pompejana* collected on East Pacific Rise at 13ºN (2) Cambon-Bonavita et. al; unpublished results). They have also been found in a microbial mat from an active hydrothermal vent system in Hawaii (Moyer, Dobbs and Karl; unpublished results).

Table 1: Similarity of selected Bush Hill 16S RNA sequences with those present at the National Center for Biotechnology Information.

Sequence Type	Closest match or clone name	% identity	Phylogenetic affiliation
BH8	Uncultured hydrocarbon seep clone (AF154101)	97%	ε-*Proteobacteria*
BH10	Nankai Trough cold seep clone (AB013263.1)	96%	ε-*Proteobacteria*
BH13	Nankai Trough cold seep clone (AB013263.1)	96%	ε-*Proteobacteria*
BH23	Cariaco Basin anoxic zone (AF224803.1)	96%	ε-*Proteobacteria*
BH15	Nankai Trough cold seep clone (AB013269.1)	97%	**Holophaga**
BH25	Santa Barbara Basin cold seep clone (AF354158)	94%	δ-*Proteobacteria* (*Desulfosarcinales*)

Many cultured vent □-*Proteobacteria,* such as *Sulfurimonas autotrophica*, grow chemolithoautotrophically with elemental sulfur, sulfide and thiosulfate as sole electron donors and oxygen as electron acceptor, while others are able to grow oxidizing hydrogen and using sulfur, thiosulfate or nitrate as an electron acceptor (2, 11, Takai et al.; unpublished results). The latter physiological mode could be operating within anoxic cold-seep sediments, such as those from which our Bush Hill sample was obtained.

The ε̃*Proteobacteria* cold-seep group has been observed in many clone libraries obtained from seep or probable seep environments. These include the anoxic zone of the Cariaco Basin where *Euryarchaeota* sequences implicated in anaerobic methane oxidation (AMO) have also been noted (18). The Cariaco Basin is known to be rich in methane (29). Other sites include the Nankai Trough at a depth of 3.8 km where AMO communities have been found and a model for AMO presented (14, 15), various depths and locations within the Japan Trench (10, 15), and methane-rich borehole fluid obtained from Ocean Drilling Project borehole 892b off the coast of

Oregon (3). Many of our clones also display high similarity to sequences derived from a hydrocarbon seep environment not yet described (O'Neill et. al; unpublished results, see accession number AF154101 for example). In the case of one Japan Trench cold seep study it was discovered that shallow sediments of 2-4 cm contained mostly □-*Proteobacteria* whereas deeper sediments of 8-10 and 14-16 cm contained increasing proportions of □-*Proteobacteria* (10).

The δ-*Proteobacteria* clones are all closely related to the putative AMO syntrophic group, such as those previously described by the DeLong research group in Eel River Basin seep sediments and in the Santa Barbara Basin (23). They are also similar to clones obtained from anoxic sediments from marine salinity meromictic lakes and a coastal meromictic marine basin, Vestfold Hilds, in eastern Antarctica (5). These microbes have been hypothesized to function as sulfate-reducing partners with anaerobic methane-oxidizing Archaea (see for example (30).

The last additional bacterial group observed in our sample belonged to the little-known *Holophaga/AcidobacteriumGeothrix* phylum and the genus *Holophaga*. This genus has been detected in diverse 16S rRNA gene libraries retrieved from diverse soil, sediment and aquatic environments (17). Little is know about the physiological properties of Holophaga except that its one cultured member, *H. foetida*, is an obligate anaerobe, isolated from a black anoxic freshwater mud sample, and it degrades aromatic compounds to acetate (16). *Holophaga* clones have previously been detected in cold-seep sediments of the Nankai Trough (14), sediment samples collected at Hornsund off the coast of Spitsbergen, in the Arctic Ocean (26), Eastern Antarctica anoxic sediments (5), and in anaerobic marine sediments enriched with organic carbon (27). Curiously, *Holophaga* is related to *Geopsychrobacter multivorans* which is being evaluated for electricity production by as a marine sediment fuel cell (Holmes et. al; unpublished results, see accession number AY579996.1).

The pore fluid data indicate that although sulfate reduction and anaerobic methane oxidation is regionally pervasive, methane (plus other hydrocarbons) upward advection is mostly focused at BH; the intensity and frequency of focused sites increases at and adjacent to the hydrate mound. This is manifested in the very high alkalinity concentrations, > 40 mM at and near the mound, and the low δ^{13}C-DIC values, shown in Figure 1, a cross plot of δ^{13}C-DIC (‰) versus alkalinity (mM). Most interesting is the observation that unlike at north and south Hydrate Ridge, for example, where δ^{13}C-DIC values range from -25 to -49‰, the most negative δ^{13}C-DIC value at BH (Fig. 1) is ~ -22‰. This indicates that at BH crude oil serves as the primary electron-donor and metabolic substrate for anaerobic sulfate reduction. Calcium, Mg, and Sr concentration profiles indicate *in situ* carbonate precipitation, some of the sulfide precipitates as Fe sulfides, and Cl concentrations indicate *in situ* methane hydrate formation at and adjacent to the main BH mound and methane seep. The high chlorinities in the pore fluids are localized in specific horizons of active hydrate formation, are not pervasive throughout the concentration-depth profiles, thus, do not suggest that brines are controlling the stability of the BH hydrate mound.

Water column methane concentration (Fig. 2) and isotope data show that at the main plume methane concentrations are high, and even in the uppermost 5 meters of the water column seawater is considerably supersaturated (150-200 times) with respect to methane, hence, methane escapes into the atmosphere.The methane flux at this and other plume sites in the Gulf of Mexico is as yet unknown. Away from the plume methane concentrations decrease rapidly (Fig. 2) and the δ^{13}C-CH_4 values indicate aerobic methanotrophy is widespread, following the reaction:

$$CH_4 + 2O_2 \rightarrow CO_2 + H_2O$$

In addition to depleting dissolved oxygen concentrations, this reaction effects the δ^{13}C-DIC values of the bottom waters at and near the BH mound and main plume, where methane concentrations are high, therefore also the C isotope values of benthic carbonates.

Conclusions:

All of the microbial phylotypes discovered through this study are related to clones present in other hydrocarbon seep environments. Their presence suggests that active hydrocarbon (in particular methane) consumption is taking place at the study site. Considering the prevalence of □-*Proteobacteria* cold seep group clones, AMO syntrophic SRB group □-*Proteobacteria* and *Holophaga* species in many seep environments, including that of Bush Hill, future studies should be directed at their culturing and physiological characterization. Genomic and functional genomic studies of the bacterial components of seep environments is also likely to reveal new insights into microbial influences on hydrocarbon gases and hydrates.

The intense anaerobic sulfate reduction and AMO in the subsurface strongly influence the pore fluid chemical environment, thus the microbiology. Methane and other hydrocarbon fluxes at BH are highly focused. At and near seeps pore fluid chemistry indicates that in addition to the coupled reactions of anaerobic sulfate reduction and AMO, methane hydrate, authigenic carbonates, and Fe-sulfides precipitate *in situ.* The pore fluids DIC □ ^{13}C values indicate that at BH crude oil serves as the primary electron-donor and metabolic substrate for anaerobic sulfate reduction. Much methane escapes across the sediment-water interface; analysis of the fluxes of methane and other solutes across the seafloor is in progress. In the water column aerobic methanotrophy is suggested by the dissolved methane C isotope values. Where methane fluxes are high this reaction utilizes dissolved oxygen, thus its concentration, and also the □ ^{13}C-DIC values. At and adjacent the main BH methane plume, methane escapes into the atmosphere.

List of References:

1. **Aharon, P., and F. Baoshun.** 2000. Microbial sulfate reduction rates and sulfur and oxygen isotope fractionations at oil and gas seeps in deepwater Gulf of Mexico. Geochim. Cosmochim. Acta **64**:233-246.
2. **Alain, K., M. Olagnon, D. Desbruyeres, A. Page, G. Barbier, S. K. Juniper, J. Quellerou, and M. A. Cambon-Bonavita.** 2002. Phylogenetic characterization of the bacterial assemblage associated with mucous secretions of the hydrothermal vent polychaete *Paralvinella palmiformis*. FEMS Micro. Ecol. **42:**463-476.
3. **Alain, K., M. Zbinden, N. Le Bris, F. Lesongeur, J. Querellou, F. Gaill, and M. A. Cambon-Bonavita.** 2004. Early steps in microbial colonization processes at deep-sea hydrothermal vents. Environ. Microbiol. **6:**227-241.
4. **Bidle, K. A., M. Kastner, and D. H. Bartlett.** 1999. A phylogenetic analysis of microbial commuities associated with methane hydrate containing marine fluids and sediments in the Cascadia Margin (ODP site 892b). FEMS Microbiol. Lett. **177:**101-108.
5. **Boetius, A., K. Ravenschlag, C. J. Schubert, D. Rickert, F. Widdel, A. Gieseke, R. I. Amann, B. B. Jørgensen, U. Witte, and O. Pfannkuche.** 2000. A marine microbial consortium apparently mediating anaerbic oxidation of methane. Nature **407:**623-26.
6. **Bowman, J. P., S. M. Rea, S. A. McCammon, and T. A. McMeekin.** 2000. Diversity and community structure within anoxic sediment from marine salinity meromictic lakes and a coastal meromictic marine basin, Vestfold Hilds, Eastern Antarctica. Env. Microbiol. **2:**227-237.
7. **Brooks, J.M., M.E. Field, and M.C. Kennicut.** 1991. Observations of gas hydrates in marine sediments, offshore northern California. Mar. Geol. **96**, 103-109.
8. **Carson, B., M. Kastner, D. Bartlett, J. Jaeger, H. Jannasch, and Y. Weinstein.** 2003. Implications of carbon flux from the Cascadia accretionary prism: results from long-term, in situ measurements at ODP Site 892B. Mar. Geol. **198:**159-180.
9. **DeLong, E. F.** 1992. Archaea in coastal marine environments. Proc. Natl. Acad. Sci. U. S. A. **89:**5685-5689.
10. **Hansen, L. B., K. Finster, H. Fossing, and N. Iversen.** 1998. Anerobic methane oxidation in sulfate depleted sediments: effects of sulfate and molybdate additions. Aquat. Microbiol. Ecol. **14:**195-204.
11. **Hinrichs, K.-U., J. M. Hayes, S. P. Sylva, P. G. Brewer, and E. F. DeLong.** 1999. Methane-consuming archaebacteria in marine sediments. Nature **398:**802-805.
12. **Inagaki, F., Y. Sakihama, A. Inoue, C. Kato, and K. Horikoshi.** 2002. Molecular phylogenetic analyses of reverse-transcribed bacterial rRNA obtained from deep-sea cold seep sediments. Environ. Microbiol. **4:**277-286.
13. **Inagaki, F., K. Takai, K. I. Hideki, K. H. Nealson, and K. Horikishi.** 2003. *Sulfurimonas autotrophica gen. nov., sp nov*., a novel sulfur-oxidizing epsilon-proteobacterium isolated from hydrothermal sediments in the Mid-Okinawa Trough. Int. J. Syst. Evol. Microbiol. **53:**1801-1805.
14. **Kastner, M., K.A. Kvenvolden, and T. Lorenson.** Chemistry, isotopic composition, and origin of methane hydrogen sulfide hydrate at the Cascadia subduction zone. Earth Planet. Sci. Lett., **156**:173-183.
15. **Kruger, M., A. Meyerdierks, F. O. Glockner, R. Amann, F. Widdel, M. Kube, R. Reinhardt, R. Kahnt, R. Bocher, R. K. Thauer, and S. A. Shima.** 2003. conspicuous nickel protein in microbial mats that oxidize methane anaerobically. Nature **426:**878-881.
16. **Kvenvolden, K.A., G.D. Ginsburg, and V.A. Soloviev.** 1993. Worldwide distribution of subaquatic hydrates. Geo-Mar. lett., **13**:32-40.

17. **Lanoil, B. D., R. Sassen, M. T. La Duc, S. T. Sweet, and K. H. Nealson.** 2001. Bacteria and Archaea physically associated with Gulf of Mexico gas hydrates. Appl. Env. Microbiol. **67:**5143-5153.
18. **Li, L., J. Guezennec, P. Nichols, P. Henry, M. Yanagibayashi, and C. Kato.** 1999. Microbial diversity in Nankai Trough sediments at a depth of 3,843 m. J. Oceanography **55:**635-642.
19. **Li, L., and C. Kato.** 1999. Microbial diversity in the sediments collected from cold-seep areas and from different depths of the Deep-sea., Extremophiles in deep-sea environments., vol. pp.55-89. Springer-Verlag, Tokyo.
20. **Liesack, W., F. Bak, J. U. Kreft, and E. Stackebrandt.** 1994. *Holophaga foetida gen. nov., sp. nov*., a new, homoacetogenic bacterium degrading methoxylated aromatic compounds. Arch. Microbiol. **162:**85-90.
21. **Ludwig, W., S. H. Bauer, M. Bauer, I. Held, G. Kirchhof, R. Schulze, I. Huber, S. Spring, A. Hartmann, and K. H. Schleifer.** 1997. Detection and *in situ* identification of representatives of a widely distributed new bacterial phylum. FEMS Microbiol. Lett., **153:**181-190.
22. **MacDonald, I.R., N.L. Guinasso Jr., R. Sassen, J.M. Brooks, L.Lee, and K.T. Scott.** 1994. Gas hydrate that breaches the sea floor on the continental slope of the Gulf of Mexico. Geology **22**:699-702.
23. **Madrid, V. M., G. T. Taylor, M. I. Scranton, and A. Y. Chistoserdov.** 2001. Phylogenetic diversity of bacterial and archaeal communities in the anoxic zone of the Cariaco Basin. Appl. Env. Microbiol. **67:**1663-1674.
24. **Marchesi, J. R., A. J. Weightman, B. A. Cragg, R. J. Parkes, and J. C. Fry.** 2001. Methanogen and bacterial diversity and distribution in deep gas hydrate sediments from the Cascadia Margin as revealed by 16S rRNA moleculae analysis. FEMS Microbiol. Ecol. **34:**221-228.
25. **Michaelis, W., R. Seifert, K. Nauhaus, T. Treude, V. Thiel, M. Blumenberg, K. Knittel, A. Gieseke, K. Peterknecht, T. Pape, A. Boetius, R. Amann, B. B. Jorgensen, F. Widdel, J. R. Peckmann, N. V. Pimenov, and M. B. Gulin.** 2002. Microbial reefs in the Black Sea fueled by anaerobic oxidation of methane. Science **297:**1013-1015.
26. **Mills, H. J., C. Hodges, K. Wilson, I. R. MacDonald, and P. A. Sobecky.** 2003. Microbial diversity in sediments associated with surface-breaching gas hydrate mounds in the Gulf of Mexico. FEMS Micro. Ecol. **46:**39-52.
27. **Nauhaus, K., A. Boetius, M. Kruger, and F. Widdel.** 2002. *In vitro* demonstration of anaerobic oxidation of methane coupled to sulphate reduction in sediment from a marine gas hydrate area. Env. Microbiol. **4:**296-305.
28. **Orphan, V. J., K. U. Hinrichs, W. I. Ussler, C. K. Paull, L. T. Taylor, S. P. Sylva, J. M. Hayes, and E. F. DeLong.** 2001. Comparative analysis of methane-oxidizing archaea and sulfate-reducing bacteria in anoxic marine sediments. Appl. Environ. Microbiol. **67:**1922-1934.
29. **Orphan, V. J., C. H. House, K. U. Hinrichs, K. McKeegan, and E. F. DeLong.** 2001. Methane-consuming archaea revealed by directly coupled isotopic and phylogenetic analysis. Science **293:**484-487.
30. **Orphan, V. J., C. H. House, K. U. Hinrichs, K. D. McKeegan, and E. F. DeLong.** 2002. Multiple archaeal groups mediate methane oxidation in anoxic cold seep sediments. Proc. Natl. Acad. Sci. U. S. A. **99:**7663-7668.
31. **Ravenschlag, K., K. Sahm, J. Pernthaler, and R. Amann.** 1999. High bacterial diversity in permanently cold marine sediments. Appl. Environ. Microbiol. **65:**3982-3989.

32. **Rossello-Mora, R., B. Thamdrup, H. Schafer, R. Weller, and R. Amann.** 1999. The response of the microbial community of marine sediments to organic carbon input under anaerobic conditions. Syst. Appl. Microbiol. **22:**237-248.
33. **Sassen, R., S. Joye, S. T. Sweet, D. A. DeFreitas, A. V. Milkov, and I. R. MacDonald.** 1999. Thermogenic gas hydrates and hydrocarbon gases in complex chemosynthetic communities, Gulf of Mexico continental slope. Organic Geochem. **30:**485-497.
34. **Sassen, R., I.R. MacDonald, N.L. Guinasso, S. Joye, A.G., Requejo, S.T. Sweet, J. Alcala-Herrera, D.A. DeFreitas, D.R. Schink.** 1998. Bacterial methane oxidation in sea-floor gas hydrate: significance to life in extreme environments. Geology. **26**:851-854.
35. **Scranton, M. I.** 1988. Temporal variations in the methane content of the Cariaco Trench. Deep Sea Res. **35:**1511-1523.
36. **Suess, E., M.E. Torres, G. Bohrmann, R.W. Collier, J. Greinert, P. Linke, G. Rehder, A. Trehu, K. Wallmann, G. Winckler, and E. Zuleger**. 1999. Gas hydrate destabilization: enhanced dewatering, benthic material turnover and large methane plumes at the Cascadia convergent margin. Earth Planet Sci. Lett., **170**:1-15.
37. **Widdel, F., A. Boetius, and R. Rabus.** 2004. Anaerobic biodegradation of Hydrocarbons including methane. *In* M. E. A. Dworken (ed.), The Prokaryotes: An Evolving Electronic Resource for the Microbiological Community, 3rd edition, release 3.16, http://link.springer-ny.com/link/service/books/10125/. Springer-Verlag, New York.

Figure 1.

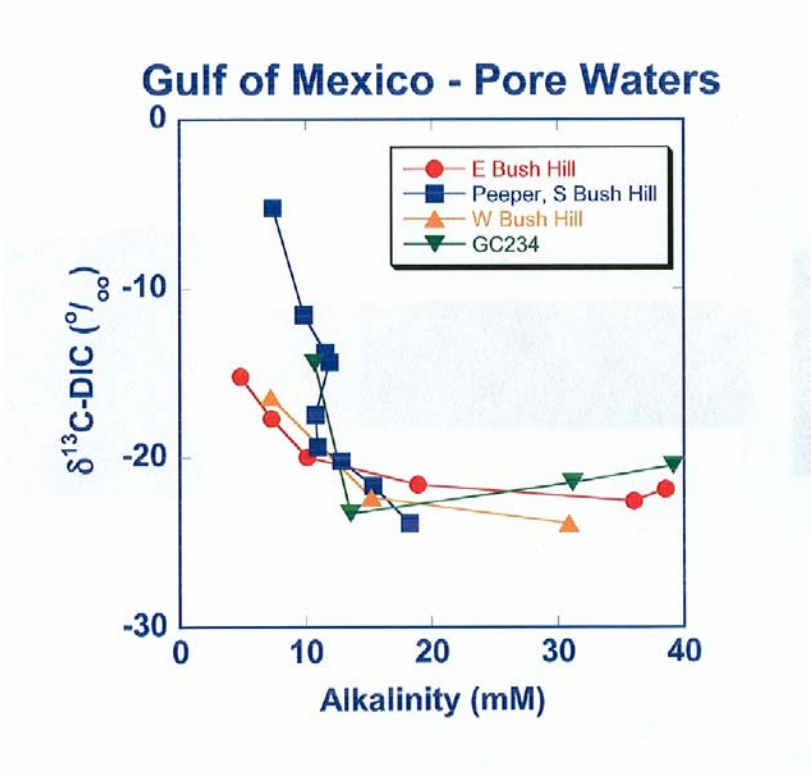
Gulf of Mexico - Pore Waters
E Bush Hill
Peeper, S Bush Hill
W Bush Hill
GC234
δ13C-DIC (°/oo)
0
-10
-20
-30
0
10
20
30
40
Alkalinity (mM)

Figure 2.

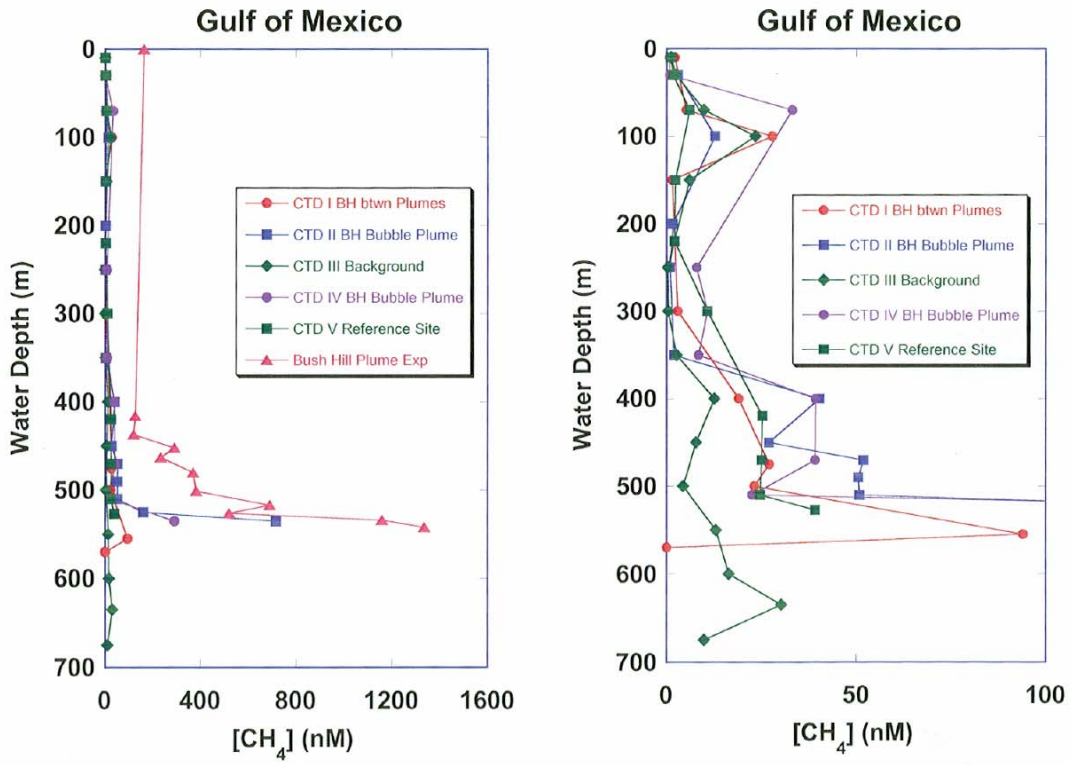
Gulf of Mexico
Water Depth (m)
[CH4] (nM)
CTD I BH btwn Plumes
CTD II BH Bubble Plume
CTD III Background
CTD IV BH Bubble Plume
CTD V Reference Site
Bush Hill Plume Exp
Gulf of Mexico
Water Depth (m)
[CH4] (nM)
CTD I BH btwn Plumes
CTD II BH Bubble Plume
CTD III Background
CTD IV BH Bubble Plume
CTD V Reference Site

List of Acronyms and Abbreviations:

AMO:	Anaerobic methane oxidation
δ:	delta
ε:	epsilon
rRNA:	ribosomal RNA
SRB:	sulfate-reducing bacteria
DIC:	Dissolved inorganic carbon
MOSQUITO:	Multiple Orifice Sampler and Quantitative Injection Tracer Observer
GOM:	Gulf of Mexico
BH:	Bush Hill

Establishing the Parameters Required for Spatial Models of Gas Hydrate Collections

Report of Findings: December 2003

DOE Cooperative Agreement DE-FC26-00NT40920

Joel S. Kuszmaul and Emily Strack
Department of Geology and Geological Engineering
The University of Mississippi
University, MS 38677

ABSTRACT

Global observations of gas hydrates provide a basis for characterizing and modeling the spatial continuity of gas hydrate environments. Indicator variography and logistic regression were applied to gas hydrate samples reported in published data sets. Each data set included sites where gas hydrates were observed or where drilling occurred without gas hydrate contact. The spatial distribution of the deposits within two study areas were characterized by preparing multiple experimental indicator variograms with values assigned as one for hydrate presence and zero for hydrate absence. The spatial distribution of gas hydrate deposits on a global scale was modeled using logistic regression. A best-fit model was determined based on the significance of multiple model variables.

An isotropic variogram with an active lag of 180 km and a uniform interval of 5 km produced the clearest structure for the Gulf of Mexico study area. The isotropic variogram was fit with an spherical model with a correlation length of 65 km, a sill value of 0.0396, and a relative nugget of 58.1%. The maximum direction of spatial continuity trends approximately 43° with the minimum axis at approximately 133°. Sampled sites are correlated at a distance of 35 km in the direction of maximum continuity and 25 km in the direction of minimum continuity. The sill value for an anisotropic spherical model was 0.0396 with a relative nugget effect of 63.1%.

An isotropic variogram with an active lag of 180 km and a uniform interval of 5 km produced the clearest structure for the Nigerian continental margin study area. The isotropic variogram was fit with a spherical model with a range of 110 km, a sill value of 0.035, and a relative nugget effect of 3.0%. No significant spatial anisotropy was evident in the Nigerian continental margin for the data set as a whole.

The nugget effect observed in the variogram models of both study areas is likely attributable to our definition of a find and may also be a consequence of the sampling procedures used to establish each data set. The maximum direction of spatial continuity derived from the Gulf of Mexico data set corresponds with the alignment of gas hydrate samples. The alignment suggests an underlying structural control on hydrate formation. Additional analysis, and perhaps additional sampling, is required for investigations of anisotropy in the Gulf of Guinea case. Indicator variograms suggest a spatial relationship does exist between gas hydrate locations as a function of both distance and direction. The stability of the spatial structure suggests a sufficient stationarity of hydrate forming processes that can be used for spatial prediction with stochastic models.

A best-fit logistic regression model for determining the conditional probability of gas hydrate occurrence includes two independent variables, water depth and temperature. The model accurately classifies the presence of gas hydrate at approximately 80% of the known gas hydrate locations. An improved dataset including all recently discovered gas hydrates as well as more observations where gas hydrates have not been found would serve to further verify the value of a logistic regression model.

List of Figures

Figure 1: Isotropic experimental variogram and best-fit model for the Gulf of Mexico

Figure 2: Anisotropic experimental variogram and best-fit model for the Gulf of Mexico

Figure 3: Isotropic experimental variogram and best-fit model for the Gulf of Guinea

Figure 4: Isotropic conditional probability map of gas hydrate occurrences: Gulf of Mexico

Figure 5: Residual plots for logistic models

Figure 6: Predictive ability of the selected logistic regression model

List of Tables

Table 1: Isotropic model results for the Gulf of Mexico and the Gulf of Guinea

Table 2: Anisotropic model results for the Gulf of Mexico

Table 3: Logistic regression model statistics

Table 4: Classification table based on the logistic regression model

INTRODUCTION

Environments conducive to natural gas hydrate formation occur worldwide in both polar and marine environments. Globally, gas hydrates have been discovered in nineteen regions, including the continental slopes of the Gulf of Mexico and offshore Nigeria (Kvenvolden, 1993). Research into the occurrence, distribution, and detection of gas hydrate deposits has escalated in the past decade because (1) gas hydrates represent a potential energy source, (2) gas hydrate formation and destabilization alters the geotechnical properties of surrounding sediments potentially causing mass movements and offshore drilling difficulty, and (3) the dissociation of gas hydrate may be a significant factor in global climate change.

The objectives of our study focused on (1) summarizing the controls on hydrate formation in marine sediments, (2) describing how the spatial continuity of gas hydrate deposits change as a function of distance and direction, and (3) determine the best-fit model to describe the relation between gas hydrate occurrences and properties of the surrounding environment. The purpose of this modeling was to characterize the spatial continuity of gas hydrate depositional environments. This characterization should prove valuable in the study of the distribution of gas hydrate deposits and may be valuable in assisting in improving the ability to predict the location of future finds of these deposits.

The analysis begins with isotropic variograms to define the distance parameters that produce the clearest structure. Anisotropic variograms are investigated to determine the directional dependence or pattern in the spatial continuity of the area. Models based on the sample variograms were used in indicator kriging to estimate the conditional probability of finding gas hydrate locations within the study areas.

A logistic regression analysis was used to determine a best-fit model that describes gas hydrate occurrences based on environmental properties associated with known gas hydrate deposits. The logistic model takes account of our binary dependent variable and can be used to calculate the conditional probability of observing gas hydrate at unsampled locations.

CONTROLS ON GAS HYDRATE FORMATION

Natural gas hydrates form a class of chemical compounds known as clathrates (Kaplan, 1974). Gas hydrates consist of a rigid structure of a low-molecular weight gas (typically methane) surrounded by water molecules. The water molecules form rings joined by hydrogen bonds which host gas molecules, producing a stabilized crystalline structure.

Stability Regime

Gas hydrate formation depends on a specific pressure-temperature regime. Hydrate deposits form where pressures are relatively high and bottom-temperatures approach 0°C. Adequate temperatures for hydrate deposition generally range from -8 to 12°C (Malone, 1994). The geothermal gradient of a region controls the maximum lower limit of temperatures facilitating hydrate formation. Fluctuations in bottom-water temperatures occur due to seasonal changes, propagation of warm water across slopes, and heat flow into sediments and the sea floor from the subsurface. Pressures conducive to hydrate formation range from approximately 3-60 MPa. The presence of higher molecular weight hydrocarbons serves to stabilize gas hydrates at higher temperatures and/or lower pressures (Brooks et al., 1986).

Gas Hydrate Stability Zone (GHSZ)

Variables used to predict the hydrate stability zone include bottom-water temperature, geothermal gradient, water depth, and gas availability and composition (Brooks et al., 1986). The sea floor forms the upper limit of the GHSZ in outer continental margin sediments (Kvenvolden and McMenamin., 1980). The intersection of the geothermal gradient and the projected hydrate phase boundary form the base of the GHSZ. Local controls influence the

actual location of the base of the GHSZ for a given area. In areas where the geothermal gradient is relatively constant, the thickness of the GHSZ increases with increasing water depth (Kvenvolden and McMenamin, 1980). The zone of actual gas hydrate accumulation often differs from the theoretical gas hydrate stability zone. The presence of gas hydrate above a regional phase boundary suggests additional factors other than pressure, temperature, and gas composition influence gas hydrate accumulation (Booth et al., 1996).

Water Depth and Sediment Depth

Marine bathymetry and sediment thickness also influence gas hydrate deposition. Studies in the Gulf of Mexico report gas hydrate observations in water depths ranging from 300-2400 meters, typically encountered at less than 1000 meters (Malone, 1994). Brooks et al., (1999) report gas hydrate occurrences offshore Nigeria in water depths ranging from 560-770 meters. Bottom-water temperature, water salinity, gas availability, and gas composition control the minimum water depth associated with gas hydrate stability (Brooks et al., 1986). Equilibrium conditions for gas hydrate occur in shallow sediments less than 6 meters below the sea floor. Seasonal changes in temperature may only affect gas hydrate stability in the upper 1-2 meters of sediment (Milkov and Sassen, 2000). Deeper deposits of gas hydrate form approximately 100-1000 meters below the sea floor. However, deposits in the Orca Basin occur at depths as low as 20-40 meters below the sea floor. Shallow marine sediments of continental slopes and abyssal plains typically exhibit a pressure-temperature envelope conducive to gas hydrate formation (Malone, 1994).

Depositional Environment

Environments associated with natural gas hydrate deposition typically exhibit high sedimentation rates and a continuous supply of methane (Cox, 1983). High rates of sediment supply and accretion promote gas hydrate formation in primarily two ways. First, proper mixtures of sediments containing organic matter can be quickly buried to the pressure-temperature regime required for gas hydrate formation. Second, a high sediment flux supports methane recycling (Cox, 1983).

The methane supply of an environment controls the preservation of natural gas hydrates. Methane gas concentrations must exceed the amount necessary to saturate pore waters in order for gas hydrate to form (Tucholke et al., 1977). Studies identify two sources of methane including microbial and thermogenic origins. Microbial, or biogenic, hydrocarbon gases form through degradation of organic matter in the absence of oxygen and sulfates (Booth et al., 1996 Thermogenic methane forms through catalytic reactions at temperatures exceeding 50°C (Kvenvolden and McMenamin, 1980).

Structural Controls

Geologic features commonly associated with gas hydrate deposits include mass movements, salt deformation, and active normal and growth faults. Mass movements may occur due to gas hydrate decomposition (Malone, 1994). Decomposition occurs based on several factors including fluctuations in seawater temperature, changes in sea level, and variable rates of methane gas concentration. Hydrate decomposition poses safety hazards in drilling and pipeline construction.

Piston cores and marine seismic records establish a strong association between shallow salt, active faulting, and gas hydrate deposits (Sassen et al., 1999). Gas hydrates coincide with diapiric crests and deep faults on flanks of diapirs. Faults resulting from the upward movement of diapirs produce lateral extension and fracturing. These mechanisms provide conduits for gas migration from deeper horizons into the pressure-temperature envelope of gas hydrate formation. Tectonics associated with salt diapirs and natural gas hydrate layers may also produce structural traps for hydrocarbons (Brooks et al., 1986). Sassen et al. (1994) report gas

hydrate observations along rims of salt-withdrawal basins and over salt ridges. Salt related fracture zones and faults provide pathways for heat flow and warm fluids from the subsurface to the sea floor, altering bottom-water temperatures, and modifying the hydrate stability zone (Booth et al., 1996). The relation between active geologic features and gas hydrate deposits suggests conditions other than regional temperatures and pressures dictate the vertical distribution of hydrate accumulation zones.

Properties of Host Sediments and Gas Hydrate Deposits

Gas hydrate formation affects diagenetic processes of sediments by producing unique migration pathways, products, and sedimentation rates that allow seeps and oil and gas traps to form. Gas hydrate deposition prevents normal sedimentation and obstructs diffusion and dissolution of ions in interstitial waters. Initial hydrate formation may occur along fractures, faults, and/or within cavities of coarse-grained sediment (Brooks et al. 1986). Previous discoveries show an irregular distribution of gas hydrates in ocean sediments (Brooks et al., 1986). However, limitations on reliable data on the in situ nature of gas hydrates exist due to poor core recovery techniques.

The textures of host sediments present a potential influence on the nature of hydrate occurrences. Booth et al. (1996) describe two general types of gas hydrate occurrences. The first type includes laminae, layers, plates, and mats suggesting crystallization parallel to bedding planes and faults. The second type includes nodules and massive deposits that form large particles capable of deforming bedding planes. Grain sizes observed with hydrate deposits range from coarse to very fine-grained sediments. Examples include medium to coarse-grained volcanic ash, sandy layers, carbonate rubble, silty mudstones, calcareous clay oozes, and high porosity silty sediments (Brooks et al., 1986). Booth et al. (1998) report the following associations between hydrate habit and host sediments: (1) layers or laminae of hydrate deposits are commonly observed in fine sediments, (2) granules and nodules are observed in fine sediments and coarse grain-size sediments, and (3) Hydrates formed within the matrix of sediments as cementation agents are strongly associated with coarser sediments. Biogenic hydrates primarily form crystal and small nodules, whereas thermogenic hydrates form nodules to thick layers to massive mounds (Brooks et al., 1986). Booth et al. (1998) report the porosity of gas hydrate host sediments ranges from 40-75 % with an average of 55%. Thicker accumulations of pure gas hydrate typically occur in higher porosity sediments. Sassen et al. (2001) report outcrops of gas hydrate mounds on the sea floor in the Gulf of Mexico. Research submersible observations establish a strong association between gas hydrate mounds and active vent sites. Gas hydrates rarely develop uniformly in nature or in a solid mass.

Observations on the Louisiana slope in the northern Gulf of Mexico exhibit gas hydrates in many forms including small to medium sized nodules (0.5-50 mm), interspersed layers (1-10 mm), and as solid masses (>150 mm) (Brooks et al., 1986). Other observations of hydrate samples contain carbonate concretions approximately 1 cm in diameter and fine-grained sediments stained with biodegraded crude oil (Cox, 1983). Oil-stained cores typically infer a thermogenic methane origin. However, some biogenic hydrates also contain oil stains (Brooks et al., 1986). Gas hydrates sampled from offshore Nigeria include large nodules (1-1.5 cm) and thin interspersed layers (Brooks et al., 1999).

ANALYSIS OF SPATIAL CONTINUITY USING INDICATOR VARIOGRAPHY

Methods

The spatial distribution of gas hydrate deposits within the two study regions was characterized by preparing indicator variograms. The data sets were compiled from multiple sources and include (1) sites where gas hydrates were either sampled directly or observed and (2) sites drilled without contact with gas hydrates. The data considered for each study area

included gas hydrate sampled locations reported by Sassen et al. (2001) and Milkov et al. (2000) for the Gulf of Mexico and Brooks et al. (1994) for the Gulf of Guinea. Sampling locations where hydrate was not observed were provided by TDI-Brooks International, Inc. as part of the 1997-2000 Gulf Program for surface geochemical exploration (SGE) and the 1996-2000 Nigeria Consortium Program. The Gulf SGE Program provided over 1000 core locations spanning the western and central sections of the Gulf of Mexico. The Nigerian Consortium Program provided close to 500 core locations.

The first study area includes a section of the continental margin of the Gulf of Mexico, located offshore southeast United States. The area is approximately 400 by 1000 km. The second study area includes a section of the continental margin of the Gulf of Guinea, located offshore Nigeria, West Africa. The area is approximately 350 by 550 km.

Sampled locations were assigned values based on an indicator function (Isaaks and Srivastava, 1989):

$$\mathrm{I}(\mathrm{x}) = \mathrm{I}(\mathrm{V_x} \mid \mathrm{H_x}) = \begin{cases} 1 & \mathrm{V_x} = \mathrm{H_x} \\ 0 & \text{otherwise} \end{cases}.$$

An indicator value of one was assigned to locations where gas hydrates were present and a value of zero where gas hydrates were absent. GS+ software (Robertson, 2000) was used to generate both isotropic and anisotropic sample variograms based on the indicator values. Multiple isotropic variograms were examined to establish the appropriate distance parameters in each study area. The lag spacing and distance over which the variance was calculated was adjusted to produce a variogram with clear structure. The lag spacing (δ) and lag distance (L) satisfied the following conditions:

δ > minimum distance between points

$L = K\delta$

where $K\delta \approx \frac{1}{4}$ maximum distance between points and L is less the than maximum distance between points. The nugget, sill and range of the isotropic variogram model were adjusted to determine the best-fit model. Variograms with an active lag and a uniform interval ranging from 100-500 km and 2-20 km, respectively, were used in the comparison process. The isotropic analysis provided a description of the spatial continuity as a function of distance. Model parameters including a regression coefficients (R^2) and residual sums of squares (RSS) calculated by GS+ provided a measure of the model fit to the variogram data.

A contour map of the variogram surface identified the orientation of the anisotropy axes used in modeling the directional trends in the data. The principal axis defined the direction of least variation across the variogram surface, or direction of maximum continuity. Multiple directional variograms based on the principle axis were generated using different offset angles. The structure, fit, and number of pairs for each point of the directional variograms were compared to obtain a suitable offset tolerance. The nugget, sill and correlation length of the anisotropic variogram model were adjusted to determine the best-fit model.

The isotropic variogram model was used to indicator krige unsampled locations on a uniform grid of the Gulf of Mexico study area. Indicator kriging provides a useful non-parametric estimation technique and assumes the distribution is constant across the study area. Indicator kriging calculates the probability of sampling gas hydrate as conditioned by the value, location, and separation distance between neighboring sampled sites and the site to be predicted. The equations used for indicator kriging include (Isaaks and Srivastava, 1989):

$$\sum_{j=1}^{N} w_j C_{ij} + \mu = C_{i0}$$

$$\sum_{i=1}^{N} w_i = 1$$

where w_i corresponds to the weight assigned to each known point and C_{ij} defines the covariance function between neighboring pairs. The predicted value, or local average of an indicator, was calculated using (Isaaks and Srivastava, 1989):

$$\hat{I}(V_{(x_0)}) = \sum_{i=1}^{N} w_i I(V_{(x_i)}).$$

The predicted indicator value represents the probability of sampling gas hydrate based on a conditional expected value:

$$E\left\langle \hat{I}(V_{(x_0)} \mid V_{(x_i)} \right\rangle = P\left(V_{(x)} \leq V \mid V_{(x_i)}\right).$$

Results and Discussion

The isotropic variogram with an active lag of 180 km and a uniform interval of 5 km produced the clearest structure for the Gulf of Mexico study area (Figure 1). The isotropic variogram was fit with a spherical model with a correlation length of 65 km, a sill value of 0.0396, and a relative nugget of 58.1% (Table 1). The maximum direction of spatial continuity trends approximately 43° with the minimum axis at approximately 133°. Directional variograms along the maximum and minimum anisotropic axes with an offset tolerance of 10° were fit with a spherical model (Figure 2). Sampled sites are correlated at a distance of 35 km in the direction of maximum continuity and 25 km in the direction of minimum continuity. The sill value for the anisotropic spherical model was 0.0396 with a relative nugget effect of 63.1% (Table 2).

The isotropic variogram with an active lag of 180 km and a uniform interval of 5 km produced the clearest structure for the Gulf of Guinea study area (Figure 3). The isotropic variogram was fit with a spherical model with a range of 110 km, a sill value of 0.035, and a relative nugget effect of 2.9% (Table 1). No significant spatial anisotropy was evident in the Nigerian continental margin for the data set as a whole.

A contour map of the conditional probability provides a summary of the spatial continuity of gas hydrate deposits derived from the indicator kriging process. Figure 4 is a conditional probability map for the Gulf of Mexico and represents the likelihood of sampling gas hydrates within the area. To include geometric constraints associated with the shore line, soft data points were assigned a value of zero at locations with water depths too shallow to allow hydrate formation. Core locations with their corresponding indicator values are shown for reference.

Isotropic variograms for both study areas show a strong variance structure. The increased variance observed above the sample variance and the slightly erratic nature of the points beyond the correlation length suggest a regional trend is present in both data sets. Gas hydrate forming processes appear similar in both environments when comparing spatial structure. The correlation length is shorter in the Gulf of Mexico than in the Gulf of Guinea, suggesting gas hydrate deposits are correlated over a shorter distance in the Gulf of Mexico.

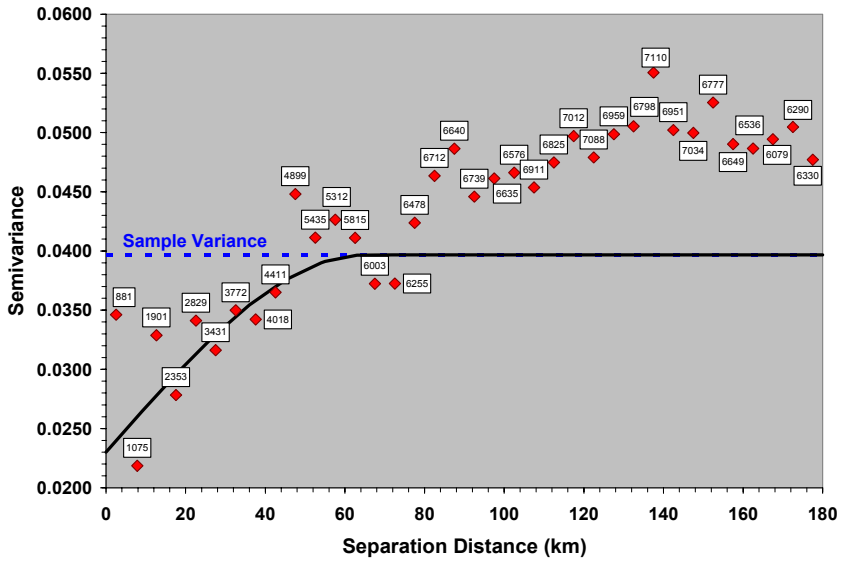

Figure 1
Isotropic experimental variogram and best-fit model for the Gulf of Mexico

Table 1

Isotropic Model Results		
Site	**Gulf of Mexico**	**Gulf of Guinea**
Model	spherical	spherical
Lag Distance (km)	180	180
Lag Class Interval (km)	5	5
Correlation Length (km)	65	110
Nugget	0.023	0.001
Sill	0.0396	0.034
R^2	0.637	0.747
RSS	0.001938	0.002200

Table 2

Anisotropic Variogram Results	
Site	**Gulf of Mexico**
Model	spherical
Max Continuity Direction	43°
Min Continuity Direction	133°
Lag Distance (km)	180
Lag Class Interval (km)	5
Major Axis Correlation Length (km)	35
Minor Axis Correlation Length (km)	25
Nugget	0.025
Sill	0.0396

R^2	0.314
RSS	0.0262

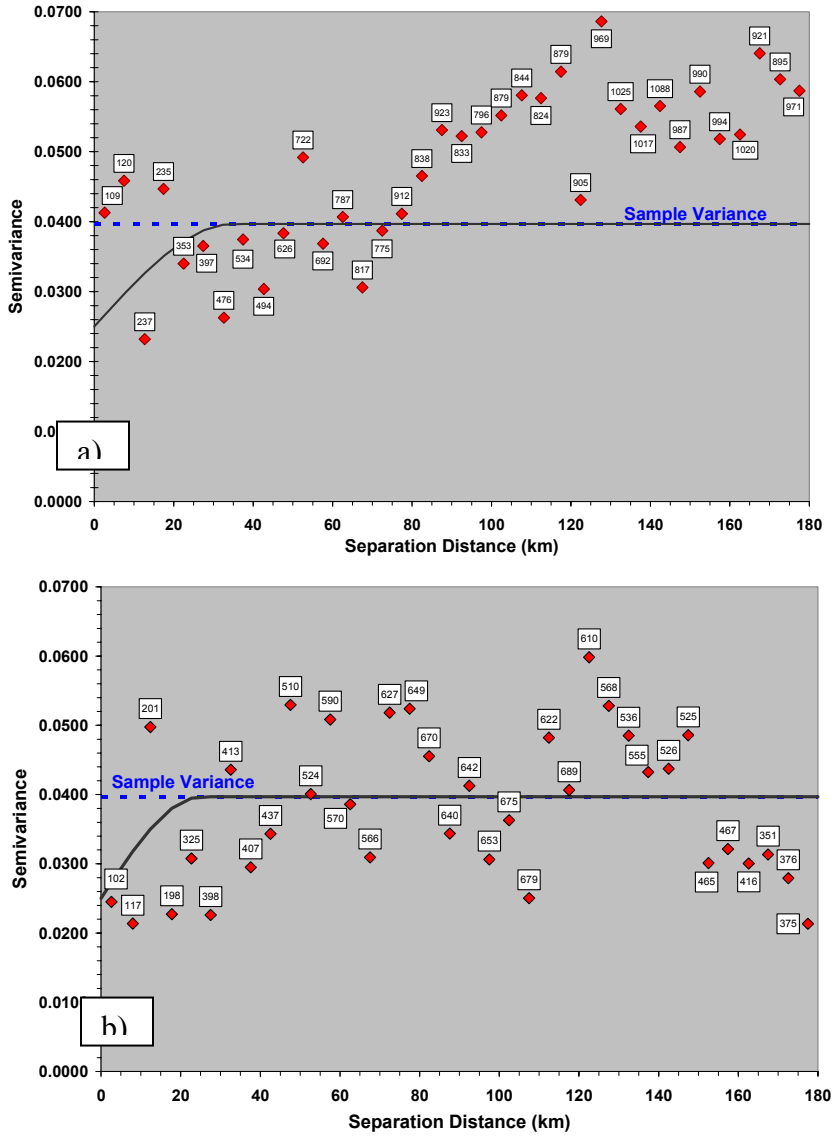

Figure 2
Anisotropic experimental variograms and best-fit models for a) maximum direction of continuity and b) minimum direction of continuity

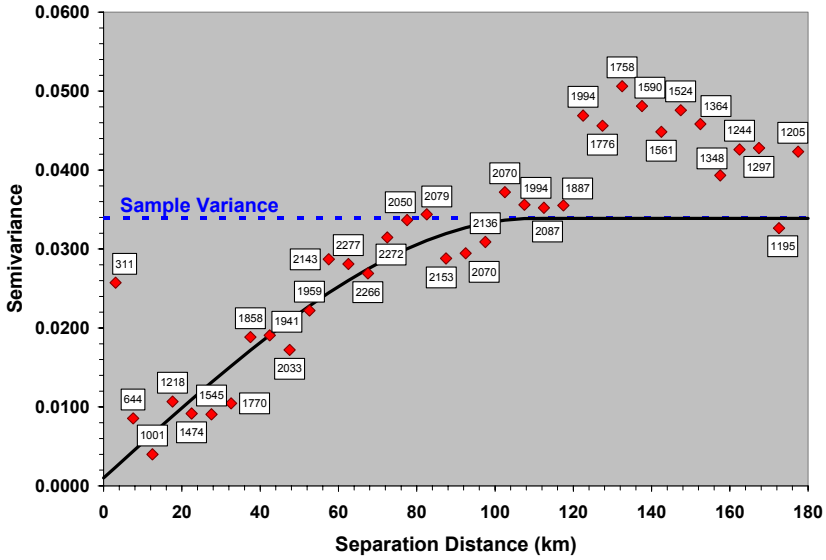

Figure 3
Isotropic experimental variogram and best-fit model for the Gulf of Guinea

The anisotropic variograms also show a degree of structure, but require a more rigorous analysis to determine the true patterns related to gas hydrate deposits, especially in the Gulf of Guinea study area. The maximum direction of spatial continuity identified in the Gulf of Mexico corresponds with the alignment of gas hydrate locations, suggesting an underlying structure control on gas hydrate formation. Gas hydrates have been reported to form localized deposits along faults and edges of salt diapers in the Gulf of Mexico.

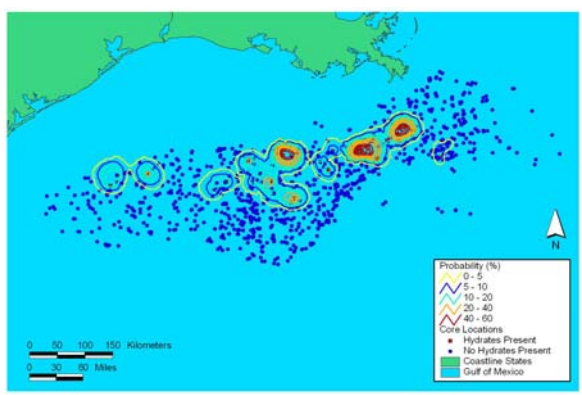

Figure 4
Isotropic conditional probability map of gas hydrate occurrences: Gulf of Mexico

Conclusion

Indicator variograms suggests a strong spatial continuity exists between gas hydrate locations as a function of both distance and direction from neighboring sampled locations. The nugget effect observed in the variograms is likely a result of bias sampling procedures. The nugget effect produces weights in the kriging process that are more equally distributed, inducing a source of error in the analysis. Additional analysis, and perhaps additional sampling, is required for investigations of anisotropy in the Gulf of Guinea case. Anisotropic variograms can be used to more accurately assign weights to sampled sites, increasing the weight for sites in

the direction of maximum continuity. The stability of the spatial variance structure suggests a sufficient stationarity of hydrate forming processes that can be used for spatial prediction with stochastic models.

Basic knowledge of the nature of gas hydrate deposits contributes to an overall understanding of worldwide gas hydrate environments. Analysis of gas hydrate geology provides information for safe and efficient exploration and exploitation of economic resources and provides data for models of climatic change.

LOGISTIC REGRESSION ANALYSIS OF GAS HYDRATE OCCURRENCES

Methods

Logistic regression analysis was used to estimate the parameters of a regression model using a binary dependent variable. The dataset includes a subset of offshore gas hydrate samples compiled from published observations and measurements recorded from 1982-1994 (Booth and Rowe, 1996). The properties recorded for each observation include:

- Geographic location
- Water depth
- Subbottom depth
- Temperature at hydrate sample

The water depths, recorded directly from the referenced literature, are reported for each sample site. The subbottom depth refers to the vertical distance from the seafloor to the position of the gas hydrate sample or the top of the sampled gas hydrate zone. The temperature is reported at the depth of each gas hydrate sample, commonly based on downhole temperature data. Hydrates occurring at the seafloor report the bottom water temperature. The gas hydrate offshore database (Booth and Rowe, 1996) provided a total of 31 observations from 12 distinct regions.

Additional observations were compiled from log data obtained through the Ocean Drilling Program. These observations also include water depth, subbottom depth, and temperature measurements (downhole data) but denote locations where gas hydrates were not drilled. ODP records provided 100 observations selected at random. The analysis included a total of 131 observations.

Sampled locations were assigned values based on an indicator function (Isaaks and Srivastava, 1989):

$$I(x) = I(V_x \mid H_x) = \begin{cases} 1 & V_x = H_x \\ 0 & otherwise \end{cases}.$$

An indicator value of one was assigned to locations where gas hydrates were present and a value of zero where gas hydrates were absent. The Excel program XLSTAT-Pro 6.1.9 (Addinsoft Software, 2003) was used to conduct the logistic regression analysis for multiple combinations of the three identified parameters.

Logistic regression is a non-linear transformation of the linear regression model. It is commonly used for (1) estimating the outcome of a categorical variable or (2) when the assumptions of classical linear regression do not apply to a dataset. The logistic regression model provides the conditional probability that an event (gas hydrate occurrence) will occur based on the following function:

$$P\langle Y = 1 \mid X \rangle = P = \frac{\exp(a + BX)}{1 + \exp(a + BX)}$$

where *a* is the coefficient on the constant term, *B* is the coefficient(s) on the independent variable(s), and *X* is the independent variable(s) (Hosmer and Lemeshow, 1989). The logistic

distribution is an S-shaped distribution function that constrains the estimated probabilities between 0 and 1. The dependent variable of a logistic regression model is interpreted as the natural logarithm of the odds that the dependent binary variable is equal to 1 rather than 0. The parameters of logistic regression are interpreted as the expected change in the "log of the odds" of the binary dependent variable. The antilogarithms of the coefficient values provide an expected change in the "odds" of the binary dependent variable associated with a one unit change in the independent variable (Hosmer and Lemeshow, 1989). The error associated with the logistic regression model follows a binomial distribution.

Model statistics used to determine the significance of each estimator and model include the chi-square statistic, log likelihood, Pearson's chi-square, log ratio chi-square, and a modified determination coefficient, R^2. The chi-square statistics are similar to the F statistic used in ordinary regression analysis; the higher the statistic the more significant the estimator or model. Probabilities for the chi-square statistic provide the probability of being wrong when saying that the explanatory variables bring significant information to (1) explain the observed values or (2) compared to the independent model. The log likelihood value is the log of the likelihood function that is used to maximize the probability estimates. High log likelihood values indicate a more significant estimator or model. The McFadden Pseudo R^2 is the proportion of the variance in the dependent variable which is explained by the variance in the independent variables.

Results

Three models were tested in the logistic regression analysis to determine the most significant predictor variables for modeling the occurrence of gas hydrates. Table 3 describes each model and lists the resulting statistics used to choose the best-fit model.

Table 3
Logistic regression model statistics

Model	Parameters	P > Chi-square	Log Likelihood	Pearson's Chi-square	P > Chi-square	L.R. Chi-square	P > L.R. Chi-square	Pseudo R^2
A	Water Depth (m)	0.003	-60.718	278.427	< 0.0001	21.925	< 0.0001	0.152936
	Subbottom Depth (m)	0.246						
	Temp (C)	0.091						
B	Water Depth (m)	0.000	-61.524355	270.709189	< 0.0001	20.31174	< 0.0001	0.141683
	Temp (C)	0.029						
C	Temp (C)	0.008	-58.941668	286.917002	< 0.0001	25.47712	< 0.0001	0.177714
	Log Pressure (MPa)	< 0.0001						

Model A describes a full model that includes all three parameters thought to influence gas hydrate deposition. The significance of each independent variable is evaluated by the P > Chi-square value. The probability associated with subbottom depth is significantly higher compared to the water depth and temperature parameters. This suggests subbottom depth is not a statistically significant independent variables for predicting gas hydrate occurrences.

Model B excludes the subbottom depth variable to examine the effect of the variable in the model. The test statistics and probabilities for Model B are similar to the results of Model A,

showing only slight differences in the fit of the models. The subbottom depth variable used in Model A does not appear to increase the significance of the model and can be eliminated from the analysis.

Model C uses temperature and the log of pressure (derived from water depth). These parameters are commonly used to determine the phase boundary of gas hydrates. Model C tests whether these independent variables might also be useful in a regression analysis for determining gas hydrate presence. The significance of each independent variable suggests these parameters could accurately model hydrate occurrence, but the test statistics and probabilities show Model C to be less significant than Model A or Model B.

Figure 5 shows the standardized residuals for each model. The residuals are similar for each model, with an increase in error for observation numbers 27-31. Figure 6 considers the predictive ability of Model B. The conditional probabilities calculated from the model are compared to known observations with 100% corresponding to the presence of gas hydrate and 0% corresponding to the absence of gas hydrate. The overall accuracy of the model when applied to the dataset with which the model was developed was 89.3% (calculated as 117 correct predictions for the 131 observations within the dataset) (Table 4). The accuracy of the model was assessed by establishing an arbitrary 40% conditional probability threshold.

Conclusions

Model B is the recommended model to use for estimating the conditional probability of encountering gas hydrates given water depth and temperature. Model B produces the lowest P-values, a higher log likelihood value, the lowest Pearson's chi-square value, and comparable L.R. chi-square and Pseudo R^2 values. Model B produced the following probability equation for estimating the global occurrence of gas hydrate deposits:

$$P = \frac{1}{1 + \exp(-(1.029 - 7.425(WaterDepth) - 0.123(Temperature)))}$$

with water depth measured in meters and temperature measured in °C. An improved dataset including all recently discovered gas hydrates as well as more observations where gas hydrates have not been found would serve to further justify the use of a logistic regression model.

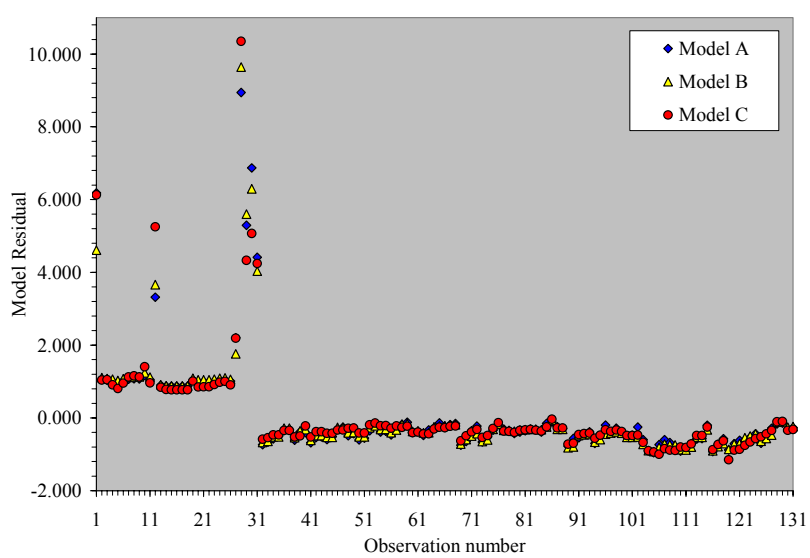

Figure 5: Residual plot for each logistic model considered

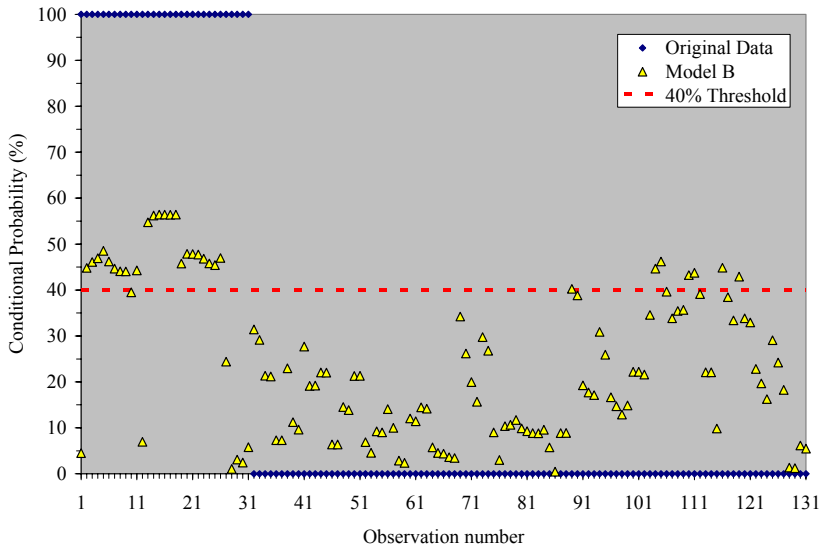

Figure 6: Predictive ability of the selected logistic regression model

Table 4: Classification table based on the logistic regression model

		Hydrate Occurrence		Accuracy of Model Prediction
Model Prediction		YES	NO	89.3 %
	YES	23	6	
	NO	8	94	

REFERENCES

Booth, J.S., and Rowe, M.M., 1996. Offshore gas hydrate sample database with an overview and preliminary analysis. USGS Open-File Report 96-272: Massachusetts, 17 p.

Booth, J. S., Winters, W.J., Dillon, W.P., Clennell, M.B., and Rowe, M.M., 1998, Major Occurrences and Reservoir Concepts of Marine Clathrate Hydrates: Implications of Field Evidence, *in* J. P. Henriet, and Mienhert, J., ed., Gas Hydrates: Relevance to World Margin Stability and Climate Change, London, Geological Society, p. 113-127.

Brooks, J. M., B.H. Cox, W.R. Bryant, M.C. Kennicutt III, R.G. Mann, T.J. McDonald, 1986, Association of Gas Hydrates and Oil Seepage in the Gulf of Mexico: Organic Geochemistry, v. 10, p. 221-234.

Brooks, J. M., Bryant, W.R., Bernard, B.B., and Cameron, N.R., 1999, The Nature of Gas Hydrates on the Nigerian Continental Slope: Annals of the New York Academy of Sciences, v. 912, p. 76-93.

Brooks, J.M., Anderson, A.L., Sassen, R., MacDonald, I.R., Kennicutt, M.C. II, and Guinasso, N.L., Jr., 1994, Hydrate occurrences in shallow subsurface cores from continental slope sediments, *in* Sloan, E.D., Jr., Happel, John, Hnatow, and Miguel A., ed., International Conference on Natural Gas Hydrates: Annals of the New York Academy of Sciences, v. 715, p. 381-391

Cox, J. L., 1983, Natural Gas Hydrates: Properties, Occurrence, and Recovery: Woburn, Butterworth Publishers, 125 p.

Hosmer, David, and Lemeshow, Stanley, 1989. Applied Logistic Regression: New York, Wiley, 307p.

Isaaks, E. H., and Srivastava, M.R., 1989, An Introduction to Applied Geostatistics: New York City, Oxford University Press, 561 p.

Kaplan, I. R., 1974, Natural Gases in Marine Sediments, v. 3: New York, Plenum Press, 317 p.

Kvenvolden, K. A., Mark A. McMenamin, 1980, Hydrates of Natural Gas: A Review of Their Geologic Occurrence, Reston, U.S. Geological Survey.

Kvenvolden, K. A., Ginsburg, G.D., and Soloviev, V.A., 1993, Worldwide Distribution of Subaquatic Gas Hydrates: Geo-Marine Letters, v. 12, p. 32-40.

Malone, R., 1994, Overview: Gas Hydrate Geology and Geography: Annals of the New York Academy of Sciences, v. 715, p. 225-231.

Milkov, A. V., and Sassen, R., 2000, Thickness of the Gas Hydrate Stability Zone, Gulf of Mexico Continental Slope: Marine and Petroleum Geology, v. 17, p. 981-991.

Robertson, G. P., 2000, GS+: Geostatistics for the Environmental Sciences, Plainwell, Michigan, Gamma Design Software.

Sassen, R., I.R. MacDonald, 1994, Evidence of Structure H Hydrate, Gulf of Mexico Continental Slope: Organic Geochemistry, v. 22, p. 1029-1032.

Sassen, R., S.T. Sweet, A.V. Milkov, D.A. DeFreitas, G.G. Salata, E.C. McDade, 1999, Geology and Geochemistry of Gas Hydrates, Central Gulf of Mexico Continental Slope: Transactions - Gulf Coast Association of Geological Societies, v. 49, p. 485-497.

Sassen, R., Sweet, S., Milkov, A. V., DeFreitas, D. A., Kennicutt II, M.C., and Roberts, H., 2001, Stability of Thermogenic Gas Hydrate in the Gulf of Mexico: Constraints on Models of Climate Change, *in* C. K. Paull, and Dillon, William P., ed., Natural Gas Hydrates: Occurrence, Distribution, and Detection: Geophysical Monograph Series, Washington, DC, American Geophysical Union, p. 131-143.

Tucholke, B. E., Bryan, George M., and Ewing, John, 1977, Gas Hydrate Horizons Detected in Seismic-Profiler Data from the Western North Atlantic: AAPG Bulletin, v. 61, p. 698-700.